Die dissimilatorische APS-Reduktase

-Vorkommen, Phylogenie, Struktur und Anwendung

in der funktionellen Genanalyse

Dissertation

zur Erlangung des Grades eines

Doktors der Naturwissenschaften

- Dr. rer. nat. -

dem Fachbereich Biologie/Chemie der

Universität Bremen vorgelegt von

Birte Meyer

aus Daverden

Bremen 2008

1. Gutachter: Prof. Dr. Friedrich Widdel

2. Gutachter: Dr. Jan Küver

Tag des Promotionskolloquiums: 02.03.2009

INHALTSVERZEICHNIS

Abkürzungsverzeichnis

Å	Angström (Einheit der Länge, verwendet in der Kristallographie)
AAPB	Aerobe anoxygene phototrophe Bakterien
AmoA	Ammonium-Monooxygenase, α-Untereinheit
APAT	Adenylylsulfat:Phosphat-Adenylyltransferase
AprBA	dissimilatorische Adenosin-5`-Phosphosulfat-Reduktase, α- und β-Untereinheit
AprM	potentielle, membranverankernde Untereinheit der reversen dissimilatorischen APS-Reduktase in SOP
APS	Adenosin-5`-Phosphosulfat
ATCC	American Type Culture Collection
BP	before the present
Cdt.	Canditatus
cf.	conferre („vergleiche“)
CysC	APS-Kinase
CysH	assimilatorische PAPS-Reduktase
DGGE	Denaturierende Gradienten-Gelelektrophorese
DMSP	Dimethylsulfoniopropionat
DoxDA	Thiosulfat:Chinon-Oxidoreduktase (Thiosulfatdehydrogenase)
DSM(Z)	Deutsche Sammlung von Mikroorganismen und Zellkulturen
DsrAB	dissimilatorische Sulfitreduktase, α- und β-Untereinheit
DsrMKJOP	Transmembran-Redoxkomplex, der funktionell mit der dissimilatorischen Sulfitreduktase assoziiert ist
FccAB	Flavocytochrom c Sulfiddehydrogenase
FeS(-Zentrum)	Eisen-Schwefel(-Zentrum)
f. *thios.*	forma *thiosulfatophilum*
Ga	giga annus (Giga-Jahr, entspricht 1.000.000.000 Jahren)
Hdr	Heterodisulfidreduktase (HdrABC bzw. HdrDE)
Kb	Kilobasen
kDa	Kilodalton
LGT	lateraler Gentransfer (Synonym: horizontaler Gentransfer, HGT)
Mb	Megabasen

MIF	massenunabhängige Schwefel-Isotopenfraktionierung (^{33}S Schwefel-Isotop)
NCIB	National Center for Biotechnology Information
Nk	Nukleotide
ORF	open reading frame
PAL	present atmospheric level
PAPS	3`-Phosphoadenosin-5`-Phosphosulfat
QmoABC	quinone-interacting membrane-bound oxidoreductase, potentielle Menachinol:APS-Reduktase-Oxidoreduktase, A-, B- und C-Untereinheit
16S rRNA	ribosomale Ribonukleinsäure
SAOR	Sulfit:Akzeptor-Oxidoreduktase (Synonym: Sulfitdehydrogenase)
Sat	dissimilatorische ATP-Sulfurylase
SDO	Schwefel-Dioxygenase
SIF	massenabhängige Schwefel-Isotopenfraktionierung
SOP	schwefeloxidierende Prokaryonten
SorAB	Sulfit:Akzeptor-Oxidoreduktase von *Starkeya novella*, A- und B-Untereinheit
Sox System	thiosulfat-/schwefeloxidierendes Multienzymsystem (die vier periplasmatischen Enzymkomplexe SoxXY, SoxYZ, SoxB, $Sox(CD)_2$ bilden das katalytisch-aktive Sox Enzymsystem)
SoxB	Sulfat-Thiol-Hydrolase (Komponente des Sox Systems)
SoxCD	Schwefeldehydrogenase (Komponente des Sox Systems)
s(p)p.	Spezies
SQR	sulfide:quinone oxidoreductase, Sulfid:Chinon-Oxidoreduktase
SRP	dissimilatorisch sulfatreduzierende Prokaryonten
ssp.	Subspezies
TOMES	thiosulfatoxidierendes Multienzymsystem von *Paracoccus* spp.
UASB	upflow anaerobic sludge badge

Summary

Within this doctoral thesis, the distribution, phylogeny and structure of the dissimilatory APS reductase (AprBA) of sulfate-reducing and sulfur-oxidizing prokaryotes (SRP and SOP) has been analyzed. An assay for *aprA*-based functional gene analysis was developed for determination of the SRP and SOP diversity in environmental samples. In addition, the distribution of the sulfate thiol hydrolase (SoxB, a component of the thiosulfate-oxidizing multi-enzyme system Sox) in SOP was investigated.

1. The reverse dissimilatory APS reductase is restrictedly distributed among the photo- and chemotrophic SOP; the absence of the AprBA in many sulfate-producing species points to the general existence and essential physiological relevance of alternative sulfite-oxidizing enzymes (e. g. the sulfite:acceptor oxidoreductase) in SOP.

2. The congruent topologies of the AprB and AprA trees indicate a shared evolutionary path for the APS reductase subunits by vertical inheritance (speciation) and concomitant lateral gene transfer (LGT) of the *aprBA* among the SRP and SOP. Novel LGT events across the SRP divisions were detected comprising *Desulfobacca acetoxidans* and *Thermacetogenium phaeum*. The latter species is the first validated sulfate-reducer proven to have been affected by a recent lateral *aprBA* gene transfer (as a putative effect of long-term co-cultivation with *Thermodesulfovibrio* spp.). In the AprBA trees, the SOP are divided into two phylogenetically distant lineages, Apr lineage I and II. The proteins of Apr lineage II (sequences of *Chlorobiaceae* and some photo- and chemotrophic *Beta-* and *Gammaproteobacteria*) are in closer affiliation to the proteins of the SRP indicating several, independant events of lateral *aprBA* gene transfer from the SRP to the SOP lineages. Some beta- and gammaproteobacterial SOP species harbour an „authentic“ as well as a SRP-related, laterally transferred *apr* gene locus, whereas others possess exclusively the xenologous gene locus as a result of orthologous *aprBA* gene replacement („xenologous gene displacement“). The two-*aprBA*-gene state in some species might be an intermediate state in the genome evolution process.

3. The phylogenetic separation into three major Apr lineages (1) proteobacterial sulfur-oxidizers (orthologous SOP Apr lineage I), (2) bacterial sulfate-reducers (including xenologous SOP (SOP Apr lineage II) and *Archaeoglobus* spp.), and (3) crenarchaeal SRP (*Caldivirga* spp.) correlates with the differing presence of AprM, Qmo and Hdr encoding genes in the genomes of SRP and SOP. The AprBA-congruent phylogenies of the AprM

and Qmo proteins point to their coevolution to the dissimilatory APS reductase as functionally associated proteins. The dissimilatory APS reductase might have originated as an enzyme working in the oxidative direction for detoxification of the DsrAB product, sulfite, within ancestors of the modern sulfur-oxidizing anoxygenic phototrophic bacteria.

4. The three-dimensional APS reductase models from SRP and SOP demonstrate a generally high structural conformity (with the exception of the presumably non-functional enzymes of *Pyrobaculum* spp.). This indicates an identical catalytic reaction mechanism for the sulfite oxidation/APS reduction in all dissimilatory APS reductases. The alterations within the AprB models represent structural adaptations of the β-subunits to the aforementioned different interacting partners. Thus, the structural differences between the proteins correlate with the phylogeny but not with the metabolism type of the enzyme.

5. The *aprA*-specific universal primer pair allows the simultaneous analysis of the SRP and SOP diversity in environmental samples. In contrast to the 16S rRNA and *dsrAB* gene analysis, the application of the *aprA* as functional marker in molecular ecological surveys allows the definite identification of (novel) SRP. In consequence of the restricted distribution of the *apr* genes among the photo- and chemotrophic SOP, the *apr*-based analysis will only detect a certain species spectrum of the SOP diversity of a habitat. With regard to the various microbial sulfur oxidation pathways, a simultaneous determination of the entire SOP complexity within an environmental sample by using a single functional marker gene is generally impossible.

6. The *aprA*-based gene analysis of environmental samples collected from the area of the Lesser Antilles volcanic arc, Caribbean Sea, demonstrated the photic regions of the water column and oxic sediment layers to have been dominated by sulfur-oxidizing, putatively chemolithoheterotrophic Alphaproteobacteria. The microbial community inhabiting the manganese crust surfaces revealed a higher phylogenetic diversity and complexity of sulfur-oxidizers comprising chemolithoheterotrophic and -autotrophic representatives of *Alpha*-, *Beta*- and *Gammaproteobacteria* as well as a potential novel SOP lineage.

7. The 16S rRNA, *aprA*- and *amoA*-based gene analysis of the caribbean deep-sea sponge, *Polymastia* cf. *corticata*, demonstrated the presence of a phylogenetically divergent and complex microbial community (*Porifera*-/*P.* cf. *corticata*-specific microorganisms as well as „contaminants“ acquired by its filtration activity from the environment); in context with other studies, the results of this work demonstrate the sponge species specificity of the associated microbial community. The spatial distribution of a species within the *P.* cf.

corticata sponge body correlated with its phylogenetic affiliation, classification as sponge-specific or -unspecific, and potential ecophysiological function. On the basis of the *aprA* gene analysis, a sponge-specific, endosymbiotic sulfur cycle is postulated to exist in the *P.* cf. *corticata.*

8. The presence of the *soxB* gene in all thiosulfate-oxidizing, obligately sulfur globules [S^0] forming photo- and chemotrophs examined in this study indicates the general involvement of the Sox system in the initial thiosulfate oxidation step. The Sox system represents the most widespread enzymatic pathway for the oxidation of anorganic sulfur compounds among bacterial SOP. Therefore, *soxB* is a suitable molecular marker for the detection of (thiosulfate-oxidizing) SOP (with the exception of acidophilic species). The 16S rRNA-incongruent SoxB tree topology points to several events of LGT across the SOP divisions (e. g. *soxB* gene transfer from representatives of the *Epsilonproteobacteria* to species of the *Aquificae* and *Thermus*). The *soxB*-xenologous *Chromatiaceae*, *Ectothiorhodospiraceae* and *Chlorobiaceae* points to an acquisition of their Sox system-mediated thiosulfate oxidation capability from putatively different chemotrophic donors of the *Gammaproteobacteria* lineage. The SoxB phylogeny indicates an (epsilon-)proteobacterial origin of the *soxB* gene within a aerobic, chemothiotrophic microorganism.

Zusammenfassung

Im Rahmen der Doktorarbeit wurde die Verbreitung, Phylogenie und Struktur der dissimilatorischen APS-Reduktase (AprBA) von sulfatreduzierenden und schwefel-oxidierenden Prokaryonten (SRP und SOP) analysiert. Eine *aprA*-basierende funktionelle Genanalyse wurde zur Diversitätsbestimmung von SRP und SOP in Umweltproben eingesetzt. Des Weiteren wurde die Verbreitung der Sulfat-Thiol-Hydrolase (SoxB, Komponente des thiosulfatoxidierenden Multienzymsystems Sox) in SOP untersucht.

1. Die reverse dissimilatorische APS-Reduktase ist in den photo- und chemotrophen SOP begrenzt verbreitet; das Fehlen der AprBA in vielen sulfatproduzierenden Spezies ist ein Hinweis auf die generelle Präsenz und essentielle physiologische Bedeutung von alternativen sulfitoxidierenden Enzyme (z. B. Sulfit:Akzeptor-Oxidoreduktasen) in SOP.

2. Die AprB und AprA Stammbaum-Topologien sind kongruent und weisen auf einen gemeinsamen Evolutionsweg über vertikale Vererbung (Speziation) und simultanen lateralen Gentransfer (LGT) der kodierenden Gene in SRP und SOP hin. Neue *aprBA* LGT-Vorgänge zwischen den SRP Linien betreffen *Desulfobacca acetoxidans* und *Thermacetogenium phaeum*. Letztere Spezies ist der erste validierte Sulfatreduzierer, für den ein rezenter lateraler *aprBA* Gentransfer nachgewiesen werden konnte (als Folge einer langzeitlichen Kokultivierung mit *Thermodesulfovibrio* spp.). Die SOP sind in den AprBA Stammbäumen in zwei phylogenetisch separate Linien aufgetrennt, SOP Apr Linie I und II. Die Proteine der SOP Apr Linie II (Sequenzen der *Chlorobiaceae* und einiger photo- und chemotropher *Beta-* und *Gammaproteobacteria*) sind verwandt zu den Proteinen der SRP; dies weist auf mehrere, unabhängige laterale Transfervorgänge der *aprBA* Gene von den SRP zu den SOP hin. Einige beta- und gammaproteobakterielle SOP besitzen sowohl einen „authentischen“ als auch einen SRP-verwandten, lateral-transferierten *apr* Genlocus, während andere nah verwandte Spezies durch den Ersatz der orthologen *aprBA* Gene (SOP Apr Linie I) nur noch einen xenologen Genlocus enthalten („xenologous gene displacement“). Die Existenz beider homologen *aprBA* Gene in einigen Spezies könnte ein genomischer Übergangszustand sein.

3. Die phylogenetische Auftrennung in drei Apr Hauptgruppen (1) proteobakterielle SOP (orthologe SOP Apr Linie I), (2) bakterielle SRP (einschließlich xenologer SOP (SOP Apr Linie II) und *Archaeoglobus* spp.) und (3) crenarchaeelle SRP (*Caldivirga* spp.) korreliert mit der jeweiligen An-/ Abwesenheit von AprM-, Qmo- und Hdr-kodierenden Genen in

den Genomen der SRP und SOP. Die AprBA-kongruenten Phylogenien der AprM und QmoABC verdeutlichen ihre Koevolution zur dissimilatorischen APS-Reduktase als funktionell assoziierte Proteine. Die APS-Reduktase könnte als ein in oxidativer Richtung arbeitendes Enyzm in Vorläufern der heutigen schwefeloxidierenden anoxygenen phototrophen Bakterien zur Detoxifikation des DsrAB-Endproduktes, Sulfit, entstanden sein.

4. Die dreidimensionalen APS-Reduktase Strukturmodelle von SRP und SOP zeigen eine allgemein hohe strukturelle Konformität (mit Ausnahme der vermutlich funktionsunfähigen Enzyme der *Pyrobaculum* spp.), d. h. der katalytische Reaktionsmechanismus der Sulfitoxidation/APS-Reduktion ist in allen dissimilatorischen APS-Reduktasen identisch. Die Unterschiede in den AprB Modellen stellen vermutlich strukturelle Adaptationen der β-Untereinheiten an die o. g. unterschiedlichen physiologischen Interaktionspartnern dar. Die Strukturunterschiede zwischen den Proteinen korrelieren demnach mit der Phylogenie, aber nicht mit dem Metabolismus-Typ des Enzyms.

5. Das *aprA*-spezifische universelle Primerpaar ermöglicht eine simultane Analyse der SRP und SOP Diversität in Umweltproben. Im Gegensatz zur 16S rRNA und *dsrAB* erlaubt die *aprA* Genanalyse eine zweifelfreie Identifizierung von (neuen) SRP. Aufgrund der limitierten Verbreitung der *apr* Gene in SOP kann über die *apr*-basierende Genanalyse allerdings nur ein bestimmtes Spezies-Spektrum der SOP Diversität eines Habitates erfasst werden. Aufgrund der unterschiedlichen mikrobiellen Schwefeloxidationswege ist eine simultane Bestimmung der gesamten SOP Komplexität einer Umweltprobe über die Analyse eines einzelnen funktionellen Genes generell nicht möglich.

6. Die *aprA*-basierende Genanalyse von Umweltproben des vulkanischen Inselbogens der Kleinen Antillen, Karibisches Meer, zeigte die Dominanz von schwefeloxidierenden, möglicherweise chemolithoheterotrophen Alphaproteobakterien in der photischen Wasserzone und den oxischen Sedimentschichten. Die mikrobielle Gemeinschaft der Mangankrustenoberflächen wies eine höhere phylogenetische Diversität und Komplexität an Schwefeloxidierern auf, die chemolithoheterotrophe und -autotrophe Vertreter der *Alpha*-, *Beta*- und *Gammaproteobacteria* sowie eine möglicherweise neue SOP Linie umfasste.

7. Die 16S rRNA, *aprA*- und *amoA*-basierenden Genanalysen des karibischen Tiefsee-Schwammes *Polymastia* cf. *corticata* zeigten die Präsenz einer phylogenetisch divergenten und komplexen mikrobiellen Gemeinschaft (*Porifera*-/*P*. cf. *corticata*-

spezifische Mikroorganismen sowie über Filtrationsaktivität aus der Umgebung aufgenommene „Kontaminanten“); im Kontext mit weiteren Studien weisen die Daten auf die generelle Schwamm-Spezies-Spezifität von Schwamm-assoziierten mikrobiellen Gemeinschaften hin. Innerhalb des *P*. cf. *corticata* Schwammkörpers korrelierte die räumliche Verteilung einer Spezies mit ihrer phylogenetischen Zugehörigkeit und Klassifikation als Schwamm-spezifisch bzw. -unspezifisch sowie der damit in Zusammenhang stehenden ökophysiologischen Funktion. Auf der Basis der *aprA* Genanalyse wurde die Existenz eines Schwamm-spezifischen, endosymbiotischen Schwefelkreislaufs in *P*. cf. *corticata* postuliert.

8. Die Präsenz des *soxB* Gens in allen thiosulfatoxidierenden, obligat [S^0] Intermediat-bildenden Photo- und Chemotrophen, die in dieser Arbeit untersucht wurden, spricht für eine generelle Involvierung des Sox Systems in den initialen Thiosulfatoxidationsschritt dieser SOP. Das Sox System stellt damit den am weitesten verbreiteten Enzymweg für die Oxidation anorganischer Schwefelverbindungen innerhalb der bakteriellen SOP dar. Das *soxB* kann demnach als molekularer Marker für die Detektion von (thiosulfat-oxidierenden) SOP verwendet werden (Ausnahmen: acidophile Spezies). Die 16S rRNA-inkongruente SoxB Stammbaum-Topologie deutet auf mehrere LGT-Vorgänge zwischen phylogenetisch divergenten SOP Linien (z. B. *soxB* Gentransfer von Vertretern der *Epsilonproteobacteria* zu Spezies der *Aquificae* und *Thermus*). Die *soxB*-xenologen *Chromatiaceae*, *Ectothiorhodospiraceae* und *Chlorobiaceae* haben ihre Sox-abhängige Thiosulfatoxidationsfähigkeit vermutlich über LGT von verschiedenen chemotrophen Donatoren der *Gammaproteobacteria* Linie erworben. Die SoxB Phylogenie der SOP weist auf einen (epsilon-)proteobakteriellen Ursprung des *soxB* Gens in einem möglicherweise aeroben, chemothiotrophen Mikroorganismus hin.

1 Einleitung

1.1 Der dissimilatorische Schwefelkreislauf

In der Natur kann das Element Schwefel in den Oxidationsstufen zwischen +VI und -II existieren, wobei seine abundantesten Formen die Oxidationsstufen +VI (Sulfate, Sulfatester), 0 (Elementarschwefel) und -II (Sulfide, Thiol-Gruppen organischer Schwefelverbindungen) sind. Bedingt durch vielfältige (geo-)chemische und biologische Oxidations- und Reduktionsprozesse ist der Schwefelkreislauf sehr komplex. Organismen sind am Schwefelkreislauf über assimilatorische und dissimilatorische Transformationen beteiligt. Der dissimilatorische Teil des biologischen Schwefelkreislaufs ist ausschließlich den Prokaryonten vorbehalten, die die anorganischen Schwefelverbindungen als Elektronendonatoren bzw. -akzeptoren für die energieerzeugenden und CO_2-fixierenden Prozesse verwenden (Brüser *et al.*, 2000a; Siegel, 1975; Trudinger, 1979).

1.1.1 Sulfatreduzierende Prokaryonten

Die dissimilatorisch sulfatreduzierenden Prokaryonten (SRP) bilden physiologisch und phylogenetisch betrachtet eine sehr heterogene Gruppe. Viele SRP können neben Sulfat auch weitere anorganische Schwefelverbindungen wie Sulfit und Thiosulfat als terminale Elektronenakzeptoren nutzen; zur dissimilatorischen Reduktion von elementarem Schwefel sind hingegen nur wenige Spezies befähigt (Rabus *et al.*, 2000; Thauer *et al.*, 2007; Widdel, 1992; Widdel & Bak, 1992). Einige SRP vermögen Energie alternativ zur anaeroben Respiration durch Disproportionierung von Thiosulfat, Sulfit und elementarem Schwefel zu gewinnen (Bak & Cypionka, 1987; Bak & Pfennig, 1987; Cypionka *et al.*, 1998; Finster *et al.*, 1998; Pikuta *et al.*, 2003). In Abwesenheit von anorganischen Schwefelverbindungen reduzieren einige metabolisch vielseitige Organismen alternative Elektronenakzeptoren wie z. B. Nitrat oder Schwermetalle (DeWeerd *et al.*, 1990; Jonkers *et al.*, 1996; Lie *et al.*, 1996; Lovley *et al.*, 2004; Muyzer & Stams, 2008; Szewzyk & Pfennig, 1987; van der Maarel *et al.*, 1996). Das Spektrum ihrer verwertbaren Elektronendonatoren reicht von einfachen Verbindungen wie molekularem Wasserstoff, Kohlenmonoxid, Formiat und Acetat über Alkane und *n*-Alkene bis hin zu Phosphit und Fe; die niedermolekularen organischen Verbindungen können von vielen SRP auch fermeniert werden (Berg *et al.*, 2007; Muyzer & Stams, 2008; Rabus *et al.*, 2000; Thauer *et al.*, 2007; Widdel & Bak, 1992; Widdel *et al.*, 2007). Aufgrund ihrer großen physiologischen Diversität sind SRP in aquatischen und terrestrischen Ökosystemen weit verbreitet; in marinen Sedimenten stellt die dissimilatorische

Sulfatreduktion sogar den dominierenden anaeroben Prozess der C-Mineralisierung dar (Jørgensen, 1982; Thamdrup & Canfield, 1996).

Die SRP sind polyphyletisch (fünf bakterielle und zwei archaeelle Phyla) (siehe Abbildung 1 zur phylogenetischen Übersicht). Innerhalb der *Bacteria* gehört die Mehrheit der bisher kultivierten Sulfatreduzierer in die Klasse der *Deltaproteobacteria* (Phylum *Proteobacteria*). Diese umfasst die SRP-enthaltenden Ordnungen *Desulfovibrionales (Desulfovibrionaceae*, *Desulfomicrobiaceae*, *Desulfohalobiaceae* und *Desulfonatronumaceae)*, *Desulfobacterales (Desulfobacteraceae* und *Desulfobulbaceae)*, *Syntrophobacterales* (*Syntrophobacteraceae* und *Syntrophaceae)*, *Desulfarcales* sowie die noch nicht klassifizierte, eigenständige Linie von „*Desulfobacterium anilini*“ und nah verwandten, marinen, sulfatreduzierenden Stämmen (Kuever *et al.*, 2005). Im Phylum *Firmicutes* werden die Gram-positiven SRP momentan den *Peptococcaceae* (*Clostridiales*) und „*Thermoanaerobacteraceae*“ („*Thermoanaerobacterales*“) innerhalb der Klasse *Clostridia* zugeordnet (Hattori *et al.*, 2000; Huber *et al.*, 1996; Kaksonen *et al.*, 2007b; Spring & Rosenzweig, 2005; Widdel, 1992); die Klassifikationen einiger neu beschriebener Gram-positiver SRP sind allerdings noch nicht ausreichend geklärt (z. B. *Desulfurispora thermophila* (Kaksonen *et al.*, 2007a)), während die aktuellen Zuordnungen anderer Spezies gemäß dem „Bergey`s taxonomic outline“ (Garrity *et al.*, 2004) im Widerspruch zu ihren phylogenetischen Positionen im 16S rRNA Stammbaum stehen (z. B. *Cdt.* Desulforudis audaxviator (Chivian *et al.*, 2008)). Innerhalb der Phyla *Thermodesulfobacteria* und *Nitrospira* bilden *Thermodesulfobacterium*, *Thermodesulfatator* (Moussard *et al.*, 2004) sowie *Thermodesulfovibrio* (Haouari *et al.*, 2008; Henry *et al.*, 1994; Sonne-Hansen & Ahring, 1999) zwei separate Linien thermophiler SRP. Der thermophile Sulfatreduzierer *Thermodesulfobium narugense* ist der bisher einzige Vertreter der „*Thermodesulfobiaceae*“ (Mori *et al.*, 2003), deren exakte phylogenetische Zuordnung noch unzureichend geklärt ist. Die momentane taxonomische Klassifikation als Familie innerhalb der „*Thermoanaerobacterales“* (Garrity *et al.*, 2004) stimmt nicht mit ihrer phylogenetischen Position im 16S rRNA Stammbaum überein (nächstverwandte Spezies sind Vertreter der „Candidate Division OP9“ (Hugenholtz *et al.*, 1998)), so dass eine taxonomische Reklassifizierung der „*Thermodesulfobiaceae*“ möglicherweise auf Phylum-Niveau gerechtfertigt sein würde. Innerhalb der *Archaea* ist die Fähigkeit zur dissimilatorischen Sulfatreduktion nur von drei hyperthermophilen Gattungen bekannt, *Archaeoglobus* (Phylum *Euryarchaeota*), *Caldivirga* und *Thermocladium* (Phylum *Crenarchaeota*) (Hartzell & Reed, 2003; Huber *et al.*, 2002; Itoh *et al.*, 1999; Mori *et al.*, 2008). Viele der sulfatreduzierenden Spezies sind nah verwandt zu Arten, die nicht zur dissimilatorischen Sulfatreduktion befähigt sind bzw. nur

Sulfit und/oder Thiosulfat dissimilatorisch zu Sulfid zu reduzieren vermögen (insbesondere innerhalb der *Firmicutes*, z. B. *Sporotomaculum, Pelotomaculum* und *Desulfitobacterium* spp. (Imachi *et al.*, 2007; Qiu *et al.*, 2003; Spring & Rosenzweig, 2005).

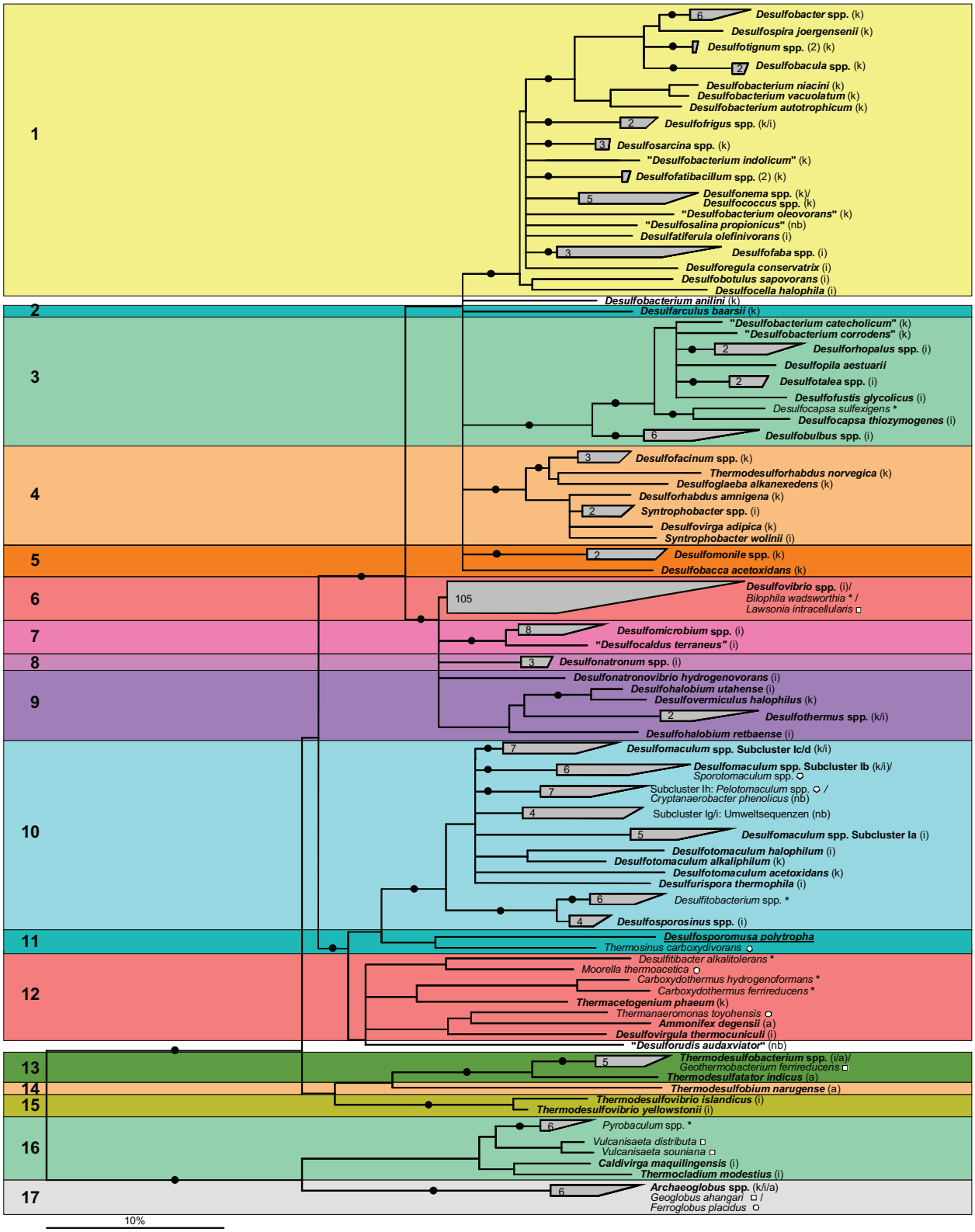

1: *Desulfobacteraceae*, **2:** *Desulfarculaceae*, **3:** *Desulfobulbaceae*, **4:** *Syntrophobacteraceae*,
5: *Syntrophaceae*, **6:** *Desulfovibrionaceae*, **7:** *Desulfomicrobiaceae*, **8:** *Desulfonatronumaceae*,
9: *Desulfohalobiaceae*, **10:** *Peptococcaceae*, **11:** *Acidaminococcaceae*, **12:** *Thermoanaerobacteraceae*,
13: *Thermodesulfobacteriaceae*, **14:** *Thermodesulfobiaceae*, **15:** *Nitrospiraceae*, **16:** *Thermoproteaceae*,
17: *Archaeoglobaceae*

Abbildung 1. Phylogenetischer Konsensus-Baum basierend auf den 16S rRNA Sequenzen (~1400 Nk Länge) bekannter SRP sowie nah verwandter, nicht-sulfatreduzierender Spezies. Spezies einer gemeinsamen Gattung wurden zusammengefasst. Multifurkationen geben nicht-eindeutige Topologien der einzelnen Berechnungsverfahren (Neighbour-joining, Maximum-parsimony und Maximum-likelihood Methode) wieder. Interne Verzweigungen, die durch Bootstrap-Werte von > 75 % bestätigt werden (Maximum-likelihood Analyse), sind durch schwarze Kreise markiert. Der Größenbalken gibt 10 % Sequenzunterschied an. Sulfatreduzierende Spezies bzw. Gattungen, welche ausschließlich sulfatreduzierende Spezies umfassen, sind fett gedruckt; die nicht-validierten Spezies sind in Anführungszeichen gesetzt (C-Metabolismus der SRP: k, komplett-Oxidierer; i, inkomplett-Oxidierer; nb, nicht bekannt; a, autotrophes Wachstum). Nicht-sulfatreduzierende Spezies sind gemäß ihrer Fähigkeit zur dissimilatorischen Reduktion von anderen anorganischen Schwefelverbindungen folgendermaßen gekennzeichnet: (Sternchen) Sulfitreduktion nachgewiesen (*dsr* vorhanden), (Kreis) Thiosulfatreduktion nachgewiesen (*dsr* bei *Moorella thermoacetica* vorhanden), (Fünfeck) keine Sulfit-/Thiosulfatreduktion nachweisbar (*dsr* aber vorhanden), (Quadrat) keine Sulfit-/Thiosulfatreduktion nachweisbar (*dsr* nicht vorhanden). Die Einteilung der Gattungen in die verschiedenen Familien (1-17) ist durch unterschiedlich farbige Blöcke hervorgehoben.

1.1.2 Schwefeloxidierende Prokaryonten

Reduzierte anorganische Schwefelverbindungen wie Sulfid, elementarer Schwefel, Sulfit, Thiosulfat oder auch Polythionate werden von anoxygenen phototrophen und chemotrophen schwefeloxidierenden Prokaryonten (SOP) als Elektronendonatoren zur Generierung von Reduktionsäquivalenten für die autotrophe CO_2-Fixierung bzw. respiratorische Energiegewinnung genutzt (Brüser *et al.*, 2000a; Brune, 1995; Friedrich, 1998).

Anoxygene phototrophe SOP. Auf der Grundlage von strukturellen, physiologischen und ökologischen Eigenschaften sowie molekularen Analysen (16S rRNA) werden die anoxygenen phototrophen Prokaryonten momentan in die Gruppen der (1) Grünen Schwefelbakterien, (2) Purpurbakterien, (3) filamentösen anoxygenen phototrophen Bakterien, (4) Heliobakterien und (5) phototrophen Acidobakterien (*Cdt.* Chloracidobacterium thermophilum (Bryant *et al.*, 2007)) unterschieden (Frigaard & Dahl, 2008) (siehe Abbildung 2 zur phylogenetischen Übersicht). Als photosynthetische Elektronendonatoren werden neben H_2, Fe(II) und einigen einfachen organischen Verbindungen charakteristischerweise reduzierte Schwefelverbindungen (hauptsächlich Sulfid) genutzt. Die Fähigkeit, Sulfid photolithoautotroph komplett zu Sulfat zu oxidieren bzw. anorganische Schwefelverbindungen wie Sulfit oder Thiosulfat (intermediäre Schwefel-Oxidationsstufen) als Elektronendonatoren zu verwenden, ist innerhalb der anoxygenen phototrophen Prokaryonten allerdings begrenzt auf Vertreter der Purpurbakterien und Grünen Schwefelbakterien.

Die strikt anaeroben, obligat phototrophen Grünen Schwefelbakterien stellen eine kohärente taxonomische Gruppe dar, die ein eigenes Phylum innerhalb der *Bacteria* bildet (Phylum *Chlorobi*). Die frühere, von morphologisch/phänotypischen Eigenschaften bestimmte Taxonomie und Nomenklatur der *Chlorobiaceae* wurde auf der Grundlage von 16S rRNA und Protein Phylogenien revidiert. Zurzeit sind vier Gattungen (*Chlorobium*, *Chlorobaculum*, *Prosthecochloris* und *Chloroherpeton*) mit 16 Spezies validiert (Alexander *et al.*, 2002; Imhoff, 2003; Vogl *et al.*, 2006). Neben Sulfid können die meisten Arten auch Thiosulfat, Schwefel und H_2 als Elektronendonatoren für das photoautotrophe Wachstum verwenden; Sulfid und Thiosulfat werden unter intermediärer Akkumulation von extrazellulär gelagertem „elementarem Schwefel“ (Schwefelkugeln) komplett zu Sulfat oxidiert (Beatty *et al.*, 2005; Overmann, 2000) (für Details siehe Tabelle 1, Anhang). Die Purpurbakterien, die phylogenetisch zu den *Alpha-*, *Beta-* und *Gammaproteobacteria* zählen, werden in die Schwefel-Purpurbakterien, schwefelfreien Purpurbakterien und aeroben anoxygenen phototrophen Bakterien (AAPB) unterteilt. Die Schwefel-Purpurbakterien bilden die taxonomischen Gruppen der *Chromatiaceae* und *Ectothiorhodospiraceae* innerhalb der *Gammaproteobacteria*. Erstere umfasst nach der aktuellen Taxonomie 22 Gattungen (Asao *et al.*, 2007; Guyoneaud *et al.*, 1998; Imhoff *et al.*, 1998; Imhoff, 2001b); ihre Vertreter lagern die während der Oxidation von Sulfid, Polysulfid oder Thiosulfat zu Sulfat intermediär gebildeten Schwefelkugeln periplasmatisch ab (Tabelle 1). Die meisten kleinzelligen Spezies (z. B. *Thiocapsa roseopersicina*) sind metabolisch vielseitig und können neben (an-)organischen Schwefelverbindungen auch Fe(II) und Nitrit als photosynthetische Elektronendonatoren verwenden (Ehrenreich & Widdel, 1994; Griffin *et al.*, 2007); einige Vertreter vermögen aerob chemolithoautotroph oder auch photo-/chemoorganoheterotroph ohne reduzierte Schwefelverbindungen zu wachsen (Kondrateva *et al.*, 1981). Die *Ectothiorhodospiraceae* umfassen die (extrem) halophilen und haloalkaliphilen Schwefel-Purpurbakterien (vier validierte Gattungen *Ectothiorhodospira*, *Halorhodospira*, *Thiorhodospira* und *Ectothiorhodosinus*); sie lagern den intermediär gebildeten „elementaren Schwefel“ außerhalb der Zelle ab (Bryantseva *et al.*, 1999; Gorlenko *et al.*, 2004; Imhoff, 1999; Tourova *et al.*, 2007) (Tabelle 1). Die schwefelfreien Purpurbakterien (ehemals „*Rhodospirillaceae*“) gehören zu den *Alpha-* und *Betaproteobacteria* (Imhoff, 2001c; Imhoff, 2001d). Ihre Vertreter bevorzugen photoheterotrophes Wachstum mit verschiedenen organischen Verbindungen. Ihre Möglichkeiten zur Nutzung von anorganischen Schwefelverbindungen sind im Vergleich zu den Schwefel-Purpurbakterien eingeschränkt; zudem tolerieren sie nur sehr niedrige Sulfidkonzentrationen. Dennoch sind die meisten Vertreter metabolisch äußerst flexibel, da

sie zwischen anaerober anoxygener Photosynthese, (an-)aerober Respiration und fermentativem Stoffwechsel wechseln können. Einige alphaproteobakterielle Arten vermögen photolithoautotroph mit Sulfid und/oder Thiosulfat als photosynthetischem Elektronendonator zu wachsen. Sulfid wird in den meisten dieser Spezies nur bis zur Oxidationsstufe von elementarem Schwefel oxidiert, der in Form von Schwefelpräzipitaten außerhalb der Zelle akkumuliert. In *Rhodovulum* spp., *Rhodopseudomonas palustris*, *Rhodopseudomonas julia*, *Blastochloris sulfoviridis* und *Rhodobacter veldkampii* ist Sulfat als Endprodukt der Sulfidoxidation nachgewiesen. Thiosulfat wird entweder zu Tetrathionat (*Rhodopila globiformis*) oder komplett zu Sulfat (*Rhodovulum* spp.) oxidiert (Brune, 1995; Imhoff, 2001c; Srinivas *et al.*, 2007). Die AAPB (anoxygene Photosynthese nur unter oxischen Bedingungen) zählen mehrheitlich zu den *Alphaproteobacteria*, bilden aber innerhalb dieser phylogenetischen Linie keine kohärente Gruppe, sondern sind mit verschiedenen anaeroben anoxygenen phototrophen und nicht-phototrophen Spezies verwandt (Yurkov, 2000; Yurkov & Beatty, 1998). Alle Vertreter bevorzugen aerobes, chemoorganoheterotrophes Wachstum (keine Spezies ist zu einer ausschließlich phototrophen Lebensweise befähigt); einige AAPB können anorganische Schwefelverbindungen photolithoheterotroph nutzen (Boldareva *et al.*, 2007; Sorokin *et al.*, 2000; Yurkov, 2000). Für viele der AABP Spezies fehlen noch genaue Analysen zu ihrer Schwefeloxidationsfähigkeit. Den in ozeanischen Habitaten abundanten Vertretern der alphaproteobakteriellen *Roseobacter* Linie und SAR11 Gruppe (u. a. *Cdt.* Pelagibacter ubique) wird eine wichtige Rolle im Abbau organischer Schwefelverbindungen wie z. B. Dimethylsulfoniopropionat (DMSP, Osmolyt verschiedener Phytoplanktongruppen) zugeschrieben (Buchan *et al.*, 2005; Giovannoni & Sting, 2005; Giovannoni *et al.*, 2005b; Gonzalez *et al.*, 2000; Howard *et al.*, 2006; Malmstom *et al.*, 2004; Moran *et al.*, 2003).

Abbildung 2. Maximum-likelihood Baum basierend auf vollständigen 16S rRNA Sequenzen (~1400 Nk Länge) von anaeroben/aeroben anoxygenen phototrophen Bakterien. Zur Berechnung des phylogenetischen Baumes wurden die anoxygenen phototrophen Typenstämme der *Chromatiaceae*, *Ectothiorhodospiraceae* und *Chlorobiaceae* verwendet, wohingegen von den anoxygenen phototrophen Vertretern der *Heliobacteriaceae*, *Chloroflexi*, *Alpha-* und *Betaproteobacteria* nur die Typenspezies der einzelnen Gattungen einbezogen wurden. Alle aeroben anoxygenen phototrophen Bakterien sind mit Sternchen markiert. Der Größenbalken gibt 10 % Sequenzunterschied an. Spezies, die Sulfid komplett bis zur Oxidationsstufe Sulfat oxidieren, sind fett gedruckt. Spezies die (zusätzlich) die Fähigkeit zur Thiosulfatoxidation zu Sulfat besitzen, sind mit der Abkürzung „TS“ gesondert gekennzeichnet. Die Einteilung der Spezies in die verschiedenen Klassen (1-7) ist durch unterschiedlich farbige Blöcke hervorgehoben.

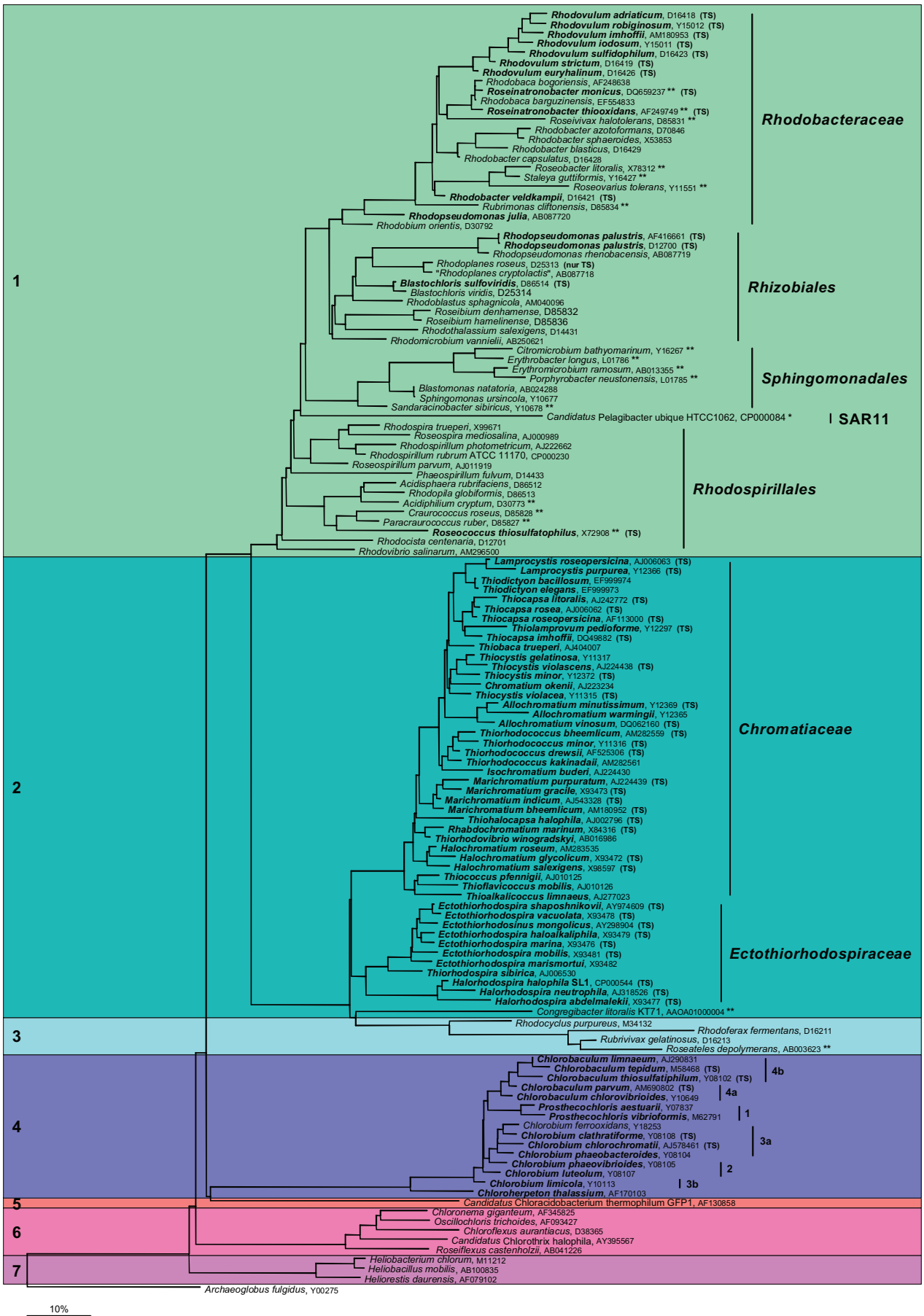

1: *Alphaproteobacteria*, **2:** *Gammaproteobacteria*, **3:** *Betaproteobacteria*, **4:** *Chlorobia*, **5:** *Acidobacteria*, **6:** *Chloroflexi*, **7:** *Heliobacteriaceae* (*Clostridia*)

Chemotrophe SOP. In Sulfid-Sauerstoff-Transitionszonen nutzen die nicht-phototrophen („farblosen“) schwefeloxidierenden Prokaryonten reduzierte anorganische Schwefelverbindungen als Elektronendonatoren für ein obligat oder fakultativ chemolitho-autotrophes, aerobes Wachstum; einige Vertreter vermögen unter anoxischen Bedingungen Nitrat als terminalen Elektronenakzeptor zu nutzen (fakultativ anaerob). Die extreme phänotypische und metabolische Vielfältigkeit der chemotrophen SOP spiegelt sich in der großen phylogenetischen Diversität dieser Gruppe wider (*Proteobacteria*, *Firmicutes* und *Aquificae* sowie *Sulfolobales*, Phylum *Crenarchaeota*, siehe Abbildung 3 und Tabelle 2, Anhang) (Brüser *et al.*, 2000a; Friedrich, 1998; Huber & Prangishvili, 2000; Huber & Eder, 2002; Krasil'nikova *et al.*, 1998; Skirnisdottir *et al.*, 2001). Hinsichtlich der Intermediat-Bildung während der Thiosulfatoxidation lassen sich die Chemotrophen generell in Organismen unterscheiden, die entweder keine Zwischenprodukte bilden oder obligat Tetrathionat bzw. „elementaren Schwefel“ bilden (Brüser *et al.*, 2000a; Friedrich, 1998; Friedrich *et al.*, 2005; Kelly *et al.*, 1997). Die dissimilatorische Nutzung von anorganischen Schwefelverbindungen wie Thiosulfat und Sulfit (intermediäre Oxidationsstufen) konnte auch für chemoheterotrophe Vertreter der *Roseobacter* Linie nachgewiesen werden (z. B. *Silicibacter pomeryoi*, *Sulfitobacter pontiacus*), die primär als organische Schwefelverbindungen-abbauende Mikroorganismen galten (Buchan *et al.*, 2005; Gonzalez *et al.*, 1999; Gonzalez *et al.*, 2003; Moran *et al.*, 2003; Sorokin, 1995). Diese sowie weitere obligat heterotrophe Thiosulfatoxidierer, die diese Verbindung nur bis zu Tetrathionat umsetzen (z. B. *Pseudomonas stutzeri* ssp., *Halomonas* spp.) (Sorokin *et al.*, 1996; Sorokin, 2003), scheinen im Hinblick auf ihre Abundanz in den unterschiedlichsten Habitaten, eine wichtige Funktion in den oxidativen Teilprozessen des marinen Schwefelkreislaufs einzunehmen (Teske *et al.*, 2000; Tuttle & Jannasch, 1976). Generell bleibt anzumerken, dass bei vielen heterotrophen Mikroorganismen die metabolische Fähigkeit, reduzierte anorganische Schwefelverbindungen als Elektronendonatoren für respiratorische Prozesse zu nutzen, noch nicht untersucht worden ist.

Abbildung 3. Schematischer 16S rRNA Stammbaum zur Übersicht über die Verteilung der verschiedenen Typen der Schwefelverbindungen-metabolisierenden Prokaryonten innerhalb der phylogenetischen Hauptgruppen. Die metabolische Fähigkeit zur Umsetzung und energetischen Nutzung von organischen Schwefelverbindungen wie z. B. DMSP ist weit verbreitet in Prokaryonten (nur selektiv in den phylogenetischen Linien gezeigt).

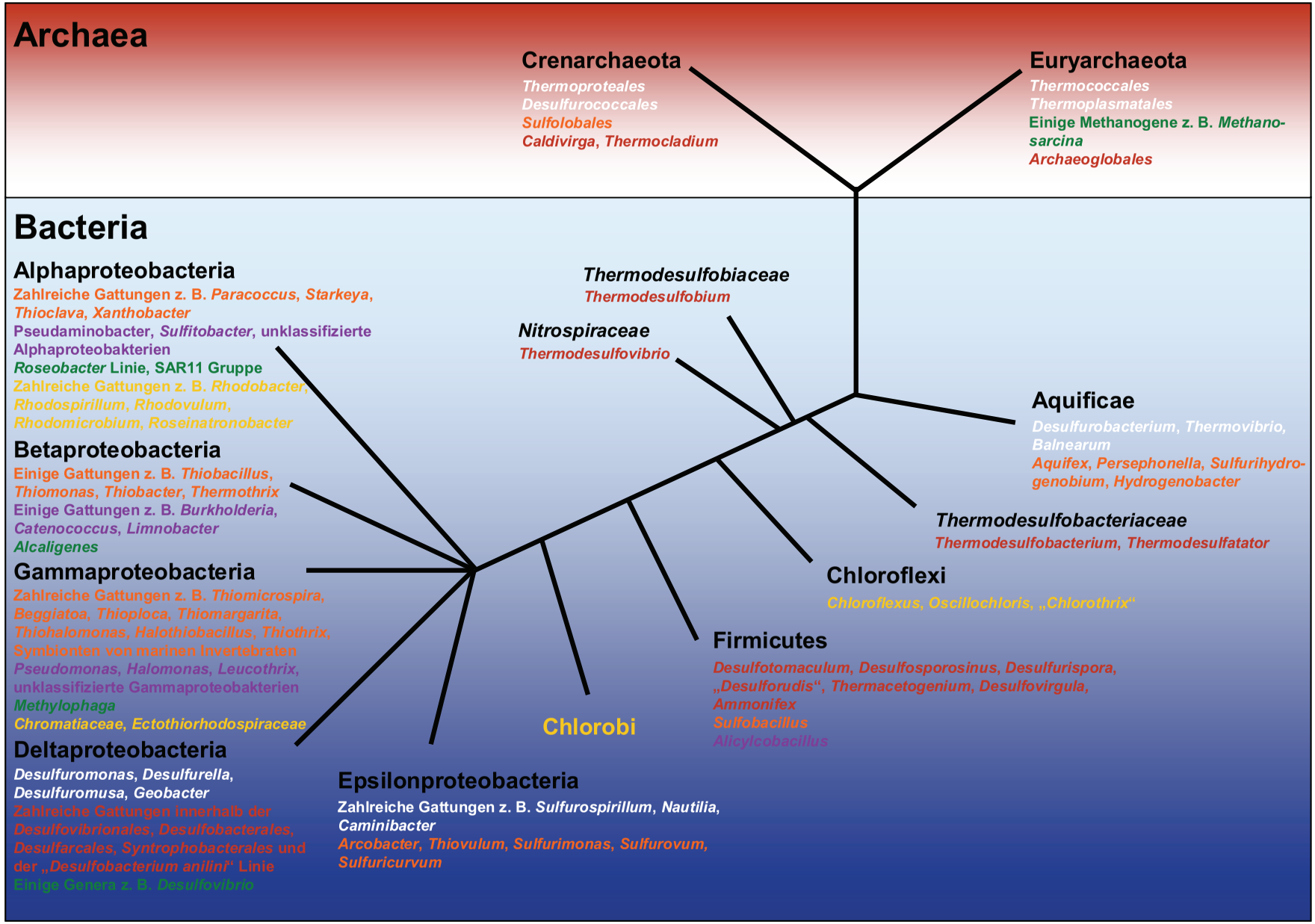

Photolithoautotrophe SOP | Chemolithoautotrophe SOP | Chemolithoheterotrophe SOP | Schwefelreduzierer | SRP | Organische Schwefelverbindungen nutzende Prokaryonten

1.2 Dissimilatorische Reduktion von Sulfat zu Sulfid

Die dissimilatorische Reduktion von Sulfat zu Sulfid ist ein Acht-Elektronen-Übertragungsprozess, der in drei enzymatischen Reaktionsschritten über die Intermediate Adenosin-5`-Phosphosulfat (APS) und Sulfit verläuft. Der Prozess wird von den cytoplasmatischen Enzymen ATP-Sulfurylase (Sat), APS-Reduktase (Apr) und Sulfitreduktase (Dsr) katalysiert (Abbildung 4), die bisher in allen diesbezüglich untersuchten SRP gefunden wurden. Diesen dissimilatorischen Enzymen stehen konvergente ATP-Sulfurylase-, APS-Reduktase- und Sulfitreduktase-Entwicklungslinien gegenüber, die den analogen Weg der assimilatorischen Sulfatreduktion sowohl in Prokaryonten als auch in Pilzen, Hefen und Pflanzen katalysieren (Carroll *et al.*, 2005; Chartron *et al.*, 2006; Crane & Getzoff, 1996; Kopriva *et al.*, 2008; Taguchi *et al.*, 2004; Yu *et al.*, 2007).

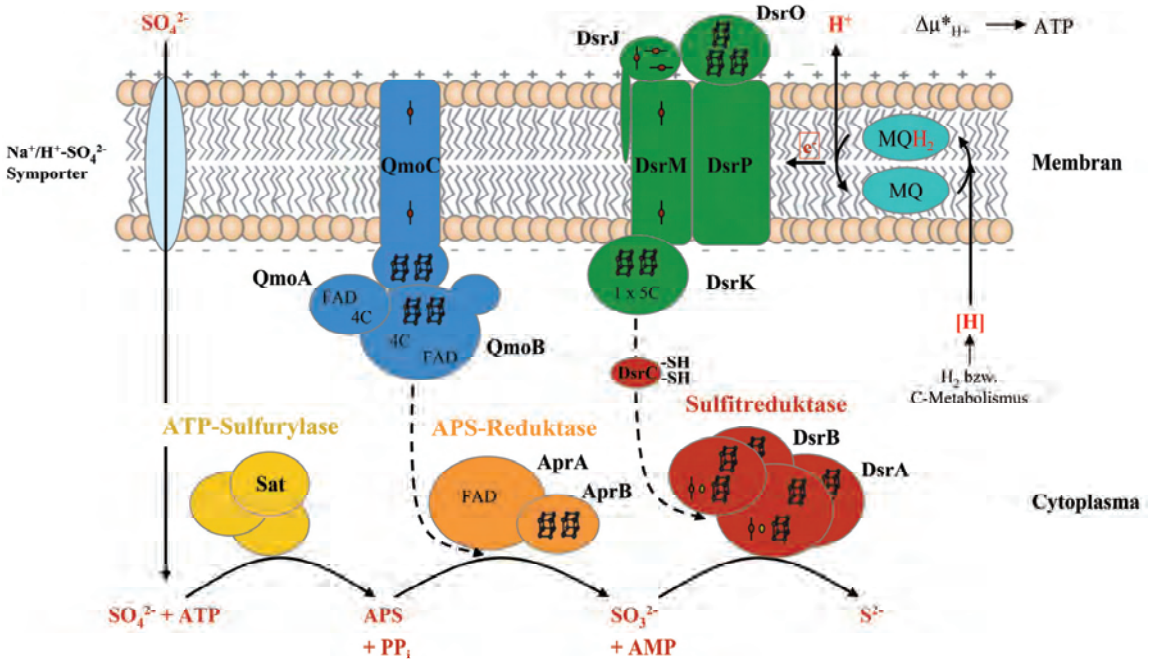

Abbildung 4. Schematische Darstellung des enzymatischen Ablaufs der dissimilatorischen Sulfatreduktion in SRP (für Protein-Abkürzungen siehe Text).

1.2.1 Sulfataufnahme und –aktivierung

Die Sulfataufnahme erfolgt in den Sulfatreduzierern über einen Symport mit Protonen (in Süßwasser-Spezies) oder Natrium-Ionen (in marinen Spezies). Zwei unterschiedliche Transportsysteme wurden näher charakterisiert, ein Niedrig- und ein Hoch-Affinitäts-Transportsystem (Stahlmann *et al.*, 1991). Da das Sulfat-Anion chemisch inert ist, wird es zunächst über einen Adenylierungsschritt unter Bildung von APS aktiviert. Diese Reaktion wird von den *sat*-kodierten, homooligomeren ATP-Sulfurylasen katalysiert (Gavel *et al.*,

1998; Sperling *et al.*, 1998; Sperling *et al.*, 2001) und ist endergon unter Standardbedingungen ($\Delta G°` = 46$ kJ/mol; $K_{Gw}= 10^{-8}$ bei pH 8.0 und 37°C) (Thauer *et al.*, 2007).

$$SO_4^{2-} + ATP + 2\ H^+ \longleftrightarrow APS + PP_i$$

$$PP_i + H_2O \longleftrightarrow 2\ P_i$$

Die thermodynamische Bedeutung der Pyrophosphat-Spaltung ($\Delta G°` = -22$ kJ/mol) für die Bildung von APS ist noch ungeklärt, da anorganische Pyrophosphatasen nicht in allen SRP nachgewiesen wurden (Rabus *et al.*, 2000).

1.2.2 APS-Reduktion

Die Aktivierung von Sulfat zu APS erhöht das Standard-Redoxpotential von -516 mV für SO_4^{2-}/HSO_3^- auf -60 mV für das Redoxpaar APS/HSO_3^- + AMP (Thauer *et al.*, 2007). Die in der S-O-P Anhydrid-Bindung vorhandene Energie (-80 kJ/mol) ermöglicht die reduktive Transformation von APS zu AMP und Sulfit.

$$APS + 2\ e^- + 2\ H^+ \longleftrightarrow HSO_3^- + AMP$$

Die molekularen Eigenschaften der dissimilatorischen APS-Reduktase wie Masse, Untereinheiten-Zusammensetzung und Kofaktor-Stöchiometrie blieben lange Zeit kontrovers diskutiert (Bramlett & Peck, 1975; Dahl & Trüper, 2001; Lampreia *et al.*, 1994; Speich & Trüper, 1988; Speich *et al.*, 1994; Verhagen *et al.*, 1994). Erst durch neuere Isolierungs- und Reinigungsverfahren unter strikt anoxischen Bedingungen konnte die Struktur zweifelsfrei geklärt werden (Fritz *et al.*, 2000; Fritz *et al.*, 2002b): Die funktionelle Einheit des Enzyms ist ein $\alpha_1\beta_1$-Heterodimer. Die katalytische α-Untereinheit enthält eine FAD-Gruppe als Kofaktor, hat eine molekulare Masse von 70-75 kDa und gehört zur Fumaratreduktase Proteinfamilie, während die elektronentransferierende β-Untereinheit zwei [Fe_4-S_4] Cluster als prosthetische Gruppen trägt, eine molekulare Masse von 18-23 kDa aufweist und strukturell mit den bakteriellen Ferredoxinen verwandt ist (Fritz *et al.*, 2000; Fritz *et al.*, 2002b) (für weitere Details siehe Kapitel 1.4). Die Untereinheiten werden durch die *aprA* und *aprB* Gene kodiert (Fritz *et al.*, 2000; Hipp *et al.*, 1997; Speich *et al.*, 1994) (in einigen Publikationen auch als *apsAB* bezeichnet (Friedrich, 2002)).

Der physiologische Elektronendonator der dissimilatorischen APS-Reduktase scheint der respiratorische Membrankomplex Qmo („quinone-interacting membrane-bound oxidoreductase“) zu sein (Pires *et al.*, 2003) (Abbildung 4). Dieser Redoxkomplex ist zusammengesetzt aus drei Untereinheiten, die homolog zu einzelnen Proteinkomponenten der Heterodisulfidreduktasen von Methanogenen sind (HdrABC und HdrDE (Hamann *et al.*,

2007; Hedderich *et al.*, 1999; Hedderich *et al.*, 2005)) (siehe Abbildung 5). QmoA und QmoB sind cytoplasmatische Flavo-FeS-Proteine; QmoA zeigt Sequenzähnlichkeit zum N-terminalen HdrA-Proteinbereich, während QmoB ein Fusionsprotein aus HdrA und MvhD (Delta-Untereinheit der F_{420}-nicht-reduzierenden Hydrogenase (Stojanowic *et al.*, 2003)) darstellt. Das membrangebundene QmoC besteht aus zwei Domänen, einem cytoplasmatisch ausgerichteten, zwei [Fe_4-S_4] Cluster-tragenden N-Terminus mit Sequenzähnlichkeit zu HdrC und einem sechs Transmembranhelices-enthaltenden, zwei Häm b-Gruppen-tragenden C-Terminus mit Sequenzähnlichkeit zum membranintegralen HdrE. Die Häm b-Gruppen Positionierung im QmoC Protein könnte den Aufbau eines Protonengradienten via Redoxschleife (vektorieller Protonentransport) ermöglichen (Abbildung 5). Die *in vitro* Reduktion der QmoC Häm-Gruppen durch Menadiol deutet darauf hin, dass Menachinol als nativer Elektronendonator des QmoABC fungiert. Ein direkter Elektronentransfer zwischen Qmo Komplex und APS-Reduktase konnte noch nicht nachgewiesen werden (Pereira, 2008; Pires *et al.*, 2003). Die potentielle Funktion des QmoABC als Menachinol:APS-Reduktase-Oxidoreduktase der SRP beruht deshalb bisher nur auf indirekten experimentellen Hinweisen (Haveman *et al.*, 2004; Hippe *et al.*, 1997; Mussmann *et al.*, 2005; Pires *et al.*, 2003) und Genomdatenanalysen (siehe Tabelle 3, Anhang).

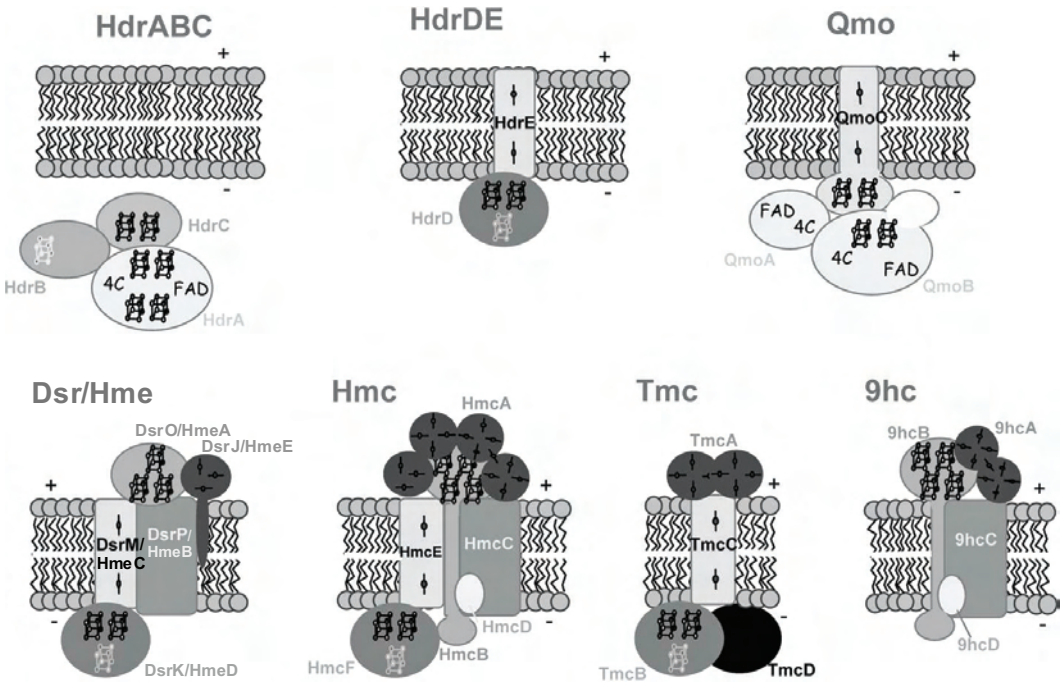

Abbildung 5. Schematische Präsentation der Heterodisulfidreduktasen von Methanogenen (HdrABC, HdrDE) und der membrangebundenen Redoxkomplexe von SRP (Qmo, Dsr, Hme, Hmc, Tmc und 9hc). Strukturell-verwandte Untereinheiten sind durch gleichen Grauton hervorgehoben. Das potentielle, katalytische [Fe_4-S_4] Cluster in HdrB, HdrD, DsrK, HmeD, HmcF und TmcB ist in hellem Grau markiert (nach (Pereira, 2008), modifiziert).

Die homooligomeren assimilatorischen APS-Reduktasen der Prokaryonten, Hefen und Pflanzen sind nicht homolog zu den *aprBA*-kodierten dissimilatorischen APS-Reduktasen, sondern verwandt zu den *cysH*-kodierten PAPS-Reduktasen (25-30 % Sequenzidentität) (Kopriva *et al.*, 2008). Die assimilatorische APS-Reduktion erfolgt unter Ausbildung eines enzymgebundenen Cystein-S-Sulfat (Synonym: Cystein-Thiosulfonat). Sulfit wird aus dem Intermediat durch reduziertes Thioredoxin (essentielles akzessorisches Protein) freigesetzt, welches über eine Thioredoxinreduktase (Elektronendonator Glutathion) wieder in seine reduzierte Form überführt wird (Carroll *et al.*, 2005; Chartron *et al.*, 2006; Chartron *et al.*, 2007; Weber *et al.*, 2000). Die signifikanten Unterschiede in den Enzymstrukturen, verwendeten Kofaktoren und Reaktionsmechanismen spiegeln die konvergente Evolution der isofunktionellen assimilatorischen und dissimilatorischen APS-Reduktase-Typen wider.

1.2.3 Sulfitreduktion

Die Reduktion von Sulfit zu Sulfid ($E^{\circ`}$ = -116 mV) (Thauer *et al.*, 2007) wird von der dissimilatorischen Sulfitreduktase katalysiert.

$$HSO_3^- + 6\ e^- + 6\ H^+ \longleftrightarrow HS^- + 3\ H_2O$$

Die dissimilatorische Sulfitreduktase hat eine $\alpha_2\beta_2$-Heterotetramerstruktur; ihre α- und β-Untereinheiten weisen molekulare Massen von 47-54 kDa bzw. 42-45 kDa auf und werden durch die *dsrA* und *dsrB* Gene kodiert, die vermutlich durch eine evolutionär-frühe Genduplikation entstanden sind (Dahl *et al.*, 1993; Hipp *et al.*, 1997; Larsen *et al.*, 1999). Das Holoenzym besteht aus zwei katalytisch-unabhängigen Heterodimeren, die pro αβ-Proteinkomplex zwei kovalent gekoppelte Sirohäm-[Fe_4-S_4]-Komplexe besitzen; jede α- und β-Untereinheit trägt zusätzlich ein zweites [Fe_4-S_4] Cluster (Ferredoxin-Domäne) (Fritz *et al.*, 2008; Schiffer *et al.*, 2008). Das DsrC Protein (11 kDa) wurde bei einigen SRP Spezies (*Desulfovibrio* spp. und *Desulfosarcina variabilis*) als Holoenzym-assoziierte γ-Untereinheit isoliert (Arendsen *et al.*, 1993); eine koordinierte Expression des *dsrC* Gens mit den *dsrAB* Genen liegt allerdings nicht vor (Fritz *et al.*, 2008; Schiffer *et al.*, 2008).

Der physiologische Elektronendonator der dissimilatorischen Sulfitreduktase scheint der respiratorische Transmembrankomplex DsrMKJOP (HmeABCDE in *Archaeoglobus fulgidus*) zu sein (Mander *et al.*, 2002; Pires *et al.*, 2006) (Abbildung 4). Dieser Redoxkomplex weist ebenfalls Untereinheiten auf, die homolog zu Hdr Proteinen sind (siehe Abbildung 5). DsrM ist ein Cytochrom b-ähnliches Membranprotein wie HdrE und der C-terminale Bereich von QmoC. DsrK ist ein cytoplasmatisches FeS-Protein, das homolog zu den katalytischen Untereinheiten der Heterodisulfidreduktasen, HdrD und HdrB (Hamann *et al.*, 2007;

Hedderich *et al.*, 2005), ist. In Analogie zu den Transmembrankomplexen Hmc, 9Hc und Tmc (Elektronentransfer-Mediatoren zwischen der periplasmatischen H_2-Oxidation und der cytoplasmatischen Sulfatreduktion in *Desulfovibrio* spp. (Matias *et al.*, 2005; Pereira, 2008)) könnte der Dsr Komplex durch seinen modulartigen Aufbau (DsrMK, DsrJOP) als bifunktionelle Menachinoloxidase/Menachinonreduktase bzw. bidirektionelle Menachinoloxidase fungieren (Abbildung 5). Der cytoplasmatische Elektronenakzeptor könnte hinsichtlich der HmcF- und TmcB-Ähnlichkeit des DsrK Proteins das Disulfid-Brücke-enthaltende DsrC sein (Cort *et al.*, 2001; Fritz *et al.*, 2008; Mander *et al.*, 2005; Schiffer *et al.*, 2008), welches zu Thiolen reduziert wiederum der DsrAB Sulfitreduktase als Elektronendonator dienen würde (mobiler Elektronenüberträger) (Mander *et al.*, 2002; Pires *et al.*, 2006). Die exakte physiologische Rolle des DsrMKJOP Komplexes in SRP ist allerdings noch nicht bekannt, da es bisher nur indirekte Hinweise gibt, die auf eine Funktion im Sulfitreduktionsprozess schließen lassen (z. B. Genomdatenanalyse von sulfat-/sulfitreduzierenden Prokaryonten, siehe Tabelle 4, Anhang).

1.3 Dissimilatorische Oxidation anorganischer Schwefelverbindungen zu Sulfat

Entsprechend der phylogenetischen und physiologischen Heterogenität der SOP gibt es keinen einheitlichen Enzymweg zur Oxidation anorganischer Schwefelverbindungen. Zudem können alternative Enzymsysteme zum Abbau derselben Schwefelverbindung in einem einzelnen Organismus vorhanden sein, die in Adaptation an die vorherrschenden Umweltbedingungen exprimiert und verwendet werden (Brüser *et al.*, 2000a; Brune, 1995; Friedrich, 1998; Friedrich *et al.*, 2001; Friedrich *et al.*, 2005; Frigaard & Dahl, 2008; Kappler & Dahl, 2001; Kappler *et al.*, 2001; Kelly *et al.*, 1997; Kelly, 1999; Kletzin, 2008).

1.3.1 Sulfid- und Elementarschwefeloxidation in Bakterien

Sulfidoxidation. Für die Oxidation von Sulfid zu Elementarschwefel bzw. gespeichtertem Schwefel [S^0] sind in photo- und chemotrophen schwefeloxidierenden Bakterien drei periplasmatische Enzym(system)e verantwortlich: (1) die Flavocytochrom c Sulfiddehydrogenase (FccAB) (Kostanjevecki *et al.*, 2000; Verte *et al.*, 2002; Visser *et al.*, 1997), (2) die Sulfid:Chinon-Oxidoreduktase („sulfide:quinone oxidoreductase“, SQR) (Brune, 1995; Friedrich, 1998; Griesbeck *et al.*, 2000; Sorokin & Kuenen, 2005; Wakai *et al.*, 2004) und (3) das Sox System. Letzteres katalysiert in *Rhodovulum sulfidophilum*, *Paracoccus pantotrophus* sowie *Pseudaminobacter salicylatoxidans* eine Sulfidoxidation, in

der keine Intermediate, sondern nur das Endprodukt Sulfat freigesetzt wird (Appia-Ayme *et al.*, 2001; Friedrich *et al.*, 2001; Lahiri *et al.*, 2006; Rother *et al.*, 2001). Das Primärprodukt der SQR und Fcc Reaktionen ist lösliches Disulfid, aus welchem sich Polysulfide verschiedener Kettenlängen durch abiotische Disproportionierungsreaktionen bilden (Steudel, 1996). In anoxygenen Phototrophen wie *Rhodobacter capsulatus*, die Sulfid nicht zu Sulfat oxidieren können, zerfällt das Endprodukt der Sulfidoxidation, Polysulfid, nach Diffusion in den extrazellulären Raum zu Elementarschwefel (S_8^0 Präzipitat) und Sulfid. In photo- und chemotrophen SOP, die Sulfid obligat über [S^0] zu Sulfat oxidieren, werden die Polysulfide in Form von intra- bzw. extrazellulären Schwefelkugeln gespeichert (Pattaragulwanit *et al.*, 1998). In Vertretern der *Chromatiaceae*, *Ectothiorhodospiraceae* und *Chlorobiaceae* besteht dieser Schwefel aus langkettigen organischen Polysulfanen, dessen organischer Bestandteil Glutathionamid oder eine ähnliche niedermolekulare Verbindung ist (Prange *et al.*, 2002). Als Träger-Molekül (Perthiol-Gruppe) gewährleistet es vermutlich auch den Schwefeltransfer vom Ort der Speicherung zur finalen Oxidation ins Cytoplasma (Pott & Dahl, 1998). In Gram-negativen acidophilen Chemotrophen (*Acidithiobacillus ferrooxidans* und *Acidiphilium acidophilum*) wird eine periplasmatische Präzipitation des Endprodukts der Sulfidoxidation durch Reaktion mit den Thiol-Gruppen spezieller Außenmembranproteine verhindert, wobei als Persulfid gebundener Sulfanschwefel entsteht (dieser kann in Form von Polythionaten gespeichert werden) (Rohwerder & Sand, 2003).

Elementar/[S^0]-Oxidation. Für die nicht-[S^0]-bildenden *R. sulfidophilum*, *P. pantotrophus* und *P. salicylatoxidans* ist die Oxidation von elementarem Schwefel über das multifunktionelle Sox Enzymsystem *in vitro* nachgewiesen (Appia-Ayme *et al.*, 2001; Lahiri *et al.*, 2006; Rother *et al.*, 2001). Für die acidophilen *A. ferrooxidans*, *A. acidophilum* und *Sulfobacillus thermosulfidooxidans* wurde hingegen ein periplasmatischer Oxidationsweg propagiert, in dem der proteingebundene Sulfanschwefel über eine Schwefel-Dioxygenase (SDO) und Sulfit:Akzeptor-Oxidoreduktase (SAOR) zu Sulfat oxidiert wird (letzteres Enyzm reduziert freie Cytochrome) (Rohwerder & Sand, 2003; Rohwerder & Sand, 2007; Valenzuela *et al.*, 2008). Für *Allochromatium vinosum* als Vertreter der phototrophen [S^0] Intermediat-bildenden SOP konnte anhand von *dsrAB*-Deletionsmutanten gezeigt werden, dass die cytoplasmatische, reverse dissimilatorische Sulfitreduktase essentiell für die Oxidation des gespeicherten Schwefels ist (Pott & Dahl, 1998). Die aus lithoautotrophen *A. vinosum* und *Thiobacillus denitrificans* Kulturen isolierten Enzyme sind homolog zu den dissimilatorischen Sulfitreduktasen der SRP (Hipp *et al.*, 1997) und besitzen ähnliche physikochemische Eigenschaften (Schedel & Trüper, 1979; Schedel *et al.*, 1979). Aus dem ins Cytoplasma

transportierten Perthiol wird durch die NADH:Akzeptor-Oxidoreduktase, DsrL, reduktiv Sulfid freigesetzt (Dahl *et al.*, 2005; Grimm *et al.*, 2008), welches dann von der reversen DsrAB zu Sulfit oxidiert wird (Abbildung 6). DsrL sowie ein aus den Untereinheiten DsrEFH bestehender Komplex sind in *A. vinosum* mit den DsrAB Proteinen assoziiert; ihre kodierenden Gene sind ausschließlich in Genomen von SOP zu finden (Dahl *et al.*, 2005; Grimm *et al.*, 2008). Da DsrMKJOP und DsrC essentiell für das photolithoautotrophe Wachstum von *A. vinosum* mit Polysulfid bzw. Elementarschwefel sind (Dahl *et al.*, 2005; Sander *et al.*, 2006), verläuft der Elektronentransfer zwischen DsrAB und der photosynthetischen Elektronentransportkette vermutlich über einen SRP-homologen Weg. DsrM und DsrP könnten als Chinonreduktase bzw. -oxidase fungieren, während das reduzierte DsrJ-Cytochrom c möglicherweise die Elektronen auf den primären Elektronendonator des photosynthetischen Zentrums überträgt (Dahl *et al.*, 2005; Sander *et al.*, 2006). Die experimentellen Ergebnisse von Dahl et al. (Dahl *et al.*, 1999) sowie Genomdatenanalysen (siehe Tabelle 4, Anhang) deuten darauf hin, dass das reverse Sulfitreduktionssystem auch eine essentielle Bedeutung für die [S^0]-Oxidation in anderen Vertretern der *Chlorobiaceae*, *Chromatiaceae* und *Ectothiorhodospiraceae* haben könnte (Abbildung 6).

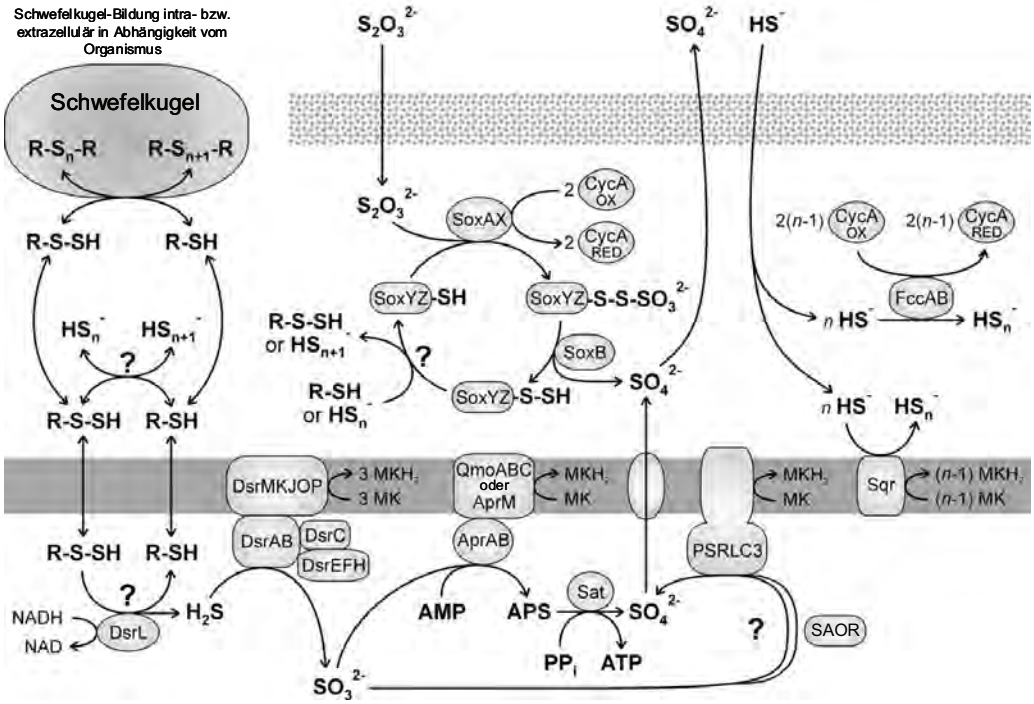

Abbildung 6. Schematische Übersicht über die potentiellen enzymatischen Oxidationswege für reduzierte anorganische Schwefelverbindungen in Vertretern der anoxygenen phototrophen *Chromatiaceae*, *Ectothiorhodospiraceae* und *Chlorobiaceae* (nach (Frigaard & Dahl, 2008), modifiziert).

In [S^0] Intermediat-bildenden Chemotrophen könnten diese Enzym(komplex)e ebenfalls operativ sein. Für *T. denitrificans* ist ihre Beteiligung sowohl bei anaerober als auch bei

aerober Lebensweise experimentell belegt (Beller *et al.*, 2006; Schedel & Trüper, 1980). Generell bleibt aber anzumerken, dass die Sulfid- bzw. Elementar/[S^0]-Oxidationswege der meisten neutro- bzw. alkaliphilen chemotrophen SOP kaum untersucht wurden, und systematische Analysen bisher vollständig fehlen.

1.3.2 Sulfitoxidation in Bakterien

Zwei unterschiedliche Sulfitoxidationswege sind in SOP vorhanden: (1) die indirekte, AMP-abhängige Oxidation via reverser dissimilatorischer APS-Reduktase und ATP-Sulfurylase (bzw. Adenylylsulfat:Phosphat-Adenylyltransferase, APAT (Brüser *et al.*, 2000b)) und (2) die direkte Oxidation via Sulfit:Akzeptor-Oxidoreduktase (Synonym: Sulfitdehydrogenase) (Kappler & Dahl, 2001; Kappler, 2008) (Abbildung 7). Ein weiterer direkter Sulfitoxidationsweg verläuft vermutlich über das periplasmatische Sox System, welches *in vitro* Sulfit als Substrat akzeptiert und zu Sulfat umsetzt (Appia-Ayme *et al.*, 2001; Rother *et al.*, 2001).

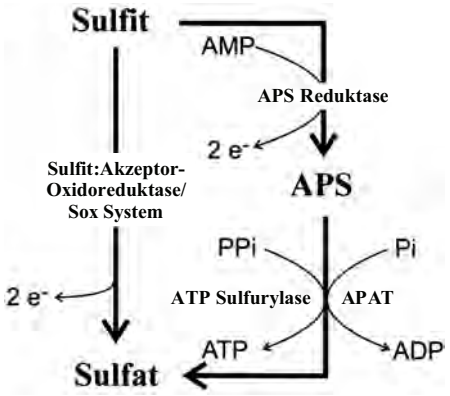

Abbildung 7. Direkter und indirekter Sulfitoxidationsweg in schwefeloxidierenden Prokaryonten

Reverse dissimilatorische APS-Reduktase und ATP-Sulfurylase. Die aus autotrophen Kulturen von *A. vinosum* und *T. denitrificans* (DSM 807) isolierten reversen dissimilatorischen APS-Reduktasen sind homolog zu den Enzymen der SRP und weisen ähnliche physikochemische Eigenschaften auf (Fritz *et al.*, 2000; Fritz *et al.*, 2002a; Schwenn & Biere, 1979; Taylor, 1994); die APS-Reduktasen einiger *Chromatiaceae* Spezies (*A. vinosum*, *Allochromatium warmingii*, *Thiocapsa roseopersicina* ssp.) sind allerdings mit der Cytoplasmamembran assoziiert (Dahl & Trüper, 1989; Dahl & Trüper, 1994). Die Proteine, die in SOP den Elektronentransfer zwischen der cytoplasmatischen APS-Reduktase und der Elektronentransportkette gewährleisten, sind noch unbekannt. APS-Reduktase Aktivität wurde bisher in den anoxygenen phototrophen *T. roseopersicina* ssp. (Dahl & Trüper, 1989; Trüper & Rogers, 1971), *Thiocystis violacea*, *Allochromatium minutissimum* (Trüper & Fischer, 1982), *Chlorobium limicola* DSM 245 (Kirchhoff & Trüper, 1974), *Chlorobaculum*

parvum NCIB 8346 (Khanna & Nicholas, 1983), *Chlorobium limicola* DSM 257, *Chlorobaculum thiosulfatiphilum* DSM 249 (Bias & Trüper, 1987) und *Chlorobium phaeovibrioides* DSM 270 (Thiele, 1968) gefunden. In chemotrophen Spezies konnte APS-Reduktase Aktivität in autotrophen Kulturen von *Thiobacillus thioparus* (Taylor, 1994), *Beggiatoa* sp. Stamm MS-81-1c (Hagen & Nelson, 1997; Teske & Nelson, 2004), *Thiothrix ramosa* (Odintsova *et al.*, 1993), thiotrophen Endosymbionten von marinen Invertebraten (Cavanaugh *et al.*, 2004; Nelson & Fisher, 1995) einschließlich einiger nah verwandter, freilebender SOP (Kuever *et al.*, 2002), *Acidianus ambivalens* (Zimmermann *et al.*, 1999) sowie in chemolitho-heterotrophen Kulturen von *Leucothrix mucor* DSM 2157 (Grabovich *et al.*, 1999), *Leucothrix thiophila* ssp. (Grabovich *et al.*, 2002) und *S. thermosulfooxidans* (Krasil'nikova *et al.*, 1998) nachgewiesen werden. Systematische Untersuchungen zum Vorkommen dieses Enzyms in SOP sind bisher allerdings nicht durchgeführt worden. SRP-homologe, reverse dissimilatorische ATP-Sulfurylasen sind aus *Endoriftia persephone* und *A. vinosum* isoliert worden (Beynon *et al.*, 2001; Frigaard & Dahl, 2008). Die funktionelle Bedeutung der APAT im Schwefelmetabolismus von SOP ist noch ungeklärt (Brune, 1995; Dahl & Trüper, 1994; Khanna & Nicholas, 1983; Trüper & Fischer, 1982).

Sulfit:Akzeptor-Oxidoreduktase. Die SAORs (Molybdopterin-Kofaktor im aktiven Zentrum) oxidieren Sulfit ohne Intermediat-Bildung zu Sulfat und transferieren die Elektronen *in vitro* auf Cytochrom c oder Ferricyanid (Kappler & Dahl, 2001; Kappler, 2008). Biochemische Analysen zeigten, dass Sulfit:Akzeptor-Oxidoreduktasen in photo- und chemotrophen SOP weit verbreitet sind und auch in denjenigen sulfatproduzierenden Spezies nachgewiesen werden konnten, die keine APS-Reduktase besitzen (wie z. B. *A. ferrooxidans*, *A. acidophilum* (Kappler & Dahl, 2001; Rohwerder & Sand, 2003), *Beggiatoa leptomitiformis* (Grabovich *et al.*, 1998), *Leucothrix* sp. (Grabovich *et al.*, 2002) und *Thioalkalivibrio* spp. (Sorokin & Kuenen, 2005), schwefelfreie Purpurbakterien wie *B. sulfoviridis*, *Rhodovulum adriaticum* und *R. veldkampii* (Neutzling *et al.*, 1985) und Schwefel-Purpurbakterien wie *Marichromatium* spp. und *Ectothiorhodospiraceae* (Brune, 1995; Trüper & Fischer, 1982)). Sulfit:Akzeptor-Oxidoreduktasen wurden auch in Vertretern der Organosulfonat-abbauenden Bakterien wie z. B. *Sulfitobacter* spp., *S. pomeroyi* und *Comomonas acidivorans* gefunden (Cook *et al.*, 2008; Denger *et al.*, 2006; Reichenbecher *et al.*, 1999; Sorokin, 1995). Die bestuntersuchte bakterielle SAOR ist das periplasmatische, heterodimere Enzym von *Starkeya novella* (SorAB). Die Katalyse erfolgt über einen nukleophilen Angriff des Sulfit S-Atoms auf einen O-Liganden des Mo(VI) im Molybdopterin-Kofaktor der SorA Untereinheit; die Elektronen werden vom reduzierten Mo(IV) über die mono-Häm Cytochrom c Untereinheit

(SorB) *in vitro* auf ein periplasmatisches Cytochrom c_{550} übertragen (Kappler & Dahl, 2001; Kappler, 2008). Weitere SAORs wurden bisher nur von acido- und neutrophilen chemotrophen SOP charakterisiert; sie unterscheiden sich hinsichtlich ihrer Untereinheiten-Zusammensetzung, molekularen Masse, zellulären Lokalisierung (frei und periplasmatisch oder membrangebunden und cytoplasmatisch) und katalytischen Eigenschaften (Kappler & Dahl, 2001; Kappler, 2008). Die SAORs der anoxygenen phototrophen SOP sind cytoplasmatische, membranassoziierte Enzyme (Dahl & Trüper, 1994; Kappler & Dahl, 2001; Neutzling *et al.*, 1985); genetische Informationen zu diesen Proteinen fehlen aber bisher (keine *sorAB*-homologen Gene in Genomen vorhanden).

1.3.3 Thiosulfatoxidation in Bakterien: Das Sox Enzymsystem

Thiosulfat ist unter neutralen bis alkalischen Bedingungen eine stabile anorganische Schwefelverbindung, die eine wichtige Funktion im Schwefelkreislauf einnimmt (Jørgensen & Bak, 1991; Jørgensen & Nelson, 2004; Sorokin *et al.*, 1996; Tuttle & Jannasch, 1976); sie wird von vielen photo- und chemotrophen SOP zu Sulfat umgesetzt (siehe Tabellen 1 und 2, Anhang). Es existieren drei enzymatische Thiosulfatoxidationswege in bakteriellen SOP: (1) der Sox Enzymsystem-katalysierte, periplasmatische Weg ohne freie Intermediate („Sox Weg“) (2) der „verzweigte“, d. h. der über zwei räumlich getrennte Enzymsysteme ablaufende Weg unter Ausbildung von freien Intermediaten ([S^0] und Sulfit), und (3) der über Tetrathionat als obligates Intermediat verlaufende „S_4I Weg“.

Das Sox System von *P. pantotrophus* umfasst 15 Gene, die in drei polycistronischen Operons (*soxRS*, *soxVW*, *soxXYZABCDEFGH*) organisiert sind (Friedrich *et al.*, 2001; Friedrich *et al.*, 2005; Friedrich *et al.*, 2008; Rother *et al.*, 2001). Die vier periplasmatischen Enzymkomplexe SoxXA, SoxYZ, SoxB, $Sox(CD)_2$ bilden das katalytisch-aktive $SoxXAYZB(CD)_2$ System (siehe Abbildung 8). Im aktuellen Modell des Thiosulfat-oxidationszyklus stellt das substratbindende SoxYZ den zentralen, redoxaktiven Enzym-komplex dar, welcher mit SoxXA, $Sox(CD)_2$ und SoxB interagiert (Elektronen werden auf Cytochrom c-Redoxpotentialniveau in die Atmungskette eingeschleust) (Quentmeier *et al.*, 2003; Sauve *et al.*, 2007). Der Reaktionsverlauf der Sulfid-, Elementarschwefel-, Sulfit- und Tetrathionatoxidation über das Sox System ist hingegen noch nicht geklärt; eine Thiosulfat-analoge, oxidative Verknüpfung dieser Verbindungen mit SoxY wird vermutet (Friedrich *et al.*, 2001; Quentmeier & Friedrich, 2001; Sauve *et al.*, 2007). Die Deletion der *sox* Gene führte in *P. pantotrophus*, *R. sulfidophilum* und *P. salicylatoxidans* zum vollständigen Verlust der Fähigkeit, Thiosulfat und Sulfid dissimilatorisch zu Sulfat zu oxidieren (Appia-Ayme *et al.*, 2001; Friedrich *et al.*, 2001; Lahiri *et al.*, 2006; Rother *et al.*, 2001). Das Sox

Enzymsystem wurde als der am weitesten verbreitete Thiosulfatoxidationsweg innerhalb der *Bacteria* postuliert (Friedrich *et al.*, 2001; Friedrich *et al.*, 2005; Friedrich *et al.*, 2008).

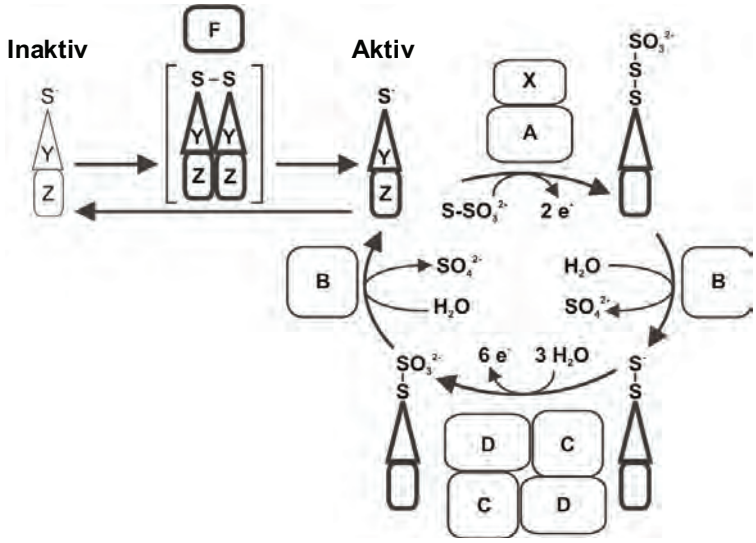

Abbildung 8. Modell des Reaktionszyklus der Thiosulfatoxidation über das Sox System von *P. pantotrophus* einschließlich der Reaktivierung von SoxYZ durch das Flavoprotein SoxF (die einzelnen Sox Enzymkomplexe sind durch Großbuchstaben gekennzeichnet). Die aktive Form des zentralen, substratbindenden Enzymkomplexes SoxYZ im Reaktionszyklus ist fett dargestellt; das SoxY-$Y(Z)_2$ stellt ein hypothetischen Intermediat dar, welches in der Transition von der inaktiven zur aktiven SoxYZ-Form entsteht, die durch SoxF katalysiert wird (Friedrich *et al.*, 2008).

Bedeutend weniger Informationen existieren über die Thiosulfatoxidation in obligat [S^0] Intermediat-bildenden SOP (Schwefel-Purpurbakterien, Grüne Schwefelbakterien sowie einige chemotrophe Beta- und Gammaproteobakterien; siehe Tabellen 1 und 2, Anhang). Studien mit radioaktiv markiertem Thiosulfat verdeutlichten, dass der Sulfonschwefel in Schwefel-Purpurbakterien periplasmatisch zu Sulfat umgesetzt wird, während der Sulfanschwefel zunächst in den Schwefelkugeln akkumuliert, bevor er im Cytoplasma zu Sulfat weiteroxidiert wird („verzweigter" Oxidationsweg) (Trüper & Pfennig, 1966). Von Friedrich und Mitarbeitern wurde postuliert, dass das Sox Enzymsystem auch in den Thiosulfatoxidationsprozess der [S^0]-formenden SOP involviert ist (Friedrich *et al.*, 2001; Friedrich *et al.*, 2005). In erster Bestätigung dieser These konnte gezeigt werden, dass die genetische Inaktivierung des SoxY bzw. der SoxXAYZB Proteine in *Chlorobaculum tepidum* und *A. vinosum* zum vollständigen Verlust ihrer Thiosulfatoxidationsfähigkeit führte, während die Sulfid- bzw. [S^0]-Oxidation zu Sulfat in beiden Organismen unbeeinflusst blieb (Hanson & Tabita, 2003; Hensen *et al.*, 2006). Für *A. vinosum* wurde deshalb ein „verzweigter" Oxidationsweg vorgeschlagen, in dem das SoxXAYZB System die periplasmatische Sulfonschwefeloxidation katalysiert: Der SoxXA Enzymkomplex verknüpft Thiosulfat

oxidativ mit SoxYZ zu SoxY-Thiocystein-S-Sulfat, aus welchem die Sulfonat-Gruppe durch das SoxB Protein als Sulfat freigesetzt wird. Der am SoxY verbleibende Sulfanschwefel des Thiosulfates kann aufgrund der fehlenden SoxCD Schwefeldehydrogenase-Komponente nicht im Periplasma weiteroxidiert werden und wird in Form von Schwefelkugeln intermediär gespeichert. Die [S^0]-Oxidation erfolgt im Cytoplasma über die revers-arbeitenden Enzyme des Sulfatreduktionsweges (Dsr, Apr und Sat/APAT oder SAOR, Abbildung 6) (Friedrich *et al.*, 2005; Grimm *et al.*, 2008; Hensen *et al.*, 2006). Eine Beteiligung der Sox Proteine am initialen Thiosulfat-Abbau ist auch beim chemotrophen, [S^0] Intermediat-bildenden *T. denitrificans* wahrscheinlich (Beller *et al.*, 2006). Systematische Analysen zum Vorkommen der *sox* Gene in thiosulfatoxidierenden, [S^0] Intermediat-bildenden SOP, die die Hypothese von Friedrich et al. (Friedrich *et al.*, 2001; Friedrich *et al.*, 2005) bestätigen würden, fehlen aber bisher.

Im „S_4I Weg“ einiger chemotropher SOP (siehe Tabelle 2, Anhang) wird Thiosulfat initial über eine Thiosulfatdehydrogenase zu Tetrathionat oxidiert, welches durch eine Tetrathionathydrolase wiederum zu Thiosulfat, Sulfat und elementaren Schwefel umgesetzt wird; letzteres kann über SDO und SAOR zu Sulfat weiteroxidiert werden, während Thiosulfat rezyklisiert wird (Kanao *et al.*, 2007; Kelly *et al.*, 1997; Meulenberg *et al.*, 1993; Rohwerder & Sand, 2007). Der genaue Reaktionsablauf dieses Weges sowie die Zusammensetzung und zelluläre Lokalisation der involvierten Enzyme sind noch nicht geklärt (Brüser *et al.*, 2000a; Kanao *et al.*, 2007; Rohwerder & Sand, 2007).

1.3.4 Sulfid-, Elementarschwefel-, Sulfit- und Thiosulfatoxidation in Archaeen

Im thermoacidophilen *A. ambivalens* (*Sulfolobales*) wird elementarer Schwefel über einen cytoplasmatischen Enzymweg (Schwefel-Oxygenase-Reduktase, SQR und SAOR) zu Sulfat oxidiert (Kletzin, 2008). Von Kletzin und Mitarbeitern wurde postuliert, dass dieser Organismus zusätzlich zur SAOR-katalysierten Reaktion eine Sulfitoxidation via APS Intermediat durchführen kann (Zimmermann *et al.*, 1999); eine Adenylylsulfat:Phosphat-Adenylyltransferase bzw. reverse dissimilatorische APS-Reduktase konnte aber bisher nicht isoliert werden (Kletzin, 2008). Thiosulfat, welches als Nebenprodukt der Oxidationsprozesse abiotisch entsteht, wird über eine membranintegrale Thiosulfat:Chinon-Oxidoreduktase (Müller *et al.*, 2004) und cytoplasmatische Tetrathionathydrolase zu Thiosulfat, elementarem Schwefel und Sulfat umgesetzt (Kletzin, 2008).

1.4 Molekulare Charakterisierung der dissimilatorischen APS-Reduktase

Zurzeit sind durch (Meta-)Genomsequenzierungen *aprBA* Komplettsequenzen von 31 validierten SRP und SOP in den Datenbanken frei zugänglich (siehe Tabelle 3, Anhang). Mit Ausnahme von *T. denitrificans* besitzen alle SRP und SOP Spezies nur einen AprBA-kodierenden Genlocus im Genom (Abbildung 9). Die Gen-Anordnung, *aprB-aprA*, ist in allen *apr* Operons streng konserviert, wobei die Gensequenzen von *A. vinosum*, *Cdt.* P. ubique und *T. denitrificans* (*apr*-Genlocus I) im *aprB*-Stopp-/*aprA*-Startcodon überlagern.

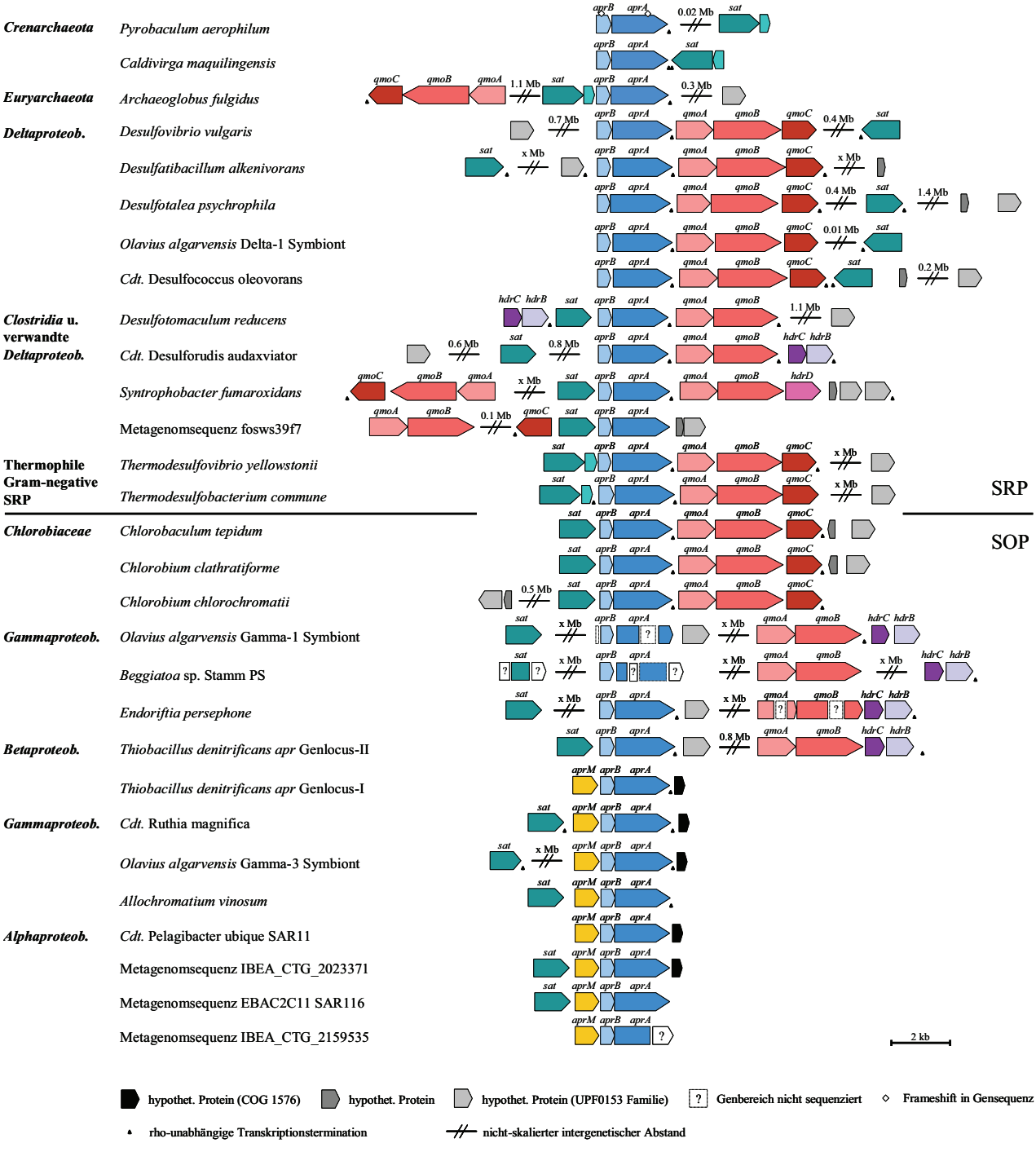

Abbildung 9. Schematische Darstellung der Genomorganisation der *sat*, *apr*, *qmo* und *hdr* Gene in ausgewählten validierten und potentiellen SRP und SOP (für GenBank Zugangsnummern der proteinkodierenden Gene siehe Tabelle 3, Anhang).

Die Röntgenstrukturanalyse der dissimilatorischen APS-Reduktase von *A. fulgidus* ergab, dass die α-Untereinheit in drei Domänen gegliedert ist (helikale, Capping- und FAD-Bindungs-Domäne) (Fritz *et al.*, 2000; Fritz *et al.*, 2002b). Die β-Untereinheit ist in drei Segmente unterteilt, von denen nur das erste Segment (B2-B68, beide [Fe_4-S_4] Cluster beinhaltend) strukturell zu Ferredoxinen verwandt ist, während die Segmente 2 und 3 (B69-B104, B105-B148) keine Sequenzähnlichkeit zu anderen Proteinen bzw. Proteindomänen zeigen. Der globuläre Teil der β-Untereinheit (erstes und zweites Segment) ist eingebettet in eine Spalte zwischen der FAD-Bindungs- und Capping-Domäne; der unstrukturierte C-Terminus (50 Å) windet sich um die α-Untereinheit und vergrößert damit den Oberflächenkontakt zwischen AprA und AprB (Stabilisierung des αβ-Heterodimers) (Fritz *et al.*, 2002b; Schiffer *et al.*, 2006) (Abbildung 10).

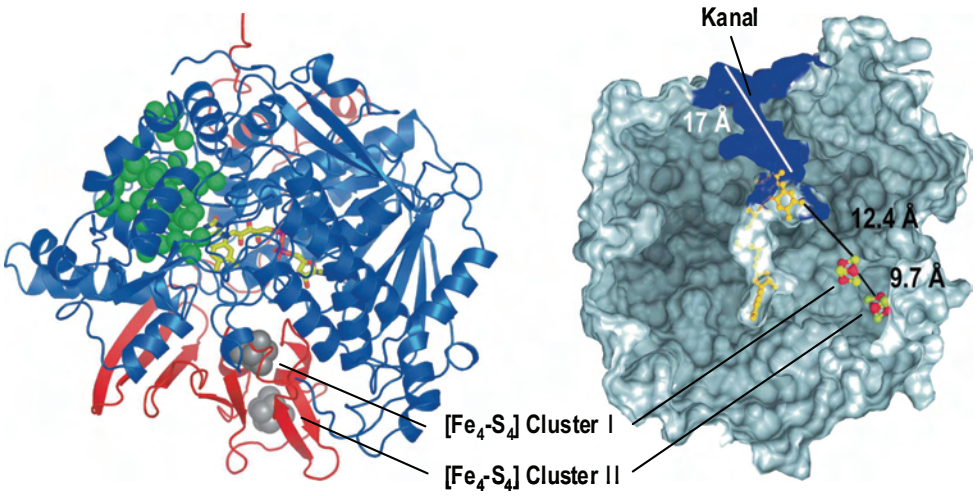

Abbildung 10. Links: Die dreidimensionale Struktur der dissimilatorischen APS-Reduktase von *A. fulgidus* (αβ-Heterodimer). Die α-Untereinheit, die den FAD-Kofaktor (gelb) enthält, ist in blauer Farbe gezeigt, während die β-Untereinheit, die die zwei [Fe_4-S_4] Cluster (grau) trägt, in roter Farbe dargestellt ist. Die Position und Form des Substratbindungskanals wird durch 35 Wasser Moleküle (grün) hervorgehoben, die durch das starke elektrostatische Feld innerhalb des Kanals gebunden sind. **Rechts:** Querschnitt durch die molekulare Oberfläche der APS-Reduktase von *A. fulgidus*, die den Weg des Elektronentransfers ausgehend von den [Fe_4-S_4] Clustern (gelb/rot) zur FAD-Gruppe (gelb) des aktiven Zentrums zeigt (Fritz *et al.*, 2002b; Schiffer *et al.*, 2006).

Die beiden FeS-Zentren der *A. fulgidus* APS-Reduktase weisen signifikante Unterschiede in ihren Redoxpotentialen auf (Fritz *et al.*, 2000; Fritz *et al.*, 2002a; Fritz *et al.*, 2008; Lampreia *et al.*, 1994; Verhagen *et al.*, 1994). Diese werden durch die unterschiedliche Anzahl von polaren Interaktionen zwischen FeS-Zentrum I bzw. II und der sie jeweils um-

gebenden Proteinmatrix verursacht (Abbildung 11). Durch die Mehrzahl an Interaktionen mit lokalen Dipolen wird der reduzierte Zustand des zur α-Untereinheit ausgerichteten [Fe_4-S_4] Cluster I stabilisiert, wodurch dessen Redoxpotential (-57 ± 5 mV) im Vergleich zu den Redoxpotentialen anderer Ferredoxin-[Fe_4-S_4] Cluster (-200 bis -500 mV) sehr hoch ist. Der geringe Abstand der Asp-B11 Carboxyl-Gruppe zum Säure-labilen S2-Atom des exponiert gelegenen [Fe_4-S_4] Cluster II (< 3 Å) führt hingegen zur Stabilisierung des oxidativen Zustandes dieses FeS-Zentrums (-520 ± 10 mV) (Fritz *et al.*, 2002b; Fritz *et al.*, 2008).

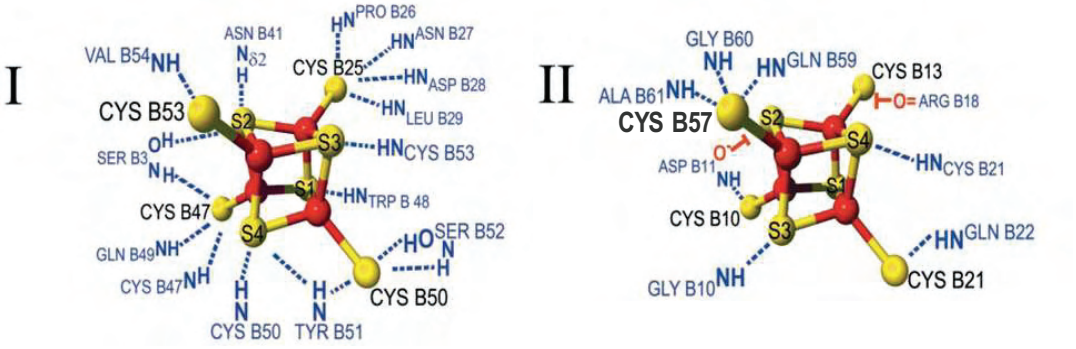

Abbildung 11. Schematische Darstellung der [Fe_4-S_4] Cluster Bindungsstellen in der β-Untereinheit der APS-Reduktase von *A. fulgidus*. Beide Cluster sind durch die Thiol-Gruppen von jeweils 4 Cysteinen kovalent gebunden. Die größere Anzahl an polaren Interaktionen zwischen Cluster I und der Proteinmatrix verglichen mit Cluster II ist verantwortlich für die signifikante Redoxpotentialdifferenz (nach (Fritz *et al.*, 2002b), korrigiert).

Das Redoxpotential des FAD-Kofaktors wird von der APS-Reduktase-Proteinmatrix über den Isoalloxazin-Beugungswinkel (N5-N10 Achse) moduliert. Die gebogene Isoalloxazin-Konformation („butterfly", ca. 25°; Abbildung 12) führt zu einer Stabilisierung des reduzierten Zustandes und zur Erhöhung des Redoxpotentials der FAD-Gruppe (-45 ± 10 mV) im Vergleich zu freiem FAD (-220 mV) (Fritz *et al.*, 2002b; Fritz *et al.*, 2008).

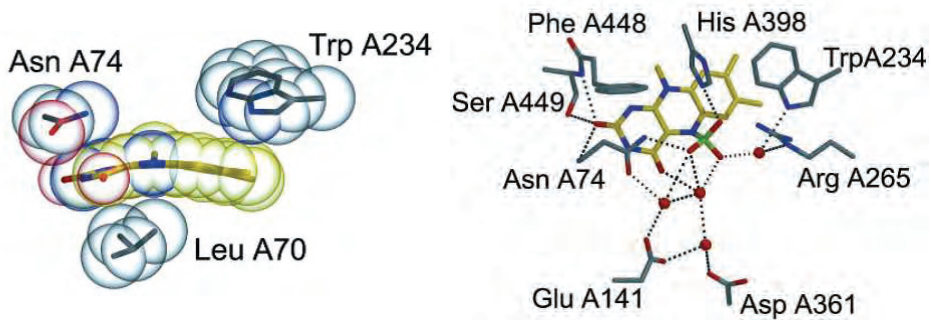

Abbildung 12. Der FAD-Kofaktor der APS-Reduktase *A. fulgidus*. **Links:** Der Isoalloxazin-Ring des FAD (Blick entlang der N5-N10 Achse) ist in seiner gebogenen Konformation (25°) gezeigt, die durch die Interaktionen mit der Proteinmatrix (hauptsächlich Asn-A74, Trp-A234 (*re*-Seite) und Leu-A70 (*si*-Seite)) bevorzugt wird. **Rechts:** Die Interaktionen der Sulfit-Gruppe des FAD-Sulfit-Adduktes mit den katalytisch-aktiven Aminosäuren His-A398, Arg-A265 und Asn-A74 sind gezeigt (Wassermoleküle sind als rote Kugeln dargestellt) (Fritz *et al.*, 2002b).

Die Elektronen werden einzeln via Cluster II und Cluster I auf den Isoalloxazin-Ring des FAD übertragen (siehe Abbildung 10); ein effektiver Elektronentransfer zwischen dem S3-Atom des Cluster I und der FAD-Methyl-Gruppe auf der *si*-Seite des FAD (12.4 Å Distanz) wird dabei durch den Indol-Ring eines zwischen beiden Kofaktoren positionierten Tryptophans ermöglicht (Fritz *et al.*, 2002b; Schiffer *et al.*, 2006). Nach Bindung des Substrates APS an der *re*-Seite des FAD erfolgt der nukleophile Angriff des N5-Atoms auf das Sulfat-S-Atom des APS und die Ausbildung eines kurzlebigen FAD-APS Intermediates. Die Katalyse wird dabei von der erhöhten Nukleophilie des N5-Atoms (durch die Deprotonierung des N1-Atoms) und der Elektrophilie des APS-S-Atoms (durch Wasserstoffbrückenbindungen im aktiven Zentrum, Abbildung 12) begünstigt. Während des FAD-APS-Übergangszustandes behält der Isoalloxazin-Ring seine gebogene Konformation bei, wird aber durch Rotation um ca. 0.6 Å in Richtung des Kanalinneraumes verschoben; dies führt dazu, dass sich der Isoalloxazin-Ring, Teile der Polypeptidkette und das APS-Molekül im Enzym-Substrat-Komplex in einer gespannten Konformation befinden. Dieser energiereiche Zustand wird durch Elektronen-Umlagerungen relaxiert und führt zur Abspaltung der AMP-Gruppe und Ausbildung eines FAD-Sulfit-Adduktes an der N5-Position des Isoalloxazin-Ringes. Die anschließende Spaltung des Adduktes in Sulfit und oxidierten FAD-Kofaktor wird vermutlich durch Protonierung der Sulfit-Gruppe beschleunigt (Fritz *et al.*, 2002b; Fritz *et al.*, 2008; Schiffer *et al.*, 2006).

1.5 Molekulare Charakterisierung der Sulfat-Thiol-Hydrolase des Sox Systems (SoxB)

Die aus *P. pantotrophus* und *A. vinosum* isolierten SoxB Proteine sind periplasmatische, monomere, di-Mangan-enthaltende Enzyme (ca. 60 kDa) (Epel *et al.*, 2005; Friedrich *et al.*, 2001; Hensen *et al.*, 2006), die eine signifikante Sequenzidentität (~30 %) zu den Zink-enthaltenden 5`-Nukleotidasen aufweisen (Friedrich *et al.*, 2001; Verte *et al.*, 2002). Das SoxB Protein ist nur in Assoziation mit den anderen Komponenten des Sox Systems katalytisch aktiv und fungiert als Sulfat-Thiol-Hydrolase, indem es die Sulfonat-Gruppe vom SoxY-(Thio-)Cystein-S-Sulfat hydrolytisch abspaltet (Friedrich *et al.*, 2001; Verte *et al.*, 2002). Der genaue Reaktionsmechanismus ist noch unbekannt; in Analogie zur Zink-enthaltenden 5`-Nukleotidase von *E. coli* (Knöfel & Sträter, 1999) wurde postuliert, dass die Mn^{2+}-Ionen in die Bindung eines Wassermoleküls und der von SoxY kovalent gebundenen Sulfonat-Gruppe involviert sind. Polare Interaktionen mit der SoxB Proteinmatrix könnten die Nukleophilie des Wassermoleküls erhöhen, um den initialen Angriff auf die S-SO_3^{2-}-Bindung

im SoxY-(Thio-)Cystein-S-Sulfat zu ermöglichen (Bagchi & Ghosh, 2005). Das *soxB* ist in den Genomen der SOP stets mit anderen Sox-kodierenden Genen assoziiert (Friedrich *et al.*, 2001; Friedrich *et al.*, 2005; Friedrich *et al.*, 2008).

1.6 Protein Phylogenie

1.6.1 Dissimilatorische APS-Reduktase und Sulfitreduktase

Die Phylogenie der dissimilatorischen APS-Reduktase wurde bisher nur in zwei Publikationen thematisch erörtert (Boucher *et al.*, 2003; Friedrich, 2002). Die Arbeit von Friedrich (Friedrich, 2002) stellte die erste systematische Untersuchung der APS-Reduktase Phylogenie von SRP dar. Für diese Publikation wurden 900 Nk-lange *aprA* Genfragmente von 60 sulfatreduzierenden Spezies mittels Gen-spezifischer PCR Primer amplifiziert (Primerpaar APS7-F und APS8-R; leicht modifizierte Sequenzen der Original-Primer von (Deplancke *et al.*, 2000; Zinkevich & Beech, 2000)). Ihre Anwendung erzielte bei einigen SRP kein Amplifikationsprodukt (z. B. von *Desulfotomaculum halophilum*, *Desulfosporosinus orientis*, *Thermodesulfovibrio yellowstonii*, *Desulfotalea psychrophila* sowie *Desulfobacca acetoxidans*). Die phylogenetische Analyse der 60 AprA Partialsequenzen verdeutlichte den Einfluss des lateralen Gentransfers (LGT; Synonym: „horizontaler Gentransfer“) auf die Evolution der dissimilatorischen APS-Reduktase in SRP (xenologe, d. h. 16S rRNA-inkongruente *apr* Gene in *Syntrophobacteraceae*, „*Nitrospinaceae*“, *Thermodesulfobacterium* und *Archaeoglobus* spp. sowie *Thermodesulfovibrio islandicus* (Friedrich, 2002)).

Im Vergleich zur APS-Reduktase ist die Phylogenie der dissimilatorischen Sulfitreduktase von SRP bereits wesentlich detaillierter untersucht worden (Hipp *et al.*, 1997; Klein *et al.*, 2001; Wagner *et al.*, 1998; Wagner *et al.*, 2005). Die Analysen der DsrAB Sequenzen zeigten mehrere unabhängige laterale *dsrAB* Transfervorgänge zwischen den SRP: *Thermodesulfobacterium* und *Archaeoglobus* spp., *Moorella thermoacetica*, *Ammonifex degensii* sowie die Vertreter der *Desulfotomaculum* Subcluster Ib, Ic Id und Ie (inklusive *Sporotomaculum* spp.) besitzen xenologe *dsrAB* Gene (Imachi *et al.*, 2006; Klein *et al.*, 2001; Larsen *et al.*, 1999; Loy *et al.*, 2008; Nielsen *et al.*, 2006; Wagner *et al.*, 1998; Zverlov *et al.*, 2005). Die orthologe „*Desulfobacterium anilini*“-Gruppe stellt die potentielle *dsrAB* Donator-Linie der xenologen Gram-positiven Sulfat-/Sulfitreduzierer dar (Zverlov *et al.*, 2005).

Die Phylogenien der reversen dissimilatorischen APS- und Sulfitreduktase von photo- und chemotrophen SOP sind aufgrund fehlender systematischer Untersuchungen ungeklärt. Phylogenetische Analysen einzelner (meta-)genomischer DsrAB Sequenzen von Schwefeloxidierer im gemeinsamen Datensatz mit Sequenzen von SRP weisen auf eine frühe

evolutionäre Trennung der oxidativ- bzw. reduktiv-arbeitenden Enzyme des dissimilatorischen Sulfitreduktionsprozesses hin (Boucher *et al.*, 2003; Hipp *et al.*, 1997; Loy *et al.*, 2008; Molitor *et al.*, 1998; Sabehi *et al.*, 2005). So zeigen die DsrAB Stammbäume eine basale trichotome Topologie: (1) DsrAB von bakteriellen Schwefeloxidierern, (2) DsrAB von bakteriellen Sulfat-/Sulfitreduzierern (einschließlich *Archaeoglobus* spp.) und (3) DsrAB von crenarchaeellen Sulfat-/Sulfitreduzierern.

1.6.2 Sulfat-Thiol-Hydrolase (SoxB)

Die Phylogenie des SoxB wurde bisher nur in einer Studie untersucht (Petri *et al.*, 2001). Der publizierte SoxB Stammbaum zeigte eine 16S rRNA-konforme Topologie (basale Position von *Aquifex aeolicus* (*Aquificae*) sowie monophyletische Gruppen der *Alpha*-, *Beta*- und *Gammaproteobacteria* und *Chlorobia*); es wurden keine LGT-Vorgänge zwischen validierten SOP Spezies festgestellt. [Anmerkung: Das postulierte xenologe *soxB* Gen des Isolates „*Thiomicrospira crunogena*“ Stamm HY-62 (Petri *et al.*, 2001) erwies sich in dieser Arbeit als Genfragment einer alphaproteobakteriellen Kontaminante der *Thiomicrospira* Kultur.] Der SoxB Datensatz von Petri et al. umfasste lediglich 18 thiosulfatoxidierende Spezies von z. T. unzureichend klassifizierten Isolaten (fünf Komplettsequenzen aus Genomdaten sowie 13 PCR-amplifizierte Partialsequenzen), so dass diese Studie keine systematische Analyse zur Verbreitung und Phylogenie dieses Proteins in SOP darstellt.

1.7 Funktionelle Genanalyse

Die Polyphylie der SRP und SOP (siehe Kapitel 1.1) erschwert ihre Identifikation über 16S rRNA-basierende Methoden (es gibt keine universellen 16S rRNA Gen-spezifischen Primer und Sonden) (Amann *et al.*, 1995; Brinkhoff *et al.*, 1998; Daly *et al.*, 2000; Joulian *et al.*, 2001; Lücker *et al.*, 2007; Manz *et al.*, 1998; Maukonen *et al.*, 2006; Stahl *et al.*, 2007; Wieringa *et al.*, 2000). Eine simultane 16S rRNA-basierende Identifikation von Sulfatreduzierern ist bisher nur über DNA Micro-Arrays möglich (SRP Phylo-Chips, gleichzeitige Hybridisierung der DNA-Umweltprobe mit 200 Gattungs- oder Spezies-spezifischen Sonden) (Loy *et al.*, 2002; Loy *et al.*, 2004; Stahl *et al.*, 2007). Die tatsächliche SRP Diversität in einem Habitat kann aber durch die 16S rRNA Analyse sowohl unterschätzt als auch überschätzt werden, da 16S rRNA Gen-spezifische Primer bzw. Sonden nicht zwischen den verwandten sulfatreduzierenden und nicht-sulfatreduzierenden Spezies (siehe Kapitel 1.1.1) diskriminieren. Als weitere wesentliche Einschränkung der 16S rRNA Analytik ist anzumerken, dass die 16S rRNA aufgrund ihrer konservativen Natur keine Diversitätsbestimmung unterhalb der Spezies-Ebene ermöglicht, d. h. es kann nicht zwischen

Stämmen hoher 16S rRNA Sequenzähnlichkeit unterschieden werden, die aber über unterschiedliche phänotypische Eigenschaften verfügen können und damit auch verschiedene ökologische Nischen besetzen (Vandamme *et al.*, 1996). Funktionelle Gene erlauben dagegen eine direkte Verknüpfung zwischen phylogenetischer Position und ökophysiologischer Funktion eines unbekannten, Umweltsequenz-detektierten Organismus. Zur Diversitätsanalyse von SRP wurden Primer zur PCR-Amplifikation von *dsrAB* und *aprA* Genfragmenten entwickelt (Deplancke *et al.*, 2000; Friedrich, 2002; Klein *et al.*, 2001; Loy *et al.*, 2004; Wagner *et al.*, 1998; Wagner *et al.*, 2005; Zinkevich & Beech, 2000; Zverlov *et al.*, 2005). Insbesondere die *dsrAB* Genanalyse ist bisher vielfach zur Untersuchung der SRP Diversität angewandt worden (über 30 Studien; *dsrAB* Analyse über Klonierung (Baker *et al.*, 2003; Castro *et al.*, 2002; Dhillon *et al.*, 2003; Kaneko *et al.*, 2007; Kjeldsen *et al.*, 2007a; Kjeldsen *et al.*, 2007b; Leloup *et al.*, 2006; Leloup *et al.*, 2007; Loy *et al.*, 2004; Schmalenberger *et al.*, 2007); *dsrA*/*dsrB* Analyse über DGGE (Dar *et al.*, 2007; Geets *et al.*, 2006; Karr *et al.*, 2005)). Die generelle Bevorzugung der *dsrAB* gegenüber der *aprA* Genanalyse steht im Zusammenhang mit der (1) größeren Datenmenge, die für die phylogenetisch Analyse zur Verfügung steht, und der (2) umfassenderen SRP Referenzstamm-Datenbank, die eine genauere phylogenetische Zuordnung der Umweltsequenzen ermöglichen. *apr* Gen-basierende Analysen wurden bisher nur in zwei medizinischen Studien zur SRP Diversitätsbestimmung verwendet (*aprA* Analyse über Klonierung (Zinkevich & Beech, 2000); *aprA* Analyse über DGGE (Deplancke *et al.*, 2000)).

Für SOP existieren bisher noch keine *dsr*- bzw. *apr*-spezifischen Primer, PCR Protokolle oder umfassende Referenzstamm-Datensätze. Dementsprechend gibt es bisher keine Studie, in der diese funktionellen Gene zur Diversitätsanalyse von Schwefeloxidierern benutzt wurden.

1.8 Zielsetzung der Arbeit

1. **Quantitative und qualitative Erweiterung der bestehenden Sequenz-Datenbasis für die dissimilatorischen APS-Reduktase von sulfatreduzierenden Prokaryonten.** Durch die Entwicklung neuer *aprB*- und *aprA*-spezifischer PCR Primer sollte möglichst der gesamte AprB- und AprA-kodierende Genbereich der phylogenetischen Analyse zugänglich gemacht werden. Zudem sollte durch die Sequenzierung weiterer sulfatreduzierender Referenzstämme die Datenbasis erweitert und vervollständigt werden, da einige phylogenetische Linien im Datensatz von Friedrich unterrepräsentiert waren. Durch die vergrößerte phylogenetisch-informative Datenmenge und das erweiterte Spezies-

Spektrum sollte die Auflösung in den Apr Stammbaum-Topologien verbessert werden, um eine genauere phylogenetische Zuordnung von Umweltsequenzen zu ermöglichen.

2. **Analyse des Vorkommens der dissimilatorische APS-Reduktase-kodierenden Gene in schwefeloxidierenden Prokaryonten und gleichzeitiger Aufbau einer Sequenz-Datenbasis für die dissimilatorische APS-Reduktase von SOP.** Durch die Entwicklung neuer *aprB*- und *aprA*-spezifischer PCR Primer sollte die Verbreitung der APS-Reduktase in photo- und chemotrophen SOP systematisch untersucht werden, um Aufschluss darüber zu bekommen, ob die *apr* Gene auch als molekulare Marker für SOP einsetzbar sind. Über Gensequenzierungen von Referenzstämmen sollte eine neue Datenbasis für dissimilatorische APS-Reduktasen von SOP aufgebaut werden.
3. **Analyse des Vorkommens des SoxB-kodierenden Gens in schwefeloxidierenden Prokaryonten und gleichzeitige Erweiterung der bestehenden Sequenz-Datenbasis für die Sulfat-Thiol-Hydrolase (SoxB) Komponente des Sox Systems von SOP.** Analog zum Modell für *A. vinosum* (Friedrich *et al.*, 2005; Grimm *et al.*, 2008; Hensen *et al.*, 2006) könnte das Sox System generell in die Thiosulfatoxidation von [S^0] Intermediat-bildenden SOP involviert sein; Studien, die diese Hypothese bestätigen würden, existieren aber bisher nicht. Eine essentielle Funktion des Sox Systems in der Sulfitoxidation konnte zudem für einige SOP experimentell belegt werden (Appia-Ayme *et al.*, 2001; Friedrich *et al.*, 2001; Lahiri *et al.*, 2006; Rother *et al.*, 2001). Ziel dieses Teilprojektes war es daher, die von Petri et al. (Petri *et al.*, 2001) publizierten *soxB*-spezifischen Primer zu nutzen, um die Verbreitung des Gens in photo- und chemotrophen SOP systematisch zu untersuchen. Eine ubiquitäre Verbreitung des Sox Systems in Schwefeloxidierern würde bedeuten, dass das *soxB* als alternativer molekularer Marker für SOP genutzt werden könnte. Durch Gensequenzierung weiterer photo- und chemotropher Referenzstämme sollte die bestehende SoxB Datenbasis (Petri *et al.*, 2001) erweitert werden.
4. **Phylogenetische Analyse der AprBA und SoxB Sequenzen im Vergleich zur 16S rRNA Phylogenie der SRP und SOP.** Durch Vergleich der 16S rRNA und AprBA/SoxB Stammbaum-Topologien sollte die Evolution der dissimilatorischen APS-Reduktase und Sulfat-Thiol-Hydrolase untersucht werden, um potentielle LGT-Vorgänge innerhalb der SOP/SRP bzw. zwischen SOP und SRP aufzudecken.
5. **Strukturanalyse über Homologie Modellierung der dissimilatorischen APS-Reduktase von SRP und SOP.** Die Röntgenstrukturdaten von Kroneck und Mitarbeitern (Fritz *et al.*, 2002b; Schiffer *et al.*, 2006) sollten zur Homologie Modellierung weiterer APS-Reduktasen genutzt werden, um die strukturellen Unterschiede zwischen den

oxidativen bzw. reduktiven APS-Reduktasen von SOP und SRP (auch im Hinblick auf den katalytischen Prozess der Sulfitoxidation bzw. APS-Reduktion) zu ermitteln.

6. **Funktionelle Genanalyse mit *aprA* als molekularem Marker.** Das von Deplancke et al. publizierte Primerpaar zur molekularökologischen Untersuchung von SRP Populationen (Deplancke *et al.*, 2000) zeigte in nachfolgenden Studien ein eingeschränktes Spezies-Amplifikationsspektrum (Friedrich, 2002) (eigene Resultate). Ziel dieses Teilprojektes war es deshalb, ein neues, universelles Primerpaar zu konstruieren, welches von allen bekannten *apr* Gen-besitzenden SOP und SRP eine *aprA* Partialsequenz amplifiziert, um eine simultane Analyse der SRP und SOP Diversität in Umweltproben zu ermöglichen.
7. **Vergleichende 16S rRNA und *aprA* Genanalyse zur Untersuchung der SRP und SOP Diversität in Umweltproben aus dem vulkanischen Inselbogen der Kleinen Antillen, Karibisches Meer.** Im Rahmen des CARIBFLUX Projektes (Nr. 03 G 0154: „Hydrothermal processes and material fluxes in the area of the Lesser Antilles volcanic arc, Caribbean Sea“) sollte die mikrobielle Diversität des dissimilatorischen Schwefelkreislaufes in Umweltproben aus dem Karibischen Meer über *aprA* Genanalysen bestimmt und mit den Ergebnissen aus 16S rRNA Genanalysen verglichen werden.

2 Ergebnisse und Diskussion

Im Folgenden werden die Ergebnisse der einzelnen Publikationen zusammengefasst und im Zusammenhang diskutiert. Dieser Abschnitt kann jedoch nicht die Diskussionen in den einzelnen Veröffentlichungen ersetzen, weshalb für eine ausführliche Betrachtung der Ergebnisse auf diese verwiesen sei. Einzelne Aspekte, die in den Publikationen nicht oder nur kurz behandelt wurden, sollen hingegen näher erläutert werden.

2.1 Dissimilatorische APS-Reduktase in sulfatreduzierenden und schwefeloxidierenden Prokaryonten: Verbreitung, Phylogenie und Strukturanalyse

Im Rahmen dieser Doktorarbeit wurden *aprBA*- bzw. *aprA*-spezifische PCR Primerpaare entwickelt, die den *aprBA* Genlocus in einer Gesamtlänge von 2.2-2.4 Kb bzw. 2.1-2.3 Kb (92-94 % bzw. 92-93 % der proteinkodierenden Genregionen) von SRP und SOP amplifizieren (Publikation 1 und 2). Die separate phylogenetische Analyse der AprB und AprA zeigte, dass sich die *aprB* und *aprA* Gene durch vertikale Transmission (Speziation) und parallele laterale Transfervorgänge (als *aprBA*-Operon) in den untersuchten SRP und SOP entwickelt haben (Koevolution) (Publikation 1 und 2). Die koordinierte Evolutionsrate beider Untereinheiten (identische Stammbaum-Topologien) rechtfertigte ihre Nutzung in einem gemeinsamen Datensatz analog zur Berechnungsweise der DsrAB Phylogenie (Klein *et al.*, 2001; Larsen *et al.*, 1999; Larsen *et al.*, 2000; Wagner *et al.*, 1998). [Anmerkung: Die zur phylogenetischen Analyse verfügbare Datenmenge des 1.9 Kb-langen *dsrAB* Genfragments umfasst nur 76-79 % der proteinkodierenden Genregionen der SRP.]

2.1.1 Sulfatreduzierende Prokaryonten

Insgesamt konnten von 75 phylogenetisch divergenten SRP Spezies 2.2-2.4 Kb-lange *aprBA* Partialsequenzen generiert werden, während von 27 weiteren sulfatreduzierenden Referenzstämmen kürzere *aprBA*/*aprA* Genfragmente sequenziert wurden (Publikation 1). Die publizierte Sequenz-Datenbasis für dissimilatorische APS-Reduktasen von SRP (Friedrich, 2002) konnte somit sowohl quantitativ als auch qualitativ signifikant erweitert werden. Die Datensätze beider Studien überschneiden sich lediglich in 30 Spezies.

Phylogenie der dissimilatorischen APS-Reduktase. Die Vergleiche der AprB/A- und 16S rRNA-basierenden SRP Stammbaum-Topologien dieser Arbeit bestätigten die postulierten LGTs von Vertretern der *Syntrophobacterales*, *Thermodesulfovibrio*, *Thermodesulfobacterium* und *Archaeoglobus* spp. sowie von „*Desulfobacterium anilini*“ und

Desulfarculus baarsii (Friedrich, 2002), deuten aber auch gleichzeitig auf einen primär durch vertikale Transmission geprägten Evolutionsweg der dissimilatorischen APS-Reduktase in SRP hin. Durch das erweiterte Spezies-Spektrum dieser Arbeit (72 bisher noch nicht untersuchte Spezies) konnte erstmals die 16S rRNA-übereinstimmende inter- und intrafamiliäre Gliederung z. B. der *Desulfovibrionales* und *Peptococcaceae* auf der Basis der Apr Sequenzen gezeigt werden. Aufgrund der vergrößerten phylogenetisch-informativen Datenmenge (92-94 % der AprBA-kodierenden Genregionen im Vergleich zu 45 % in der Friedrich Veröffentlichung) wurde außerdem eine verbesserte Stammbaum-Auflösung erreicht, die verdeutlichte, dass die LGT-Vorgänge zwischen den Gram-positiven SRP als *aprBA* Donator-Linie und den xenologen *Syntrophobacteraceae*, *Desulfarculaceae*, *Desulfomonile tiedjei* („*Syntrophaceae*“) und der „*Desulfobacterium anilini*“-Gruppe unabhängig voneinander abgelaufen sind (Publikation 1). Neue laterale *apr* Gentransfers zwischen entfernt verwandten SRP Linien wurden ebenfalls detektiert: So besitzen *Desulfobacca acetoxidans* („*Syntrophaceae*“) und *Thermacetogenium phaeum* („*Thermoanaerobacteraceae*“) xenologe, *Thermodesulfovibrio*-verwandte *apr* Gene (Publikation 1). [Anmerkung: Die Platzierung der sulfatreduzierenden „*Thermoanaerobacteraceae*“-Spezies *Desulfovirgula thermocuniculi* (Kaksonen *et al.*, 2007b) im Apr Stammbaum ist 16S rRNA-kongruent (neue *apr* Sequenzdaten)]. Die separaten Positionen der „*Desulfobacterium anilini*“-Gruppe sowie der Vertreter der „*Syntrophaceae*“ im AprBA Stammbaum stehen in Übereinstimmung mit der 16S rRNA Phylogenie (Kuever *et al.*, 2005) (siehe auch Abbildung 1) und würden ihre Reklassifizierung als eigenständige SRP Linien auf taxonomischem Niveau von Ordnungen bzw. Familien innerhalb der *Deltaproteobacteria* rechtfertigen; diese taxonomische Revision wäre auch durch die DsrAB Phylogenie belegt (Klein *et al.*, 2001; Loy *et al.*, 2008; Zverlov *et al.*, 2005). Interessanterweise stellt die *apr*-xenologe, aber *dsr*-orthologe „*Desulfobacterium anilini*“-Gruppe die potentielle *dsrAB* Donator-Linie der *dsr*-xenologen, aber *apr*-orthologen Gram-positiven Sulfat-/Sulfitreduzierer dar (Imachi *et al.*, 2006; Loy *et al.*, 2008; Nielsen *et al.*, 2006; Zverlov *et al.*, 2005), d. h. der laterale Transfer der Sulfitreduktase-kodierenden Gene zwischen diesen Gruppen ist vermutlich in umgekehrter Richtung zum lateralen Transfer der APS-Reduktase-kodierenden Gene erfolgt.

Thermacetogenium phaeum (Hattori *et al.*, 2000) ist bisher der einzige sulfatreduzierende Referenzstamm, für den ein rezenter lateraler Transfer der *apr* Gene nachgewiesen werden konnte; letzterer ist vermutlich das Resultat einer langzeitlichen Kokultivierung mit *Thermodesulfovibrio* spp. (Sekiguchi *et al.*, 1998) in einem UASB Reaktor. Da *T. phaeum* innerhalb der „*Thermoanaerobacteraceae*“ mit den sulfitreduzierenden, *dsrAB*-orthologen

Carboxydothermus hydrogenoformans, *C. ferrireducens* (Henstra & Stams, 2004; Slobodkin *et al.*, 2006) und *Desulfitibacter alkalitolerans* (Nielsen *et al.*, 2006) verwandt ist (Abbildung 1), könnte der Vorläufer dieser Spezies ursprünglich ebenfalls ein Sulfitreduzierer gewesen sein. Der simultane Transfer und die funktionelle Integration der Enzyme des Sulfatreduktionsschrittes in die Atmungskette des sulfitrespirierenden Vorläuferorganismus könnten sowohl durch den engen Zellkontakt innerhalb der granulären Pellets (Sekiguchi *et al.*, 1998) als auch durch gewisse genetische und physiologische Voraussetzungen im Donator und Akzeptor ermöglicht worden sein (siehe Publikation 1 für Details). Da die Position von *T. phaeum* im DsrAB Baum noch unbekannt ist, einige Vertreter der „*Thermoanaerobacteraceae*"-Linie wie *A. degensii* und *M. thermoacetica* (nur sulfitreduzierend) aber lateraltransferierte *dsrAB* Gene besitzen (Imachi *et al.*, 2006; Loy *et al.*, 2008; Nielsen *et al.*, 2006), könnte diese SRP Spezies alternativ durch einen gleichzeitigen Erwerb der Sulfat- und Sulfitreduktionsfähigkeit von *Thermodesulfovibrio* Donatoren entstanden sein. Obwohl die Genaufnahme von *T. phaeum* vermutlich durch die gesonderten konstanten Bedingungen im Habitat „UASB Reaktor" ermöglicht und begünstigt worden ist, spiegelt dieser „künstlich" generierte LGT-Vorgang dennoch den stetig ablaufenden, natürlichen Prozess des lateralen Generwerbs (via Konjugation, Transduktion und Transformation (Zaneveld *et al.*, 2008)) und Genverlustes in Genomen freilebender Prokaryonten wider (Boucher *et al.*, 2003; Choi & Kim, 2007; Doolittle *et al.*, 2003; Gogarten & Townsend, 2005; Ochman & Davalos, 2006; Thomas & Nielsen, 2005).

Die innovative Bedeutung des LGT für die mikrobielle Genomevolution und die damit einhergehende Möglichkeit zur physiologischen Adaptation an neue Umweltbedingungen (ökologische Nischen) wurde bereits in zahlreichen Studien nachgewiesen (Daubin *et al.*, 2003; Jain *et al.*, 2003; Lerat *et al.*, 2005; Mira *et al.*, 2002; Zhaxybayeva & Gogarten, 2004; Zhaxybayeva *et al.*, 2004). Sein Einfluss auf die Entstehung und Evolution der polyphyletischen SRP ist auch an den Diskrepanzen zwischen den AprBA und DsrAB Stammbaum-Topologien erkennbar (Publikation 1): Die abweichenden Positionen der *Thermodesulfovibrio* spp. deuten darauf hin, dass der Vorläufer dieser Linie ursprünglich ein Sulfitreduzierer gewesen sein könnte, der erst im späteren Verlauf der Evolution, die Fähigkeit zur Sulfatrespiration durch LGT erlangt hat. [Anmerkung: Dieser Entwicklungsweg trifft möglicherweise auch für die *Thermodesulfobiaceae* zu (neue *apr* Sequenzdaten).] Gemäß den übereinstimmenden xenologen Platzierungen der *Thermodesulfobacterium* bzw. *Archaeoglobus* spp. im AprBA und DsrAB Stammbaum könnten sich diese SRP Linien nach simultaner Übertragung der *dsr* und *apr* Gene von deltaproteobakteriellen bzw. Gram-

positiven sulfatreduzierenden Donatoren aus ursprünglich Fe(III)-reduzierenden bzw. methanogenen Organismen (Hartzell & Reed, 2003; Kashefi *et al.*, 2002) entwickelt haben. Die xenologen Positionierungen einiger deltaproteobakterieller bzw. Gram-positiver Gruppen in den AprBA und DsrAB Stammbäumen resultieren hingegen vermutlich aus dem Austausch des ursprünglichen, orthologen Gens durch ein lateral-transferiertes, xenologes *apr* bzw. *dsr* Gen in den jeweiligen sulfatreduzierenden Vorläufern (bezeichnet als „xenologous gene displacement" oder „orthologous gene replacement" (Koonin *et al.*, 2001)). Tatsächlich ist diese Form des LGT häufig (Coenye & Vandamme, 2005; Koonin *et al.*, 2001; Omelchenko *et al.*, 2003) und betrifft 10-15 % der orthologen Gene innerhalb der bakteriellen Domäne (Novichkov *et al.*, 2004). Die *apr*-xenologen *Syntrophobacterales* könnten ihre Sulfatreduktionsfähigkeit aber auch sekundär (d. h. erst nach Verlust der orthologen *apr* Gene) wiedererworben haben. Im allgemeinen sind die lateralen Gentransfers willkürliche und nicht gezielt ablaufende Vorgänge; der Ersatz eines orthologen, Spezies-spezifisch optimierten Proteins und die Etablierung eines xenologen, strukturell und regulatorisch nicht-optimierten Proteins innerhalb einer Population erfordert aber positive Selektion (Hao & Golding, 2006; Kurland *et al.*, 2003; Lercher & Pal, 2008; Pal *et al.*, 2005). Der Selektionsvorteil, den die xenologen *apr*/*dsr* Gene dem Metabolismus der entsprechenden Sulfatreduzierer geboten haben, ist dabei nicht offensichtlich. Der Grund dafür, dass diese LGT-Form vornehmlich in den *Syntrophobacterales* und Gram-positiven Sulfat- bzw. Sulfitreduzierern aufgetreten ist, könnte in den syntrophen, fermentierenden bzw. sporulierenden Fähigkeiten dieser Organismen liegen (Imachi *et al.*, 2006; Kuever *et al.*, 2005; Rabus *et al.*, 2000; Widdel, 1992), die ihnen eine gewisse Unabhängigkeit von den noch nicht optimierten Genen der Sulfatreduktion erlaubt und damit die Fixierung und Etablierung der xenologen Gene innerhalb der Vorläuferpopulationen ermöglicht haben könnten. Über Genomsequenz-Vergleiche wurde zwischen Vertretern der *Proteobacteria* und *Firmicutes* eine generell hohe LGT-Frequenz, insbesondere von metabolischen Genen festgestellt („LGT-highways") (Aguilar *et al.*, 2004; Beiko *et al.*, 2005). Die zahlreichen nahen Verwandtschaften von nicht-sulfat-/nicht-sulfitreduzierenden Spezies mit SRP (Abbildung 1) sind vermutlich die Folge der physiologischen Adaptationen von ursprünglich sulfatreduzierenden Stämmen an neue ökologische Nischen wie z. B. sulfatarme, methanogene Habitate. Dieser Adaptationsprozess resultiert offensichtlich zunächst im Verlust der *apr* Gene. Der häufig zu verzeichnende Verbleib der *dsr* Gene und Sulfitreduktionsfähigkeit in den entstandenen nicht-SRP Linien (siehe weitere Verbreitung der *dsr* gegenüber den *apr* Genen; vgl. Tabelle 3 und 4, Anhang) könnte die Folge der ubiquitären Präsenz von Organosulfonaten sein (Cook & Denger, 2002;

Cook *et al.*, 2006; Cook *et al.*, 2008), deren Sulfonat-Gruppe nach Abspaltung und Abbau der organischen Bestandteile als Elektronenakzeptor dient.

2.1.2 Schwefeloxidierende Prokaryonten

Die Ergebnisse der genetischen Analyse dieser Arbeit zeigten, dass die reverse dissimilatorische APS-Reduktase innerhalb der photo- und chemotrophen SOP begrenzt verbreitet ist. Zu den *aprBA*-besitzenden SOP zählen die *Chromatiaceae* (Ausnahmen: *Isochromatium* und *Marichromatium* spp.), einige *Chlorobiaceae* Spezies der Subcluster 3 und 4b (Alexander *et al.*, 2002; Imhoff, 2003), *Thiobacillus* spp. (*Betaproteobacteria*), *Thiothrix* spp. sowie thiotrophe Endosymbionten von diversen Invertebraten einschließlich einiger ihrer freilebenden Verwandten (*Gammaproteobacteria*); einzelne positive Enzymaktivitätsnachweise früherer Studien (Brune, 1995; Grabovich *et al.*, 1999; Grabovich *et al.*, 2002; Khanna & Nicholas, 1983; Kirchhoff & Trüper, 1974; Thiele, 1968; Zimmermann *et al.*, 1999) wurden durch die neuen, molekularen Daten sogar widerlegt (Publikation 2). Ein neuer Sequenzabgleich zwischen den verwendeten Primern und *apr* Genen von SOP (aktualisierte Daten siehe Tabelle 3, Anhang) ergab, dass mit Ausnahme der *apr* Gene von Vertretern der SAR11 Gruppe (Giovannoni *et al.*, 2005b; Rappe *et al.*, 2002) keine Primer-Zielsequenz-Fehlpaarungen im 3`-terminalen Primerbereich vorlagen, die eine verringerte PCR-Amplifikationseffizienz hätten verursachen können (Kwok *et al.*, 1990; Simsek & Adnan, 2000). Die unerwartet negativen Amplifikationsresultate, insbesondere von vielen Vertretern der sulfatproduzierenden *Chlorobiaceae* spiegeln deshalb die tatsächliche Abwesenheit der *apr* Gene in den jeweiligen Spezies wider (verifiziert durch zusätzliche molekulare Analysen und Genomdaten, siehe Publikation 2). Insgesamt konnten von 44 phylogenetisch divergenten SOP Spezies 2.1-2.3 Kb-lange *aprBA* Partialsequenzen generiert werden, während von neun weiteren schwefeloxidierenden Referenzstämmen kürzere Genbereiche sequenziert wurden (Publikation 2). Je zwei *aprBA* Genloci unterschiedlicher Sequenz sind in drei *Chromatiaceae* und drei *Thiobacillus* Spezies sowie dem Gamma-4 Symbionten von *Inanidrilus exumae* vorhanden (Publikation 2).

Verbreitung der reversen dissimilatorischen APS-Reduktase in photo- und chemotrophen SOP. Die Abwesenheit der *apr* Gene (sowie der *sat* und *dsr*) bei gleichzeitiger Präsenz des *sox* Genclusters in den heterotrophen bzw. fakultativ autotrophen Alpha- und Betaproteobakterien, die Sulfid ohne Intermediat-Bildung zu Sulfat oxidieren (z. B. „schwefelfreie“ Purpurbakterien wie *Rhodopseudomonas palustris*) (Publikationen 2 und 4), liefert einen ersten Hinweis darauf, dass diese photo- und chemotrophen SOP vermutlich generell einen *P. pantotrophus*-homologen Weg zur Oxidation anorganischer Schwefel-

verbindungen benutzen (Friedrich *et al.*, 2001; Friedrich *et al.*, 2005; Friedrich *et al.*, 2008). Die Multifunktionalität des Sox Enzymsystem ist bereits für einige Spezies experimentell nachgewiesen (Appia-Ayme *et al.*, 2001; Lahiri *et al.*, 2006; Rother *et al.*, 2001). In Anbetracht der o. g. Resultate ist die Präsenz von *apr* Genen in einigen aeroben Alphaproteobakterien wie den Spezies der SAR11 Gruppe einschließlich *Cdt.* P. ubique (Giovannoni *et al.*, 2005a; Giovannoni *et al.*, 2005b; Rappe *et al.*, 2002) und Vertretern der SAR116 Gruppe (Stingl *et al.*, 2007) (Publikation 2) interessant. In ozeanischen Systemen wird insbesondere der abundanten SAR11 Gruppe eine wichtige Funktion im Abbau von organischen Schwefelverbindungen wie DMSP zugeschrieben (Giovannoni *et al.*, 2005a; Howard *et al.*, 2006; Malmstom *et al.*, 2004; Vila-Costa *et al.*, 2007). Da die Proteorhodopsin-enthaltenden, heterotrophen *Cdt.* P. ubique ssp. über keine weiteren Gene des reversen Sulfatreduktionsweges bzw. des Sox Systems verfügen (Publikation 4), ist eine dissimilatorische Nutzung der dabei anfallenden anorganischen Schwefelverbindungen (Buchan *et al.*, 2005; Gonzalez *et al.*, 1999; Moran *et al.*, 2003) unwahrscheinlich. Da andererseits in den Genomen der SAR11 Gruppe häufig Gene vorhanden sind, die für Organosulfonat-transportierende und -abbauende Proteine kodieren, könnte die reverse dissimilatorische APS-Reduktase zur Detoxifizierung von Sulfit dienen, welches im Cytoplasma während des Abbaus von z. B. Taurin oder Methansulfonat akkumuliert (Cook & Denger, 2002; Cook *et al.*, 2006; Cook *et al.*, 2008). Die Nutzung einer revers-arbeitenden APS-Reduktase gegenüber einer SAOR wäre in diesem Fall vorteilhaft, da der generierte APS-Pool wiederum zur Synthese von PAPS (via CysC APS-Kinase) verwendet werden kann; PAPS stellt in vielen Prokaryonten das zentrale Intermediat für die Biosynthese von Sulfat-Gruppen-modifizierten Sekundärmetaboliten dar (katalysiert von Sulfotransferasen) (Abola *et al.*, 1999; Kopriva *et al.*, 2008; Williams *et al.*, 2002). Tatsächlich fehlen den *Cdt.* P. ubique spp. bis auf *cysC* alle weiteren Gene zur assimilatorischen Sulfatreduktion (einschließlich *cysH*) (Tripp *et al.*, 2008). Für eine essentielle Funktion der reversen dissimilatorischen APS-Reduktase im Metabolismus von SAR11 Organismen spricht (1) die hohe Abundanz und weite geographische Verbreitung des *apr* Genlocus in Vertretern der SAR11 Gruppe (siehe Abbildung 13 und Tabelle 3, Anhang) sowie (2) das komprimierte, auf ein Minimum von Genen reduzierte Genom der *Cdt.* P. ubique ssp. („streamlined genome“, Genome bestehen zu 95 % aus ORFs und haben keine Pseudogene (Giovannoni *et al.*, 2005a; Giovannoni *et al.*, 2005b; Rappe *et al.*, 2002)).

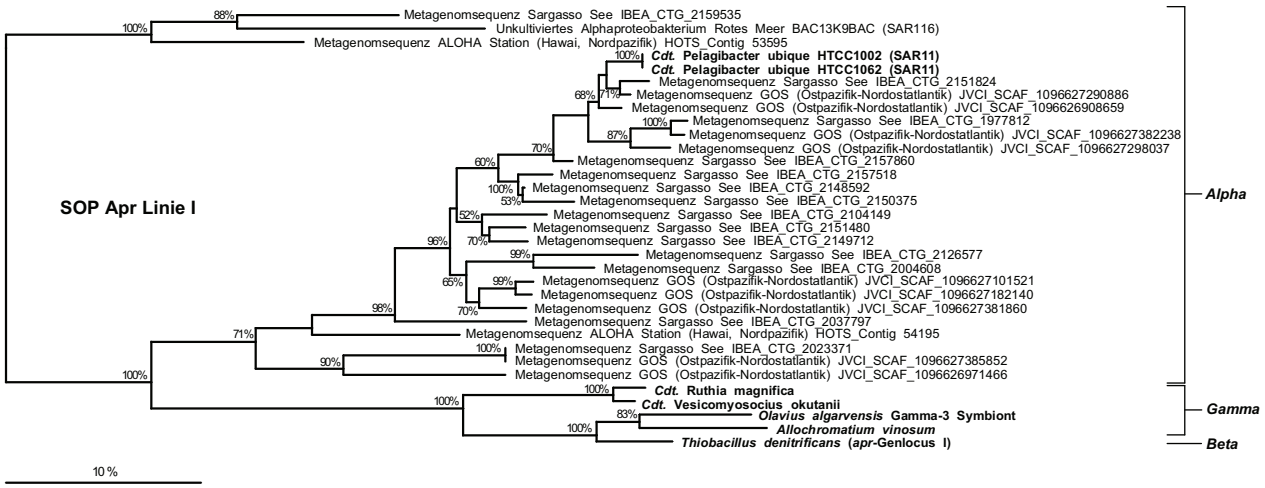

Abbildung 13. Maximum-likelihood Baum basierend auf den (meta-)genomischen AprBA Sequenzen der SOP Apr Linie I (Sequenzen aus validierten SOP Spezies sind fett hervorgehoben). Partialsequenzen wurden nachträglich über Parsimonie eingefügt (Ludwig *et al.*, 2004). An den Verzweigungen sind die Bootstrap-Werte (> 50 %), die über Maximum-likelihood Analyse mit 1000 Wiederholungen berechnet wurden, angegeben. Der Größenbalken gibt 10 % Sequenzunterschied an.

Die experimentellen Ergebnisse von Dahl und Mitarbeitern (Dahl *et al.*, 1999; Dahl *et al.*, 2005; Grimm *et al.*, 2008; Pott & Dahl, 1998; Sander *et al.*, 2006) sowie die Genomdaten (für aktualisierte Daten siehe Tabelle 4, Anhang) weisen darauf hin, dass die reverse DsrAB und der Redoxkomplex DsrMKJOP die [S^0]-Oxidation in *Chromatiaceae*, *Ectothiorhodospiraceae* und *Chlorobiaceae* Spezies katalysieren (eine systematische Analyse über das Vorkommen der kodierenden Gene fehlt bisher aber noch). Die Verbreitung der reversen dissimilatorischen APS-Reduktase innerhalb dieser Gruppen ist hingegen begrenzt (Publikation 2). Die Sulfitoxidation via APS wird von den Schwefel-Purpurbakterien und Grünen Schwefelbakterien vermutlich nur als alternativer, zusätzlicher Weg zur essentiellen AMP-unabhängigen Sulfitoxidation benutzt. Die Enzyme, die die direkte Sulfitoxidation in diesen Gruppen katalysieren, sind aber noch unzureichend charakterisiert. Für *A. vinosum* konnte die Präsenz einer molybdänhaltigen, cytoplasmatischen Sulfit:Akzeptor-Oxidoreduktase experimentell gezeigt werden. Ihre essentielle funktionelle Bedeutung für die photolithoautotrophe Sulfitoxidation wurde zudem durch die unverminderten Oxidations- und Wachstumsraten von *aprBA*-Deletionsmutanten im Vergleich zum Wildtyp-Stamm nachgewiesen (Dahl, 1996; Sanchez *et al.*, 2001). Tatsächlich konnten in allen diesbezüglich untersuchten *Chromatiaceae*, *Ectothiorhodospiraceae* und *Chlorobiaceae* Spezies (unabhängig zum Vorkommen der APS-Reduktase) Aktivitäten von cytoplasmatischen bzw. membrangebundenen SAORs detektiert werden (Brune, 1995; Dahl & Trüper, 1989; Dahl & Trüper, 1994; Trüper & Fischer, 1982). Molekulare Daten zu diesen potentiellen SAORs fehlen allerdings bisher

(keine *sorA*-homologen Sequenzen in den Genomen vorhanden, Publikation 4). Von Frigaard und Dahl (Frigaard & Dahl, 2008) wurde deshalb auf der Basis von Genomdaten-Vergleichen ein Polysulfidreduktase-ähnlicher Komplex, PSRLC3, als alternatives Sulfitoxidationsenzymsystem der nicht-*apr*/*sat*-besitzenden *Chlorobiaceae* und *Halorhodospira halophila* propagiert. Das System ist homolog zur periplasmatischen PsrABC Polysulfidreduktase von *Wollinella succinogenes* (Krafft *et al.*, 1995), im Gegensatz zu letzterer aber vermutlich invers orientiert und damit cytoplasmatisch ausgerichtet (Frigaard & Dahl, 2008). Experimentelle Beweise für diese postulierte Funktion fehlen allerdings bisher; zudem befinden sich keine PSRLC3-homologen Gene im Genom von *Chlorobaculum parvum* DSM 263, in welchem auch das Sat-Apr-katalysierte Sulfitoxidationssystem fehlt. In Analogie zu den sulfatproduzierenden anoxygenen phototrophen Alphaproteobakterien wurde auch das Sox System als weiterer möglicher Kandidat für die Sulfitoxidation in *Chromatiaceae*, *Ectothiorhodospiraceae* und *Chlorobiaceae* diskutiert; aufgrund seines auf die thiosulfatoxidierenden Spezies dieser Gruppen begrenzten Vorkommens (Publikation 4) ist eine solche Funktion aber unwahrscheinlich. Die zusätzliche Präsenz eines Sulfitoxidationsweges via APS bietet den Schwefel-Purpurbakterien und Grünen Schwefelbakterien möglicherweise unter bestimmten Umwelt-/Wachstumsbedingungen (z. B. bei Molybdän-Limitierung oder chemolithoautotrophem Wachstum, siehe *Thiocapsa roseopersicina* ssp. (Dahl & Trüper, 1989)) einen Selektionsvorteil (Publikation 2).

Bei den chemotrophen SOP wurden die *apr* Gene ausschließlich in neutrophilen, obligat [S^0] Intermediat-bildenden, autotrophen Spezies gefunden, die zumeist zur fakultativ anaeroben Lebensweise befähigt sind (*Thiobacillus* und *Thiothrix* spp., Invertebraten-Symbionten und deren freilebende Verwandte (Publikation 2) sowie marine *Beggiatoa* spp. (Mussmann *et al.*, 2007)). Möglicherweise wird das reverse Sulfatreduktionsenzymsystem von diesen Organismen analog zum [S^0]-Oxidationsweg der anoxygenen Phototrophen genutzt wird; ein *dsr* und *sat* Gen-Nachweis fehlt allerdings noch für die meisten der o. g. *apr*-besitzenden Spezies. Die Beteiligung der reversen Dsr, Apr und Sat ist momentan nur für (an-)aerobe *T. denitrificans* Kulturen (Beller *et al.*, 2006; Schedel & Trüper, 1980) und *Endoriftia pachyptila* bei anaerober Lebensweise (Markert *et al.*, 2007) experimentell belegt. Die Abwesenheit der *apr* Gene in den meisten der untersuchten chemotrophen SOP (Publikation 2) verdeutlicht, dass die Nutzung anderer sulfitoxidierender Enzym(system)e auch in dieser physiologischen Gruppe weit verbreitet ist. Unabhängig zur Präsenz einer APS-Reduktase konnten in vielen [S^0]-formenden Chemotrophen SAOR Enzymaktivitäten (siehe Kapitel 1.3.2) sowie *sorAB*-homologe Sequenzen (Publikation 4) nachgewiesen werden. In

den Gram-negativen acidophilen Chemotrophen ist die SAOR mit der SDO essentiell für den Sulfitoxidationsprozess (Rohwerder & Sand, 2003; Rohwerder & Sand, 2007; Valenzuela *et al.*, 2008). Eine Erklärung für die fehlenden Gendaten zu einigen SAORs (z. B. von *T. denitrificans* und *A. ferrooxidans*, aber auch von anoxygenen phototrophen SOP) einschließlich der beobachteten Enzym-Heterogenitäten (Denger *et al.*, 2006; D'Errico *et al.*, 2006; Di Salle *et al.*, 2006; Kappler & Dahl, 2001; Kappler, 2008; Loschi *et al.*, 2004; Myers & Kelly, 2005; Reichenbecher *et al.*, 1999) könnte die konvergente Entwicklung von isofunktionellen Proteinen sein. Ein Sox System-abhängiger Sulfitoxidationsweg wurde hingegen für die obligat autotrophen *T. crunogena* und *S. denitrificans* propagiert, da diesen *dsr*, *apr* und *sat* Gene fehlen (Scott *et al.*, 2006; Sievert *et al.*, 2008). Möglicherweise hat das Sox Enzymsystem in vielen weiteren [S^0] Intermediat-bildenden, nicht-*dsr*/*apr*-enthaltenden chemotrophen SOP ebenfalls eine essentielle Funktion für die Sulfit- bzw. Schwefeloxidation (z. B. *Halothiobacillus* spp., *L. mucor*; Publikationen 2 und 4). Die für das *P. pantotrophus* Sox System-untypische Intermediat-Bildung in *T. crunogena* wird vermutlich durch die unabhängige Regulation der *sox* Gene, die im Genom getrennt voneinander positioniert sind, verursacht (Scott *et al.*, 2006). Die Nutzung des reversen dissimilatorischen Sulfatreduktionssystems anstatt des Sox bzw. SDO/SAOR Enzymweges könnte in chemothioautotroph wachsenden Organismen insbesondere unter O_2-limitierenden Bedingungen energetische Vorteile liefern (z. B. auf Chinon-Redoxpotentialniveau in die Elektronentransportkette eingeschleuste Elektronen, zusätzlicher Energiegewinn durch Substratstufenphosphorylierung etc., Publikation 2).

Phylogenie der reversen dissimilatorischen APS-Reduktase. Im Gegensatz zu den monophyletischen DsrAB Sequenzen (Publikation 2, siehe auch (Boucher *et al.*, 2003; Hipp *et al.*, 1997; Sabehi *et al.*, 2005; Sander *et al.*, 2006)) trennen sich die AprBA Sequenzen der SOP in zwei divergente Linien, Apr Linie I und II. Die DsrAB-kongruente SOP Apr Linie I umfasst die Sequenzen von chemo- und phototrophen *Alpha-*, *Beta-* und *Gammaproteobacteria* und stellt vermutlich die authentische Position der proteobakteriellen SOP im AprBA Stammbaum dar. Die SOP Apr Linie II, die die Sequenzen der *Chlorobiaceae* (IIa) sowie einiger chemo- bzw. phototropher *Beta-* und *Gammaproteobacteria* (IIb) umfasst, weist hingegen eine DsrAB-inkongruente nähere Verwandtschaft zu den Proteinen der SRP auf, die sich nur durch mehrfache, unabhängige laterale Transfers der *aprBA* Gene von SRP zu SOP erklären lässt (Publikation 2).

Die *Chlorobiaceae* haben die Fähigkeit zur AMP-abhängigen Sulfitoxidation möglicherweise über einen simultanen lateralen Transfer des *sat-aprBA-qmoABC* Genlocus von einem

Thermodesulfovibrio-Vorläufer neu erworben (bestätigt durch ihre AprBA-übereinstimmende xenologe Position in Sat- und QmoABC-basierenden Stammbäumen, Publikation 3). Die funktionelle Integration des Sulfatreduktionssystems in die photosynthetischen Elektronentransportprozesse könnte durch bestimmte genetische und physiologische Voraussetzungen im Donator und Akzeptor ermöglicht worden sein (siehe Publikation 2 für Details). Der Transfer erfolgte entweder zum Vorläufer der Chlorobien (mit nachfolgendem Verlust des SRP-ähnlichen Sulfitoxidationssystems in den meisten Spezies) oder aber erst nach Diversifikation zu den Subcluster-Linien 3 und 4.

Die Xenologie der proteobakteriellen Apr Linie IIb wird durch das begrenzte Auftreten dieser Sequenzen in Beta- und Gammaproteobakterien bekräftigt, von denen mehrere Spezies neben dem xenologen zusätzlich noch einen zweiten, „authentischen“ (nicht-lateral-transferierten) *apr* Genlocus besitzen (Publikation 2). Der *apr* Donator dieser Gruppe ist unbekannt; die übereinstimmende Gen-Zusammensetzung (*qmoAB-hdrCB*) sowie die Sequenzähnlichkeit der Qmo und Hdr Proteine weisen auf Gram-positive SRP als Donatoren der *qmo-hdr* Gene hin (Publikation 2 und 3). Die Akquisition der *apr* Gene ist vermutlich durch mehrere, unabhängig voneinander abgelaufene Transfervorgänge zu den Vorläufern der *Thiobacillus*-, *Thiothrix*-, Invertebraten-Symbionten-, *Thiocystis*-, *Thiorhodococcus*- und *Thiocapsa-Thiodictyon-Lamprocystis*-Linien erfolgt. Nach Diversifikation in diesen Linien ist der „authentische“, DsrAB-orthologe *apr* Genlocus dann in der Mehrzahl dieser Spezies durch den homologen, SRP-verwandten Genlocus ersetzt worden („xenologous gene displacement“). Der zwei-*apr*-Genlocus-Zustand in einigen chemo- bzw. phototrophen Beta- und Gammaproteobakterien stellt dabei möglicherweise noch den genomischen Übergangszustand der Vorläuferorganismen dar, der eine Adaptation des lateral-erworbenen Gens im Genom ermöglichte, bevor das orthologe Gen entweder durch das xenologe Gen ausgetauscht (*Thiocapsa pendens*) oder letzteres wieder aus dem Genom eliminiert wurde (*Thiolamprovum pedioforme*) (Publikation 2). Die vermutlich ubiquitäre Präsenz alternativer, konvergent-entwickelter Sulfitoxidationsenzym(system)e in SOP (siehe vorheriger Abschnitt) könnte für die erfolgreiche funktionelle Integration der fremden Gene/Proteine eine entscheidende Bedeutung gehabt haben. Die Voraussetzung für einen Genaustausch zwischen Vertretern der SRP und SOP war/ist durch ihr gemeinsames Auftreten in verschiedenen Habitaten und ihre synergistischen Interaktionen gegeben (Blazejak *et al.*, 2005; Bright & Giere, 2005; Dubilier *et al.*, 2001; Imhoff, 2001b; Koizumi *et al.*, 2004; Markert *et al.*, 2007; Overmann, 2000; Tonolla *et al.*, 2004; van den Ende *et al.*, 1996; van den Ende *et al.*, 1997; Visscher *et al.*, 1992; Woyke *et al.*, 2006). Der Erwerb der SRP-Typ dissimilatorischen APS-Reduktase

(einschließlich des Qmo Komplexes) muss für den Metabolismus einiger Schwefeloxidierer ein Selektionsvorteil gewesen sein, da die Etablierung des xenologen, strukturell sowie regulatorisch nicht-optimierten Proteins positive Selektion voraussetzt (Hao & Golding, 2006; Lercher & Pal, 2008; Pal *et al.*, 2005). Tatsächlich sind die Vertreter der *Chromatiaceae*, die über eine SRP-ähnliche APS-Reduktase verfügen, physiologisch vielseitiger, da sie u. a. zwischen photo- und chemolithoautotropher Lebensweise wechseln können (Imhoff, 2001b; Kämpf & Pfennig, 1980). Der Verbleib beider *aprBA* Genloci in einigen *Chromatiaceae* Spezies wie z. B. *Thiocapsa roseopersicina* (unbewegliche Zellen) erlaubt möglicherweise eine Adaptation des Sulfitoxidationsprozesses an wechselnde Umweltbedingungen im Habitat. Eine SRP-homologe Elektronenübertragung auf Chinone via Qmo/Hdr-Redox-komplex bei der APS-Reduktase-katalysierten Sulfitoxidation könnte insbesondere bei chemolithoautotrophem Wachstum energetisch vorteilhaft sein und würde auch den häufigen Ersatz der orthologen *apr* Gene durch die homologen SRP Gene in chemotrophen SOP erklären (Publikation 2). Die Involvierung der SRP-Typ dissimilatorischen APS-Reduktase im oxidativen Schwefelmetabolismus (auch in Präferenz gegenüber dem zusätzlich vorhandenen, orthologen Enzym) wurde für *T. roseopersicina*, *T. denitrificans* und *E. persephone* indirekt nachgewiesen (Beller *et al.*, 2006; Dahl & Trüper, 1989; Dahl & Trüper, 1994; Markert *et al.*, 2007).

2.1.3 Strukturunterschiede der dissimilatorischen APS-Reduktase (Homologie Modellierung) und funktionell assoziierte Proteine Qmo, Hdr und AprM in Korrelation zur Apr Phylogenie

Die Topologien der AprBA Stammbäume weisen basal eine trichotome Verzweigungsstruktur auf: (1) AprBA der proteobakteriellen SOP (orthologe SOP Apr Linie I), (2) AprBA der bakteriellen SRP (einschließlich der xenologen Proteine von *Archaeoglobus* spp. und Schwefeloxidierern der SOP Apr Linie II) und (3) AprBA der crenarchaeellen SRP (*Caldivirga maquilingensis* einschließlich der nicht-sulfat-/nicht-sulfitreduzierenden *Pyrobaculum* Spezies) (Publikationen 1, 2 und 3). Diese phylogenetische Auftrennung in drei Apr Hauptgruppen korreliert mit der jeweiligen An-/Abwesenheit von AprM-, Qmo- und Hdr-kodierenden Genen in den (Meta-)Genomen der SRP und SOP (siehe Abbildung 14) (Publikationen 1, 2 und 3).

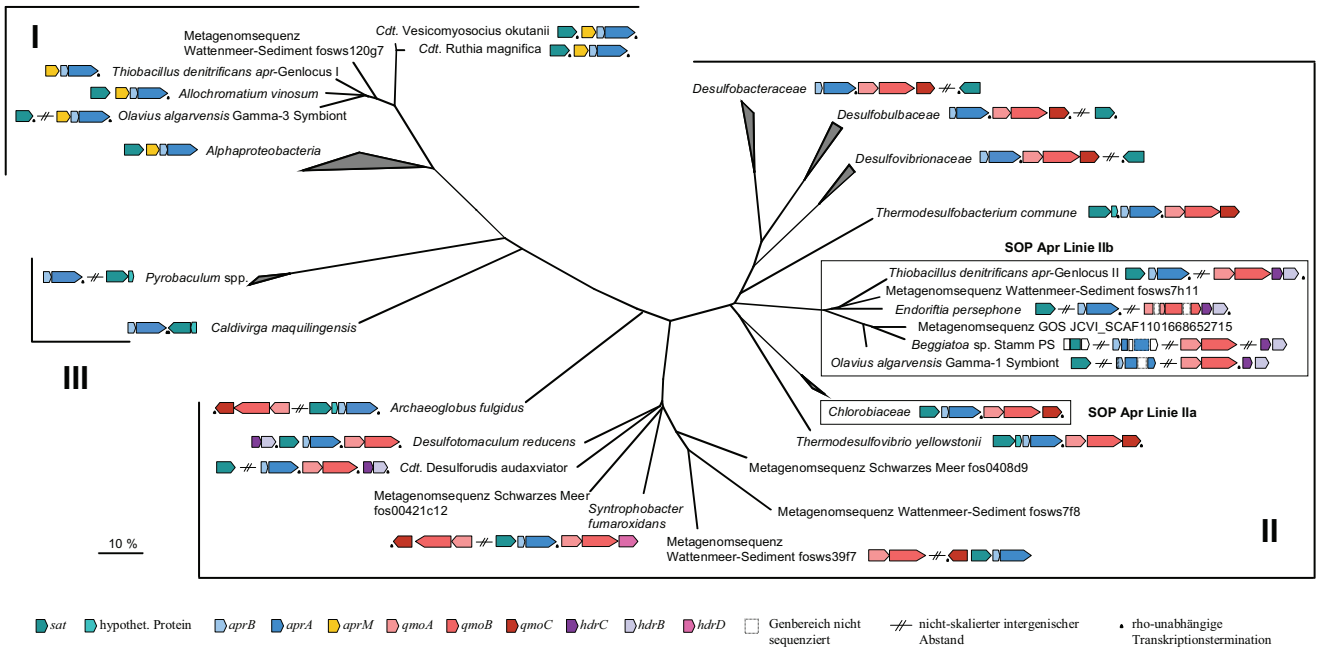

Abbildung 14. Maximum-likelihood Baum basierend auf AprBA Sequenzen aus SOP und SRP (Meta-) Genomen (siehe Tabelle 3, Anhang); Partialsequenzen wurden nachträglich über Parsimonie eingefügt (Ludwig *et al.*, 2004). Die trichotome Trennung der SRP und SOP in die Apr Hauptgruppen I-III (siehe Text) ist gezeigt (die xenologen SOP Linien sind durch Umrandungen gesondert hervorgehoben). Die *sat-apr-qmo*/*hdr* Genlocus-Zusammensetzung und –Anordnung in den validierten SRP und SOP ist schematisch dargestellt (homologe Gene sind gleichfarbig dargestellt, siehe Legende). Der Größenbalken gibt 10 % Sequenzunterschied an.

Die *aprBA* Gene, die für die reversen APS-Reduktasen der „authentischen“ SOP Apr Linie I kodieren, werden stets mit *aprM*-homologen Genen kotranskribiert; *qmo*-homologe Gene fehlen in den Genomen der SOP der Apr Linie I (Tabelle 3; Anhang). Im Hinblick auf ihre Koevolution (vgl. Abbildungen 13 und 15) könnte das Transmembranhelices-enthaltende AprM möglicherweise als essentielle membranverankernde Untereinheit der Typ-I oxidativen APS-Reduktase fungieren (Publikationen 1, 2 und 3); in Übereinstimmung dazu wurden die APS-Reduktasen von *Chromatiaceae* Spezies, die Apr Linie I-Sequenzen besitzen (z. B. *A. vinosum* und *A. warmingii*), als membrangebunden charakterisiert (Dahl & Trüper, 1989; Dahl & Trüper, 1994). Analog zur Menachinol:Fumarat-Oxidoreduktase (Cecchini *et al.*, 2002; Lancaster, 2003a; Lancaster, 2003b) könnte das AprM neben seiner Funktion als Strukturkomponente auch direkt in den Elektronentransfer zwischen cytoplasmatischer APS-Reduktase und membrangebundenem Elektronenakzeptor involviert sein (Publikation 2). Die Proteine, die den Elektronentransfer zur photosynthetischen bzw. respiratorischen Elektronentransportkette in diesen SOP gewährleisten, sind zurzeit noch unbekannt.

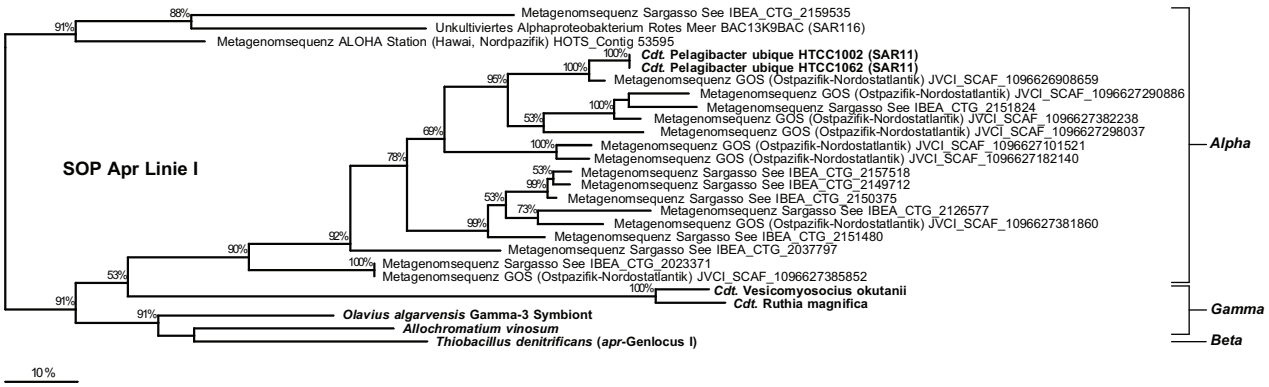

Abbildung 15. Maximum-likelihood Baum basierend auf den (meta-)genomischen AprM Sequenzen der SOP Apr Linie I (Sequenzen aus validierten SOP sind fett hervorgehoben). Partialsequenzen wurden nachträglich über Parsimonie eingefügt (Ludwig *et al.*, 2004). An den Verzweigungen sind die Bootstrap-Werte (> 50 %), die über Maximum-likelihood Analyse mit 1000 Wiederholungen berechnet wurden, angegeben. Der Größenbalken gibt 10 % Sequenzunterschied an.

In Bestätigung der postulierten Funktion als potentielle Menachinol:APS-Reduktase-Oxidoreduktase (Haveman *et al.*, 2004; Pereira, 2008; Pires *et al.*, 2003) sind die *aprBA* Gene der SRP in den Genomen häufig direkt mit Qmo-kodierenden Genen assoziiert. Die Möglichkeit eines Elektronentransfers von Menachinol (-70 mV) zu APS ($E^{\circ`}$ APS/SO_3^{2-} = -60 mV) via Qmo ist durch die Redoxpotentiale der beiden Häm b-Gruppen des membranintegralen QmoC (z. B. in *Desulfovibrio desulfuricans*: -20 bzw. +75 mV) gewährleistet (Pereira, 2008). Der genaue Mechanismus der Elektronenübertragung zwischen QmoA oder QmoB und AprB ist allerdings noch vollkommen ungeklärt (Pereira, 2008; Pires *et al.*, 2003); die Beteiligung eines zusätzlichen Redoxpartners (z. B. Thiole) ist nach den bisherigen Ergebnissen aus APS-Reduktase Reaktivitätsanalysen auszuschließen (Fritz *et al.*, 2008). Im Verlauf der SRP Evolution haben sich offensichtlich zwei Qmo Komplex-Typen entwickelt (Abbildung 14): So sind die *qmoAB* Gene der Gram-positiven SRP (einschließlich des *apr*-xenologen *Syntrophobacter fumaroxidans*) mit *hdrCB* bzw. *hdrD* Genen assoziiert (z. T. ein Operon formend), während *qmoC*-homologe Gene fehlen. In Analogie zur postulierten Interaktion zwischen DsrMKJOP und DsrAB via DsrC (Cort *et al.*, 2001; Dahl *et al.*, 2005; Fritz *et al.*, 2008; Pereira, 2008; Pires *et al.*, 2006) könnte der Elektronentransfer zwischen Membran und dem cytoplasmatischen QmoAB-HdrCB-Komplex über redoxaktive Thiol/Disulfidpaare erfolgen (Publikationen 1 und 2). Im Gegensatz dazu besitzen die deltaproteobakteriellen und die thermophilen SRP (einschließlich *A. fulgidus*) *qmoC*-assoziierte *qmoAB* Genloci; die Elektronen werden vom Menachinonpool vermutlich direkt über die Cytochrom b-Domäne des QmoC auf den Qmo Komplex transferiert. Die xenologen, SRP-verwandten *aprBA* Gene der SOP sind in den Genomen ebenfalls mit *qmoABC* (*Chlorobiaceae*) bzw. *qmoAB-hdrCB*

Genen (*Beta*- und *Gammaproteobacteria*) assoziiert, während *aprM*-homologe Gene fehlen. Eine SRP-homologe Elektronenübertragung könnte generell in denjenigen Schwefeloxidierern vorliegen, die über Typ-II oxidative APS-Reduktasen verfügen (Publikationen 2 und 3); APS-Reduktasen dieser Linie sind wie die Enzyme der SRP als cytoplasmatisch beschrieben worden (Dahl & Trüper, 1989; Dahl & Trüper, 1994). Interessanterweise sind in den Genomen der *aprBA*-besitzenden *C. maquilingensis* und *Pyrobaculum* spp. weder *aprM*- noch *qmoABC*/*hdrCBD*-homologe Sequenzen vorhanden; dies deutet auf einen bisher unbekannten Weg des Elektronentransfers in den crenarchaeellen SRP hin (Publikation 3).

Der Vergleich der über Homologie Modellierung (Fiser *et al.*, 2001; Krieger *et al.*, 2003; Marti-Renom *et al.*, 2000) berechneten AprA und AprB Modelle zeigte eine allgemein hohe strukturelle Konformität zwischen den dissimilatorischen APS-Reduktasen der SRP und SOP (Publikation 3). Die Unterschiede zwischen den AprA Modellen beschränkten sich hauptsächlich auf Bereiche der Proteinoberfläche, die die individuellen, Spezies-spezifischen Adaptationen zwischen den Untereinheiten repräsentieren (Publikation 3). Die den FAD-Kofaktor umgebenden bzw. den Substratbindungskanal und das aktive Zentrum formenden Proteinmatrices waren in den AprA Modellen der oxidativen und reduktiven APS-Reduktasen hoch konserviert; dies deutet auf einen revers zum APS-Reduktionsprozess der SRP (Fritz *et al.*, 2002a; Fritz *et al.*, 2002b; Schiffer *et al.*, 2006) verlaufenden Sulfitoxidationsmechanismus in SOP hin (Publikation 3). Auf der Basis der AprB Modelle konnten keine signifikanten Unterschiede zwischen den FeS-Zentren umgebenden und Redoxpotential modulierenden Proteinmatrices der APS-Reduktasen festgestellt werden, die einen generell inversen Elektronentransfer innerhalb der β-Untereinheit von oxidativen APS-Reduktasen begünstigen würden (Publikation 3). Die Modelle der Schwefeloxidierer-APS-Reduktasen lieferten demnach keinen strukturellen Hinweis darauf, dass die SOP Enzyme präferentiell die Oxidationsreaktion katalysieren. Allerdings zeigten die AprB Modelle von SRP und SOP Strukturunterschiede, die die o. g. phylogenetische Trennung der Enzyme und die damit korrelierende Entwicklung unterschiedlicher Enzym(system)e zur Kopplung der APS-Reduktase mit der Elektronentransportkette widerspiegeln (Publikation 3). So wiesen alle AprB Modelle der Apr Hauptgruppe II eine exponiert gelegene Proteinschleife nahe des FeS-II Zentrums auf, die möglicherweise eine strukturelle Adaptation an den physiologischen Interaktionspartner QmoABC bzw. QmoAB-HdrCB Komplex ist (möglicher QmoA- oder QmoB-Kontaktbereich). Die AprB Modelle der Apr Hauptgruppe I besaßen stattdessen eine exponiert gelegene Proteinschleife im zweiten Segment, die möglicherweise den physikalischen Kontakt der Typ-I oxidativen APS-Reduktase zu ihrem potentiellen

Membrananker AprM und dem noch unbekannten, membranständigen Elektronenakzeptor gewährleistet. Die AprB Modelle der crenarchaeellen SRP (Apr Hauptgruppe III) enthielten keinen dieser potentiellen Qmo/AprM-Proteinandockbereiche (Publikation 3). Die AprB Modelle deuteten zudem darauf hin, dass die *apr*-kodierten Proteinsequenzen der *Pyrobaculum* spp. keine funktionsfähigen Enzyme bilden (siehe Publikation 3 für weitere Details); die in Pseudogenen generell erhöhte Mutationsrate (Lerat & Ochman, 2005; Ochman & Davalos, 2006) würde auch die separaten Positionen der *Pyrobaculum* spp. und *C. maquilingensis* im AprBA Stammbaum erklären. Tatsächlich gibt es bisher keinen validierten *Pyrobaculum* Stamm, der zur dissimilatorischen Sulfatreduktion befähigt ist (Amo *et al.*, 2002; Huber *et al.*, 2002; Sako *et al.*, 2001).

2.2 Sulfat-Thiol-Hydrolase (SoxB) in schwefeloxidierenden Prokaryonten: Verbreitung und Phylogenie

In der genetischen Analyse dieser Arbeit wurde die Präsenz von *soxB* Genen in 57 photo- und chemotrophen SOP nachgewiesen (Publikation 4). Ein neuer Sequenzabgleich zwischen den Primern (Petri *et al.*, 2001) und *soxB* Genen zeigte, dass nur in einzelnen SOP Gruppen Primer-Zielsequenz-Fehlpaarungen vorlagen, die vermutlich zu den falsch-negativen PCR-Amplifikationsresultaten für die 13 thiosulfatoxidierenden *Thiomicrospira* spp., *Calyptogena* und *Bathymodiolus* Symbionten sowie *Rhodoblastus acidophilus* führten (Brinkhoff *et al.*, 1999; Cavanaugh *et al.*, 2004; Imhoff, 2001a; Imhoff, 2001c; Kuwahara *et al.*, 2007; Newton *et al.*, 2007). Die negativen Amplifikationsresultate der übrigen getesteten 59 Schwefeloxidierer korrelierten mit der fehlenden Fähigkeit zur Thiosulfatoxidation in der jeweiligen Spezies und gaben deshalb die tatsächliche Abwesenheit der *soxB* Gene wieder (verifiziert durch zusätzliche molekulare Analysen und Genomdaten, Publikation 4). Insgesamt konnte die bestehende *soxB* Datenbasis (Petri *et al.*, 2001) um 50 Sequenzen von phylogenetisch divergenten SOP Referenzstämmen erweitert werden (Publikation 4).

Verbreitung der SoxB in photo- und chemotrophen SOP. Da *soxB* als genetischer Indikator für die Präsenz des *sox* Genclusters genutzt werden kann, weisen die genetischen und genomischen Analysen dieser Arbeit auf eine weite Verbreitung des Sox Enzymsystems innerhalb der thiosulfatoxidierenden SOP der Domäne *Bacteria* hin (*sox* Gene wurden in 117 Vertretern der *Chlorobiaceae*, *Alpha*-, *Beta*-, *Gamma*-, *Delta*- und *Epsilonproteobacteria*, *Spirochaeta* sowie thermophilen *Aquifex* und *Thermus* spp. gefunden) (Publikation 4) und bestätigen damit die Hypothese von Friedrich et al. (Friedrich *et al.*, 2001; Friedrich *et al.*, 2005). Ein *P. pantotrophus*-homologer Thiosulfatoxidationsweg (Friedrich *et al.*, 2001;

Friedrich *et al.*, 2005; Friedrich *et al.*, 2008) wird vermutlich von allen Photo- und Chemotrophen verwendet, die Thiosulfat ohne Intermediat-Bildung zu Sulfat umsetzen (siehe Tabelle 2, Anhang), da in den bisher sequenzierten Genomen dieser SOP vollständige *sox* Gencluster (*soxXAYZBCD*) vorliegen (Publikation 4) [bestätigt durch neue Genomdaten von *Epsilonproteobacteria* und *Aquificae* (Aguiar *et al.*, 2004; Campbell *et al.*, 2006; Deckert *et al.*, 1998; Inagaki *et al.*, 2004; Miller *et al.*, 2007; Nakagawa *et al.*, 2007; Nunoura *et al.*, 2008; Sievert *et al.*, 2008)]. Die Abwesenheit von *sat*-, *apr*- und *dsr*-homologen Genen weist zudem darauf hin, dass das *P. pantotrophus*-SoxXAYZB(CD)$_2$ System in diesen SOP auch essentiell für die Oxidation anderer anorganischer Schwefelverbindungen ist. Die Existenz des *sox* Genclusters in vielen heterotrophen Spezies, deren schwefelmetabolisierende Fähigkeiten noch nicht untersucht worden sind (z. B. *Aurantimonas*, *Polaromonas*; Publikation 4), zeigt, dass die Möglichkeit zur chemolithoheterotrophen Lebensweise (Energiegewinnung via Sox System) nicht nur auf die bisher bekannten Vertreter aus der *Roseobacter* Linie beschränkt ist (Buchan *et al.*, 2005; Moran *et al.*, 2003; Moran *et al.*, 2007), sondern weiter verbreitet ist als bisher vermutet wurde.

Die Ergebnisse dieser Arbeit lieferten auch einen ersten Hinweis darauf, dass das Sox Enzymsystem generell in die Thiosulfatoxidation der [S^0] Intermediat-bildenden SOP involviert ist (*Chlorobiaceae*, *Chromatiaceae* und *Ectothiorhodospiraceae* sowie einige chemolithoautotrophe *Beta*- und *Gammaproteobacteria*) (Publikation 4). Die negative Korrelation zwischen der Präsenz der *dsrAB*/*dsrKMJOP* und *soxCD* Gene in den Genomen (Publikation 4) deutet zudem darauf hin, dass das postulierte „verzweigte“ Oxidationsmodell (Grimm *et al.*, 2008; Hensen *et al.*, 2006) für diejenigen [S^0] Intermediat-bildenden SOP Spezies Gültigkeit besitzt, die über die revers-arbeitenden Enzyme des dissimilatorischen Sulfatreduktionsweges (oder zumindest die reverse DsrAB) verfügen (Publikation 4). Die funktionelle Kopplung des Sox an das reverse Sulfatreduktionsenzymsystem zur cyto- statt periplasmatischen Sulfanschwefeloxidation bietet möglicherweise energetische Vorteile, da die Dsr und Apr die Einschleusung der freiwerdenden Elektronen auf Redoxpotentialniveau von Chinon statt Cytochrom c erlauben; dies könnte insbesondere für obligat chemolithoautotrophe SOP von Bedeutung sein. Zusätzlich könnte die Nutzung des Sox Systems den Vorteil eines schnellen Thiosulfat-Umsatzes bei gleichzeitiger [S^0] Intermediat-Bildung als Reserve-Energiequelle bringen (Publikation 4). Aufgrund der eingeschränkten Verbreitung des reversen Sulfatreduktionssystems in strikt aeroben chemotrophen SOP (Publikation 2 und 4) könnte der *P. pantotrophus*-homologe Oxidationsweg wie in *T. crunogena* (Scott *et al.*, 2006) auch von vielen weiteren [S^0] Intermediat-bildenden, obligat autotrophen SOP (wie

z. B. *Thioalkalivibrio* spp. (Sorokin & Kuenen, 2005) und *Thiobacter subterraneus* (Hirayama *et al.*, 2005), siehe Tabelle 2, Anhang) zur Oxidation von anorganischen Schwefelverbindungen genutzt werden und damit in Chemotrophen generell weiter verbreitet sein als der „verzweigte" Oxidationsweg. Die in *T. crunogena* beobachtete [S^0] Intermediat-Bildung während der Thiosulfatoxidation ist vermutlich das Resultat differentieller *soxXAYZ*, *soxB* und *soxCD* Genexpression (Scott *et al.*, 2006).

Einige photo- und chemotrophen SOP verfügen offensichtlich auch über alternative Enzym(system)e zur Thiosulfatoxidation, die in Adaptation an die physikochemischen Bedingungen genutzt werden (Brüser *et al.*, 2000a; Hensen *et al.*, 2006; Kelly *et al.*, 1997; Kelly, 1999). So konnte die Existenz von *sox* Genen in acidophilen und halophilen Chemotrophen nachgewiesen werden (Publikation 4), für die eine Thiosulfatoxidation über den „S_4I Weg" postuliert wurde (Brüser *et al.*, 2000a; Kelly *et al.*, 1997; Rohwerder & Sand, 2003; Rohwerder & Sand, 2007).

Phylogenie der SoxB. Die topologischen Diskrepanzen zwischen den SoxB- und 16S rRNA-basierenden SOP Stammbäumen weisen auf mehrere, unabhängige laterale *soxB* Transfervorgänge sowohl innerhalb als auch zwischen den verschiedenen SOP Linien hin (Publikation 4) [bestätigt durch neue Genomdaten (Campbell *et al.*, 2006; Miller *et al.*, 2007; Nakagawa *et al.*, 2007; Nunoura *et al.*, 2008; Sievert *et al.*, 2008)]. Die Ähnlichkeit der *soxB* Sequenzcharakteristika zwischen den xenologen *Spirochaeta* sp., *Thiovirga sulfuroxydans* (Dubinina *et al.*, 2004; Friedrich *et al.*, 2002; Ito *et al.*, 2005) und deren potentiellen Donatoren (*Sulfitobacter* bzw. *Ralstonia* spp.) spricht für rezente LGTs. Die Thiosulfatoxidationsfähigkeit via Sox Enzymsystem ist vermutlich von den meisten *soxB*-xenologen SOP (*Aquificae*, *Thermus* spp., *Anaeromyxobacter* spp., *Acetobacteraceae*, *Chlorobiaceae*, *Chromatiaceae* und *Ectothiorhodospiraceae*) neu erworben worden; für eine simultane Aufnahme des gesamten *sox* Genclusters über einen einzelnen LGT-Vorgang sprechen ihre SoxB-übereinstimmenden xenologen Positionen in den SoxAYZCD Stammbäumen (Publikation 4). Die Akquisition eines einzelnen *soxB* Gens sowie dessen Verbleib im Genom hätte keinen Selektionsvorteil bedeutet, da das SoxB Protein nur in Assoziation mit den übrigen Komponenten des Sox Systems als Sulfat-Thiol-Hydrolase aktiv ist, und eine weitere enzymatische Funktion bisher nicht bekannt ist (Epel *et al.*, 2005; Friedrich *et al.*, 2005). Die gleichzeitige Präsenz in einem Habitat als Voraussetzung für den Genaustausch ist für viele der Akzeptor- und Donator-Linien/Spezies nachgewiesen worden (z. B. *Ectothiorhodospira* spp. und deren potentielle Donatoren *Halothiobacillus* spp. (Imhoff, 1999; Kelly & Wood, 2000)). Nach Transfer und erfolgreicher Integration des neu erworbenen, „chemotrophen"

soxXAYZBCD Genlocus in den Vorläufern der anoxygenen phototrophen *Ectothiorhodospiraceae*, *Chromatiaceae* und *Chlorobiaceae* ist das periplasmatische Sox System durch funktionelle Kopplung an das bereits präsente reverse Sulfatreduktionssystem vermutlich um die Schwefeldehydrogenase-Komponente (SoxCD) reduziert worden (mit dem Resultat der Entstehung des „verzweigten" Thiosulfatoxidationsweges und Akkumulation von [S^0] als obligates Intermediat in diesen SOP); alternativ könnte dieser Prozess auch vor den Transfervorgängen in den jeweiligen chemotrophen Donator-Linien abgelaufen sein. Nach Diversifikation der Purpur-Schwefelbakterien und Grünen Schwefelbakterien sind die *sox* Genloci aus einigen Vertretern wie den metabolisch spezialisierten Gattungen *Thiococcus* und *Prosthecochloris* wieder verlorengegangen (Publikation 4).

2.3 Evolution des dissimilatorischen Schwefelkreislaufs

2.3.1 Evolutionäres Szenario zur Entstehung und Entwicklung des dissimilatorischen Sulfatreduktionsweges

Die Präsenz und metabolische Aktivität von SRP wurde basierend auf Daten zur massenabhängigen ^{34}S und ^{32}S Schwefel-Isotopenfraktionierung (SIF) auf einen Zeitpunkt von vor 3.46 Milliarden Jahren (3.46 Ga BP) datiert (Shen *et al.*, 2001; Shen & Buick, 2004). Der weltweite Erhalt von $\Delta^{33}S$ Anomalien (massenunabhängige ^{33}S Schwefel-Isotopenfraktionierung, MIF, verursacht durch Photolyse von vulkanischem SO_2 und H_2S Gasen in S_8^0 und SO_4^{2-} Aerosole mit positiver $\Delta^{33}S$ bzw. negativer $\Delta^{33}S$ Signatur) in sedimentären Sulfiden und Sulfaten, die älter als 2.5 Ga sind, verdeutlicht aber, dass der Sauerstoffgehalt der Atmosphäre während des Archaikums (4.0-2.4 Ga BP) sehr niedrig war ($pO_2 < 10^{-5}$ PAL), so dass der ozeanische „Schwefelkreislauf" in diesem Erdzeitalter von den atmosphärischen Prozessen dominiert wurde, da das photolytisch gebildete Sulfat den einzig signifikanten abiotischen Sulfateintrag darstellte (Farquhar *et al.*, 2000; Farquhar *et al.*, 2002; Farquhar & Wing, 2003; Farquhar *et al.*, 2007; Mojzsis *et al.*, 2003; Ono *et al.*, 2003; Pavlov & Kasting, 2002; Strauss, 2003). Die Mehrheit der Archaikum-datierten SIF-Daten (Canfield *et al.*, 2000; Canfield, 2005; Strauss, 2003) weist ebenfalls auf die Abwesenheit eines aktiven globalen Schwefelkreislaufes in den Ozeanen hin (Sulfatgehalt unter 200 µM) (Canfield & Raiswell, 1999; Canfield *et al.*, 2000; Canfield, 2005; Habicht *et al.*, 2002). Auf der Basis neuerer Untersuchungen wurden die $+\Delta^{33}S$ Anomalien der $-\delta^{34}S$ Sulfide aus den 3.46 Ga-alten Baritablagerungen (Shen *et al.*, 2001; Shen & Buick, 2004) von Philippot et al. als Nachweis für die archaische Aktivität von disproportionierenden Bakterien ausgelegt (den $+\Delta^{33}S$

Elementarschwefel zu -δ^{34}S Sulfid und +δ^{34}S Sulfat umsetzend) (Philippot *et al.*, 2007). Eine quantitativ bedeutende metabolische Aktivität von SRP hätte Philippot et al. zufolge zu –δ^{34}S Sulfiden mit -Δ^{33}S Anomalien führen müssen (Philippot *et al.*, 2007; Philippot *et al.*, 2008). Eine alternative Erklärung für die Entstehung der +Δ^{33}S/–δ^{34}S Sulfide könnte aber auch sein, dass +Δ^{33}S Elementarschwefel zunächst durch frühe anoxygene phototrophe schwefeloxidierende Bakterien umgesetzt wurde (ohne SIF (Canfield *et al.*, 1998; Fry *et al.*, 1986; Habicht *et al.*, 1998; Habicht & Canfield, 2001)), so dass an vereinzelten Standorten und in räumlich-begrenzten Zonen größere Mengen an +Δ^{33}S Sulfat/Sulfit entstanden, die dann von Sulfat-/Sulfitreduzierern zu den MIF und SIF Signatur-tragenden Sulfiden (Philippot *et al.*, 2007; Philippot *et al.*, 2008; Shen *et al.*, 2001; Shen & Buick, 2004) umgesetzt wurden (Publikation 1). Tatsächlich ist die Existenz solcher von anoxygenen phototrophen Bakterien dominierten, photosynthetischen mikrobiellen Matten für das Archaikum nachgewiesen worden (auf 3.4 Ga BP datiert) (Tice & Lowe, 2004). Aufgrund der niedrigen ozeanischen Sulfatkonzentrationen im Archaikum können die SRP nur in Koexistenz zu den sulfit-/ sulfatproduzierenden SOP evolviert sein (Publikation 1).

In Übereinstimmung mit dem letzten Szenario weisen die Dsr und Apr Phylogenien auf einen Ursprung der Proteine als oxidativ-arbeitende Enzyme und eine sukzessive Evolution des dissimilatorischen Sulfatreduktionssystems in anoxygenen phototrophen schwefeloxidierenden Bakterien hin (Publikation 1). Die Entwicklung der reversen DsrAB (möglicherweise aus einem monomeren assimilatorischen Enzym von Methanogenen (Dahl *et al.*, 1993; Dhillon *et al.*, 2005)) einschließlich des funktionell-assoziierten DsrMKJOP Redoxkomplexes (möglicherweise aus Hdr-Untereinheiten der Methanogenen (Dahl *et al.*, 2005; Hedderich *et al.*, 2005; Mander *et al.*, 2002; Pereira, 2008; Pires *et al.*, 2006)) könnte ferrotrophen anoxygenen Phototrophe (Ehrenreich & Widdel, 1994; Heising *et al.*, 1999; Straub *et al.*, 1999; Widdel *et al.*, 1993) ermöglicht haben, den in küstennahen Ozeanbereichen abgelagerten, atmosphärischen Elementarschwefel (oder auch durch Hydrothermalquellen eingetragenes Sulfid) als photosynthetischen Elektronendonator zu nutzen (Oxidation bis zu Sulfit). Die archaischen mikrobiellen Matten („Stromatolite“ (Awramik, 1992; Grassineau *et al.*, 2001; Nisbet & Fowler, 1999; Nisbet & Sleep, 2001; Nisbet & Fowler, 2003)) bildeten möglicherweise wie ihre modernen Formen (Molin & Tolker-Nielsen, 2003; Sorensen *et al.*, 2005) „hot spots“ für die metabolische Diversifikation der mikrobiellen Gemeinschaft. Durch lateralen Transfer der *dsr* Gene zu Nicht-Phototrophen könnten zunächst sulfitrespirierende Vorläuferorganismen der rezenten SRP Linien entstanden sein, die Sulfit durch adaptive Umkehr des oxidativen Dsr Systems zu respiratorischen Zwecken genutzt haben (Publikation

1) (siehe auch Kapitel 2.1.1). Eine oxidativ-operierende APS-Reduktase könnte dann von den anoxygenen phototrophen schwefeloxidierenden Bakterien entwickelt worden sein, um die cytoplasmatische Akkumulation des toxischen DsrAB-Endproduktes, Sulfit, zu verringern bzw. zu verhindern. Das Enzym hatte vermutlich zunächst eine ausschließlich detoxifizierende Funktion, die durch die (möglicherweise simultane) Entwicklung einer ATP-Sulfurylase (Boucher *et al.*, 2003; Sperling *et al.*, 2001) zusätzlich Energiegewinn über Substratstufenphosphorylierung ermöglichte (Publikation 1). Durch LGT der *aprBA* zu den Sulfitreduzierern könnten schließlich die Vorläufer der polyphyletischen SRP Linien entstanden sein. Erst nach Diversifikation in den oxidativen und die zwei reduktiven Enzymtypen (analog zur Evolution der DsrAB) erfolgte vermutlich die Kopplung der cytoplasmatischen Sulfitoxidation/APS-Reduktion an die Elektronentransportkette durch (1) die sukzessive Entwicklung der QmoAB-HdrCB/QmoABC Redoxkomplexe in den sulfitreduzierenden Vorläufern der bakteriellen SRP Linien und (2) die Entwicklung eines AprM-gekoppelten Elektronentransfersystems in den Vorläufern der schwefeloxidierenden, anoxygenen phototrophen Proteobakterien. Eine dem ursprünglichen, nicht an die Elektronentransportkette gekoppelten Enzym ähnliche APS-Reduktase könnte noch in den crenarchaeellen Sulfatreduzierern wie *C. maquilingensis* vorhanden sein (Publikation 1 und 3). Die physiologische Gruppe der SRP gewann vermutlich erst durch die Entwicklung der oxygenen Photosynthese (2.7 Ga BP) (Brocks *et al.*, 2003; Kopp *et al.*, 2005) und die beginnende Oxygenierung der Erdatmosphäre und Ozeanoberfläche zu Anfang des Proterozoikums (ab 2.45 Ga BP; „great oxygenation event“) (Catling & Claire, 2005; Holland, 2002; Johnson *et al.*, 2008; Kaufman *et al.*, 2007; Scott *et al.*, 2008) an ökologischer Bedeutung. Die steigenden ozeanischen Sulfatkonzentrationen (Anbar & Knoll, 2002; Canfield, 2005; Gellatly & Lyons, 2005; Habicht *et al.*, 2002; Kah *et al.*, 2004) hatten die Unabhängigkeit der SRP von der Versorgung mit SOP-produziertem Elektronenakzeptoren und Radiation der SRP Linien zur Folge. Die zunehmende SRP-Produktivität führte zur Beendigung der BIFs („banded iron formations“) und Ausbildung des sogenannten „Canfield-Ozeans“ mit global anoxischen, sulfidhaltigen Tiefenwassern im Verlauf des Proterozoikums (Anbar & Knoll, 2002; Anbar & Roiixel, 2007; Arnold *et al.*, 2004; Johnson *et al.*, 2008; Poulton *et al.*, 2004; Scott *et al.*, 2008; Shen *et al.*, 2003). Die Akkumulation von Sulfid könnte im Gegenzug die Unabhängigkeit der anoxygenen phototrophen SOP von den lokal-begrenzten, abiogenen Schwefelquellen gefördert haben mit der Folge der ubiquitären Präsenz dieser Gruppe als Primärproduzenten im Bakterioplankton während dieses Erdzeitalters (Brocks *et al.*, 2005; Canfield & Raiswell, 1999). Die im Neoproterozoikum (ab 1.05 Ga BP) ansteigenden

Sauerstoffkonzentrationen in Atmosphäre und Ozeanen (> 10 % PAL) (Anbar & Knoll, 2002; Canfield, 1998; Canfield *et al.*, 2000; Canfield, 2005; Canfield *et al.*, 2007; Kah *et al.*, 2004; Scott *et al.*, 2008) könnten die anoxygenen phototrophen SOP zu Adaptationen ihrer Schwefeloxidationssysteme gezwungen haben. Im Verlauf dieser Entwicklungsprozesse wurden die an anoxische Umweltbedingungen angepassten, FeS-Zentren-enthaltenden Proteine (wie die reverse AprBA) durch Redoxpotential-unempfindlichere, isofunktionelle Enzyme (SAOR) ausgetauscht bzw. neue, alternative metabolische Strategien (wie das Sox System) entwickelt (Dupont *et al.*, 2006; Imlay, 2006). Der Rückzug in SRP-dominierte anoxische und sulfidreiche Habitate könnte die beobachteten LGTs zwischen SRP und SOP begünstigt haben (Publikation 2).

2.3.2 Evolutionäres Szenario zur Entstehung und Entwicklung des Sox Weges

Für die Erdzeitalter Archaikum und Mesoproterozoikum kann eine quantitativ bedeutende (a)biogene Bildung von anorganischen Schwefelverbindungen wie Thiosulfat (Falkowski, 1997; Schippers & Jørgensen, 2001; Schippers & Jørgensen, 2002) aufgrund der globalen anoxischen bzw. euxinischen Bedingungen in den Ozeanen (Anbar & Knoll, 2002; Anbar & Roiixel, 2007; Arnold *et al.*, 2004; Canfield, 2005; Poulton *et al.*, 2004; Scott *et al.*, 2008; Shen *et al.*, 2003) ausgeschlossen werden. Die erst ab dem Neoproterozoikum auftretenden hohen SIF-Werte, die die metabolische Aktivität von schwefeldisproportionierenden Bakterien geochemisch belegen (Canfield & Teske, 1996; Canfield *et al.*, 1998; Canfield, 2005; Canfield *et al.*, 2007), spiegeln diese evolutionär-späte Bioverfügbarkeit wider. Der Ursprung und die Diversifikation von nicht-photosynthetischen, (fakultativ) aeroben SOP einschließlich der globalen Etablierung der oxischen Schwefeltransformationsprozesse wird auf 0.75-0.62 Ga BP datiert (Canfield & Teske, 1996; Canfield, 1998; Canfield *et al.*, 2000; Canfield, 2005). Im Verlauf dieser Entwicklung könnte der Sox System-katalysierte Oxidationsweg in den o. g. Organismen zur Nutzung von Thiosulfat entstanden sein. Die Phylogenie der SoxB Komponente (einschließlich weiterer Sox Proteine) weist dabei auf einen möglichen Ursprung in aeroben, chemotrophen, (epsilon-)proteobakteriellen SOP hin (Publikation 4). Bis auf wenige, fakultativ anaerobe chemolithoautotrophe Spezies der *Beta-* und *Gammaproteobacteria* (z. B. *Thiobacillus* spp., *Thiothrix* spp., Publikation 2) wurde in den meisten chemotrophen SOP das reverse Sulfatreduktionssystem durch das Sox System ersetzt. In Adaptation an die oxischen Umweltbedingungen in ihren Habitaten könnten die anoxygenen phototrophen SOP die metabolische Fähigkeit zur Thiosulfatoxidation erst durch

LGT des *sox* Gencluster von chemotrophen SOP erworben haben; die anschließende Kopplung des SoxCD-defizienten Sox Systems an das reverse Sulfatreduktionssystem hätte eine effiziente funktionelle Integration der neuen Enzyme in das Protein-Netzwerk bedeutet (Hao & Golding, 2006; Lercher & Pal, 2008; Pal *et al.*, 2005) (Publikation 4).

2.4 Bestimmung der SRP und SOP Diversität über funktionelle Genanalyse mit aprA als molekularem Marker Gen

Im Rahmen dieser Arbeit wurde ein universelles *aprA*-spezifisches Primerpaar konstruiert, das die simultane Bestimmung der SRP und SOP Diversität in Umweltproben über die DGGE-Analytik ermöglichte (Publikation 5). Das Screening phylogenetisch divergenter SRP und SOP Referenzstämme in Einzeltemplate-PCRs, die Multitemplate-PCRs mit definierten Template-Mischungsverhältnissen sowie die vergleichenden Analysen diverser Umweltproben verdeutlichten das vergrößerte Spezies-Amplifikationsspektrum und die höhere Phylotyp-Detektionssensitivität des neuen Primerpaares im direkten Vergleich zum publizierten Primerpaar von Deplancke et al. (Deplancke *et al.*, 2000). Ein neuer Sequenzabgleich mit dem *aprBA* Datensatz (einschließlich aller zurzeit verfügbaren Genomdaten, z. B. *Cdt.* D. audaxviator, *C*. *maquilingensis*) bestätigt die Komplementarität der neuen Primer zu den *aprA* Genen von SRP und SOP („universelle“ Primer). Die unterschiedlichen Resultate der mikrobiellen Matten der Toyoha Mine (Publikation 5) weisen allerdings darauf hin, dass die Nutzung von mehr als einem *aprA*-spezifischen Primerpaar ein vollständigeres Bild der Diversität eines Habitates liefern kann (aufgrund der generellen methodischen Limitierungen der PCR und DGGE (Muyzer *et al.*, 1995; Polz & Cavanaugh, 1998; Suzuki & Giovannoni, 1996; von Wintzingerode *et al.*, 1997)).

Das im Rahmen dieser Arbeit neu konstruierte *aprA*-spezifische Primerpaar wurde bereits erfolgreich zur SRP und SOP Diversitätsbestimmung in marinen Invertebraten eingesetzt (Blazejak *et al.*, 2006; Duperron *et al.*, 2007; Duperron *et al.*, 2008; Musat *et al.*, 2007).

2.4.1 Vergleich zwischen *aprA*, 16S rRNA und *dsrAB* Genanalyse

Die Beurteilung der Vor- und Nachteile der *aprA*, 16S rRNA und *dsrAB* Genanalysen zur Untersuchung der SRP und SOP Diversität war durch den direkten Vergleich der Ergebnisse von (1) Gewebematerial aus Echinoiden (*aprA*/16S rRNA Vergleich) und (2) mikrobiellen Matten aus der Toyoha Mine (*aprA*/*dsrAB* Vergleich) möglich (Publikation 5 und (Gomes da Silva *et al.*, 2006; Nakagawa *et al.*, 2002)). In *Echinocardium cordatum* bilden die mikrobiellen Symbionten im Verdauungstrakt periphere Biofilme um die Detrituspartikel

(Thorsen, 1999; Thorsen *et al.*, 2003). Die über 16S rRNA Sequenzen postulierte Präsenz von „*Desulfobacterium catecholicum*"-, *Desulfobacula toluolica*- und *Desulfotomaculum acetoxidans*-verwandten Sulfatreduzierern (Gomes da Silva *et al.*, 2006) konnte durch die *aprA* Genanalyse nicht bestätigt werden. [Anmerkung: Die *aprA* Amplifikation der entspechenden Referenzstämme mit dem neuen Primerpaar wurde aber experimentell verifiziert.] Die detektierten Organismen können demnach keine SRP gewesen sein, da die dissimilatorische APS-Reduktase essentiell für den Sulfatreduktionsprozess ist (Publikation 5). Im Zusammenhang mit der zunehmenden Anzahl von SRP-verwandten nicht-sulfatreduzierenden Stämmen (siehe Kapitel 1.1.1) verdeutlichen diese Resultate, dass 16S rRNA Gen-basierende Methoden keine eindeutigen Ergebnisse für die Analyse von SRP Gemeinschaften liefern können (siehe Kapitel 1.7). Die Problematik der SRP Diversitätsüberschätzung in 16S rRNA Gen-basierenden Studien (selbst bei der Nutzung von gruppenspezifischen Primern und Sonden) ist auch aus anderen Publikationen bekannt (Hristova *et al.*, 2000; Imachi *et al.*, 2006; Joulian *et al.*, 2001; Lücker *et al.*, 2007; Stahl *et al.*, 2007; Stubner, 2002). Im Gegensatz dazu ermöglichen die *aprA* Gene eine direkte Verknüpfung zwischen phylogenetischer Position und ökophysiologischer Funktion eines Umweltsequenz-detektierten Organismus und sind deshalb trotz der nachgewiesenen LGT-Vorgänge als molekulare Marker für molekularökologische Studien geeignet (Publikation 5).

Die Resultate der geothermalen mikrobiellen Matten zeigten, dass die *aprA* gegenüber der *dsrAB* Genanalyse (Nakagawa *et al.*, 2002) ein exakteres Bild der präsenten SRP Gemeinschaft lieferte: Die *aprA* Genanalyse wies auf die Anwesenheit von *Thermodesulfobacterium*-verwandten SRP hin, die über die *dsrAB* Gene nicht detektiert wurden (möglicherweise als Folge der SRP Linien/Gattungs-Spezifität der *dsrAB*-spezifischen Primer (Loy *et al.*, 2004; Wagner *et al.*, 1998; Zverlov *et al.*, 2005)), während die DsrAB-postulierte Existenz von zwei neuen Gram-positiven SRP Linien nicht verifiziert werden konnte (Publikation 5). Da die „SRP-spezifischen" Primer auch komplementär zu den *dsrAB* Genen von Sulfitreduzierern (z. B. *Desulfitobacterium* spp.) und Nicht-Sulfitreduzierern (z. B. *Pelotomaculum thermopropionicum*) sind, ist in der *dsrAB* Genanalyse keine Diskriminierung zwischen diesen Organismengruppen möglich. Im Hinblick auf die steigende Anzahl an neu beschriebenen sulfit- und nicht-sulfitreduzierenden (aber *dsr*-besitzenden) Spezies, die sich vermutlich aus sulfatreduzierenden Spezies in Adaptation an sulfatarme, methanogene Standorte entwickelt haben (*dsr* Gene stellen „genetische Relikte" des früheren Metabolismus dar), ist die zweifelfreie Identifikation von SRP in Umweltproben demnach nur über *apr* Gen-basierende Analysen gegeben (Publikation 5). Vermutlich sind viele der nur anhand von DsrAB Umwelt-

sequenzen postulierten SRP Stämme aus diversen Studien (Bagwell *et al.*, 2006; Bahr *et al.*, 2005; Baker *et al.*, 2003; Castro *et al.*, 2002; Chang *et al.*, 2001; Dhillon *et al.*, 2003; Fishbain *et al.*, 2003; Kaneko *et al.*, 2007; Karr *et al.*, 2005; Kjeldsen *et al.*, 2007a; Kjeldsen *et al.*, 2007b; Kondo & Butani, 2007; Leloup *et al.*, 2006; Leloup *et al.*, 2007; Loy *et al.*, 2004; Nakagawa *et al.*, 2002; Nakagawa *et al.*, 2004; Nercessian *et al.*, 2005a; Schmalenberger *et al.*, 2007; Thomsen *et al.*, 2001) keine Sulfatreduzierer, sondern noch uncharakterisierte Sulfit- bzw. Organosulfonatreduzierer oder sekundär-entstandene, syntrophe Fermentierer.

Im Gegensatz zu den *dsrAB*-basierenden Analysen ermöglichte die *aprA* Genanalyse die simultane Bestimmung der Diversität von SRP und SOP (z. B. in mikrobiellen Matten des „Hydrate Ridge“ (Publikation 5), siehe auch (Blazejak *et al.*, 2006) und Publikation 6). Aufgrund der begrenzten Verbreitung der *apr* Gene in SOP erlaubt die *apr* Genanalyse allerdings nur die selektive Detektion bestimmter schwefeloxidierender Organismengruppen (Publikation 2), d. h. die tatsächliche phylogenetische Diversität und Komplexität der Mikroorganismen, die in die Schwefeloxidationsprozesse eines Habitates involviert sind, kann über die *aprA* Genanalyse nicht vollständig erfasst werden. Die phylogenetische Zuordnung einzelner SOP-Typ Umweltsequenzen wird zudem durch die LGT-Vorgänge zwischen SOP/SRP und SOP sowie durch die Existenz von mehr als einem *apr* Genlocus in einigen Spezies der *Beta*- und *Gammaproteobacteria* erschwert (Publikation 2); letzteres verhindert auch eine exakte Quantifizierung der *apr* Gen-detektierten SOP (Publikation 5). Die Ergebnisse dieser Arbeit verdeutlichen, dass eine *soxB*-spezifische Genanalyse zur SOP Diversitätsbestimmung geeigneter ist, da chemotrophe Schwefeloxidierer sowie thiosulfatoxidierende Schwefel-Purpurbakterien und Grüne Schwefelbakterien detektiert werden können (Publikationen 2 und 4). Aufgrund der unterschiedlichen Schwefeloxidationswege in SOP ist eine vollständige Erfassung der SOP Komplexität über die Analyse eines einzelnen funktionellen Gens aber generell nicht möglich.

2.4.2 Phylogenetische Diversität der SRP und SOP in Umweltproben aus der Region des vulkanischen Inselbogens der Kleinen Antillen, Karibisches Meer

Die 16S rRNA Genanalysen der Karibik-Umweltproben (CARIBFLUX, 2003) aus Wassersäule und Tiefsee-Sedimenten (Probenentnahme-Standorte siehe Abbildung 16) zeigte eine für subtropische, photische Wasserzonen bzw. nicht-hydrothermale, oxische Tiefsee-Sedimente typische mikrobielle Komplexität und Diversität; die 16S rRNA-basierende Genanalyse ermöglichte keine Rückschlüsse auf die mikrobielle Gemeinschaft des Schwefel-

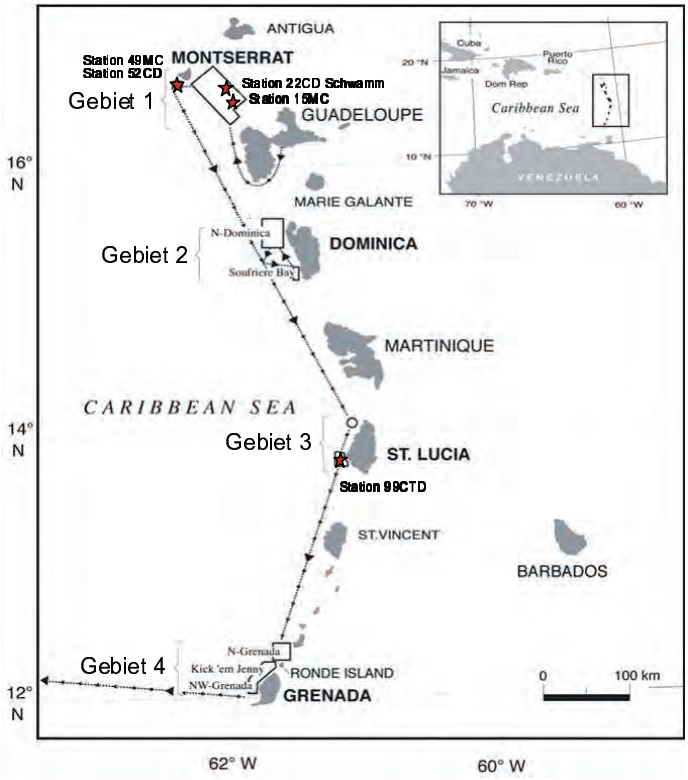

Abbildung 16. Fahrtroute und Arbeitsgebiete der Forschungsfahrt RV Sonne SO-154 (CARIBFLUX Projekt) im Karibischen Meer (die Probenentnahme-Standorte sind durch rote Sterne markiert (MC, Multicorer; CD, „chain bag dredge"; CTD, Kranzwasserschöpfer).

kreislaufs an diesen Standorten (Publikation 5). Die *aprA* Genanalysen zeigten, dass die thiotrophen mikrobiellen Gemeinschaften der photischen Wasserzone und oxischen Sedimentschichten von chemolithoheterotrophen, schwefeloxidierenden Alphaproteobakterien dominiert waren (Publikation 5). Die Präsenz ähnlicher Apr Umweltsequenzen in den Metagenom-Datensätzen der „Sargasso See" (Nordatlantik), „Station ALOHA" (Nordpazifik) und „Global Ocean Sampling" (GOS) (DeLong *et al.*, 2006; Rusch *et al.*, 2007; Venter *et al.*, 2004; Yooseph *et al.*, 2007) verdeutlicht die globale Verbreitung dieser *apr* Gen-besitzenden potentiellen SOP Linien (siehe Abbildungen 13 und 15). Tatsächlich sind viele Vertreter der alphaproteobakteriellen *Roseobacter* Linie zur lithoheterotrophen Lebensweise mit anorganischen Schwefelverbindungen wie Sulfit, die durch den zellinternen Abbau von DMSP und Organosulfonaten entstehen, befähigt (Buchan *et al.*, 2005; Gonzalez *et al.*, 2003; Moran *et al.*, 2003; Sorokin, 1995). Thiosulfatoxidierende, chemolithoheterotrophe Stämme dieser Linie sind auch in Tiefsee-Sedimenten anderer nicht-hydrothermaler Standorte abundant (Sorokin, 2003; Teske *et al.*, 2000; Tuttle & Jannasch, 1976). Die *aprA*-detektierten, potentiellen SOP könnten Vertreter der *Roseobacter* Gruppe gewesen sein; *apr* Gene wurden aber bisher noch nicht in Spezies dieser Linie gefunden (einschließlich der in dieser Arbeit isolierten Stämme; Publikation 5). Eine mögliche alternative Funktion der „dissimilatorischen" APS-Reduktase im Metabolismus dieser Organismen wurde bereits am Beispiel von *Cdt.* Pelagibacter ubique erläutert (Kapitel 2.1.2).

Die mikrobielle Diversität des Schwefelkreislaufes in den untersuchten Mangankrusten-oberflächenschichten (Abbildung 17) konnte ebenfalls nur über die Analyse des *aprA* Gens erfasst werden. In Übereinstimmung mit den geochemischen Daten, die auf subrezente (vermutlich hydrothermale) externe Einträge anorganischer Schwefelverbindungen hinwiesen

(CARIBFLUX, 2003), wurde eine hohe phylogenetische Diversität und Komplexität an potentiellen SOP festgestellt. Basierend auf den detektierten AprA Umweltsequenzen (fünf Phylotypen) umfasste die thiotrophe mikrobielle Gemeinschaft (1) chemolithoautotrophe, schwefeloxidierende Stämme der *Gamma*- und *Betaproteobacteria* (nah verwandt zu kultivierten SOP aus Hydrothermalsystemen (Kuever *et al.*, 2002; Nercessian *et al.*, 2005b)), (2) chemolithoheterotrophe Schwefeloxidierer der *Alphaproteobacteria* (verwandt zu den Phylotypen der Tiefsee-Sedimente) sowie (3) potentielle SOP einer neuen, phylogenetisch noch nicht zugeordneten Linie (Publikation 5). Im Hinblick auf die Abwesenheit von *apr* Genen z. B. in den abundanten Vertretern der *Epsilonproteobacteria* und *Thiomicrospira* (Schwefeloxidation über das Sox Enzymsystem (siehe Kapitel 2.1.2 und 2.2)) ist zu vermuten, dass nur ein Teil des SOP-Spektrums der Mangankrusten erfasst wurde (Publikation 5).

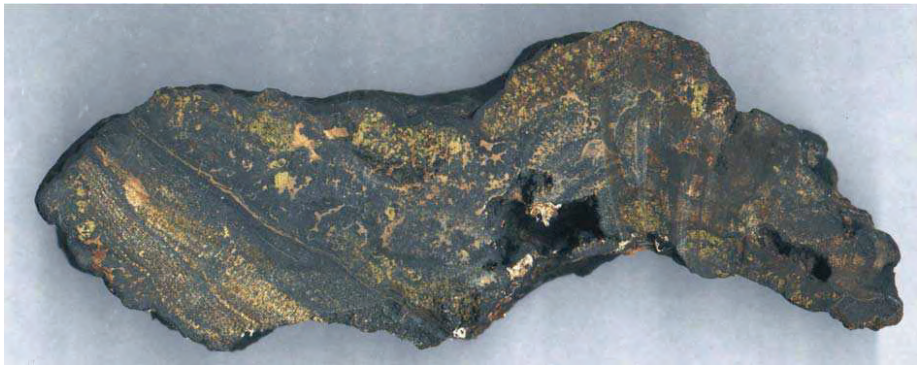

Abbildung 17. Querschnitt durch die massiven Mangan-Eisen-Präzipitate (Mangankrusten) von Station 52CD, Montserrat Ridge, Karibisches Meer.

2.4.3 Phylogenetische Diversität der SRP und SOP im karibischen Tiefsee-Schwamm *Polymastia* cf. *corticata*

In Übereinstimmung mit den Resultaten von marinen Flachwasser-Schwämmen (z. B. (Hentschel *et al.*, 2006; Hill *et al.*, 2006; Taylor *et al.*, 2007) war auch die mikrobielle Gemeinschaft des karibischen Tiefsee-Schwammes *Polymastia* cf. *corticata* (Boury-Esnault, 2002; Morrow & Boury-Esnault, 2000) (Station 22CD, Abbildung 16) phylogenetisch komplexer als das planktonische Konsortium der umgebenden Wassersäule (Publikation 6): Von den insgesamt 38 identifizierten 16S rRNA Phylotypen gehörten 53 % zu den monophyletischen, *Porifera*-spezifischen Sequenzclustern (klassifiziert als „Schwamm-Assoziate“ (Hentschel *et al.*, 2002; Holmes & Blanch, 2007; Lee *et al.*, 2003; Taylor *et al.*, 2004; Thiel *et al.*, 2007b)), während 26 % bzw. 21 % der detektierten Phylotypen *Polymastia* cf. *corticata* „Spezialisten“ bzw. Schwamm-unspezifische, Bakterioplankton-verwandte „Generalisten“ repräsentierten. Letztere könnten basierend auf den 16S rRNA-kongruenten AmoA

Sequenzdaten ammonifizierende *Nitrosospira* spp. gewesen sein (Freitag & Prosser, 2004; Kowalchuk & Stephen, 2001; Lam *et al.*, 2004; O`Mullan & Ward, 2005) (Publikation 6). Im Kontext mit anderen 16S rRNA-basierenden Studien (Li *et al.*, 2007; Ridley *et al.*, 2005; Taylor *et al.*, 2004; Taylor *et al.*, 2007; Thiel *et al.*, 2007a; Thiel *et al.*, 2007b; Webster *et al.*, 2004; Weisz *et al.*, 2007) weisen die Daten darauf hin, dass die phylogenetische Zusammensetzung und Komplexität der Schwamm-assoziierten mikrobiellen Gemeinschaft nicht mit dem geographischen Standort und Habitat des Schwammes korreliert, sondern abhängig von der Schwamm Spezies und deren internen Faktoren ist; sie widersprechen der ursprünglichen Hypothese einer generell einheitlichen mikrobiellen Signatur in marinen Schwämmen (Hentschel *et al.*, 2002).

Abbildung 18. Links: Tiefsee-Schwamm *Polymastia* cf. *corticata* (1127 m) aus Kahouanne Basin, Karibisches Meer. **Rechts:** Querschnitt durch Schwammgewebe (Kompartimentierung in die morphologisch abgrenzbaren Sektionen Papillen, Kortex und Choanosom ist angezeigt).

Unterschiedliche mikrobielle Konsortien waren mit den verschiedenen Gewebesektionen des Tiefsee-Schwammes (Papillen, äußerer und innerer Kortex sowie Choanosom, siehe Abbildung 18) assoziiert (unterschiedliche „Mikrohabitate“). Die räumliche Verteilung einer Spezies innerhalb des *P.* cf. *corticata* Schwammkörpers korrelierte mit der phylogenetischen Zugehörigkeit, der Klassifikation als Schwamm-Assoziat, Spezialist oder Generalist sowie der damit im Zusammenhang stehenden ökologischen Funktion im Schwamm (Publikation 6). Die *Porifera*-spezifischen Crenarchaeoten, Deltaproteo-, Acido- und Actinobakterien waren ausschließlich im Choanosom und innerem Kortex zu finden; ihre Assoziationen mit *P.* cf. *corticata* stellen vermutlich mutualistische Schwamm-Symbionten-Interaktionen dar (die Deltaproteobakterien und Actinobakterien könnten den Schwämmen als Sekundärmetabolit-Produzenten (Li & Liu, 2006; Montalvo *et al.*, 2005; Schirmer *et al.*, 2005; Schmidt *et al.*, 2000) z. B. zur Abwehr von Prädatoren gedient haben). Diese *Porifera*-spezifischen Bakteriengruppen (einschließlich der *Nitrospira* Vertreter (Koops & Pommerening-Röser, 2001)) wurden vermutlich vom Schwamm vertikal transmittiert (Enticknap *et al.*, 2006;

Schmitt *et al.*, 2007; Sharp *et al.*, 2007). Die auf der Schwammoberfläche und äußeren Kortexschicht befindlichen Crenarchaeoten, Alpha- und Gammaproteobakterien waren im Gegensatz dazu nur „spezifisch“ für die Spezies *P.* cf. *corticata* (nach heutiger 16S rRNA Sequenz-Datenbasis). Wie die o. g. Generalisten sind diese „Spezialisten“ vom Schwamm entweder passiv (durch Besiedlung mit freilebenden, opportunistischen Bakterioplankton-populationen) oder aktiv (durch Filtration) erworben worden; tatsächlich können Schwämme im Filtrierungsprozess nicht zwischen Schwamm-spezifischen und Schwamm-unspezifischen Mikroorganismen (Symbionten bzw. Kontaminanten) unterscheiden (Wehrl *et al.*, 2007). Die Generalisten und Spezialisten stellen vermutlich kommensalische, vorübergehend assoziierte Populationen dar (Publikation 6).

Die *aprA* Genanalyse ermöglichte Rückschlüsse auf die mikrobielle Gemeinschaft des Schwefelkreislaufs in *P.* cf. *corticata*, da die Präsenz von schwefeloxidierenden Alpha- und Gammaproteobakterien (fünf Phylotypen) sowie einem sulfatreduzierenden Euryarchaeon nachgewiesen werden konnte. Die räumliche Verteilung der SOP und SRP im Schwamm-gewebe korrelierte ebenfalls mit ihrer (1) Spezifität für Schwämme und (2) möglichen öko-physiologischen Rolle in *P.* cf. *corticata*. Die meisten alphaproteobakteriellen SOP Stämme waren als Generalisten im gesamten Schwammkörper zu finden, während die *Porifera*-/*P.* cf. *corticata*-spezifischen SOP und SRP ausschließlich im Choanosom vertreten waren (Publikation 6). Über 16S rRNA-basierende Methoden wurden potentielle Sulfatreduzierer bisher ebenfalls nur in den Choanosom-Bereichen von Flachwasser-Schwämmen nach-gewiesen (Hoffmann *et al.*, 2005; Manz *et al.*, 2000). Diese Schwamm-SRP-Assoziationen könnten synergistische Interaktionen darstellen: So entstehen durch alternierende Pump-Aktivitäten des Schwammes im Schwammkörper vorübergehend anoxische Gewebezonen, in denen die SRP die metabolischen Endprodukte der fermentierenden Schwammzellen umsetzen; die dadurch entstehende mikrobielle Biomasse wird wiederum von den Schwamm-zellen konsumiert („bacterial farming“) (Hentschel *et al.*, 2006; Hoffmann *et al.*, 2005; Taylor *et al.*, 2007). Eine entsprechende Funktion könnte das sulfatreduzierende Euryarchaeon in *P.* cf. *corticata* innegehabt haben; die Stoffwechselendprodukte der SRP könnten wiederum den chemolithoauto-/heterotrophen SOP (*P.* cf. *corticata*-/*Porifera*-spezifische Organismen sowie Generalisten) sowohl unter oxischen als auch anoxischen Bedingungen als Elektronen-donatoren gedient haben. Die Ergebnisse der *aprA* Genanalyse weisen somit auf die Präsenz eines Schwamm-spezifischen, endosymbiontischen Schwefelkreislaufes im Tiefsee-Schwamm *P.* cf. *corticata* hin (ähnliche endosymbiontische Schwefelkreisläufe wurden auch für marine Oligochaeten postuliert (Blazejak *et al.*, 2005; Dubilier *et al.*, 2001)).

3 Literaturverzeichnis

Abola, A. P., Willits, M. G., Wang, R. C. & Long, S. R. (1999). Reduction of adenosine-5 '-phosphosulfate instead of 3 '-phosphoadenosine-5 '-phosphosulfate in cysteine biosynthesis by *Rhizobium meliloti* and other members of the family *Rhizobiaceae*. *J Bacteriol* **181**, 5280-5287.

Aguiar, P., Beveridge, T. J. & Reysenbach, A. L. (2004). *Sulfurihydrogenibium azorense*, sp. nov., a thermophilic hydrogen-oxidizing microaerophile from terrestrial hot springs in the Azores. *Int J Syst Evol Micr* **54**, 33-39.

Aguilar, D., Aviles, F. X., Querol, E. & Sternberg, M. J. E. (2004). Analysis of phenetic trees based on metabolic capabilites across the three domains of life. *J Mol Biol* **340**, 491-512.

Albuquerque, L., Santos, J., Travassos, P., Nobre, M. F., Rainey, F. A., Wait, R., Empadinhas, N., Silva, M. T. & da Costa, M. S. (2002). *Albidovulum inexpectatum* gen. nov., sp. nov., a nonphotosynthetic and slightly thermophilic bacterium from a marine hot spring that is very closely related to members of the photosynthetic genus *Rhodovulum*. *Appl Environ Microb* **68**, 4266-4273.

Albuquerque, L., Tiago, I., Verissimo, A. & da Costa, M. S. (2006). *Tepidimonas thermarum* sp. nov., a new slightly thermophilic betaproteobacterium isolated from the Elisenquelle in Aachen and emended description of the genus *Tepidimonas*. *Syst Appl Microbiol* **29**, 450-456.

Alexander, B., Andersen, J. H., Cox, R. P. & Imhoff, J. F. (2002). Phylogeny of green sulfur bacteria on the basis of gene sequences of 16S rRNA and of the Fenna-Matthews-Olson protein. *Arch Microbiol* **178**, 131-140.

Amann, R. I., Ludwig, M. L. & Schleifer, K.-H. (1995). Phylogenetic identification and *in situ* detection of individual microbial cells without cultivation. *Microbiol Rev* **59**, 143-169.

Amo, T., Paje, M. L. F., Inagaki, A., Ezaki, S., Atomi, H. & Imanaka, T. (2002). *Pyrobaculum calidifontis* sp. nov., a novel hyperthermophilic archaeon that grows in atmospheric air. *Archaea* **1**, 113-121.

Anandham, R., Indiragandhi, P., Madhaiyan, M., Kim, K., Yim, W., Saravanan, V. S., Chung, J. & Sa, T. (2007). Thiosulfate oxidation and mixotrophic growth of *Methylobacterium oryzae*. *Can J Microbiol* **53**, 869-876.

Anbar, A. D. & Knoll, A. H. (2002). Proterozoic ocean chemistry and evolution: A bioinorganic bridge? *Science* **297**, 1137-1142.

Anbar, A. D. & Roiixel, O. (2007). Metal stable isotopes in paleoceanography. *Annu Rev Earth Pl Sc* **35**, 717-746.

Appia-Ayme, C., Little, P. J., Matsumoto, Y., Leech, A. P. & Berks, B. C. (2001). Cytochrome complex essential for photosynthetic oxidation of both thiosulfate and sulfide in *Rhodovulum sulfidophilum*. *J Bacteriol* **183**, 6107-6118.

Arendsen, A. F., Verhagen, M. F. J. M., Wolbert, R. B. G., Pierik, A. J., Stams, A. J. M., Jetten, M. S. M. & Hagen, W. R. (1993). The dissimilatory sulfite reductase from *Desulfosarcina variabilis* is a desulforubidin containing uncoupled metalated sirohemes and S = 9/2 iron-sulfur clusters. *Biochemistry* **32**, 10323-10330.

Arnold, G. L., Anbar, A. D., Barling, J. & Lyons, T. W. (2004). Molybdenum isotope evidence for widespread anoxia in mid-proterozoic oceans. *Science* **304**, 87-90.

Arunasri, K., Sasikala, C., Ramana, C. V., Suling, J. & Imhoff, J. F. (2005). *Marichromatium indicum* sp. nov., a novel purple sulfur gammaproteobacterium from mangrove soil of Goa, India. *Int J Syst Evol Micr* **55**, 673-679.

Asao, M., Takaichi, S. & Madigan, M. T. (2007). *Thiocapsa imhoffii* sp. nov., an alkaliphilic purple sulfur bacterium of the family *Chromatiaceae* from Soap Lake, Washington (USA). *Arch Microbiol* **188**, 665-675.

Awramik, S. M. (1992). The history and significance of stromatolites. In *Early organic evolution: implications for mineral and energy resources*, pp. 435-449. Edited by M. Schidlowski. Berlin Heidelberg: Springer.

Bagchi, A. & Ghosh, T. C. (2005). A structural study towards the understanding of the interactions of SoxY, SoxZ, and SoxB, leading to the oxidation of sulfur anions via the novel global sulfur oxidizing (*sox*) operon. *Biochem Bioph Res Co* **335**, 609-615.

Bagwell, C. E., Liu, X., Wu, L. & Zhou, J. (2006). Effects of legacy nuclear waste on the compositional diversity and distributions of sulfate-reducing bacteria in a terrestrial subsurface aquifer. *FEMS Microbiol Ecol* **55**, 424-431.

Bahr, M., Crump, B. C., Klepac-Ceraj, V., Teske, A., Sogin, M. L. & Hobbie, J. E. (2005). Molecular characterization of sulfate-reducing bacteria in a New England salt marsh. *Environ Microbiol* **7**, 1175-1185.

Bak, F. & Cypionka, H. (1987). A novel type of energy metabolism involving fermentation of inorganic sulfur compounds. *Nature* **326**, 891-892.

Bak, F. & Pfennig, N. (1987). Chemolithotrophic growth of *Desulfovibrio sulfodismutans* sp. nov. by disproportionation of inorganic compounds. *Arch Microbiol* **147**, 184-189.

Baker, B. J., Moser, D. P., MacGregor, B. J., Fishbain, S., Wagner, M. & Fry, N. K. (2003). Related assemblages of sulfate-reducing bacteria associated with ultradeep gold mines of South Africa and deep basalt aquifers of Washington State. *Environ Microbiol* **5**, 267-277.

Beatty, J. T., Overmann, J., Lince, M. T., Manske, A. K., Lang, A. S., Blankenship, R. E., van Dover, C. L., Martinson, T. A. & Plumley, F. G. (2005). An obligately photosynthetic bacterial anaerobe from a deep-sea hydrothermal vent. *PNAS* **102**, 9306-9310.

Beiko, R. G., Harlow, T. J. & Ragan, M. A. (2005). Highways of gene sharing in prokaryotes. *P Natl Acad Sci USA* **102**, 14332-14337.

Beller, H. R., Letain, T. E., Chakicherla, A., Kane, S. R., Legler, T. C. & Coleman, M. A. (2006). Whole-genome transcriptional analysis of chemolithoautotrophic thiosulfate oxidation by *Thiobacillus denitrificans* under aerobic versus denitrifying conditions. *J Bacteriol* **188**, 7005-7015.

Berg, I. A., Kockelkorn, D., Buckel, W. & Fuchs, G. (2007). A 3-Hydroxypropionate/4-Hydroxybutyrate autotrophic carbon dioxide assimilation pathway in archaea. *Science* **318**, 1782-1786.

Beynon, J. D., MacRae, I. J., Huston, S. L., Nelson, D. C., Segel, I. H. & Fisher, A. J. (2001). Crystal structure of ATP sulfurylase from the bacterial symbiont of the hydrothermal vent tubeworm *Riftia pachyptila*. *Biochemistry* **40**, 14509-14517.

Bias, U. & Trüper, H. G. (1987). Species-specific release of sulfate from adenylyl sulfate by ATP sulfurylase or ADP sulfurylase in the green sulfur bacteria *Chlorobium limicola* and *Chlorobium vibrioforme*. *Arch Microbiol* **147**, 406-410.

Blazejak, A., Erseus, C., Amann, R. & Dubilier, N. (2005). Coexistence of bacterial sulfide oxidizers, sulfate reducers, and spirochetes in a gutless worm (Oligochaeta) from the Peru margin. *Appl Environ Microb* **71**, 1553-1561.

Blazejak, A., Kuever, J., Erseus, C., Amann, R. & Dubilier, N. (2006). Phylogeny of 16S rRNA, ribulose 1,5-biphosphate carboxylase/oxygenase and adenosine-5`-phosphosulfate reductase genes from gamma- and alphaproteobacterial symbionts in gutless marine worms (Oligochaeta) from Bermuda and the Bahamas. *Appl Environ Microb* **72**, 5527-5536.

Boldareva, E. N., Bryantseva, I. A., Tsapin, A., Nelson, K., Sorokin, D. Y., Tourova, T. P., Boichenko, V. A., Stadnichuk, I. N. & Gorlenko, V. M. (2007). The new alkaliphilic bacteriochlorophyll a-containing bacterium *Roseinatronobacter monicus* sp. nov. from the hypersaline soda Mono Lake (California, United States). *Microbiology* **76**, 82-92.

Boucher, Y., Douady, C. J., Papke, R. T., Walsh, D. A., Boudreau, M. E. R., Nesbo, C. L., Case, R. J. & Doolittle, W. F. (2003). Lateral gene transfer and the origins of prokaryotic groups. *Annu Rev Genet* **37**, 283-328.

Boury-Esnault, N. (2002). Family *Polymastiidae* Gray, 1867. In *Systema Porifera: a guide to the classification of sponges*, pp. 201-219. Edited by N. J. A. Hooper & R. W. M. van Soest. New York: Kluwer Academic, Plenum Publishers, New York.

Bramlett, R. N. & Peck, H. D. (1975). Some physical and kinetic properties of adenylylsulfate reductase from *Desulfovibrio vulgaris*. *J Biol Chem* **250**, 2979-2986.

Bright, M. & Giere, O. (2005). Microbial symbiosis in Annelida. *Symbiosis* **38**, 1-45.

Brinkhoff, T., Santegoeds, C. M., Sahm, K., Kuever, J. & Muyzer, G. (1998). A polyphasic approach to study the diversity and vertical distribution of sulfur-oxidizing *Thiomicrospira* species in coastal sediments of the German Wadden Sea. *Appl Environ Microb* **64**, 4650-4657.

Brinkhoff, T., Muyzer, G., Wirsen, C. O. & Kuever, J. (1999). *Thiomicrospira kuenenii* sp. nov., and *Thiomicrospira frisia* sp. nov., two mesophilic obligately chemolithoautotrophic sulfur-oxidizing bacteria isolated from an intertidal mud flat. *Int J Syst Bacteriol* **49**, 385-392.

Brocks, J. J., Buick, R., Summons, R. E. & Logan, G. A. (2003). A reconstruction of Archean biological diversity based on molecular fossils from the 2.78 to 2.45 billion-year-old Mount Bruce Supergroup, Hamersley Basin, Western Australia. *Geochim Cosmochim Ac* **67**, 4321-4335.

Brocks, J. J., Love, G. D., Summons, R. E., Knoll, A. H., Logan, G. A. & Bowden, S. A. (2005). Biomarker evidence for green and purple sulphur bacteria in a stratified Palaeoproterozoic sea. *Nature* **437**, 866-870.

Brüser, T., Lens, P. N. L. & Trüper, H. G. (2000a). The biological sulfur cycle. In *Environmental Technologies to Treat Sulfur Pollution*, pp. 47-86. Edited by P. N. L. Lens & L. H. Pol. London: IWA Publishing.

Brüser, T., Selmer, T. & Dahl, C. (2000b). "ADP sulfurylase" from *Thiobacillus denitrificans* is an adenylylsulfate:phosphate adenylyltransferase and belongs to a new family of nucleotidyltransferases. *J Biol Chem* **275**, 1691-1698.

Brune, D. C. (1995). Sulfur compounds as photosynthetic electron donors. In *Anoxygenic Photosynthetic Bacteria*, pp. 847-870. Edited by R. E. Blankenship, M. T. Madigan & C. E. Bauer. Dordrecht: Kluwer Academic Publishers.

Bryant, D. A., Costas, A. M. G., Maresca, J. A. & other authors (2007). *Candidatus* Chloracidobacterium thermophilum: An aerobic phototrophic acidobacterium. *Science* **317**, 523-526.

Bryantseva, I., Gorlenko, V. M., Kompantseva, E. I., Imhoff, J. F., Suling, J. & Mityushina, L. (1999). *Thiorhodospira sibirica* gen. nov., sp. nov., a new alkaliphilic purple sulfur bacterium from a Siberian soda lake. *Int J Syst Bacteriol* **49**, 697-703.

Buchan, A., Gonzalez, J. M. & Moran, M. A. (2005). Overview of the marine *Roseobacter* lineage. *Appl Environ Microb* **71**, 5665-5677.

Campbell, B. J., Engel, A. S., Porter, M. L. & Takai, K. (2006). The versatile epsilon-proteobacteria: key players in sulphidic habitats. *Nat Rev Genet* **4**, 458-468.

Canfield, D. E. & Teske, A. (1996). Late Proterozoic rise in atmospheric oxygen concentration inferred from phylogenetic and sulphur-isotope studies. *Nature* **382**, 127-132.

Canfield, D. E. (1998). A new model for Proterozoic ocean chemistry. *Nature* **396**, 450-453.

Canfield, D. E., Thamdrup, B. & Fleischer, S. (1998). Isotope fractionation and sulfur metabolism by pure and enrichment cultures of elemental sulfur-disproportionating bacteria. *Limnol Oceanogr* **43**, 253-264.

Canfield, D. E. & Raiswell, R. (1999). The evolution of the sulfur cycle. *Am J Sci* **299**, 697-723.

Canfield, D. E., Habicht, K. S. & Thamdrup, B. (2000). The Archean sulfur cycle and the early history of atmospheric oxygen. *Science* **288**, 658-661.

Canfield, D. E. (2005). The early history of atmospheric oxygen: Homage to Robert A. Garrels. *Annu Rev Earth Pl Sc* **33**, 1-36.

Canfield, D. E., Poulton, S. W. & Narbonne, G. M. (2007). Late-Neoproterozoic deep-ocean oxygenation and the rise of animal life. *Science* **315**, 92-95.

CARIBFLUX (2003). Abschlußbericht Caribflux Projekt. Hydrothermale Prozesse und Massenflüsse im Bereich des vulkanischen Inselbogens der Kleinen Antillen (Karibik). pp. 1-103. Berlin.

Carroll, K. S., Gao, H., Chen, H., Stout, C. D., Leary, J. A. & Bertozzi, C. R. (2005). A conserved mechanism for sulfonucleotide reduction. *Plos Biol* **3**, 1418-1435.

Castro, H., Reddy, K. R. & Ogram, A. (2002). Composition and function of sulfate-reducing prokaryotes in eutrophic and pristine areas of Florida Everglades. *Appl Environ Microb* **68**, 6129-6137.

Catling, D. C. & Claire, M. W. (2005). How Earth's atmosphere evolved to an oxic state: A status report. *Earth Planet Sc Lett* **237**, 1-20.

Cavanaugh, C. M., McKiness, Z. P., Newton, I. L. G. & Stewart, F. J. (2004). Marine chemosynthetic symbioses. In *The prokaryotes An evolving electronic resource for the microbial community*. Edited by M. Dworkin, E. Falkow, E. Rosenberg, K.-H. Schleifer & E. Stackebrandt. New York, N. Y.: Springer Verlag.

Cecchini, G., Schröder, I., Gunsalus, R. P. & Maklashina, E. (2002). Succinate dehydrogenase and fumarate reductase from *Escherichia coli*. *Biochim Biophys Acta* **1553**, 140-157.

Chang, Y. J., Peacock, A. D., Long, P. E., Stephen, J. R., McKinley, J. P., Macnaughton, S. J., Hussain, A. K. M. A., Saxton, A. M. & White, D. C. (2001). Diversity and characterization of sulfate-reducing bacteria in groundwater at a uranium mill tailings site. *Appl Environ Microb* **67**, 3149-3160.

Chartron, J., Carroll, K. S., Shiau, C., Gao, H., Leary, J. A., Bertozzi, C. R. & Stout, C. D. (2006). Substrate recognition, protein dynamics, and iron-sulfur cluster in *Pseudomonas aeruginosa* adenosine-5 '-phosphosulfate reductase. *J Mol Biol* **364**, 152-169.

Chartron, J., Shiau, C., Stout, C. D. & Carroll, K. S. (2007). 3 '-phosphoadenosine-5 '-phosphosulfate reductase in complex with thioredoxin: A structural snapshot in the catalytic cycle. *Biochemistry* **46**, 3942-3951.

Chivian, D., Brodie, E. L., Alm, E. J. & other authors (2008). Environmental genomics reveals a single-species ecosystem deep within earth. *Science* **322**, 275-278.

Choi, I. G. & Kim, S. H. (2007). Global extent of horizontal gene transfer. *P Natl Acad Sci USA* **104**, 4489-4494.

Coenye, T. & Vandamme, P. (2005). Displacement of epsilon-proteobacterial core genes by horizontally transferred homologous genes. *Res Microbiol* **156**, 738-747.

Cook, A. M. & Denger, K. (2002). Dissimilation of the C_2 sulfonates. *Arch Microbiol* **179**, 1-6.

Cook, A. M., Denger, K. & Smits, T. H. M. (2006). Dissimilation of C_3 sulfonates. *Arch Microbiol* **185**, 83-90.

Cook, A. M., Smits, T. H. M. & Denger, K. (2008). Sulfonates and organotrophic sulfite metabolism. In *Microbial sulfur metabolism*, pp. 170-183. Edited by C. Dahl & C. G. Friedrich. Berlin Heidelberg: Springer Verlag.

Cort, J. R., Mariappan, S. V. S., Kim, C. Y., Park, M. S., Peat, T. S., Waldo, G. S., Terwilliger, T. C. & Kennedy, M. A. (2001). Solution structure of *Pyrobaculum aerophilum* DsrC, an archaeal homologue of the gamma subunit of dissimilatory sulfite reductase. *Eur J Biochem* **268**, 5842-5850.

Crane, B. R. & Getzoff, E. D. (1996). The relationship between structure and function for the sulfite reductases. *Curr Opin Struc Biol* **6**, 744-756.

Cypionka, H., Smock, A. M. & Böttcher, M. E. (1998). A combined pathway of sulfur compound disproportionation in *Desulfovibrio desulfuricans*. *FEMS Microbiol Lett* **166**, 181-186.

Dahl, C. & Trüper, H. G. (1989). Comparative enzymology of sulfite oxidation in *Thiocapsa roseopersicina* strain 6311, strain M1 and strain BBS under chemotropic and phototrophic conditions. *Z Naturforsch C* **44**, 617-622.

Dahl, C., Kredich, N. M., Deutzmann, R. & Trüper, H. G. (1993). Dissimilatory sulfite reductase from *Archaeoglobus fulgidus* - physicochemical properties of the enzyme and cloning, sequencing and analysis of the reductase genes. *J Gen Microbiol* **139**, 1817-1828.

Dahl, C. & Trüper, H. G. (1994). Enzymes of dissimilatory sulfide oxidation in phototrophic sulfur bacteria. In *Methods Enzymol*, pp. 400-421.

Dahl, C. (1996). Insertional gene inactivation in a phototrophic sulphur bacterium: APS-reductase-deficient mutants of *Chromatium vinosum*. *Microbiol-Uk* **142**, 3363-3372.

Dahl, C., Rakhely, G., Pott-Sperling, A. S. & other authors (1999). Genes involved in hydrogen and sulfur metabolism in phototrophic sulfur bacteria. *FEMS Microbiol Lett* **180**, 317-324.

Dahl, C. & Trüper, H. G. (2001). Sulfite reductase and APS reductase from *Archaeoglobus fulgidus*. In *Methods Enzymol*, pp. 427-441.

Dahl, C., Engels, S., Pott-Sperling, A. S., Schulte, A., Sander, J., Lubbe, Y., Deuster, O. & Brune, D. C. (2005). Novel genes of the dsr gene cluster and evidence for close interaction of Dsr proteins during sulfur oxidation in the phototrophic sulfur bacterium *Allochromatium vinosum*. *J Bacteriol* **187**, 1392-1404.

Daly, K., Sharp, R. J. & McCarthy, A. J. (2000). Development of oligonucleotide probes and PCR primers for detecting phylogenetic subgroups of sulphate-reducing bacteria. *Microbiology* **146**, 1693-1705.

Dam, B., Mandal, S., Ghosh, W., Das Gupta, S. K. & Roy, P. (2007). The S4-intermediate pathway for the oxidation of thiosulfate by the chemolithoautotroph *Tetrathiobacter kashmirensis* and inhibition of tetrathionate oxidation by sulfite. *Res Microbiol* **158**, 330-338.

Dar, S. A., Yao, L., van Dongen, U., Kuenen, G. J. & Muyzer, G. (2007). Analysis of diversity and activity of sulfate-reducing bacterial communities in sulfidogenic bioreactors using 16S rRNA and *dsrB* genes as molecular markers. *Appl Environ Microb* **73**, 594-604.

Daubin, V., Moran, N. A. & Ochman, H. (2003). Phylogenetics and the cohesion of bacterial genomes. *Science* **301**, 829-832.

Deb, C., Stackebrandt, E., Pradella, S., Saha, A. & Roy, P. (2004). Phylogenetically diverse new sulfur chemolithotrophs of alpha-proteobacteria isolated from Indian soils. *Curr Microbiol* **48**, 452-458.

Deckert, G., Warren, P. V., Gaasterland, T. & other authors (1998). The complete genome of the hyperthermophilic bacterium *Aquifex aeolicus*. *Nature* **392**, 353-358.

DeLong, E. F., Preston, C. M., Mincer, T. & other authors (2006). Community genomics among stratified microbial assemblages in the ocean`s interior. *Nature* **311**, 496-503.

Denger, K., Smits, T. H. M. & Cook, A. M. (2006). L-Cysteate sulpho-lyase, a widespread pyridoxal 5 '-phosphate-coupled desulphonative enzyme purified from *Silicibacter pomeroyi* DSS-3. *Biochem J* **394**, 657-664.

Deplancke, B., Hristova, K. R., Oakley, H. A., McCracken, V. J., Aminov, R., Mackie, R. I. & Gaskins, H. R. (2000). Molecular ecological analysis of the succession and diversity of sulfate-reducing bacteria in the mouse gastrointestinal tract. *Appl Environ Microb* **66**, 2166-2174.

D'Errico, G., Di Salle, A., La Cara, F., Rossi, M. & Cannio, R. (2006). Identification and characterization of a novel bacterial sulfite oxidase with no heme binding domain from *Deinococcus radiodurans*. *J Bacteriol* **188**, 694-701.

DeWeerd, K. A., Mandelco, L., Tanner, R. S., Woese, C. R. & Suflita, J. M. (1990). *Desulfomonile tiedjei* gen. nov. and sp. nov., a novel, anaerobic, dehalogenating, sulfate-reducing bacterium. *Arch Microbiol* **154**, 23-30.

Dhillon, A., Teske, A., Dillon, J., Stahl, D. A. & Sogin, M. L. (2003). Molecular characterization of sulfate-reducing bacteria in the Guaymas Basin. *Appl Environ Microb* **69**, 2765-2772.

Dhillon, A., Goswami, S., Riley, M., Teske, A. & Sogin, M. (2005). Domain evolution and functional diversification of sulfite reductases. *Astrobiology* **5**, 18-29.

Di Salle, A., D'Errico, G., La Cara, F., Cannio, R. & Rossi, M. (2006). A novel thermostable sulfite oxidase from *Thermus thermophilus*: characterization of the enzyme, gene cloning and expression in *Escherichia coli*. *Extremophiles* **10**, 587-598.

Doolittle, W. F., Boucher, Y., Nesbo, C. L., Douady, C. J., Andersson, J. O. & Roger, A. J. (2003). How big is the iceberg of which organellar genes in nuclear genomes are but the tip? *Philos T Roy Soc B* **358**, 39-57.

Dubilier, N., Mulders, C., Ferdelman, T. & other authors (2001). Endosymbiotic sulphate-reducing and sulphide-oxidizing bacteria in an oligochaete worm. *Nature* **411**, 298-302.

Dubinina, G. A., Grabovich, M. Y. & Chernyshova, Y. Y. (2004). The role of oxygen in the regulation of the metabolism of aerotolerant Spirochetes, a major component of "*Thiodendron*" bacterial sulfur mats. *Microbiology* **73**, 725-733.

Duperron, S., Fiala-Medioni, A., Caprais, J. C., Olu, K. & Sibuet, M. (2007). Evidence for chemoautotrophic symbiosis in a Mediterranean cold seep clam (*Bivalvia*: *Lucinidae*): comparative sequence analysis of bacterial 16S rRNA, APS reductase and RubisCO genes. *FEMS Microbiol Ecol* **59**, 64-70.

Duperron, S., Laurent, M. C. Z., Gaill, F. & Gros, O. (2008). Sulphur-oxidizing extracellular bacteria in the gills of *Mytilidae* associated with wood falls. *FEMS Microbiol Ecol* **63**, 338-349.

Dupont, C. L., Yang, S., Palenik, B. & Bourne, P. E. (2006). Modern proteomes contain putative imprints of ancient shifts in trace metal geochemistry. *P Natl Acad Sci USA* **103**, 17822-17827.

Ehrenreich, A. & Widdel, F. (1994). Anaerobic oxidation of ferrous iron by purple bacteria, a new-type of phototrophic metabolism. *Appl Environ Microb* **60**, 4517-4526.

Enticknap, J. J., Kelly, M., Peraud, O. & Hill, R. T. (2006). Characterization of a culturable alphaproteobacterial symbiont common to many sponges and evidence for vertical transmission via sponge larvae. *Appl Environ Microb* **72**, 3724-3732.

Epel, B., Schafer, K. O., Quentmeier, A., Friedrich, C. & Lubitz, W. (2005). Multifrequency EPR analysis of the dimanganese cluster of the putative sulfate thiohydrolase SoxB of *Paracoccus pantotrophus*. *J Biol Inorg Chem* **10**, 636-642.

Falkowski, P. G. (1997). Evolution of the nitrogen cycle and its influence on the biological sequestration of CO_2 in the ocean. *Nature* **387**, 272-275.

Farquhar, J., Bao, H. M. & Thiemens, M. (2000). Atmospheric influence of Earth's earliest sulfur cycle. *Science* **289**, 756-758.

Farquhar, J., Wing, B. A., McKeegan, K. D., Harris, J. W., Cartigny, P. & Thiemens, M. H. (2002). Mass-independent sulfur of inclusions in diamond and sulfur recycling on early earth. *Science* **298**, 2369-2372.

Farquhar, J. & Wing, B. A. (2003). Multiple sulfur isotopes and the evolution of the atmosphere. *Earth Planet Sc Lett* **213**, 1-13.

Farquhar, J., Peters, M., Johnston, D. T., Strauss, H., Masterson, A., Wiechert, U. & Kaufman, A. J. (2007). Isotopic evidence for Mesoarchaean anoxia and changing atmospheric sulphur chemistry. *Nature* **449**, 706-U705.

Finster, K., Liesack, W. & Thamdrup, B. (1998). Elemental sulfur and thiosulfate disproportionation by *Desulfocapsa sulfoexigens* sp. nov., a new anaerobic bacterium isolated from marine surface sediment. *Appl Environ Microb* **64**, 119-125.

Fiser, A., Sanchez, R., Melo, F. & Sali, A. (2001). Comparative protein structure modeling. In *Computational Biochemistry and Biophysics*, pp. 275-312. Edited by M. Watanabe, B. Roux, A. D. MacKerell & O. Becker.

Fishbain, S., Dillon, J. G., Gough, H. L. & Stahl, D. A. (2003). Linkage of high rates of sulfate reduction in Yellowstone hot springs to unique sequence types in the dissimilatory sulfate respiration pathway. *Appl Environ Microb* **69**, 3663-3667.

Freitag, T. E. & Prosser, J. I. (2004). Differences between betaproteobacterial ammonia-oxidizing communities in marine sediments and those in overlying water. *Appl Environ Microb* **70**, 3789-3793.

Friedrich, C. G. (1998). Physiology and genetics of sulfur-oxidizing bacteria. In *Advances in Microbial Physiology*, pp. 235-289. Edited by R. K. Poole: Academic Press.

Friedrich, C. G., Rother, D., Bardischewsky, F., Quentmeier, A. & Fischer, J. (2001). Oxidation of reduced inorganic sulfur compounds by bacteria: Emergence of a common mechanism? *Appl Environ Microb* **67**, 2873-2882.

Friedrich, C. G., Bardischewsky, F., Rother, D., Quentmeier, A. & Fischer, J. (2005). Prokaryotic sulfur oxidation. *Curr Opin Microbiol* **8**, 253-259.

Friedrich, C. G., Quentmeier, A., Bardischewsky, F., Rother, D., Orawski, G., Hellwig, P. & Fischer, J. (2008). Redox control of chemotrophic sulfur oxidation of *Paracoccus pantotrophus*. In *Microbial sulfur metabolism*, pp. 139-150. Edited by C. Dahl & C. G. Friedrich. Berlin Heidelberg: Springer Verlag.

Friedrich, M., Schmidt, M., Kuever, J. & Schulz, H. H. (2002). Sulfidoxidation in kommunalen Abwasser. *unpubliziert*.

Friedrich, M. W. (2002). Phylogenetic analysis reveals multiple lateral transfers of adenosine-5'-phosphosulfate reductase genes among sulfate-reducing microorganisms. *J Bacteriol* **184**, 278-289.

Frigaard, N. U. & Dahl, C. (2008). Sulfur metabolism in phototrophic sulfur bacteria. In *Sulfur metabolism in phototrophic sulfur bacteria*, pp. 283-356. Edited by R. Hell, C. Dahl, D. Knaff & T. Leustek. New York: Springer.

Fritz, G., Buchert, T., Huber, H., Stetter, K. O. & Kroneck, P. M. H. (2000). Adenylylsulfate reductases from archaea and bacteria are 1 : 1 alpha beta-heterodimeric iron-sulfur flavoenzymes - high similarity of molecular properties emphasizes their central role in sulfur metabolism. *FEBS Lett* **473**, 63-66.

Fritz, G., Buchert, T. & Kroneck, P. M. H. (2002a). The function of the [4Fe-4S] clusters and FAD in bacterial and archaeal adenylylsulfate reductases - Evidence for flavin-catalyzed reduction of adenosine 5 '-phosphosulfate. *J Biol Chem* **277**, 26066-26073.

Fritz, G., Roth, A., Schiffer, A. & other authors (2002b). Structure of adenylylsulfate reductase from the hyperthermophilic *Archaeoglobus fulgidus* at 1.6-A resolution. *P Natl Acad Sci USA* **99**, 1836-1841.

Fritz, G., Schiffer, A., Behrens, A., Büchert, T., Ermler, U. & Kroneck, P. M. H. (2008). Living on sulfate: Three-dimensional structure and spectroscopy of adenosine 5`-phosphosulfate reductase and dissimilatory sulfite reductase. In *Microbial sulfur metabolism*, pp. 13-23. Edited by C. Dahl & C. G. Friedrich. Berlin Heidelberg: Springer Verlag.

Fry, B., Cox, J., Gest, H. & Hayes, J. M. (1986). Discrimination between ^{34}S and ^{32}S during bacterial metabolism of inorganic sulfur compounds. *J Bacteriol* **165**, 328-330.

Garrity, G. M., Bell, J. A. & Lilburn, T. G. (2004). Taxonomic outline of the prokaryotes. In *Bergey`s manual of systematic bacteriology*, pp. DOI: 10.1007/bergeysoutline200405. Berlin Heidelberg New York: Springer Verlag.

Gavel, O. Y., Bursakov, S. A., Calvete, J. J., George, G. N., Moura, J. J. G. & Moura, I. (1998). ATP sulfurylases from sulfate-reducing bacteria of the genus *Desulfovibrio*. A novel metalloprotein containing cobalt and zinc. *Biochemistry* **37**, 16225-16232.

Geets, J., Borremans, B., Diels, L., Springael, D., Vangronsveld, J., van der Lelie, D. & Vanbroekhoven, K. (2006). *DsrB* gene-based DGGE for community and diversity surveys of sulfate-reducing bacteria. *J Microbiol Meth* **66**, 194-205.

Gellatly, A. M. & Lyons, T. W. (2005). Trace sulfate in mid-Proterozoic carbonates and the sulfur isotope record of biospheric evolution. *Geochim Cosmochim Ac* **69**, 3813-3829.

Ghosh, W., Bagchi, A., Mandal, S., Dam, B. & Roy, P. (2005). *Tetrathiobacter kashmirensis* gen. nov., sp. nov., a novel mesophilic, neutrophilic, tetrathionate-oxidizing, facultatively chemolithotrophic betaproteobacterium isolated from soil from a temperate orchard in Jammu and Kashmir, India. *Int J Syst Evol Micr* **55**, 1779-1787.

Ghosh, W. & Roy, P. (2007). Chemolithoautotrophic oxidation of thiosulfate, tetrathionate and thiocyanate by a novel rhizobacterium belonging to the genus *Paracoccus*. *FEMS Microbiol Lett* **270**, 124-131.

Giovannoni, S. J., Bibbs, L., Cho, J.-C. & other authors (2005a). Proteorhodopsin in the ubiquitous marine bacterium SAR11. *Nature* **438**, 82-85.

Giovannoni, S. J. & Sting, U. (2005). Molecular diversity and ecology of microbial plankton. *Nature* **437**, 343-348.

Giovannoni, S. J., Tripp, H. J., Givan, S. & other authors (2005b). Genome streamlining in a cosmopolitan oceanic bacterium. *Science* **309**, 1242-1245.

Gogarten, J. P. & Townsend, J. P. (2005). Horizontal gene transfer, genome innovation and evolution. *Nat Rev Microbiol* **3**, 679-687.

Gomes da Silva, S., Gillan, D. C., Dubilier, N. & De Ridder, C. (2006). Characterization by 16S rRNA gene analysis and *in situ* hybridization of bacteria living in the hindgut of a deposit-feeding echinoid (Echinodermata). *J Mar Biol Assoc U K* **86**, 1209-1213.

Gonzalez, J. M., Kiene, R. P. & Moran, M. A. (1999). Transformation of sulfur compounds by an abundant lineage of marine bacteria in the alpha-subclass of the class *Proteobacteria*. *Appl Environ Microb* **65**, 3810-3819.

Gonzalez, J. M., Simo, R., Massana, R., Covert, J. S., Casamayor, E. O., Pedros-Alio, C. & Moran, M. A. (2000). Bacterial community structure associated with a dimethylsulfoniopropionate-producing North-Atlantic algal bloom. *Appl Environ Microb* **66**, 4237-4246.

Gonzalez, J. M., Covert, J. S., Whitman, W. B. & other authors (2003). *Silicibacter pomeroyi* sp nov and *Roseovarius nubinhibens* sp nov., dimethylsulfoniopropionate-demethylating bacteria from marine environments. *Int J Syst Evol Micr* **53**, 1261-1269.

Gorlenko, V. M., Bryantseva, I. A., Panteleeva, E. E., Tourova, T. P., Kolganova, T. V., Makhneva, Z. K. & Moskalenko, A. A. (2004). *Ectothiorhodosinus mongolicum* gen. nov., sp. nov., a new purple bacterium from a soda lake in Mongolia. *Microbiology* **73**.

Grabovich, M. Y., Dubinina, G. A., Lebedeva, V. Y. & Churikova, V. V. (1998). Mixotrophic and lithoheterotrophic growth of the freshwater filamentous sulfur bacterium *Beggiatoa leptomitiformis* D-402. *Microbiology* **67**, 383-388.

Grabovich, M. Y., Muntyan, M. S., Lebedeva, V. Y., Ustiyan, V. S. & Dubinina, G. A. (1999). Lithoheterotrophic growth and electron transfer chain components of the filamentous gliding bacterium *Leucothrix mucor* DSM 2157 during oxidation of sulfur compounds. *FEMS Microbiol Lett* **178**, 155-161.

Grabovich, M. Y., Dul'tseva, N. M. & Dubinina, G. A. (2002). Carbon and sulfur metabolism in representatives of two clusters of bacteria of the genus *Leucothrix*: A comparative study. *Microbiology* **71**, 255-261.

Grassineau, N. V., Nisbet, E. G., Bickle, M. J., Fowler, C. M. R., Lowry, D., Mattey, D. P., Abell, P. & Martin, A. (2001). Antiquity of the biological sulphur cycle: evidence from sulphur and carbon isotopes in 2700 million-year-old rocks of the Belingwe Belt, Zimbabwe. *P Roy Soc Lond B Bio* **268**, 113-119.

Griesbeck, C., Hauska, G. & Schütz, M. (2000). Biological sulfide oxidation: sulfide-quinone reductase (SQR), the primary reaction. In *Recent research developments in microbiology*, pp. 179-203. Edited by S. G. Pandalai. Trivadrum, India: Research Signpost.

Griffin, B. M., Schott, J. & Schink, B. (2007). Nitrite, an electron donor for anoxygenic photosynthesis. *Science* **316**, 1870-.

Grimm, F., Franz, B. & Dahl, C. (2008). Thiosulfate and sulfur oxidation in purple sulfur bacteria. In *Microbial sulfur metabolism*, pp. 101-116. Edited by C. Dahl & C. G. Friedrich. Berlin Heidelberg: Springer Verlag.

Guyoneaud, R., Suling, J., Petri, R., Matheron, R., Caumette, P., Pfennig, N. & Imhoff, J. F. (1998). Taxonomic rearrangements of the genera *Thiocapsa* and *Amoebobacter* on the basis of 16S rDNA sequence analyses, and description of *Thiolamprovum* gen. nov. *Int J Syst Bacteriol* **48**, 957-964.

Habicht, K. S., Canfield, D. E. & Rethmeier, J. (1998). Sulfur isotope fractionation during bacterial reduction and disproportionation of thiosulfate and sulfite. *Geochim Cosmochim Ac* **62**, 2585-2595.

Habicht, K. S. & Canfield, D. E. (2001). Isotope fractionation by sulfate-reducing natural populations and the isotopic composition of sulfide in marine sediments. *Geology* **29**, 555-558.

Habicht, K. S., Gade, M., Thamdrup, B., Berg, P. & Canfield, D. E. (2002). Calibration of sulfate levels in the Archean Ocean. *Science* **298**, 2372-2374.

Hagen, K. D. & Nelson, D. C. (1997). Use of reduced sulfur compounds by *Beggiatoa* spp.: Enzymology and physiology of marine and freshwater strains in homogeneous and gradient cultures. *Appl Environ Microb* **63**, 3957-3964.

Hamann, N., Mander, G. J., Shokes, J. E., Scott, R. A., Bennati, M. & Hedderich, R. (2007). Cysteine-rich CCG domain contains a novel 4Fe-4S cluster binding motif as deduced from studies with subunit B of heterodisulfide reductase from *Methanothermobacter marburgensis*. *Biochemistry* **46**, 12875-12885.

Hanson, T. E. & Tabita, F. R. (2003). Insights into the stress response and sulfur metabolism revealed by proteome analysis of a *Chlorobium tepidum* mutant lacking the Rubisco-like protein. *Photosynth Res* **78**, 231-248.

Hao, W. L. & Golding, G. B. (2006). The fate of laterally transferred genes: Life in the fast lane to adaptation or death. *Genome Res* **16**, 636-643.

Haouari, O., Fardeau, M. L., Cayol, J. L., Fauque, G., Casiot, C., Elbaz-Poulichet, F., Hamdi, M. & Ollivier, B. (2008). *Thermodesulfovibrio hydrogeniphilus* sp. nov., a new thermophilic sulphate-reducing bacterium isolated from a Tunisian hot spring. *Syst Appl Microbiol* **31**, 38-42.

Hartzell, P. & Reed, D. (2003). The genus *Archaeoglobus*. In *The Prokaryotes - an evolving electronic resource for the microbiological community*. Edited by M. Dworkin, S. Falkow, E. Rosenberg, K.-H. Schleifer & E. Stackebrandt. New York, N. Y.: Springer Verlag.

Hattori, S., Kamagata, Y., Hanada, S. & Shoun, H. (2000). *Thermacetogenium phaeum* gen. nov., sp. nov., a strictly anaerobic, thermophilic, syntrophic acetate-oxidizing bacterium. *Int J Syst Evol Micr* **50**, 1601-1609.

Haveman, S. A., Greene, E. A., Stilwell, C. P., Voordouw, J. K. & Voordouw, G. (2004). Physiological and gene expression analysis of inhibition of *Desulfovibrio vulgaris* Hildenborough by nitrite. *J Bacteriol* **186**, 7944-7950.

Hedderich, R., Klimmek, O., Kroger, A., Dirmeier, R., Keller, M. & Stetter, K. O. (1999). Anaerobic respiration with elemental sulfur and with disulfides. *FEMS Microbiol Rev* **22**, 353-381.

Hedderich, R., Hamann, N. & Bennati, M. (2005). Heterodisulfide reductase from methanogenic archaea: a new catalytic role for an iron-sulfur cluster. *Biol Chem* **386**, 961-970.

Heising, S., Richter, L., Ludwig, W. & Schink, B. (1999). *Chlorobium ferrooxidans* sp. nov., a phototrophic green sulfur bacterium that oxidizes ferrous iron in coculture with a "*Geospirillum*" sp. strain. *Arch Microbiol* **172**, 116-124.

Henry, E. A., Devereux, R., Maki, J. S., Gilmour, C. C., Woese, C. R., Mandelco, L., Schauder, R., Remsen, C. C. & Mitchell, R. (1994). Characterization of a new thermophilic sulfate-reducing bacterium *Thermodesulfovibrio yellowstonii*, gen. nov. and sp. nov.: Its phylogenetic relationship to *Thermodesulfobacterium commune* and their origins deep within the bacterial domain. *Arch Microbiol* **161**, 62-69.

Hensen, D., Sperling, D., Trüper, H. G., Brune, D. C. & Dahl, C. (2006). Thiosulphate oxidation in the phototrophic sulphur bacterium *Allochromatium vinosum*. *Mol Microbiol* **62**, 794-810.

Henstra, A. M. & Stams, A. J. M. (2004). Novel physiological features of *Carboxydothermus hydrogenoformans* and *Thermoterrabacterium ferrireducens*. *Appl Environ Microb* **70**, 7236-7240.

Hentschel, U., Hopke, J., Horn, M., Friedrich, A. B., Wagner, M., Hacker, J. & Moore, B. S. (2002). Molecular evidence for a uniform microbial community in sponges from different oceans. *Appl Environ Microb* **68**, 4431-4440.

Hentschel, U., Usher, K. M. & Taylor, M. W. (2006). Marine sponges as microbial fermenters. *FEMS Microbiol Ecol* **55**, 167-177.

Hill, M., Hill, A., Lopez, N. & Harriott, O. (2006). Sponge-specific bacterial symbionts in the Caribbean sponge, *Chondrilla nucula* (*Demospongiae*, *Chondrosida*). *Mar Biol* **148**, 1221-1230.

Hipp, W. M., Pott, A. S., Thum-Schmitz, N., Faath, I., Dahl, C. & Trüper, H. G. (1997). Towards the phylogeny of APS reductases and sirohaem sulfite reductases in sulfate-reducing and sulfur-oxidizing prokaryotes. *Microbiology* **143**, 2891-2902.

Hippe, H., Hagenauer, A. & Kroppenstedt, R. M. (1997). Menadione requirement for sulfate-reduction in *Desulfotomaculum aeronauticum*, and emended species description. *Syst Appl Microbiol* **20**, 554-558.

Hirayama, H., Takai, K., Inagaki, F., Nealson, K. H. & Horikoshi, K. (2005). *Thiobacter subterraneus* gen. nov., sp. nov., an obligately chemolithoautotrophic, thermophilic, sulfur-oxidizing bacterium from a subsurface hot aquifer. *Int J Syst Evol Microbiol* **55**, 467-472.

Hoeft, S. E., Blum, J. S., Stolz, J. F., Tabita, F. R., Witte, B., King, G. M., Santini, J. M. & Oremland, R. S. (2007). *Alkalilimnicola ehrlichii* sp. nov., a novel, arsenite-oxidizing haloalkaliphilic gammaproteobacterium capable of chemoautotrophic or heterotrophic growth with nitrate or oxygen as the electron acceptor. *Int J Syst Evol Microbiol* **57**, 504-512.

Hoffmann, F., Larsen, O., Thiel, V., Rapp, H. T., Pape, T., Michaelis, W. & Reitner, J. (2005). An anaerobic world in sponges. *Geomicrobiol J* **22**, 1-10.

Holland, H. D. (2002). Volcanic gases, black smokers, and the Great Oxidation Event. *Geochim Cosmochim Ac* **66**, 3811-3826.

Holmes, B. & Blanch, H. (2007). Genus-specific associations of marine sponges with group I crenarchaeotes. *Mar Biol* **150**, 759-772.

Howard, E. C., Henriksen, J. R., Buchan, A. & other authors (2006). Bacterial taxa that limit sulfur flux from the ocean. *Science* **314**, 649-652.

Howarth, R., Unz, R. F., Seviour, E. M., Seviour, R. J., Blackall, L. L., Pickup, R. W., Jones, J. G., Yaguchi, J. & Head, I. M. (1999). Phylogenetic relationships of filamentous sulfur bacteria (*Thiothrix* spp. and Eikelboom type 021N bacteria) isolated from wastewater-treatment plants and description of *Thiothrix eikelboomii* sp. nov., *Thiothrix unzii* sp. nov., *Thiothrix fructosivorans* sp. nov. and *Thiothrix defluvii* sp. nov. *Int J Syst Bacteriol* **49**, 1817-1827.

Hristova, K. R., Mau, M., Zheng, D., Aminov, R. I., Mackie, R. I., Gaskins, H. R. & Raskin, L. (2000). *Desulfotomaculum* genus- and subgenus-specific 16S rRNA hybridization probes for environmental studies. *Environ Microbiol* **2**, 143-159.

Huber, H. & Prangishvili, D. (2000).*Sulfolobales*. In *The prokaryotes An evolving electronic resource for the microbial community*. Edited by M. Dworkin, E. Falkow, E. Rosenberg, K.-H. Schleifer & E. Stackebrandt. New York, N. Y.: Springer Verlag.

Huber, H., Huber, R. & Stetter, K. O. (2002).*Thermoproteales*. In *The prokaryotes An evolving electronic resource for the microbial community*. Edited by M. Dworkin, E. Falkow, E. Rosenberg, K.-H. Schleifer & E. Stackebrandt. New York, N. Y.: Springer Verlag.

Huber, R., Rossnagel, P., Woese, C. R., Rachel, R., Langworthy, T. A. & Stetter, K. O. (1996). Formation of ammonium from nitrate during chemolithoautotrophic growth of the extremely thermophilic bacterium *Ammonifex degensii* gen. nov. sp. nov. *Syst Appl Microbiol* **19**, 40-49.

Huber, R. & Eder, W. (2002).*Aquificales*. In *The prokaryotes An evolving electronic resource for the microbial community*. Edited by M. Dworkin, E. Falkow, E. Rosenberg, K.-H. Schleifer & E. Stackebrandt. New York, N. Y.: Springer Verlag.

Hugenholtz, P., Pitulle, C., Hershberger, K. L. & Pace, N. R. (1998). Novel division level bacterial diversity in a Yellowstone hot spring. *J Bacteriol* **180**, 366-376.

Imachi, H., Sekiguchi, Y., Kamagata, Y. & other authors (2006). Non-sulfate-reducing, syntrophic bacteria affiliated with *Desulfotomaculum* cluster I are widely distributed in methanogenic environments. *Appl Environ Microb* **72**, 2080-2091.

Imachi, H., Sakai, S., Ohashi, A., Harada, H., Hanada, S., Kamagata, Y. & Sekiguchi, Y. (2007). *Pelotomaculum propionicicum* sp. nov., an anaerobic, mesophilic, obligately syntrophic propionate-oxidizing bacterium. *Int J Syst Evol Micr* **57**, 1487-1492.

Imhoff, J. F., Suling, J. & Petri, R. (1998). Phylogenetic relationships among the *Chromatiaceae*, their taxonomic reclassification and description of the new genera *Allochromatium*, *Halochromatium*, *Isochromatium*, *Marichromatium*, *Thiococcus*, *Thiohalocapsa* and *Thermochromatium*. *Int J Syst Bacteriol* **48**, 1129-1143.

Imhoff, J. F. (1999). The family *Ectothiorhodospiraceae*. In *The prokaryotes An evolving electronic resource for the microbial community*. Edited by M. Dworkin, E. Falkow, E. Rosenberg, K.-H. Schleifer & E. Stackebrandt. New York, N. Y.: Springer Verlag.

Imhoff, J. F. (2001a). Transfer of *Rhodopseudomonas acidophila* to the new genus *Rhodoblastus* as *Rhodoblastus acidophilus* gen. nov., comb. nov. *Int J Syst Evol Micr* **51**, 1863-1866.

Imhoff, J. F. (2001b). The *Chromatiaceae*. In *The prokaryotes An evolving electronic resource for the microbial community*. Edited by M. Dworkin, E. Falkow, E. Rosenberg, K.-H. Schleifer & E. Stackebrandt. New York, N. Y.: Springer Verlag.

Imhoff, J. F. (2001c). The phototrophic alpha-Proteobacteria. In *The prokaryotes An evolving electronic resource for the microbial community*. Edited by M. Dworkin, E. Falkow, E. Rosenberg, K.-H. Schleifer & E. Stackebrandt. New York, N. Y.: Springer Verlag.

Imhoff, J. F. (2001d). The phototrophic beta-Proteobacteria. In *The prokaryotes An evolving electronic resource for the microbial community*. Edited by M. Dworkin, E. Falkow, E. Rosenberg, K.-H. Schleifer & E. Stackebrandt. New York, N. Y.: Springer Verlag.

Imhoff, J. F. (2003). Phylogenetic taxonomy of the family *Chlorobiaceae* on the basis of 16S rRNA and *fmo* (Fenna Matthews-Olson protein) gene sequences. *Int J Syst Evol Micr* **53**, 941-951.

Imlay, J. A. (2006). Iron-sulphur clusters and the problem with oxygen. *Mol Microbiol* **59**, 1073-1082.

Inagaki, F., Takai, K., Nealson, K. H. & Horikoshi, K. (2004). *Sulfurovum lithotrophicum* gen. nov., sp. nov., a novel sulfur-oxidizing chemolithoautotroph within the *Epsilonproteobacteria* isolated from Okinawa Trough hydrothermal sediments. *Int J Syst Evol Microbiol* **54**, 1477-1482.

Ito, T., Sugita, K., Yumoto, I., Nodasaka, Y. & Okabe, S. (2005). *Thiovirga sulfuroxydans* gen. nov., sp. nov., a chemolithoautotrophic sulfur-oxidizing bacterium isolated from a microaerobic waste-water biofilm. *Int J Syst Evol Micr* **55**, 1059-1064.

Itoh, T., Suzuki, K., Sanchez, P. C. & Nakase, T. (1999). *Caldivirga maquilingensis* gen. nov., sp. nov., a new genus of rod-shaped crenarchaeote isolated from a hot spring in the Philippines. *Int J Syst Bacteriol* **49**, 1157-1163.

Jain, R., Rivera, M. C., Moore, J. E. & Lake, J. A. (2003). Horizontal gene transfer accelerates genome innovation and evolution. *Mol Biol Evol* **20**, 1598-1602.

Jørgensen, B. B. (1982). Mineralization of organic matter in the sea bed - the role of sulphate reduction. *Nature* **296**, 643-645.

Jørgensen, B. B. & Bak, F. (1991). Pathways and microbiology of thiosulfate transformations and sulfate reduction in a marine sediment (Kattegat, Denmark). *Appl Environ Microb* **57**, 847-856.

Jørgensen, B. B. & Nelson, D. C. (2004). Sulfide oxidation in marine sediments: Geochemistry meets microbiology. In *Sulfur Biogeochemistry - Past and Present*, pp. 63-81. Edited by J. P. Amend, K. J. Edwards & T. W. Lyons: Geological Society of America.

Johnson, C. M., Beard, B. L. & Roden, E. E. (2008). The iron isotope fingerprints of redox and biogeochemical cycling in the modern and ancient Earth. *Annu Rev Earth Pl Sc* **36**, 457-493.

Johnson, D. B., Stallwood, B., Kimura, M. & Hallberg, K. B. (2006). Isolation and characterization of *Acidicaldus organivorus*, gen. nov., sp. nov.: a novel sulfur-oxidizing, ferric iron-reducing thermoacidophilic heterotrophic proteobacterium. *Arch Microbiol* **185**, 212-221.

Jonkers, H. M., van der Maarel, M. J. E. C., van Gemerden, H. & Hansen, T. A. (1996). Dimethylsufoxide reduction by marine sulfate-reducing bacteria. *FEMS Microbiol Lett* **136**, 283-287.

Joulian, C., Ramsing, N. B. & Ingvorsen, K. (2001). Congruent phylogenies of most common small-subunit rRNA and dissimilatory sulfite reductase gene sequences retrieved from estuarine sediments. *Appl Environ Microb* **67**, 3314-3318.

Kah, L. C., Lyons, T. W. & Frank, T. D. (2004). Low marine sulphate and protracted oxygenation of the proterozoic biosphere. *Nature* **431**, 834-838.

Kaksonen, A. H., Spring, S., Schumann, P., Kroppenstedt, R. M. & Puhakka, J. A. (2007a). *Desulfurispora thermophila* gen. nov., sp. nov., a thermophilic, spore-forming sulfate-reducer isolated from a sulfidogenic fluidized-bed reactor. *Int J Syst Evol Micr* **57**, 1089-1094.

Kaksonen, A. H., Spring, S., Schumann, P., Kroppenstedt, R. M. & Puhakka, J. A. (2007b). *Desulfovirgula thermocuniculi* gen. nov., sp. nov., a thermophilic sulfate-reducer isolated from a geothermal underground mine in Japan. *Int J Syst Evol Micr* **57**, 98-102.

Kämpf, C. & Pfennig, N. (1980). Capacity of *Chromatiaceae* for chemotrophic growth. Specific respiration rates of *Thiocystis violacea* and *Chromatium vinosum*. *Arch Microbiol* **127**, 125-135.

Kanao, T., Kamimura, K. & Sugio, T. (2007). Identification of a gene encoding a tetrathionate hydrolase in *Acidithiobacillus ferrooxidans*. *J Biotechnol* **132**, 16-22.

Kaneko, R., Hayashi, T., Tanahashi, M. & Naganuma, T. (2007). Phylogenetic diversity and distribution of dissimilatory sulfite reductase genes from deep-sea sediment cores. *Mar Biotechnol* **9**, 429-436.

Kappler, U. & Dahl, C. (2001). Enzymology and molecular biology of prokaryotic sulfite oxidation. *FEMS Microbiol Lett* **203**, 1-9.

Kappler, U., Friedrich, C. G., Trüper, H. G. & Dahl, C. (2001). Evidence for two pathways of thiosulfate oxidation in *Starkeya novella* (formerly *Thiobacillus novellus*). *Arch Microbiol* **175**, 102-111.

Kappler, U. (2008). Bacterial sulfite-oxidizing enzymes - enzymes for chemolithotrophs only? In *Microbial sulfur metabolism*, pp. 151-169. Edited by C. Dahl & C. G. Friedrich. Berlin Heidelberg: Springer Verlag.

Karavaiko, G. I., Bogdanova, T. y. I., Tourova, T. y. P., Kondrat'eva, T. F., Tsaplina, I. A., Egorova, M. A., Krasil'nikova, E. N. & Zakharchuk, L. M. (2005). Reclassification of '*Sulfobacillus thermosulfidooxidans* subsp. *thermotolerans*' strain K1 as *Alicyclobacillus tolerans* sp. nov. and *Sulfobacillus disulfidooxidans* Dufresne et al. 1996 as *Alicyclobacillus disulfidooxidans* comb. nov., and emended description of the genus *Alicyclobacillus*. *Int J Syst Evol Microbiol* **55**, 941-947.

Karr, E. A., Sattley, W. M., Rice, M. R., Jung, D. O., Madigan, M. T. & Achenbach, L. A. (2005). Diversity and distribution of sulfate-reducing bacteria in permanently frozen Lake Fryxell, McMurdo Dry Valleys, Antarctica. *Appl Environ Microb* **71**, 6353-6359.

Kashefi, K., Holmes, D. E., Reysenbach, A. L. & Lovley, D. R. (2002). Use of Fe(III) as an electron acceptor to recover previously uncultured hyperthermophiles: Isolation and characterization of *Geothermobacterium ferrireducens* gen. nov., sp. nov. *Appl Environ Microb* **68**, 1735-1742.

Kaufman, A. J., Johnston, D. T., Farquhar, J. & other authors (2007). Late Archean biospheric oxygenation and atmospheric evolution. *Geochim Cosmochim Ac* **71**, A469-A469.

Kelly, D. P., Shergill, J. K., Lu, W. P. & Wood, A. P. (1997). Oxidative metabolism of inorganic sulfur compounds by bacteria. *Anton Leeuw Int J G* **71**, 95-107.

Kelly, D. P. (1999). Thermodynamic aspects of energy conservation by chemolithotrophic sulfur bacteria in relation to the sulfur oxidation pathways. *Arch Microbiol* **171**, 219-229.

Kelly, D. P. & Wood, A. P. (2000). Reclassification of some species of *Thiobacillus* to the newly designated genera *Acidithiobacillus* gen. nov., *Halothiobacillus* gen. nov. and *Thermithiobacillus* gen. nov. *Int J Syst Evol Micr* **50**, 511-516.

Kelly, D. P., Uchino, Y., Huber, H., Amils, R. & Wood, A. P. (2007). Reassessment of the phylogenetic relationships of *Thiomonas cuprina*. *Int J Syst Evol Micr* **57**, 2720-2724.

Khanna, S. & Nicholas, D. J. D. (1983). Substrate phosphorylation in *Chlorobium vibrioforme* f. sp. *thiosulfatophilum*. *J Gen Microbiol* **129**, 1365-1370.

Kirchhoff, J. & Trüper, H. G. (1974). Adenylylsulfate reductase of *Chlorobium limicola*. *Arch Microbiol* **100**, 115-120.

Kjeldsen, K. U., Kjellerup, B. V., Egli, K., Froelund, B., Nielsen, P. H. & Ingvorsen, K. (2007a). Phylogenetic and functional diversity of bacteria in biofilms from metal surfaces of an alkaline district heating system. *FEMS Microbiol Ecol* **61**, 384-397.

Kjeldsen, K. U., Loy, A., Jakobsen, T. F., Thomsen, T. R., Wagner, M. & Ingvorsen, K. (2007b). Diversity of sulfate-reducing bacteria from an extreme hypersaline sediment, Great Salt Lake (Utah). *FEMS Microbiol Ecol* **60**, 287-298.

Klein, M., Friedrich, M., Roger, A. J., Hugenholtz, P., Fishbain, S., Abicht, H., Blackall, L. L., Stahl, D. A. & Wagner, M. (2001). Multiple lateral transfers of dissimilatory sulfite reductase genes between major lineages of sulfate-reducing prokaryotes. *J Bacteriol* **183**, 6028-6035.

Kletzin, A. (2008). Oxidation of sulfur and inorganic sulfur compounds in *Acidianus ambivalens*. In *Microbial sulfur metabolism*, pp. 184-201. Edited by C. Dahl & C. G. Friedrich. Berlin Heidelberg: Springer Verlag.

Knöfel, T. & Sträter, N. (1999). X-ray structure of the *Escherichia coli* periplasmic 5`-nucleotidase containing a dimetal catalytic site. *Nat Struct Biol* **6**, 448-453.

Koizumi, Y., Kojima, H., Oguri, K., Kitazato, H. & Fukui, M. (2004). Vertical and temporal shifts in microbial communities in the water column and sediment of saline meromictic Lake Kaiike (Japan), as determined by a 16S rDNA-based analysis, and related to physicochemical gradients. *Environ Microbiol* **6**, 622-637.

Kondo, R. & Butani, J. (2007). Comparison of the diversity of sulfate-reducing bacterial communities in the water column and the surface sediments of a Japanese meromictic lake. *Limnology* **8**, 131-141.

Kondrateva, E. N., Zhukov, V. G., Ivanovskii, R. N., Petrushkova, Y. P. & Monosov, E. Z. (1981). Light and dark metabolism in purple sulfur bacteria. *Soviet Science Reviews* **2**.

Koonin, E. V., Makarova, K. S. & Aravind, L. (2001). Horizontal gene transfer in prokaryotes: Quantification and classification. *Annu Rev Microbiol* **55**, 709-742.

Koops, H.-P. & Pommerening-Röser, A. (2001). Distribution and ecophysiology of the nitrifying bacteria emphasizing cultured species. *FEMS Microbiol Ecol* **37**, 1-9.

Kopp, R. E., Kirschvink, J. L., Hilburn, I. A. & Nash, C. Z. (2005). The paleoproterozoic snowball Earth: A climate disaster triggered by the evolution of oxygenic photosynthesis. *P Natl Acad Sci USA* **102**, 11131-11136.

Kopriva, S., Patron, N., Leustek, T. & Keeling, P. (2008). Phylogenetic analysis of sulfate assimilation and cysteine biosynthesis in phototrophic organisms. In *Sulfur metabolism in phototrophic organisms*. Edited by R. Hell, C. Dahl, D. B. Knaff & T. Leustek. New York: Springer Verlag.

Kostanjevecki, V., Brige, A., Meyer, T. E., Cusanovich, M. A., Guisez, Y. & Van Beeumen, J. (2000). A membrane-bound flavocytochrome c-sulfide dehydrogenase from the purple phototrophic sulfur bacterium *Ectothiorhodospira vacuolata*. *J Bacteriol* **182**, 3097-3103.

Kowalchuk, G. A. & Stephen, J. R. (2001). Ammonia-oxidizing bacteria: a model for molecular microbial ecology. *Annu Rev Microbiol* **55**, 485-529.

Krafft, T., Gross, R. & Kröger, A. (1995). The function of *Wollinella succinogenes psr* genes in electron transport with polysulfide as the terminal electron acceptor. *Eur J Biochem* **230**, 601-606.

Krasil'nikova, E. N., Bogdanova, T. I., Zakharchuk, L. M., Tsaplina, I. A. & Karavaiko, G. I. (1998). Metabolism of reduced sulfur compounds in *Sulfobacillus thermosulfidooxidans* strain 1269. *Microbiology* **67**, 125-132.

Krieger, E., Nabuurs, S. B. & Vriend, G. (2003). Homology modeling. In *Structural Bioinformatics*, pp. 509-523. Edited by P. E. Bourne & H. Weissig: Wiley.

Kuever, J., Sievert, S. M., Stevens, H., Brinkhoff, T. & Muyzer, G. (2002). Microorganisms of the oxidative and reductive part of the sulfur cycle at a shallow-water hydrothermal vent in the Aegean Sea (Milos, Greece). *Cah Biol Mar* **43**, 413-416.

Kuever, J., Rainey, F. A. & Widdel, F. (2005). Class IV. *Deltaproteobacteria* class nov. In *Bergey`s Manual of Systematic Bacteriology*, pp. 922-1040. Edited by D. J. Brenner, N. R. Krieg, J. T. Staley & G. M. Garrity. New York: Springer.

Kumar, P. A., Jyothsna, T. S. S., Srinivas, T. N. R., Sasikala, C., Ramana, C. V. & Imhoff, J. F. (2007a). *Marichromatium bheemlicum* sp. nov., a non-diazotrophic, photosynthetic gammaproteobacterium from a marine aquaculture pond. *Int J Syst Evol Microbiol* **57**, 1261-1265.

Kumar, P. A., Sasi Jyothsna, T. S., Srinivas, T. N. R., Sasikala, C., Ramana, C. V. & Imhoff, J. F. (2007b). Two novel species of marine phototrophic *Gammaproteobacteria*: *Thiorhodococcus bheemlicus* sp. nov. and *Thiorhodococcus kakinadensis* sp. nov. *Int J Syst Evol Microbiol* **57**, 2458-2461.

Kumar, P. A., Srinivas, T. N. R., Sasikala, C. & Ramana, C. V. (2007c). *Halochromatium roseum* sp. nov., a non-motile phototrophic gammaproteobacterium with gas vesicles, and emended description of the genus *Halochromatium*. *Int J Syst Evol Microbiol* **57**, 2110-2113.

Kurland, C. G., Canback, B. & Berg, O. G. (2003). Horizontal gene transfer: A critical view. *P Natl Acad Sci USA* **100**, 9658-9662.

Kuwahara, H., Yoshida, T., Takaki, Y. & other authors (2007). Reduced genome of the thioautotrophic intracellular symbiont in a deep-sea clam, *Calyptogena okutanii*. *Curr Biol* **17**, 881-886.

Kwok, S., Kellogg, D. E., McKinney, N., Spasic, D., Goda, L., Levenson, C. & Sninsky, J. J. (1990). Effects of primer-template mismatches on the polymerase chain reaction. *Nucleic Acids Res* **18**, 999-1005.

Lahiri, C., Mandal, S., Ghosh, W., Dam, B. & Roy, P. (2006). A novel gene cluster *soxSRT* is essential for the chemolithotrophic oxidation of thiosulfate and tetrathionate by *Pseudaminobacter salicylatoxidans* KCT001. *Curr Microbiol* **52**, 267-273.

Lam, P., Cowen, J. P. & Jones, R. D. (2004). Autotrophic ammonia oxidation in a deep-sea hydrothermal plume. *FEMS Microbiol Ecol* **47**, 191-206.

Lampreia, J., Pereira, A. S. & Moura, J. J. G. (1994). Adenylylsulfate reductases from sulfate-reducing bacteria. In *Methods Enzymol*, pp. 241-260.

Lancaster, C. R. D. (2003a). *Wolinella succinogenes* quinol : fumarate reductase and its comparison to *E. coli* succinate : quinone reductase. *FEBS Lett* **555**, 21-28.

Lancaster, C. R. D. (2003b). The structure of *Wolinella succinogenes* quinol: fumarate reductase and its relevance to the superfamily of succinate: quinone oxidoreductases. *Adv Protein Chem* **63**, 131-149.

Larsen, O., Lien, T. & Birkeland, N. K. (1999). Dissimilatory sulfite reductase from *Archaeoglobus profundus* and *Desulfotomaculum thermocisternum*: phylogenetic and structural implications from gene sequences. *Extremophiles* **3**, 63-70.

Larsen, O., Lien, T. & Birkeland, N. K. (2000). Characterization of the desulforubidin operons from *Desulfobacter vibrioformis* and *Desulfobulbus rhabdoformis*. *FEMS Microbiol Lett* **186**, 41-46.

Lee, E. Y., Lee, H. K., Lee, Y. K., Sim, C. J. & Lee, J. H. (2003). Diversity of symbiotic archaeal communities in marine sponges from Korea. *Biomol Eng* **20**, 299-304.

Leloup, J., Quillet, L., Berthe, T. & Petit, F. (2006). Diversity of the *dsrAB* (dissimilatory sulfite reductase) gene sequences retrieved from two contrasting mudflats of the Seine estuary, France. *FEMS Microbiol Ecol* **55**, 230-238.

Leloup, J., Loy, A., Knab, N. J., Borowski, C., Wagner, M. & Jørgensen, B. B. (2007). Diversity and abundance of sulfate-reducing microorganisms in the sulfate and methane zones of a marine sediment, Black Sea. *Environ Microbiol* **9**, 131-142.

Lerat, E., Daubin, V., Ochman, H. & Moran, N. A. (2005). Evolutionary origins of genomic repertoires in bacteria. *Plos Biol* **3**, 807-814.

Lerat, E. & Ochman, H. (2005). Recognizing the pseudogenes in bacterial genomes. *Nucleic Acids Res* **33**, 3125-3132.

Lercher, M. J. & Pal, C. (2008). Integration of horizontally transferred genes into regulatory interaction networks takes many million years. *Mol Biol Evol* **25**, 559-567.

Li, Z., Hu, Y., Liu, Y., Huang, Y., He, L. & Miao, X. (2007). 16S rDNA clone library-based bacterial phylogenetic diversity associated with three South China Sea sponges. *World J Microbiol Biotechnol*.

Li, Z.-Y. & Liu, Y. (2006). Marine sponge *Craniella australiensis*-associated bacterial diversity revelation based on 16S rDNA library and biologically active *Actinomycetes* screening, phylogenetic analysis. *Lett Appl Microbiol* **43**, 410-416.

Lie, T. J., Pitta, T., Leadbetter, E. R., Godchaux, W. & Leadbetter, J. R. (1996). Sulfonates: Novel electron acceptors in anaerobic respiration. *Arch Microbiol* **166**, 204-210.

Loschi, L., Brokx, S. J., Hills, T. L., Zhang, G., Bertero, M. G., Lovering, A. L., Weiner, J. H. & Strynadka, N. C. J. (2004). Structural and biochemical identification of a novel bacterial oxidoreductase. *J Biol Chem* **279**, 50391-50400.

Lovley, D. R., Holmes, D. E. & Nevin, K. P. (2004). Dissimilatory Fe(III) and Mn(IV) reduction. *Advances in Microbial Physiology* **49**, 221-286.

Loy, A., Lehner, A., Lee, N. & Adamczyk, J. (2002). Oligonucleotide microarray for 16S rRNA gene-based detection of all recognized lineages of sulphate-reducing prokaryotes in the environment. *Appl Environ Microb* **68**, 5064-5081.

Loy, A., Kusel, K., Lehner, A., Drake, H. L. & Wagner, M. (2004). Microarray and functional gene analyses of sulfate-reducing prokaryotes in low-sulfate, acidic fens reveal cooccurrence of recognized genera and novel lineages. *Appl Environ Microb* **70**, 6998-7009.

Loy, A., Duller, S. & Wagner, M. (2008). Evolution and ecology of microbes dissimilating sulfur compounds: Insights from siroheme sulfite reductases. In *Microbial sulfur metabolism*, pp. 46-59. Edited by C. Dahl & C. G. Friedrich. Berlin Heidelberg: Springer Verlag.

Ludwig, W., Strunk, O., Westram, R. & other authors (2004). ARB: a software environment for sequence data. *Nucleic Acids Res* **32**, 1363-1371.

Lücker, S., Steger, D., Kjeldsen, K. U., MacGregor, B. J., Wagner, M. & Loy, A. (2007). Improved 16S rRNA-targeted probe set for analysis of sulfate-reducing bacteria by fluorescence in situ hybridization. *J Microbiol Meth* **69**, 523-528.

Malmstom, R. R., Kiene, R. P., Cottrell, M. T. & Kirchman, D. L. (2004). Contribution of SAR11 bacteria to dissolved dimethylsulfoniopropionate and amino acid uptake in the North Atlantic Ocean. *Appl Environ Microb* **70**, 4129-4135.

Mander, G. J., Duin, E. C., Linder, D., Stetter, K. O. & Hedderich, R. (2002). Purification and characterization of a membrane-bound enzyme complex from the sulfate-reducing archaeon *Archaeoglobus fulgidus* related to heterodisulfide reductase from methanogenic archaea. *Eur J Biochem* **269**, 1895-1904.

Mander, G. J., Weiss, M. S., Hedderich, R., Kahnt, J., Ermler, U. & Warkentin, E. (2005). X-ray structure of the gamma-subunit of a dissimilatory sulfite reductase: Fixed and flexible C-terminal arms. *FEBS Lett* **579**, 4600-4604.

Manz, W., Eisenbrecher, M., Neu, T. R. & Szewzyk, U. (1998). Abundance and spatial organization of Gram-negative sulphate-reducing bacteria in activated sludge investigated by *in situ* probing with specific 16S rRNA targeted oligonucleotides. *FEMS Microbiol Ecol* **25**, 43-61.

Manz, W., Arp, G., Schumann-Kindel, G., Szewzyk, U. & Reitner, J. (2000). Widefield deconvolution epifluorescence microscopy combined with fluorescence *in situ* hybridization reveals the spatial arrangement of bacteria in sponge tissue. *J Microbiol Meth* **40**, 125-134.

Markert, S., Arndt, C., Felbeck, H. & other authors (2007). Physiological proteomics of the uncultured endosymbiont of *Riftia pachyptila*. *Science* **315**, 247-250.

Marti-Renom, M. A., Stuart, A. C., Fiser, A., Sanchez, R., Melo, F. & Sali, A. (2000). Comparative protein structure modeling of genes and genomes. *Annu Rev Biophys Biomol Struct* **29**, 291-325.

Matias, P. M., Pereira, I. A. S., Soares, C. M. & Carrondo, M. A. (2005). Sulphate respiration from hydrogen in *Desulfovibrio* bacteria: astructural biology review. *Prog Biophys Mol Bio* **89**, 292-329.

Maukonen, J., Saarela, M. & Raaska, L. (2006). *Desulfovibrionales*-related bacteria in a paper mill environment as detected with molecular techniques and culture. *J Ind Microbiol Biotechnol* **33**, 45-54.

Meulenberg, R., Scheer, E. J., Pronk, J. T., Hazeu, W., Bos, P. & Kuenen, J. G. (1993). Metabolism of tetrathionate in *Thiobacillus acidophilus*. *FEMS Microbiol Lett* **112**, 167-172.

Miller, W. G., Parker, C. T., Rubenfield, M. & other authors (2007). The complete genome sequence and analysis of the epsilonproteobacterium *Arcobacter butzleri*. *PLoS One*, e1358.

Mira, A., Klasson, L. & Andersson, S. G. E. (2002). Microbial genome evolution: sources of variability. *Curr Opin Microbiol* **5**, 506-512.

Miyake, J. H., Ichiki, S.-I., Tanabe, M., Oda, T., Kurado, H., Nishihara, H. & Sambongi, Y. (2007). Thiosulfate oxidation by a moderately thermophilic hydrogen-oxidizing bacterium, *Hydrogenophilus thermoluteus*. *Arch Microbiol* **188**, 199-204.

Mojzsis, S. J., Coath, C. D., Greenwood, J. P., McKeegan, K. D. & Harrison, T. M. (2003). Mass-independent isotope effects in Archean (2.5 to 3.8 Ga) sedimentary sulfides determined by ion microprobe analysis. *Geochim Cosmochim Ac* **67**, 1635-1658.

Molin, S. & Tolker-Nielsen, T. (2003). Gene transfer occurs with enhanced efficiency in biofilms and induces enhanced stabilisation of the biofilm structure. *Curr Opin Biotech* **14**, 255-261.

Molitor, M., Dahl, C., Molitor, I., Schafer, U., Speich, N., Huber, R., Deutzmann, R. & Trüper, H. G. (1998). A dissimilatory sirohaem-sulfite-reductase-type protein from the hyperthermophilic archaeon *Pyrobaculum islandicum*. *Microbiol-Sgm* **144**, 529-541.

Montalvo, N. F., Mohamed, N. M., Enticknap, J. J. & Hill, R. T. (2005). Novel actinobacteria from marine sponges. *Antonie Leeuwenhoek* **87**, 29-36.

Moran, M. A., Gonzalez, J. M. & Kiene, R. P. (2003). Linking a bacterial taxon to sulfur cycling in the sea: studies of the marine *Roseobacter* group. *Geomicrobiol J* **20**, 375-388.

Moran, M. A., Belas, R., Schell, M. A. & other authors (2007). Ecological genomics of marine Roseobacters. *Appl Environ Microb* **73**, 4559-4569.

Mori, K., Kim, H., Kakegawa, T. & Hanada, S. (2003). A novel lineage of sulfate-reducing microorganisms: *Thermodesulfobiaceae* fam. nov., *Thermodesulfobium narugense*, gen. nov., sp. nov., a new thermophilic isolate from a hot spring. *Extremophiles* **7**, 283-290.

Mori, K., Maruyama, A., Urabe, T., Suzuki, K. & Hanada, S. (2008). *Archaeoglobus infectus* sp. nov., a novel thermophilic, chemolithoheterotrophic archaeon isolated from a deep-sea rock collected at Suiyo Seamount, Izu-Bonin Arc, western Pacific Ocean. *Int J Syst Evol Micr* **58**, 810-816.

Morrow, C. & Boury-Esnault, N. (2000). Redescription of the type species of the genus *Polymastia* Bowerbank, 1864 (Porifera, Demospongiae, Hadromerida). *Zoosystema* **22**, 327-335.

Moussard, H., L'Haridon, S., Tindall, B. J., Banta, A., Schumann, P., Stackebrandt, E., Reysenbach, A. L. & Jeanthon, C. (2004). *Thermodesulfatator indicus* gen. nov., sp nov., a novel thermophilic chemolithoautotrophic sulfate-reducing bacterium isolated from the Central Indian Ridge. *Int J Syst Evol Micr* **54**, 227-233.

Müller, F. H., Bandeiras, T. M., Urich, T., Teixeira, M., Gomes, C. M. & Kletzin, A. (2004). Coupling of the pathway of sulphur oxidation to dioxygen reduction: characterization of a novel membrane-bound thiosulphate:quinone oxidoreductase. *Mol Microbiol* **53**, 1147-1160.

Musat, N., Giere, O., Gieseke, A., Thiermann, F., Amann, R. & Dubilier, N. (2007). Molecular and morphological characterization of the association between bacterial endosymbionts and the marine nematode *Astomonema* sp. from the Bahamas. *Environ Microbiol* **9**, 1345-1353.

Mussmann, M., Richter, M., Lombardot, T., Meyerdierks, A., Kuever, J., Kube, M., Glockner, F. O. & Amann, R. (2005). Clustered genes related to sulfate respiration in uncultured prokaryotes support the theory of their concomitant horizontal transfer. *J Bacteriol* **187**, 7126-7137.

Mussmann, M., Hu, F. Z., Richter, M. & other authors (2007). Insights into the genome of large sulfur bacteria revealed by analysis of single filaments. *Plos Biol* **5**, 1923-1937.

Muyzer, G., Teske, A., Wirsen, C. O. & Jannasch, H. W. (1995). Phylogenetic relationships of *Thiomicrospira* species and their identification in deep-sea hydrothermal vent samples by denaturing gradient gel electrophoresis of 16S rDNA fragments. *Arch Microbiol* **164**, 165-172.

Muyzer, G. & Stams, A. J. M. (2008). The ecology and biotechnology of sulphate-reducing bacteria. *Nat Rev Microbiol* **6**, 441-456.

Myers, J. D. & Kelly, D. J. (2005). A sulphite respiration system in the chemoheterotrophic human pathogen *Campylobacter jejuni*. *Microbiol-Sgm* **151**, 233-242.

Nakagawa, S., Shtaih, Z., Banta, A., Beveridge, T. J., Sako, Y. & Reysenbach, A. L. (2005). *Sulfurihydrogenibium yellowstonense* sp. nov., an extremely thermophilic, facultatively heterotrophic, sulfur-oxidizing bacterium from Yellowstone National Park, and emended descriptions of the genus *Sulfurihydrogenibium, Sulfurihydrogenibium subterraneum* and *Sulfurihydrogenibium azorense*. *Int J Syst Evol Micr* **55**, 2263-2268.

Nakagawa, S., Takaki, Y., Shimamura, S., Reysenbach, A. L., Takai, K. & Horikoshi, K. (2007). Deep-sea vent epsilon-proteobacterial genomes provide insights into emergence of pathogens. *P Natl Acad Sci USA* **104**, 12146-12150.

Nakagawa, T., Hanada, S., Maruyama, A., Marumo, K., T., U. & Fukui, M. (2002). Distribution and diversity of thermophilic sulfate-reducing bacteria within a Cu-Pb-Zn mine. *FEMS Microbiol Ecol* **41**, 199-209.

Nakagawa, T., Nakagawa, S., Inagaki, F., Takai, K. & Horikoshi, K. (2004). Phylogenetic diversity of sulfate-reducing prokaryotes in active deep-sea hydrothermal vent chimney structures. *FEMS Microbiol Lett* **232**, 145-152.

Nelson, D. C. & Fisher, C. R. (1995). Chemoautotrophic and methanoautotrophic endosymbiontic bacteria at deep-sea vents and seeps. In *Deep Sea Hydrothermal Vents*, pp. 125-167. Edited by D. M. Karl: CRC Press.

Nercessian, O., Bienvenu, N., Moreira, D., Prieur, D. & Jeanthon, C. (2005a). Diversity of functional genes of methanogens, methanotrophs and sulfate reducers in deep-sea hydrothermal environments. *Environ Microbiol* **7**, 118-132.

Nercessian, O., Fouquet, Y., Pierre, C., Prieur, D. & Jeanthon, C. (2005b). Diversity of *Bacteria* and *Archaea* associated with a carbonate-rich metalliferous sediment sample from the Rainbow vent field on the Mid-Atlantic Ridge. *Environ Microbiol* **7**, 698-714.

Neutzling, O., Pfleiderer, C. & Trüper, H. G. (1985). Dissimilatory sulfur metabolism in phototrophic non-sulfur bacteria. *J Gen Microbiol* **131**, 791-798.

Newton, I. L. G., Woyke, T., Auchtung, T. A. & other authors (2007). The *Calyptogena magnifica* chemoautotrophic symbiont genome. *Science* **315**, 998-1000.

Nielsen, M. B., Kjeldsen, K. U. & Ingvorsen, K. (2006). *Desulfitibacter alkalitolerans* gen. nov., sp. nov., an anaerobic, alkalitolerant, sulfite-reducing bacterium isolated from a district heating plant. *Int J Syst Evol Micr* **56**, 2831-2836.

Nisbet, E. G. & Fowler, C. M. R. (1999). Archaean metabolic evolution of microbial mats. *P Roy Soc Lond B Bio* **266**, 2375-2382.

Nisbet, E. G. & Sleep, N. H. (2001). The habitat and nature of early life. *Nature* **409**, 1083-1091.

Nisbet, E. G. & Fowler, C. M. R. (2003). The early history of life. In *Treatise on Geochemistry*, pp. 1-39.

Novichkov, P. S., Omelchenko, M. V., Gelfand, M. S., Mironov, A. A., Wolf, Y. I. & Koonin, E. V. (2004). Genome-wide molecular clock and horizontal gene transfer in bacterial evolution. *J Bacteriol* **186**, 6575-6585.

Nunoura, T., Miyazaki, M., Suzuki, Y., Takai, K. & Horikoshi, K. (2008). *Hydrogenivirga okinawensis* sp. nov., a thermophilic sulfur-oxidizing chemolithoautotroph isolated from a deep-sea hydrothermal field, Southern Okinawa Trough. *Int J Syst Evol Micr* **58**, 676-681.

O`Mullan, G. D. & Ward, B. B. (2005). Relationship of temporal and spatial variabilities of ammonia-oxidizing bacteria to nitrification rates in Monterey Bay, California. *Appl Environ Microb* **71**, 697-705.

Ochman, H. & Davalos, L. M. (2006). The nature and dynamics of bacterial genomes. *Science* **311**, 1730-1733.

Odintsova, E., Jannasch, H., Mamone, J. & Langworthy, T. (1996). *Thermothrix azorensis* sp. nov., an obligately chemolithoautotrophic, sulfur-oxidizing, thermophilic bacterium. *Int J Syst Bacteriol* **46**, 422-428.

Odintsova, E. V., Wood, A. P. & Kelly, D. P. (1993). Chemolithoautotrophic growth of *Thiothrix ramosa*. *Arch Microbiol* **160**, 152-157.

Omelchenko, M., Makarova, K., Wolf, Y., Rogozin, I. & Koonin, E. (2003). Evolution of mosaic operons by horizontal gene transfer and gene displacement in situ. *Genome Biol* **4**, R55.

Ono, S., Eigenbrode, J. L., Pavlov, A. A., Kharecha, P., Rumble, D., Kasting, J. F. & Freeman, K. H. (2003). New insights into Archean sulfur cycle from mass-independent sulfur isotope records from the Hamersley Basin, Australia. *Earth Planet Sc Lett* **213**, 15-30.

Overmann, J. (2000). The family *Chlorobiaceae*. In *The prokaryotes An evolving electronic resource for the microbial community*. Edited by M. Dworkin, E. Falkow, E. Rosenberg, K.-H. Schleifer & E. Stackebrandt. New York, N. Y.: Springer Verlag.

Pal, C., Papp, B. & Lercher, M. J. (2005). Adaptive evolution of bacterial metabolic networks by horizontal gene transfer. *Nat Genet* **37**, 1372-1375.

Pattaragulwanit, K., Brune, D. C., Trüper, H. G. & Dahl, C. (1998). Molecular genetic evidence for extracytoplasmic localization of sulfur globules in *Chromatium vinosum*. *Arch Microbiol* **169**, 434-444.

Pavlov, A. A. & Kasting, J. F. (2002). Mass-independent fractionation of sulfur isotopes in Archean sediments: Strong evidence for an anoxic Archean atmosphere. *Astrobiology* **2**, 27-41.

Pereira, I. A. C. (2008). Respiratory membrane complexes of *Desulfovibrio*. In *Microbial sulfur metabolism*, pp. 24-35. Edited by C. Dahl & C. G. Friedrich. Berlin Heidelberg: Springer Verlag.

Petri, R., Podgorsek, L. & Imhoff, J. F. (2001). Phylogeny and distribution of the *soxB* gene among thiosulfate-oxidizing bacteria. *FEMS Microbiol Lett* **197**, 171-178.

Philippot, P., Van Zuilen, M., Lepot, K., Thomazo, C., Farquhar, J. & Van Kranendonk, M. J. (2007). Early Archaean microorganisms preferred elemental sulfur, not sulfate. *Science* **317**, 1534-1537.

Philippot, P., Van Zuilen, M., Lepot, K., Thomazo, C., Farquhar, J. & Van Kranendonk, M. J. (2008). Response to comment on "Early Archaean microorganisms preferred elemental sulfur, not sulfate". *Science* **319**.

Pikuta, E. V., Hoover, R. B., Bej, A. K., Marsic, D., Whitman, W. B., Cleland, D. & Krader, P. (2003). *Desulfonatronum thiodismutans* sp. nov., a novel alcaliphilic, sulfate-reducing bacterium capable of lithoautotrophic growth. *Int J Syst Evol Micr* **53**, 1327-1332.

Pires, R. H., Lourenco, A. I., Morais, F., Teixeira, M., Xavier, A. V., Saraiva, L. M. & Pereira, I. A. C. (2003). A novel membrane-bound respiratory complex from *Desulfovibrio desulfuricans* ATCC 27774. *Bba-Bioenergetics* **1605**, 67-82.

Pires, R. H., Venceslau, S. S., Morais, F., Teixeira, M., Xavier, A. V. & Pereira, I. A. C. (2006). Characterization of the *Desulfovibrio desulfuricans* ATCC 27774 DsrMKJOP complex - A membrane-bound redox complex involved in the sulfate respiratory pathway. *Biochemistry* **45**, 249-262.

Polz, M. F. & Cavanaugh, C. M. (1998). Bias in template-to-product ratios in multitemplate PCR. *Appl Environ Microb* **64**, 3724-3730.

Pott, A. S. & Dahl, C. (1998). Sirohaem sulfite reductase and other proteins encoded by genes at the *dsr* locus of *Chromatium vinosum* are involved in the oxidation of intracellular sulfur. *Microbiology* **144**, 1881-1894.

Poulton, S. W., Fralick, P. W. & Canfield, D. E. (2004). The transition to a sulphidic ocean similar to 1.84 billion years ago. *Nature* **431**, 173-177.

Prange, A., Chauvistre, R., Modrow, H., Hormes, J., Trüper, H. G. & Dahl, C. (2002). Quantitative speciation of sulfur in bacterial sulfur globules: X-ray absorption spectroscopy reveals at least three different species of sulfur. *Microbiology* **148**, 267-276.

Qiu, L. Y., Sekiguchi, Y., Imachi, H., Kamagata, Y., Tseng, I. C., Cheng, S. S., Ohashi, A. & Harada, H. (2003). *Sporotomaculum syntrophicum* sp. nov., a novel anaerobic, syntrophic benzoate-degrading bacterium isolated from methanogenic sludge treating wastewater from terephthalate manufacturing. *Arch Microbiol* **179**, 242-249.

Quentmeier, A. & Friedrich, C. G. (2001). The cysteine residue of the SoxY protein as the active site of protein-bound sulfur oxidation of *Paracoccus pantotrophus* GB17. *FEBS Lett* **503**, 168-172.

Quentmeier, A., Hellwig, P., Bardischewsky, F., Grelle, G., Kraft, R. & Friedrich, C. G. (2003). Sulfur oxidation in *Paracoccus pantotrophus*: interaction of the sulfur-binding protein SoxYZ with the dimanganese SoxB protein. *Biochem Bioph Res Co* **312**, 1011-1018.

Rabus, R., Hansen, T. A. & Widdel, F. (2000). Dissimilatory sulfate- and sulfur-reducing prokaryotes. In *The prokaryotes: an evolving electronic database for the microbiological community*. Edited by M. Dworkin, K.-H. Schleifer & E. Stackebrandt. New York, N. Y.: Springer Verlag.

Rappe, M. S., Connon, S. A., Vergin, K. L. & Giovannoni, S. J. (2002). Cultivation of the ubiquitous SAR11 marine bacterioplankton clade. *Nature* **418**, 630-633.

Reichenbecher, W., Kelly, D. P. & Murrell, J. C. (1999). Desulfonation of propanesulfonic acid by *Comamonas acidovorans* strain P53: evidence for an alkanesulfonate sulfonatase and an atypical sulfite dehydrogenase. *Arch Microbiol* **172**, 387-392.

Ridley, C. P., Faulkner, D. J. & Haygood, M. G. (2005). Investigation of *Oscillatoria spongeliae*-dominated bacterial communities in four dictyoceratid sponges. *Appl Environ Microb* **71**, 7366-7375.

Rohwerder, T. & Sand, W. (2003). The sulfane sulfur of persulfides is the actual substrate of the sulfur-oxidizing enzymes from *Acidithiobacillus* and *Acidiphilium* spp. *Microbiology* **149**, 1688-1709.

Rohwerder, T. & Sand, W. (2007). Oxidation of inorganic sulfur compounds in acidophilic prokaryotes. **7**, 301-309.

Rother, D., Henrich, H. J., Quentmeier, A., Bardischewsky, F. & Friedrich, C. G. (2001). Novel genes of the *sox* gene cluster, mutagenesis of the flavoprotein SoxF, and evidence for a general sulfur-oxidizing system in *Paracoccus pantotrophus* GB17. *J Bacteriol* **183**, 4499-4508.

Rusch, D. B., Halpern, A. L., Sutton, G. & other authors (2007). The Sorcerer II Global Ocean Sampling expedition: Northwest Atlantic through Eastern Tropical Pacific. *Plos Biol* **5**, 398-431.

Sabehi, G., Loy, A., Jung, K. H., Partha, R., Spudich, J. L., Isaacson, T., Hirschberg, J., Wagner, M. & Beja, O. (2005). New insights into metabolic properties of marine bacteria encoding proteorhodopsins. *Plos Biol* **3**, 1409-1417.

Sako, Y., Nunoura, T. & Uchida, A. (2001). *Pyrobaculum oguniense* sp. nov., a novel facultatively aerobic and hyperthermophilic archaeon growing at up to 97 °C. *Int J Syst Evol Micr* **51**, 303-309.

Sanchez, O., Ferrera, I., Dahl, C. & Mas, J. (2001). In vivo role of adenosine-5 '-phosphosulfate reductase in the purple sulfur bacterium *Allochromatium vinosum*. *Arch Microbiol* **176**, 301-305.

Sander, J., Engels-Schwarzlose, S. & Dahl, C. (2006). Importance of the DsrMKJOP complex for sulfur oxidation in *Allochromatium vinosum* and phylogenetic analysis of related complexes in other prokaryotes. *Arch Microbiol* **186**, 357-366.

Sauve, V., Bruno, S., Berks, B. C. & Hemmings, A. M. (2007). The SoxYZ complex carries sulfur cycle intermediates oon a peptide swinging arm. *J Biol Chem* **282**, 23194-23204.

Schedel, M. & Trüper, H. G. (1979). Purification of *Thiobacillus denitrificans* siroheme sulfite reductase and investigation of some molecular and catalytic properties. *Biochim Biophys Acta* **568**, 454-466.

Schedel, M., Vanselow, M. & Trüper, H. G. (1979). Siroheme sulfite reductase isolated from *Chromatium vinosum* - purification and investigation of some of its molecular and catalytic properties. *Arch Microbiol* **121**, 29-36.

Schedel, M. & Trüper, H. G. (1980). Anaerobic oxidation of thiosulfate and elemental sulfur in *Thiobacillus denitrificans*. *Arch Microbiol* **124**, 205-210.

Schiffer, A., Fritz, G., Kroneck, P. M. H. & Ermler, U. (2006). Reaction mechanism of the iron-sulfur flavoenzyme adenosine-5 '-phosphosulfate reductase based on the structural characterization of different enzymatic states. *Biochemistry* **45**, 2960-2967.

Schiffer, A., Parey, K., Warkentin, E., Diederichs, K., Huber, H., Stetter, K. O., Kroneck, P. M. H. & Ermler, U. (2008). Structure of the dissimilatory sulfite reductase from the hyperthermophilic archaeon *Archaeoglobus fulgidus*. *J Mol Biol* **379**, 1063-1074.

Schippers, A. & Jørgensen, B. B. (2001). Oxidation of pyrite and iron sulfide by manganese dioxide in marine sediments. *Geochim Cosmochim Ac* **65**, 915-922.

Schippers, A. & Jørgensen, B. B. (2002). Biogeochemistry of pyrite and iron sulfide oxidation in marine sediments. *Geochim Cosmochim Ac* **66**, 85-92.

Schirmer, A., Gadkari, R., Reeves, C. D., Ibrahim, F., DeLong, E. F. & Hutchinson, C. R. (2005). Metagenomic analysis reveals diverse polyketide synthase gene clusters in microorganisms associated with the marine sponge *Discodermia dissoluta*. *Appl Environ Microb* **71**, 4840-4849.

Schmalenberger, A., Drake, H. L. & Küsel, K. (2007). High unique diversity of sulfate-reducing prokaryotes characterized in a depth gradient in an acidic fen. *Environ Microbiol* **9**, 1317-1328.

Schmidt, E. W., Obraztsova, A. Y., Davidson, S. K., Faulkner, D. J. & Haygood, M. G. (2000). Identification of the antifungal peptide-containing symbiont of the marine sponge *Theonella swinhoei* as a novel deltaproteobacterium, "*Candidatus* Entotheonella palauensis". *Mar Biol* **136**, 969-977.

Schmitt, S., Weisz, J. B., Lindquist, N. & Hentschel, U. (2007). Vertical transmission of a phylogenetically complex microbial consortium in the vivparous sponge *Ircinia felix*. *Appl Environ Microb* **73**, 2067-2078.

Schwenn, J. D. & Biere, M. (1979). APS-reductase activity in the chromatophores of *Chromatium vinosum* strain D. *FEMS Microbiol Lett* **6**, 19-22.

Scott, C., Lyons, T. W., Bekker, A., Shen, Y., Poulton, S. W., Chu, X. & Anbar, A. D. (2008). Tracing the stepwise oxygenation of the Proterozoic ocean. *Nature* **452**, 456-U455.

Scott, K. M., Sievert, S. M., Abril, F. N. & other authors (2006). The genome of deep-sea vent chemolithoautotroph *Thiomicrospira crunogena* XCL-2. *Plos Biol* **4**, 2196-2212.

Sekiguchi, Y., Kamagata, Y., Syutsubo, K., Ohashi, A., Harada, H. & Nakamura, K. (1998). Phylogenetic diversity of mesophilic and thermophilic granular sludges determined by 16S rRNA analysis. *Microbiology* **144**, 2655-2665.

Sharp, K. H., Eam, B., Faulkner, D. J. & Haygood, M. G. (2007). Vertical transmission of diverse microbes in the tropical sponge *Corticium* sp. *Appl Environ Microb* **73**, 622-629.

Shen, Y., Knoll, A. H. & Walter, M. R. (2003). Evidence for low sulphate and anoxia in a mid-Proterozoic marine basin. *Nature* **423**, 632-635.

Shen, Y. A., Buick, R. & Canfield, D. E. (2001). Isotopic evidence for microbial sulphate reduction in the early Archaean era. *Nature* **410**, 77-81.

Shen, Y. N. & Buick, R. (2004). The antiquity of microbial sulfate reduction. *Earth-Sci Rev* **64**, 243-272.

Siegel, L. M. (1975). Biochemistry of sulfur cycle. In *Metabolic pathways VII: Metabolism of sulfur compounds*, pp. 217-286. Edited by D. M. Greenberg. London: Academic Press London.

Sievert, S. M., Heidorn, T. & Kuever, J. (2000). *Halothiobacillus kellyi* sp. nov., a mesophilic, obligately chemolithoautotrophic, sulfur-oxidizing bacterium isolated from a shallow-water hydrothermal vent in the Aegean Sea, and emended description of the genus *Halothiobacillus*. *Int J Syst Evol Micr* **50**, 1229-1237.

Sievert, S. M., Scott, K. M., Klotz, M. G. & other authors (2008). Genome of the epsilonproteobacterial chemolithoautotroph *Sulfurimonas denitrificans*. *Appl Environ Microb* **74**, 1145-1156.

Simsek, M. & Adnan, H. (2000). Effect of single mismatches at 3`-end of primers on polymerase chain reaction. *Med Sci* **2**, 11-14.

Skirnisdottir, S., Hreggvidsson, G. O., Holst, O. & Kristjansson, J. K. (2001). Isolation and characterization of a mixotrophic sulfur-oxidizing *Thermus scotoductus*. *Extremophiles* **5**, 45-51.

Slobodkin, A. I., Sokolova, T. G., Lysenko, A. M. & Wiegel, J. (2006). Reclassification of *Thermoterrabacterium ferrireducens* as *Carboxydothermus ferrireducens* comb. nov., and emended description of the genus *Carboxydothermus*. *Int J Syst Evol Micr* **56**, 2349-2351.

Sonne-Hansen, J. & Ahring, B. K. (1999). *Thermodesulfobacterium hveragerdense* sp. nov., and *Thermodesulfovibrio islandicus* sp. nov., two thermophilic sulfate reducing bacteria isolated from a Icelandic hot spring. *Syst Appl Microbiol* **22**, 559-564.

Sorensen, S. J., Bailey, M., Hansen, L. H., Kroer, N. & Wuertz, S. (2005). Studying plasmid horizontal transfer in situ: A critical review. *Nat Rev Microbiol* **3**, 700-710.

Sorokin, D. Y. (1995). *Sulfitobacter pontiacus* gen. nov., sp. nov. - a new heterotrophic bacterium from the Black Sea, specialized on sulfite oxidation. *Microbiology* **64**, 295-305.

Sorokin, D. Y., Robertson, L. A. & Kuenen, J. G. (1996). Sulfur cycling in *Catenococcus thiocyclus*. *FEMS Microbiol Ecol* **19**, 117-125.

Sorokin, D. Y., Tourova, T. P., Kuznetsov, B. B., Bryantseva, I. A. & Gorlenko, V. M. (2000). *Roseinatronobacter thiooxidans* gen. nov., sp. nov., a new alkaliphilic aerobic bacteriochlorophyll-a-containing bacteria from a soda lake. *Microbiology (Moscow)* **69**, 89-97.

Sorokin, D. Y. (2003). Oxidation of inorganic sulfur compounds by obligately organotrophic bacteria. *Microbiology* **72**, 641-653.

Sorokin, D. Y. & Kuenen, G. J. (2005). Haloalkaliphilic sulfur-oxidizing bacteria in soda lakes. *FEMS Microbiol Rev* **29**, 685-702.

Sorokin, D. Y., Tourova, T. P., Lysenko, A. M. & Muyzer, G. (2006). Diversity of culturable halophilic sulfur-oxidizing bacteria in hypersaline habitats. *Microbiology* **152**, 3013-3023.

Sorokin, D. Y. (2008). Diversity of halophilic sulfur-oxidizing bacteria in hypersaline habitats. In *Microbial sulfur metabolism*, pp. 225-237. Edited by C. Dahl & C. G. Friedrich. Berlin Heidelberg: Springer Verlag.

Speich, N. & Trüper, H. G. (1988). Adenylylsulfate reductase in a dissimilatory sulfate-reducing archaebacterium. *J Gen Microbiol* **134**, 1419-1425.

Speich, N., Dahl, C., Heisig, P., Klein, A., Lottspeich, F., Stetter, K. O. & Trüper, H. G. (1994). Adenylylsulphate reductase from the sulfate-reducing archaeon *Archaeoglobus fulgidus* - cloning and characterization of the genes and comparison of the enzyme with other iron-sulfur flavoproteins. *Microbiology* **140**, 1273-1284.

Sperling, D., Kappler, U., Wynen, A., Dahl, C. & Trüper, H. G. (1998). Dissimilatory ATP sulfurylase from the hyperthermophilic sulfate reducer *Archaeoglobus fulgidus* belongs to the group of homo-oligomeric ATP sulfurylases. *FEMS Microbiol Lett* **162**, 257-264.

Sperling, D., Kappler, U., Trüper, H. G. & Dahl, C. (2001). Dissimilatory ATP sulfurylase from *Archaeoglobus fulgidus*. In *Methods Enzymol*, pp. 419-427.

Spring, S., Kampfer, P. & Schleifer, K. (2001). *Limnobacter thiooxidans* gen. nov., sp. nov., a novel thiosulfate-oxidizing bacterium isolated from freshwater lake sediment. *Int J Syst Evol Microbiol* **51**, 1463-1470.

Spring, S. & Rosenzweig, F. (2005). The genera *Desulfitobacterium* and *Desulfosporosinus*: Taxonomy. In *The Prokaryotes - an evolving electronic resource for the microbiological community*. Edited by M. Dworkin, S. Falkow, E. Rosenberg, K.-H. Schleifer & E. Stackebrandt. Heidelberg: Springer Verlag.

Srinivas, T. N. R., Kumar, P. A., Sasikala, C. & Ramana, C. V. (2007). *Rhodovulum imhoffii* sp. nov. *Int J Syst Evol Microbiol* **57**, 228-232.

Stahl, D. A., Loy, A. & Wagner, M. (2007). Molecular strategies for studies of natural populations of sulphate-reducing microorganisms. In *Sulphate-reducing bacteria: environmental and engineered systems*, pp. 39-115. Edited by L. L. Barton & W. A. Hamilton. New York: Cambridge University Press.

Stahlmann, J., Warthmann, R. & Cypionka, H. (1991). Na^+-dependent accumulation of sulfate and thiosulfate in marine sulfate-reducing bacteria. *Arch Microbiol* **155**, 554-558.

Steudel, R. (1996). Mechanism for the formation of elemental sulfur from aqueous sulfide in chemical and microbiological desulfurization processes. *Industrial & Engineering Chemistry Research* **35**, 1417-1423.

Stingl, U., Tripp, H. J. & Giovannoni, S. J. (2007). Improvements of high-throughput culturing yielded novel SAR11 strains and other abundant marine bacteria from the Oregon coast and the Bermuda Atlantic Time Series study site. *Isme Journal* **1**, 361-371.

Stojanowic, A., Mander, G. J., Duin, E. C. & Hedderich, R. (2003). Physiological role of the F_{420}-non-reducing hydrogenase (Mvh) from *Methanothermobacter marburgensis*. *Arch Microbiol* **180**, 194-203.

Straub, K. L., Rainey, F. A. & Widdel, F. (1999). *Rhodovulum iodosum* sp. nov, and *Rhodovulum robiginosum* sp. nov., two new marine phototrophic ferrous-iron-oxidizing purple bacteria. *Int J Syst Bacteriol* **49**, 729-735.

Strauss, H. (2003). Sulphur isotopes and the early Archaean sulphur cycle. *Precambrian Res* **126**, 349-361.

Stubner, S. (2002). Enumeration of 16S rDNA of *Desulfotomaculum* lineage I in rice field soil by real-time PCR with the. *J Microbiol Meth* **50**, 155-164.

Suzuki, M. T. & Giovannoni, S. J. (1996). Bias caused by template annealing in the amplification of mixtures of 16S rRNA genes by PCR. *Appl Environ Microb* **62**, 625-630.

Szewzyk, R. & Pfennig, N. (1987). Complete oxidation of catechol by the strictly anaerobic sulfate-reducing *Desulfobacterium catecholicum* sp. nov. *Arch Microbiol* **147**, 163-168.

Taguchi, Y., Sugishima, M. & Fukuyama, K. (2004). Crystal structure of a novel zinc-binding ATP sulfurylase from *Thermus thermophilus* HB8. *Biochemistry* **43**, 4111-4118.

Takai, K., Campbell, B. J., Cary, S. C. & other authors (2005). Enzymatic and genetic characterization of carbon and energy metabolisms by deep-sea hydrothermal chemolithoautotrophic isolates of *Epsilonproteobacteria*. *Appl Environ Microb* **71**, 7310-7320.

Takai, K., Suzuki, M., Nakagawa, S., Miyazaki, M., Suzuki, Y., Inagaki, F. & Horikoshi, K. (2006). *Sulfurimonas paravinellae* sp. nov., a novel mesophilic, hydrogen- and sulfur-oxidizing chemolithoautotroph within the *Epsilonproteobacteria* isolated from a deep-sea hydrothermal vent polychaete nest, reclassification of *Thiomicrospira denitrificans* as *Sulfurimonas denitrificans* comb. nov. and emended description of the genus *Sulfurimonas*. *Int J Syst Evol Micr* **56**, 1725-1733.

Taylor, B. F. (1994). Adenylylsulfate reductases from Thiobacilli. In *Methods Enzymol*, pp. 393-400. San Diego, California: Academic Press.

Taylor, M. W., Schupp, P. J., Dahllof, I., Kjelleberg, S. & Steinberg, P. D. (2004). Host specificity in marine sponge-associated bacteria, and potential implications for marine microbial ecology. *Environ Microbiol* **6**, 121-130.

Taylor, M. W., Radax, R., Steger, D. & Wagner, M. (2007). Sponge-associated microorganisms: evolution, ecology, and biotechnological potential. *Microbiol Mol Biol Rev* **71**, 295-347.

Teske, A., Brinkhoff, T., Muyzer, G., Moser, D. P., Rethmeier, J. & Jannasch, H. W. (2000). Diversity of thiosulfate-oxidizing bacteria from marine sediments and hydrothermal vents. *Appl Environ Microb* **66**, 3125-3133.

Teske, A. & Nelson, D. C. (2004). The genera *Beggiatoa* and *Thioploca*. In *The prokaryotes An evolving electronic resource for the microbial community*. Edited by M. Dworkin, E. Falkow, E. Rosenberg, K.-H. Schleifer & E. Stackebrandt. New York, N. Y.: Springer Verlag.

Thamdrup, B. & Canfield, D. E. (1996). Pathways of carbon oxidation in continental margin sediments off central Chile. *Limnol Oceanogr* **41**, 1629-1650.

Thauer, R. K., Stackebrandt, E. & Hamilton, W. A. (2007). Energy metabolism and phylogenetic diversity of sulphate-reducing bacteria. In *Sulphate-reducing bacteria: environmental and engineered systems*, pp. 1-37. Edited by L. L. Barton & W. A. Hamilton. New York: Cambridge University Press.

Thiel, V., Leininger, S., Schmaljohann, R., Brümmer, F. & Imhoff, J. F. (2007a). Sponge-specific bacterial associations of the Mediterranean sponge *Chondrilla nucula* (Demospongiae, Tetractinomorpha). *Microb Ecol*.

Thiel, V., Neulinger, S. C., Staufenberger, T., Schmaljohann, R. & Imhoff, J. F. (2007b). Spatial distribution of sponge-associated bacteria in the Mediterranean sponge *Tethya aurantium*. *FEMS Microbiol Ecol* **59**, 47-63.

Thiele, H. H. (1968). Sulfur metabolism in *Thiorhodaceae*. V. Enzymes of sulfur metabolism in *Thiocapsa floridana* and *Chromatium* species. *Antonie Leeuwenhoek* **34**, 350-356.

Thomas, C. M. & Nielsen, K. M. (2005). Mechanisms of, and barriers to, horizontal gene transfer between bacteria. *Nat Rev Microbiol* **3**, 711-721.

Thomsen, T. R., Finster, K. & Ramsing, N. B. (2001). Biogeochemical and molecular signatures of anaerobic methane oxidation in a marine sediment. *Appl Environ Microb* **67**, 1646-1656.

Thorsen, M. S. (1999). Abundance and biomass of the gut-living microorganisms (bacteria, protozoa and fungi) in the irregular sea urchin *Echinocardium cordatum* (Spatangoida: Echinodermata). *Mar Biol* **133**, 353-360.

Thorsen, M. S., Wieland, A., Ploug, A., Kragelund, C. & Nielsen, P. H. (2003). Distribution, identity and activity of symbiotic bacteria in anoxic aggregates from the hindgut of the sea urchin *Echinocardium cordatum*. *Ophelia* **57**, 1-12.

Tice, M. M. & Lowe, D. R. (2004). Photosynthetic microbial mats in the 3,416-Myr-old ocean. *Nature* **431**, 549-552.

Tonolla, M., Peduzzi, S., Demarta, A., Peduzzi, R. & Hahn, D. (2004). Phototrophic sulfur and sulfate-reducing bacteria in the chemocline of meromictic Lake Cadagno, Switzerland. *Journal of Limnology* **63**, 161-170.

Tourova, T. P., Spiridonova, E. M., Berg, I. A., Slobodova, N. V., Boulygina, E. S. & Sorokin, D. Y. (2007). Phylogeny and evolution of the family *Ectothiorhodospiraceae* based on comparison of 16S rRNA, *cbbL* and *nifH* gene sequences. *Int J Syst Evol Micr* **57**, 2387-2398.

Tripp, H. J., Kitner, J. B., Schwalbach, M. S., Dacey, J. W. H., Wilhelm, L. J. & Giovannoni, S. J. (2008). SAR11 marine bacteria require exogenous reduced sulphur for growth. **452**, 741-744.

Trudinger, P. A. (1979). The biological sulfur cycle. In *Biogeochemical cycling of mineral-forming elements*, pp. 293-313. Edited by P. A. Trudinger & D. J. Swain. Amsterdam: Elvesier.

Trüper, H. G. & Pfennig, N. (1966). Sulphur metabolism in *Thiorhodaceae*. III. Storage and turnover of thiosulphate sulphur in *Thiocapsa floridana* and *Chromatium* species. *Antonie Leeuwenhoek* **32**, 261-276.

Trüper, H. G. & Rogers, L. A. (1971). Purification and properties of adenylyl sulfate reductase from phototrophic sulfur bacterium, *Thiocapsa roseopersicina*. *J Bacteriol* **108**, 1112-&.

Trüper, H. G. & Fischer, U. (1982). Anaerobic oxidation of sulfur-compounds as electron-donors for bacterial photosynthesis. *Philos T Roy Soc B* **298**, 529-542.

Tuttle, J. H. & Jannasch, H. W. (1976). Microbial utilization of thiosulfate in deep-sea. *Limnol Oceanogr* **21**, 697-701.

Valenzuela, L., Chi, A., Beard, S., Shabanowitz, J., Hunt, D. F. & Jerez, C. A. (2008). Differential expression proteomics for the study of sulfur metabolism in the chemolithoautotrophic *Acidithiobacillus ferrooxidans*. In *Microbial sulfur metabolism*, pp. 77-86. Edited by C. Dahl & C. G. Friedrich. Berlin Heidelberg: Springer Verlag.

van den Ende, F. P., Laverman, A. M. & van Gemerden, H. (1996). Coexistence of aerobic chemotrophic and anaerobic phototrophic sulfur bacteria under oxygen limitation. *FEMS Microbiol Ecol* **19**, 141-151.

van den Ende, F. P., Meier, J. & van Gemerden, H. (1997). Syntrophic growth of sulfate-reducing bacteria and colorless sulfur bacteria during oxygen limitation. *FEMS Microbiol Ecol* **23**, 65-80.

van der Maarel, M. J. E. C., van Bergeijk, S., van Werkhoven, A. F., Laverman, A. M., Meijer, W. G., Stam, W. T. & Hansen, T. (1996). Cleavage of dimethylsulfoniopropionate and reduction of acrylate by *Desulfovibrio acrylicus*. *Arch Microbiol* **166**, 109-115.

Vandamme, P., Gillis, M., de Vos, W. M., Kersters, K. & Swings, J. (1996). Polyphasic taxonomy, a consensus approach to bacterial systematics. *Microbiol Rev* **60**, 407-438.

Venter, J. C., Remington, K., Heidelberg, J. F. & other authors (2004). Environmental genome shotgun sequencing of the Sargasso Sea. *Science* **304**, 66-74.

Verhagen, M. F. J. M., Kooter, I. M., Wolbert, R. B. G. & Hagen, W. R. (1994). On the iron-sulfur cluster of adenosine phosphosulfate reductase from *Desulfovibrio vulgaris* (Hildenborough). *Eur J Biochem* **221**, 831-837.

Verte, F., Kostanjevecki, V., De Smet, L., Meyer, T. E., Cusanovich, M. A. & Van Beeumen, J. J. (2002). Identification of a thiosulfate utilization gene cluster from the green phototrophic bacterium *Chlorobium limicola*. *Biochemistry* **41**, 2932-2945.

Vila-Costa, M., Pinhassi, J., Alonso, C., Pernthaler, J. & Simo, R. (2007). An annual cycle of dimethylsulfoniopropionate- sulfur and leucine assimilating bacterioplankton in the coastal NW Mediterranean. *Environ Microbiol* **9**, 2451-2463.

Visscher, P. T., Vandenende, F. P., Schaub, B. E. M. & Vangemerden, H. (1992). Competition between anoxygenic phototrophic bacteria and colorless sulfur bacteria in a microbial mat. *FEMS Microbiol Ecol* **101**, 51-58.

Visser, J. M., deJong, G. A. H., Robertson, L. A. & Kuenen, J. G. (1997). A novel membrane-bound flavocytochrome c sulfide dehydrogenase from the colourless sulfur bacterium *Thiobacillus* sp. W5. *Arch Microbiol* **167**, 295-301.

Vogl, K., Glaeser, J., Pfannes, K. R., Wanner, G. & Overmann, R. (2006). *Chlorobium chlorochromatii* sp. nov., a symbiotic green sulfur bacterium isolated from the phototrophic consortium "*Chlorochromatium aggregatum*". *Arch Microbiol* **185**, 363-372.

von Wintzingerode, F., Gobel, U. B. & Stackebrandt, E. (1997). Determination of microbial diversity in environmental samples: pitfalls of PCR-based rRNA analysis. *FEMS Microbiol Rev* **21**, 213-229.

Wagner, M., Roger, A. J., Flax, J. L., Brusseau, G. A. & Stahl, D. A. (1998). Phylogeny of dissimilatory sulfite reductases supports an early origin of sulfate respiration. *J Bacteriol* **180**, 2975-2982.

Wagner, M., Loy, A., Klein, M., Lee, N., Ramsing, N. B., Stahl, D. A. & Friedrich, M. W. (2005). Functional marker genes for identification of sulfate-reducing prokaryotes. *Environ Microbiol* **397**, 469-489.

Wakai, S., Kikumoto, M., Kanao, T. & Kamimura, K. (2004). Involvement of sulfide:quinone oxidoreductase in sulfur oxidation of an acidophilic iron-oxidizing bacterium, *Acidithiobacillus ferrooxidans* NASF-1. *Biosci Biotech Bioch* **68**, 2519-2528.

Weber, M., Suter, M., Brunold, C. & Kopriva, S. (2000). Sulfate assimilation in higher plants - characterization of a stable intermediate in the adenosine-5 '-phosphosulfate reductase reaction. *Eur J Biochem* **267**, 3647-3653.

Webster, N. S., Negri, A. P., Munro, M. & Battershill, C. N. (2004). Diverse microbial communities inhabit Antarctic sponges. *Environ Microbiol* **6**, 288-300.

Wehrl, M., Steinert, M. & Hentschel, U. (2007). Bacterial uptake by the marine sponge *Aplysina aerophoba*. *Microb Ecol* **53**, 355-366.

Weisz, J. B., Hentschel, U., Lindquist, N. & Martens, C. S. (2007). Linking abundance and diversity of sponge-associated microbial communities to metabolic differences in host sponges. *Mar Biol* **152**, 475-483.

Widdel, F. (1992). The genus *Desulfotomaculum*. In *The Prokaryotes*, pp. 1792-1799. Edited by A. Balows, H. G. Trüper, M. Dworkin, W. Harder & K.-H. Schleifer. New York: Springer Verlag.

Widdel, F. & Bak, F. (1992). Gram-negative mesophilic sulfate-reducing bacteria. In *The Prokaryotes*, pp. 3352-3378. Edited by A. Balows, H. G. Trüper, M. Dworkin, W. Harder & K.-H. Schleifer. New York: Springer Verlag.

Widdel, F., Schnell, S., Heising, S., Ehrenreich, A., Assmus, B. & Schink, B. (1993). Ferrous iron oxidation by anoxygenic phototrophic bacteria. *Nature* **362**, 834-836.

Widdel, F., Musat, F., Knittel, K. & Galushko, A. (2007). Anaerobic degradation of hydrocarbons with sulphate as electron acceptor. In *Sulphate-reducing bacteria: environmental and engineered systems*, pp. 265-303. Edited by L. L. Barton & W. A. Hamilton. New York: Cambridge University Press.

Wieringa, E. B. A., Overmann, J. & Cypionka, H. (2000). Detection of abundant sulphate-reducing bacteria in marine oxic sediment layers by a combined cultivation and molecular approach. *Environ Microbiol* **2**, 417-427.

Williams, S. J., Senaratne, R. H., Mougous, J. D., Riley, L. W. & Bertozzi, C. R. (2002). 5 '-Adenosinephosphosulfate lies at a metabolic branch point in mycobacteria. *J Biol Chem* **277**, 32606-32615.

Wirsen, C. O., Sievert, S. M., Cavanaugh, C. M., Molyneaux, S. J., Ahmad, A., Taylor, L. T., DeLong, E. F. & Taylor, C. D. (2002). Characterization of an autotrophic sulfide-oxidizing marine *Arcobacter* sp. that produces filamentous sulfur. *Appl Environ Microb* **68**, 316-325.

Woyke, T., Teeling, H., Ivanova, N. N. & other authors (2006). Symbiosis insights through metagenomic analysis of a microbial consortium. *Nature* **443**, 950-955.

Yooseph, S., Sutton, G., Rusch, D. B. & other authors (2007). The Sorcerer II Global Ocean Sampling expedition: Expanding the universe of protein families. *Plos Biol* **5**, 432-466.

Yu, Z., Lansdon, E. B., Segel, I. H. & Fisher, A. J. (2007). Crystal Structure of the bifunctional ATP Sulfurylase - APS kinase from the chemolithotrophic thermophile *Aquifex aeolicus*. *J Mol Biol* **365**, 732-743.

Yurkov, V. (2000). Aerobic phototrophic bacteria. In *The prokaryotes An evolving electronic resource for the microbial community*. Edited by M. Dworkin, E. Falkow, E. Rosenberg, K.-H. Schleifer & E. Stackebrandt. New York, N. Y.: Springer Verlag.

Yurkov, V. V. & Beatty, J. T. (1998). Aerobic anoxygenic phototrophic bacteria. *Microbiol Mol Biol Rev* **62**, 695-724.

Zaar, A., Fuchs, G., Golecki, J. R. & Overmann, J. (2003). A new purple sulfur bacterium isolated from a littoral microbial mat, *Thiorhodococcus drewsii* sp. nov. *Arch Microbiol* **179**, 174-183.

Zaneveld, J. R., Nemergut, D. R. & Knight, R. (2008). Are all horizontal gene transfers created equal? Prospects for mechanism-based studies of HGT patterns. *Microbiol-Sgm* **154**, 1-15.

Zhaxybayeva, O. & Gogarten, J. P. (2004). Cladogenesis, coalescence and the evolution of the three domains of life. *Trends Genet* **20**, 182-187.

Zhaxybayeva, O., Lapierre, P. & Gogarten, J. P. (2004). Genome mosaicism and organismal lineages. *Trends Genet* **20**, 254-260.

Zimmermann, P., Laska, S. & Kletzin, A. (1999). Two modes of sulfite oxidation in the extremely thermophilic and acidophilic archaeon *Acidianus ambivalens*. *Arch Microbiol* **172**, 76-82.

Zinkevich, V. & Beech, I. B. (2000). Screening of sulfate-reducing bacteria in colonoscopy samples from healthy and colitic human gut mucosa. *FEMS Microbiol Ecol* **34**, 147-155.

Zverlov, V., Klein, M., Lücker, S., Friedrich, M. W., Kellermann, J., Stahl, D. A., Loy, A. & Wagner, M. (2005). Lateral gene transfer of dissimilatory (bi)sulfite reductase revisited. *J Bacteriol* **187**, 2203-2208.

4 Publikationen

4.1 Publikationsliste mit Erläuterungen

Diese Dissertation beruht auf den folgenden aufgelisteten Publikationen. Die angefügten Erläuterungen legen den eigenen Beitrag zu der jeweiligen Arbeit dar.

1. **Phylogeny of the alpha and beta subunits of the dissimilatory adenosine-5`-phosposulfate (APS) reductase from sulfate-reducing prokaryotes –origin and evolution of the dissimilatory sulfate-reduction pathway**
   Birte Meyer und Jan Küver (2007) Microbiology. 153, 2026-2044

Entwicklung des Konzeptes mit J. Küver. Durchführung aller mikro- und molekularbiologischen Arbeiten sowie der Sequenzdatenanalyse. Phylogenetische Analyse in Zusammenarbeit mit J. Küver. Erstellung des Manuskriptes unter der redaktionellen Mitarbeit von J. Küver.

2. **Molecular analysis of the distribution and phylogeny of dissimilatory adenosine-5`-phosphosulfate (APS) reductase-encoding genes (*aprBA*) among sulfur-oxidizing prokaryotes**
   Birte Meyer und Jan Küver (2007) Microbiology. 153, 3478-3498

Entwicklung des Konzeptes mit J. Küver. Durchführung aller mikro- und molekularbiologischen Arbeiten (eigenständige Durchführung der Southern Blot-Hybridisierungsversuche nach Einführung durch C. Wawer und O. Grundmann) sowie der Sequenzdatenanalyse. Phylogenetische Analyse in Zusammenarbeit mit J. Küver. Erstellung des Manuskriptes unter der redaktionellen Mitarbeit von J. Küver.

3. **Homology modeling of dissimilatory APS reductases (AprBA) of sulfur-oxidizing and sulfate-reducing prokaryotes**
   Birte Meyer und Jan Küver (2008) PLoS ONE. 3 (1), e1514

Entwicklung des Konzeptes mit J. Küver. Durchführung der Sequenzdatenanalyse und Homologie Modellierung. Phylogenetische Analyse in Zusammenarbeit mit J. Küver. Erstellung des Manuskriptes unter der redaktionellen Mitarbeit von J. Küver.

4. **Molecular analysis of the distribution and phylogeny of the *soxB* gene among sulfur-oxidizing prokaryotes –evolution of the sulfur oxidation enzyme system**
   Birte Meyer und Jan Küver (2007) Environmental Microbiology. 153, 3478-3498

Entwicklung des Konzeptes mit J. Küver. Durchführung aller mikro- und molekularbiologischen Arbeiten sowie der Sequenzdatenanalyse. Phylogenetische Analyse in Zusammenarbeit mit J. Küver. Erstellung des Manuskriptes unter der redaktionellen Mitarbeit von J. Küver.

5. **Molecular analysis of the diversity of sulfate-reducing and sulfur-oxidizing prokaryotes in the environment, using *aprA* as functional marker gene**
   Birte Meyer und Jan Küver (2007) Applied and Environmental Microbiology. 73 (23), 7664-7679

Entwicklung des Konzeptes mit J. Küver. Durchführung aller mikro- und molekularbiologischen Arbeiten sowie der Sequenzdatenanalyse. Phylogenetische Analyse in Zusammenarbeit mit J. Küver. Erstellung des Manuskriptes unter der redaktionellen Mitarbeit von J. Küver.

6. **Phylogenetic diversity and spatial distribution of the microbial community associated with the Caribbean deep-water sponge *Polymastia* cf. *corticata* by 16S rRNA, *aprA*, and *amoA* gene analysis**
   Birte Meyer und Jan Küver (2008) Microbial Ecology. 56, 306-321

Entwicklung des Konzeptes mit J. Küver. Durchführung aller molekularbiologischen Arbeiten sowie der Sequenzdatenanalyse. Phylogenetische Analyse in Zusammenarbeit mit J. Küver. Erstellung des Manuskriptes unter der redaktionellen Mitarbeit von J. Küver.

4.2 Publikationen

4.2.1 Publikation 1

Phylogeny of the alpha and beta subunits of the dissimilatory adenosine-5`-phosposulfate (APS) reductase from sulfate-reducing prokaryotes – origin and evolution of the dissimilatory sulfate-reduction pathway

Birte Meyer und Jan Küver

Microbiology (2007). 153, 2026-2044

Microbiology (2007), **153**, 2026–2044 DOI 10.1099/mic.0.2006/003152-0

Phylogeny of the alpha and beta subunits of the dissimilatory adenosine-5′-phosphosulfate (APS) reductase from sulfate-reducing prokaryotes – origin and evolution of the dissimilatory sulfate-reduction pathway

Birte Meyer and Jan Kuever†

Max-Planck-Institute for Marine Microbiology, Celsiusstrasse 1, D-28359 Bremen, Germany

Correspondence
Jan Kuever
kuever@mpa-bremen.de

Received 5 October 2006
Revised 22 February 2007
Accepted 21 March 2007

Newly developed PCR assays were used to PCR-amplify and sequence fragments of the dissimilatory adenosine-5′-phosphosulfate (APS) reductase genes (*aprBA*) comprising nearly the entire gene locus (2·2–2·4 kb, equal to 92–94 % of the protein coding sequence) from 75 sulfate-reducing prokaryotes (SRP) of a taxonomically wide range. Comparative phylogenetic analysis included all determined and publicly available AprBA sequences from SRP and selected homologous sequences of sulfur-oxidizing bacteria (SOB). The almost identical AprB and AprA tree topologies indicated a shared evolutionary path for the *aprBA* among the investigated SRP by vertical inheritance and concomitant lateral gene transfer (LGT). The topological comparison of AprB/A- and 16S rRNA gene-based phylogenetic trees revealed novel LGT events across the SRP divisions. Compositional gene analysis confirmed *Thermacetogenium phaeum* to be the first validated strain affected by a recent lateral transfer of *aprBA* as a putative effect of long-term co-cultivation with a *Thermodesulfovibrio* species. Interestingly, the Apr proteins of SRP and SOB diverged into two phylogenetic lineages, with the SRP affiliated with the green sulfur bacteria, e.g. *Chlorobaculum tepidum*, while the *Allochromatium vinosum*-related sequences formed a distinct group. Analysis of genome data indicated that this phylogenetic separation is also reflected in the differing presence of the putative proteins functionally associated with Apr, QmoABC complex (quinone-interacting membrane-bound oxidoreductase) and AprM (transmembrane protein). Scenarios for the origin and evolution of the dissimilatory APS reductase are discussed within the context of the dissimilatory sulfite reductase (DsrAB) phylogeny, the appearance of QmoABC and AprM in the SRP and SOB genomes, and the geochemical setting of Archean Earth.

INTRODUCTION

Microbial sulfate respiration is an ancient metabolic pathway of energy conservation, which probably originated as early as 3·47 billion years ago (Shen *et al.*, 2001). Despite its suggested antiquity, the capability for dissimilatory sulfate reduction is patchily distributed, and occurs solely within members of six bacterial and two distinct archaeal lineages (Itoh *et al.*, 1999; Mori *et al.*, 2003; Moussard *et al.*, 2004; Rabus *et al.*, 1999). In all recognized sulfate-reducing prokaryotes (SRP), the dissimilatory process is mediated by three key enzymes. After the activation of the chemically inert sulfate to adenosine-5′-phosphosulfate (APS) by ATP sulfurylase (Sat), the second enzyme, APS reductase (Apr), converts APS to AMP and sulfite, which is finally reduced to sulfide by the activity of the sulfite reductase (Dsr) (Rabus *et al.*, 1999). Homologous proteins are also present in the anoxygenic photolithotrophic and chemolithotrophic sulfur-oxidizing bacteria (SOB) (Dahl & Trüper, 1994; Hipp *et al.*, 1997; Schedel & Trüper, 1979, 1980; Sperling *et al.*, 1998; Trüper & Fischer, 1982). Indeed, earlier studies have confirmed that the dissimilatory APS

†Present address: Bremen Institute for Materials Testing, Paul-Feller-Strasse 1, D-28199 Bremen, Germany.

Abbreviations: APS, adenosine-5′-phosphosulfate; DSMZ, Deutsche Sammlung von Mikroorganismen und Zellkulturen; LGT, lateral gene transfer; SOB, sulfur-oxidizing bacteria; SRB, sulfate-reducing bacterium/a; SRP, sulfate-reducing prokaryotes; TIGR, The Institute for Genomic Research.

The GenBank/EMBL/DDBJ accession numbers for the nucleotide sequence data reported in this study are EF442876–EF442976 (*apr*) and EF442977–EF442994 (16S rRNA).

Supplementary data are available with the online version of this paper.

2006/003152 © 2007 SGM Printed in Great Britain

reductases are highly conserved among SRP and SOB and form heterodimers with one alpha subunit (75–80 kDa, one FAD) and one beta subunit (18–23 kDa, two [4Fe–4S] centres) which are encoded by the *aprBA* gene loci (Fritz *et al.*, 2000; Hipp *et al.*, 1997; Lampreia *et al.*, 1994; Molitor *et al.*, 1998; Speich *et al.*, 1994). In contrast, the proteins that mediate the electron transport between the cytoplasmic AprBA and DsrAB and the quinol/quinone pool in the membrane are still poorly characterized. However, experimental evidence is accumulating that the membrane-bound redox complexes HmeABCDE [heterodisulfide reductase (Hdr)-like menaquinol-oxidizing enzyme] and homologous DsrMKJOP, as well as QmoABC (quinone-interacting membrane-bound oxidoreductase), are involved (Dahl *et al.*, 2005; Mander *et al.*, 2002; Pires *et al.*, 2003, 2006; Sander *et al.*, 2006). The Qmo redox complex from *Desulfovibrio desulfuricans* ATCC 27774 has been described as consisting of two soluble, HdrA-homologous, FAD-containing proteins, QmoA and QmoB, and membrane integral, HdrC/E-homologous protein, QmoC, containing two haem *b* groups and a putative quinone-binding site. Based on experimental results with *Desulfovibrio desulfuricans* ATCC 27774, the QmoABC complex has been postulated to be the missing link between the membrane menaquinol/menaquinone pool and the cytoplasmic reduction of APS by acting as a menaquinol/APS reductase oxidoreductase (Pires *et al.*, 2003).

Although lateral gene transfer (LGT) between distantly related phylogenetic lineages and domains is well-documented, especially for genes that encode proteins of metabolic pathways (Boucher *et al.*, 2003), the general impact of LGT as a major driving force in the genome evolution of prokaryotes is still debated (Daubin & Ochman, 2004; Gogarten & Townsend, 2005; Jain *et al.*, 2003; Kurland *et al.*, 2003; Lerat *et al.*, 2005). The evolution of the sulfate-respiration process in SRP has primarily been investigated by comparative phylogenetic studies of the dissimilatory sulfite reductase DsrAB, and this has confirmed the occurrence of multiple events of LGT of *dsrAB* among members of this physiological group (Klein *et al.*, 2001; Mussmann *et al.*, 2005; Zverlov *et al.*, 2005). A widespread dispersal via 'metabolic islands' has recently been discussed as responsible for the polyphyletic distribution of this metabolic trait (Klein *et al.*, 2001; Mussmann *et al.*, 2005). In contrast to the comprehensive analysis of DsrAB phylogeny, knowledge concerning the evolution of the dissimilatory APS reductase is currently restricted to a single phylogenetic study based on the limited sequence information of a minor part of the *aprA* gene-coding region (~0·9 kb) from 60 taxonomically different SRP species (Friedrich, 2002). The AprA tree topology of that study differed partially from the 16S rRNA gene-based tree, and led the author to suggest frequent events of inter- and intradomain LGT of the *apr* genes involving members of the Gram-positive sulfate-reducing bacteria (SRB), *Syntrophobacteraceae, Syntrophaceae* and *Archaeoglobus*, as well as the thermophilic *Thermodesulfovibrio islandicus* and representatives of the genus *Thermodesulfobacterium* (Friedrich, 2002).

The aim of this study was to increase the available genetic information for the *apr* gene locus by developing new PCR primer pairs for amplification and sequencing of nearly the entire coding region of the dissimilatory APS reductase (*aprBA*) genes from reference strains of all currently known SRP lineages. The phylogeny of both subunits AprB and AprA of the dissimilatory APS reductase from 103 different SRP (including some selected sequences of reverse-operating APS reductases of SOB) was compared with their 16S rRNA gene-based phylogeny to reveal novel events of LGT among the examined sulfate-reducing species. In addition, the results of the Apr phylogenetic analyses are discussed within the context of (1) the DsrAB phylogeny, (2) the collected genomic data concerning the presence and genomic arrangement of genes coding for putative functionally associated proteins (Qmo complex, AprM) at the *apr* gene locus of SRP and SOB, and (3) the geochemical data, in order to elucidate the origin and evolution of dissimilatory sulfate reduction/sulfite oxidation in prokaryotes.

METHODS

Micro-organisms. The investigated SRP reference strains (listed in Table 1) were obtained from the Deutsche Sammlung von Mikroorganismen und Zellkulturen (DSMZ) either as lyophilized or as actively growing cultures. If necessary, strains were cultivated as recommended by the DSMZ. Actively growing cultures of the following reference strains were provided by O. Kniemeyer (SRB strain EbS7), A. Galushko (strain NaphS2), G. Harms (strain mXyS1), H. T. Dinh ('*Desulfovibrio ferrophilus*' strain IS5, '*Desulfobacterium corrodens*' strain IS4 and SRB strain QLNR1), K. Nauhaus (*Desulfofrigus* sp. strain HRS-LA3X and *Desulfovibrio* sp. strain HRS-LA4), M. Könnecke (SRB strain JHA1) and J. Detmers (*Desulfovibio* sp. strain JD-160, *Desulfotomaculum* sp. strains JD-175 and JD-176) at the Max-Planck-Institute for Marine Microbiology, Bremen, and by H. P. Goorissen (*Desulfotomaculum solfataricum*) and T. A. Hansen (*Desulfobacterium niacini* strain PM4) at the University of Groningen. *Desulfovibrio* sp. strains LB1/LA1(H_2)/LA2/49MC/sponge tissue 85CD as well as *Desulfobulbus* sp. strain LB2 were isolated from sediment and seawater samples of the Caribbean Sea (RV Sonne cruise SO-154, Caribflux project).

DNA isolation. All general molecular techniques were performed according to the described standard methods (Sambrook *et al.*, 1989). Genomic DNAs were extracted from the investigated strains using the DNAeasy kit (Qiagen) according to the manufacturer's instructions. The DNA concentration was measured using a spectrophotometer. DNA quality was checked by PCR amplification with the 16S rRNA gene-targeting primer sets GM3F/GM4R and Arch21F/Arch958R, as described elsewhere (DeLong, 1992; Muyzer *et al.*, 1995).

PCR primers. Two sets of degenerate primers that anneal to conserved *aprBA* gene regions of SRP (Table 2) were newly designed based on comparison of *Desulfovibrio vulgaris, Desulfovibrio desulfuricans, Archaeoglobus fulgidus* (see Table 1 for GenBank accession numbers), *Allochromatium vinosum* (U84759) and *Chlorobaculum tepidum* (NC_002932) full-length *apr* sequences. Since the *aprA* alignment revealed a limited number of suitable primer target sites and a generally low degree of conserved nucleotide positions in the 3′

Table 1. PCR amplification results of *aprBA* and *aprA* gene fragments from genomic DNA of sulfate-reducing reference strains

Species*	Strain†	PCR product obtained with primer set‡			GenBank accession no.§	
		AprB-1-FW/ AprA-5-RV	AprA-1-FW/ AprA-10-RV	AprA-1-FW/ AprA-11-RV	*aprBA*	16S rRNA
Archaea						
Phylum *Crenarchaeota, Thermoprotei*						
Thermoproteaceae						
Caldivirga maquilingensis	13496^T	− (52)	− (56)	− (50)	−	AB013926
Phylum *Euryarchaeota, Archaeoglobi*						
Archaeaglobaceae						
Archaeoglobus fulgidus	4304^T	+‖		+‖	NC_000917	AE000965
Archaeoglobus profundus	5631^T	+ (60)	ND	+ (62)	**EF442876**	AF297529
Archaeoglobus veneficus	11195^T	+ (60)	ND	+ (62)	**EF442877**	AF418181
Bacteria						
Phylum *Thermodesulfobacteria, Thermodesulfobacteria*						
Thermodesulfobacteriaceae						
Thermodesulfobacterium commune	2178^T	+ (60)	+ (56)	− (50)	**EF442878**	AF418169
Thermodesulfobacterium hveragardense	12571^T	+ (58)	+ (56)	− (50)	**EF442879**	X96725
Thermodesulfatator indicus	15286^T	+ (58)	+ (56)	ND	**EF442880**	AF393376
Phylum *Nitrospira, Nitrospira*						
Nitrospiraceae						
Thermodesulfovibrio yellowstonii	11374^T	+ (60)	+ (62)	− (50)	**EF442881**	L14619
Phylum *Proteobacteria, Deltaproteobacteria*						
Desulfovibrionaceae						
Desulfovibrio acrylicus	10141^T	+ (60)	± (62)	ND	**EF442882**	U32578
Desulfovibrio oxyclinae	11498^T	+ (54)	+ (62)	ND	**EF442883**	U33316
Desulfovibrio desulfuricans strain G20	−	+‖	+‖		NC_007519	CP000112
Desulfovibrio desulfuricans ssp. *desulfuricans* strain Essex	642^T	+‖	+‖		AF226708	AF192153
'Desulfovibrio ferrophilus' strain IS5	15579	± (54)	+ (54)	ND	**EF442884**	AY274449
Desulfovibrio piger	749^T	± (56)	+ (62)	ND	**EF442885**	AF192152
Desulfovibrio profundus	11384^T	± (58)	+ (62)	ND	**EF442886**	AF418172
Desulfovibrio salexigens	2638^T	+ (58)	± (62)	ND	**EF442887**	M34401
Desulfovibrio sp.	9953	± (54)	+ (62)	ND	**EF442888**	NA
Desulfovibrio sp. strain HRS-LA4	−	+ (54)	ND	ND	**EF442889**	**EF442986**
Desulfovibrio sp. strain X	−	+ (54)	± (52)	ND	**EF442890**	**EF442979**
Desulfovibrio sp. strain JD-160	−	± (54)	+ (56)	ND	**EF442891**	AF295660
Desulfovibrio sp. strain 49MC	−	+ (54)	ND	ND	**EF442893**	**EF442988**
Desulfovibrio sp. strain LB1	−	+ (54)	ND	ND	**EF442892**	EF614447
Desulfovibrio sp. strain LA1(H_2)	−	+ (54)	ND	ND	**EF442894**	**EF442991**
Desulfovibrio sp. strain LA2	−	± (54)	ND	ND	**EF442895**	**EF442992**
Desulfovibrio sp. strain sponge tissue 85CD	−	± (54)	ND	ND	**EF442896**	**EF442989**
Desulfovibrio sulfodismutans	3969^T	+ (58)	+ (62)	ND	**EF442897**	Y17764
Desulfovibrio vulgaris ssp. *vulgaris* strain Hildenborough	644^T	+‖		+‖	NC_002937	AF418179
Desulfomicrobiaceae						
Desulfocaldus sp. strain Hobo	−	+ (60)	+ (62)	ND	**EF442898**	**EF442977**
Desulfomicrobium baculatum	4028^T	+ (60)	+ (62)	ND	**EF442899**	AF030438
Desulfohalobiaceae						
Desulfohalobium retbaense	5692^T	± (54)	+ (62)	ND	**EF442900**	U48244
Desulfonatronovibrio hydrogenovorans	9292^T	+ (56)	+ (62)	ND	**EF442902**	X99234
Desulfonauticus submarinus	15269^T	± (54)	+ (62)	ND	**EF442903**	AF524933
Desulfothermus naphthae strain TD3	13418^T	+ (58)	+ (62)	ND	**EF442901**	X80922
SRB strain 4206	4206	± (54)	+ (62)	ND	**EF442904**	SS
Desulfonatronumaceae						
Desulfonatronum lacustre	10312^T	ND	+ (62)	ND	**EF442905**	AF418171
Desulfobacteraceae						

Table 1. cont.

Species*	Strain†	PCR product obtained with primer set‡			GenBank accession no.§	
		AprB-1-FW/ AprA-5-RV	AprA-1-FW/ AprA-10-RV	AprA-1-FW/ AprA-11-RV	*aprBA*	16S rRNA
Desulfatibacillum sp. strain Pnd3	–	± (55)	+ (62)	ND	**EF442906**	Y17501
Desulfobacter postgatei	2034^T	± (54)	± (56)	ND	**EF442907**	AF418180
Desulfobacter sp.	2035	+ (55)	± (52)	ND	**EF442908**	M34415
Desulfobacter sp.	2057	+ (55)	± (52)	ND	**EF442909**	M34416
Desulfobacterium autotrophicum	3382^T	+ (58)	± (62)	ND	**EF442910**	AF418177
Desulfobacterium indolicum	3883^T	+ (58)	+ (62)	ND	**EF442911**	AJ237607
Desulfobacterium niacini	2650^T	± (57)	+ (62)	ND	**EF442912**	M34405
Desulfobacterium niacini strain PM4	–	± (54)	+ (62)	ND	**EF442913**	U51845
'*Desulfobacterium oleovorans*' strain Hxd3	6200^T	± (57)	+ (62)	ND	**EF442914**	Y17698
SRB strain JHA1	–	± (54)	± (56)	ND	**EF442915**	**EF442984**
Desulfobacterium sp.	7120^T	+ (57)	± (56)	ND	**EF442916**	**EF442994**
Desulfobacterium zeppelinii	9120	± (54)	+ (62)	ND	**EF442917**	**EF442983**
Desulfobacula phenolica	3384^T	+ (57)	+ (62)	ND	**EF442918**	AJ237606
Desulfobacula toluolica	7467^T	+ (58)	+ (62)	ND	**EF442919**	AJ441316
Desulfobotulus sapovorans	2055^T	+ (54)	+ (62)	ND	**EF442920**	M34402
Desulfocella sp.	2056^T	± (52)	± (50)	ND	**EF442921**	**EF442981**
Desulfococcus multivorans	2059^T	+ (60)	+ (62)	ND	**EF442922**	AF418173
Desulfococcus sp.	8541	+ (55)	+ (62)	ND	**EF442923**	**EF442980**
Desulfofrigus sp. strain HRS-LA3X	–	+ (54)	+ (56)	ND	**EF442924**	**EF442987**
Desulfonema limicola	2076^T	+ (57)	+ (56)	ND	**EF442925**	U45990
Desulfonema magnum	2077^T	+ (60)	+ (56)	ND	**EF442926**	U45989
Desulforegula conservatrix	13587^T	+ (58)	+ (62)	ND	**EF442927**	AF243334
Desulfosarcina variabilis	2060^T	± (58)	+ (62)	ND	**EF442928**	M34407
Desulfospira joergensenii	10085^T	± (58)	+ (62)	ND	**EF442929**	X99637
Desulfotignum balticum	7044^T	+ (57)	+ (62)	ND	**EF442930**	AF418176
Desulfobulbaceae						
Desulfobacterium catecholicum	3882^T	+ (58)	± (50)	ND	**EF442931**	AJ237602
Desulfobacterium catecholicum strain Kette	–	+ (57)	± (50)	ND	**EF442932**	**EF442982**
'*Desulfobacterium corrodens*' strain IS4	15630	+ (58)	± (52)	ND	**EF442933**	AY274450
Desulfobulbus marinus	2058^T	± (54)	+ (62)	ND	**EF442934**	M34411
Desulfobulbus propionicus	2032^T	+ (58)	± (62)	ND	**EF442935**	M34410
Desulfobulbus sp.	2033	+ (57)	+ (62)	ND	**EF442936**	**EF442993**
Desulfobulbus sp. strain LB2	–	± (54)	ND	ND	**EF442937**	**EF442990**
Desulfocapsa thiozymogenes	7269^T	± (58)	+ (62)	ND	**EF442938**	X95181
Desulfofustis glycolicus	9705^T	+ (58)	+ (62)	ND	**EF442939**	X99707
Desulforhopalus vacuolatus	9700^T	± (57)	± (62)	ND	**EF442940**	L42613
Desulfotalea psychrophila	12343^T	+ (55)	± (52)	ND	NC_006138	AF099062
SRB strain QLNR1	–	+ (58)	± (52)	ND	**EF442941**	**EF442985**
Uncertain affiliation						
Desulfobacterium anilini	4660^T	± (54)	– (52)	± (62)	**EF442942**	AJ237601
SRB strain EbS7	15769	± (55)	– (54)	+ (62)	**EF442943**	AJ430774
SRB strain NaphS2	14454	± (54)	– (54)	+ (62)	**EF442944**	AJ132804
SRB strain mXyS1	12567	+ (58)	– (52)	+ (62)	**EF442945**	AJ006853
Desulfarculaceae						
Desulfarculus baarsii	2075^T	+ (58)	ND	± (62)	**EF442946**	AF418174
Syntrophaceae						
Desulfobacca acetoxidans	11109^T	± (58)	± (50)	± (50)	**EF442947**	AF002671
Desulfomonile tiedjei	6799^T	± (55)	– (50)	± (56)	**EF442948**	M26635
Syntrophobacteraceae						
Desulforhabdus amnigena	10338^T	± (57)	ND	+ (62)	**EF442949**	X83274
Desulforhabdus sp. strain BKA11	–	+ (58)	ND	+ (62)	**EF442950**	AJ012597
Desulforhabdus sp. strain DDT	–	± (58)	ND	+ (62)	**EF442951**	**EF442978**
Syntrophobacter fumaroxidans strain MPOB	10017^T	+‖		+‖	NZ_AAJ-F01000079	X82874

Table 1. cont.

Species*	Strain†	PCR product obtained with primer set‡			GenBank accession no.§	
		AprB-1-FW/ AprA-5-RV	AprA-1-FW/ AprA-10-RV	AprA-1-FW/ AprA-11-RV	*aprBA*	16S rRNA
Thermodesulforhabdus norvegica	9990^T	+ (54)	ND	+ (62)	**EF442952**	U25627
Phylum *Firmicutes*, *Clostridia*						
Peptococcaceae						
Desulfosporosinus orientis	765^T	± (54)	ND	− (50)	**EF442953**	Y11570
Desulfosporosinus meridei	13257^T	± (54)	ND	− (50)	**EF442954**	AF076527
Desulfotomaculum acetoxidans	771^T	+ (54)	− (50)	− (50)	**EF442955**	Y11566
Desulfotomaculum australicum	11792^T	+ (56)	ND	+ (62)	**EF442956**	M96665
Desulfotomaculum geothermicum	3669^T	− (50)	ND	+ (62)	**EF442957**	Y11567
Desulfotomaculum gibsoniae	7213^T	− (50)	ND	+ (62)	**EF442958**	AJ294431
Desulfotomaculum halophilum	11559^T	± (50)	ND	± (50)	**EF442959**	U88891
Desulfotomaculum luciae	12396^T	± (56)	ND	± (62)	**EF442960**	AF069293
Desulfotomaculum reducens strain MI-1	−	+‖		+‖	NZ_AAO-P01000042	U95951
Desulfotomaculum ruminis	2154^T	± (50)	ND	± (50)	**EF442961**	Y11572
Desulfotomaculum sapomandens	3223^T	− (50)	− (50)	+ (62)	**EF442962**	AF168365
Desulfotomaculum solfataricum	14956^T	± (54)	ND	+ (62)	**EF442963**	AY084078
Desulfotomaculum sp.	7440	± (50)	ND	± (50)	**EF442964**	Y11579
Desulfotomaculum sp.	7474	+ (58)	ND	+ (62)	**EF442965**	Y11577
Desulfotomaculum sp.	7475	+ (58)	ND	± (62)	**EF442966**	Y11580
Desulfotomaculum sp.	7476	+ (58)	ND	± (62)	**EF442967**	Y11578
Desulfotomaculum sp.	8775	+ (58)	ND	± (62)	**EF442968**	U33451
Desulfotomaculum thermoacetoxidans	5813^T	± (56)	ND	± (62)	**EF442969**	Y11573
Desulfotomaculum thermobenzoicum ssp. *thermobenzoicum*	6193^T	+ (58)	ND	± (62)	**EF442970**	Y11574
Desulfotomaculum thermobenzoicum ssp. *thermosyntrophicum*	14055^T	± (56)	ND	± (62)	**EF442971**	AY007190
Desulfotomaculum thermocisternum	10259^T	± (56)	ND	± (62)	**EF442972**	U33455
Desulfotomaculum thermosapovorans	6562^T	− (50)	ND	± (62)	**EF442973**	Y11575
Desulfotomaculum sp. strain JD-175	−	− (50)	ND	± (62)	**EF442975**	AF295656
Desulfotomaculum sp. strain JD-176	−	− (50)	ND	± (62)	**EF442976**	AF295657
Thermoanaerobacteriaceae						
Thermacetogenium phaeum	12270^T	+ (58)	+ (56)	− (50)	**EF442974**	AB020336

*Taxonomic classification of investigated SRP species is according to the Taxonomic outline of the prokaryotes, *Bergey's Manual of Systematic Bacteriology*, 2nd edition, release 5.0, May 2004 (http://dx.doi.org/10.1007/bergeysoutline) and Kuever *et al.* (1999).

†DSMZ strain numbers; −, not deposited in a culture collection; T, type strain.

‡PCR amplification results with the respective primer pairs as follows: +, correct-sized PCR amplicon without byproducts; ±, correct-sized PCR amplicon with byproducts; −, no PCR amplicon obtained; ND, PCR amplification not determined. PCR annealing temperatures (°C) are in parentheses.

§*aprBA* and 16S rRNA gene sequences determined in this study are in bold type; NA, 16S rRNA gene sequence not available; SS, 16S rRNA gene sequence provided by S. Spring, DSMZ.

‖Binding of primer pair deduced from genomic *aprBA* sequence of respective SRP. +, Annealing possible; −, annealing inhibited (due to three or more mismatches).

terminal gene region, two reverse PCR primers of differing degeneracy (AprA-10-RV, AprA-11-RV) were developed that were complementary to the target site of either the *Desulfovibrio* species or the *Archaeoglobus*/Gram-positive SRB. The PCR primer pair AprB-1-FW/AprA-5-RV yielded a 1·2–1·35 kb *aprBA* amplicon from the investigated SRP, while an ~1·4 kb gene fragment of the 3′ terminal *aprA* gene region was amplified using the forward primer AprA-1-FW in combination with the reverse primers AprA-10-RV or AprA-11-RV. The *aprBA* and *aprA* PCR products overlap in sequence by ~400 bp (corresponding to *aprA* nucleotide positions 1236–1631 from *Desulfovibrio vulgaris*; Table 2).

PCR amplification of the *aprBA* gene fragments. PCR assays were performed with the RED*Taq* DNA Polymerase kit (Sigma-Aldrich). Reaction mixtures (50 µl total volume) contained 5 µl 10× RED*Taq* PCR reaction buffer, 5 µl 10× BSA solution (3 mg ml^{-1}), 200 µM dNTPs mixture, 1 µM each primer, 2·5 U RED*Taq* DNA Polymerase and 10–100 ng genomic DNA as template (water was

Table 2. PCR primers used for amplification of the *aprBA* and *aprA* gene fragments

Primer	Sequence (5′→3′)*	Primer binding site†
AprB-1-FW	TGC GTG TAY ATH TGY CC	272–288
AprA-1-FW	TGG CAG ATC ATG ATY MAY GG	1236–1256
AprA-5-RV	GCG CCA ACY GGR CCR TA	1615–1631
AprA-10-RV	CKG WAG TAG WAR CCR GGR TA	2611–2630
AprA-11-RV	CKG YRR TAG TAK CCS GGC CA	2611–2630

*Degenerate positions are in bold type.
†Corresponding nucleotide positions of the *aprBA* operon of *Desulfovibrio vulgaris* ssp. *vulgaris* strain Hildenborough (GenBank accession no. Z69372).

used as a negative control in all PCR amplifications). The gene fragments were amplified in a PCR thermocycler (Eppendorf) by using a 'touchdown' PCR protocol. Thermal cycling was carried out as follows: 5 min of initial denaturation of DNA at 95 °C, followed by 35 cycles of denaturation at 95 °C for 60 s, a 'touchdown' annealing step for 90 s (annealing temperature was decreased in the first 20 cycles by 0·5 °C in every cycle, while the subsequent 15 cycles were carried out at constant temperature), and elongation at 72 °C for 120 s. Amplification was completed by a final elongation step at 72 °C for 10 min. The initial annealing temperature for the touchdown interval (10 °C) was altered in a range between 62 and 50 °C to optimize the amplification results with respect to the different templates. Aliquots of the amplicons (10 % of the reaction volume) were visually analysed by electrophoresis on 1 % (w/v) agarose gels run in 1 × Tris/borate/EDTA (TBE) buffer followed by ethidium bromide staining (0·5 mg ml^{-1}). Amplicons of the expected gene fragment size were purified using the QIAquick PCR purification kit, the QIAquick gel extraction kit (Qiagen) or the Perfectprep Gel Cleanup kit (Eppendorf) according to the suppliers' recommendations.

Cloning of PCR products. The 1·3 kb *aprBA* gene fragment of *Thermacetogenium phaeum* was ligated into pCR 2·1-TOPO vectors (TOPO TA cloning systems, Invitrogen) and transformed into chemically competent *Escherichia coli* TOP10 cells following the manufacturer's instructions. Clone plasmids with inserts of approximately 1·3 kb were selected and screened by PCR amplification with subsequent RFLP analysis of the amplicons. RFLP patterns were visualized on 2 % (w/v) agarose gel runs in 1 × TBE buffer and stained with ethidium bromide. Plasmids of representative clones from unique RFLP patterns were recovered with the QIAprep Spin kit (Qiagen).

Nucleotide sequencing. The PCR products (*aprBA*, *aprA* and 16S rDNA amplicons) were directly sequenced in both directions using the respective PCR amplification primers and the ABI BigDye Terminator Cycle Sequencing kit (Applied Biosystems). Sequencing reactions were run on an ABI PRISM 3100 Genetic Analyzer (Applied Biosystems).

Sequence data analysis and phylogenetic tree inference. The DNA sequence data of the *aprBA* and *aprA* amplicons were assembled and manually corrected using the BioEdit (version 7.0.5) sequence alignment editor (http://www.mbio.ncsu.edu/BioEdit/bioedit.html). BLAST searches for homologous sequences were performed at the NCBI web site (http://www.ncbi.nlm.nih.gov/BLAST/). Searches on the preliminary data of ongoing sequencing projects of SRP and SOB genomes were performed at The Institute for Genomic Research (TIGR) web site (http://www.tigr.org) and at the US Department of Energy (DOE) Joint Genome Institute web site (http://img.jgi.doe.gov/cgi-bin/pub/main.cgi). The deduced partial amino acid sequences of this study and the publicly available full-length AprBA sequences (summarized in Table 3) were automatically aligned using the web server Tcoffee@igs (http://igs-server.cnrs-mrs.fr/Tcoffee/). The frameshifted *aprB/A* sequences of the *Pyrobaculum aerophilum* genome were manually corrected before inclusion into the datasets. The nucleotide sequences were aligned according to the corrected amino acid alignment. The AprB and AprA datasets were analysed separately with the phylogeny inference methods included in the ARB software package (http://www.arb-home.de). Alignment regions of insertions and deletions (indels) were not considered in the phylogenetic analysis. Unrooted phylogenetic trees were calculated based on 103 (AprB) and 555/413 (AprA) amino acid positions using the ARB implemented program package (distance matrix, Fitch analysis; maximum-parsimony, ProtPars; maximum-likelihood, ProML and PUZZLE) and the PhyML program (maximum-likelihood method; http://atgc.lirmm.fr/phyml). Maximum-likelihood trees were constructed using the WAG or JTT amino acid substitution model matrices. The robustness of inferred trees was tested by bootstrap analysis with 100 resamplings. Tree reconstruction with PUZZLE analysis was performed by 20 000 Quartet Puzzling steps employing the WAG amino acid replacement model with either a unique rate of evolution or a mixed four-category discrete gamma heterogeneity model (approximation of parameters done using a neighbour-joining tree). Predictions of potential promoters, termination sites and operons in genome data were performed using the web versions FGENESB, BPROM and BTERM of the Softberry program package available at (http://www.softberry.com/berry.phtml). Protein secondary structure analysis and transmembrane helix prediction were done using the tools available at http://us.expasy.org/tools/#secondary.

The 16S rDNA sequences from the investigated reference strains (see Table 1 for GenBank accession nos) were loaded into the ARB database and aligned using the ARB_ALIGN tool. The maximum-parsimony method with a 50 % positional conservation filter and the Kimura two-parameter model of the ARB program package was used for phylogenetic tree calculations based on 1400 nucleotide positions. Partial 16S rDNA gene sequences were added to the calculated initial trees by applying the parsimony insertion tool of ARB without allowing changes in the overall tree topology. The robustness of the inferred tree was tested by bootstrap analysis with 100 resamplings using the PhyML program.

RESULTS

Amplification of *aprBA* genes by PCR from SRP

Using the PCR primer set AprB-1-FW/AprA-5-RV, we were able to amplify an *aprBA* gene fragment and establish a new *aprB* database from 95 distinct SRP species of 103 tested (Table 1). No *aprBA* amplicon was obtained from any of the six representatives of *Desulfotomaculum*

Table 3. Homologous genes coding for dissimilatory APS reductase and functionally associated proteins and their genetic arrangement in partial or complete genome sequences of prokaryotes

Str., strain.

SRP and SOB species	Homologous ORFs in genomic sequences (gene arrangement indicated by gene locus_tag no. annotation)						
	sat	*aprM*	*aprB*	*aprA*	*qmoA*	*qmoB*	*qmoC*
Chlorobia							
Chlorobaculum tepidum str. TLS	CT0862	–	CT0864	CT0865	CT0866	CT0867	CT0868
Chlorobium phaeobacteroides str. BS1	Cphamn1-DRAFT_1538	–	Cphamn1-DRAFT_1537	Incomplete ORF: *aprA*-NTCS in Cphamn1-DRAFT_1537 following sequence*	Incomplete ORF: *qmoA*-CTCS in Cphamn1-DRAFT_0878 preceding sequence*	Incomplete ORF: *qmoB*-NTCS in Cphamn1-DRAFT_0878*	Cphamn1-DRAFT_3474
Chlorobium chlorochromatium str. CaD3	Cag_1587	–	Cag_1586	Cag_1585	Cag_1584	Cag_1583	Cag_1582
Chlorobium clathratiforme str. BU-1	Ppha-DRAFT_2470	–	Ppha-DRAFT_2471	Ppha-DRAFT_2472	Ppha-DRAFT_2473	Ppha-DRAFT_2474	Ppha-DRAFT_2475
Alphaproteobacteria							
Uncultured bacterium EBAC2C11 (SAR116)	Red2C11_59	Red2C11_60	Red2C11_61	Red2C11_62	–	–	–
'*Candidatus* Pelagibacter ubique' HTCC1002 (SAR11)	–	PU1002_02221	PU1002_02216†	PU1002_02211	–	–	–
'*Candidatus* Pelagibacter ubique' HTCC1062 (SAR11)	–	SAR11_0835	SAR11_0836	SAR11_0837	–	–	–
Betaproteobacteria							
Thiobacillus denitrificans ATCC 25259	Tbd_0874	Tbd_2284	Tbd_0873/Tbd_2283	Tbd_0872/Tbd_2282	Tbd_1648	Tbd_1647	–
Gammaproteobacteria							
Allochromatium vinosum	AAC23622‡	AAK16200‡	AAC23620‡	AAC23621‡	–	–	–
Deltaproteobacteria							
Desulfotalea psychrophila str. LSv54	DP1472	–	DP1104	DP1105†	DP1106†	DP1107	DP1108
Desulfovibrio vulgaris ssp. *vulgaris* str. Hildenborough	DVU1295	–	DVU0846	DVU0847	DVU0848	DVU0849	DVU0850
Desulfovibrio desulfuricans str. G20	Dde_2265	–	Dde_1109	Dde_1110	Dde_1111	Dde_1112	Dde_1113
Syntrophobacter fumaroxidans str. MPOB	Sfum-DRAFT_3449	–	Incomplete ORF: *aprB*-NTCS in Sfum-DRAFT_3449 following sequence*	Incomplete ORF: *aprA*-CTCS in Sfum-DRAFT_3839*	Sfum-DRAFT_3840/Sfum-DRAFT_1034	Sfum-DRAFT_3841/Sfum-DRAFT_1035	Sfum-DRAFT_1036
Uncultured sulfate-reducing bacterium fosws39f7	39f70021	–	39f70022	39f70023	39f70001	39f70002	39f70020
Uncultured sulfate-reducing bacterium fosws7f8	ws7f8_12	–	ws7f8_11	ws7f8_10	–	–	ws7f8_3
Thermodesulfobacteriaceae							
Thermodesulfobacterium commune DSM 2178	TIGR contig 486	–	TIGR contig 486	TIGR contig 486	TIGR contig 486	TIGR contig 486	TIGR contig 486
Nitrospira							
Thermodesulfovibrio yellowstonii DSM 11347	TIGR contig 173	–	TIGR contig 173	TIGR contig 173	TIGR contig 173	TIGR contig 173	TIGR contig 173

Table 3. cont.

SRP and SOB species	Homologous ORFs in genomic sequences (gene arrangement indicated by gene locus_tag no. annotation)						
	sat	*aprM*	*aprB*	*aprA*	*qmoA*	*qmoB*	*qmoC*
Clostridia							
Desulfotomaculum reducens str. MI-1	Dred-DRAFT_3079		Dred-DRAFT_3080	Dred-DRAFT_3081	Dred-DRAFT_3082	Dred-DRAFT_3083	–
Euryarchaeota							
Archaeoglobus fulgidus DSM 4304	AF1667†	–	AF1669	AF1670	AF0663	AF0662	AF0661
Crenarchaeota							
Pyrobaculum aerophilum str. IM-2	PAE2609	–	PAE2561/ PAE2562§	PAE2563/ PAE2564§	–	–	–

*Abbreviations for incomplete ORF sequences received from draft genome projects: N- or C-terminal protein coding sequence (NTCS/CTCS).
†Incorrect ORF annotation by automated protein coding gene prediction program in genome sequence.
‡GenBank protein accession no. of respective ORF.
§Frameshift in sequence of respective ORF.

subcluster Ib (for *Desulfotomaculum* subcluster assignment, see Fig. 1), *Thermodesulforhabdus norvegica* or *Caldivirga maquilingensis*, while direct nucleotide sequencing of the *Desulfosporosinus orientis*, *Desulfobacterium niacini* and '*Desulfobacterium oleovorans*' strain HxD3 amplicon was unsuccessful with the reverse primer AprA-5-RV. The second primer set, AprA-1-FW combined with AprA-10-RV or AprA-11-RV, amplified the 3′-terminal *aprA* gene fragment from 93 out of 97 tested SRP species (Table 1). No *aprA* amplification product was obtained from the investigated *Desulfosporosinus* strains, *Desulfotomaculum acetoxidans* or *Caldivirga maquilingensis*. Direct nucleotide sequencing of the *Desulfotomaculum halophilum*, *Desulforhabdus amnigena*, *Desulfotalea psychrophila*, *Desulfobacterium catecholicum*, SRB strain Kette, *Desulfocella* sp. (DSM 2056) and *Thermacetogenium phaeum aprA* amplicon resulted in only partially evaluable sequences due to sequence ambiguities. The failure to amplify and sequence *apr* gene fragments from certain SRB species indicated that they do not contain target sites fully complementary to the applied primers. In fact, compositional analysis of the *aprBA* gene locus of *Desulfotalea psychrophila* (Rabus *et al.*, 2004) revealed a deviating codon usage that resulted in four mismatches at the primer binding site of Apr-10-RV. Nevertheless, the newly developed PCR primer sets enabled the enlargement of the present 0·9 kb *aprA* database (Friedrich, 2002) to a comprehensive *aprBA* database which comprises 2·2–2·4 kb (equivalent to 91–93 %) of the coding region of the dissimilatory APS reductase from 75 SRP species over a wide taxonomical range.

Molecular characterization of the *aprBA* gene locus in SRP

The sequence data from this study and the analysis of the available SRP and SOB genome data (Table 3) revealed a strictly conserved gene locus arrangement of *aprB* preceding the *aprA* gene and the absence of terminator-like signals downstream of the *aprB* stop codon, demonstrating that both genes form a transcriptional unit. The *aprBA* genes of SRP (and *Chlorobiaceae*) are generally separated by an intercistronic sequence region (16–148 nt) of a varying, family-specific length interval. As expected for highly expressed genes, the *aprA* genes from most investigated SRP possess Shine–Dalgarno (SD) sequences with entire complementarity (GGAGG) to the anti-SD core sequence and an optimal space distance between 6 and 12 nt (Kozak, 1999). AUG is used to start translation in all *aprA* sequences, with the exception of the members of *Desulfotomaculum* subcluster Ic, which utilize the less potent initiator GUG. The alternative start codon UUG (accession no. NC_006138, nucleotide position 1 246 432 in the genome sequence) annotated for the *aprA* gene of the *Desulfotalea psychrophila* genome (Rabus *et al.*, 2004) has to be corrected in our opinion to AUG (nucleotide position 1 246 438), which fulfils the required criteria (e.g. space distance of 9 nt instead of the annotated 3 nt to the SD sequence). In contrast, no intergenetic sequence exists in the *Allochromatium vinosum*-related sequence group as a consequence of the general overlapping of the *aprB* stop codon with the start codon of *aprA* in the sequence UGAUG or UAAUG.

Phylogeny of dissimilatory APS reductases from SRP

The AprB and AprA trees presented in this study were based on 110 AprB (Fig. 2) and 93 AprA sequences (Fig. 3), with 103 and 555 compared amino acid positions, respectively. AprA subtrees were calculated (413 compared positions) to include in the phylogenetic analysis partial sequences obtained from e.g. *Desulfotomaculum* subcluster

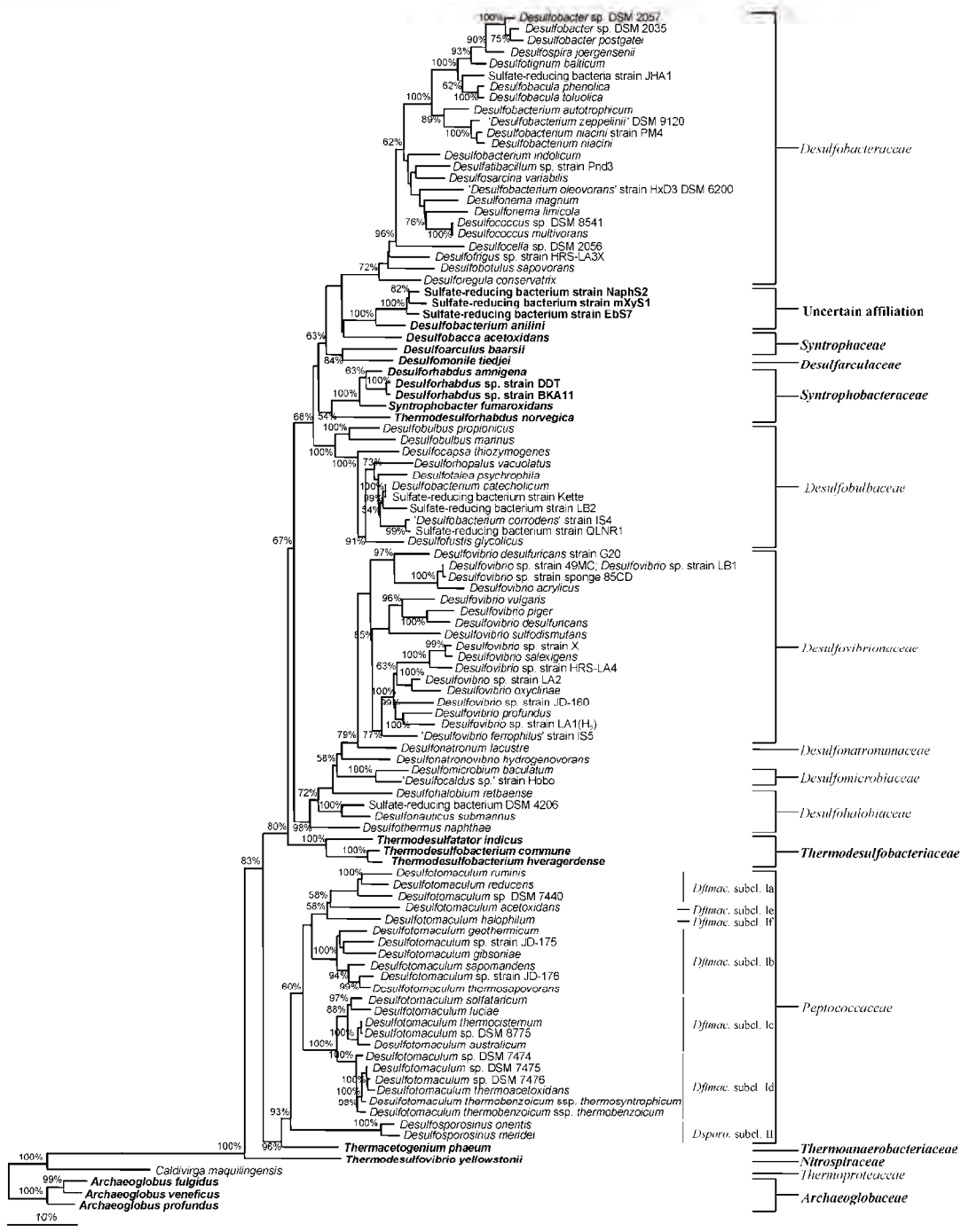

Fig. 1. Phylogenetic tree of 16S rRNA gene sequences from investigated SRP. The tree was constructed using the maximum-parsimony method with a 50 % positional conservation filter. The partial sequences of sulfate-reducing strains 49MC, LA1(H_2), LA2, LB1, sponge tissue 85CD and LB2 were inserted into the tree by applying parsimony criteria without allowing changes in the overall tree topology. *Archaeoglobus* species and *Caldivirga maquilingensis* were used as outgroup. The scale bar corresponds to 10 % estimated sequence divergence. Percentages greater than 50 % of bootstrap resampling that support each topological element are indicated near the nodes. SRP with laterally transferred *aprBA* genes are in bold type. Taxonomical classification of SRP into families and phylogenetic subclusters (subcl.) of Gram-positive SRB in the genera *Desulfotomaculum* (*Dftmac.*) and *Desulfosporosinus* (*Dsporo.*) (Kuever *et al.*, 1999) are indicated.

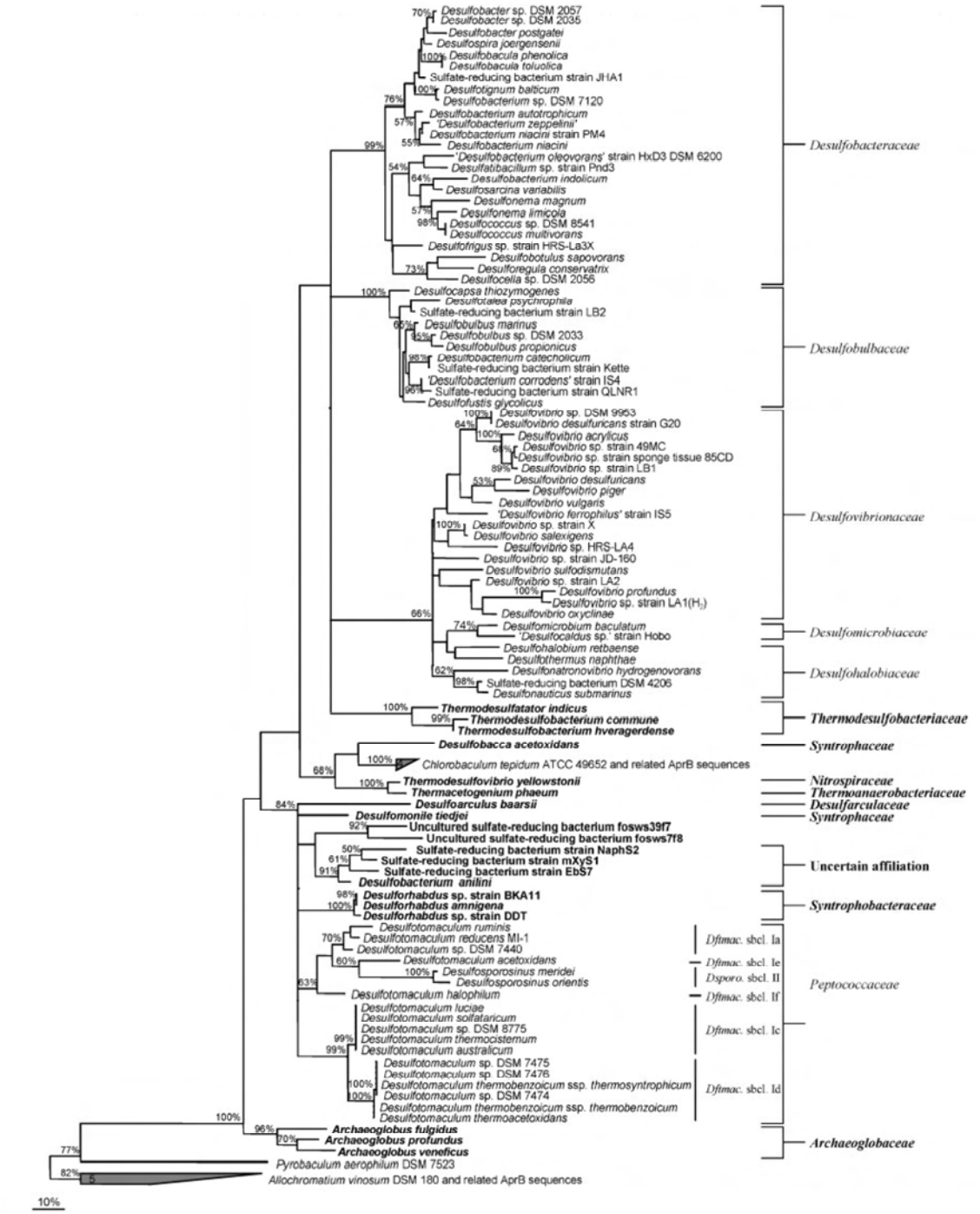

Fig. 2. Phylogenetic tree based on AprB sequences obtained from 92 investigated SRP including full-length protein sequences retrieved from public databases. The tree was inferred using PhyML (maximum-likelihood method). The *Allochromatium vinosum*-related sequences group and *Pyrobaculum aerophilum* were used as outgroup. The scale bar corresponds to 10 % estimated sequence divergence. Percentages greater than 50 % of bootstrap resampling that support each topological element are indicated near the nodes. SRP with laterally transferred *aprB* genes are in bold type. The consistent arrangements of SRP according to the 16S rRNA gene sequence-based taxonomical classification are indicated. Subcluster (sbcl.) assignment of the representatives of the genera *Desulfotomaculum* (*Dftmac.*) and *Desulfosporosinus* (*Dsporo.*) are according to Kuever *et al.* (1999).

Fig. 3. Phylogenetic tree based on AprA sequences obtained from 75 investigated SRP including full-length AprA sequences retrieved from public databases. The tree was inferred using PUZZLE analysis (maximum-likelihood method). The *Allochromatium vinosum*-related sequences group and *Pyrobaculum aerophilum* were used as outgroup. The scale bar corresponds to 10 % estimated sequence divergence. Reliability of branching order is indicated by numbers representing the quartet puzzling support values of the corresponding branches; polytomic nodes connect branches for which a relative order could not be determined unambiguously by PUZZLE. SRP with inferred laterally transferred *aprA* genes are in bold type. The 16S rRNA gene-based taxonomical classifications of the SRP species are indicated.

Ib (see Supplementary Fig. S1). The *Allochromatium vinosum*-related sequence group (including '*Candidatus* Pelagibacter ubique', uncultured bacterium EBAC2C11 and *Thiobacillus denitrificans*; see Table 3) and *Pyrobaculum aerophilum* were used to root the trees. The comparison of the AprB- and AprA-based tree topologies of the investigated SRP revealed a consistent separation into four distinct phylogenetic sequence clusters consisting of (1) *Archaeoglobus* species, (2) the Gram-positive SRB associated with members of the deltaproteobacterial *Syntrophobacterales*, *Desulfarcales* and the *Desulfobacterium anilini*-related SRB group, (3) the thermophilic SRB in affiliation with the *Chlorobaculum tepidum*-related sequences group (comprising *Chlorobium phaeobacteroides*, *Chlorobium chlorochromatium* and *Chlorobium clathratiforme*; see Table 3), and (4) the representatives of *Desulfovibrionales* and *Desulfobacterales* (Figs 2 and 3). The intracluster-branching order of taxa was consistent between the subunit trees, irrespective of the tree inference method or dataset used. However, topological discrepancies were obtained with respect to the relative ordering of the major SRP groups in the AprB and AprA trees, e.g. the varying position of the *Thermodesulfobacteriaceae* and *Archaeoglobus*. This might be explained by the limited amount of phylogenetic information contained in the smaller beta subunit, which is most likely insufficient to resolve branching orders at deeper phylogenetic levels. Nevertheless, the inferred phylogenies indicated the co-evolution of the beta and alpha subunits of the dissimilatory APS reductase in the investigated SRP.

Overall, the AprA trees presented in this work (Fig. 3, Supplementary Fig. S1) are topologically congruent with the tree of the earlier phylogenetic analysis which was based on 252 compared positions from AprA sequences of 60 SRP species and support the major LGT events postulated earlier (Friedrich, 2002). However, the AprA datasets used in the two phylogenetic studies overlap in only 30 investigated reference strains. The newly investigated genera and species, e.g. representatives of *Desulfosporosinus* and *Desulfotomaculum* subclusters Ic, Id and If (see Table 1), complete the previous Apr database for phylogenetic analyses and provide a more comprehensive framework for molecular ecology studies (Figs 2 and 3, Supplementary Fig. S1). The enlarged species coverage of this study refined and emphasized by novel results the general 16S rRNA gene congruence of the Apr-based inter- and intrafamily SRP relationships, e.g. the formation of the *Desulfovibrionaceae*, *Desulfonatronumaceae* and *Desulfomicrobiaceae* subclusters within the *Desulfovibrionales*. Interestingly, the Apr trees showed the *Desulfohalobiaceae* to be subdivided into two groups consisting of (1) *Desulfohalobium retbaense* related to the *Desulfomicrobiaceae*, and (2) *Desulfothermus naphthae*/*Desulfonatronovibrio hydrogenovorans*/*Desulfonauticus* sp. forming a basal-positioned group. The proposed 16S rRNA gene-based classification of the *Desulfotomaculum* and *Desulfosporosinus* members into the subclusters Ia–If and II (Kuever *et al.*, 1999) (Fig. 1) was supported by the Apr trees (Figs 2 and 3, Supplementary Fig. S1). In contrast with the earlier study (Friedrich, 2002), *Desulfarculus baarsii*, *Desulfomonile tiedjei* and the *Desulfobacterium anilini*-related SRB group branched separately within the Gram-positive AprB/A lineage. Furthermore, the family *Syntrophaceae* was not monophyletic, since *Desulfomonile tiedjei* formed a separate lineage within the *Desulfotomaculum* radiation, while the newly provided AprB/A sequences of *Desulfobacca acetoxidans* were by 16S rRNA gene-based phylogeny discordantly associated with the Gram-negative, thermophilic *Thermodesulfovibrio yellowstonii*. Another newly discovered deviation from the 16S rRNA gene-based phylogeny was the Apr-based, close relationship of the Gram-positive *Thermacetogenium phaeum* (Hattori *et al.*, 2000) with *Thermodesulfovibrio yellowstonii*. The cloning results of the *Thermacetogenium phaeum aprBA* amplicon demonstrated the absence of further gene copies in this reference strain. Direct nucleotide sequencing of its PCR-amplified 16S rDNA resulted in unambiguous nucleotide sequences. Indeed, the uncontaminated pure-culture status of the type strain of *Thermacetogenium phaeum* was also confirmed by the DSMZ (S. Spring, personal communication).

Additional evidence for lateral transfer of *aprBA* genes among SRP

The presence of indels at identical positions within the Apr sequences was used as additional evidence for the occurrence of the inferred LGT events. In addition, the new, enlarged *aprBA* sequence dataset was checked for recent LGTs by identification of (1) atypical *aprBA* sequence characteristics, such as significant G+C-content deviations (Lawrence & Ochman, 1997), and variations in codon usage with respect to the recipient genome and the *dsrAB* gene, and (2) sequence similarity of the *aprBA* intercistronic region between distantly related species. In this way, the separate phylogenetic position of the *Allochromatium vinosum*-related sequences group was confirmed by the presence of four unique indels in each subunit which were absent from AprB and AprA sequences of all SRP and the affiliated *Chlorobiaceae* cluster (see Supplementary Fig. S2 for amino acid sequence alignment). The proposed LGT of *aprBA* genes from Gram-positive SRB donor strains to the *Syntrophobacteraceae*, *Desulfomonile tiedjei* (including the unclassified putative SRB), the *Desulfobacterium anilini*-related SRB group, *Desulfarculus baarsii* as well as *Archaeoglobus* species were confirmed by the presence of six shared indels in the respective Apr sequences. The separate, basal branching point of the archaeal genus in AprB/A-based trees was supported by two additional unique indels. The close relationship of *Desulfobacca acetoxidans* to the *Thermodesulfovibrio–Chlorobaculum* cluster was confirmed by three unique indels located in the AprA sequence and the shared short C-terminal sequence of the AprB protein. No atypical sequence characteristics were detected in members

of the above recipient lineages that would indicate the recent occurrence of the proposed LGT events. However, the Apr-based close relationship of *Thermacetogenium phaeum* with *Thermodesulfovibrio* might be the first example of a recent LGT of *apr* genes among distantly related SRB reference strains. A recent lateral transfer of the *aprBA* gene to *Thermacetogenium phaeum* was supported by the presence of identical indel positions and lengths in the AprBA sequences of *Thermacetogenium phaeum* and *Thermodesulfovibrio* (see Supplementary Fig. S2), similar *aprBA* gene G+C content, codon usage, and the nearly identical length and nucleotide sequence of the intercistronic region.

Genomic arrangement of genes coding for the dissimilatory APS reductase and functionally associated proteins

The *sat/aprBA/qmoABC* gene organization of the available genomes reflected the phylogenetic divergence of the investigated SRP species into the four major AprBA lineages and their affiliation to the green sulfur bacteria (see Table 3 for gene locus numbers in genomes, and Fig. 4 for a graphical representation). The genomic arrangement in the thermophilic SRB, e.g. *Thermodesulfovibrio yellowstonii* and *Thermodesulfobacterium commune*, and the *Chlorobiaceae* was identical; the genes are most probably regulated in two separate operons, *sat-aprBA* and *qmoABC*. Notably, the *sat* gene is followed in all thermophilic SRP genomes by an additional ORF that encodes a protein of unknown function (*Archaeoglobus fulgidus*, AF1668; *Pyrobaculum aerophilum*, PAE2610). The *aprBA* and *qmoABC* gene arrangement in the genomes of the deltaproteobacterial representatives was similar to that of the thermophilic SRB and *Chlorobiaceae* genomes; however, the *sat* gene was separately located and regulated. Interestingly, the close relationship of the AprBA of *Syntrophobacter fumaroxidans* to the Gram-positive SRB lineage (e.g. *Desulfotomaculum reducens* MI-1) was reflected in their identical *sat-aprBA* and *qmoAB* operon structure; a sequence homologous to *qmoC* adjacent to this gene locus could not be identified in the preliminary genome data of these species. However, *Syntrophobacter fumaroxidans* harbours a second and functionally complete *qmoABC* operon that is not associated with the *sat-aprBA-qmoAB* gene cluster. A separately transcribed *qmoC* homologue is present near the *qmoAB* and *sat-aprBA* gene loci in the metagenomic sequences of the LGT-affected unclassified putative SRB strains (fosws39f7, fosws7f8) (Mussmann *et al.*, 2005). Interestingly, these strains are also closely related in the QmoA- and QmoB-based phylogenetic trees (not shown). This might indicate a concerted lateral transfer of the entire *sat-aprBA-qmoAB* gene cluster from the Gram-positive donor lineage (representative strain *Desulfotomaculum reducens*) to the deltaproteobacterial *Syntrophobacter fumaroxidans* and both uncultivated SRB strains (fosws39f7, fosws7f8), with subsequent intragenomic rearrangements (Suyama & Bork, 2001) in the uncultivated strains. Nevertheless, the presence of a (second) LGT-affected and separately located *qmoABC* gene locus in the *Syntrophobacter fumaroxidans* and *Archaeoglobus fulgidus* genomes demonstrates that independent lateral transfer of the *apr* and *qmo* genes has occurred.

The distant AprB/A-based phylogenetic relationship of the *Allochromatium vinosum*-related sequences group to the SRP and green sulfur bacteria is also reflected in the differing presence and genomic arrangement of genes that code for the functionally associated proteins. No *qmoABC*-homologous ORFs exist in the genomes of representatives of this sequence group (e.g. *Allochromatium vinosum*, '*Candidatus* Pelagibacter ubique'). Instead, the *aprBA* gene locus is always spatially associated and co-regulated with the unique gene *aprM* (encoding a putative membrane-bound protein), an arrangement that is not found in the genomes of SRP or *Chlorobiaceae*.

DISCUSSION

Phylogeny of the dissimilatory APS reductase from SRP

The consistent relative branching order of SRP taxa among the AprB and AprA trees indicates a shared evolutionary path for the *aprB* and *aprA* genes by vertical inheritance (speciation) and acquisition via concomitant LGT events, as demonstrated for the dissimilatory sulfite reductase-encoding genes *dsrA* and *dsrB* (Klein *et al.*, 2001; Molitor *et al.*, 1998; Zverlov *et al.*, 2005). The topology of the AprB/A-based trees of this study is congruent with the topology of an AprA-based tree of an earlier work (Friedrich, 2002). However, the two studies are based on different Apr datasets with respect to the SRP species coverage (102 versus 60 species) and the amount of phylogenetic information used for tree inference (2·2–2·4 kb versus 0·9 kb of the *apr* gene locus). The inferred phylogenetic positions of the Apr sequences from 72 newly investigated SRP species of this work were generally consistent with the major LGT events of *apr* genes proposed by Friedrich (2002) to have affected the sulfate-reducing members of the *Syntrophobacterales*, *Thermodesulfobacterium* and *Thermodesulfovibrio* species, as well as the archaeal genus *Archaeoglobus*. Nevertheless, the newly provided Apr sequences (Figs 2 and 3, Supplementary Fig. S1) refined and emphasized the 16S rRNA gene-congruent inter- and intrafamily clustering of the SRP taxa by the higher number of examined species. The results of this phylogenetic study prove the principal vertical transmission of the *aprBA* genes in the major SRP lineages. In contrast to the findings of the earlier analysis (Friedrich, 2002), the LGT-affected members of the *Syntrophobacteraceae*, the *Desulfobacterium anilini*-related SRB group, *Desulfomonile tiedjei* and *Desulfarculus baarsii* form four separately branching Apr lineages in affiliation with the monophyletic Gram-positive SRB group. Their separate phylogenetic placement

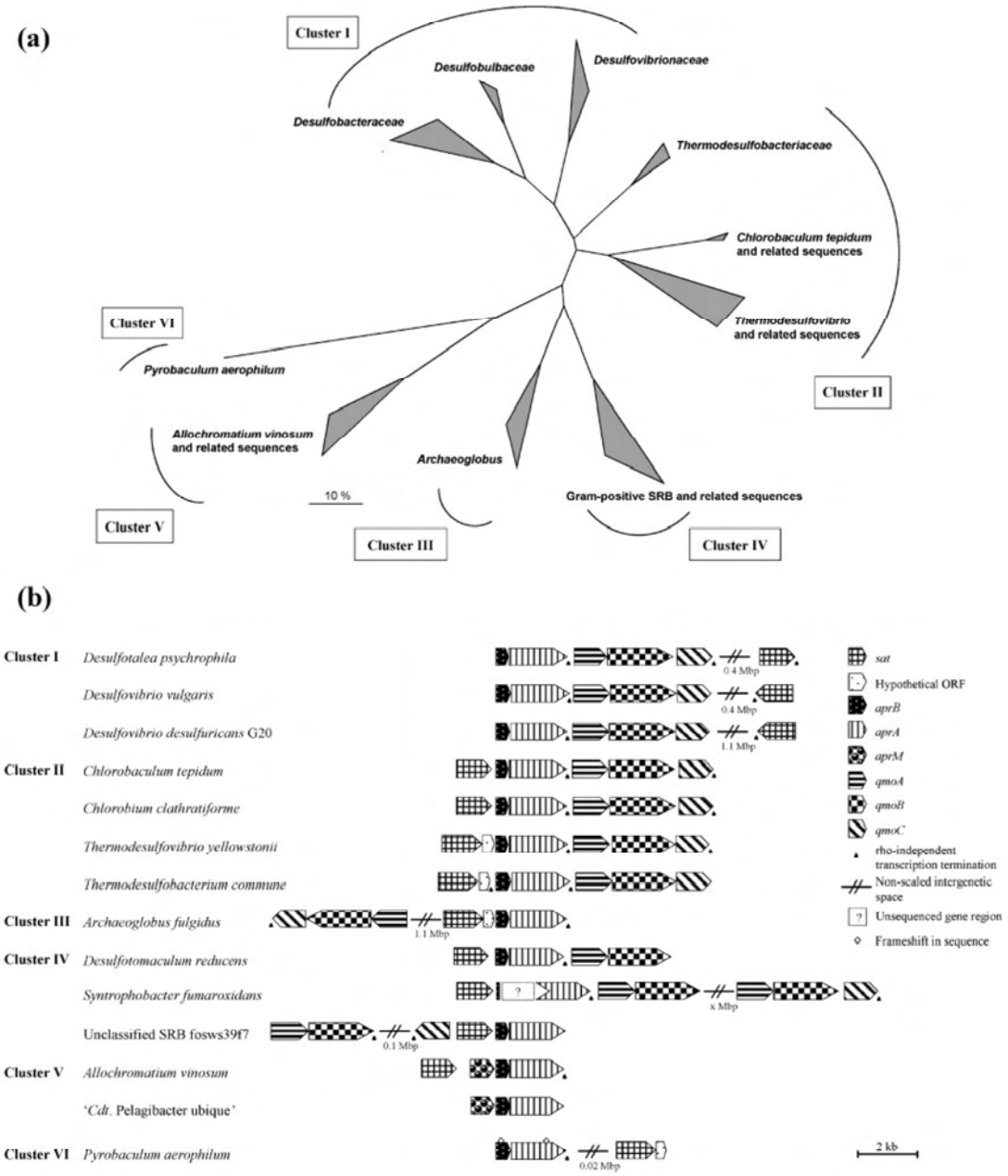

Fig. 4. (a) AprA-based phylogenetic tree of investigated SRP including full-length amino acid sequences of SRP and selected SOB received from public databases. The tree was inferred by Fitch analysis (distance matrix method). AprA sequences of SRP and SOB were graphically unified to their corresponding (16S rRNA gene-based) taxonomical groups of *Desulfovibrionales*, *Desulfobulbaceae*, *Desulfobacteraceae* (cluster I); *Thermodesulfobacteriaceae*, *Thermodesulfovibrio*, and *Chlorobaculum tepidum* and relatives (cluster II); *Archaeoglobus* (cluster III); Gram-positive SRB and LGT-affected deltaproteobacterial lineages (cluster IV); *Allochromatium vinosum*-related sequences group (cluster V); and *Pyrobaculum aerophilum* (cluster IV). The *Allochromatium vinosum*-related sequences group and *Pyrobaculum aerophilum* were used as outgroup. The scale bar corresponds to 10 % estimated sequence divergence. (b) Gene organization of the *sat*, *apr* and *qmo* loci (including predicted operon structure by Softberry) in sequenced SRP and SOB genomes and *Allochromatium vinosum*. ORFs were named based on BLASTX search results with significant homology scores. The following abbreviations were used for proposed homologous ORFs: *sat*, dissimilatory ATP sulfurylase; *aprA* and *aprB*, alpha and beta subunits of the dissimilatory APS reductase; *aprM*, putative transmembrane protein; *qmoA*, *qmoB* and *qmoC*, subunits of the putative menaquinone-oxidizing transmembrane protein complex. The cluster assignment refers to the enumeration of SRP and SOB in the AprA-based phylogenetic tree in (a).

points to four independent LGT events involving *apr* genes, most probably with different Gram-positive SRB species serving as donor strains. The different phylogenetic relationships of the xenologous *aprBA* genes from *Desulfomonile* and *Desulfobacca* indicate the incorrect systematic classification of both genera within the '*Syntrophaceae*', along with members that are not capable of sulfate or sulfite reduction (*Smithella* and *Syntrophus*) (Kuever *et al.*, 2005). Therefore, the AprB/A phylogenies support (1) the proposed taxonomical placement of *Desulfarculus baarsii* as well as *Desulfobacterium anilini* and its relatives into individual orders distinct from the *Syntrophobacterales* (Kuever *et al.*, 2005), and (2) the need for reclassification and validation of *Desulfomonile tiedjei* and *Desulfobacca acetoxidans* at the family level within the *Deltaproteobacteria*.

Two novel cases of LGT are proposed with respect to the xenologous Apr sequences of *Desulfobacca acetoxidans* and *Thermacetogenium phaeum* (also confirmed by indel pattern; see Supplementary Fig. S2). The *apr* gene composition analysis supported an ancient occurrence of the LGT event in *Desulfobacca acetoxidans*, whereas *Thermacetogenium phaeum* is the first reference strain reported to have been affected by a recent lateral transfer of *aprBA* genes. The type strain of *Thermacetogenium phaeum* was isolated from a thermophilic anaerobic methanogenic reactor (UASB), and to date is the only recognized sulfate-respiring strain within the Gram-positive *Thermoanaerobacteriales* (Hattori *et al.*, 2000). Its phylogenetic position in DsrAB-based trees has not yet been investigated and is therefore unknown. In support of a recent lateral *aprBA* transfer, the co-occurrence and predominance of *Thermacetogenium phaeum* and *Thermodesulfovibrio* species (recently classified as *Thermodesulfovibrio aggregans* and *Thermodesulfovibrio ethanolicus*; Y. Sekiguchi & H. Imachi, unpublished data) have been demonstrated by 16S rRNA analysis within the same granular sludge pellets of a thermophilic UASB reactor (Sekiguchi *et al.*, 1998). This close cell-to-cell contact would have increased the probability of interspecies LGT. The successful acquisition and functional implementation of this novel metabolic trait in the ancestor of *Thermacetogenium phaeum* might have been accelerated by certain genetic and physiological prerequisites: (1) the genomic arrangement (*sat-aprBA-qmoABC*) in the *Thermodesulfovibrio* donor strain (see genomic structure of *Thermodesulfovibrio yellowstonii*; Fig. 4b), which would have enabled a concomitant lateral transfer of all relevant genes in one single event; (2) the pre-existing capability for sulfite respiration in the ancestor of *Thermacetogenium phaeum* [see Supplementary Table S1 for the presence of *dsr* genes in the genomes of the related *Moorella thermoacetica* and *Carboxydothermus hydrogenoformans*; the capability of dissimilatory sulfite reduction has also been proven for *Carboxydothermus hydrogenoformans* (Henstra & Stams, 2004)]; and (3) the utilization of the same major membrane quinone component in the donor and recipient, menaquinone-7. The latter would have allowed an immediate linkage of the newly acquired sulfate-respiration system to the electron-transport processes in the ancestor of *Thermacetogenium phaeum*. Although the stable, specific conditions within the UASB reactor might have favoured the artificial generation of the SRB strain *Thermacetogenium phaeum*, it is a representative example of the permanently ongoing evolutionary process of gene flux among the genomes of free-living prokaryotes in nature (Daubin & Ochman, 2004; Jain *et al.*, 2003; Lerat *et al.*, 2005; Zhaxybayeva *et al.*, 2004).

Comparison of AprBA and DsrAB phylogeny from SRP

The topological comparison of AprB/A- and DsrAB-based trees revealed members of the same SRB lineages to be involved in lateral transfer of the *dsr* and *apr* genes. However, in the DsrAB-based tree, the deltaproteobacterial SRB group was monophyletic and the *Desulfobacterium anilini*-related SRB group was suggested to be the donor lineage for the xenologous *dsrAB* genes of the *Desulfotomaculum* subclusters Ib, Ic, Id and Ie, as well as *Moorella thermoacetica* (member of the *Thermoanaerobacteriales*). *Desulfosporosinus* and the *Desulfotomaculum* subclusters Ia, If and Ih have been postulated to represent the DsrAB-'authentic' Gram-positive SRB clades that were not affected by LGT (Imachi *et al.*, 2006; Klein *et al.*, 2001; Zverlov *et al.*, 2005). The xenologous gene displacements of the orthologous *dsrAB* genes in subclusters Ib–Ie are supported by the AprB/A phylogeny of this study, because *Desulfotomaculum* subclusters Ia/If and *Desulfosporosinus* consistently branch close to the root of the DsrAB- and AprB/A-based trees. According to the AprB/A phylogeny, the Gram-positive SRB species are monophyletic and present a relative branching order of taxa that is congruent with 16S rRNA and unaffected by LGT. Conversely, the acquisition of the *apr* gene of the deltaproteobacterial SRB lineages (*Syntrophobacteraceae*, the *Desulfobacterium anilini*-related SRB group, *Desulfomonile tiedjei* and *Desulfarculus baarsii*) postulated by four independent events of xenologous gene displacement is supported by the moderate relationships among their orthologous DsrAB sequences (Zverlov *et al.*, 2005). Indeed, this class of LGT has been reported to have influenced the evolutionary path of ~10–15 % of the orthologous genes in the bacterial domain (Novichkov *et al.*, 2004). The consistent xenologous branching positions from *Thermodesulfobacteriaceae* as well as *Archaeoglobus* in the AprA- and DsrAB-based trees (Klein *et al.*, 2001) point to a concerted acquisition of the novel capabilities to respire sulfite and sulfate by ancient, dual LGT events from unknown donor lineages; however, an early lateral transfer from Gram-positive SRB is suggested for the latter genus, since *Archaeoglobus* species seemed to be affiliated most closely with this lineage. In contrast, the ancestors of *Thermodesulfovibrio* might initially have been sulfite reducers, as indicated by the 16S rRNA-congruent branching of their DsrAB sequences (Klein *et al.*, 2001), and received their ability to respire

sulfate later on their evolutionary path. A donor lineage for the LGT of their *apr* genes is not apparent. Interestingly, a congruent taxonomical classification of both uncultivated putative SRB strains (fosws39f7, fosws7f8) (Mussmann *et al.*, 2005) was not possible on the basis of the Dsr and Apr sequences. A distinct origin is proposed for their xenologous *apr* and *dsr* genes, which are arranged as a metabolic island.

Correlation between Apr phylogeny and presence of proteins functionally associated with AprBA (Qmo and AprM) in SRP and SOB

The genome analysis indicated the development of two unrelated protein (complexes), AprM and QmoABC, mediating the electron transfer between the cytoplasmic sulfite oxidation/APS reduction process and the membrane quinone pool in correlation with the Apr phylogeny-based divergence of the SRP and SOB. The membrane-bound redox complex QmoABC that has been investigated and characterized from *Desulfovibrio desulfuricans* ATCC 27774 is proposed to act as a menaquinol/APS reductase oxidoreductase (Pires *et al.*, 2003). In support, further experimental studies have demonstrated the coordinated down-regulation of the *apr* and *qmo* gene sets in a *Desulfovibrio vulgaris* strain Hildenborough mutant in the presence of nitrite (Haveman *et al.*, 2004), and the dependence of the sulfate-reduction capability of *Desulfotomaculum aeronauticum* on amendment with the quinone precursor menadione (Hippe *et al.*, 1997). Indeed, (1) the presence of the *qmoABC* genes and their close proximity to the *aprBA* genes in all genomes of SRP (see Table 3, Fig. 4) (whereas they are absent in sulfite- or thiosulfate-reducing species which lack the *aprBA* genes; Supplementary Table S1), and (2) the congruent protein phylogenies (trees not shown), support the proposed functional association of the Qmo complex and the APS reductase in SRP. The presence of SRP-related *apr* and *qmo* genes in *Chlorobiaceae* genomes is an indication of an electron transfer system similar to that of SRP in the green sulfur bacteria. In contrast, in genomes of SOB harbouring *Allochromatium vinosum*-related Apr sequences, the *aprBA* genes are always co-regulated with a preceding *aprM* (encoding a membrane-integral protein), whereas ORFs homologous to *qmoABC* are absent (see Table 3, Fig. 4b). The strictly conserved arrangement and the AprBA-congruent AprM tree topology (not shown) point to an essential role for AprM in *Allochromatium vinosum* and other Apr-related SOB. An *in vivo* function as a structural component (membrane anchor) for the cytoplasmic APS reductase or even a direct functional involvement in electron transfer, by analogy with the menaquinol : fumarate oxidoreductase of *E. coli* (Cecchini *et al.*, 2002; Lancaster, 2003), are possible.

Unlike the APS reductase, the transmembrane redox complex that is functionally associated with the dissimilatory sulfite reductase (DsrAB) seems to be identical among the SRP and SOB. The homologous HmeABCDE and DsrMKJOP protein complexes have been proposed to operate in the electron transfer pathway between cytoplasmic DsrAB and the membrane-integral quinol/quinone pool (Dahl *et al.*, 2005; Mander *et al.*, 2002; Pires *et al.*, 2006; Sander *et al.*, 2006). The genome analyses in this study revealed DsrMKJOP homologues to be present in all sulfate- and sulfite-reducing as well as several sulfur-oxidizing bacteria (Supplementary Table S1).

Evolutionary scenario for the dissimilatory APS reductase as a key enzyme of the sulfate-reduction pathway in the light of Apr and Dsr phylogeny and geochemical data of Archean Earth

The global appearance of mass-independent isotope fractionation (MIF) in sedimentary sulfides and sulfates older than 2·45 billion years is consistent with low oxygen levels in the atmosphere ($pO_2 < 10^{-5}$ present atmospheric level; PAL) and a global sulfur cycle dominated by atmospheric reactions during the Archean era (4·0–2·4 billion years ago) (Farquhar *et al.*, 2000). Atmospheric sulfate generated by photolysis of SO_2 would have represented the only significant abiogenic sulfate load of the ocean (Canfield, 2005; Farquhar *et al.*, 2000; Strauss, 2003). Consistently, the absence of significant mass-dependent isotope fractionation between Archean sulfate and sulfide is an indication of a global sulfate concentration below 200 μM (Canfield *et al.*, 2000; Canfield, 2001; Habicht *et al.*, 2002) and the absence of an active global sulfur cycle in the Archean hydrosphere (Strauss, 2003). Sulfate in concentrations sufficient for energy conservation by sulfate respiration could have only been supplied by the metabolic activity of sulfur-oxidizing anoxygenic phototrophic bacteria (Canfield & Raiswell, 1999; Shen *et al.*, 2001). Indeed, photosynthetic microbial mats dominated by anoxygenic phototrophic bacteria existed at 3·4 billion years ago (Tice & Lowe, 2004). The ancestors of the modern SRP could have originated in dependence on the favourable conditions provided by the sulfur-oxidizing anoxygenic phototrophic bacteria, and the sulfate-reduction process might have become established and geochemically expressed as early as 3·4 billion years ago (Shen *et al.*, 2001) at local, restricted sites.

In agreement with the proposed geochemical setting of the Archean Earth, the Dsr and Apr phylogenies (Boucher *et al.*, 2003; this study) consistently point to their origin and evolution as oxidative-operating enzymes. Since the DsrAB has been suggested to be of ancient origin (Dhillon *et al.*, 2005), the reverse sulfate-reduction pathway might have evolved successively (sulfite reductase preceding the APS reductase and ATP sulfurylase) in an ancestral anoxygenic phototrophic bacterium. The development of DsrAB and its functionally associated DsrMKJOP complex (Dahl *et al.*, 2005; Mander *et al.*, 2002; Sander *et al.*, 2006) would have allowed the utilization of hydrothermal-derived sulfide as a

reductant for anoxygenic photosynthesis. The subsequent phylogenetic divergence into three DsrAB lineages (Boucher *et al.*, 2003) might have been the result of two early, independent LGTs of the progenotic *dsrAB* (in concert with the *dsrMKJOP* genes) from the ancestral sulfide-oxidizing bacterial donor lineage to the ancestors of SRP and sulfur-respiring archaeal *Pyrobaculum*. In the same way as their modern equivalents, the ancient microbial mats might have presented hot spots for the metabolic diversification of the microbial community by LGT (Molin & Tolker-Nielsen, 2003; Sorensen *et al.*, 2005). The ancestors of the SRB lineages might initially have been sulfite respirers by adaptive reversal of the oxidative-operating Dsr protein sets. The SRP-related DsrMKJOP of the *Chlorobiaceae* (Sander *et al.*, 2006) might have arisen from an early xenologous replacement of the *dsrMKJOP* genes of an ancestral green sulfur bacterium with those from a sulfite reducer.

Since the end product of Dsr-mediated sulfide/sulfur oxidation is sulfite, the reverse APS reductase might primarily have been developed by the ancestral sulfide oxidizers for detoxification instead of energy conservation. Indeed, a sulfite-oxidation pathway via the intermediate APS would have allowed the simultaneous generation of energy (ATP) by substrate phosphorylation, which would have contributed to relieving energy limitation in a primitive anoxygenic phototrophic bacterium. Two conflicting scenarios would explain the DsrAB-incongruent AprBA tree topology and the appearance of two different membrane protein(s) systems that interact with APS reductase. First, after phylogenetic separation of the progenotic detoxifying APS reductase into the lineages of the anoxygenic phototrophic green and purple sulfur bacteria, the protein sets QmoABC and AprM emerged independently in these groups and allowed the utilization of sulfite as a reductant in anoxygenic photosynthesis. The concurrent presence of *apr* and *qmo* genes in *Chlorobiaceae* and SRP genomes would have been the result of a subsequent, concerted LGT from an ancestral green sulfur bacterial donor to the sulfite-respiring ancestors of the SRP lineages. The second, alternative scenario implies an early divergence of the progenotic detoxifying AprBA into the phylogenetic lineages of the SOB and the SRP analogous to the postulated evolutionary path of DsrAB (Boucher *et al.*, 2003; Molitor *et al.*, 1998). The Qmo complex would then have originated within an ancestral sulfite-reducing bacterial lineage and not in an ancestor of the green sulfur bacteria, whereas AprM developed in ancestral purple sulfur bacteria. Because of the restricted distribution of the *apr* and *qmo* genes within the *Chlorobiaceae* (B. Meyer and J. Kuever, unpublished results), their ancestors either never possessed or lost their ancestral *apr* genes due to functional replacement by convergently evolved proteins. Indeed, a thermophilic sulfate-reducing lineage (e.g. *Thermodesulfovibrio*) could have served as donor for the later acquisition or reacquisition of the entire gene locus by LGT. Irrespective of possible evolutionary scenarios, the basal branching AprBA lineage of *Pyrobaculum aerophilum* might represent the APS reductase type most closely related to the progenotic detoxifying form, because no gene coding for any of the proposed functionally associated proteins is present in the genome. The patchy and polyphyletic distribution of the sulfate-reduction pathway among prokaryotes and the late diversification of the major SRP lineages, despite the postulated early origin of the respiration process (Shen *et al.*, 2001), might be the result of the persistently low sulfate content of ocean waters until 2·4 billion years ago (Canfield *et al.*, 2000; Canfield, 2005; Farquhar *et al.*, 2000; Habicht *et al.*, 2002; Strauss, 2003), which restricted the abundance and ecological significance of this physiological group in the Archean era. The radiation of the SRP might have started with the beginning of the oxygenation of the atmosphere (Canfield *et al.*, 2000; Canfield, 2005; Farquhar *et al.*, 2000), which resulted in an increasing oceanic sulfate concentration during the Proterozoic era (2·5–0·54 billion years ago) (Canfield, 2005; Kah *et al.*, 2004). A widespread lateral distribution of the sulfate-reduction pathway via mobilizable metabolic islands has been suggested (Friedrich, 2002; Mussmann *et al.*, 2005). However, (1) the absence of characteristic mobility elements indicative of classical genomic islands in the metagenome sequences (Mussmann *et al.*, 2005), (2) the generally scattered arrangement of the *dsr* and *apr* genes in the genomes of validated SRP, and (3) the differing phylogenies of DsrAB (Boucher *et al.*, 2003; Klein *et al.*, 2001; Zverlov *et al.*, 2005) compared with those of AprBA (this study) and Sat (Sperling *et al.*, 1998) caused by non-parallel LGT events, seem to contradict this hypothesis for the evolution of the dissimilatory sulfate-reduction pathway.

NOTE ADDED IN PROOF

While this paper was under review, *sat*, *aprBA* and *qmoABC* gene sequences of further SRB were made available in public databases by the (meta)genome sequencing projects of *Desulfovibrio vulgaris* strain DP4 (NC_008751), deltaproteobacterium strain MLMS-1 (NZ_AAFQ01000037, NZ_AAFQ01000064 and NZ_AAFQ01000396) and *Desulfosarcina/Desulfonema*-related symbionts of *Olavius algarvensis* (AASZ_01000000). The gene arrangements in the genomes of these SRB are identical to those of *Desulfovibrio* spp. and *Desulfotalea psychrophila* as presented in this work.

ACKNOWLEDGEMENTS

This study was supported by grants of the Bundesministerium für Bildung und Forschung (BMBF) (project 'Caribflux' under contract no. 03G0154C), the Deutsche Forschungsgemeinschaft (DFG) (under contract no. KU 916/8-1) and the Max Planck Society, Munich.

REFERENCES

Boucher, Y., Douady, C. J., Papke, R. T., Walsh, D. A., Boudreau, M. E. R., Nesbo, C. L., Case, R. J. & Doolittle, W. F. (2003). Lateral gene

transfer and the origins of prokaryotic groups. *Annu Rev Genet* **37**, 283–328.

Canfield, D. E. (2001). Isotope fractionation by natural populations of sulfate-reducing bacteria. *Geochim Cosmochim Acta* **65**, 1117–1124.

Canfield, D. E. (2005). The early history of atmospheric oxygen: homage to Robert A. Garrels. *Annu Rev Earth Planet Sci* **33**, 1–36.

Canfield, D. E. & Raiswell, R. (1999). The evolution of the sulfur cycle. *Am J Sci* **299**, 697–723.

Canfield, D. E., Habicht, K. S. & Thamdrup, B. (2000). The Archean sulfur cycle and the early history of atmospheric oxygen. *Science* **288**, 658–661.

Cecchini, G., Schröder, I., Gunsalus, R. P. & Maklashina, E. (2002). Succinate dehydrogenase and fumarate reductase from *Escherichia coli*. *Biochim Biophys Acta* **1553**, 140–157.

Dahl, C. & Trüper, H. G. (1994). Enzymes of dissimilatory sulfide oxidation in phototrophic sulfur bacteria. *Methods Enzymol* **243**, 400–421.

Dahl, C., Engels, S., Pott-Sperling, A. S., Schulte, A., Sander, J., Lubbe, Y., Deuster, O. & Brune, D. C. (2005). Novel genes of the *dsr* gene cluster and evidence for close interaction of Dsr proteins during sulfur oxidation in the phototrophic sulfur bacterium *Allochromatium vinosum*. *J Bacteriol* **187**, 1392–1404.

Daubin, V. & Ochman, H. (2004). Bacterial genomes as new gene homes: the genealogy of ORFans in *E. coli*. *Genome Res* **14**, 1036–1042.

DeLong, E. F. (1992). Archaea in coastal marine environments. *Proc Natl Acad Sci U S A* **89**, 5685–5689.

Dhillon, A., Goswami, S., Riley, M., Teske, A. & Sogin, M. (2005). Domain evolution and functional diversification of sulfite reductases. *Astrobiology* **5**, 18–29.

Farquhar, J., Bao, H. M. & Thiemens, M. (2000). Atmospheric influence of Earth's earliest sulfur cycle. *Science* **289**, 756–758.

Friedrich, M. W. (2002). Phylogenetic analysis reveals multiple lateral transfers of adenosine-5′-phosphosulfate reductase genes among sulfate-reducing microorganisms. *J Bacteriol* **184**, 278–289.

Fritz, G., Buchert, T., Huber, H., Stetter, K. O. & Kroneck, P. M. H. (2000). Adenylylsulfate reductases from archaea and bacteria are 1 : 1 alpha beta-heterodimeric iron-sulfur flavoenzymes – high similarity of molecular properties emphasizes their central role in sulfur metabolism. *FEBS Lett* **473**, 63–66.

Gogarten, J. P. & Townsend, J. P. (2005). Horizontal gene transfer, genome innovation and evolution. *Nat Rev Microbiol* **3**, 679–687.

Habicht, K. S., Gade, M., Thamdrup, B., Berg, P. & Canfield, D. E. (2002). Calibration of sulfate levels in the Archean ocean. *Science* **298**, 2372–2374.

Hattori, S., Kamagata, Y., Hanada, S. & Shoun, H. (2000). *Thermacetogenium phaeum* gen. nov., sp. nov., a strictly anaerobic, thermophilic, syntrophic acetate-oxidizing bacterium. *Int J Syst Evol Microbiol* **50**, 1601–1609.

Haveman, S. A., Greene, E. A., Stilwell, C. P., Voordouw, J. K. & Voordouw, G. (2004). Physiological and gene expression analysis of inhibition of *Desulfovibrio vulgaris* Hildenborough by nitrite. *J Bacteriol* **186**, 7944–7950.

Henstra, A. M. & Stams, A. J. M. (2004). Novel physiological features of *Carboxydothermus hydrogenoformans* and *Thermoterrabacterium ferrireducens*. *Appl Environ Microbiol* **70**, 7236–7240.

Hipp, W. M., Pott, A. S., Thum-Schmitz, N., Faath, I., Dahl, C. & Trüper, H. G. (1997). Towards the phylogeny of APS reductases and sirohaem sulfite reductases in sulfate-reducing and sulfur-oxidizing prokaryotes. *Microbiology* **143**, 2891–2902.

Hippe, H., Hagenauer, A. & Kroppenstedt, R. M. (1997). Menadione requirement for sulfate-reduction in *Desulfotomaculum aeronauticum*, and emended species description. *Syst Appl Microbiol* **20**, 554–558.

Imachi, H., Sekiguchi, Y., Kamagata, Y., Loy, A., Qiu, Y. L., Hugenholtz, P., Kimura, N., Wagner, M., Ohashi, A. & Harada, H. (2006). Non-sulfate-reducing, syntrophic bacteria affiliated with *Desulfotomaculum* cluster I are widely distributed in methanogenic environments. *Appl Environ Microbiol* **72**, 2080–2091.

Itoh, T., Suzuki, K., Sanchez, P. C. & Nakase, T. (1999). *Caldivirga maquilingensis* gen. nov., sp. nov., a new genus of rod-shaped crenarchaeote isolated from a hot spring in the Philippines. *Int J Syst Bacteriol* **49**, 1157–1163.

Jain, R., Rivera, M. C., Moore, J. E. & Lake, J. A. (2003). Horizontal gene transfer accelerates genome innovation and evolution. *Mol Biol Evol* **20**, 1598–1602.

Kah, L. C., Lyons, T. W. & Frank, T. D. (2004). Low marine sulphate and protracted oxygenation of the proterozoic biosphere. *Nature* **431**, 834–838.

Klein, M., Friedrich, M., Roger, A. J., Hugenholtz, P., Fishbain, S., Abicht, H., Blackall, L. L., Stahl, D. A. & Wagner, M. (2001). Multiple lateral transfers of dissimilatory sulfite reductase genes between major lineages of sulfate-reducing prokaryotes. *J Bacteriol* **183**, 6028–6035.

Kozak, M. (1999). Initiation of translation in prokaryotes and eukaryotes. *Gene* **234**, 187–208.

Kuever, J., Rainey, F. A. & Hippe, H. (1999). Description of *Desulfotomaculum* sp. Groll as *Desulfotomaculum gibsoniae* sp. nov. *Int J Syst Bacteriol* **49**, 1801–1808.

Kuever, J., Rainey, F. A. & Widdel, F. (2005). The deltaproteobacterial orders *Desulfovibrionales, Desulfobacterales, Desulfarcales* and *Syntrophobacterales*. In *Bergey's Manual of Systematic Bacteriology*, pp. 925–1040. Edited by G. Garrity. New York: Springer.

Kurland, C. G., Canback, B. & Berg, O. G. (2003). Horizontal gene transfer: a critical view. *Proc Natl Acad Sci U S A* **100**, 9658–9662.

Lampreia, J., Pereira, A. S. & Moura, J. J. G. (1994). Adenylylsulfate reductases from sulfate-reducing bacteria. *Methods Enzymol* **243**, 241–260.

Lancaster, C. R. D. (2003). *Wolinella succinogenes* quinol : fumarate reductase and its comparison to *E. coli* succinate : quinone reductase. *FEBS Lett* **555**, 21–28.

Lawrence, J. G. & Ochman, H. (1997). Amelioration of bacterial genomes: rates of change and exchange. *J Mol Evol* **44**, 383–397.

Lerat, E., Daubin, V., Ochman, H. & Moran, N. A. (2005). Evolutionary origins of genomic repertoires in bacteria. *PLoS Biol* **3**, e130.

Mander, G. J., Duin, E. C., Linder, D., Stetter, K. O. & Hedderich, R. (2002). Purification and characterization of a membrane-bound enzyme complex from the sulfate-reducing archaeon *Archaeoglobus fulgidus* related to heterodisulfide reductase from methanogenic archaea. *Eur J Biochem* **269**, 1895–1904.

Molin, S. & Tolker-Nielsen, T. (2003). Gene transfer occurs with enhanced efficiency in biofilms and induces enhanced stabilisation of the biofilm structure. *Curr Opin Biotechnol* **14**, 255–261.

Molitor, M., Dahl, C., Molitor, I., Schafer, U., Speich, N., Huber, R., Deutzmann, R. & Trüper, H. G. (1998). A dissimilatory sirohaem-sulfite-reductase-type protein from the hyperthermophilic archaeon *Pyrobaculum islandicum*. *Microbiology* **144**, 529–541.

Mori, K., Kim, H., Kakegawa, T. & Hanada, S. (2003). A novel lineage of sulfate-reducing microorganisms: *Thermodesulfobiaceae* fam. nov., *Thermodesulfobium narugense*, gen. nov., sp. nov., a new thermophilic isolate from a hot spring. *Extremophiles* **7**, 283–290.

Moussard, H., L'Haridon, S., Tindall, B. J., Banta, A., Schumann, P., Stackebrandt, E., Reysenbach, A. L. & Jeanthon, C. (2004).

Thermodesulfatator indicus gen. nov., sp. nov., a novel thermophilic chemolithoautotrophic sulfate-reducing bacterium isolated from the Central Indian Ridge. *Int J Syst Evol Microbiol* **54**, 227–233.

Mussmann, M., Richter, M., Lombardot, T., Meyerdierks, A., Kuever, J., Kube, M., Glockner, F. O. & Amann, R. (2005). Clustered genes related to sulfate respiration in uncultured prokaryotes support the theory of their concomitant horizontal transfer. *J Bacteriol* **187**, 7126–7137.

Muyzer, G., Teske, A., Wirsen, C. O. & Jannasch, H. W. (1995). Phylogenetic relationships of *Thiomicrospira* species and their identification in deep-sea hydrothermal vent samples by denaturing gradient gel electrophoresis of 16S rDNA fragments. *Arch Microbiol* **164**, 165–172.

Novichkov, P. S., Omelchenko, M. V., Gelfand, M. S., Mironov, A. A., Wolf, Y. I. & Koonin, E. V. (2004). Genome-wide molecular clock and horizontal gene transfer in bacterial evolution. *J Bacteriol* **186**, 6575–6585.

Pires, R. H., Lourenco, A. I., Morais, F., Teixeira, M., Xavier, A. V., Saraiva, L. M. & Pereira, I. A. C. (2003). A novel membrane-bound respiratory complex from *Desulfovibrio desulfuricans* ATCC 27774. *BBA Bioenergetics* **1605**, 67–82.

Pires, R. H., Venceslau, S. S., Morais, F., Teixeira, M., Xavier, A. V. & Pereira, I. A. C. (2006). Characterization of the *Desulfovibrio desulfuricans* ATCC 27774 DsrMKJOP complex – a membrane-bound redox complex involved in the sulfate respiratory pathway. *Biochemistry* **45**, 249–262.

Rabus, R., Hansen, T. A. & Widdel, F. (1999). Dissimilatory sulfate- and sulfur-reducing prokaryotes. In *The Prokaryotes: an Evolving Electronic Database for the Microbiological Community*, pp. 1–87. Edited by M. Dworkin, K.-H. Schleifer & E. Stackebrandt. New York: Springer.

Rabus, R., Ruepp, A., Frickey, T., Rattei, T., Fartmann, B., Stark, M., Bauer, M., Zibat, A., Lombardot, T. & other authors (2004). The genome of *Desulfotalea psychrophila*, a sulfate-reducing bacterium from permanently cold Arctic sediments. *Environ Microbiol* **6**, 887–902.

Sambrook, J., Fritsch, E. F. & Maniatis, T. (1989). *Molecular Cloning: a Laboratory Manual*, 2nd edn. Cold Spring Harbor, NY: Cold Spring Harbor Laboratory.

Sander, J., Engels-Schwarzlose, S. & Dahl, C. (2006). Importance of the DsrMKJOP complex for sulfur oxidation in *Allochromatium vinosum* and phylogenetic analysis of related complexes in other prokaryotes. *Arch Microbiol* **186**, 357–366.

Schedel, M. & Trüper, H. G. (1979). Purification of *Thiobacillus denitrificans* siroheme sulfite reductase and investigation of some molecular and catalytic properties. *Biochim Biophys Acta* **568**, 454–466.

Schedel, M. & Trüper, H. G. (1980). Anaerobic oxidation of thiosulfate and elemental sulfur in *Thiobacillus denitrificans*. *Arch Microbiol* **124**, 205–210.

Sekiguchi, Y., Kamagata, Y., Syutsubo, K., Ohashi, A., Harada, H. & Nakamura, K. (1998). Phylogenetic diversity of mesophilic and thermophilic granular sludges determined by 16S rRNA analysis. *Microbiology* **144**, 2655–2665.

Shen, Y. A., Buick, R. & Canfield, D. E. (2001). Isotopic evidence for microbial sulphate reduction in the early Archaean era. *Nature* **410**, 77–81.

Sorensen, S. J., Bailey, M., Hansen, L. H., Kroer, N. & Wuertz, S. (2005). Studying plasmid horizontal transfer in situ: a critical review. *Nat Rev Microbiol* **3**, 700–710.

Speich, N., Dahl, C., Heisig, P., Klein, A., Lottspeich, F., Stetter, K. O. & Trüper, H. G. (1994). Adenylylsulphate reductase from the sulfate-reducing archaeon *Archaeoglobus fulgidus* – cloning and characterization of the genes and comparison of the enzyme with other iron-sulfur flavoproteins. *Microbiology* **140**, 1273–1284.

Sperling, D., Kappler, U., Wynen, A., Dahl, C. & Trüper, H. G. (1998). Dissimilatory ATP sulfurylase from the hyperthermophilic sulfate reducer *Archaeoglobus fulgidus* belongs to the group of homo-oligomeric ATP sulfurylases. *FEMS Microbiol Lett* **162**, 257–264.

Strauss, H. (2003). Sulphur isotopes and the early Archaean sulphur cycle. *Precambrian Res* **126**, 349–361.

Suyama, M. & Bork, P. (2001). Evolution of prokaryotic gene order: genome rearrangements in closely related species. *Trends Genet* **17**, 10–13.

Tice, M. M. & Lowe, D. R. (2004). Photosynthetic microbial mats in the 3,416-Myr-old ocean. *Nature* **431**, 549–552.

Trüper, H. G. & Fischer, U. (1982). Anaerobic oxidation of sulfur-compounds as electron-donors for bacterial photosynthesis. *Philos Trans R Soc Lond B Biol Sci* **298**, 529–542.

Zhaxybayeva, O., Lapierre, P. & Gogarten, J. P. (2004). Genome mosaicism and organismal lineages. *Trends Genet* **20**, 254–260.

Zverlov, V., Klein, M., Lücker, S., Friedrich, M. W., Kellermann, J., Stahl, D. A., Loy, A. & Wagner, M. (2005). Lateral gene transfer of dissimilatory (bi)sulfite reductase revisited. *J Bacteriol* **187**, 2203–2208.

Edited by: G. Muyzer

Supplementary material

Supplementary Table S1. Homologous genes coding for dissimilatory sulfite reductase and functionally associated transmembrane complex proteins, and their genetic arrangement in partial or complete genome sequences of prokaryotes

SRP and SOB species	Homologous ORFs in genomic sequences (gene arrangement indicated by gene locus_tag no. annotation)						
	dsrA	*dsrB*	*dsrM/ hmeC*	*dsrK/ hmeD*	*dsrJ/ hmeE*	*dsrO/ hmeA*	*dsrP/ hmeB*
Chlorobia							
Chlorobaculum tepidum str. TLS	CT2249/ CT0852	CT2248/ CT0853	CT2244	CT2243	CT2242	CT2241	CT2240
Chlorobium phaeobacteroides DSM 266	Cpha266_1136	Cpha266_1135	Cpha266_2458	Cpha266_2457	Cpha266_2456	Cpha266_2455	Cpha266_2454
Chlorobium phaeobacteroides str. BS1	Cphamn1DRAFT_1219	Cphamn1DRAFT_1220	Cphamn1DRAFT_1547	Cphamn1DRAFT_1548	Cphamn1DRAFT_1549	Cphamn1DRAFT_1545	Cphamn1DRAFT_1544
Chlorobium limicola DSM 245	ClimDRAFT_0782	ClimDRAFT_0783	ClimDRAFT_0790	ClimDRAFT_0791	ClimDRAFT_0792	ClimDRAFT_0793	ClimDRAFT_0794
Chlorobium chlorochromatium str. CaD3	Cag_1956	Cag_1955	Cag_1948	Cag_1947	Cag_1946	Cag_1945	Cag_1944
Prosthecochloris aestuarii DSM 271	PaesDRAFT_0605	PaesDRAFT_0606	PaesDRAFT_0613	PaesDRAFT_0614	PaesDRAFT_0615	PaesDRAFT_0616	PaesDRAFT_0617
Chlorobium phaeovibrioides DSM 265	CvibDRAFT_0869	CvibDRAFT_0868	CvibDRAFT_0861	CvibDRAFT_0860	CvibDRAFT_0859	CvibDRAFT_0858	CvibDRAFT_0857
Chlorobium luteolum DSM 273	Plut_0036	Plut_0037	Plut_0044	Plut_0045	Plut_0046	Plut_0047	Plut_0048
Chlorobium clathratiforme str. BU-1	PphaDRAFT_1185	PphaDRAFT_1184	PphaDRAFT_1177	PphaDRAFT_1176	PphaDRAFT_1197	PphaDRAFT_1175	PphaDRAFT_1174
Alphaproteobacteria							
Magnetospirillum magneticum str. AMB-1	amb3367	amb3368	amb3373	amb3374	amb3376	amb3377	amb3378
Magnetospirillum magnetotacticum str. MS-1	Magn03007648	Magn03007649	Magn03007102	Magn03007103 (NTCS) + Magn03009258 (CTCS)†	Magn03009256	Magn03009255	Magn03009254-Magn03009252[b]
Betaproteobacteria							
Thiobacillus denitrificans ATCC 25259	Tbd_1369/ Tbd_1309/ Tbd_2485	Tbd_2484	Tbd_2479	Tbd_2478	Tbd_2476	Tbd_2475	Tbd_2474
Gammaproteobacteria							
Allochromatium vinosum DSM 180	AAC35394*	AAC35395*	AAC35400*	AAC35401*	AAG13083 *	AAG13084 *	AAG13085 *
Alkalilimnicola ehrlichei str. MLHE-1	MlgDRAFT_2359	MlgDRAFT_2358	MlgDRAFT_2353	MlgDRAFT_2352	MlgDRAFT_2350	MlgDRAFT_2349	MlgDRAFT_2348
Halorhodospira halophila str. SL1	HhalDRAFT_2336	HhalDRAFT_2337	HhalDRAFT_2342	HhalDRAFT_2343	HhalDRAFT_2345	HhalDRAFT_2346	HhalDRAFT_2347
Deltaproteobacteria							
Desulfotalea psychrophila str. LSv54	DP0797	DP0798	DP3075	DP3074	DP3073	DP3072 (NTCS) +DP3071 (CTCS)†	DP3070
Desulfovibrio vulgaris ssp. *vulg.* str. Hildenborough	DVU0402	DVU0403	DVU1290	DVU1289	DVU1288	DVU1287	DVU1286
Desulfovibrio desulfuricans str. G20	Dde_0526	Dde_0527	Dde_2271	Dde_2272	Dde_2273	Dde_2274	Dde_2275
Syntrophobacter fumaroxidans str. MPOB	SfumDRAFT_ 0104 (CTCS)†	SfumDRAFT_ 0103	SfumDRAFT_ 2761	SfumDRAFT_ 2760	SfumDRAFT_ 2759	SfumDRAFT_ 2758	incomplete ORF: NTCS present in SfumDRAFT_ 2758 following sequence†
Uncultured sulfate-reducing bacterium fosws39f7	39f70003	39f70004	39f70011	39f70012	39f70013	39f70014	39f70015
Uncultured sulfate-reducing bacterium fosws7f8	ws7f8_26	ws7f8_24	ws7f8_16	ws7f8_15	ws7f8_14	ws7f8_28	ws7f8_29
Thermodesulfobacteria							
Thermodesulfobacterium commune DSM 2178	TIGR contig 486	TIGR contig 486	TIGR contig 486	TIGR contig 486	TIGR contig 486	TIGR contig 486	TIGR contig 486
Nitrospira							
Thermodesulfovibrio yellowstonii DSM 11347	TIGR contig 173	TIGR contig 173	TIGR contig 173	TIGR contig 173	TIGR contig 173	TIGR contig 173	TIGR contig 173
Clostridia							
Desulfotomaculum reducens str. MI-1	DredDRAFT_0635	DredDRAFT_0634	DredDRAFT_0647	DredDRAFT_0646	-	-	-
Desulfitobacterium hafniense str. Y51	DSY0309	DSY0310	DSY0312	DSY0313	DSY0314	DSY0315	DSY0316
Desulfitobacterium hafniense str. DFB-2	DhafDRAFT_1141	DhafDRAFT_1142	DhafDRAFT_1145	DhafDRAFT_1146	DhafDRAFT_1147	DhafDRAFT_1148	DhafDRAFT_1149
Carboxydothermus hydrogenoformans str. Z-2901	CHY_2410	CHY_2409	CHY_2404	CHY_2403	-	-	-
Moorella thermoacetica ATCC 39073	Moth_1601	Moth_1600	Moth_1602	Moth_1606	Moth_1605	Moth_1604	Moth_1603
Unclassified bacteria							
Magnetococcus sp. str. MC-1	Mmc1DRAFT_ 2356	Mmc1DRAFT_ 2357	Mmc1DRAFT_ 0053	Mmc1DRAFT_ 0054	Mmc1DRAFT_ 0153	Mmc1DRAFT_ 0152	incomplete ORF: NTCS present in Mmc1DRAFT_ 0152 following sequence[b]
Uncultured bacterium BAC13K9BAC	AAY89969*	AAY89968*	AAY89963*	AAY89962*	AAY89960*	AAY89959*	AAY89958*
Euryarchaeota							
Archaeoglobus fulgidus DSM 4304	AF0423	AF0424	AF0501	AF0502	AF0503	AF0499	AF500
Crenarchaeota							
Pyrobaculum aerophilum str. IM-2	PAE2572/ PAE2596	PAE2571/ PAE2597	PAE2614	PAE2616	-	-	-

* GenBank protein accession no. of respective ORF.
† Incorrect ORF annotation by automated protein coding gene prediction program in genome sequence (abbreviations used to determine incomplete ORF sequences: NTCS/ CTCS for N- or C-terminal protein coding sequence).

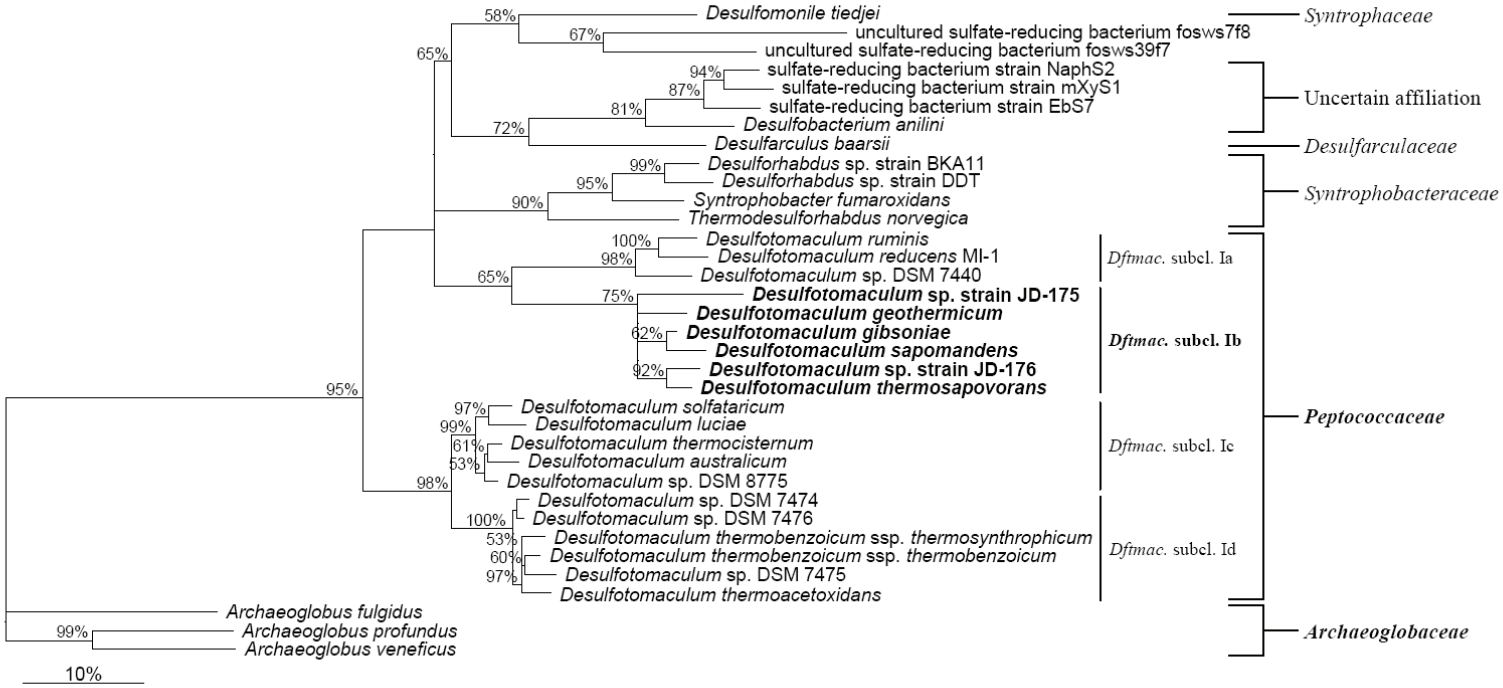

Supplementary Fig. S1. Phylogenetic tree based on partial AprA sequences presenting the orthologous Apr lineage of the Gram-positive SRB including the *Desulfotomaculum* subcluster Ib (in bold type) with related, xenologous deltaproteobacterial SRB. The subtree was inferred using PUZZLE analysis (maximum-likelihood method). *Archaeoglobus* spp. were used as outgroup. The scale bar corresponds to 10 % estimated sequence divergence. Reliability of branching order is indicated by numbers representing the quartet puzzling support values of the corresponding branches; polytomic nodes connect branches for which a relative order could not be determined unambiguously by PUZZLE. The topological congruence with the subcluster classification of the genus *Desulfotomaculum* (*Dftmac*. sbcl. Ia-d) based on the 16S rRNA gene phylogeny (Kuever *et al*., 1999) is indicated.

Supplementary Fig. S2. AprB and AprA alignment showing indels among selected representatives of the major lineages of SRP and SOB supporting the inferred lateral *aprBA* gene transfers in SRP and the separate phylogenetic position of the *Allochromatium vinosum*-related sequences group

Identical indel positions in AprB/A sequences are indicated by grey-shaded boxes.

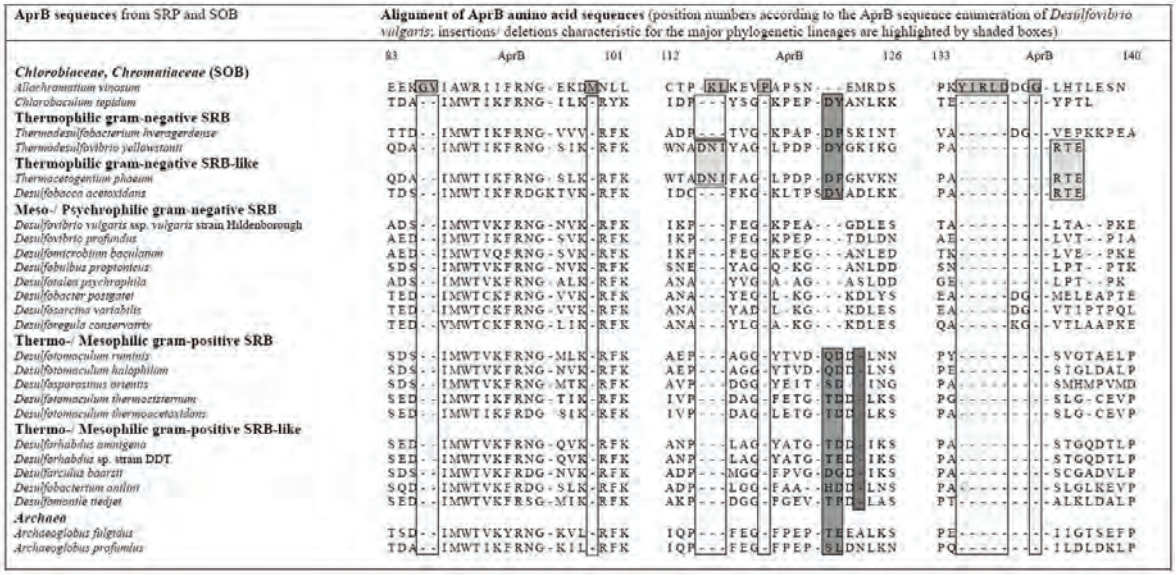

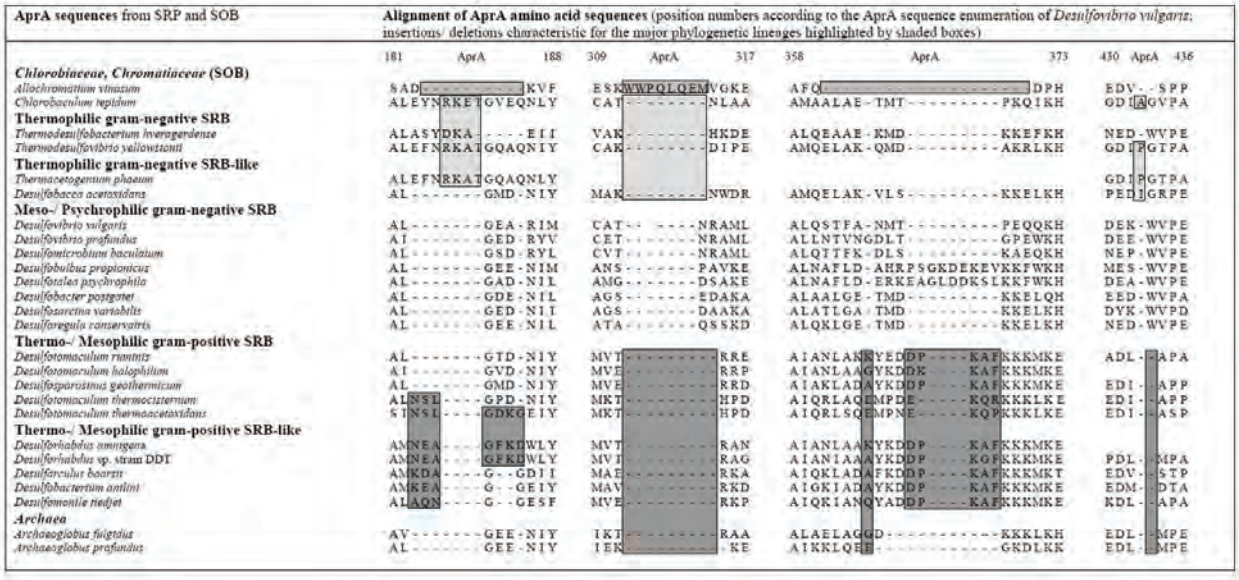

4.2.2 Publikation 2

Molecular analysis of the distribution and phylogeny of dissimilatory adenosine-5`-phosphosulfate (APS) reductase-encoding genes (aprBA) among sulfur-oxidizing prokaryotes

Birte Meyer und Jan Küver

Microbiology (2007). 153, 3478-3498

Microbiology (2007), **153**, 3478–3498 DOI 10.1099/mic.0.2007/008250-0

Molecular analysis of the distribution and phylogeny of dissimilatory adenosine-5′-phosphosulfate reductase-encoding genes (*aprBA*) among sulfur-oxidizing prokaryotes

Birte Meyer and Jan Kuever†

Max-Planck-Institute for Marine Microbiology, Celsiusstrasse 1, D-28359 Bremen, Germany

Correspondence
Jan Kuever
kuever@mpa-bremen.de

Dissimilatory adenosine-5′-phosphosulfate (APS) reductase (AprBA) is a key enzyme of the dissimilatory sulfate-reduction pathway. Homologues have been found in photo- and chemotrophic sulfur-oxidizing prokaryotes (SOP), in which they are postulated to operate in the reverse direction, oxidizing sulfite to APS. Newly developed PCR assays allowed the amplification of 92–93 % (2.1–2.3 kb) of the APS reductase locus *aprBA*. PCR-based screening of 116 taxonomically divergent SOP reference strains revealed a distribution of *aprBA* restricted to photo- and chemotrophs with strict anaerobic or at least facultative anaerobic lifestyles, including *Chlorobiaceae*, *Chromatiaceae*, *Thiobacillus*, *Thiothrix* and invertebrate symbionts. In the AprBA-based tree, the SOP diverge into two distantly related phylogenetic lineages, Apr lineages I and II, with the proteins of lineage II (*Chlorobiaceae* and others) in closer affiliation to the enzymes of the sulfate-reducing prokaryotes (SRP). This clustering is discordant with the dissimilatory sulfite reductase (DsrAB) phylogeny and indicates putative lateral *aprBA* gene transfer from SRP to the respective SOB lineages. In support of lateral gene transfer (LGT), several beta- and gammaproteobacterial species harbour both *aprBA* homologues, the DsrAB-congruent 'authentic' and the SRP-related, LGT-derived gene loci, while some relatives possess exclusively the SRP-related *apr* genes as a possible result of resident gene displacement by the xenologue. The two-gene state might be an intermediate in the replacement of the resident essential gene. Collected genome data demonstrate the correlation between the AprBA tree topology and the composition/arrangement of the *apr* gene loci (occurrence of *qmoABC* or *aprM* genes) from SRP and SOP of lineages I and II. The putative functional role of the SRP-related APS reductases in photo- and chemotrophic SOP is discussed.

Received 21 March 2007
Revised 15 June 2007
Accepted 25 June 2007

†Present Address: Bremen Institute for Materials Testing, Paul-Feller-Strasse 1, D-28199 Bremen, Germany.

Abbreviations: APAT, adenylylsulfate : phosphate adenylyltransferase; APS, adenosine-5′-phosphosulfate; DGGE, denaturing gradient gel electrophoresis; DG-DGGE, double-gradient DGGE; LGT, lateral gene transfer; SAOR, sulfite : acceptor oxidoreductase; SDR, sulfur dioxygenase; SOB, sulfur-oxidizing bacteria; SOP, sulfur-oxidizing prokaryotes; SQR, sulfide : quinone oxidoreductase; SRP, sulfate-reducing prokaryotes.

The GenBank/EMBL/DDBJ accession numbers for the *aprBA* and 16S rRNA sequences of the species examined in this study are EF641902–EF641963 and EF675611–EF675615, respectively.

A supplementary table of the presence of genes encoding dissimilatory sulfite reductase and its functionally associated proteins in genome sequences of SOB, and two supplementary figures showing a phylogenetic consensus tree based on 16S rRNA gene sequences from the *apr*-containing SOB reference strains, and an AprB and AprA alignment showing indels among selected representatives of the major phylogenetic SOB lineages, are available with the online version of this paper.

INTRODUCTION

Microbial sulfur oxidation is a key process in the oxidative half of the sulfur cycle in soil and water, and dominates as the major reaction, especially in extreme environments such as volcanic hot springs, solfataras and deep-sea hydrothermal vents. Reduced inorganic sulfur compounds such as sulfide, polysulfides, sulfur, sulfite, thiosulfate and various polythionates can serve as electron donors for the energy-generating systems in many photo- and chemotrophic species of the domain *Bacteria*, whereas this metabolic capability is restricted in the domain *Archaea* to representatives of the thermoacidophilic order *Sulfolobales* (Brune, 1995; Brüser *et al.*, 2000; Friedrich, 1998; Huber & Prangishvili, 2000; Nelson & Fisher, 1995; Overmann & Garcia-Pichel, 2001). The sulfur-oxidizing prokaryotes (SOP) are phylogenetically and physiologically diverse, differing in their abilities to utilize the various reduced sulfur compounds. As a consequence, the enzymic

pathways used for dissimilatory sulfur oxidation have been found to be widely variable and may involve different intermediates (Brune, 1995; Brüser *et al.*, 2000; Friedrich, 1998; Friedrich *et al.*, 2001; Kletzin *et al.*, 2004; Nelson & Fisher, 1995). The oxidation of sulfide generally results in the formation of periplasmic and extracellular sulfur globules mediated by the activity of the ubiquitous enzyme sulfide : quinone oxidoreductase (SQR) (Griesbeck *et al.*, 2000; Theissen *et al.*, 2003). Its further oxidation to sulfate has been suggested to be mediated by the reverse-operating enzymes of the sulfate-reduction process, comprising the dissimilatory ATP sulfurylase, adenosine-5′-phosphosulfate (APS) reductase and sulfite reductase, which are ubiquitously present in the sulfate-reducing prokaryotes (SRP). Homologues have been shown to exist in several anoxygenic phototrophic and facultative anaerobic chemotrophic sulfur-oxidizing bacteria (SOB) (Dahl & Trüper, 1994; Hipp *et al.*, 1997; Taylor, 1994; Trüper & Fischer, 1982). Experimental evidence is accumulating that the reverse-acting sulfite reductase (DsrAB) and its functionally associated transmembrane redox complex DsrMKJOP are essential for the oxidation of sulfide or intermediately stored sulfur to sulfite (Dahl *et al.*, 2005; Sander *et al.*, 2006). Its subsequent oxidation to sulfate can be mediated by two different enzymes in SOB: (1) the APS reductase (Apr), catalysing the oxidative binding of sulfite to AMP, which generates APS as product; and (2) the sulfite : acceptor oxidoreductase (SAOR), catalysing the AMP-independent oxidation to sulfate without formation of intermediates (Brune, 1995; Brüser *et al.*, 2000; Kappler & Dahl, 2001). Sulfate is released from APS by the activity either of ATP sulfurylase (Sat) or adenylylsulfate : phosphate adenylyltransferase (APAT). Energy is yielded by substrate phosphorylation, with the former enzyme transferring the AMP moiety of APS onto pyrophosphate, which leads to ATP formation, while the latter enzyme uses phosphate for replacement and produces ADP (Brune, 1995; Brüser *et al.*, 2000).

Recent studies have confirmed that the dissimilatory APS reductases (irrespective of metabolic type) consist of two different subunits, which are proposed to form a 1 : 1 $\alpha\beta$-heterodimeric iron–sulfur flavoenzyme (AprBA). Only the α subunit, AprA, has structural similarity to the flavoprotein subunits of the succinate-dehydrogenase/fumarate-reductase family; however, this structural relationship is not reflected in sequence similarity (Fritz *et al.*, 2000, 2002; Schiffer *et al.*, 2006). The encoding genes, *aprBA*, have been cloned from sulfur-oxidizing *Allochromatium vinosum*; comparative sequence analysis confirmed their homology to the dissimilatory APS reductase of bacterial and archaeal SRP (Hipp *et al.*, 1997). However, the *in vivo* role of the reverse APS reductase, compared to that of the SAOR, in the dissimilatory oxidative sulfur metabolism of photo- and chemotrophic SOP (Dahl, 1996; Sanchez *et al.*, 2001) and its functional linkage to the photosynthetic and respiratory electron transport chain are still unresolved. For SRP, there is increasing evidence that the Qmo redox complex, consisting of one membrane-integral (QmoC) and two cytoplasmic (QmoAB) proteins, acts as a menaquinol/APS reductase oxidoreductase (Haveman *et al.*, 2004; Pires *et al.*, 2003).

Previous phylogenetic analyses of enzymes of the sulfate-reduction pathway (Apr and Dsr) have been restricted to SRP, and have revealed that multiple lateral gene transfer (LGT) events have affected their evolutionary path (Friedrich, 2002; Klein *et al.*, 2001) (Meyer & Kuever, 2007). The aims of this study were (1) the comprehensive molecular investigation of *aprBA* distribution among SOP by examining 116 representatives of photo- and chemotrophic sulfur-oxidizing *Archaea* and *Bacteria*, and (2) the phylogenetic analysis of the AprBA sequences to reveal potential LGTs affecting the SOP and to elucidate the origin and evolution of the sulfite-oxidation process. Accordingly, novel PCR assays were developed that enabled the amplification and direct sequencing of 92–93 % (equivalent to 2.1–2.3 kb) of the reverse APS reductase gene region to establish a new *aprBA* database from the major taxonomic lineages of SOP. The results of this work also provide a framework for future molecular ecological studies to investigate the microbial community of the sulfur cycle by functional gene analysis.

METHODS

Micro-organisms. The investigated reference strains of photo- and chemotrophic SOB (listed in Table 1) were obtained from the DSMZ (Braunschweig, Germany). Genomic DNA of *Chlorobiaceae* and several *Chromatiaceae* were received from the culture collection of J. Imhoff (University of Kiel) Extracted genomic DNAs of invertebrate tissues were provided by N. Dubilier, Max-Planck-Institute for Marine Microbiology, (*Inanidrilus* spp., *Bathymodiolus azoricus* and *Bathymodiolus brevior*), A. D. Nussbauer, University of Vienna, (*Riftia pachyptila*, *Bathymodiolus thermophilus*, *Calyptogena magnifica* and *Oasisia* sp.) and C. Borowski, Max-Planck-Institute for Marine Microbiology, (*Ifremeria nautilei*). Harvested cells of *Beggiatoa* spp., *Aquaspirillum* spp., *Macromonas bipunctata* strain D-408 and *Spirochaeta* spp. were received from G. Dubinina, Winogradsky Institute of Microbiology. The SOB strain 'manganese crust' was isolated from enrichment cultures of sediment and seawater samples from the Caribbean Sea (Caribflux project, SO-154).

DNA isolation. Genomic DNA from the investigated reference strains was obtained by applying the DNAeasy kit (Qiagen) or the NUCLEOBOND kit (Macherey–Nagel) according to the manufacturers' instructions. The DNA concentration and quality were estimated spectrophotometrically, while its integrity was examined visually by gel electrophoresis on 0.8 % (w/v) agarose gels run in 1 × Tris/borate/EDTA (TBE) buffer and followed by ethidium bromide staining (0.5 $\mu g\ ml^{-1}$).

PCR amplification of *aprBA* and 16S rRNA genes. The forward primers AprB-1-FW and AprB-3-FW (with different target sites in the *aprB* gene) were used in combination with the reverse primer AprA-5-RV for amplification of a 1.2–1.3 kb and a 1.2–1.1 kb *aprBA* gene fragment, respectively. The forward primer AprA-1-FW was combined with the reverse primers AprA-9-RV or AprA-10-RV (identical target site in the *aprA* gene), which yielded a 1.4 kb *aprA* amplicon from the 5′-terminal region of *aprA*. The *aprBA* and *aprA* amplicons

Table 1. cont.

Species*	Strain†	PCR product obtained with primer set‡			Phylogenetic affiliation and length of the *aprBA* sequence§		GenBank accession no. *aprBA*
		AprB-1-FW/ AprA-5-RV	AprB-3-FW/ AprA-5-RV	AprA-1-FW/ AprA-9-RV or AprA-10-RV	Apr lineage I	Apr lineage II	
Thiolamprovum pedioforme	3802^T	+ (60)	+ (63)	+ (63)	I: 2163	–	EF641941
Thiorhodococcus minor	11518^T	+ (63)	+ (63)	± (55)	I: 1205	II: 1250	EF641950, EF641913
Thiorhodovibrio winogradskyi	6702^T	+ (63)	ND	+ (63)	I: 2094	–	EF641946
Ectothiorhodospiraceae							
Ectothiorhodospira mobilis†	4180	– (54)	ND	– (54)	–	–	–
Ectothiorhodospira shaposhnikovii	243^T	– (54)	ND	– (54)	–	–	–
Halothiobacillaceae							
Halothiobacillus kellyi	13162^T	– (50)	– (50)	– (50)	–	–	–
Halothiobacillus neapolitanus	581^T	– (50)	– (50)	– (50)	–	–	–
Thiovirga sulfuroxydans sp. strain A7	–	– (58)	ND	ND	–	–	–
Thiotrichaceae							
Beggiatoa alba	1416^T	– (54)	ND	– (54)	–	–	–
Beggiatoa leptomitiformis strain D-401	–	– (54)	ND	– (54)	–	–	–
Beggiatoa leptomitiformis strain D-402	–	– (54)	ND	– (54)	–	–	–
Leucothrix mucor	2157^T	– (55)	– (50)	– (50)	–	–	–
Leucothrix mucor	621	– (55)	– (50)	– (50)	–	–	–
Macromonas bipunctata strain D-408	–	– (55)	ND	– (55)	–	–	–
Thiothrix nivea	5205^T	+ (54)	– (63)	+ (56)	–	II: 2277	EF641919
Thiothrix sp.	12730	+ (54)	– (63)	+ (56)	–	II: 2318	EF641918
Piscirickettsiaceae							
Thiomicrospira frisia	12351^T	– (54)	ND	– (54)	–	–	–
Thiomicrospira kuenenii	12350^T	– (54)	ND	– (54)	–	–	–
Thiomicrospira sp.	13163	– (54)	ND	– (54)	–	–	–
Thiomicrospira sp.	13164	– (54)	ND	– (54)	–	–	–
Thiomicrospira sp.	13189	– (54)	ND	– (54)	–	–	–
Thiomicrospira sp.	13190	– (54)	ND	– (54)	–	–	–
Uncertain affiliation							
'*Thiobacillus prosperus*'	5130^T	– (50)	– (50)	– (50)	–	–	–
Invertebrate symbionts and free-living relatives							
Bathymodiolus azoricus symbiont	–	± (54)	ND	± (54)	I: 2142	–	EF641959
Bathymodiolus brevior symbiont	–	± (54)	ND	± (54)	I: 2163	–	EF641958
Bathymodiolus thermophilus symbiont	–	± (54)	ND	± (54)	I: 2169	–	EF641960
Calyptogena magnifica symbiont	–	± (55)	ND	± (55)	I: 982	–	EF669484
Ifremeria nautilei symbiont	–	+ (55)	+ (55)	± (55)	–	II: 1304	EF641929
Inanidrilus exumae symbiont	–	+ (57)	ND	± (52)	I: 1198	II: 1331	EF641957, EF641927
Inanidrilus leukodermatus symbiont	–	+ (57)	ND	± (52)	–	II: 2225	EF641926
Inanidrilus makropetalos symbiont	–	+ (57)	ND	± (52)	–	II: 2249	EF641925
Oasisia sp. symbiont	–	± (54)	ND	± (52)	I: 396	–	EF641962
Riftia pachyptila symbiont	–	+ (57)	ND	± (55)	–	II: 2210	EF641928
Sulfur-oxidizing bacterium OAII2#	–	± (54)	ND	± (53)	I: 2105	–	EF641953
Sulfur-oxidizing bacterium OBII5	–	± (54)	ND	± (53)	–	–	–
Sulfur-oxidizing bacterium ODIII5	–	+ (55)	ND	± (55)	I: 2161	–	EF641951
Sulfur-oxidizing bacterium ODI4	–	– (55)	ND	– (54)	–	–	–
Sulfur-oxidizing bacterium NDII1.2		– (55)	ND	– (54)	–	–	–
Sulfur-oxidizing bacterium 'manganese crust'	–	± (50)	ND	± (50)	I: 1288	–	EF641930

Table 1. cont.

Species*	Strain†	PCR product obtained with primer set‡			Phylogenetic affiliation and length of the *aprBA* sequence§		GenBank accession no. *aprBA*
		AprB-1-FW/ AprA-5-RV	AprB-3-FW/ AprA-5-RV	AprA-1-FW/ AprA-9-RV or AprA-10-RV	Apr lineage I	Apr lineage II	
Rhodobiaceae							
Rhodobium marinum	2698^T	− (54)	ND	− (54)	−	−	−
Phylum *Proteobacteria*, *Betaproteobacteria*							
Hydrogenophilaceae							
Thiobacillus aquaesulis	4255^T	+ (55)	+ (63)	± (63)	−	II: 2314	EF641916
Thiobacillus denitrificans	12475^T	+ (55)	+ (63)	± (63)	I: 1197	II: 2262	EF641952, EF641924
Thiobacillus denitrificans	739	± (63)	+ (63)	± (63)	I: 553	II: 2218	EF641955, EF641923
Thiobacillus denitrificans¶	807	± (63)	ND	± (63)	−	II: 2215	EF641922
Thiobacillus plumbophilus	6690^T	± (55)	± (63)	± (63)	I: 1183	II: 2317	EF641956, EF641917
Thiobacillus thioparus¶	505^T	± (55)	+ (63)	+ (63)	I: 1152	II: 2275	EF641954, EF641920
Neisseriaceae							
Aquaspirillum sp. strain D-412	−	− (55)	ND	− (55)	−	−	−
Aquaspirillum sp. strain D-415	−	− (55)	ND	− (55)	−	−	−
Phylum *Proteobacteria*, *Gammaproteobacteria*							
Chromatiaceae							
Allochromatium minutissimum‖	1376^T	± (63)	+ (63)	± (63)	I: 2090	−	EF641963
Allochromatium vinosum‖	180^T	+ (63)	+ (63)	+ (63)	I: 2168	−	−
Allochromatium warmingii‖	173^T	± (55)	+ (63)	± (63)	I: 2140	−	EF641931
*Chromatium okenii***	*6010*	± (63)	+ (63)	± (63)	I: 2122	−	EF641935
Halochromatium glycolicum	11080^T	± (63)	± (63)	+ (63)	I: 2142	−	EF641934
Halochromatium salexigens	4395^T	+ (63)	± (63)	+ (63)	I: 2127	−	EF641933
Isochromatium buderi	176^T	− (55)	ND	− (54)	−	−	−
*Isochromatium buderi***	*5612*	− (55)	ND	− (54)	−	−	−
*Lamprocystis purpurea***	4197^T	+ (63)	+ (63)	− (55)	−	II: 1285	EF641909
*Lamprocystis roseopersicina***	*4510*	+ (63)	ND	+ (63)	I: 2159	−	EF641939
Marichromatium gracile	203^T	− (55)	ND	− (54)	−	−	−
Marichromatium purpuratum	1591^T	− (55)	ND	− (54)	−	−	−
Rhabdochomatium marinum	5261^T	+ (63)	+ (63)	± (63)	I: 2159	−	EF641947
Thermochromatium tepidum	3771^T	± (63)	+ (63)	+ (63)	I: 2121	−	EF641936
Thiocapsa pendens	236^T	+ (55)	ND	− (55)	−	II: 1298	EF641914
*Thiocapsa rosea***	235^T	− (57)	− (63)	− (55)	I: 371	−	EF641961
Thiocapsa roseopersicina	217^T	+ (63)	+ (63)	+ (63)	I: 1197	II: 2285	EF641937, EF641907
*Thiocapsa roseopersicina***	*4210*	+ (63)	+ (63)	+ (63)	I: 1197	II: 2298	EF641938, EF641908
*Thiococcus pfennigii***	226^T	+ (63)	ND	± (63)	I: 2129	−	EF641942
Thiococcus pfennigii	227	+ (63)	+ (63)	+ (63)	I: 2138	−	EF641943
Thiococcus pfennigii	228	± (63)	+ (63)	± (63)	I: 2126	−	EF641944
Thiocystis gelatinosa	215^T	+ (63)	+ (55)	+ (63)	−	II: 2327	EF641911
Thiocystis violacea‖	207^T	+ (63)	+ (63)	+ (63)	I: 1197	II: 2238	EF641948, EF641912
Thiocystis violacea	214	+ (63)	ND	+ (63)	I: 2128	−	EF641949
Thiocystis violascens	198^T	+ (63)	+ (63)	+ (55)	−	II: 2251	EF641910
*Thiodictyon bacillosum***	234^T	+ (63)	ND	+ (55)	−	II: 2155	EF641915
Thiodictyon sp. strain F4	−	± (50)	ND	± (50)	−	II: 2321	EF641921
Thiohalocapsa halophila	6210^T	+ (63)	+ (63)	+ (63)	I: 2172	−	EF641932

Table 1. cont.

Species*	Strain†	PCR product obtained with primer set‡			Phylogenetic affiliation and length of the *aprBA* sequence§		GenBank accession no. *aprBA*
		AprB-1-FW/ AprA-5-RV	AprB-3-FW/ AprA-5-RV	AprA-1-FW/ AprA-9-RV or AprA-10-RV	Apr lineage I	Apr lineage II	
Thiolamprovum pedioforme	3802^T	+ (60)	+ (63)	+ (63)	I: 2163	–	EF641941
Thiorhodococcus minor	11518^T	+ (63)	+ (63)	± (55)	I: 1205	II: 1250	EF641950, EF641913
Thiorhodovibrio winogradskyi	6702^T	+ (63)	ND	+ (63)	I: 2094	–	EF641946
Ectothiorhodospiraceae							
Ectothiorhodospira mobilis†	4180	– (54)	ND	– (54)	–	–	–
Ectothiorhodospira shaposhnikovii	243^T	– (54)	ND	– (54)	–	–	–
Halothiobacillaceae							
Halothiobacillus kellyi	13162^T	– (50)	– (50)	– (50)	–	–	–
Halothiobacillus neapolitanus	581^T	– (50)	– (50)	– (50)	–	–	–
Thiovirga sulfuroxydans sp. strain A7	–	– (58)	ND	ND	–	–	–
Thiotrichaceae							
Beggiatoa alba	1416^T	– (54)	ND	– (54)	–	–	–
Beggiatoa leptomitiformis strain D-401	–	– (54)	ND	– (54)	–	–	–
Beggiatoa leptomitiformis strain D-402	–	– (54)	ND	– (54)	–	–	–
Leucothrix mucor	2157^T	– (55)	– (50)	– (50)	–	–	–
Leucothrix mucor	621	– (55)	– (50)	– (50)	–	–	–
Macromonas bipunctata strain D-408	–	– (55)	ND	– (55)	–	–	–
Thiothrix nivea	5205^T	+ (54)	– (63)	+ (56)	–	II: 2277	EF641919
Thiothrix sp.	12730	+ (54)	– (63)	+ (56)	–	II: 2318	EF641918
Piscirickettsiaceae							
Thiomicrospira frisia	12351^T	– (54)	ND	– (54)	–	–	–
Thiomicrospira kuenenii	12350^T	– (54)	ND	– (54)	–	–	–
Thiomicrospira sp.	13163	– (54)	ND	– (54)	–	–	–
Thiomicrospira sp.	13164	– (54)	ND	– (54)	–	–	–
Thiomicrospira sp.	13189	– (54)	ND	– (54)	–	–	–
Thiomicrospira sp.	13190	– (54)	ND	– (54)	–	–	–
Uncertain affiliation							
'*Thiobacillus prosperus*'	5130^T	– (50)	– (50)	– (50)	–	–	–
Invertebrate symbionts and free-living relatives							
Bathymodiolus azoricus symbiont	–	± (54)	ND	± (54)	I: 2142	–	EF641959
Bathymodiolus brevior symbiont	–	± (54)	ND	± (54)	I: 2163	–	EF641958
Bathymodiolus thermophilus symbiont	–	± (54)	ND	± (54)	I: 2169	–	EF641960
Calyptogena magnifica symbiont	–	± (55)	ND	± (55)	I: 982	–	EF669484
Ifremeria nautilei symbiont	–	+ (55)	+ (55)	± (55)	–	II: 1304	EF641929
Inanidrilus exumae symbiont	–	+ (57)	ND	± (52)	I: 1198	II: 1331	EF641957, EF641927
Inanidrilus leukodermatus symbiont	–	+ (57)	ND	± (52)	–	II: 2225	EF641926
Inanidrilus makropetalos symbiont	–	+ (57)	ND	± (52)	–	II: 2249	EF641925
Oasisia sp. symbiont	–	± (54)	ND	± (52)	I: 396	–	EF641962
Riftia pachyptila symbiont	–	+ (57)	ND	± (55)	–	II: 2210	EF641928
Sulfur-oxidizing bacterium OAII2#	–	± (54)	ND	± (53)	I: 2105	–	EF641953
Sulfur-oxidizing bacterium OBII5	–	± (54)	ND	± (53)	–	–	–
Sulfur-oxidizing bacterium ODIII5	–	+ (55)	ND	± (55)	I: 2161	–	EF641951
Sulfur-oxidizing bacterium ODI4	–	– (55)	ND	– (54)	–	–	–
Sulfur-oxidizing bacterium NDII1.2		– (55)	ND	– (54)	–	–	–
Sulfur-oxidizing bacterium 'manganese crust'	–	± (50)	ND	± (50)	I: 1288	–	EF641930

Table 1. cont.

Species*	Strain†	PCR product obtained with primer set‡			Phylogenetic affiliation and length of the *aprBA* sequence§		GenBank accession no. *aprBA*
		AprB-1-FW/ AprA-5-RV	AprB-3-FW/ AprA-5-RV	AprA-1-FW/ AprA-9-RV or AprA-10-RV	Apr lineage I	Apr lineage II	
Phylum *Proteobacteria, Epsilonproteobacteria*							
Helicobacteraceae							
Sulfurimonas denitrificans	1251^T	− (54)	ND	− (54)	−	−	−
Phylum *Spirochaeta, Spirochaetes*							
Spirochaetaceae							
Spirochaeta sp. strain P	−	− (55)	ND	− (55)	−	−	−
Spirochaeta sp. strain BM	−	− (55)	ND	− (55)	−	−	−
Spirochaeta sp. strain M-6	−	− (55)	ND	− (55)	−	−	−

*Taxonomic classification of investigated SRP species according to the Taxonomic outline of the prokaryotes, Bergey's Manual of Systematic Bacteriology, 2nd edition, release 5.0, May 2004 (http://dx.doi.org/10.1007/bergeysoutline); genomic DNA of sulfur-oxidizing reference strains marked with ** were received from J. Imhoff's laboratory (Kiel, Germany).

†DSMZ strain numbers of investigated species (Imhoff laboratory internal numbers in italic type); −, not deposited in a culture collection; T, type strain.

‡PCR amplification results with the respective primer pair: +, correct-sized amplicon without by-products; ±, correct-sized amplicon with by-products; −, no amplicon obtained; ND, PCR amplification not determined. The initial PCR annealing temperature (°C) is given in parentheses.

§Length of assembled *aprBA* gene fragment PCR product and phylogenetic assignment of the deduced AprBA sequence to the Apr lineages I and II.

‖Proposed presence of dissimilatory APS reductase in respective species based on enzyme activity assay (see Dahl & Trüper, 1994, and references therein).

¶Proposed presence of dissimilatory APS reductase in respective species based on enzyme activity assay (see Taylor, 1994, and references therein).

#Proposed presence of dissimilatory APS reductase in respective species based on enzyme activity assay (see Kuever *et al.*, 2002).

††Uncertain taxonomic classification (synonym *Ectothiorhodospira marismortui*).

overlap in sequence by ~390 bp (corresponding to nucleotide positions 3471–3859 in the *sat–aprMBA* operon of *Allochromatium vinosum*; Table 2).

PCR assays were performed with the RED*Taq* DNA polymerase kit (Sigma–Aldrich). Reaction mixtures (50 µl total volume) contained 5 µl 10 × RED*Taq* PCR reaction buffer (with 11 mM $MgCl_2$), 5 µl 10 × BSA solution (3 mg ml^{-1}), 200 µM deoxynucleoside triphosphates (dNTPs) mixture, 1 µM of each primer and 10–100 ng genomic DNA as template (water was used as a negative control in all PCR amplifications). PCR amplification was performed in a thermocycler (Eppendorf) with an initial denaturation step of 95 °C for 5 min followed by the addition of 2.5 U RED*Taq* DNA polymerase to each PCR assay (hot start PCR). Subsequently, a 'touchdown' thermal profile was performed (35 cycles in total): 95 °C for 60 s (denaturation), 63 °C for 90 s ('touchdown': the annealing temperature was lowered at every cycle of the first 20 cycles by 0.5 °C to a final temperature of 53 °C, after which 15 additional cycles were carried out) and 72 °C for 120 s (elongation). Amplification was completed by a final elongation step at 72 °C for 10 min. The initial annealing temperature of the 'touchdown' was altered in a range between 63 and 55 °C to optimize the amplification results.

16S rRNA gene fragments were amplified using the primer sets GM3F/GM4R and GM5F-GC clamp/907R [for subsequent denaturing gradient gel electrophoresis (DGGE) analysis] with the PCR conditions described elsewhere (Muyzer *et al.*, 1995).

Double-gradient (DG) DGGE analysis of PCR-amplified 16S rRNA gene fragments. DG-DGGE was applied to improve the quality of 16S rDNA band separation and resolution. An acrylamide gradient from 6 to 8 % acrylamide/bisacrylamide stock solution, 37.5 : 1 (v/v) (Bio-Rad), was superimposed over a collinear denaturant gradient from 20 to 70 % of denaturant [100 % denaturant corresponds to 7 M urea and 40 % formamide (v/ v), deionized with AG501-X8 mixed bed resin (Bio-Rad)]. Gradients were formed using a Bio-Rad Gradient Former model 385. PCR samples were applied to the gels in aliquots of 20 µl per lane. Further analysis was performed as described elsewhere (Muyzer *et al.*, 1995) using the D-CODE and D-GENE systems (Bio-Rad) for electrophoresis runs in 1 × Tris/acetate/EDTA (TAE) buffer at 60 °C for 3.5 h at 200 V. After staining with ethidium bromide (0.5 µg ml^{-1}), DNA bands were visualized on a UV transillumination table (Biometra), excised from the polyacrylamide gel, eluted in 50 µl Tris/HCl, pH 8.0, and reamplified using the original PCR conditions and primer pair without a GC clamp.

Cloning of PCR products. The *aprBA* and 16S rRNA amplicons were ligated into pCR2.1-TOPO vectors (TOPO TA cloning systems; Invitrogen) and transformed into chemically competent *Escherichia coli* TOP10 cells as recommended by the manufacturer. Clone plasmids were screened for correct-sized inserts by PCR amplification followed by RFLP analysis of the amplicons. Cloned plasmids with different digestion patterns were selected for sequencing and recovered with the QIAprep spin kit (Qiagen).

Nucleotide sequencing. The *aprBA*, *aprA* and 16S rDNA PCR products of the expected sizes were purified using QIAquick PCR purification, the QIAquick gel extraction kit (Qiagen) or the

Table 2. PCR primers utilized for amplification of the *aprBA* and *aprA* gene fragments

Primer	Sequence (5′→3′)*	Primer binding site†	Reference
AprB-1-FW	TGC GTG TAY ATH TGY CC	2653–2669	‡
AprB-3-FW	ACM WGT GCT GGG AGT GCT AC	2726–2745	This study
AprA-1-FW	TGG CAG ATC ATG ATY MAY GG	3471–3490	‡
AprA-5-RV	GCG CCA ACY GGR CCR TA	3843–3859	‡
AprA-9-RV	CKG WAG TAG TAR CCS GGS YA	4811–4831	This study
AprA-10-RV	CKG WAG TAG WAR CCR GGR TA	4811–4831	‡

*Degenerate positions are in bold type.
†Corresponding nucleotide positions of the *sat–aprMBA* operon of *Allochromatium vinosum* (GenBank accession no. U84759).
‡Meyer & Kuever (2007).

Perfectprep gel cleanup sample kit (Eppendorf,), following the suppliers' recommendations. All PCR products were sequenced directly in both directions using the respective amplification primers and the ABI BigDye terminator cycle sequencing kit (Applied Biosystems). Sequencing reactions were run on an ABI PRISM 3100 Genetic Analyzer (Applied Biosystems).

Sequence analysis tools and phylogenetic tree inference. The nucleotide sequence data for the *aprBA* and *aprA* amplicons were assembled (2.1–2.3 kb total length) and manually corrected using the BioEdit (version 7.0.5) sequence alignment editor (http://www.mbio.ncsu.edu/BioEdit/BioEdit.html). BLAST searches for homologues (AprBA and DsrAB) were performed at the NCBI website (http://www.ncbi.nlm.nih.gov/BLAST/). Searches on the preliminary sequence data of ongoing SOB and SRP genome sequencing projects were performed at The Institute for Genomic Research website (http://www.tigr.org) and at the US Department of Energy (DOE) Joint Genome Institute website (http://img.jgi.doe.gov/cgi-bin/pub/main.cgi). The AprBA and DsrAB sequences were aligned by using the web server Tcoffee@igs (http://igs-server.cnrs-mrs.fr/Tcoffee/). The AprBA and DsrAB datasets were phylogenetically analysed with the tree inference methods included in the ARB software package (http://www.arb-home.de). Alignment regions of insertions and deletions (indels) were not considered. Unrooted phylogenetic trees were calculated based on two AprBA datasets of 379 and 701, and a DsrAB dataset of 740 compared amino acid positions, using the ARB implemented program package (distance matrix, Fitch analysis; maximum-parsimony, ProtPars; maximum-likelihood, ProML) and the PhyML program (maximum-likelihood method; http://atgc.lirmm.fr/phyml). Maximum-likelihood trees were constructed using the Whelan and Goldman (WAG) or Jones, Taylor and Thornton (JTT) amino acid substitution model matrices. The robustness of inferred trees was tested by bootstrap analysis with 100 resamplings using the PhyML program.

Prediction of potential promoters, termination sites and gene arrangement in operons was performed using the web versions FGENESB, BPROM and BTERM of the Softberry program package (http://www.softberry.com/berry.phtml). Secondary structure analysis and transmembrane helix prediction were done using programs available at http://us.expasy.org/tools/#secondary.

Southern blot analysis. Identical amounts of genomic DNA (5 μg) from sulfur-oxidizing and sulfate-reducing bacteria (Table 3) were digested at 37 °C with *Hin*dIII and *Eco*RI overnight, precipitated by ethanol, electrophoresed on 0.8 % 1 × TAE buffer at 100 V for 3 h, transferred to positively charged nylon membranes (Hybond-N+ filter, Amersham) by capillary neutral transfer and immobilized by UV cross-linking (Transilluminator; Biometra). The *aprA* gene DNA probes (0.4 kb in length) were radioactively labelled with [α-^{32}P]dCTP by the random-priming method using the HexaLabel DNA labelling kit (MBI Fermentas) according to the manufacturer's instructions. The membranes were placed into glass hybridization bottles and prehybridized in 5 × SSC (1 × SSC is 0.15 M NaCl, 0.015 M sodium citrate, pH 8.0), 50 % formamide, 0.1 % sarcosyl, 7 % SDS, 50 mM phosphate buffer, pH 7.0, and 2 % casein ('Church' hybridization solution) at 50 °C for 1 h in a hybridization oven (Biometra). Subsequently, a freshly denaturated, labelled DNA probe was added to the prehybridization solution followed by incubation for 12–16 h at 50 °C under slow-speed rotation. The membranes were washed twice at 50 °C for 30 min in 0.1 × SSC/0.1 % SDS, exposed to PhosphorImaging screen cassettes (Molecular Dynamics), scanned with a Typhoon Variable Mode Imager and processed with ImageQuant software (Amersham). The membranes were stripped by two incubations for 15 min in probe-stripping solution (consisting of 0.4 M NaOH and 0.1 % SDS) at 37 °C under permanent agitation and reprobed, starting from the prehybridization step of the hybridization procedure.

RESULTS

Amplification of *aprBA* genes by PCR from SOB

In this study, 116 archaeal or bacterial, photo- or chemolithotrophic reference strains were investigated for the presence of *aprBA* genes. Previous studies have reported the association of invertebrates with a single thiotrophic symbiont phylotype (Blazejak *et al.*, 2006; Bright & Giere, 2005; Cavanaugh *et al.*, 2001; Nelson & Fisher, 1995), which is supported by the single Apr sequences obtained from the investigated species (except *Inanidrilus exumae*). The results of the PCR-based survey are summarized in Table 1 and demonstrate the high species diversity coverage of the primers. In general, the four different primer sets yielded correct-sized PCR products when higher annealing temperatures (>55 °C) were applied in the assays. However, in some cases (e.g. invertebrate symbionts) the annealing temperature had to be lowered (from 55 to 50 °C) to obtain a sufficient amount of *apr* amplicons for direct sequencing. The comparison of the primer sequences to newly available genomic *aprBA* sequences (e.g. *Candidatus* Ruthia magnifica

Table 3. Determination of *apr* gene locus number in SOB

Cloning assay results for the *aprBA* amplicons from SOB species for which direct sequencing failed are shown; the potential presence of contaminants in the investigated SOB cultures was checked by cloning and DGGE analysis of PCR-amplified 16S rRNA gene fragments.

Species	DSM*	Gene locus number according to sequence analysis of cloned *aprBA* amplicons†	DGGE analysis and cloning assay results of 16S rRNA gene amplicons‡	
		AprB-1-FW or AprB-3-FW/AprA-5-RV§	GM5F-GC clamp/907R§	GM3F/GM4R§
Gammaproteobacteria				
Thiocapsa roseopersicina	217	2 (Apr lineages I and II)	Four DGGE bands‖	ND
Thiocapsa roseopersicina	*4210***	2 (Apr lineages I and II)	Two DGGE bands‖	ND
Thiocystis violacea	207	2 (Apr lineages I and II)	Two DGGE bands: seq. nearly identical to reference strain	Two seq. nearly identical to reference strain
Thiorhodococcus minor	11518	2 (Apr lineages I and II)	Two DGGE bands: seq. nearly identical to reference strain	Two seq. nearly identical to reference strain
Invertebrate symbionts				
Inanidrilus exumae	–	2 (Apr lineages I and II)	Two DGGE bands‖	ND
Betaproteobacteria				
Thiobacillus denitrificans	12475	2 (Apr lineages I and II)	One DGGE band: seq. identical to reference strain	One seq. identical to reference strain
Thiobacillus denitrificans	739	2 (Apr lineages I and II)	One DGGE band: seq. identical to reference strain	ND
Thiobacillus plumbophilus	6690	2 (Apr lineages I and II)	One DGGE band: seq. identical to reference strain	One seq. identical to reference strain
Thiobacillus thioparus	505	2 (Apr lineages I and II)	One DGGE band: seq. identical to reference strain	ND

*Cultures obtained from culture collection of J. Imhoff (laboratory internal numbers in italic type) are marked with **; –, not deposited in a culture collection.

†Phylogenetic assignment of AprBA sequences to Apr lineages I and II in parentheses.

‡Abbreviations: ND, 16S rDNA amplicon cloning assays of respective SOB species were not performed; seq., sequence(s).

§Primer sets used to generate amplicons. For primer sets GM5F/907R and GM3F/GM4R, see Muyzer *et al.* (1995).

‖No pure culture of reference strains according to 16S rDNA-based DGGE analysis: besides the sulfur-oxidizing reference strain, additional 16S rDNA sequence(s) indicated the presence of non-sulfur-oxidizing species (BLAST search results) in the investigated cultures.

and *Olavius algarvensis* symbionts) (Newton *et al.*, 2007; Woyke *et al.*, 2006) revealed the presence of single mismatches to the strictly conserved target sites. However, as reported for 16S rRNA-based studies (Kwok *et al.*, 1990; Simsek & Adnan, 2000), the presence of single mismatches at internal or 5′-end sequence positions in the novel PCR primers did not affect their PCR efficiency. Thus, the absence of *apr* amplicons most likely reflects the absence of the APS reductase genes in the respective SOB species. Overall, the occurrence of *aprBA* genes in SOB seemed to be restricted to most *Chromatiaceae* species, a few representatives of the *Chlorobiaceae*, *Thiobacillus* spp. (*Betaproteobacteria*), *Thiothrix* spp. and the sulfur-oxidizing symbionts, including their free-living relatives (*Gammaproteobacteria*).

Number of *apr* gene loci in SOB

Interestingly, direct nucleotide sequencing of *aprBA* and *aprA* amplicons of some SOB species (Table 3) failed due to high levels of sequence ambiguities. Investigation of the genome of *Thiobacillus denitrificans* ATCC 25259 (Beller *et al.*, 2006) revealed the existence of two *apr* gene loci of differing sequence. Therefore, the previous SOB species were checked for the presence of multiple *apr* genes by cloning assays of the *aprBA* PCR products and subsequent RFLP analysis of the recombinant plasmids. The assays revealed the existence of two *aprBA* genes of differing sequence in genomic DNA from *Thiocapsa roseopersicina* (DSM 217 and *4210*), *Thiocystis violacea* and *Thiorhodococcus minor*, *Thiobacillus denitrificans* (DSM 12475 and 739), *Thiobacillus thioparus* and *Thiobacillus plumbophilus* cultures, and the Gamma-4 symbiont of *Inanidrilus exumae* (see Table 3). The GM3F/GM4R-amplified 16S rRNA gene fragments of these species were analysed by cloning assays (followed by RFLP analysis), while all investigated SOB cultures were checked by 16S rDNA-based DGGE analysis; the results confirmed the absence of putative sulfur-oxidizing, *apr*-harbouring contaminants in the examined reference strain cultures of this study.

Unexpectedly, PCR amplification of *apr* gene fragments was unsuccessful for most studied *Chlorobiaceae* (see Table 1). Therefore, Southern blot experiments were performed with *Chlorobium* spp. [subclusters 2a and 3b (Imhoff, 2003)] by using different, radioactively labelled *aprA* probes (Table 4; *aprA* probe sequence was verified by direct sequencing of an identical non-labelled PCR product). The Southern blot analyses confirmed the results of the PCR assays for the *Chlorobiaceae*. In addition, the appearance of two distinct hybridization signals with the *Thiocapsa roseopersicina*-specific probe supported the existence of two *aprA* genes in *Thiocapsa roseopersicina*, as suggested by the PCR and cloning assays (Table 1).

Phylogeny of dissimilatory APS reductase of SOB

The 63 partial (Table 1) and 27 full-length AprBA sequences of sulfur-oxidizing reference strains (from public databases; Table 5) were integrated into the pre-existing AprBA database of SRP species (Meyer &, 2007). Phylogenetic trees were constructed based on (1) 379 compared positions (sequence data of the *aprBA* amplicon) (Fig. 1) and (2) 701 compared positions (assembled sequence data of the *aprBA* and *aprA* amplicons) (Fig. 2). In contrast to the DsrAB phylogeny, which clearly demonstrates the evolutionary divergence of the proteins from sulfate/sulfite reducers and sulfur oxidizers into two separate clusters (Fig. 3), the AprBA sequences of SOB separated into two distinct lineages, Apr lineages I and II. While the oxidative-operating AprBA proteins of lineage I formed a distinct, DsrAB-congruent cluster of SOB (less than 43.5 % sequence identity to the SRP and affiliated SOB Apr lineage II sequences), the oxidative-operating AprBA proteins of lineage II were DsrAB-discordantly placed in closer affiliation with the reductive-operating enzymes of the SRP, which was indicative of LGT events. Within these major Apr lineages, the SOB taxa clustered consistently with their 16S rRNA-gene-based classification into the *Chlorobiaceae* and individual classes of the *Proteobacteria* (see Supplementary Fig. S1, available with the online version of this paper) (Cavanaugh *et al.*, 2001; Imhoff, 2001a, 2003; Kelly & Wood, 2000; Kuever *et al.*, 2002; Polz *et al.*, 1996; Robertson & Kuenen, 2001). In Apr lineage I, the *Alphaproteobacteria* formed a basal branching group separated into (1) the SAR11 clade, comprising *Pelagibacter ubique* (Giovannoni *et al.*, 2005) and closely related environmental sequences, and (2) the SAR116 clade [environmental sequences derived from shotgun sequencing of Sargasso and Red Sea water samples (Venter *et al.*, 2004; G. Sabehi and O. Beja, unpublished data)]. However, the close relatedness of *Thiobacillus plumbophilus* to the *Alphaproteobacteria* is discordant with its 16S rRNA-gene-based betaproteobacterial position. The second group of Apr lineage I consisted of the *Gammaproteobacteria*, with distinct clusters formed by (1) the symbiotic and related, free-living chemotrophic SOB (e.g. symbionts of *Calyptogena magnifica* and *Bathymodiolus* spp., strain OAII2) that are 16S rRNA-discordantly in close affiliation with the group of betaproteobacterial *Thiobacillus* spp., and (2) the anoxygenic phototrophic *Chromatiaceae*. The Apr-based intrafamily branching order of the *Chromatiaceae* taxa was partially incongruent with the 16S rRNA-gene-based phylogeny (Imhoff, 2001a) and indicated putative LGT events among members of the *Chromatiaceae* (e.g. marine *Thiococcus pfennigii* strains were in closer affiliation with freshwater *Allochromatium* spp. than with salt-requiring *Rhabdochromatium* or halophilic *Halochromatium* spp.). In agreement with its 16S rRNA-gene-based

Table 4. Results of Southern blot assays with radioactively labelled *aprA*-specific probes and genomic DNA of SOB and SRB

Genomic DNA of SOB species (*Eco*RI/*Hind*III digestion)	DSM*	Southern blot hybridization results with *aprA*-specific probe†			
		Chlorobium limicola 1855	*Chlorobium clathratiforme* 5477	*Thiocapsa roseopersicina 4210***	*Desulfomicrobium baculatum* 4028
Gammaproteobacteria					
Thiocapsa roseopersicina	217	+‡	+	++‡	+
Thiocapsa roseopersicina	*4210***	+‡	+	++‡	+
Chlorobia					
Chlorobium limicola	245**	−	−	−	−
Chlorobium limicola	248**	−	−	−	−
Chlorobium limicola	1855**	++	+	+	+
Chlorobium luteolum	262**	−	−	−	−
Chlorobium luteolum	273**	−	−	−	−
Deltaproteobacteria					
Desulfomicrobium baculatum	4028	++	+	+	++

*Cultures obtained from culture collection of J. Imhoff (laboratory internal numbers in italic type) are marked with **.

†Quality of hybridization results: −, no hybridization; +, hybridization signal; ++, strong hybridization signal.

‡Two hybridization signals obtained with genomic DNA of reference strain *Thiocapsa roseopersicina* DSM 217 and strain *4210* (culture collection of J. Imhoff).

Table 5. Presence of *sat*, *apr* and *qmo* homologues coding for the dissimilatory ATP sulfurylase, the APS reductase and its putative functionally associated proteins (AprM and QmoABC) in genome sequences of SOB (the genomic arrangement of the genes is indicated by the GenBank accession numbers of the encoded proteins)

Environm. seq., environmental sequence.

SOB species	GenBank accession numbers of genome sequences	Homologues present in the SOB genome*						
		Sat	AprM	AprB	AprA	QmoA	QmoB	QmoC
Chlorobia								
Chlorobium clathratiforme str. BU-1	AAIK01000013	ZP_00589416	–	ZP_00589417	ZP_00589418	ZP_00589419	ZP_00589420	ZP_00589421
Chlorobium chlorochromatii str. CaD3	NC_007514	YP_379885	–	YP_379884	YP_379883	YP_379882	YP_379881	YP_379880
Chlorobium phaeobacteroides str. BS1	NZ_AAIC01000057, NZ_AAIC01000606, NZ_AAIC01000002	ZP_00532500	–	ZP_00532499	ZP_00532499‡	ZP_005333969†	ZP_005333969†	ZP_00530754
Chlorobaculum tepidum str. TLS	NC_002932	NP_661756	–	NP_661758	NP_661759	NP_661760	NP_661761	NP_661762
Alphaproteobacteria								
SAR11 clade								
Pelagibacter ubique HTCC1002	NC_007205	–	ZP_01264008	ZP_01264007†	ZP_01264006	–	–	–
Pelagibacter ubique HTCC1062	AACY01002870	–	YP_266255	YP_266256	YP_266257	–	–	–
Environm. seq. IBEA_CTG_2004608	AACY01050991	–	EAK63329‡	EAK63329	EAK63328	–	–	–
Environm. seq. IBEA_CTG_2148592	AACY01000596	–	EAJ52712‡	EAJ52712	EAJ52711	–	–	–
Environm. seq. IBEA_CTG_1977812	AACY01023675	–	EAK69056‡	EAK69056	EAK69055‡	–	–	–
Environm. seq. IBEA_CTG_2104149	AACY01055405	–	EAK12872‡	EAK12872	EAK12873	–	–	–
Environm. seq. IBEA_CTG_2157860	AACY01021098	–	–	EAJ42062	EAJ42063	–	–	–
Environm. seq. IBEA_CTG_2023371	NC_007205	EAK19071	EAK19072	EAK19073	EAK19074	–	–	–
Environm. seq. IBEA_CTG_2151824	AACY01077644	–	EAI88884	EAI88883	EAI88882	–	–	–
Environm. seq. IBEA_CTG_2037797	AACY01013231	–	EAK37254	EAK37255	EAK37256	–	–	–
Environm. seq. IBEA_CTG_2149712	AACY01043919	–	EAJ68379	EAJ68380	EAJ68381	–	–	–
Environm. seq. IBEA_CTG_2157518	AACY01120224	–	EAH91106	EAH91107	EAH91108	–	–	–
Environm. seq. IBEA_CTG_2150375	AACY01003082	–	EAK62842	EAK62843	EAK62844	–	–	–
Environm. seq. IBEA_CTG_2126577	AACY01037195	–	EAJ82119	EAJ82118	EAJ82117	–	–	–
Environm. seq. IBEA_CTG_2151480	AACY01061995	–	EAJ26240†	EAJ26241	EAJ26242	–	–	–
SAR116 clade								
Uncultured bacterium EBAC2C11	AY744399	AAV31643	AAV31644	AAV31645	AAV31646	–	–	–
Environm. seq. IBEA_CTG_2159535	AACY01013150	–	EAK37449	EAK37448	EAK37447‡	–	–	–

Table 5. cont.

SOB species	GenBank accession numbers of genome sequences	Homologues present in the SOB genome*						
		Sat	AprM	AprB	AprA	QmoA	QmoB	QmoC
Betaproteobacteria								
Thiobacillus denitrificans ATCC 25259	NC_007404	YP_314632	YP_316042	YP_314631/ YP_316041	YP_314630/ YP_316040	YP_315406	YP_315405	–
Gammaproteobacteria								
Allochromatium vinosum	U84759§	AAC23622	AAK16200	AAC23620	AAC23621	–	–	–
Olavius algarvensis Gamma-3 symbiont	AASZ_01000200	+	+	+	+	–	–	–
Olavius algarvensis Gamma-1 symbiont	AASZ_01004101, AASZ_01004100, AASZ_01000461	ND	–	+‡	+‡	+	+	–
Endoriftia persephone	AASF_01001200, AASF_01001506, AASF_01002103, AASF_01001775, AASF_01001739	+‡	–	+	+	+‡	+‡	–
Cdt. Ruthia magnifica str. CM	NC_008610	YP_903355	YP_903356	YP_903357	YP_903358			

*The presence of protein encoding *sat*, *aprBA*, *aprM* and *qmoABC* homologues in the SOB genome is indicated by the GenBank accession number of the respective protein (or by + for the metagenomic sequences of the gammaproteobacterial symbiont of *Olavius algarvensis*).
†Incorrect gene annotation by automated protein coding gene prediction program in genome sequence.
‡Incomplete gene sequences obtained from unfinished genome/environmental metagenome sequencing projects.
§Partial genome sequence obtained by cloning experiments.

phylogenetic assignment as a member of the genus *Allochromatium*, the AprBA-based trees confirmed the incorrect classification of SOB strain DSM 214 as a *Thiocystis violacea* subspecies.

The *dsrAB*-discordant branching position of Apr lineage II in the Apr trees points to putative lateral transfer of *apr* genes among SRP and SOB. This lineage comprised the proteins of the green sulfur bacteria and several members of the *Chromatiaceae*, *Thiobacillus* and invertebrate symbionts. While some of these beta- and gammaproteobacterial SOB harbour a second *apr* gene locus that codes for the putative resident, 'authentic' homologue (Apr lineage I), the majority exclusively possess *aprBA* genes of the SRP-related Apr lineage II. In this lineage, the green sulfur bacteria formed a monophyletic group (sequence identity >80.9 %) in closer affiliation with the reductive-operating Apr of the *Thermodesulfovibrio–Desulfobacca* cluster than with the other oxidative-acting APS reductases of the proteobacterial SOB. The latter group diverged in agreement with the 16S rRNA phylogeny into (1) the chemotrophic betaproteobacterial SOB (*Thiobacillus*), and (2) the chemo- and phototrophic gammaproteobacterial SOB (*Thiothrix*, symbionts from *Riftia*, *Inanidrilus* and *Ifremeria* and seven *Chromatiaceae* species). However, the AprBA-based basal branching of the phototrophic Fe(II)-oxidizing *Thiodictyon* sp. strain F4 in closest affiliation with the *Thiobacillus* spp. was not consistent with its 16S rRNA-gene-based classification (Ehrenreich & Widdel, 1994).

Additional evidence for LGT of *aprBA*

The presence of indels at identical positions in the AprBA alignments provides additional evidence for LGT events. In addition, the sequences were checked for recent LGT events by identification of atypical sequence characteristics (Lawrence & Ochman, 1997), e.g. significant deviations in mol% G+C content and codon usage between the LGT-derived gene and respective SOB genome, as well as the corresponding *dsrAB* genes.

The separate phylogenetic position of Apr lineage I was confirmed by the presence of nine unique indels in the sequences of both subunits (see grey-shaded boxes in AprBA alignment, Supplementary Fig. S2 available with the online version of this paper). The separation into the alphaproteobacterial and the beta/gammaproteobacterial SOB group in the Apr lineage I was stressed by single, group-specific indels, whereas the 16S rRNA-discordant

Fig. 1. Phylogenetic tree based on comparative analysis of 379 amino acid positions of 104 AprBA sequences from investigated SOB, including full-length AprBA sequences retrieved from public databases of SOB (genomic, metagenomic and PCR analysis-derived sequences are indicated by ●, ■ and ▲, respectively) and selected SRP. The tree was inferred using the maximum-likelihood method. The DsrAB-congruent, presumably 'authentic' AprBA lineage I (Apr-lin. I) was used as the outgroup reference. SOB with DsrAB-discordant, putative laterally transferred *aprBA* genes are in bold type (Apr lineage II; Apr-lin. II), while the reference strains with two *apr* copies are indicated with boxes. Proposed LGT events are indicated by letters (a–h). The taxonomic classifications of investigated SOB based on the 16S rRNA gene phylogeny are indicated. The scale bar corresponds to 10 % estimated sequence divergence. Cdt., Candidatus; str., strain.

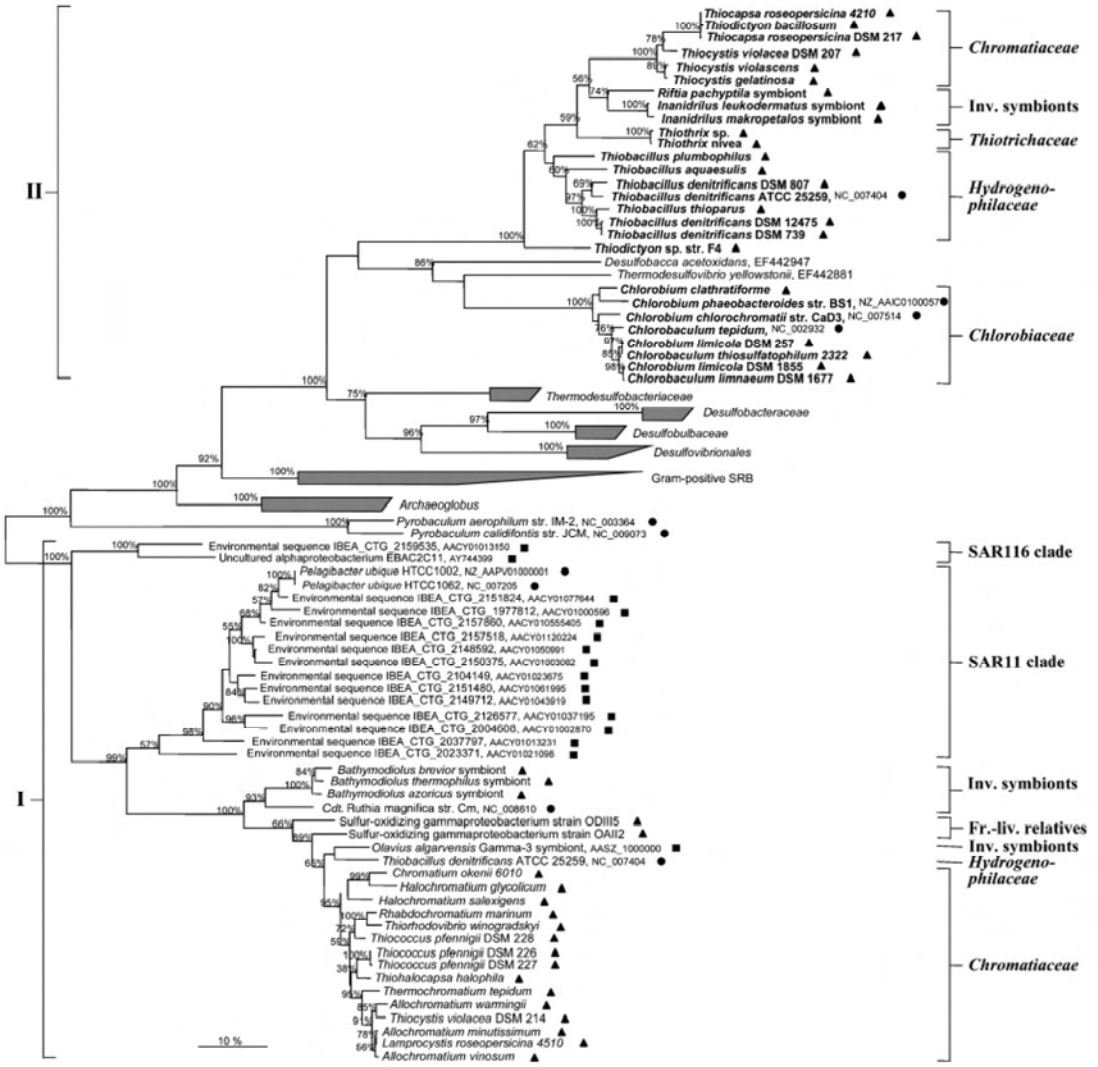

Fig. 2. Phylogenetic tree based on comparative analysis of 701 amino acid positions of 89 AprBA sequences from investigated SOB, including full-length AprBA sequences retrieved from public databases of SOB (genomic, metagenomic and PCR analysis-derived sequences are indicated by ●, ■ and ▲, respectively) and selected SRP. The tree was inferred using the maximum-likelihood method. The DsrAB-congruent, presumably 'authentic' AprBA lineage I was used as the outgroup reference. SOB with DsrAB-discordant, putative laterally transferred *aprBA* genes are in bold type (Apr lineage II). The taxonomic classifications of investigated SOB based on the 16S rRNA gene phylogeny are indicated. The scale bar corresponds to 10% estimated sequence divergence. Cdt., Candidatus; str., strain; Inv., invertebrate; Fr.-liv., free-living.

branching positions of *Thiobacillus plumbophilus* and symbionts of *Bathymodiolus* spp. in the AprBA trees were supported by group-intermixed indels and further unique insertions in each subunit sequence. The affiliation of *Chlorobiaceae* and *Thermodesulfovibrio* AprBA proteins was confirmed by the presence of four shared indels, while their phylogenetic separation from the proteobacterial Apr sequences in Apr lineage II was proven by the existence of five unique indels. In addition, the 16S rRNA-discordant closest affiliation of the *Thiodictyon* sp. strain F4 with the investigated chemotrophic SOB of the *Beta-* and *Gammaproteobacteria* was supported by three shared indels. The compositional similarity of the LGT-derived *aprBA* sequences of Apr lineage II to the respective recipient genomes points to an ancient timing of all inferred LGTs that affected the investigated SOB. This is also stressed by the strong congruence of the mol% G+C content and codon usage of the corresponding *aprBA* sequences of those SOB that contain two *apr* gene loci, despite their distant relationship.

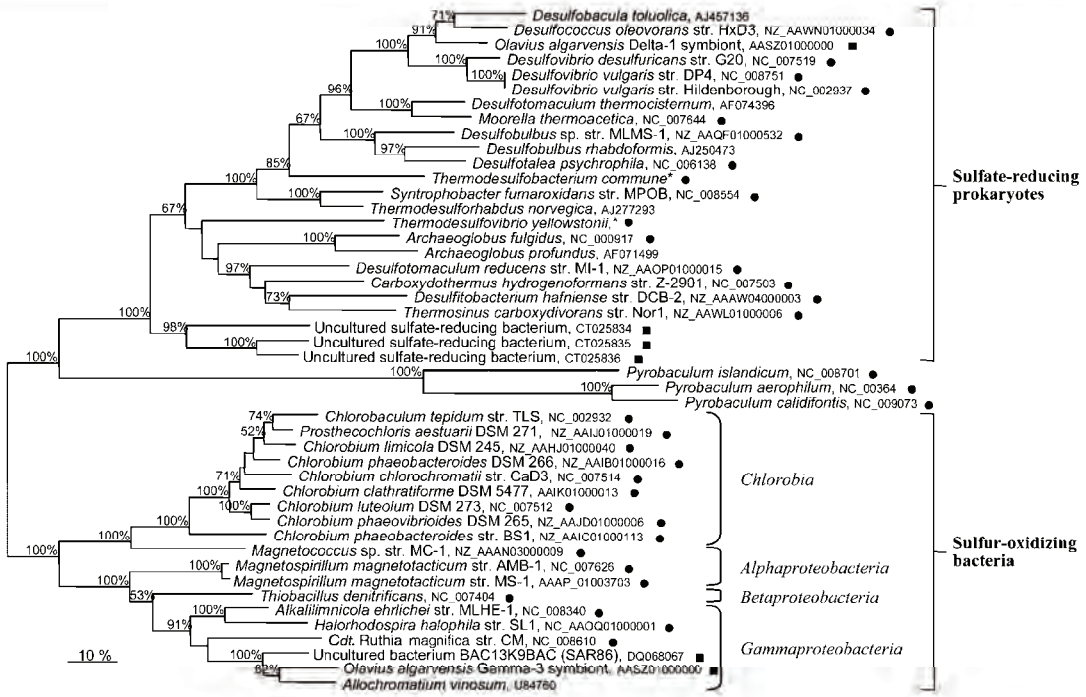

Fig. 3. Phylogenetic tree based on comparative analysis of 740 amino acid positions of 46 DsrAB sequences from full-length sequences retrieved from public databases of SOB and SRP (genomic and metagenomic sequences are indicated by ● and ■, respectively). The tree was inferred using the maximum-likelihood method. The DsrAB lineage of SOB was used as the outgroup reference. The taxonomic classifications of SOB based on the 16S rRNA gene phylogeny are indicated. The scale bar corresponds to 10% estimated sequence divergence. Cdt., Candidatus; str., strain.

Genomic arrangement of *aprBA* and functionally associated genes in SOB

Interestingly, the phylogenetic divergence of the oxidative-operating APS reductases into two distantly related lineages is reflected in the deviating presence and arrangement of *sat*, *aprM*, *qmoABC* and heterodisulfide reductase-encoding (*hdr*) genes and other hypothetical proteins (UPF0153 and COG1576) in the SOB genomes (see Fig. 4, Table 5). The presumably LGT-unaffected, 'authentic' *aprBA* gene loci (Apr lineage I) of the photo- and chemotrophic *Proteobacteria* are always preceded by and co-transcribed with an *aprM* homologue which is not found in the genomes of SRP, *Chlorobiaceae*, *Endoriftia persephone* or *Olavius algarvensis* Gamma-1 symbiont, or adjacent to the LGT-affected *apr* gene locus II from *Thiobacillus denitrificans*. The native electron acceptor and transfer mechanism to the electron transport chain is unknown for the APS reductases of Apr lineage I. However, comparative sequence analysis predicts the protein AprM to contain five transmembrane helices with no sequence similarity to any currently known conserved domain or cofactor binding site in the databases. An essential structural function of AprM as a membrane anchor that allows the spatial and functional association of this type of oxidative APS reductase with the membrane has been postulated (Meyer & Kuever, 2007).

In accordance with their affiliated AprBA proteins, the *sat-aprBA-qmoABC* genomic arrangement of the *Chlorobiaceae* is nearly identical to the gene organization of *Thermodesulfovibrio yellowstonii* (Fig. 4). The additional ORF located downstream of the *sat* gene in the genomes of thermophilic SRP is missing in the *Chlorobiaceae*; however, unusually long intergenic distances separate the *sat* and *aprB* genes in the latter, indicating the potential loss of this ORF after the transfer event. Interestingly, the gene composition and arrangement of the presumably LGT-derived *apr* gene loci from *Olavius algarvensis* Gamma-1 symbiont, *Endoriftia persephone* and *Thiobacillus denitrificans* are more similar to the SRP than to the *Chlorobiaceae*. The *qmo* operons are truncated to a *qmoAB* gene locus (compare to *Desulfotomaculum reducens* and *Syntrophobacter fumaroxidans*, Fig. 4), but are located in a genomic position distant to that of the *sat–aprBA* operon. A separately transcribed *qmoC* homologue could not be identified; however, *hdrC* and *hdrB* homologues (coding for functional subunits of the heterodisulfide reductase) are present near the *qmoAB* of *Thiobacillus denitrificans*, *Olavius algarvensis* Gamma-1 symbiont and *Endoriftia*

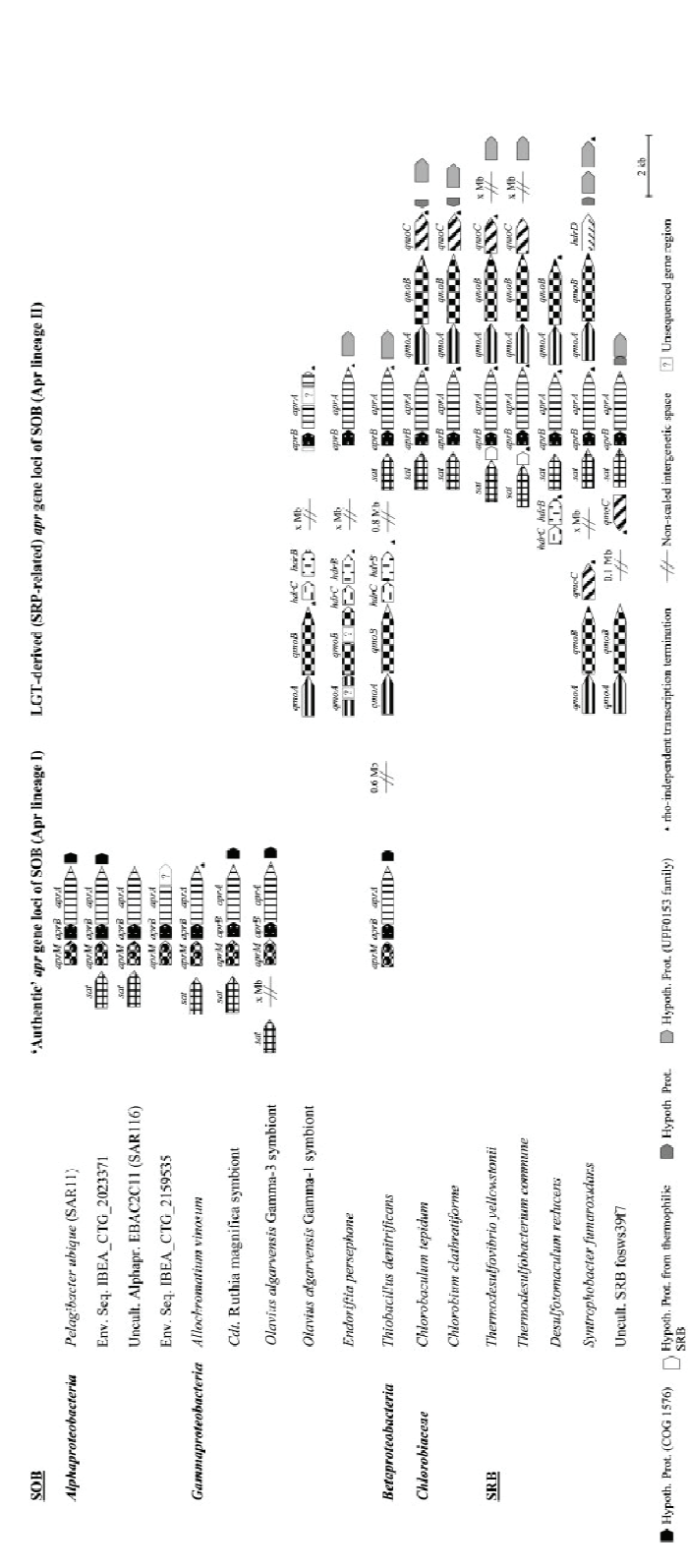

Fig. 4. Diagrammatic comparison of the genomic organization of the *sat*, *apr* and *qmo* genes in selected SOB and SRP (operon structure prediction by Softberry) in support of the inferred LGTs of the entire gene locus from SRP to certain SOB lineages. ORFs were designated based on BLASTX search results with significant homology scores. Loci: *sat*, dissimilatory ATP sulfurylase; *aprA* and *aprB*, α and β subunits of the dissimilatory APS reductase; *aprM*, putative transmembrane protein; *qmoA*, *qmoB* and *qmoC*, subunits of the putative APS : menaquinone oxidoreductase; *hdrB*, *hdrC* and *hdrD*, subunits of heterodisulfide reductase. Abbreviations: Cdt., Candidatus; Env. Seq., environmental sequence; Uncult. Alphapr., uncultured alphaproteobacterium; Hypoth. Prot., hypothetical protein.

persephone (see also *Desulfotomaculum reducens* and *Syntrophobacter fumaroxidans*, Fig. 4). Interestingly, the *qmoAB*, *hdrC* and *hdrB* genes of *Thiobacillus denitrificans* and *Endoriftia persephone* have been predicted to be co-transcribed. This might indicate that the electron transfer from cytoplasmic sulfite oxidation to the membrane quinone pool might be mediated by an SRP-like linking mechanism (Pires *et al.*, 2003) in the Apr lineage II protein-containing SOB.

DISCUSSION

Distribution of *apr* genes among anoxygenic phototrophic SOB

In *Allochromatium vinosum*, the oxidation of intermediately stored sulfur globules has been demonstrated to depend on the activity of the reverse-acting sulfite reductase and membrane-spanning DsrMKJOP complex (Dahl *et al.*, 2005; Pott & Dahl, 1998; Sander *et al.*, 2006). In support of a general, essential role in the oxidative sulfur metabolism of the *Chlorobiaceae*, *Chromatiaceae* and *Ectothiorhodospiraceae* (1) the *dsrAB* and *dsrMKJOP* genes are present in all currently sequenced genomes from representatives of the previous SOB lineages (Dahl *et al.*, 2005; Sabehi *et al.*, 2005; Sander *et al.*, 2006) (see also Supplementary Table S1 available with the online version of this paper), and (2) the existence of *dsr* operons has been confirmed by Southern blot assays in several further members (Dahl *et al.*, 1999). The subsequent oxidation of sulfite can be mediated by either the reverse-operating APS reductase (Apr) or SAOR (Brune, 1995; Brüser *et al.*, 2000; Kappler & Dahl, 2001). Although the reverse-acting Apr has been demonstrated to be constitutively expressed, an essential *in vivo* role for this enzyme in the sulfur metabolism of *Allochromatium vinosum* has recently been questioned (Dahl, 1996; Sanchez *et al.*, 2001). In support of the former results, the PCR-based analysis of this study indicated a generally restricted distribution of the dissimilatory APS reductase-encoding genes among the investigated anoxygenic phototrophic SOB (Table 1). While the presence of *apr* genes could be proven for most *Chromatiaceae* spp. (except marine *Isochromatium* and *Marichromatium*), they are absent in the investigated *Ectothiorhodospiraceae* species and restricted in the *Chlorobiaceae* to members of subclusters 3 and 4b (Imhoff, 2003). Generally, the results of our molecular analysis are in agreement with those of earlier enzyme activity studies (Brune, 1995; Dahl & Trüper, 1994; Trüper & Fischer, 1982); however, the reported APS reductase activity in cell extracts of *Chlorobium limicola* DSM 245, '*Chlorobium vibrioforme* f. *thiosulfatophilum*' NCIB 8346 (*Chlorobaculum parvum 2352* in Table 1) and *Chlorobium phaeovibrioides* DSM 270 (Brune, 1995; Dahl & Trüper, 1994) are not supported. Because all available AprBA sequences of green sulfur bacteria are highly similar in sequence (>80.9 % sequence identity) and possess complementary primer target sites, amplification failure can be excluded. In addition, the proposed absence of *apr* genes of several *Chlorobiaceae* species of subcluster 2b and 3b was confirmed by Southern blot analysis using an *aprA* probe that encompassed the strictly conserved gene region coding for the APS/ sulfite binding site (see hybridization results with *Desulfomicrobium baculatum*, Table 4). Therefore, the existence of *apr* genes that encode functional enzymes could be excluded for the investigated reference strains. Further evidence for the correctness of our PCR results is given by the consistent negative BLAST search results for the currently sequenced genomes of *C. limicola* DSM 245, *Chlorobium luteolum* DSM 273 and *Chlorobium ferrooxidans*.

Growth experiments with *aprBA*-deficient strains of *Allochromatium vinosum* showed that the loss of reverse APS reductase activity had no effect on the specific growth rate and sulfite-oxidizing ability. The sulfite oxidation has been calculated to rely to 69–100 % on the activity of the coexisting SAOR under photolithoautotrophic conditions (Sanchez *et al.*, 2001). Because all green and purple sulfur bacteria investigated in this study are capable of complete sulfide/sulfur oxidation to sulfate, the observed lack of *apr* genes in most examined species might be indirect evidence for the presence and functional importance of the AMP-independent pathway in the oxidative sulfur metabolism of SOB. Indeed, the existence of an SAOR has been established by enzyme assays for several representatives that do not possess the APS pathway, e.g. *Marichromatium* spp. (Trüper & Fischer, 1982). The SAOR of *Allochromatium vinosum* has been suggested to be a molybdenum-containing protein (Dahl, 1996), like the well-documented enzyme of *Starkeya novella*, SorAB (Kappler & Dahl, 2001; Kappler & Bailey, 2005). With regard to its functional association with the essential reverse sulfite reductase (Pott & Dahl, 1998), a cytoplasmically localized SAOR is postulated for the anoxygenic phototrophic SOB. Indeed, periplasmic SorAB-encoding homologues could not be identified in the currently sequenced genomes of *Chlorobiaceae* and *Ectothiorhodospiraceae*. The presence of an additional sulfite-oxidation pathway via APS-reductase (and ATP sulfurylase) besides the SAOR would allow molybdenum-independent sulfite oxidation and might be a selective advantage under certain photolithotrophic conditions (e.g. allowing a greater supply of reducing equivalents at saturating irradiances), or during chemolithoautotrophic growth (observed for several *Chromatiaceae*; Imhoff, 2001a).

In accordance with earlier results based on enzyme assays (Brune, 1995; Friedrich, 1998; Trüper & Fischer, 1982), *apr* genes were not detected in the investigated phototrophic *Alphaproteobacteria* (Table 1). Indeed, their representatives have been reported to prefer a photoorganoheterotrophic mode of growth and to vary considerably in their ability to use reduced sulfur compounds as photosynthetic electron donors (Brune, 1995; Imhoff, 2001b). If utilized, sulfide is primarily converted (by SQR) to elemental sulfur instead

of sulfate (Griesbeck *et al.*, 2000). The absence of *apr* and *dsr* genes in their genomes confirms their use of a different enzymic sulfur oxidation system compared to the cytoplasmic pathway of the previously discussed SOB lineages. Interestingly, the only members of the *Alphaproteobacteria* that harbour *apr* genes in their genomes (Table 5) are *Pelagibacter ubique* subsp. (SAR11) and an uncultured putative SOB of the SAR116 clade. Since they lack *sat* and *dsrAB* genes, a dissimilatory function of the APS reductase in their sulfur metabolism can be excluded. The reverse-acting APS reductase might primarily be used for detoxification of sulfite to prevent its cytoplasmic accumulation during the degradation of organic sulfur compounds. Indeed, members of the SAR11 clade have been demonstrated to dominate the assimilation of dissolved dimethylsulfoniopropionate (DMSP) in the surface ocean (Malmstrom *et al.*, 2004).

Distribution of *apr* genes among chemotrophic SOB

Diverse enzymic systems have been suggested to be involved in the aerobic oxidation of sulfide/sulfur to sulfate in the phylogenetically divergent chemotrophic SOB, comprising primarily the periplasmic enzymes SQR, sulfur dioxygenase (SDR) and SAOR (Brüser *et al.*, 2000; Friedrich, 1998; Griesbeck *et al.*, 2000; Kappler & Dahl, 2001; Kelly, 1999; Rohwerder & Sand, 2003; Suzuki, 1994; Takai *et al.*, 2005; Teske & Nelson, 2004; Theissen *et al.*, 2003). Consistently, this study revealed the *apr* genes to be restricted among the chemotrophic SOB to representatives of *Thiobacillus*, *Thiothrix* and invertebrate symbionts, including some of their free-living relatives, in accordance with earlier enzyme activity studies (Friedrich, 1998; Nelson & Fisher, 1995; Odintsova *et al.*, 1993; Taylor, 1994). Furthermore, APS reductase activity has been found in obligate chemolithoautotrophic, marine *Beggiatoa* subspecies but seems to be absent in mixo- or even heterotrophic freshwater strains (Teske & Nelson, 2004) as confirmed by this molecular analysis. In congruence to the results of this study (Table 1), no APS reductase has been reported to be involved in the oxidative sulfur metabolism of *Thiomicrospira* spp. (Nelson & Fisher, 1995), *Sulfurimonas denitrificans* (Takai *et al.*, 2005) and acidophilic SOB (Brüser *et al.*, 2000). The sulfur metabolism of *Aquaspirillum*, *Macromonas* and *Spirochaeta* spp. (Dubinina *et al.*, 2004; LaRiviere & Schmidt, 2001) has not yet been investigated by enzyme studies.

Interestingly, most chemotrophic SOB that possess *apr* genes are facultative anaerobes with the ability to switch between aerobic and anaerobic modes of growth (Brüser *et al.*, 2000; Cavanaugh *et al.*, 2001; Kuever *et al.*, 2002; Nelson & Fisher, 1995; Robertson & Kuenen, 2001). The cytoplasmic enzyme system (Dsr, Apr and Sat/APAT) might operate in these chemotrophic SOB in a manner analogous to that of the anoxygenic phototropic *Chromatiaceae* (and *Chlorobiaceae*), with significant energetic advantages for chemothioautotrophic growth under oxygen limitation (electron transport phosphorylation-coupled sulfur oxidation; electrons enter the electron transport chain at the energetic level of quinones with a higher number of coupling sites available to drive ATP synthesis and lower energy demand for reverse electron flow; substrate phosphorylation-coupled sulfite oxidation). Indeed, the expression and involvement of Dsr, Apr and Sat in the sulfur oxidation process has been confirmed for anaerobically grown cultures of *Thiobacillus denitrificans* (Beller *et al.*, 2006; Schedel & Trüper, 1980) and the endosymbiont of *Riftia pachyptila* (Markert *et al.*, 2007). A general involvement of the latter pathway was suggested by Kelly (1999), based on the greater molar growth yields of *Thiobacillus denitrificans* compared to *Sulfurimonas denitrificans* even under aerobic conditions. In contrast, the involvement of an extracytoplasmic sulfur-oxidation pathway (via SQR, SDR and SAOR) might in principle be more advantageous (no requirement for energy-demanding sulfur compound permease systems; no cytoplasmic accumulation of toxic substrates or products; no acidification of the cytoplasm while the extracytoplasmic localization of substrate oxidation contributes to the proton gradient).

The enzymes of the archaeal sulfur-oxidation pathway (e.g. the unique sulfur oxygenase reductase) represent convergent evolutionary lines compared to the bacterial proteins (Brüser *et al.*, 2000; Kletzin *et al.*, 2004). Based on enzyme activity assays, an involvement of the reverse APS reductase in the sulfite oxidation of *Acidianus ambivalens* has been postulated, despite high levels of non-enzymic background (Zimmermann *et al.*, 1999). In contrast, the results of our molecular study do not support its involvement in the oxidative sulfur metabolism of *Sulfolobales* representatives, including *Acidianus ambivalens*.

Phylogeny of dissimilatory APS reductase from SOB indicates lateral transfer of *aprBA* genes between SRP and SOB

The DsrAB phylogeny presents the oxidative-operating sulfite reductases of SOB as monophyletic and distantly related to the reductive enzyme type of the SRP (Fig. 3). In contrast, the reverse APS reductases of photo- and chemotrophic SOB appear to have diverged into two distinct phylogenetic clusters, comprising the DsrAB-congruent Apr lineage I and the DsrAB-discordant Apr lineage II (Figs 1 and 2). Accumulating experimental evidence confirms the postulated essential function of the reverse sulfite reductase (including the DsrMKJOP transmembrane redox complex) in the dissimilatory sulfur metabolism of SOB (Beller *et al.*, 2006; Dahl *et al.*, 1999, 2005; Pott & Dahl, 1998; Sander *et al.*, 2006) (also reflected by the ubiquitous presence of *dsr* homologues in genomes; Supplementary Table S1). Thus, the DsrAB-congruent phylogenetic placement most likely represents the 'authentic', LGT-unaffected position of SOB in the Apr tree. The most reasonable explanation for the presence of the

SRP-related *apr* genes (Apr lineage II) in *Chlorobiaceae* and several *Beta-* and *Gammaproteobacteria* (in some representatives in addition to the 'authentic' *apr* gene locus) is the occurrence of multiple LGT events between SRP and SOB. In analogy, the SRP-affiliated *dsrMKJOP* genes of green sulfur bacteria have recently been postulated to have been acquired via lateral transfer from an unknown SRP donor (Sander *et al.*, 2006). Because the AprBA proteins of *Chlorobiaceae* are more closely related to the *Thermodesulfovibrio–Desulfobacca* cluster than to the *Beta-* and *Gammaproteobacteria* (Figs 1 and 2), these SOB groups will have received their LGT-derived *apr* genes independently. Although direct SRP donor lineages are not apparent, putative thermophilic strains might have transferred their *apr* genes concurrently to ancestral strains of the aforementioned groups. A direct lateral transfer of the entire gene locus from the *Thermodesulfovibrio* donor lineage to the *Chlorobiaceae* is supported by (1) the similarity of their indel pattern (Supplementary Fig. S2 available with the online version of this paper), (2) the congruent arrangement of the *sat*, *apr* and *qmoABC* genes in the genomes (Fig. 4), as well as (3) the Apr-consistent topologies of the Sat and QmoABC phylogenetic trees (not shown). The restricted distribution of the *apr* genes among the green sulfur bacteria might indicate that the LGT occurred after their diversification into marine and freshwater strains (Imhoff, 2003). The LGT-derived character of proteobacterial proteins of Apr lineage II is supported by the fact that the SRP-affiliated proteins are restricted to a few beta- and gammaproteobacterial genera and mainly comprise species that harbour two *aprBA* gene loci of which one codes for a presumably 'authentic' protein (Tables 1 and 3). Additional support for an SRP origin of the Apr lineage II proteins in *Proteobacteria* is given by (1) the similar gene locus composition and organization in the betaproteobacterial *Thiobacillus denitrificans* and *Olavius algarvensis* Gamma-1 symbiont compared to the SRP (Table 5 and Fig. 4), and (2) their close relationship on the basis of the QmoA/B proteins (tree not shown). The *apr* genes might have been received via at least seven independent LGT events by the ancestors of *Thiobacillus*, *Thiothrix*, the invertebrate Gamma-1 and -4 symbionts, the *Thiocapsa–Thiodictyon–Lamprocystis* cluster, *Thiocystis* and *Thiorhodococcus*. After diversification, the resident, 'authentic' *apr* gene might have been replaced in several species by its SRP-affiliated xenologue (xenologous gene displacement), causing the observed polyphyly of the *Beta-* and *Gammaproteobacteria* in the Apr-based tree. Indeed, close associations and synergistic interactions between those SOB species that harbour SRP-related *aprBA* genes and SRP have been reported from various habitats and even in invertebrate tissues (Bright & Giere, 2005; Imhoff, 2001a; Markert *et al.*, 2007; Overmann & Garcia-Pichel, 2001; Tonolla *et al.*, 2004; Visscher *et al.*, 1992). Microbial biofilms and mats have been demonstrated to be especially hot spots for LGT involving different physiological groups of prokaryotes (Molin & Tolker-Nielsen, 2003; Sorensen *et al.*, 2005).

Notably, some inferred relationships in the Apr lineage I subtree are discordant with the 16S rRNA-gene-based species phylogeny and indicate the occurrence of putative lateral transfers even among the SOB, e.g. the SAR116-affiliated AprBA proteins of *Thiobacillus plumbophilus*. Furthermore, the correlation of the salt requirement-correlated *Chromatiaceae* classification is not reflected in the Apr-based tree (Imhoff, 2001a). Interestingly, the Apr-based intrafamily branching order is confirmed by the sulfate thiohydrolase (SoxB)-based phylogeny (Meyer *et al.*, 2007). In contrast to the 16S rRNA-gene-based phylogeny (Cavanaugh *et al.*, 2001), the AprBA proteins of *Bathymodiolus* spp. and *Calyptogena magnifica* symbionts form a basal-branching group in the Apr lineage I distinct from their closest relatives *Olavius algarvensis* Gamma-1 symbiont, and SOB strains OAII2 and ODIII5 (Kuever *et al.*, 2002). This might be a result of their vertical mode of transmission (Cary & Giovannoni, 1993; Hurtado *et al.*, 2003), which disconnects the mussel- and bivalve-inhabiting SOB populations from their free-living counterparts and causes elevated evolutionary rates and genetic drift in the symbiotic population by co-adaptation to the host (Peek *et al.*, 1998). The symbiotic bacteria of vestimentiferan tube worms and gastropods that are instead environmentally acquired by their hosts from free-living populations (Bright & Giere, 2005; Cavanaugh *et al.*, 2001; Nelson & Fisher, 1995) have had a higher probability of interspecies gene exchange with the environmental microbial community and harbour xenologous *apr* genes (Fig. 1). A recent 16S rRNA gene analysis of thiotrophic symbionts in *Inanidrilus* spp. (oligochaetes) has revealed the presence of Gamma-4 symbionts in *Inandrilus exumae* (Bergin *et al.*, 2006), which replace the sulfur-oxidizing Gamma-1 symbionts found in other *Inanidrilus* spp. (Blazejak *et al.*, 2006; Bright & Giere, 2005). The distant relationship of the *Inandrilus exumae* Gamma-4 symbiont is reflected in the Apr-based tree and in the presence of two *apr* gene loci that encode proteins of both lineages.

Putative functional importance of SRP-related APS reductases in SOB

The postulated distinct electron-transfer strategies via AprM or Qmo/Hdr are supported by observed differences in the degrees of membrane binding of lineage I and II APS reductases in the photo- and chemotrophic SOB species (Brüser *et al.*, 2000; Dahl & Trüper, 1994; Friedrich, 1998). Interestingly, in *Chromatiaceae* species that contain *apr* genes which code for lineage I proteins (e.g. *Allochromatium vinosum* and *Allochromatium warmingii*), the APS reductases have been reported to be firmly membrane-bound, whereas they have been described as being soluble in those species that harbour the SRP-related *apr* genes encoding the lineage II proteins (e.g. *Thiocapsa roseopersicina*). A functionally important role for the LGT-derived APS reductases in SOB is indicated by the preferential expression of the SRP-related *apr* gene locus compared to the concurrent 'authentic' one in cells of

Thiocapsa roseopersicina (only the soluble APS reductase form is detected in culture; Dahl & Trüper, 1994) and *Thiobacillus denitrificans* (transcriptional analysis; Beller *et al.*, 2006). Recent proteome analysis of *Endoriftia persephone* has confirmed the essential role of the SRP-related APS reductase in the sulfur-dependent energy metabolism of that micro-organism (Markert *et al.*, 2007). Interestingly, *Thiobacillus denitrificans*, *Olavius algarvensis* Gamma-1 symbiont and *Endoriftia persephone* harbour SRP-related *qmoAB* and *hdrCB* homologues in their genomes, indicating the presence of an SRP-related mechanism linking cytoplasmic sulfite oxidation to the membrane quinone pool (Fig. 4). Indeed, *qmoB* has been demonstrated to be expressed in addition to *aprBA* in chemolithoautotrophically growing *Endoriftia persephone* (Markert *et al.*, 2007). By analogy with the postulated interaction of DsrAB and transmembrane complex DsrMKJOP via conserved cysteine residues in DsrC proteins (Dahl *et al.*, 2005; Pires *et al.*, 2006), the SRP-related reverse APS reductase and the QmoAB–HdrCB complex might couple the cytoplasmic sulfite/APS redox process to the electron transport chain by reversible disulfide/thiol interchanges. With regard to the multiple xenologous *aprBA* gene displacements, e.g. in chemotrophic *Thiobacillus* spp. and gammaproteobacterial SOB, the SRP-related APS reductase and electron transfer mechanism might be more advantageous for chemolithotrophic growth. Indeed, the members of the *Chromatiaceae* genera that contain SRP-related *apr* gene loci (Table 1) have been demonstrated to be physiologically versatile, e.g. by their ability to switch between photo- and chemolithoautotrophic lifestyles (Imhoff, 2001a). The two-gene state might be an intermediate in the replacement of the resident essential gene by the LGT-derived foreign homologue. However, the genomic persistence of both gene loci might allow the adaptation of the energy conservation process when growing (1) in dynamic and unstable habitats such as microbial mats with diurnal oscillating sulfide and oxygen concentrations, or (2) in competition with chemotrophic SOB (Imhoff, 2001a; Overmann & Garcia-Pichel, 2001), and might be a selective advantage, especially for non-motile species such as *Thiocapsa roseopersicina* (Imhoff, 2001a).

ACKNOWLEDGEMENTS

This study was supported by grants of the BMBF (project 'Caribflux' under contract no. 03G0154C), the DFG (under contract no. KU 916/8-1) and the Max Planck Society, Munich.

REFERENCES

Beller, H. R., Chain, P. S. G., Letain, T. E., Chakicherla, A., Larimer, F. W., Richardson, P. M., Coleman, M. A., Wood, A. P. & Kelly, D. P. (2006). The genome sequence of the obligately chemolithoautotrophic, facultatively anaerobic bacterium *Thiobacillus denitrificans*. *J Bacteriol* **188**, 1473–1488.

Bergin, C., Berwig, N., Blazejak, A., Rühland, C. & Dubilier, N. (2006). *Novel Symbiont in the Gutless Marine Oligochaete Inanidrilus exumae*. Poster no. P037 presented at the International Symposium on Microbial Sulfur Metabolism (ISMSM), Münster, 29 June to 2 July 2006.

Blazejak, A., Kuever, J., Erseus, C., Amann, R. & Dubilier, N. (2006). Phylogeny of 16S rRNA, ribulose 1,5-bisphosphate carboxylase/oxygenase and adenosine 5′-phosphosulfate reductase genes from gamma- and alphaproteobacterial symbionts in gutless marine worms (Oligochaeta) from Bermuda and the Bahamas. *Appl Environ Microbiol* **72**, 5527–5536.

Bright, M. & Giere, O. (2005). Microbial symbiosis in Annelida. *Symbiosis* **38**, 1–45.

Brune, D. C. (1995). Sulfur compounds as photosynthetic electron donors. In *Anoxygenic Photosynthetic Bacteria*, pp. 847–870. Edited by R. E. Blankenship, M. T. Madigan & C. E. Bauer. Dordrecht: Springer.

Brüser, T., Lens, P. N. L. & Trüper, H. G. (2000). The biological sulfur cycle. In *Environmental Technologies to Treat Sulfur Pollution*, pp. 47–86. Edited by P. N. L. Lens & L. H. Pol. London: IWA Publishing.

Cary, S. C. & Giovannoni, S. J. (1993). Transovarial inheritance of endosymbiotic bacteria in clams inhabiting deep-sea hydrothermal vents and cold seeps. *Proc Natl Acad Sci U S A* **90**, 5695–5699.

Cavanaugh, C. M., McKiness, Z. P., Newton, I. L. G. & Stewart, F. J. (2001). Marine chemosynthetic symbioses. In *The Prokaryotes an Evolving Electronic Resource for the Microbial Community*. Edited by M. Dworkin, E. Falkow, E. Rosenberg, K.-H. Schleifer & E. Stackebrandt. New York: Fischer Verlag.

Dahl, C. (1996). Insertional gene inactivation in a phototrophic sulphur bacterium: APS-reductase-deficient mutants of *Chromatium vinosum*. *Microbiology* **142**, 3363–3372.

Dahl, C. & Trüper, H. G. (1994). Enzymes of dissimilatory sulfide oxidation in phototrophic sulfur bacteria. In *Inorganic Microbial Sulfur Metabolism* (Methods in Enzymology, vol. 243), pp. 400–421. Edited by H. Peck Jr., J. LeGall, J Abelson & M. Simon. San Diego, CA: Academic Press.

Dahl, C., Rakhely, G., Pott-Sperling, A. S., Fodor, B., Takacs, M., Toth, A., Kraeling, M., Gyorfi, K., Kovacs, A. & other authors (1999). Genes involved in hydrogen and sulfur metabolism in phototrophic sulfur bacteria. *FEMS Microbiol Lett* **180**, 317–324.

Dahl, C., Engels, S., Pott-Sperling, A. S., Schulte, A., Sander, J., Lubbe, Y., Deuster, O. & Brune, D. C. (2005). Novel genes of the *dsr* gene cluster and evidence for close interaction of Dsr proteins during sulfur oxidation in the phototrophic sulfur bacterium *Allochromatium vinosum*. *J Bacteriol* **187**, 1392–1404.

Dubinina, G. A., Grabovich, M. Y. & Chernyshova, Y. Y. (2004). The role of oxygen in the regulation of the metabolism of aerotolerant Spirochetes, a major component of "*Thiodendron*" bacterial sulfur mats. *Microbiologiia* **73**, 725–733 (in Russian).

Ehrenreich, A. & Widdel, F. (1994). Anaerobic oxidation of ferrous iron by purple bacteria, a new type of phototrophic metabolism. *Appl Environ Microbiol* **60**, 4517–4526.

Friedrich, C. G. (1997). Physiology and genetics of sulfur-oxidizing bacteria. In *Advances in Microbial Physiology*, 39, pp. 235–289. Edited by R. K. Poole. San Diego, CA: Academic Press.

Friedrich, M. W. (2002). Phylogenetic analysis reveals multiple lateral transfers of adenosine-5′-phosphosulfate reductase genes among sulfate-reducing microorganisms. *J Bacteriol* **184**, 278–289.

Friedrich, C. G., Rother, D., Bardischewsky, F., Quentmeier, A. & Fischer, J. (2001). Oxidation of reduced inorganic sulfur compounds by bacteria: emergence of a common mechanism? *Appl Environ Microbiol* **67**, 2873–2882.

Fritz, G., Buchert, T., Huber, H., Stetter, K. O. & Kroneck, P. M. H. (2000). Adenylylsulfate reductases from archaea and bacteria are 1:1 $\alpha\beta$-heterodimeric iron–sulfur flavoenzymes – high similarity of

molecular properties emphasizes their central role in sulfur metabolism. *FEBS Lett* **473**, 63–66.

Fritz, G., Roth, A., Schiffer, A., Buchert, T., Bourenkov, G., Bartunik, H. D., Huber, H., Stetter, K. O., Kroneck, P. M. H. & Ermler, U. (2002). Structure of adenylylsulfate reductase from the hyperthermophilic *Archaeoglobus fulgidus* at 1.6-Å resolution. *Proc Natl Acad Sci U S A* **99**, 1836–1841.

Giovannoni, S. J., Tripp, H. J., Givan, S., Podar, M., Vergin, K. L., Baptista, D., Bibbs, L., Eads, J., Richardson, T. H. & other authors (2005). Genome streamlining in a cosmopolitan oceanic bacterium. *Science* **309**, 1242–1245.

Griesbeck, C., Hauska, G. & Schütz, M. (2000). Biological sulfide oxidation: sulfide-quinone reductase (SQR), the primary reaction. In *Recent Research Developments in Microbiology*, 4, pp. 179–203. Edited by S. G. Pandalai. Trivadrum, India: Research Signpost.

Haveman, S. A., Greene, E. A., Stilwell, C. P., Voordouw, J. K. & Voordouw, G. (2004). Physiological and gene expression analysis of inhibition of *Desulfovibrio vulgaris* Hildenborough by nitrite. *J Bacteriol* **186**, 7944–7950.

Hipp, W. M., Pott, A. S., Thum-Schmitz, N., Faath, I., Dahl, C. & Trüper, H. G. (1997). Towards the phylogeny of APS reductases and sirohaem sulfite reductases in sulfate-reducing and sulfur-oxidizing prokaryotes. *Microbiology* **143**, 2891–2902.

Huber, H. & Prangishvili, D. (2000). *Sulfolobales.* In *The Prokaryotes an Evolving Electronic Resource for the Microbial Community.* Edited by M. Dworkin, E. Falkow, E. Rosenberg, K.-H. Schleifer & E. Stackebrandt. New York: Fischer Verlag.

Hurtado, L. A., Mateos, M., Lutz, R. A. & Vrijenhoek, R. C. (2003). Coupling of bacterial endosymbiont and host mitochondrial genomes in the hydrothermal vent clam *Calyptogena magnifica*. *Appl Environ Microbiol* **69**, 2058–2064.

Imhoff, J. F. (2001a). The *Chromatiaceae.* In *The Prokaryotes an Evolving Electronic Resource for the Microbial Community.* Edited by M. Dworkin, E. Falkow, E. Rosenberg, K.-H. Schleifer & E. Stackebrandt. New York: Springer Verlag.

Imhoff, J. F. (2001b). The phototrophic alpha-Proteobacteria. In *The Prokaryotes an Evolving Electronic Resource for the Microbial Community.* Edited by M. Dworkin, E. Falkow, E. Rosenberg, K.-H. Schleifer & E. Stackebrandt. New York: Springer Verlag.

Imhoff, J. F. (2003). Phylogenetic taxonomy of the family *Chlorobiaceae* on the basis of 16S rRNA and *fmo* (Fenna-Matthews-Olson protein) gene sequences. *Int J Syst Evol Microbiol* **53**, 941–951.

Kappler, U. & Bailey, S. (2005). Molecular basis of intramolecular electron transfer in sulfite-oxidizing enzymes is revealed by high resolution structure of a heterodimeric complex of the catalytic molybdopterin subunit and a *c*-type cytochrome subunit. *J Biol Chem* **280**, 24999–25007.

Kappler, U. & Dahl, C. (2001). Enzymology and molecular biology of prokaryotic sulfite oxidation. *FEMS Microbiol Lett* **203**, 1–9.

Kelly, D. P. (1999). Thermodynamic aspects of energy conservation by chemolithotrophic sulfur bacteria in relation to the sulfur oxidation pathways. *Arch Microbiol* **171**, 219–229.

Kelly, D. P. & Wood, A. P. (2000). Reclassification of some species of *Thiobacillus* to the newly designated genera *Acidithiobacillus* gen. nov., *Halothiobacillus* gen. nov. and *Thermithiobacillus* gen. nov. *Int J Syst Evol Microbiol* **50**, 511–516.

Klein, M., Friedrich, M., Roger, A. J., Hugenholtz, P., Fishbain, S., Abicht, H., Blackall, L. L., Stahl, D. A. & Wagner, M. (2001). Multiple lateral transfers of dissimilatory sulfite reductase genes between major lineages of sulfate-reducing prokaryotes. *J Bacteriol* **183**, 6028–6035.

Kletzin, A., Urich, T., Muller, F., Bandeiras, T. M. & Gomes, C. M. (2004). Dissimilatory oxidation and reduction of elemental sulfur in thermophilic archaea. *J Bioenerg Biomembr* **36**, 77–91.

Kuever, J., Sievert, S. M., Stevens, H., Brinkhoff, T. & Muyzer, G. (2002). Microorganisms of the oxidative and reductive part of the sulfur cycle at a shallow-water hydrothermal vent in the Aegean Sea (Milos, Greece). *Cah Biol Mar* **43**, 413–416.

Kwok, S., Kellogg, D. E., McKinney, N., Spasic, D., Goda, L., Levenson, C. & Sninsky, J. J. (1990). Effects of primer-template mismatches on the polymerase chain reaction. *Nucleic Acids Res* **18**, 999–1005.

LaRiviere, J. W. M. & Schmidt, K. (2001). Morphologically conspicuous sulfur-oxidizing *Eubacteria.* In *The Prokaryotes an Evolving Electronic Resource for the Microbial Community.* Edited by M. Dworkin, E. Falkow, E. Rosenberg, K.-H. Schleifer & E. Stackebrandt. New York: Fischer Verlag.

Lawrence, J. G. & Ochman, H. (1997). Amelioration of bacterial genomes: rates of change and exchange. *J Mol Evol* **44**, 383–397.

Malmstrom, R. R., Kiene, R. P., Cottrell, M. T. & Kirchman, D. L. (2004). Contribution of SAR11 bacteria to dissolved dimethylsulfoniopropionate and amino acid uptake in the North Atlantic Ocean. *Appl Environ Microbiol* **70**, 4129–4135.

Markert, S., Arndt, C., Felbeck, H., Becher, D., Sievert, S. M., Hügler, M., Albrecht, D., Robidart, J., Bench, S., Feldman, R. A., Hecker, M. & Schweder, T. (2007). Physiological proteomics of the uncultured endosymbiont of *Riftia pachyptila*. *Science* **315**, 247–250.

Meyer, B. & Kuever, J. (2007). Phylogeny of the alpha and beta subunits of the dissimilatory adenosine-5'-phosphosulfate (APS) reductase from sulfate-reducing prokaryotes – origin and evolution of the dissimilatory sulfate-reduction pathway. *Microbiology* **153**, 2026–2044.

Meyer, B., Imhoff, J. F. & Kuever, J. (2007). Molecular analysis of the distribution and phylogeny of the *soxB* gene among sulfur-oxidizing bacteria – evolution of the Sox sulfur oxidation enzyme system. *Environ Microbiol* (in press).

Molin, S. & Tolker-Nielsen, T. (2003). Gene transfer occurs with enhanced efficiency in biofilms and induces enhanced stabilisation of the biofilm structure. *Curr Opin Biotechnol* **14**, 255–261.

Muyzer, G., Teske, A., Wirsen, C. O. & Jannasch, H. W. (1995). Phylogenetic relationships of *Thiomicrospira* species and their identification in deep-sea hydrothermal vent samples by denaturing gradient gel electrophoresis of 16S rDNA fragments. *Arch Microbiol* **164**, 165–172.

Nelson, D. C. & Fisher, C. R. (1995). Chemoautotrophic and methanoautotrophic endosymbiontic bacteria at deep-sea vents and seeps. In *Microbiology of Deep Sea Hydrothermal Vents*, pp. 125–167. Edited by D. M. Karl. Boca Raton, FL: CRC Press.

Newton, I. L. G., Woyke, T., Auchtung, T. A., Dilly, G. F., Dutton, R. J., Fisher, M. C., Fontanez, K. M., Lau, E., Stewart, F. J. & other authors (2007). The *Calyptogena magnifica* chemoautotrophic symbiont genome. *Science* **315**, 998–1000.

Odintsova, E. V., Wood, A. P. & Kelly, D. P. (1993). Chemolithoautotrophic growth of *Thiothrix ramosa*. *Arch Microbiol* **160**, 152–157.

Overmann, J. & Garcia-Pichel, F. (2001). The phototrophic way of life. In *The Prokaryotes an Evolving Electronic Resource for the Microbial Community.* Edited by M. Dworkin, E. Falkow, E. Rosenberg, K.-H. Schleifer & E. Stackebrandt. New York: Fischer Verlag.

Peek, A. S., Vrijenhoek, R. C. & Gaut, B. S. (1998). Accelerated evolutionary rate in sulfur-oxidizing endosymbiotic bacteria associated with the mode of symbiont transmission. *Mol Biol Evol* **15**, 1514–1523.

Pires, R. H., Lourenco, A. I., Morais, F., Teixeira, M., Xavier, A. V., Saraiva, L. M. & Pereira, I. A. C. (2003). A novel membrane-bound respiratory complex from *Desulfovibrio desulfuricans* ATCC 27774. *Bba-Bioenergetics* **1605**, 67–82.

Pires, R. H., Venceslau, S. S., Morais, F., Teixeira, M., Xavier, A. V. & Pereira, I. A. C. (2006). Characterization of the *Desulfovibrio desulfuricans* ATCC 27774 DsrMKJOP complex – a membrane-bound redox complex involved in the sulfate respiratory pathway. *Biochemistry* **45**, 249–262.

Polz, M. F., Odintsova, E. V. & Cavanaugh, C. M. (1996). Phylogenetic relationships of the filamentous sulfur bacterium *Thiothrix ramosa* based on 16S rRNA sequence analysis. *Int J Syst Bacteriol* **46**, 94–97.

Pott, A. S. & Dahl, C. (1998). Sirohaem sulfite reductase and other proteins encoded by genes at the *dsr* locus of *Chromatium vinosum* are involved in the oxidation of intracellular sulfur. *Microbiology* **144**, 1881–1894.

Robertson, L. A. & Kuenen, G. J. (2001). The genus *Thiobacillus*. In *The Prokaryotes An Evolving Electronic Resource for the Microbial Community*. Edited by M. Dworkin, E. Falkow, E. Rosenberg, K.-H. Schleifer & E. Stackebrandt. New York: Fischer Verlag.

Rohwerder, T. & Sand, W. (2003). The sulfane sulfur of persulfides is the actual substrate of the sulfur-oxidizing enzymes from *Acidithiobacillus* and *Acidiphilium* spp. *Microbiology* **149**, 1699–1710.

Sabehi, G., Loy, A., Jung, K. H., Partha, R., Spudich, J. L., Isaacson, T., Hirschberg, J., Wagner, M. & Beja, O. (2005). New insights into metabolic properties of marine bacteria encoding proteorhodopsins. *PLoS Biol* **3**, 1409–1417.

Sanchez, O., Ferrera, I., Dahl, C. & Mas, J. (2001). In vivo role of adenosine-5′-phosphosulfate reductase in the purple sulfur bacterium *Allochromatium vinosum*. *Arch Microbiol* **176**, 301–305.

Sander, J., Engels-Schwarzlose, S. & Dahl, C. (2006). Importance of the DsrMKJOP complex for sulfur oxidation in *Allochromatium vinosum* and phylogenetic analysis of related complexes in other prokaryotes. *Arch Microbiol* **186**, 357–366.

Schedel, M. & Trüper, H. G. (1980). Anaerobic oxidation of thiosulfate and elemental sulfur in *Thiobacillus denitrificans*. *Arch Microbiol* **124**, 205–210.

Schiffer, A., Fritz, G., Kroneck, P. M. H. & Ermler, U. (2006). Reaction mechanism of the iron–sulfur flavoenzyme adenosine-5′-phosphosulfate reductase based on the structural characterization of different enzymatic states. *Biochemistry* **45**, 2960–2967.

Simsek, M. & Adnan, H. (2000). Effect of single mismatches at 3′-end of primers on polymerase chain reaction. *Med Sci (Paris)* **2**, 11–14.

Sorensen, S. J., Bailey, M., Hansen, L. H., Kroer, N. & Wuertz, S. (2005). Studying plasmid horizontal transfer in situ: a critical review. *Nat Rev Microbiol* **3**, 700–710.

Suzuki, I. (1994). Sulfur-oxidizing enzymes. In *Inorganic Microbial Sulfur Metabolism* (Methods in Enzymology, 243), pp. 455–462. San Diego, CA: Academic Press.

Takai, K., Campbell, B. J., Cary, S. C., Suzuki, M., Oida, H., Nunoura, T., Hirayama, H., Nakagawa, S., Suzuki, Y. & other authors (2005). Enzymatic and genetic characterization of carbon and energy metabolisms by deep-sea hydrothermal chemolithoautotrophic isolates of *Epsilonproteobacteria*. *Appl Environ Microbiol* **71**, 7310–7320.

Taylor, B. F. (1994). Adenylylsulfate reductases from thiobacilli. In *Inorganic Microbial Sulfur Metabolism* (Methods in Enzymology, 243), pp. 393–400. San Diego, CA: Academic Press.

Teske, A. & Nelson, D. C. (2004). The genera *Beggiatoa* and *Thioploca*. In *The Prokaryotes An Evolving Electronic Resource for the Microbial Community*. Edited by M. Dworkin, E. Falkow, E. Rosenberg, K.-H. Schleifer & E. Stackebrandt. New York: Springer Verlag.

Theissen, U., Hoffmeister, M., Grieshaber, M. & Martin, W. (2003). Single eubacterial origin of eukaryotic sulfide: quinone oxidoreductase, a mitochondrial enzyme conserved from the early evolution of eukaryotes during anoxic and sulfidic times. *Mol Biol Evol* **20**, 1564–1574.

Tonolla, M., Peduzzi, S., Demarta, A., Peduzzi, R. & Hahn, D. (2004). Phototrophic sulfur and sulfate-reducing bacteria in the chemocline of meromictic Lake Cadagno, Switzerland. *Journal of Limnology* **63**, 161–170.

Trüper, H. G. & Fischer, U. (1982). Anaerobic oxidation of sulfur-compounds as electron-donors for bacterial photosynthesis. *Philos Trans R Soc Lon B Biol Sci* **298**, 529–542.

Venter, J. C., Remington, K., Heidelberg, J. F., Halpern, A. L., Rusch, D., Eisen, J. A., Wu, D. Y., Paulsen, I., Nelson, K. E. & other authors (2004). Environmental genome shotgun sequencing of the Sargasso Sea. *Science* **304**, 66–74.

Visscher, P. T., Prins, R. A. & van Gemerden, H. (1992). Rates of sulfate reduction and thiosulfate consumption in a marine microbial mat. *FEMS Microbiol Ecol* **86**, 283–294.

Woyke, T., Teeling, H., Ivanova, N. N., Huntemann, M., Richter, M., Gloeckner, F. O., Boffelli, D., Anderson, I. J., Barry, K. W. & other authors (2006). Symbiosis insights through metagenomic analysis of a microbial consortium. *Nature* **443**, 950–955.

Zimmermann, P., Laska, S. & Kletzin, A. (1999). Two modes of sulfite oxidation in the extremely thermophilic and acidophilic archaeon *Acidianus ambivalens*. *Arch Microbiol* **172**, 76–82.

Edited by: G. Muyzer

Supplementary Material

Supplementary Table S1. Presence of *dsr* homologs coding for the dissimilatory sulfite reductase including its functionally associated proteins DsrMKJOP in genome sequences of SOB

SOB species	GenBank accession numbers of genome sequences	*dsrAB*	*dsrMKJOP/ hmeABCDE*
Chlorobia			
Chlorobium clathratiforme str. BU-1	AAIK01000013	+	+
Chlorobium chlorochromatii str. CaD3	NC_007514	+	+
Chlorobium phaeobacteroides str. BS1	NZ_AAIC01000113, NZ_AAIC01000957	+	+
Chlorobaculum tepidum str. TLS	NC_002932	+	+
Chlorobium phaeobacteroides DSM 266	NZ_AAIB01000016, NZ_AAIB01000004	+	+
Prosthecochloris aestuarii DSM 271	NZ_AAIJ01000019	+	+
Prosthecochloris vibrioformis DSM 265	NZ_AAJD01000006	+	+
Pelodictyon luteolum DSM 273	NC_007512	+	+
Chlorobium limicola DSM 245	NZ_AAHJ01000040	+	+
Alphaproteobacteria			
Magnetococcus sp. MC-1	NZ_AAAN03000009, NZ_AAAN03000063, NZ_AAAN03000064, NZ_AAAN03000091	+	+
Magnetospirillum magneticum AMB-1	NC_007626	+	+
Magnetospirillum magnetotacticum MS-1	NZ_AAAP01003703, NZ_AAAP01003586, NZ_AAAP01003833	+	+
Betaproteobacteria			
Thiobacillus denitrificans ATCC 25259	NC_007404	+	+
Gammaproteobacteria			
Allochromatium vinosum	U84760	+	+
Olavius algarvensis Gamma 3 symbiont	AASZ_01000111, AASZ_01004984	+	+
Olavius algarvensis Gamma 1 symbiont	AASZ_01001690	+	+
Endoriftia persephone	AASF_01001644, AASF_01001547, AASF_01001341	+	+
Cdt. *Ruthia magnifica* str. CM	NC_008610	+	+
Alkalilimnicola ehrlichei MLHE-1	NC_008340	+	+
Halorhodospira halophila SL1	NZ_AAOQ01000001	+	+
SAR86			
Uncultured bacterium BAC13K9BAC	DQ068067	+	+

Supplementary Fig. S1

Supplementary Fig. S1. Consensus tree based on 16S rRNA gene sequences from the *apr* gene-containing SOB referenc strains including SRP species. Branching orders that were not supported by all treeing methods are shown as multifurcations. Partial sequences were individually added to the reconstructed consensus tree without allowing changes in the overall tree topology. The sequences of *Archaeoglobus fulgidus*, *A. profundus* and *A. veneficus* were used as outgroup reference. Bootstrap values shown were calculated by the maximum likelihood method; the scale bar corresponds to 10% estimated sequence divergence. SOB species with laterally transferred *apr* genes are in boldface, while the reference strains with two *apr* gene copies are highlighted by boxes. The proposed LGT events are indicated by letters (see Fig. 1).

Supplementary Fig. S2. AprB and AprA alignment showing indels among selected representatives of the major phylogenetic SOB lineages supporting (1) their Apr-based divergence into the distinct protein lineages I and II, as well as (2) the postulated LGTs of *aprBA* between SRP and SOB and among SOB. Amino acid positions are according to the enumeration of *Allochromatium vinosum* proteins. Identical indel positions in AprB/A sequences are indicated by boxes (characteristic indels of Apr lineage I-sequences are highlighted by grey-shading).

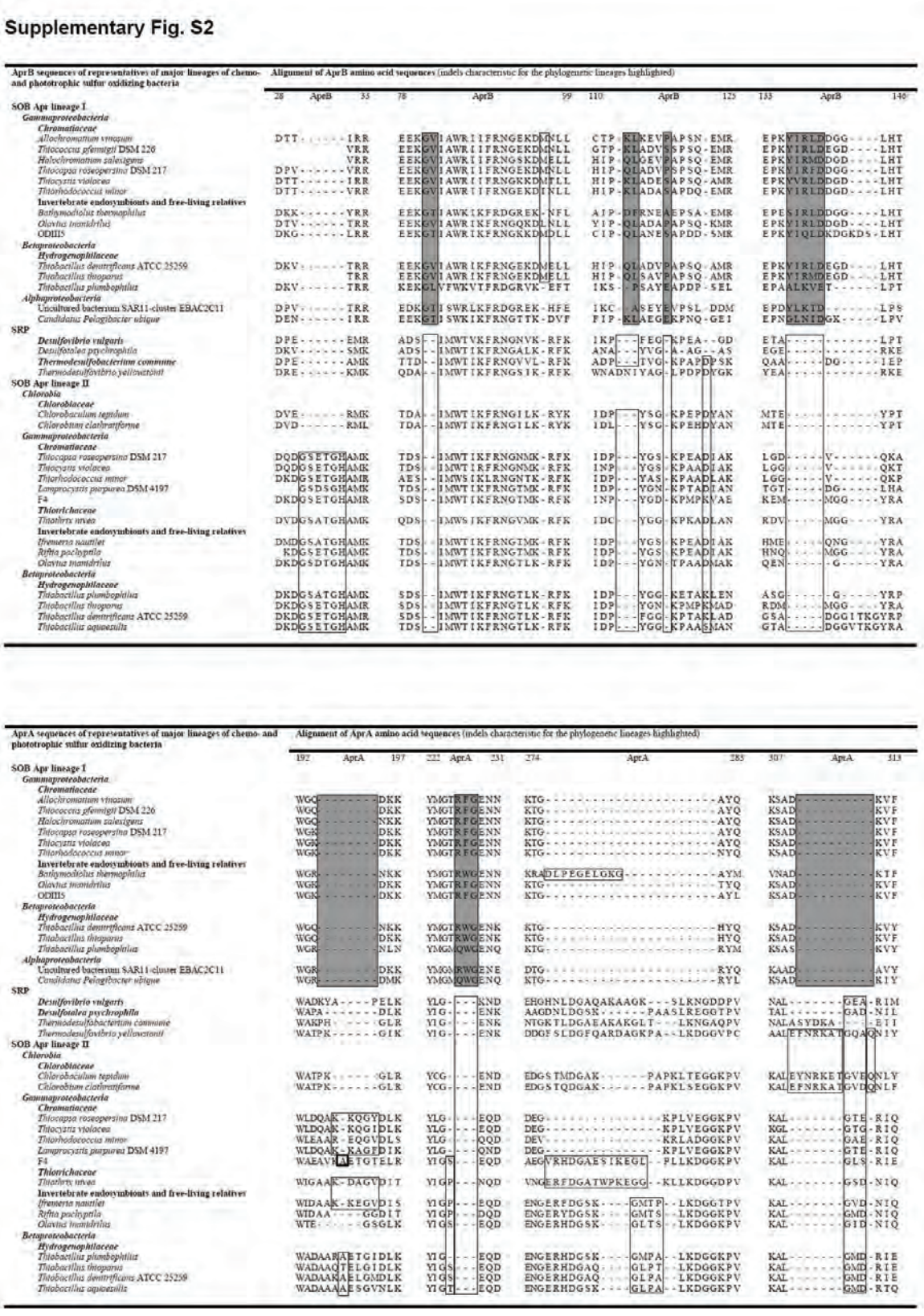

4.2.3 Publikation 3

Homology modeling of dissimilatory APS reductases (AprBA) of sulfur-oxidizing and sulfate-reducing prokaryotes

Birte Meyer und Jan Küver

PLoS ONE (2008). 3 (1), e1514

OPEN ACCESS Freely available online

PLoS one

Homology Modeling of Dissimilatory APS Reductases (AprBA) of Sulfur-Oxidizing and Sulfate-Reducing Prokaryotes

Birte Meyer, Jan Kuever¤*

Max Planck Institute for Marine Microbiology, Bremen, Germany

***Background*.** The dissimilatory adenosine-5′-phosphosulfate (APS) reductase (cofactors flavin adenine dinucleotide, FAD, and two [4Fe-4S] centers) catalyzes the transformation of APS to sulfite and AMP in sulfate-reducing prokaryotes (SRP); in sulfur-oxidizing bacteria (SOB) it has been suggested to operate in the reverse direction. Recently, the three-dimensional structure of the *Archaeoglobus fulgidus* enzyme has been determined in different catalytically relevant states providing insights into its reaction cycle. ***Methodology/Principal Findings*.** Full-length AprBA sequences from 20 phylogenetically distinct SRP and SOB species were used for homology modeling. In general, the average accuracy of the calculated models was sufficiently good to allow a structural and functional comparison between the beta- and alpha-subunit structures (78.8–99.3% and 89.5–96.8% of the AprB and AprA main chain atoms, respectively, had root mean square deviations below 1 Å with respect to the template structures). Besides their overall conformity, the SRP- and SOB-derived models revealed the existence of individual adaptations at the electron-transferring AprB protein surface presumably resulting from docking to different electron donor/acceptor proteins. These structural alterations correlated with the protein phylogeny (three major phylogenetic lineages: (1) SRP including LGT-affected Archaeoglobi and SOB of Apr lineage II, (2) crenarchaeal SRP *Caldivirga* and *Pyrobaculum*, and (3) SOB of the distinct Apr lineage I) and the presence of potential APS reductase-interacting redox complexes. The almost identical protein matrices surrounding both [4Fe-4S] clusters, the FAD cofactor, the active site channel and center within the AprB/A models of SRP and SOB point to a highly similar catalytic process of APS reduction/sulfite oxidation independent of the metabolism type the APS reductase is involved in and the species it has been originated from. ***Conclusions*.** Based on the comparative models, there are no significant structural differences between dissimilatory APS reductases from SRP and SOB; this might be indicative for a similar catalytic process of APS reduction/sulfite oxidation.

Citation: Meyer B, Kuever J (2008) Homology Modeling of Dissimilatory APS Reductases (AprBA) of Sulfur-Oxidizing and Sulfate-Reducing Prokaryotes. PLoS ONE 3(1): e1514. doi:10.1371/journal.pone.0001514

INTRODUCTION

ATP sulfurylase, adenosine-5′-phosphosulfate (APS) reductase and sulfite reductase mediate the process of dissimilatory sulfate reduction and, therefore, represent key enzymes in the energy metabolism of the phylogenetically diverse sulfate-reducing prokaryotes (SRP). Sulfate is activated to APS by ATP sulfurylase (Sat) at the expense of ATP; hereafter, APS reductase (Apr) converts APS to AMP and sulfite which is subsequently reduced to sulfide by the activity of sulfite reductase (Dsr) [1–4]. Homologous proteins have been shown to exist in several anoxygenic phototrophic and chemotrophic, facultative anaerobic sulfur-oxidizing bacteria (SOB) [3,5–11] in which they were suggested to operate in the reverse direction oxidizing sulfide to sulfate. In SRP as well as in SOB, these enzymes appeared to be located in the cytoplasm or at the cytoplasmic site of the inner membrane [3,7,8,10,11].

The enzyme APS reductase has been investigated from several SRP and SOB with respect to the molecular parameters, e.g. mass, subunit composition and cofactor stoichiometry; the results confirmed its general conformity although the enzyme was involved in different metabolic pathways (oxidative/reductive) and was isolated from phylogenetically distant species [7,8,12,13]. Its functional unit is suggested to be a 1:1 heterodimeric complex composed of a FAD-containing alpha-subunit with a molecular mass of 70–75 kDa and a two [4Fe-4S] clusters-containing beta-subunit of 18–23 kDa [12,13]. There is increasing evidence that a quinone-interacting membrane-bound oxidoreductase, QmoABC, represents the native electron donor in SRP [14,15]. Recent phylogenetic analyses of AprBA sequences of sulfate-reducers and sulfur-oxidizers demonstrated that their encoding genes, *aprBA*, have been frequently affected by lateral gene transfer (LGT) events [16,17] which are reflected in the existence of two distantly related oxidative APS reductase types in SOB: Most members of the *Chromatiaceae* possess a homologue (SOB Apr lineage I) distinct to the reductive protein type of the SRP, whereas members of certain SOB families and genera, e.g. *Chlorobiaceae* and betaproteobacterial *Thiobacillus*, harbor SRB-related, putatively LGT-acquired *aprBA* genes (SOB Apr lineage II) [17]. Genome data demonstrated that the composition/arrangement of the *apr* gene loci (occurrence of *qmoABC* or *aprM* genes) of the distinct SOB lineages I and II correlates with the AprBA phylogeny. Based on the concomitant presence of the *apr* and *qmo* genes, the Qmo redox complex has been suggested to act as a functional link between the APS reductase and the membrane quinone pool also in those SOB that harbor SRP-

Academic Editor: Hany El-Shemy, Cairo University, Egypt

Received October 9, 2007; **Accepted** December 17, 2007; **Published** January 30, 2008

Copyright: © 2008 Meyer, Kuever. This is an open-access article distributed under the terms of the Creative Commons Attribution License, which permits unrestricted use, distribution, and reproduction in any medium, provided the original author and source are credited.

Funding: This study was funded by the Max-Planck-Society and the German Research Foundation.

Competing Interests: The authors have declared that no competing interests exist.

* **To whom correspondence should be addressed.** E-mail: kuever@mpa-bremen.de

¤ **Current address:** Bremen Institute for Materials Testing, Bremen, Germany

related *apr* gene loci (SOB Apr lineage II) [17] as proposed for the SRP [14]. The native electron donor of the SOB Apr lineage I type APS reductase is still unknown; interestingly, the corresponding genes are always co-transcribed with a conserved ORF, *aprM*, coding for a membrane-integral protein [17].

The X-ray structure of the dissimilatory APS reductase isolated from *Archaeoglobus fulgidus* has been elucidated at 1.6 Å resolution by Fritz and coworkers [18]: Its beta-subunit can be subdivided in three segments comprising a bacterial ferredoxin-like segment that envelopes both [4Fe-4S] clusters (amino acids B1-B68), followed by a three-stranded antiparallel beta-sheet (B69-B104) and a tail with a length of 50 Å (B105-B148) (see Fig. 1). The structure of the alpha-subunit can be grouped into the FAD cofactor-binding (amino acids A2-A261 and A394-A487), the capping (A262-A393) and the helical domains (A488-A643) (see Fig. 1); its overall structure classifies this subunit of the APS reductase as member of the fumarate reductase family [18–20]. The global part of the beta-subunit is embedded into a broad cleft of the alpha-subunit, while its long tail wraps around the latter increasing the contact surface between both subunits [18] (see Fig. 1). The reaction mechanism of APS reductase has been under debate [21,22]; Schiffers and coworkers recently determined the X-ray structures of *A. fulgidus* APS reductases in different enzymatic states [23] that confirmed the proposed catalytic mechanism via a nucleophilic attack of the N5 atom of reduced FAD on the sulfur of APS. A covalent FAD-APS intermediate is formed that decomposes spontaneously to AMP and to the FAD-sulfite adduct which is subsequently cleaved, and sulfite is finally liberated [23,24]. The two electrons required for the reduction of APS were postulated to be transferred one by one over 30 Å via [4Fe-4S] cluster II at the surface of the protein, cluster I and Trp-B48 to the isoalloxazine ring of the buried FAD [18,23,24] (see Fig. 1).

The aim of this study was to investigate the structural differences of oxidative and reductive APS reductases present in the phylogenetically and physiologically diverse SRP and SOB based on homology modeling-built protein models. The theoretical protein structure prediction method homology (or comparative) modeling [25–27] relies on the observation that the structural conformation of a protein is more highly conserved than its amino acid sequence, and that small or medium changes in sequence typically result in only small changes in the 3D structure [28]. In general, reliable homology models are constructed if the sequence identity exceeds 30% [25–27]. The results are discussed in context to the AprBA-based phylogeny and the presence/absence of the Qmo redox complex-encoding genes.

ANALYSIS

Sequence analysis and phylogenetics

PSI-BLAST (www.ncbi.nlm.nih.gov/BLAST/) was used to search the non-redundant version of current public databases of the National Center for Biotechnology Information (NCBI) for homologous, full-length sequences of QmoABC and AprBA. The AprBA sequences were implemented into the persisting multiple alignment of SRP- and SOB-derived sequences [16,17] using the Bioedit (version 7.0.5) sequence alignment editor (http://www.mbio.ncsu.edu/BioEdit/bioedit.html, email:). The QmoA, QmoB, and QmoC proteins were automatically aligned with the web server 3DCoffee@igs (http://igs-server.cnrs-mrs.fr/Tcoffee/) [29,30]; the initial alignments were refined manually by visual inspection. Phylogenetic analysis of the AprBA, QmoA, QmoB, and QmoC data sets (119, 21, 22, and 18 sequences) was performed with the online version of PhyML (http://atgc.lirmm.fr/phyml) [31]. Maximum likelihood-based phylogenetic trees were constructed using the global rearrangement and randomized species input order options as well as the JTT matrix as amino acid replacement model; regions of insertions and deletions (indels) were omitted from the calculations yielding finally 701, 392, 715,

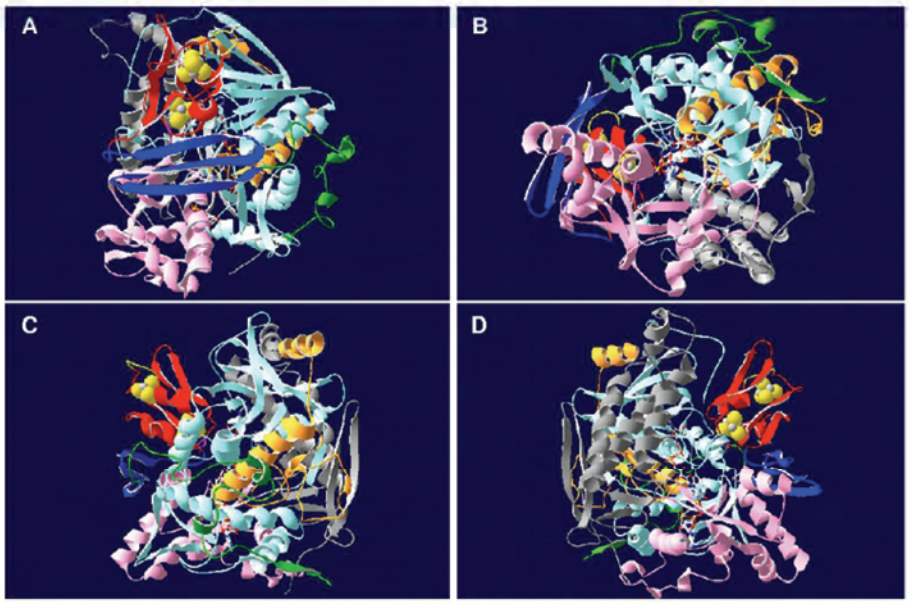

Figure 1. Three-dimensional ribbon structure of APS reductase from *A. fulgidus*. The beta-subunit segments are colored red (ferredoxin segment), blue (3 antiparallel beta-sheets segment), and green (tail segment); the alpha-subunit domains are colored light blue and orange (FAD-binding domain I and II), pink (capping domain), and grey (helical domain). The [4Fe-4S] clusters, FAD and substrate APS are shown as ball-and-stick representations; tryptophan Trp-B48 of AprB is highlighted by violet color. Ribbon structure is shown from (A) top view, (B) bottom view (substrate channel), (C) front view, and (D) back view.
doi:10.1371/journal.pone.0001514.g001

and 357 compared amino acid positions, respectively. Statistical support for the protein trees is given by bootstrap analysis with 100 resamplings.

Homology modeling

The AprBA sequences of *Pyrobaculum calidifontis* (YP_929769-70), *Pyrobaculum aerophilum* (NP_560098-101), *Caldivirga maquilingensis* (ZP_01711818-9), *Chlorobaculum tepidum* (NP_661758-9), *Pelagibacter ubique* HTCC1062 (YP_266256-7), uncultured alphaproteobacterium EBAC2C11 (AAV31645-6), *Thiobacillus denitrificans* ATCC 25259 (YP_314630-1, YP_316040-1), *Allochromatium vinosum* (AAC23620-1), *Candidatus* Ruthia magnifica (YP_903357-8), *Desulfovibrio vulgaris* str. Hildenborough (YP_010067-8), *Desulfovibrio desulfuricans* ATCC 29577 (AAF36689-90), *Desulfotalea psychrophila* (YP_064840-1), *Desulfobulbus* sp. str. MLMS-1 (ZP_01288426-7), *Olavius algarvensis* Delta1 symbiont (AASZ_01000974), *Syntrophobacter fumaroxidans* (YP_845176-7), uncultured sulfate-reducing bacterium fosws7f8 and fosws39f7 (CAJ31201-2; CAJ31179-80) [32], *Desulfotomaculum reducens* str. MI-1 (ZP_011499890-1), *Thermodesulfobacterium commune* and *Thermodesulfovibrio yellowstonii* (genome sequencing database of The Institute of Genome Research, http://www.tigr.org) were selected to create three-dimensional models of dissimilatory APS reductases from a phylogenetically and physiologically diverse range of SRB and SOB. Comparative modeling by assembly of rigid bodies [25–27] was performed with the SWISS-MODEL/ProModII online server for automated protein homology modeling (http://swissmodel.expasy.org) [33,34] using the recently determined AprBA structures of *Archaeoglobus fulgidus* [18,23] as templates (Brookhaven Protein Data Bank, PDB, entries 1jnrA/B, 2FJA, 2FJB, 2FJD, 2FJE). The input alignments (SWISS-MODEL "alignment mode") were based on a structural multiple alignment calculated by 3DCoffee which was manually refined to result in optimal pair wise target-template alignments (to be modeled SOB/SRB AprBA versus the *A. fulgidus* sequence). Model construction by the ProModII program included complete backbone and side chain building, loop building, verification of model quality, including packing, and subsequent energy minimization [33,34] using the Gromos96 force field [35]. The stereochemical and energetic parameters of the initial 3D protein models were evaluated by the WHATCH-ECK [36], PROSAII [37], ANOLEA [38], and Verify3D [39] analysis reports provided by the SWISS-MODEL server. The protein structure visualization program DeepView (Swiss-PdbViewer, version 3.7.; available from the ExPASy server http://www.expasy.org/spdbv) [33,40] was used to optimize the placement of the insertions and deletions considering the template structure context and conservation of structural features with a functional role. The "project mode" of SWISS-MODEL was used to iteratively improve the output 3D models of each SOB and SRB species on the basis of the evaluation software embedded within ProModII. Docking of the [4Fe-4S] clusters, FAD cofactor and substrate APS into the structure of modeled dissimilatory APS reductase was performed by superimposition with the template. The quality of the final model was determined from the B-score values provided by SWISS-MODEL and the root mean square (RMS) deviation values between equivalenced atoms in the amino acids of modeled and template protein. The models were also analyzed for violations of main chain Phi/Psi dihedral bond angle ratios and backbone/side chain steric conflicts. The molecular surface including the electrostatic potential as well as the accessible surface areas were calculated using the corresponding tools implemented into the DeepView program. The figures were generated using the Render3D mode of DeepView.

RESULTS AND DISCUSSION

In general, the average homology model accuracy is a function of the template-target sequence similarity: The dispersion of the model-target structural overlap increases with the decrease in sequence identity between template and target. Errors in models can be divided into five categories: (1) errors in side chain packing, (2) distortions and shifts of a region that is aligned correctly with the template structure, (3) distortions and shifts of a region that does not have an equivalent segment in any of the template structures, (4) distortions and shifts of a region that is aligned incorrectly with the template structures, and (5) a misfolded structure that results from using an incorrect template. Errors 3–5 are relatively infrequent when sequences with more than 40% identity to the templates are modeled; in such a case, approximately 90% of the main chain atoms are likely to be modeled with an RMS deviation of about 1 Å between template and target proteins; the structural differences are usually limited to loops and side chains [25–27]. Overall, these models are almost as good as medium-resolution experimental structures, because the proteins at this level of similarity are likely to be as similar to each other as are the structures for the same protein determined by different experimental techniques under different conditions, see [25–27] and references therein. When the sequence identity is between 30 and 40%, the structural differences become larger resulting in an increase of the main chain RMS errors to about 1.5 Å for about 80% of residues. The rest of the residues are modeled with large errors because the homology modeling methods generally fail to model structural distortions and rigid body shifts, and are unable to recover from misalignments [25–27].

In this study, full-length Apr sequences from 20 phylogenetically distinct SRP and SOB species were used for homology modeling that ranged in their sequence identity values to the *A. fulgidus* templates between 38.6 to 62.6% (beta-subunit) and 47.6 to 60.7% (alpha-subunit) (see supplementary data material Table S1 and S3). The lowest identity values were found for the sequences of SOB Apr lineage-I members, e.g. *Pelagibacter ubique*, (AprB: 38.6 to 45.8%; AprA: 47.7 to 51.5%) and the sequences of crenarchaeal *Pyrobaculum* spp. (38.7 to 42.4%; AprA: 47.6%) which is in accordance to the AprBA phylogeny (see Fig. 2A). The APS reductases of SRB species possessed sequence identities to the *A. fulgidus* templates that ranged between 53.1 to 62.6% (AprB) and 49.5 to 60.7% (AprA) with the highest values received for the Gram-positive SRB and the LGT-affected deltaproteobacterial members [16]; the APS reductases of SOB Apr lineage II had 49.0 to 61.4% (AprB) and 50.2 to 54.0% (AprA) sequence identity to the templates. The overall accuracy of all AprA and most AprB comparative models could be assumed to be sufficiently good to allow their structural and functional comparison (in the models, 78.8 to 99.3% (AprB) and 89.5 to 96.8% (AprA) of the main chain atoms had RMS deviations below 1 Å, see supplementary data material Table S1 and S3).

Structural comparison of the beta-subunit (AprB) comparative models of the dissimilatory APS reductase among SRP and SOB

The three segment-subdivision of the *A. fulgidus* beta-subunit described by Fritz and coworkers [18,23] is reflected in all comparative models of the dissimilatory APS reductase irrespective of species metabolism type and phylogenetic affiliation. While the presence and orientation of the secondary structure elements are strictly conserved in the functionally important first and second segment of the models (ferredoxin-like and alpha-subunit interface region), the third, the tail segment, is more variable among the investigated SRP and SOB (see Fig. 3 for AprB models of selected

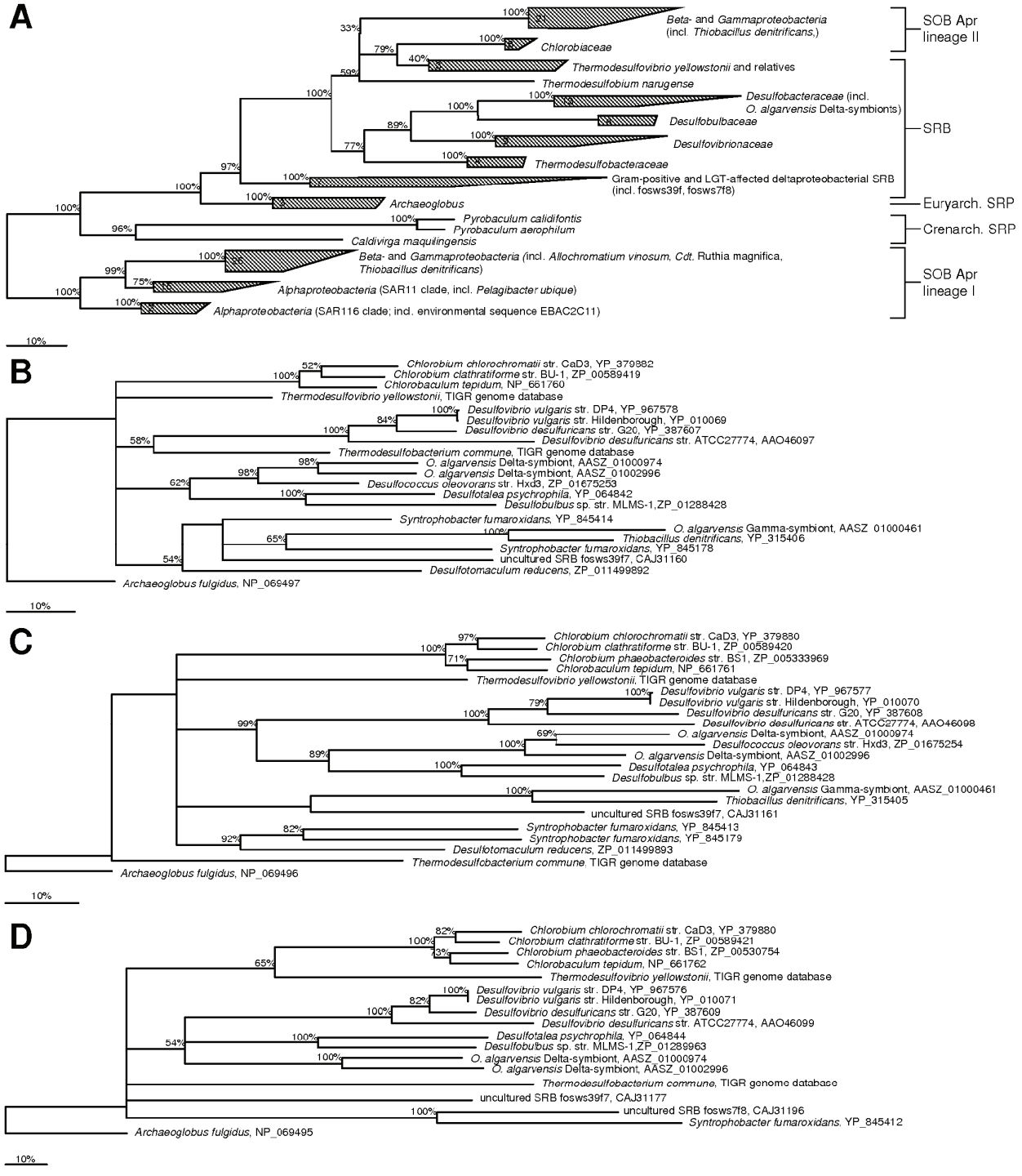

Figure 2. Phylogenetic trees based on (A) AprBA, (B) QmoA, (C) QmoB, and (D) QmoC sequences. The trees were inferred using PhyML (maximum likelihood method). The SOB Apr lineage-I sequence group (A) and the *Archaeglobus fulgidus* QmoABC sequences (B–D) were used as outgroup, respectively. The scale bar corresponds to 10% estimated sequence divergence. Branching orders that were only supported by bootstrap resampling values below 50% are shown as multifurcations; percentages greater than 50% of bootstrap resampling supporting a topological element are indicated near the nodes.

doi:10.1371/journal.pone.0001514.g002

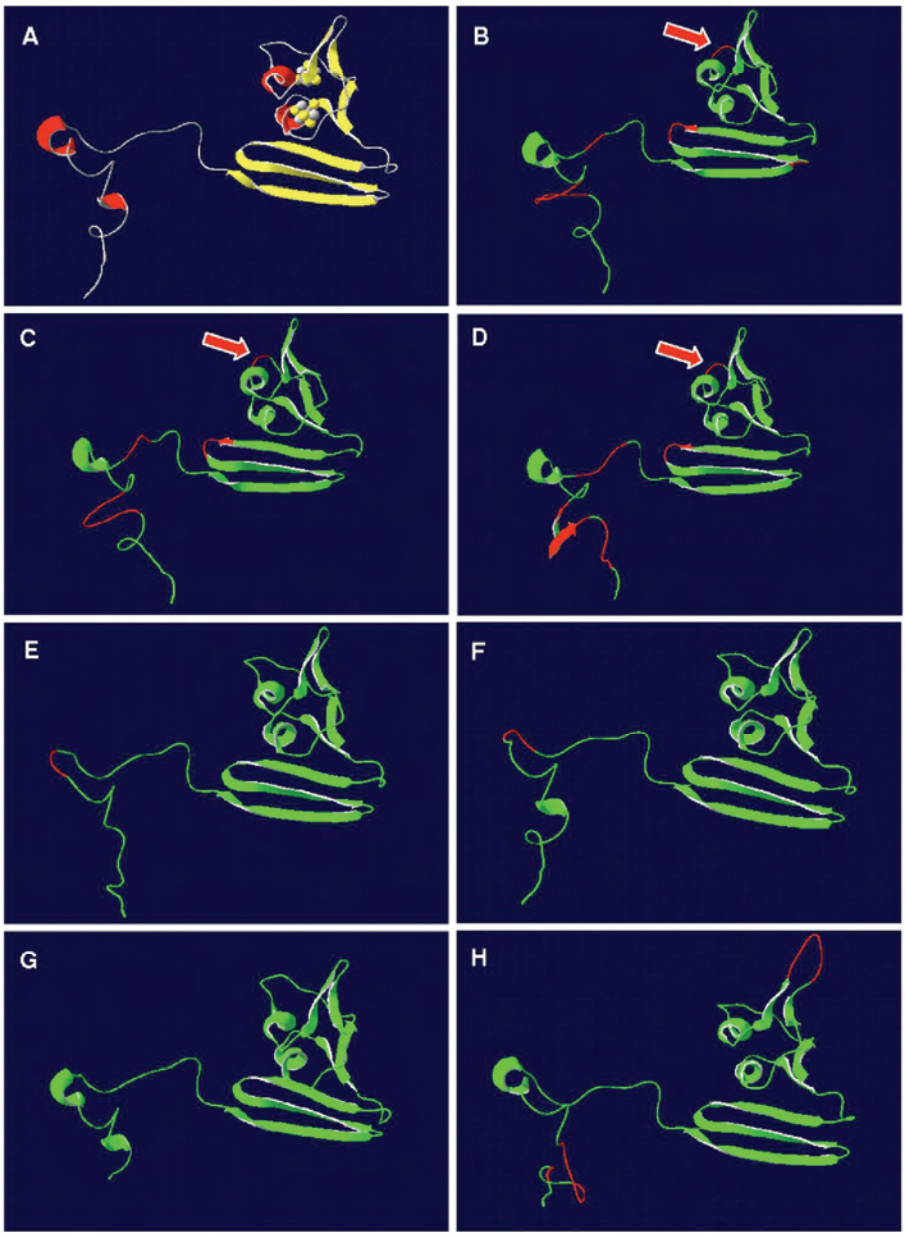

Figure 3. Three-dimensional structure of AprB from *A. fulgidus* (A) and selected, homology modeling-based AprB models from *Allochromatium vinosum* (B) and *Pelagibacter ubique* (C) (as representatives of SOB from Apr lineage-I), *Pyrobaculum calidifontis* (D) (as representative of crenarchaeal SRP), *Desulfotomaculum reducens* (E) (as representative of Gram-positive SRB and LGT-affected deltaproteobacterial SRB), *Desulfovibrio vulgaris* (F) (as representative of non-LGT-affected deltaproteobacterial SRB), *Chlorobaculum tepidum* (G) and *Thiobacillus denitrificans* (H) (as representatives of LGT-affected SOB from Apr lineage-II). Ribbon structure shown from front view (positions of [4Fe-4S] clusters indicated in *A. fulgidus* AprB). Ribbon structure of *A. fulgidus* AprB (A) colored by secondary structure elements; ribbon structures of AprB models (B–H) colored by model confidence factor provided by SWISS-MODEL (green, respective region of model and reference structure superpose; red, respective region of model deviates from the reference structure). The missing flexible loop between Cys-B13 and Gly-B19 (enumeration based on *A. fulgidus* sequence) in models of SOB from Apr lineage-I and *Pyrobaculum* spp. is marked by red arrows.
doi:10.1371/journal.pone.0001514.g003

SRP/SOB; all AprB models are presented in supplementary material Table S1 and Figure S1). Significantly higher main chain atom RMS deviations of up to 3.28 Å to the *A. fulgidus* template were present in this protein region in comparison with the low values of the first segments that ranged between 0.00 and 0.84 Å (see Table 1). The tail region has been proposed to be responsible for the tightening of the subunit interaction and, thus, a stable heterodimer formation by increasing the contact surface between both subunits [18,23]. The differing presence of secondary structure elements in the tail segments of the models is a result of the high variability in sequence and length. The structural dispersion of the tail regions might reflect the process of speciation

Table 1. Root mean square deviations (RMSD) of AprB and AprA comparative models from SRP and SOB with respect to the *A. fulgidus* template structure.

Spezies	AprB				AprA	
	1.+2. segment		3. segment			
	AA	RMSD for backbone/Cα atoms in Å (no. of atoms involved in calculation)	AA	RMSD for backbone/Cα atoms in Å (no. of atoms involved in calculation)	AA	RMSD for backbone/Cα atoms in Å (no. of atoms involved in calculation)
SOB Apr lineage I						
Allochromatium vinosum	2-102	0.63 (392)/0.47 (98)	103-156	1.50 (184)/1.27 (46)	2-620	0.88 (2424)/0.84 (606)
Thiobacillus denitrificans	2-102	0.62 (392)/0.46 (98)	103-156	1.22 (184)/1.14 (46)	2-622	0.79 (2432)/0.73 (608)
Cdt. Ruthia magnifica	2-101	0.59 (392)/0.41 (98)	102-155	1.46 (184)/1.30 (46)	2-625	0.96 (2432)/0.94 (608)
Pelagibacter ubique	2-101	0.55 (392)/0.35 (98)	102-153	1.56 (184)/1.37 (46)	2-614	1.16 (2400)/1.15 (600)
EBAC2C11	2-101	0.53 (392)/0.34 (98)	102-153	1.53 (184)/1.28 (46)	2-614	1.46 (2400)/1.48 (600)
Crenarchaeal SRP						
Caldivirga maquilingensis	2-104	0.82 (392)/0.68 (98)	105-154	1.69 (180)/1.56 (45)	2-627	0.88 (2460)/0.82 (615)
Pyrobaculum calidifontis	2-101	0.59 (392)/0.44 (98)	102-151	3.28 (168)/3.23 (42)	2-627	1.16 (2440)/1.17 (610)
SRB and related SOB Apr lineage-II						
Desulfotomaculum reducens	2-104	0.08 (412)/0.05 (103)	105-147	2.11 (172)/2.20 (45)	2-624	0.82 (2456)/0.78 (614)
Syntrophobacter fumaroxidans	2-104	0.08 (412)/0.06 (103)	105-147	0.83 (172)/0.78 (43)	2-634	0.71 (2476)/0.65 (619)
fosws7f8	2-104	0.09 (412)/0.07 (103)	105-146	0.87 (180)/0.95 (45)	2-630	0.66 (2480)/0.62 (620)
fosws39f7	2-104	0.00 (412)/0.00 (103)	105-146	0.00 (168)/0.00 (42)	2-634	0.70 (2484)/0.64 (621)
Thermodesulfobacterium commune	2-104	0.08 (412)/0.06 (103)	105-152	0.61 (184)/0.50 (46)	2-664	0.97 (2524)/0.92 (631)
Desulfovibrio vulgaris	2-104	0.08 (412)/0.06 (103)	105-148	0.67 (176)/0.61 (44)	2-664	1.54 (2512)/1.53 (628)
Desulfovibrio desulfuricans	2-104	0.08 (412)/0.06 (103)	105-148	0.65 (176)/0.60 (44)	2-662	1.01 (2520)/0.98 (630)
Desulfotalea psychrophila	2-104	0.08 (412)/0.06 (103)	105-138	3.21 (140)/3.18 (35)	2-671	1.04 (2512)/1.00 (628)
Desulfobulbus sp. MLMS1	2-104	0.08 (412)/0.06 (103)	105-139	3.21 (140)/3.18 (35)	2-669	1.14 (2516)/1.11 (629)
O. algarvensis Delta 1 symbiont	2-104	0.09 (412)/0.06 (103)	105-147	1.31 (172)/1.36 (43)	2-659	1.20 (2504)/1.18 (626)
Thermodesulfovibrio yellowstonii	2-104	0.08 (412)/0.06 (103)	105-142	1.46 (140)/1.28 (35)	2-662	1.05 (2492)/1.00 (623)
Chlorobaculum tepidum	2-104	0.09 (412)/0.06 (103)	105-140	0.09 (144)/0.07 (36)	2-658	0.91 (2492)/0.88 (623)
Thiobacillus denitrificans	2-110	0.38 (412)/0.22 (103)	111-157	1.81 (176)/1.89 (44)	2-666	0.82 (2492)/0.79 (623)

doi:10.1371/journal.pone.0001514.t001

by individual structural adaptations at the interacting surface between the beta- and alpha-subunit of each species. Indeed, the tail segment is the only sequence section of the beta-subunit that contains sufficient phylogenetic information to allow inter- and intrafamily differentiation among the SRP and SOB sequences.

Besides their overall conformity in the secondary structure element positioning, the first and the second segment of the comparative models showed significant differences in distinct loop regions resulting from insertions and deletions (see Fig. 3 and 4; for details see supplementary data material Table S1 and Figure S1). Interestingly, these structural differences reflected the AprBA-based phylogeny in its separation into three major phylogenetic AprBA clusters: (1) the SRB including the LGT-affected Archaeoglobi and SOB of Apr lineage II, (2) the *Caldivirga-Pyrobaculum* group of putative crenarchaeal sulfate-reducers, and (3) the SOB of distinct Apr lineage I (see Fig. 2A). Furthermore, the presence/absence of certain loops among the AprB models of each cluster correlated with the absence/presence of the Qmo redox complex and AprM protein encoding genes in the investigated SRP and SOB genomes [16,17] and might reflect their different functional linkage to the electron transport chain in the membrane. (1) In all comparative AprB models of SRB, *A. fulgidus* and the SOB of Apr lineage II, there is a flexible loop conservatively located between Cys-B13 and Gly-B19 which comprised predominantly charged amino acids of the following general sequence, K G X D/E K/R (see Fig. 3 and 4; for sequence details see supplementary data material Table S1). This loop is absent in the beta-subunit models of SOB from Apr lineage I and the *Caldivirga-Pyrobaculum* group (see Fig. 3B–D and supplementary data material Figure S1). Especially the conserved Lys-B14 and Glu/Asp-B17 are located at exposed, solvent-accessible positions in this loop (see Fig. 4 and supplementary data material Figures S1, panels G/H); they might be responsible for the functional docking of the putative redox partner QmoABC/QmoAB(-HdrBC) to the AprB protein surface adjacent to the [4Fe-4S] cluster II. The Qmo complex presumably operates as physiological electron carrier between the membrane-integral quinone/quinol pool and the cytoplasmic APS reductase in the SRP as well as in the sulfite-oxidizing *Chlorobiaceae* and *Beta-* and *Gammaproteobacteria* that harbor a SRB-related enzyme (SOB Apr lineage II) [17]. *Thiobacillus denitrificans* possessed a second exposed loop of six amino acids positioned between the beta-alpha-beta structure motifs of the ferredoxin-like segment; however, its functional or structural role is not apparent. (2) The crenarchaeal *Caldivirga maquilingensis* and putative sulfate-reducing *Pyrobaculum* spp. did not harbor *qmo* homologous sequences in their genomes [17]; in agreement to the previous proposal, an elongated loop between secondary structure element 2 and 3 was absent in their AprB comparative models (see Fig. 3D and supplementary material Figure S1). The putative physiological electron donor for the dissimilatory APS reductase in these species is unknown;

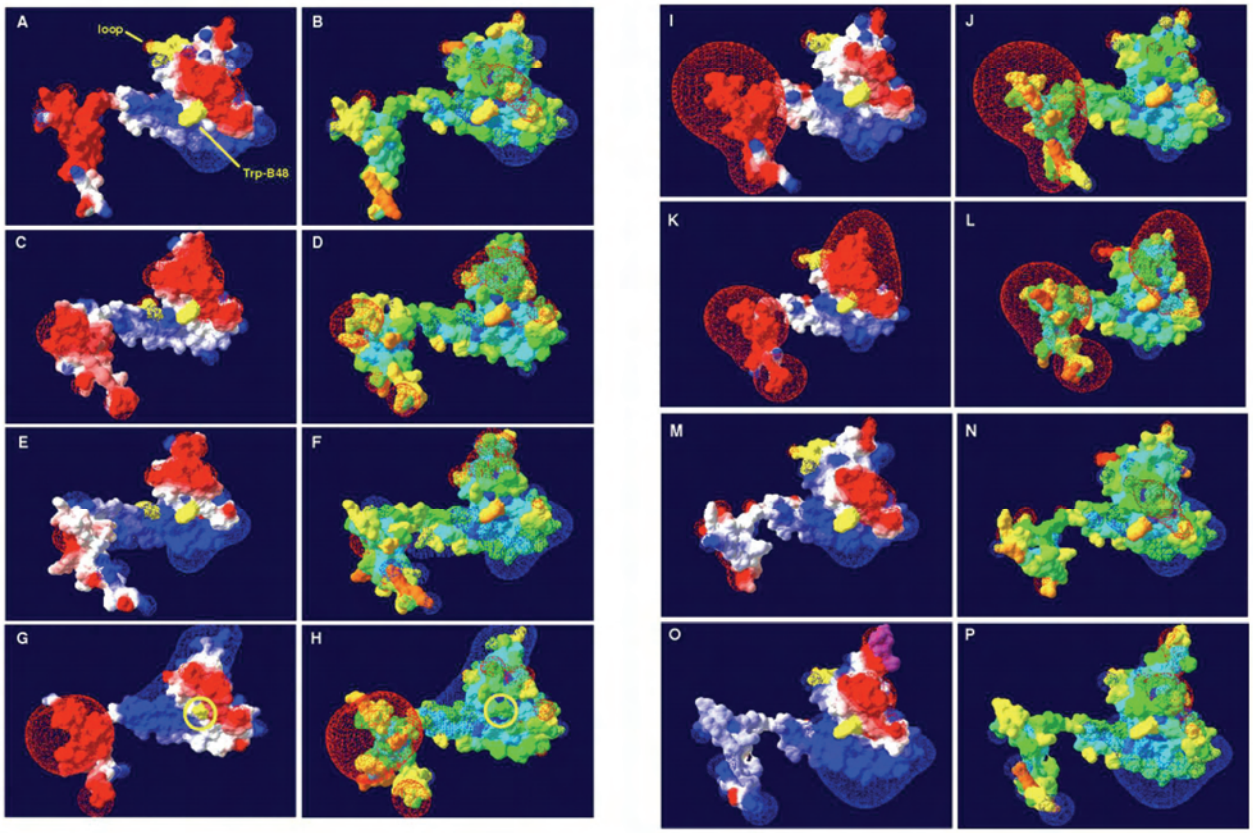

Figure 4. Three-dimensional structure of AprB from *A. fulgidus* (A, B) and selected, homology modeling-based AprB models from *Allochromatium vinosum* (C, D), *Pelagibacter ubique* (E, F), *Pyrobaculum calidifontis* (G, H), *Desulfotomaculum reducens* (I, J), *Desulfovibrio vulgaris* (K, L), *Chlorobaculum tepidum* (M, N) and *Thiobacillus denitrificans* (O, P). Protein molecular surface colored by calculated electrostatic potential are shown in panels A, C, E, G, I, K, M, O (electric charge at the molecular surface is colored with a red (negative), white (neutral), and blue (positive) color gradient; electric field extending into the solvent is shown); the differently present, negatively charged loops in the models of SRP and SOB are marked by yellow color (the additional loop of *Thiobacillus denitrificans* is shown in violet); the electron-transferring Trp-B43/-B48 is marked by yellow color (*Pyrobaculum calidifontis*: Trp-substituting Ala-B43 is highlighted in G and H). Protein molecular surface colored by calculated solvent accessibility are shown in panels B, D, F, H, J, L, N, P.
doi:10.1371/journal.pone.0001514.g004

however, naphtoquinones have been described from *Pyrobaculum* species [41,42]. The electrostatic potential at the protein surface of the crenarchaeal AprB models differed significantly from the other SRP and SOB which might be an indication that the potential interacting redox partner and the electron transfer process of the aforementioned are different and unrelated to the latter (see Fig. 4 and supplementary data material Figures S1, panels E/F). Interestingly, both *Pyrobaculum* APS reductases missed the strictly conserved, electron transfer-relevant Trp-B48 that was substituted by an Ala-B43 residue at the corresponding AprB model position (see Fig. 4 panel G for the *Pyrobaculum calidifontis* AprB model). In all other Apr comparative models, the Trp-B48/43 was located between the S3 of cluster I and the methyl C8M of FAD (distance 12.4 Å) and in van der Waals contact with both redox centers; its indole ring was locked in its position by Thr-A233 and Arg-A232. The electron transfer function of trytophan residues located between two redox centers has been frequently documented [43,44]; an analogous functional role, however, has not been reported for alanine residues. In consequence, the *Pyrobaculum* spp. APS reductases might have lost their structural ability for electron transfer between both subunits (essential for APS reduction) and, thus, their enzymes will not be functional anymore (see also the structural comparison of the alpha-subunits). Indeed, no cultivated *Pyrobaculum* species has been described to be capable of dissimilatory sulfate reduction [45,46]; notably, the *aprBA* sequences of the *Pyrobaculum aerophilum* genome are frame-shifted [47] which might be a result of elevated mutation rate in irrelevant enzymes/metabolic pathways. (3) Like the beta-subunits of the crenarchaeal putative sulfate-reducers, the AprB comparative models of the SOB Apr lineage-I sulfur-oxidizers did not contain an elongated loop between secondary structure element 1 and 2 (see Fig. 3B and C and supplementary material Figure S1). Consistently, the genomes of the respective species did not include *qmo* homologues; however, their *aprBA* genes were always preceded and co-transcribed by a membrane-integral protein encoding gene, *aprM*. Interestingly, all AprB models of the SOB Apr lineage I possessed in the antiparallel beta-sheet segment an elongated loop by amino acid insertion between the secondary structure element 8 and 9 that comprised predominantly negatively charged residues (see Fig. 4 panels C and E; supplementary data material Table S1 and Figure S1, compare panels E/F). The latter were exposed to the solvent (see Fig. 4 panels D and F and supplementary data material Figure S1, compare panels G/H) and might function as an interface region for docking the AprBA

enzyme to the AprM protein that anchors the dissimilatory APS reductase to the membrane and enables its physical contact to the yet unknown electron receptor. The presumed differing functional linkage of the cytoplasmic SOB Apr lineage I-type APS reductases to the membrane (not involving Qmo complex homologues) was also reflected in the deviating electrostatic potential at the protein surface when compared to the SRB-type AprB models (supplementary data material Figure S1, compare panels E/F).

The [4Fe-4S] clusters surrounding protein matrix in the AprB models of SRP and SOB

The [4Fe-4S] clusters of APS reductases from several sulfate reducing strains have been documented to differ significantly in their reduction potential (approximately −500 mV for cluster II and −60 mV for cluster I) [18,23,24]. Based on the X-ray structure of *A. fulgidus*, the large reduction potential difference of the two clusters was explained by their distinctly different surrounding protein matrix (see Fig. 5 panel A). Generally, local dipole in close proximity to the acid-labile sulfur and cysteinyl sulfur atoms modulate the reduction potential of a [4Fe-4S] cluster: Its reduced state can be stabilized by NH-S hydrogen bonds and backbone amide dipoles that shift the reduction potential of an iron-sulfur center to a more positive value. In the *A. fulgidus* APS reductase, the number of polar interactions between the sulfur atoms of cluster I compared to cluster II and the backbone amides at a distance of less than 3.5 Å (17 versus 7) is substantially increased and proposed to be responsible for the high reduction potential of cluster I. In contrast, the close proximity of the negatively charged Asp-B11-carboxylate group to an acid-labile sulfur of the cluster II was suggested to stabilize its oxidized state with the result of a low reduction potential [18,23] (see Fig. 5 panel A; see also supplementary material Figure S2 for details).

The DeepView program does not allow the calculation of potential interactions between the modeled protein and enzyme-associated cofactors; the structural comparison of the different comparative models and the *A. fulgidus* template was therefore restricted to distance analyses between the [4Fe-4S] clusters and their surrounding protein matrix. Notably, there were no significant structural differences between the comparative models of SRP and those of SOB (see Table 2, see Fig. 5 for AprB models of selected SRP/SOB; for details see supplementary data material Figure S2 and Table S2). Indeed, the protein environments of the clusters from sulfur-oxidizers of Apr lineage II, e.g. *Chlorobaculum tepidum* and *Thiobacillus denitrificans*, were more similar to those of SRP than to those of Apr lineage I sulfur-oxidizers (compare residues in a distance of less than 3.5 Å to the clusters, Table 2). In consequence, there was no increased number of polar interactions between cluster II compared with cluster I and backbone amides in the aforementioned SOB that would modulate the iron-sulfur center reduction potentials in order to favor the reverse "oxidative" electron transfer in these species. According to the models, the structural differences in the [4Fe-4S] ambient protein matrix rather correlated with the AprBA phylogeny: In contrast to the models of SRB including affiliated Archaeoglobi and SOB of Apr lineage II, the Apr lineage I SOB and crenarchaeal SRP models revealed a deviating successive appearance of amino acids near both clusters (see supplementary data material Figure S2 and Table S2). As a result of the missing elongated loop between secondary structure 1 and 2, Ile-B24 and Thr-B3 came very close (2.0 and 3.0 Å, respectively) to the [4Fe-4S] cluster I, whereas cluster II exhibited an increased number of backbone amide contacts at a distance of less than 3.0 Å in contrast to cluster I. Besides the carboxylate group of Asp-B11 (in some cases substituted by Glu-B54), the side chain of a histidine residue (His-B15/54/55) was positioned in proximity (3.5 Å) to cluster II in most AprB models of Apr lineage I SOB (Table 2 and supplementary data material Figure S2 and Table S2). However, if this positively charged surrounding is appropriate to stabilize the reduced state of cluster II and, thus, to shift its reduction potential to more positive values remains to be proven experimentally. Noteworthy, both *Pyrobaculum* spp. AprB models contained two positively charged amino acids adjacent to the acid labile sulfur and cysteinyl sulfur atoms of cluster II that would not favor oxidized state of the latter as proposed to be essential for the intrinsic electron transfer in the SRP-type proteins (see Fig. 5 panel D for *Pyrobaculum calidifontis*). Indeed, this feature might be another indication for the presence of a non-functional enzyme in the investigated *Pyrobaculum* species.

Structural comparison of the alpha-subunit (AprA) comparative models of the dissimilatory APS reductase among SRP and SOB

The *A. fulgidus* alpha-subunit has been described to be subdivided into three domains, the FAD-binding (A2-261, A394-487), capping (A262-393), and the helical domain (A488-643) (see Fig. 1 and 6). The FAD-binding domain constitutes the center, while the capping and helical domains form the periphery of the alpha-subunit (the helical domain is firmly attached to the first whereas the capping domain is partly exposed from the core region). The FAD-binding domain is composed of a central six-stranded parallel beta-sheet (sec. str. elm. 1, 3, 11, 12, 13, 14) that is flanked by four alpha-helices on one side (sec. str. elm. 2, 6, 10, 36) and by a four-stranded mixed beta-sheet on the other (sec. str. elm. 15, 17, 19, 32) (see Fig. 6 panel B). The capping domain is inserted into the polypeptide chain of the aforementioned domain and consists of a four-stranded antiparallel beta-sheet (sec. str. elm. 20. 22, 27, 31) surrounded by eight (mostly short) alpha-helices (see Fig. 6 panel C), whereas the helical domain is primarily composed of three long alpha-helices (sec. str. elm. 39, 41, 42) (see Fig. 6 panel D) [18,23]. This general fold scheme was present in all comparative AprA models of APS reductases from SOB and SRP (irrespective of species metabolism type and protein phylogenetic affiliation) (see Fig. 7, for details see supplementary data material Table S3 and Figure S3). The conserved nature of the AprA structure was reflected in the low main chain atom RMS deviations from the template structure that ranged between 0.66 Å (uncultured SRB fosws7f8) and 1.20 Å (*O. algarvensis* Delta 1 symbiont) in the SRB and SOB Apr lineage II models (except the model of *Desulfovibrio vulgaris* with 1.54 Å RMSD), between 0.79 Å (*Thiobacillus denitrificans*) and 1.46 Å (environmental sequence EBAC2C11) in the SOB Apr lineage I, and in the crenarchaeal SRP group between 0.88 Å (*Caldivirga maquilingensis*) and 1.16 Å (*Pyrobaculum calidifontis*) (see Table 1). The helical domain which has been suggested to mainly build up the interface region between two $\alpha\beta$-heterodimers [18,23] constituted the most highly conserved protein region in the AprA models with regard to the presence and orientation of the secondary structure elements (RMSD from 0.06 to 0.99 Å; see supplementary data material Table S3 and Figure S3). In contrast, the FAD-binding and the capping domains of the comparative AprA models showed more structural differences; nevertheless, these alterations were predominantly restricted to certain loop amino acid stretches (e.g. between sec. str. elm. 10 and 11 or 36 and 37) and short secondary structure elements (e.g. alpha-helices, sec. str. elm. 23, 24 or 33) located at the protein surface (see supplementary data material Table S3 and Figure S3). As mentioned in a previous section, the

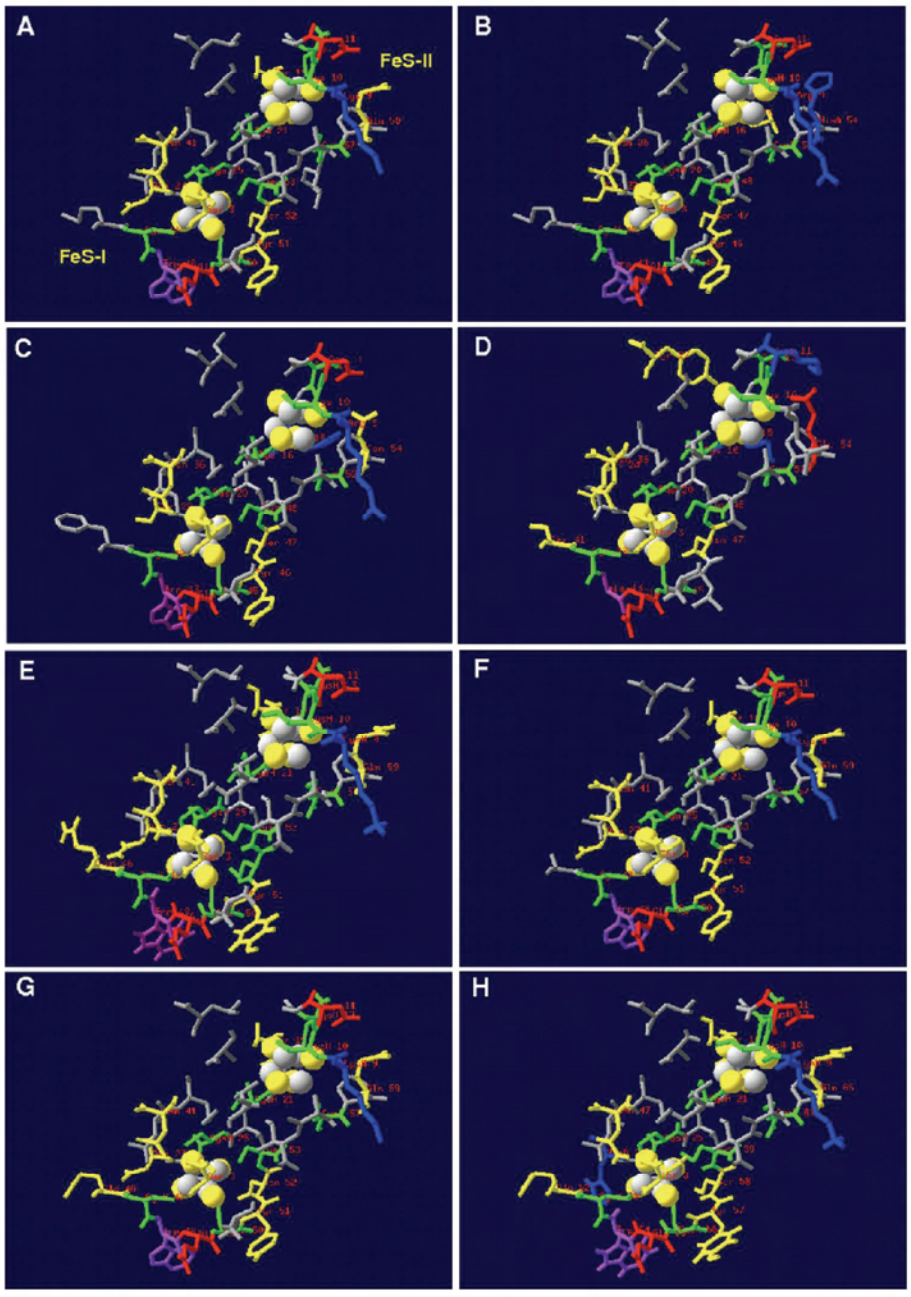

Figure 5. AprB protein matrix surrounding the [4Fe-4S] cluster I and II (residues in a distance of less than 5.0 Å are shown) in the three-dimensional structure from *A. fulgidus* (A) and selected, homology modeling-based models from *Allochromatium vinosum* (B), *Pelagibacter ubique* (C), *Pyrobaculum calidifontis* (D), *Desulfotomaculum reducens* (E), *Desulfovibrio vulgaris* (F), *Chlorobaculum tepidum* (G), and *Thiobacillus denitrificans* (H). Charged and polar residues are marked (positively charged AA, blue; negatively charged AA, red; polar AA, yellow); tryptophan (Trp-B48/-B43) and cysteine residues are highlighted by violet and green color.
doi:10.1371/journal.pone.0001514.g005

higher structural variability among the latter might reflect the individual adaptations at the contact areas between both APS reductase subunits of each species because these domains comprise the AprA interface areas to the second and third segment of AprB. Overall, the alpha-subunit core region was conserved and structurally uniform among the enzymes of sulfur-oxidizers and sulfate-reducers. Notably, the comparative models of *Thermodesulfovibrio yellowstonii*, *Thermodesulfobacterium commune*, the non-LGT-affected deltaproteobacterial SRB and the SOB of Apr lineage II contained 17 to 21 amino acids long insertions between the secondary structure elements 7 and 8; the inserted amino acid stretches were predicted by SWISS-MODEL to primarily form two extended, antiparallel beta-sheets that are exposed from the core region (see Fig. 7 panel E to H, see also supplementary data material Table S3 and Figure S3). The accuracy of the proposed structures in this AprA model area is highly speculative because of

Table 2. AprB amino acid residues surrounding the [4Fe-4S] clusters and cysteinyl sulfur atoms in a distance of less than 3.5 Å (sorted by chemical nature of the amino acid side chain)

	Reference structure	SOB of Apr lineage I					Crenarchaeal SRP			SRB and SOB of related Apr lineage II		
[4Fe-4S] cluster	*Archaeoglobus fulgidus*	*Allochromatium vinosum*	*Thiobacillus denitrificans*	*Cdt.* Ruthia magnifica	*Pelagibacter ubique*	EBAC2C11	*Caldivirga maquilingensis*	*Pyrobaculum calidifontis*	*Pyrobaculum aerophilum*	*Chlorobaculum tepidum*	*Thermodesulfo-vibrio yellowstonii*	*Thiobacillus denitrificans*
Cluster I	Cys25, Cys47, Cys50, Cys53	Cys20, Cys42, Cys45, Cys48	Cys20, Cys42, Cys45, Cys48	Cys20, Cys42, Cys45, Cys48	Cys20, Cys42 Cys45, Cys48	Cys20, Cys42, Cys45, Cys48	Cys20, Cys45, Cys48, Cys51	Cys20, Cys42, Cys45, Cys48	Cys20, Cys42, Cys45, Cys48	Cys25, Cys47, Cys50, Cys53	Cys25, Cys47, Cys50, Cys53	Cys25, Cys53, Cys56, Cys59
	Ser3, Asn41, Asn27, Tyr51, Ser52	Thr3, Ser22, Tyr46, Ser47	Thr3, Ser22, Tyr46, Ser47	Thr3, Ser22, Asn23, Tyr46, Ser47	Thr3, Ser22, Tyr46, Ser47	Thr3, Ser22, Tyr46, Ser47	Ser3, Ser22, Tyr49, Asn50	Thr3, Asn24, Asn47	Thr3, Asn24, Asn47	Ser3, Tyr51, Asn52	Ser3, Tyr51, Asn52	Thr3, Tyr57, Ser58
	Asp28, Glu49	Asp23, Glu44	Asp23, Glu44	Glu44	Asp23, Glu44	Asp23, Glu44	Glu47	Asp23, Glu44	Glu49, Glu44	Glu28, Glu49	Asp28, Glu49	Asp28, Glu55
							His23					His27
	Leu29, Val54	Ile24, Pro21, Val49	Pro21, Ile24, Val49	Pro21, Ile24, Val49	Ile24, Val49	Pro21, Ile24, Val49	Pro21, Ile24, Val52, Ile62	Leu46, Val49	Leu46, Val49	Leu29, Val54	Leu29, Val54	Val60
Cluster II	Cys10, Cys21, Cys57, Cys13	Cys13, Cys10, Cys16, Cys52	Cys13, Cys10, Cys16, Cys52	Cys13, Cys10, Cys16, Cys52	Cys13, Cys10 Cys16, Cys52	Cys13, Cys10, Cys16, Cys52	Cys13, Cys10, Cys16, Cys55	Cys13, Cys10, Cys16, Cys52	Cys13, Cys10, Cys16, Cys52	Cys10, Cys13, Cys21, Cys57	Cys10, Cys13, Cys21, Cys57	Cys10, Cys13, Cys21, Cys63
	Gln59	Asn55	Tyr15	Gln55	Asn54	Asn55	Thr11	Tyr27	Tyr27	Gln60	Gln22, Gln60	Gln66
	Asp11, Glu22	Asp11	Asp11, Asp55	Asp11	Asp11	Asp11		Glu54	Glu54	Asp11	Asp11	Asp11
		His54		His15, Arg33	His55	His15		Lys11, His55	Lys11, His55			
	Gly12, Gly60, Ala61	Gly12, Gly14, Val17, Ala56, Ile57	Gly12, Gly14, Val17, Met54, Ala56, Ile57	Gly12, Gly14, Val17, Ala56, Ile57	Gly12, Gly14, Val17, Ala56, Ile57	Gly12, Gly14, Val17, Ala56, Ile57	Gly12, Gly14, Val17, Phe27, Gly58, Ala59	Gly12, Gly14, Val17, Ala56	Gly12, Gly14, Val17, Ala56	Gly12, Ala20, Met22, Ala61	Gly12, Ala20, Ala61	Gly12, Ala20, Met22, Ala67

	Reference structure	SRB									
[4Fe-4S] cluster	*Archaeoglobus fulgidus*	*Desulfotomaculum reducens*	*Syntrophobacter fumaroxidans*	fosws39f	foswsf8	*Thermodesulfobac-terium commune*	*Desulfovibrio desulfuricans*	*Desulfovibrio vulgaris*	*Desulfotalea psychrophila*	*Desulfobulbus* sp.	*O. algarvensis* Delta 1 symbiont
Cluster I	Cys25, Cys47, Cys50, Cys53	Cys25, Cys47, Cys50, Cys53	Cys25, Cys47, Cys50, Cys53	Cys25, Cys47, Cys50, Cys53	Cys25, Cys47, Cys50, Cys53	Cys25, Cys47, Cys50, Cys53	Cys25, Cys47, Cys50, Cys53	Cys25, Cys47, Cys50, Cys53	Cys25, Cys47, Cys50, Cys53	Cys25, Cys47, Cys50, Cys53	Cys25, Cys47, Cys50, Cys53
	Ser3, Asn41, Asn27, Tyr51, Ser52	Ser3, Asn27, Tyr51	Ser3, Asn27, Tyr51, Asn52	Ser3, Asn27, Asn41, Tyr51, Ser52	Ser3, Tyr51	Ser3, Tyr51, Ser52	Thr3, Tyr51, Ser52	Thr3, Tyr51, Ser52	Ser3, Tyr51, Ser52	Ser3, Tyr51, Ser52	Ser3, Ser52
	Asp28, Glu49	Asp28, Glu49	Asp28, Glu49	Asp28, Glu49	Asp28, Glu49	Glu49	Glu49	Glu49	Asp28, Glu49	Asp28, Glu49	Glu49
	Leu29, Val54	Pro26, Leu29, Cys52, Val54	Leu29, Val54	Leu29, Val54	Leu29, Cys52, Val54	Leu29, Val54	Leu29, Val54	Leu29, Val54	Leu29, Val54	Leu29, Val54	Leu29, Phe51, Val54
Cluster II	Cys10, Cys21, Cys57, Cys13	Cys10, Cys13, Cys21, Cys57	Cys10, Cys13, Cys21, Cys57	Cys10, Cys21, Cys57, Cys13	Cys10, Cys13, Cys21, Cys57	Cys10, Cys13, Cys21, Cys57	Cys10, Cys13, Cys21, Cys57	Cys10, Cys13, Cys21, Cys57	Cys10, Cys13, Cys21, Cys57	Cys10, Cys13, Cys21, Cys57	Cys10, Cys13, Cys21, Cys57
	Gln59	Gln60	Gln60	Gln22, Gln60	Gln22, Gln60						Gln22, Thr59, Gln60
	Asp11, Glu22	Asp11	Asp11	Asp11	Asp11	Asp11	Asp11	Asp11	Asp11	Asp11	Asp11
	Gly12, Gly60, Ala61	Gly12, Ala20, Met22, Ala61, Ile62	Gly12, Ala20, Met22, Ala61	Gly12, Met38, Val59, Ala61	Gly12, Ala20, Val59, Ala61	Gly12, Val20, Met22, Gly60, Ala61	Gly12, Ala20, Met22, Gly60, Ala61, Ile62	Gly12, Ala20, Met22, Gly60, Ala61, Ile62	Gly12, Ala20, Met22, Gly60, Ala61, Ile62	Gly12, Ala20, Met22, Gly60, Ala61	Gly12, Ala20, Ala61, Ile62

doi:10.1371/journal.pone.0001514.t002

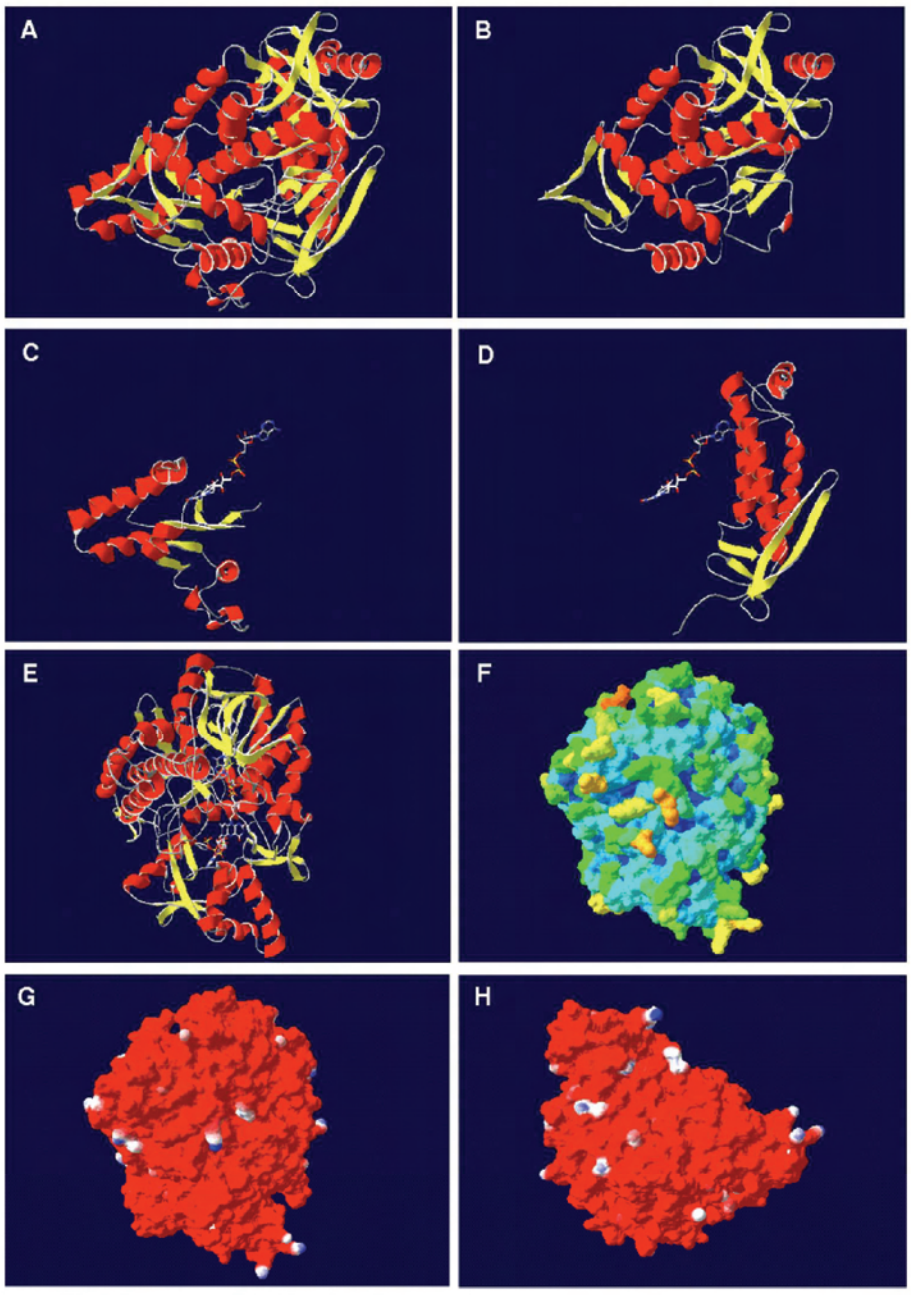

Figure 6. Structure of AprA from *A. fulgidus*. (A–E) Ribbon structure colored by secondary structure elements (position of FAD cofactor indicated), (A) entire model from front view, (B) only FAD-binding domain, (C) only capping domain, (D) only helical domain, and (E) entire protein from top view (position of APS molecule indicated additionally); (F) protein molecular surface colored by calculated solvent accessibility shown from top view; (G, H) protein molecular surface colored by calculated electrostatic potential shown from top and back view (electric charge at the molecular surface is colored with a red (negative), white (neutral, and blue (positive) color gradient).
doi:10.1371/journal.pone.0001514.g006

the current computational limitations in calculating the correct fold of loop regions encompassing more than eight residues. Its solvent-exposed location at the AprB-interacting site of the alpha-subunit might be an indication for an involvement in stabilizing the contact between the native electron donor/acceptor protein and the electron-transferring smaller subunit of APS reductase.

FAD cofactor surrounding protein matrix in the AprA models of SRP and SOB

The reductive reaction mechanism of the dissimilatory APS reductase proceeds via a nucleophilic attack of the N5 atom (isoalloxazine moiety) of the reduced FAD on the sulfur of APS [18,23,24]. According to the AprA comparative models, 35 to 36

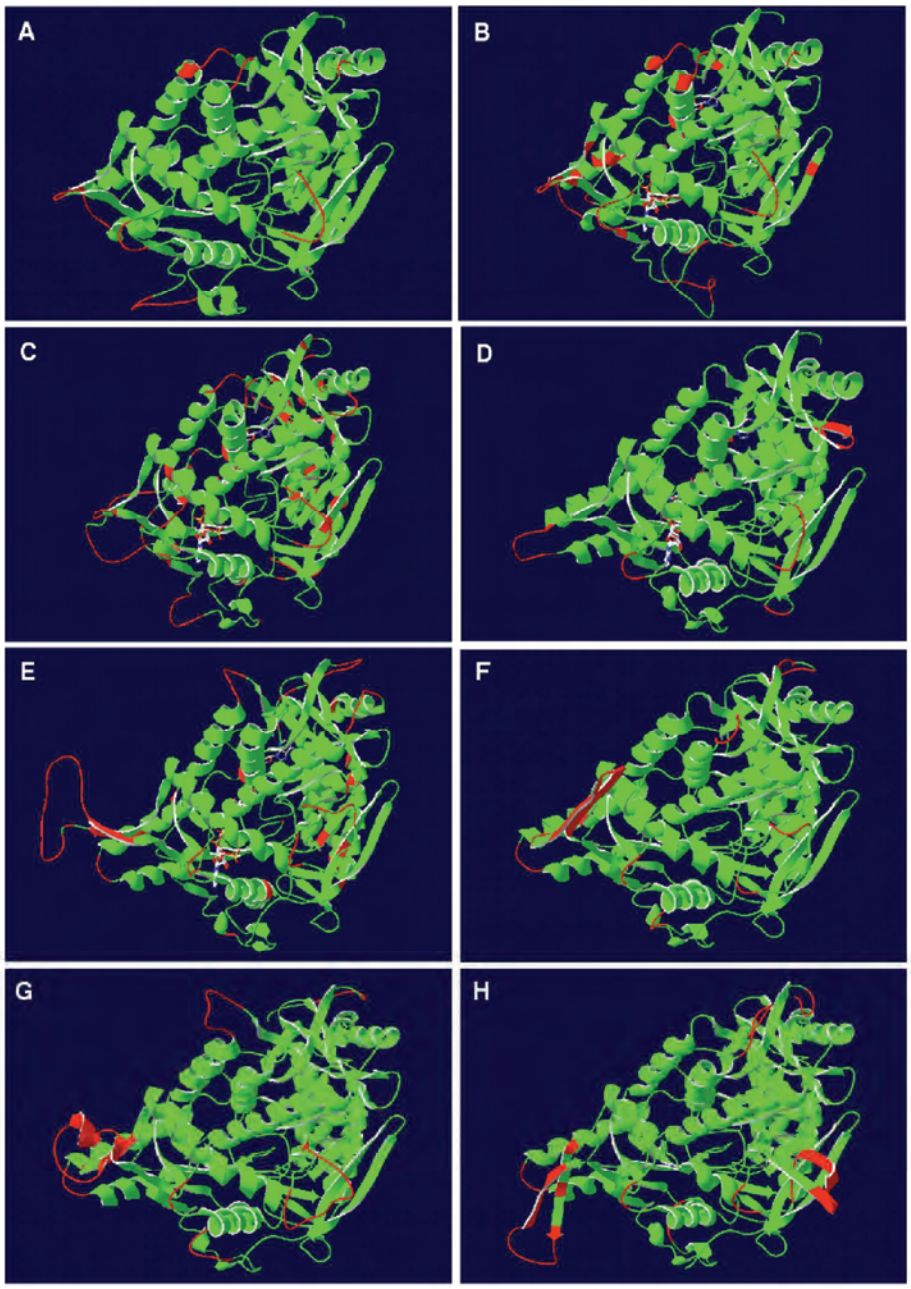

Figure 7. Selected, homology modeling-based AprA models from *Allochromatium vinosum* (A) and *Pelagibacter ubique* (B) (as representatives of SOB from Apr lineage-I), *Pyrobaculum calidifontis* (C) (as representative of crenarchaeal SRP), *Desulfotomaculum reducens* (D) (as representative of Gram-positive SRB and LGT-affected deltaproteobacterial SRB), *Thermodesulfobacterium commune* (E) (as representative of thermophilic SRB), *Desulfovibrio vulgaris* (F) (as representative of non-LGT-affected deltaproteobacterial SRB), *Chlorobaculum tepidum* (G) and *Thiobacillus denitrificans* (H) (as representatives of LGT-affected SOB from Apr lineage-II). Ribbon structure shown from front view (position of FAD cofactor and substrate APS are indicated). Ribbon structure of AprA models colored by model confidence factor provided by SWISS-MODEL (green, respective region of model and reference structure superpose; red, respective region of model deviates from the reference structure).
doi:10.1371/journal.pone.0001514.g007

mostly conserved amino acids are located at a distance of less than 4.1 Å to the FAD cofactor (comprising residues of sec. str. elm. 1 to 2, 3 to 4, 11, 14 to 15, 16 to 18, 31 to 32, and 35 to 36 including the interjacent loop regions, see Fig. 8; for details see also supplementary data material Figure S3, panels G/H, and supplementary data material Table S4); thus, the cofactor-surrounding protein matrices are highly conserved among the APS reductases of SOB and SRP. As revealed by the *A. fulgidus* 3D protein structure, a pronounced feature of the $FADH^-$ state in the enzyme is the substantial bend of the isoalloxazine ring along the N5-N10 axis by an angle of 25° (Fig. 9 and 10). In general, the protein matrix could have a considerable influence on the bending

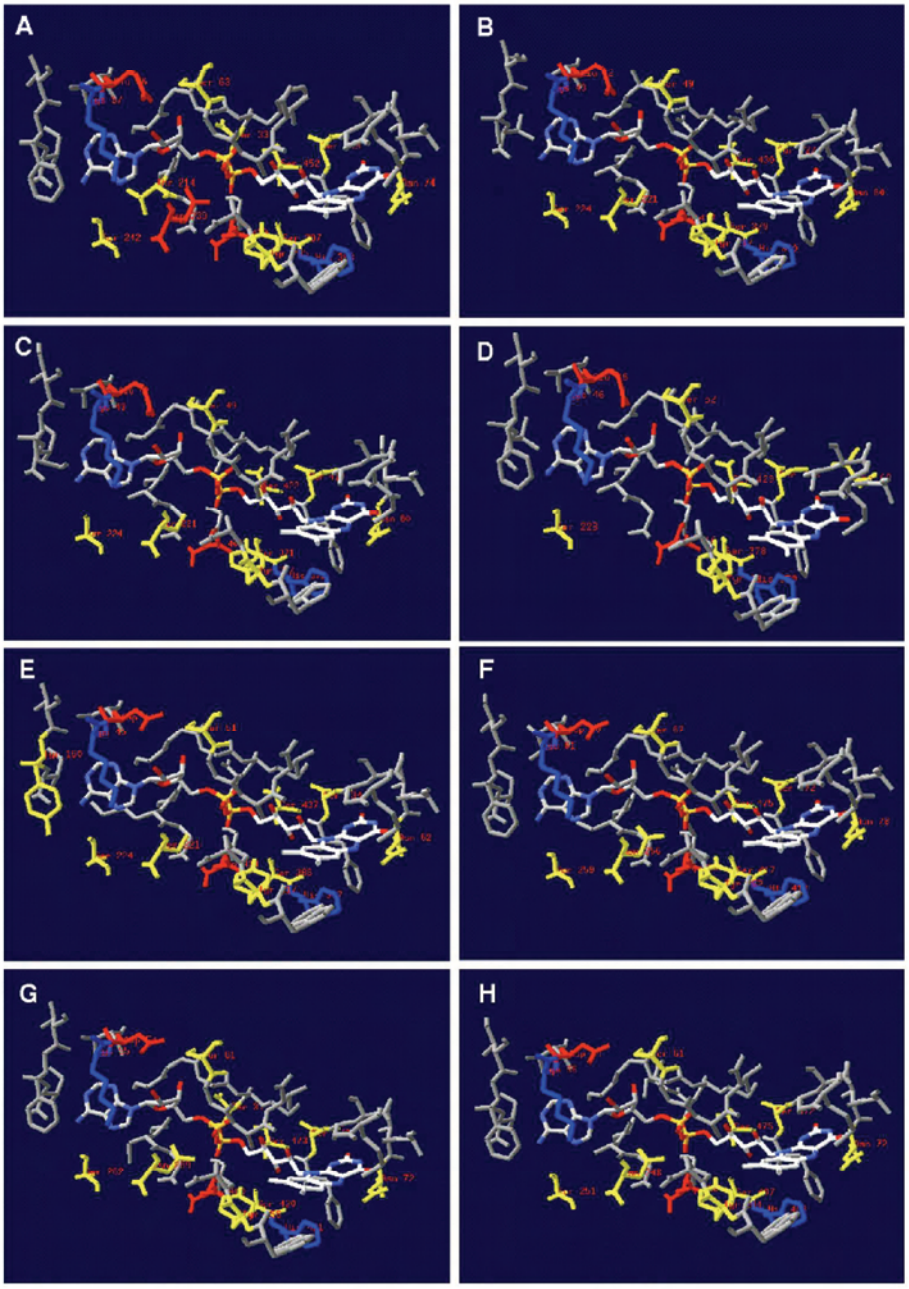

Figure 8. AprA protein matrix surrounding the FAD cofactor (residues in a distance of less than 4.1 Å are shown) in the three-dimensional structure from *A. fulgidus* (A) and selected, homology modeling-based models from *Allochromatium vinosum* (B), *Pelagibacter ubique* (C), *Pyrobaculum calidifontis* (D), *Desulfotomaculum reducens* (E), *Desulfovibrio vulgaris* (F), *Chlorobaculum tepidum* (G), and *Thiobacillus denitrificans* (H). Charged and polar residues are marked (positively charged AA, blue; negatively charged AA, red; polar AA, yellow; uncharged/-polar AA, grey).
doi:10.1371/journal.pone.0001514.g008

angle of the latter and thereby affect the redox potential of FAD; a flat conformation of FAD (0–10°) favors the oxidized state and a bent "butterfly" conformation (15–30°) favors the reduced state. In the *A. fulgidus* APS reductase, the side chains of Asn-A74 and Trp-A234 that are located at the *re*-face of FAD enforce a shift of the dimethylbenzene and pyrimidine rings toward the *si*-face of the FAD, whereas the pyrazine ring is held in position by Leu-A70 which protrudes toward the *si*-face of FAD (Fig. 9 panels A and B). The induced stabilization of the reduced form of FAD agrees with the experimentally determined higher reduction potentials of ~−45 mV in APS reductases of several SRP compared to ~−220 mV of free FAD [18,23,24]. Notably, the aforementioned residues are strictly conserved and strongly fixed at their positions in all AprA models of the sulfate reducers (except *Pyrobaculum calidifontis*, see Fig. 9 panels C and D) and even the sulfur-oxidizers (see supplementary data material Figure S4 for details) which

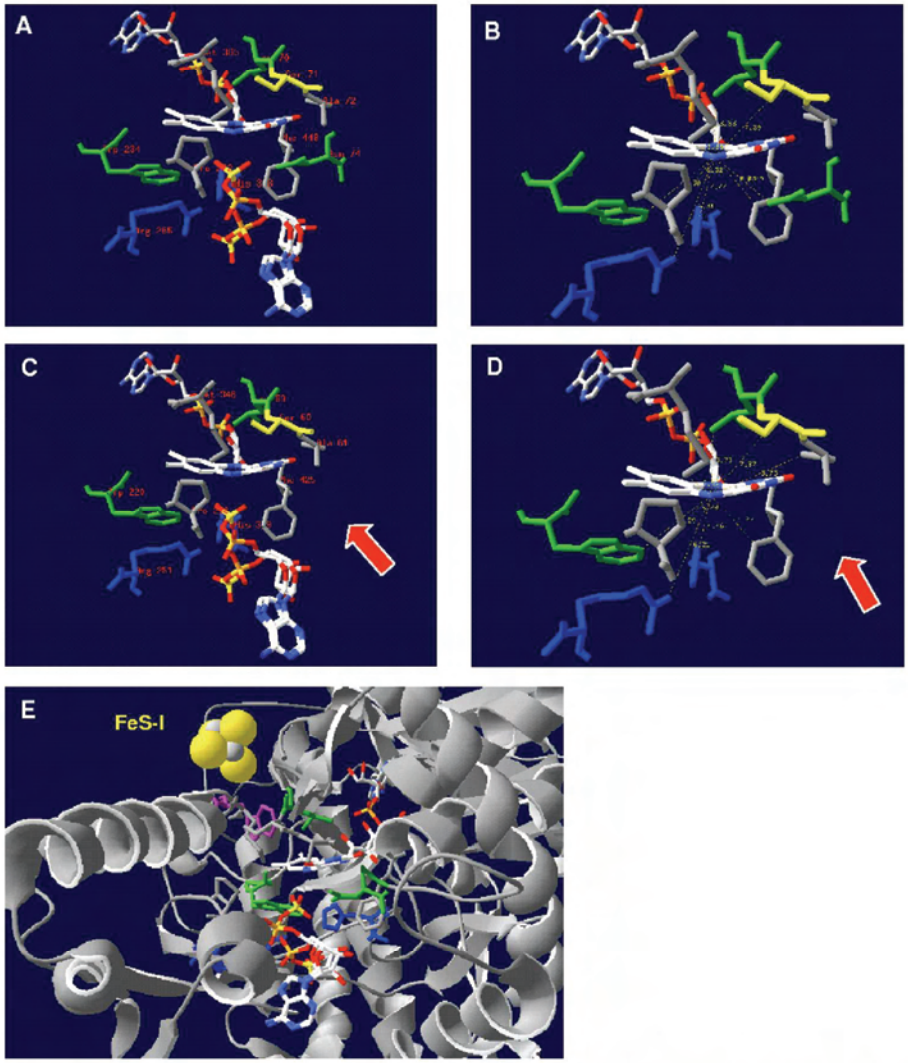

Figure 9. AprA active center from the protein of *A. fulgidus* (A, B) and the homology modeling-based model of *Pyrobaculum calidifontis* (C, D) (residues in a distance of less than 6.5 Å to the N5 atom of FAD cofactor are shown). FAD cofactor and substrate APS (in two conformations) are shown as ball-and-stick representations. Residues involved in the isoalloxazine binding (e.g. *A. fulgidus*: Leu-A70, Asn-A74, Trp-A234) are highlighted by green color (missing Asn-A63 in the *Pyrobaculum calidifontis* AprA model is marked by an arrow), the invariant, positively charged residues His-A398 and Arg-A265 of the active site are blue colored (other AA are colored in grey). Distances are given in Å (B, D). (E) The position of the electron-transferring [4Fe-4S] cluster I and Trp-B48 (highlighted by violet color) of AprB to the FAD cofactor in the AprA protein of *A. fulgidus* is shown (ribbon structure is colored in grey).
doi:10.1371/journal.pone.0001514.g009

might indicate that this cofactor is also present in a bent conformation in the SOB-type APS reductases although the coplanar arrangement of the three aromatic rings would be the energetical favorable conformation in the oxidized state. Indeed, the isoalloxazine ring system of *A. fulgidus* APS reductase revealed an identical bending angle in the oxidized as in the reduced FAD state [18,23,24] i.e. the butterfly conformation is maintained in the *A. fulgidus* protein independent of the redox potential of the FAD cofactor and direction of catalytic reaction (Fig. 10). This is also demonstrated by the AprA models of this study that encompassed reductive and oxidative type APS reductases from distinct SRP and SOB. In contrast, other enzymes e.g. thioredoxin reductase [48], alternate the FAD conformation with respect to their oxidized and reduced states. The AprA model of *Pyrobaculum calidifontis* lacked the structurally essential Asn-A63 at the re-face of FAD (see Fig. 9 panels C and D). However, the strained conformation of the isoalloxazine moiety was suggested to be important for efficient electron flow between the redox centers by facilitating the reduction of the oxidized FAD via the [4Fe-4S] clusters. In agreement with the AprB model-derived results, this missing structural feature might be another indication for the non-functionality of the APS reductase present in the investigated *Pyrobaculum* species.

Active site channel and active center in the AprA models of SRP and SOB

According to the *A. fulgidus* 3D structure, the active site of APS reductase is deeply buried into the protein interior and is only accessible from the outside through a 17 Å long channel of 10 Å

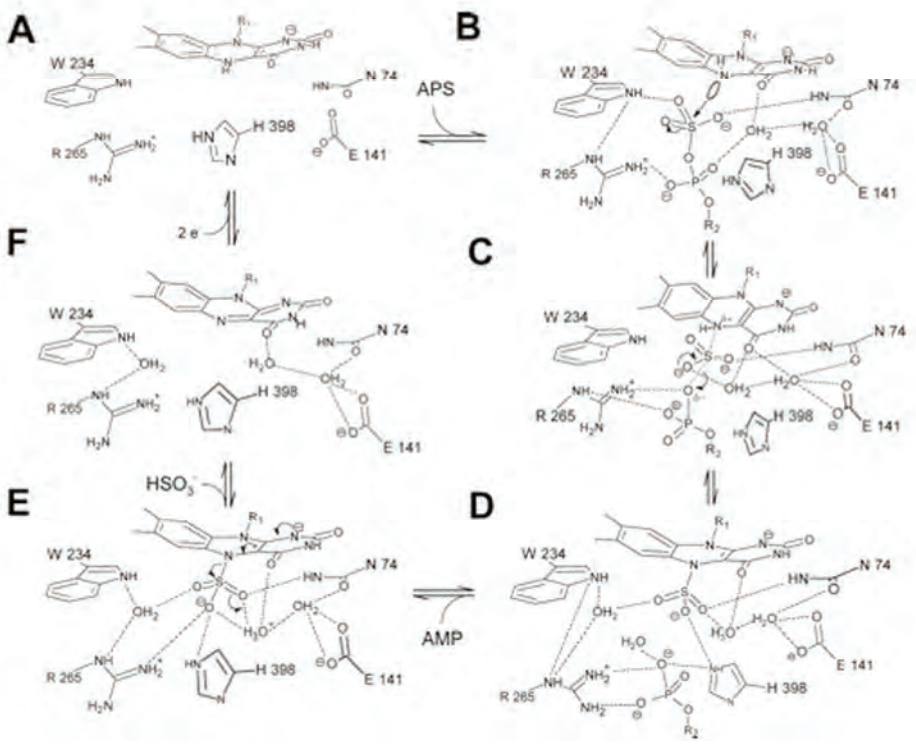

Figure 10. Reaction cycle of the dissimilatory APS reductase from *A. fulgidus* (Schiffer et al., 2006).
doi:10.1371/journal.pone.0001514.g010

diameter which is formed at the interface between the FAD-binding and capping domains [18,23,24] (see Fig. 1B and 9E). The entrance of the substrate-binding channel is surrounded by five positively charged residues (Arg-A85, Lys-A281, Lys-A283, Arg-A294, and Arg-A317) attracting negatively charged molecules such as APS, sulfite and AMP. With the exception of Lys-A281 and the AMP-moiety-interacting Arg-A317, the previous residues were not well-conserved among the AprA comparative models of SRP and SOB but were substituted by other positively charged residues of varying positions at the opening of the channel (data not shown). The channel itself has been proposed to be pre-built prior to substrate binding by a hydrophobic cluster of residues (Tyr-A95, Trp-A144, Trp-A234, Phe-A261, Val-A273, Gly-A274, Phe-A277, Leu-A278, Phe-A448) [18,23,24] that would allow fast catalysis which is essential especially for SRP that rely on efficient transformation of sulfate to sulfite for energy conservation. Indeed, the aforementioned residues are strictly conserved among the AprA models (note: Tyr-A95 and Phe-A261 are substituted by the hydrophobic amino acids methionine in most deltaproteobacterial SRB and isoleucine in SOB of Apr lineage I proteins; see supplementary data material Table S5). Structural analyses of different states of the *A. fulgidus* enzyme indicated, that substrate binding induces a shift of the isoalloxazine ring towards the channel bottom thereby producing a compressed enzyme-substrate complex. While the conformations of the adenine and ribose ring of APS are well-defined in the active site channel, phosphate and, particularly, the sulfate group appeared to be conformationally rather flexible. Before reduction, the molecule APS is present in a strained conformation with its sulfate moiety directly positioned in front of the pyrazine ring of $FADH^-$ (distance of ~3.4 Å between the sulfur and the N5 atoms). In this position, the sulfate O1 atom has been predicted to interact with the ND2 atom of Asn-A74, its O2 atom with NE2 atom of His-A398, and its O3 atom via a water molecule with Arg-A265 and Trp-A234 and via two water molecules with Glu-A141, Asp-A361, and Asn-A74 (Fig. 10) [18,23,24]. Indeed, Asn-A74, Trp-A234, Arg-A265, and His-A398 corresponding residues were predicted to be located in the active sites of all comparative models (except *Pyrobaculum calidifontis*, see previous section) at nearly identical positions and distances to the sulfate group of APS/sulfite and the N5 atom of FAD (see supplementary data material Figure S4 and Table S6). In agreement with the *A. fulgidus* structure, the phosphate and ribose moiety of APS/AMP might be connected with Arg-A265, Val-A273, and Gly-A274 as well as Tyr-A95 and His-A446 corresponding residues in the substrate-binding channel of SRP- and SOB-type models. The adenine ring of APS/AMP is most likely fixed in its position in the models as proposed for the APS reductase of *A. fulgidus* (clamped between Arg-A317 and Leu-A278) [18,23,24] (see supplementary material Table S5). Upon APS/AMP binding of the *A. fulgidus* APS reductase, the Arg-A317 residues has been predicted to largely change its conformation by swinging into the channel to form a coplanar arrangement of its guanidine group to the adenine ring [18,23,24]. In conclusion, the active site channel including the active center appeared to be structural highly conserved among the APS reductases of SRP and even SOB with only minor alterations by single amino acid substitutions.

Reaction mechanism of APS reduction and sulfite oxidation

The enzyme-bound APS is held in a strained conformation by the Arg-A317/Leu-A278 clamp fixation of the adenine ring and the curved APS conformation. This energy-rich state has been

postulated to become relaxed during the sulfonation reaction via a nucleophilic attack of the N5 atom of reduced FAD on the sulfur atom of APS; in consequence, a covalent FAD-APS intermediate is formed. The energy liberated upon cleavage of the S-O-P mixed anhydride bond of APS is high (80 kJ mol^{-1}); catalysis will be supported by an increase in the nucleophilicity of N5 due to the deprotonated N1 atom and of the electrophilicity of the sulfur due to hydrogen bonds between the four sulfate oxygens of APS and Asn-A74, Trp-A234, Arg-A265, and His-A398. Rearrangements of electrons result in the release of AMP accompanied by formation of the N5-sulfite adduct. Subsequent dissociation of the latter to yield oxidized FAD and sulfite might be enzymatically triggered by protonation of the sulfite moiety (via His-A398) (see Fig. 10). Finally, the product sulfite is released and oxidized FAD reduced via the two [4Fe-4S] clusters. Concerning the backward reaction, the oxidative formation of APS from sulfite and AMP, it is assumed that the nucleophile sulfite adds to the N5 atom of oxidized FAD as most electrophilic position of the cofactor followed by a shift of the negative charge on the sulfite sulfur toward the flavin ring. This enables a nucleophilic attack of the charged phosphate oxygen of AMP on the sulfur atom of the FAD-sulfite adduct. After rearrangement of electrons, APS is eliminated and FAD becomes reduced by two electrons, which are subsequently transferred to the iron-sulfur clusters [18,23,24].

With respect to the comparative models-based assumption of nearly identical protein matrices surrounding the FAD cofactor, the active site channel and center in the SRP- and SOB-type alpha-subunits, the overall catalytic process of APS reduction/sulfite oxidation in SRP and SOB appeared to be identical irrespective of metabolism type the APS reductase is involved in or species it has been originated from. Indeed, as experimentally proven by enzyme assays [12,18,21,23,24] and demonstrated by the common occurrence of sulfur isotope fractionation during microbial-mediated sulfate reduction [49–51], the forward but also the backward reaction is generally catalyzed by enzymes of the SRP-type (note the sulfite-oxidation unfavorable redox potential of cofactors as determined for the *A. fulgidus* protein). However, the data of UV-vis difference spectra of APS reductases from *A. fulgidus*, *Desulfovibrio desulfuricans*, and *Desulfovibrio vulgaris* (upon addition of sulfite and AMP) indicated the presence of an anionic flavosemiquinone after FAD-sulfite adduct decay and reduction of the flavin. In contrast, the enzyme isolated from the sulfur-oxidizer *Thiobacillus denitrificans* (DSM 807) did not form a stable flavosemiquinone under the same conditions, and the FAD and [4Fe-4S] clusters became immediately reduced. It has been postulated that the presence/absence of this anionic flavin radical might reflect the preferential direction of catalysis in sulfate-reducing and sulfur-oxidizing organisms [18,23,24]. On the basis of the comparative models, there appeared to be no significant structural differences between APS reductases of sulfate-reducers and sulfur-oxidizers that would be indicative for a favored oxidation reaction in the SOB-type enzymes (e.g. reverse modulation of redox potential of FAD and iron-sulfur centers) in comparison to the SRP-type proteins.

SUPPORTING INFORMATION

Figure S1
Found at: doi:10.1371/journal.pone.0001514.s001 (8.23 MB DOC)

Figure S2
Found at: doi:10.1371/journal.pone.0001514.s002 (2.17 MB DOC)

Figure S3
Found at: doi:10.1371/journal.pone.0001514.s003 (8.75 MB DOC)

Figure S4
Found at: doi:10.1371/journal.pone.0001514.s004 (1.17 MB DOC)

Table S1
Found at: doi:10.1371/journal.pone.0001514.s005 (0.76 MB DOC)

Table S2
Found at: doi:10.1371/journal.pone.0001514.s006 (0.21 MB DOC)

Table S3
Found at: doi:10.1371/journal.pone.0001514.s007 (2.10 MB DOC)

Table S4
Found at: doi:10.1371/journal.pone.0001514.s008 (0.18 MB DOC)

Table S5
Found at: doi:10.1371/journal.pone.0001514.s009 (0.18 MB DOC)

Table S6
Found at: doi:10.1371/journal.pone.0001514.s010 (0.19 MB DOC)

ACKNOWLEDGMENTS

Author Contributions

Conceived and designed the experiments: JK BM. Performed the experiments: BM. Analyzed the data: JK BM. Contributed reagents/materials/analysis tools: JK. Wrote the paper: JK BM.

REFERENCES

1. Rabus R, Hansen TA, Widdel F (1999) Dissimilatory sulfate- and sulfur-reducing prokaryotes. In: Dworkin M, Schleifer K-H, Stackebrandt E, eds. The prokaryotes: an evolving electronic database for the microbiological community. New York, N. Y.: Springer. pp 1–87.
2. Hansen TA (1994) Metabolism of sulfate-reducing prokaryotes. Antonie Van Leeuwenhoek International Journal of General and Molecular Microbiology 66: 165–185.
3. Brüser T, Lens PNL, Trüper HG (2000) The biological sulfur cycle. In: Lens PNL, Pol LH, eds. Environmental Technologies to Treat Sulfur Pollution. London: IWA Publishing. pp 47–86.
4. Dahl C, Trüper HG (2001) Sulfite reductase and APS reductase from *Archaeoglobus fulgidus*. Methods in Enzymology. pp 427–441.
5. Hipp WM, Pott AS, Thum-Schmitz N, Faath I, Dahl C, et al. (1997) Towards the phylogeny of APS reductases and sirohaem sulfite reductases in sulfate-reducing and sulfur-oxidizing prokaryotes. Microbiology-Uk 143: 2891–2902.
6. Trüper HG, Fischer U (1982) Anaerobic oxidation of sulfur-compounds as electron-donors for bacterial photosynthesis. Philosophical Transactions of the Royal Society of London Series B-Biological Sciences 298: 529–542.
7. Dahl C, Trüper HG (1994) Enzymes of dissimilatory sulfide oxidation in phototrophic sulfur bacteria. Methods in Enzymology. pp 400–421.
8. Taylor BF (1994) Adenylylsulfate reductases from Thiobacilli. Methods in Enzymology. San Diego, California: Academic Press. pp 393–400.
9. Schedel M, Trüper HG (1980) Anaerobic oxidation of thiosulfate and elemental sulfur in *Thiobacillus denitrificans*. Archives of Microbiology 124: 205–210.
10. Brune DC (1995) Sulfur compounds as photosynthetic electron donors. In: Blankenship RE, Madigan MT, Bauer CE, eds. Anoxygenic Photosynthetic Bacteria. Dordrecht: Kluwer Academic Publishers. pp 847–870.
11. Sperling D, Kappler U, Truper HG, Dahl C (2001) Dissimilatory ATP sulfurylase from *Archaeoglobus fulgidus*. Methods in Enzymology. pp 419–427.

12. Lampreia J, Pereira AS, Moura JJG (1994) Adenylylsulfate reductases from sulfate-reducing bacteria. Methods in Enzymology. pp 241–260.
13. Fritz G, Buchert T, Huber H, Stetter KO, Kroneck PMH (2000) Adenylylsulfate reductases from archaea and bacteria are 1:1 alpha beta-heterodimeric iron-sulfur flavoenzymes - high similarity of molecular properties emphasizes their central role in sulfur metabolism. FEBS Letters 473: 63–66.
14. Pires RH, Lourenco AI, Morais F, Teixeira M, Xavier AV, et al. (2003) A novel membrane-bound respiratory complex from *Desulfovibrio desulfuricans* ATCC 27774. Biochimica Et Biophysica Acta-Bioenergetics 1605: 67–82.
15. Haveman SA, Greene EA, Stilwell CP, Voordouw JK, Voordouw G (2004) Physiological and gene expression analysis of inhibition of *Desulfovibrio vulgaris* Hildenborough by nitrite. Journal of Bacteriology 186: 7944–7950.
16. Meyer B, Kuever J (2007) Phylogeny of the alpha and beta subunits of the dissimilatory adenosine-5′-phosphosulfate (APS) reductase from sulfate-reducing prokaryotes - origin and evolution of the dissimilatory sulfate-reduction pathway. Microbiology 153: 2026–2044.
17. Meyer B, Kuever J (2007) Molecular analysis of the distribution and phylogeny of dissimilatory adenosine-5′-phosphosulfate reductase-encoding genes (*aprBA*) among sulfur-oxidizing prokaryotes. Microbiology 153: 3478–3498.
18. Fritz G, Roth A, Schiffer A, Buchert T, Bourenkov G, et al. (2002) Structure of adenylylsulfate reductase from the hyperthermophilic *Archaeoglobus fulgidus* at 1.6-A resolution. Proceedings of the National Academy of Sciences of the United States of America 99: 1836–1841.
19. Lancaster CRD (2003) The structure of Wolinella succinogenes quinol: Fumarate reductase and its relevance to the superfamily of succinate: Quinone oxidoreductases. Membrane Proteins 63: 131–149.
20. Lancaster CRD (2003) *Wolinella succinogenes* quinol : fumarate reductase and its comparison to *E. coli* succinate : quinone reductase. FEBS Letters 555: 21–28.
21. Peck HD, Deacon TE, Davidson JT (1965) Studies on Adenosine 5′-Phosphosulfate Reductase from *Desulfovibrio desulfuricans* and *Thiobacillus thioparus*. I. Assay and Purification. Biochimica Et Biophysica Acta 96: 429–446.
22. Michaels GB, Davidson JT, Peck HD (1970) A Flavin-Sulfite Adduct as an Intermediate in Reaction Catalyzed by Adenylyl Sulfate Reductase from *Desulfovibrio vulgaris*. Biochemical and Biophysical Research Communications 39: 321–&.
23. Schiffer A, Fritz G, Kroneck PMH, Ermler U (2006) Reaction mechanism of the iron-sulfur flavoenzyme adenosine-5′-phosphosulfate reductase based on the structural characterization of different enzymatic states. Biochemistry 45: 2960–2967.
24. Fritz G, Buchert T, Kroneck PMH (2002) The function of the [4Fe-4S] clusters and FAD in bacterial and archaeal adenylylsulfate reductases - Evidence for flavin-catalyzed reduction of adenosine 5′-phosphosulfate. Journal of Biological Chemistry 277: 26066–26073.
25. Marti-Renom MA, Stuart AC, Fiser A, Sanchez R, Melo F, et al. (2000) Comparative protein structure modeling of genes and genomes. Annual Review of Biophysics and Biomolecular Structure 29: 291–325.
26. Fiser A, Sanchez R, Melo F, Sali A (2001) Comparative protein structure modeling. In: Watanabe M, Roux B, MacKerell AD, Becker O, eds. Computational Biochemistry and Biophysics. pp 275–312.
27. Krieger E, Nabuurs SB, Vriend G (2003) Homology modeling. In: Bourne PE, Weissig H, eds. Structural Bioinformatics Wiley.
28. Lesk AM, Cothia C (1986) The response of protein structures to amino-acid sequence changes. Philosophical Transactions of the Royal Society of London B Biological Sciences 317: 345–356.
29. Poirot O, Suhre K, Abergel C, O'Toole E, Notredame C (2004) 3DCoffee@igs: a web server for combining sequences and structures into a multiple sequence alignment. Nucleic Acids Research 32: W37–W40.
30. Poirot O, O'Toole E, Notredame C (2003) Tcoffee@igs: a web server for computing, evaluating and combining multiple sequence alignments. Nucleic Acids Research 31: 3503–3506.
31. Guindon S, Lethiec F, Duroux P, Gascuel O (2005) PHYML Online -a web server for fast maximum likelihood-based phylogenetic inference. Nucl Acids Res 33: W557–559.
32. Mussmann M, Richter M, Lombardot T, Meyerdierks A, Kuever J, et al. (2005) Clustered genes related to sulfate respiration in uncultured prokaryotes support the theory of their concomitant horizontal transfer. Journal of Bacteriology 187: 7126–7137.
33. Guex N, Peitsch MC (1997) SWISS-MODEL and the Swiss-PdbViewer: An environment for comparative protein modeling. Electrophoresis 18: 2714–2723.
34. Schwede T, Kopp J, Guex N, Peitsch MC (2003) SWISS-MODEL: an automated protein homology-modeling server. Nucl Acids Res 31: 3381–3385.
35. van Gunsteren WF, Billeter SR, Eising AA, Hünenberger PH, Krüger P, et al. (1996) Biomolecular simulations: GROMOS96 Manual and User Guide. Zurich, Switzerland: VdF Hochschulverlag ETHZ.
36. Hooft RWW, Sander C, Vriend G (1996) Verification of protein structures: sidechain planarity. Journal of Applied Crystallography 29: 714–716.
37. Sippl MJ (1993) Recognition of errors in three-dimensional structures of proteins. Proteins 17: 355–362.
38. Melo F, Feytmans E (1998) Assessing protein structures with a non-local atomic interaction energy. Journal of Molecular Biology 277: 1141–1152.
39. Luthy R, Bowie JU, Eisenberg D (1992) Assessment of protein models with three-dimensional profiles. Nature 356: 83–85.
40. Schwede T, Diemand A, Guex N, Peitsch MC (2000) Protein structure computing in the genomic era. Research in Microbiology 151: 107–112.
41. Tindall BJ, Wray V, Huber R, Collins MD (1991) A novel, fully saturated cyclic menaquinone in the archaeabacterium *Pyrobaculum organotrophum*. Systematic and Applied Microbiology 14: 218–221.
42. Itoh T (2003) Taxonomy of nonmethanogenic hyperthermophilic and related thermophilic archaea. Journal of Bioscience and Bioengineering 96: 203–212.
43. Deisenhofer J, Michel H (1989) The photosynthetic reaction centre from the purple bacterium *Rhodopseudomonas viridis*. EMBO (European Molecular Biology Organization) Journal 8: 2149–2170.
44. Pelletier H, Kraut J (1992) Crystal structure of a complex between electron transfer partners, cytochrome c peroxidase and cytochrome c. Science 258: 1748–1755.
45. Huber H, Huber R, Stetter KO (2002) *Thermoproteales*. In: Dworkin M, Falkow E, Rosenberg E, Schleifer K-H, Stackebrandt E, eds. The prokaryotes An evolving electronic resource for the microbial community. New York, N. Y.: Fischer Verlag.
46. Amo T, Paje MLF, Inagaki A, Ezaki S, Atomi H, et al. (2002) *Pyrobaculum calidifontis* sp. nov., a novel hyperthermophilic archaeon that grows in atmospheric air. Archaea 1: 113–121.
47. Fitz-Gibbon ST, Ladner H, Kim UJ, Stetter KO, Simon MI, et al. (2002) Genome sequence of the hyperthermophilic crenarchaeon *Pyrobaculum aerophilum*. Proceedings of the National Academy of Sciences of the United States of America 99: 984–989.
48. Lennon BW, Williams CH, Ludwig ML (1999) Crystal structure of reduced thioredoxin reductase from *Escherichia coli*: Structural flexibility in the isoalloxazine ring of the flavin adenine dinucleotide cofactor. Protein Science 8: 2366–2379.
49. Habicht KS, Canfield DE (2001) Isotope fractionation by sulfate-reducing natural populations and the isotopic composition of sulfide in marine sediments. Geology 29: 555–558.
50. Habicht KS, Salling LL, Thamdrup B, Canfield DE (2005) Effect of low sulfate concentrations on lactate oxidation and isotope Fractionation during sulfate reduction by *Archaeoglobus fulgidus* strain Z. Applied and Environmental Microbiology 71: 3770–3777.
51. Canfield DE (2001) Biogeochemistry of sulfur isotopes. In: Valley JW, Cole DR, eds. Stable Isotope Geochemistry: Reviews in Mineralogy and Geochemistry. Washington, DC: Mineralogy Society of America. pp 607–636.

Supplementary Material

Siehe Anhang

4.2.4 Publikation 4

Molecular analysis of the distribution and phylogeny of the *soxB* gene among sulfur-oxidizing prokaryotes –evolution of the sulfur oxidation enzyme system

Birte Meyer und Jan Küver

Environmental Microbiology (2007). 153, 3478-3498

Environmental Microbiology (2007) 9(12), 2957–2977 doi:10.1111/j.1462-2920.2007.01407.x

Molecular analysis of the distribution and phylogeny of the *soxB* gene among sulfur-oxidizing bacteria – evolution of the Sox sulfur oxidation enzyme system

Birte Meyer,[1] Johannes F. Imhoff[2] and Jan Kuever[1*†]
[1]*Max-Planck-Institute for Marine Microbiology, Celsiusstrasse 1, D-28359 Bremen, Germany.*
[2]*Marine Microbiology, IFM-GEOMAR, Düsternbrooker Weg 20, D-24105 Kiel, Germany.*

Summary

The *soxB* gene encodes the SoxB component of the periplasmic thiosulfate-oxidizing Sox enzyme complex, which has been proposed to be widespread among the various phylogenetic groups of sulfur-oxidizing bacteria (SOB) that convert thiosulfate to sulfate with and without the formation of sulfur globules as intermediate. Indeed, the comprehensive genetic and genomic analyses presented in the present study identified the *soxB* gene in 121 phylogenetically and physiologically divergent SOB, including several species for which thiosulfate utilization has not been reported yet. In first support of the previously postulated general involvement of components of the Sox enzyme complex in the thiosulfate oxidation process of sulfur-storing SOB, the *soxB* gene was detected in all investigated photo- and chemotrophic species that form sulfur globules during thiosulfate oxidation (*Chromatiaceae*, *Chlorobiaceae*, *Ectothiorhodospiraceae*, *Thiothrix*, *Beggiatoa*, *Thiobacillus*, invertebrate symbionts and free-living relatives). The SoxB phylogeny reflected the major 16S rRNA gene-based phylogenetic lineages of the investigated SOB, although topological discrepancies indicated several events of lateral *soxB* gene transfer among the SOB, e.g. its independent acquisition by the anaerobic anoxygenic phototrophic lineages from different chemotrophic donor lineages. A putative scenario for the proteobacterial origin and evolution of the Sox enzyme system in SOB is presented considering the phylogenetic, genomic (*sox* gene cluster composition) and geochemical data.

Received 13 February, 2007; accepted 27 June, 2007. *For correspondence. E-mail kuever@mpa-bremen.de; Tel. (+49) 0421 5370870; Fax (+49) 0421 5370810. †Present address: Bremen Institute for Materials Testing, Paul-Feller-Strasse 1, D-28199 Bremen, Germany.

Introduction

The sulfur compound thiosulfate has been suggested to fulfil a key role in the biological sulfur cycle in nature (Joergensen and Nelson, 2004; Zopfi *et al.*, 2004). A variety of photo- and chemotrophic sulfur-oxidizing prokaryotes (SOP) are able to use thiosulfate besides sulfide and sulfur as electron donor for their photosynthetic and respiratory energy-generating systems (Brune, 1995; Nelson and Fisher, 1995; Kelly *et al.*, 1997; Imhoff, 1999; 2001a,b; 2003; Brüser *et al.*, 2000; Robertson and Kuenen, 2002; Kletzin *et al.*, 2004; Takai *et al.*, 2005). In consequence of the phylogenetic and physiological diversity of SOP, several different enzymatic systems and pathways appear to be involved in the dissimilatory oxidation of thiosulfate. While the thiosulfate-converting enzymes of the archaeal sulfur oxidizers, e.g. *Acidianus ambivalens* (Kletzin *et al.*, 2004), represent a convergently evolved system, at least three thiosulfate oxidation pathways are postulated to exist in the sulfur-oxidizing bacteria (SOB) (Kelly *et al.*, 1997; Brüser *et al.*, 2000; Friedrich *et al.*, 2001; 2005). (i) The thiosulfate degradation process via polythionate intermediates involves the enzymes thiosulfate dehydrogenase and tetrathionate hydrolase and appears to be common in chemotrophic SOB living in extreme habitats, such as *Acidithiobacillus*, *Thermothiobacillus* and *Halothiobacillus* (Pronk *et al.*, 1990; Meulenberg *et al.*, 1993; Kelly *et al.*, 1997); in addition, some *Pseudomonas* and *Halomonas* species use the formation of tetrathionate from thiosulfate as supplemental energy source (Sorokin, 2003). However, no conclusive model for the formerly termed 'tetrathionate pathway' exists and the central role of tetrathionate has recently been disputed (Brüser *et al.*, 2000; and references therein). In addition, a different model not involving tetrathionate has been developed for the oxidation of elemental sulfur in acidophilic SOB (Rohwerder and Sand, 2003). (ii) The multienzyme complex system (Sox)-mediated pathway has been demonstrated to operate in photo- and chemotrophic *Alphaproteobacteria* that convert thiosulfate to sulfate without sulfur globule formation as free intermediate

© 2007 The Authors
Journal compilation © 2007 Society for Applied Microbiology and Blackwell Publishing Ltd

(Mukhopadhyaya *et al.*, 2000; Appia-Ayme *et al.*, 2001; Friedrich *et al.*, 2001; Kappler *et al.*, 2001). The current model of the Sox enzyme system comprises the four periplasmic complexes SoxXA, SoxYZ, SoxB and $Sox(CD)_2$ that catalyse the thiosulfate oxidation according to the following mechanism. First, the SoxXA complex oxidatively couples the sulfane sulfur of thiosulfate to a SoxY-cysteine-sulfhydryl group of the SoxYZ complex from which the terminal sulfone group is subsequently released by the activity of the SoxB component. Subsequently, the sulfane sulfur of the residual SoxY-cysteine persulfide is further oxidized to cysteine-S-sulfate by the $Sox(CD)_2$ sulfur dehydrogenase complex from which the sulfonate moiety is again hydrolysed off by SoxB, thereby restoring SoxYZ; each of the previous proteins alone is catalytically inactive (Friedrich *et al.*, 2001; 2005). The primary structure of the SoxB is about 30% identical to zinc-containing 5′-nucleotidases; however, besides its essential enzymatic activity as sulfate thioesterase component in the Sox enzyme system, no other *in vivo* function has been reported for this monomeric, dimanganese-containing protein (Epel *et al.*, 2005). (iii) The branched thiosulfate oxidation pathway was postulated to operate in those bacteria that form sulfur globules during thiosulfate oxidation. This pathway proceeds via the interaction of two spatially separated enzyme systems; the sulfone sulfur is rapidly converted to sulfate in the periplasm, whereas the sulfane sulfur accumulates as intracellularly or periplasmically deposited sulfur [S^0] before further oxidation by cytoplasmic enzymes. Previously, the thiosulfate oxidation was suggested to be initiated by the activity of periplasmic thiosulfate reductases or rhodaneses via a reductive cleavage of the molecule (Brune, 1995; Brüser *et al.*, 2000). Increasing experimental data indicate that components of the Sox enzyme system are instead involved in the initial step of the branched thiosulfate oxidation pathway of some sulfur-storing bacteria (Hanson and Tabita, 2003; Friedrich *et al.*, 2005; Hensen *et al.*, 2006). In consequence, the oxidation of reduced inorganic sulfur compounds via components of the Sox enzyme system was postulated to be a widespread mechanism among the SOB (Friedrich *et al.*, 2001; 2005; Hensen *et al.*, 2006). However, a comprehensive investigation of the phylogentically diverse SOB had not been performed to confirm this proposal. In first support, Petri and coworkers (2001) proved the presence of SoxB encoding genes in eight thiosulfate-utilizing reference strains from the *Alpha-, Beta-* and *Gammaproteobacteria* as well as *Chlorobia* lineage. Their presented SoxB phylogenetic tree was based on a limited dataset not including representatives of several major SOB lineages, e.g. *Chromatiaceae*, *Ectothiorhodospiraceae*, *Thiotrichaceae*, invertebrate symbionts and their free-living relatives, as well as *Sulfurimonas denitrificans* (Takai *et al.*, 2006).

To evaluate the former postulation by Friedrich and coworkers, the previously published polymerase chain reaction (PCR) assays (Petri *et al.*, 2001) were used to investigate the *soxB* distribution among 116 different photo- and chemotrophically SOB strains considering especially the thiosulfate-oxidizing, sulfur-storing species. The comparison of the SoxB- and 16S rRNA gene-based tree topologies indicated the occurrence of several putative lateral gene transfer (LGT) events of the *soxB* gene among the SOB. A potential scenario for the origin and evolution of the microbial thiosulfate oxidation processes is presented in context with the gene composition of the *sox* gene loci in SOB genomes and the geochemical data.

Results

Amplification of soxB *genes by PCR from SOB*

The PCR-based analysis confirmed the presence of the *soxB* gene for 50 different photo- and chemotrophic sulfur-oxidizing species from 116 investigated reference strains (see Table 1 for details of PCR results; potential contamination of the examined reference strains could be excluded by 16S rRNA gene-based analyses). In general, the amplification with soxB693F/soxB1446R and soxB693F/soxB1164B (Table 2) resulted in single, correct-sized PCR products (~750 bp and ~470 bp, respectively), whereas the primer pair soxB432F/soxB1446R (Table 2) frequently generated two amplicons of nearly identical length (~1000 bp) with the consequence of ambiguous direct sequencing results. Analysis of genome data revealed that the highly degenerated primers are complementary to the target sites of *Chlorobiaceae*, *Betaproteobacteria* and most *Gamma-* and *Alphaproteobacteria soxB* sequences. Therefore, the negative amplification results obtained from several proven SOB species of, e.g. *Chromatiaceae* and *Chlorobiaceae* with the three different primer sets were most probably not caused by inhibited primer annealing but are indicative for the absence of this gene in the respective strain (see Table 1). The results of the PCR-based analysis are supported by: (i) the Southern blot assays resulting in no hybridization signal for the examined *Chlorobiaceae* species of the subclusters 2a and 3b (except *Chlorobium limicola* DSM 1855) irrespective of *soxB* probes used (see Table 3; probe specificities and stringency of hybridization conditions verified by the negative hybridization results obtained with genomic DNA from non-thiosulfate-oxidizing *Desulfomicrobium baculatum*); and (ii) genome data (Table 4). In contrast, the target sites of *Hyphomicrobiaceae* and *Rhodopseudomonas* spp. (*Alphaproteobacteria*), *Thiomicrospira crunogena* and '*Candidatus* Ruthia magnifica' (*Gammaproteobacteria*), as well as *S. denitrificans* (*Epsilonproteobacteria*), harboured two or more mismatches at the 3′-end

© 2007 The Authors
Journal compilation © 2007 Society for Applied Microbiology and Blackwell Publishing Ltd,

Table 1. Polymerase chain reaction (PCR) amplification results of *soxB* gene fragments from genomic DNA of sulfur-oxidizing reference strains.

Species[a]	Strain[b]	PCR product obtained with primer set[c] soxB432F soxB1446B	soxB693F soxB1446B	soxB693F soxB1164B	Length of obtained *soxB* sequence	GenBank accession no. *soxB*
Archaea						
Crenarchaeota phylum, *Thermoprotei*						
Sulfolobaceae						
Acidianus ambivalens	3772	–	–	n.d.	–	–
Metallosphaera sedulae[d]	5348^T	–	–	n.d.	–	–
Metallosphaera prunae[d]	10039	–	–	n.d.	–	–
Sulfolobus metallicus[d]	6482	–	–	n.d.	–	–
Bacteria						
Chloroflexi phylum, *Chloroflexi*						
Chloroflexaceae						
Chloroflexus aggregans[d]	9485	–	–	n.d.	–	–
Chlorobi phylum, *Chlorobia*						
Chlorobiaceae						
1 *Prosthecochloris aestuarii*[e,d]	271^T	–	–	n.d.	–	–
Prosthecochloris sp.[e,d]	*2K*	–	–	n.d.	–	–
Prosthecochloris vibrioforme[e,d]	260	–	–	n.d.	–	–
Prosthecochloris vibrioforme[e,d]	1678	–	–	n.d.	–	–
2a *Chlorobium luteolum*[e,d]	273^T	–	–	n.d.	–	–
Chlorobium luteolum[e,d]	262	–	–	n.d.	–	–
2b *Chlorobium phaeovibrioides*[e,d]	269^T	–	–	n.d.	–	–
Chlorobium phaeovibrioides[e,f]	265	+	+	n.d.	database	AJ294321
Chlorobium phaeovibrioides[e,d]	261	–	–	n.d.	–	–
Chlorobium phaeovibrioides[e,d]	270	–	–	n.d.	–	–
3a *Chlorobium phaeobacteroides*[e,d]	266^T	–	–	n.d.	–	–
Chlorobium clathratiforme[e]	5477^T	+	+	n.d.	database	AJ294323
'Chlorobium ferrooxidans'[d]	13031^T	–	–	n.d.	–	–
3b *Chlorobium limicola*[e,d]	245^T	–	–	n.d.	–	–
Chlorobium limicola[e]	246	–	–	n.d.	–	–
Chlorobium limicola[e]	*2323*	+	+	+	1002	EF618588
Chlorobium limicola[e,f]	1855	+	+	n.d.	1026	EF618591
Chlorobium limicola[e]	257	+	+	+	1026	EF618579
Chlorobium limicola[e,d]	247	–	–	n.d.	–	–
Chlorobium limicola[e,d]	248	–	–	n.d.	–	–
4a *Chlorobaculum parvum*[e]	263^T	+	+	n.d.	database	AJ294320
Chlorobaculum parvum[e]	*2352*	+	+	n.d.	1026	EF618589
4b *Chlorobaculum limnaeum*[e,f]	1677	+	+	n.d.	1026	EF618590
Chlorobaculum thiosulfatiphilum[e]	249^T	n.d.	n.d.	n.d.	database	AAL68888
Chlorobaculum thiosulfatiphilum[e]	*2322*	+	+	+	959	EF618587
Proteobacteria phylum, *Alphaproteobacteria*						
Rhodospirillaceae						
Rhodospirillum photometricum	122^T	+	–	n.d.	918	EF618569
Rhodobacteraceae						
Rhodothalassium salexigens	2132^T	±	±	n.d.	679	EF618585
Rhodovulum adriaticum	2781	±	+	n.d.	972	EF618592
Rhodovulum sulfidophilum	1374^T	+	+	n.d.	database	AAF99435
Bradyrhizobiaceae						
Rhodoblastus acidophilus	137^T	–	–	n.d.	–	–
Hyphomicrobiaceae						
Blastochloris viridis[d]	133^T	–	–	n.d.	–	–
Rhodobiaceae						
Rhodobium marinum[d]	2698^T	–	–	n.d.	–	–
Proteobacteria phylum, *Betaproteobacteria*						
Hydrogenophilaceae						
Thiobacillus aquaesulis	4255^T	+	+	n.d.	999	EF618597
Thiobacillus denitrificans	12475^T	+	+	n.d.	981	EF618607
Thiobacillus denitrificans	739	n.d.	n.d.	n.d.	–	–
Thiobacillus denitrificans	807	n.d.	n.d.	+	501	EF618581
Thiobacillus plumbophilus	6690^T	+	+	n.d.	765	EF618604
Thiobacillus thioparus	505^T	+	n.d.	n.d.	database	AJ294326
Neisseriaceae						
Aquaspirillum sp. strain D-412[d]	–	–	–	n.d.	–	–
Aquaspirillum sp. strain D-415[d]	–	–	–	n.d.	–	–

© 2007 The Authors
Journal compilation © 2007 Society for Applied Microbiology and Blackwell Publishing Ltd, *Environmental Microbiology*, **9**, 2957–2977

Table 1. *cont.*

Species[a]	Strain[b]	PCR product obtained with primer set[c] soxB432F soxB1446B	soxB693F soxB1446B	soxB693F soxB1164B	Length of obtained *soxB* sequence	GenBank accession no. *soxB*
Proteobacteria phylum, *Gammaproteobacteria*						
Chromatiaceae						
Allochromatium minutissimum	1376^T	+	+	n.d.	1008	EF618582
Allochromatium vinosum	180^T	±	+	n.d.	1017	EF618570
Allochromatium warmingii[d]	173^T	–	–	n.d.	–	–
Chromatium okenii[e]	*6010*	±	+	n.d.	729	EF618602
Halochromatium glycolicum	11080^T	+	+	n.d.	966	EF618605
Halochromatium salexigens	4395^T	+	+	n.d.	1018	EF618598
Isochromatium buderi[d]	176^T	–	–	n.d.	–	–
Lamprocystis purpurea[e]	4197^T	+	±	n.d.	919	EF618595
Marichromatium gracile	203^T	±	+	n.d.	1017	EF618572
Marichromatium purpuratum	1591^T	+	+	n.d.	1017	EF618584
Rhabdochomatium marinum	5261^T	±	–	+	713	EF618601
Thermochromatium tepidum[d]	3771^T	–	–	–	–	–
Thiocapsa pendens	236^T	+	+	–	990	EF618577
Thiocapsa rosea[e]	235^T	±	n.d.	–	–	–
Thiocapsa roseopersicina	217^T	+	+	n.d.	1023	EF618576
Thiocapsa roseopersicina[e]	*4210*	+	+	n.d.	1023	EF618596
Thiococcus pfennigii[e,d]	226^T	–	–	n.d.	–	–
Thiococcus pfennigii[d]	227	–	–	–	–	–
Thiococcus pfennigii[d]	228	–	–	–	–	–
Thiocystis gelatinosa[f]	215^T	+	n.d.	–	950	EF618575
Thiocystis violacea	207^T	+	n.d.	+	984	EF618573
Thiocystis violacea	214	+	+	n.d.	1008	EF618574
Thiocystis violascens	198^T	+	+	+	987	EF618571
Thiodictyon bacillosum[e,d]	234^T	–	n.d.	n.d.	–	–
Thiodictyon sp. strain F4[d]	–	–	–	–	–	–
Thiohalocapsa halophila	6210^T	+	n.d.	+	981	EF618603
Thiolamprovum pedioforme	3802^T	+	n.d.	+	993	EF618593
Thiorhodococcus minor	11518^T	+	n.d.	+	1029	EF618606
Thiorhodovibrio winogradskyi[d]	6702^T	–	–	–	–	–
Ectothiorhodospiraceae						
Ectothiorhodospira mobilis[g]	4180	+	+	n.d.	1011	EF618594
Ectothiorhodospira shaposhnikovii[f]	243^T	+	+	n.d.	1011	EF618578
Halothiobacillaceae						
Halothiobacillus hydrothermalis	7121^T	–	+	n.d.	database	AJ294325
Halothiobacillus kellyi	13162^T	+	+	n.d.	954	EF618609
Halothiobacillus neapolitanus	581^T	+	+	n.d.	database	AJ294332
Thiovirga sulfuroxydans sp. strain A7	–	+	+	n.d.	735	EF618610
Thiotrichaceae						
Beggiatoa alba	1416^T	+	+	n.d.	858	EF618583
Beggiatoa leptomitiformis strain D-401[d]	–	n.d.	n.d.	n.d.	–	–
Beggiatoa leptomitiformis strain D-402	–	n.d.	n.d.	n.d.	–	–
Leucothrix mucor	2157^T	–	+	+	465	EF618586
Leucothrix mucor[f]	621	–	+	+	669	EF618580
Macromonas bipunctata strain D-408[d]	–	±	–	n.d.	–	–
Thiothrix nivea	5205^T	n.d.	+	n.d.	738	EF618600
Thiothrix sp.	12730	n.d.	+	n.d.	765	EF618608
Piscirickettsiaceae						
Thiomicrospira frisia	12351^T	–	–	–	–	–
Thiomicrospira kuenenii	12350^T	–	–	–	–	–
Thiomicrospira sp.	13163	–	n.d.	–	–	–
Thiomicrospira sp.	13164	–	n.d.	–	–	–
Thiomicrospira sp.	13189	–	n.d.	–	–	–
Thiomicrospira sp.	13190	–	n.d.	–	–	–
Uncertain affiliation						
'Thiobacillus prosperus'	5130^T	+	n.d.	–	447	EF618599
Invertebrate symbionts and free-living relatives						
Bathymodiolus azoricus symbiont	–	–	–	–	–	–
Bathymodiolus brevior symbiont	–	–	–	–	–	–
Bathymodiolus thermophilus symbiont	–	–	–	n.d.	–	–
Calyptogena magnifica symbiont	–	–	–	n.d.	–	–
Ifremeria nautilei symbiont[f]	–	+	+	n.d.	766	EF618614

© 2007 The Authors
Journal compilation © 2007 Society for Applied Microbiology and Blackwell Publishing Ltd, *Environmental Microbiology*, **9**, 2957–2977

Table 1. *cont.*

Species[a]	Strain[b]	PCR product obtained with primer set[c] soxB432F soxB1446B	soxB693F soxB1446B	soxB693F soxB1164B	Length of obtained *soxB* sequence	GenBank accession no. *soxB*
Inanidrilus exumae symbiont[d]	–	–	–	n.d.	–	–
Inanidrilus leukodermatus symbiont[d]	–	–	–	n.d.	–	–
Inanidrilus makropetalos symbiont[d]	–	–	–	n.d.	–	–
Oasisia sp. symbiont[d]	–	–	–	n.d.	–	–
Riftia pachyptila symbiont	–	+	+	n.d.	756	EF618617
sulfur-oxidizing bacterium OAII2	–	+	n.d.	n.d.	993	EF618611
sulfur-oxidizing bacterium OBII5	–	+	+	n.d.	975	EF618612
sulfur-oxidizing bacterium ODIII5	–	–	–	n.d.	–	–
sulfur-oxidizing bacterium ODI4	–	+	n.d.	+	936	EF618613
sulfur-oxidizing bacterium NDII1.2	–	–	n.d.	+	501	EF618616
sulfur-oxidizing bacterium 'manganese crust'	–	+	n.d.	n.d.	972	EF618615
Proteobacteria phylum, *Epsilonproteobacteria* *Helicobacteraceae*						
Sulfurimonas denitrificans	1251[T]	–	–	–	database	YP_392780
Spirochaeta phylum, *Spirochaetes* *Spirochaetaceae*						
Spirochaeta sp. strain P[d]	–	±	±	n.d.	–	–
Spirochaeta sp. strain BM[d]	–	±	±	n.d.	–	–
Spirochaeta sp. strain M-6[f]	–	±	±	n.d.	927	EF618568

a. Taxonomic classification of investigated SRP species according to the taxonomic outline of the prokaryotes, Bergey's Manual of Systematic Bacteriology, 2nd edition, release 5.0 May 2004 (http://dx.doi.org/10.1007/bergeysoutline); genomic DNA of sulfur-oxidizing reference strains signed with **e** were received from the culture collection of J. Imhoff, University of Kiel.
b. DSM identification numbers of investigated species (laboratory-internal numbers of culture collection from J. Imhoff in italic type); (–) not deposited in a culture collection; T, type strain.
c. *soxB* gene PCR results obtained from genomic DNA of sulfur-oxidizing reference strains are summarized with the following abbreviations: (–) no amplicon; (+) correct-sized amplicon; (±) correct-sized amplicon with byproducts; (n.d.) PCR amplification not determined.
d. Thiosulfate-oxidizing ability not experimentally proven for respective species (Brune, 1995; Nelson and Fisher, 1995; Brinkhoff *et al.*, 1999; Howarth *et al.*, 1999; Imhoff, 1999; 2001a,b,c; 2003; Kelly and Wood, 2000; Kuever *et al.*, 2002; Cavanaugh *et al.*, 2004; Dubinina *et al.*, 2004; Kletzin *et al.*, 2004; Teske and Nelson, 2004; Takai *et al.*, 2006).
f. Thiosulfate-oxidizing ability of *soxB* gene-harbouring SOB species not experimentally proven (Nelson and Fisher, 1995; Imhoff, 1999, 2001a; 2003; Kuever *et al.*, 2002; Cavanaugh *et al.*, 2004; Dubinina *et al.*, 2004; Teske and Nelson, 2004).
g. Uncertain taxonomic classification (synonym *Ectothiorhodospira marismortui*).

sequence position of one or both primers of the applied primer sets. While internally or at the 5′-end located, single mismatches have only a limited effect on the primer annealing efficiency (Kwok *et al.*, 1990; Simsek and Adnan, 2000), their position at the 3′-end of the primer sequence severely affects the PCR efficiency. In consequence, the *soxB* PCR primer combinations used will have failed to amplify gene fragments from certain examined genera, e.g. *Thiomicrospira* spp. and related symbionts of the Vesicomyid mussels and Mytilid clam, *S. denitrificans* and putatively *Rhodoblastus acidophilus*.

Phylogeny of sulfate thioesterase (SoxB) of SOB

The SoxB consensus tree presented in this work (Fig. 1) is based on 124 sequences obtained from genetic and genomic analyses (Tables 1 and 4). The integration of 50 novel SoxB partial sequences from sulfur-storing photo- and chemotrophic bacteria, e.g. *Chromatiaceae*, *Ectothiorhodospiraceae*, *Thiotrichaceae*, thiotrophic symbiont of invertebrates and their free-living relatives (Table 1) which were previously not considered (Petri *et al.*, 2001), allowed new insights into the evolutionary

Table 2. Polymerase chain reaction (PCR) primers used for amplification of *soxB* gene fragments.

Primer[a]	Sequence (in 5′→3′ direction)[b]							Primer binding site[c]
soxB432F	GAY	GGN	GGN	GAY	ACN	TGG		432–450
soxB693F	ATC	GGN	CAR	GCN	TTY	CCN	TA	693–713
soxB1164B	AAR	TTN	CCN	CGN	CGR	TA		1181–1166
soxB1446B	CAT	GTC	NCC	NCC	RTG	YTG		1446–1428

a. Source: Petri *et al.* (2001).
b. Degenerate positions are in boldface.
c. *soxB* primer binding sites are enumerated according to the nucleotide sequence of *Paracoccus denitrificans* str. GB 17 (GenBank accession no. CAA55824).

© 2007 The Authors
Journal compilation © 2007 Society for Applied Microbiology and Blackwell Publishing Ltd,

Table 3. Results of Southern blot assays with radioactively labelled *soxB*-specific probes and genomic DNA of sulfur-oxidizing and sulfate-reducing bacteria.

Genomic DNA of SOB and SRB species (*Eco*RI/*Hind*III digestion)	Strain[a]	Southern blot hybridization results with *soxB*-specific probe[b]			
		Chlorobium limicola 1855	*Chlorobium limicola* 257	*Chlorobium clathrathiforme* 5477	*Thiocapsa roseopersicina 4210*
Gammaproteobacteria					
Thiocapsa roseopersicina	217	±	±	±	++
Thiocapsa roseopersicina	*4210*[c]	±	±	±	++
Chlorobia					
Chlorobium limicola	245[c]	–	–	–	–
Chlorobium limicola	248[c]	–	–	–	–
Chlorobium limicola	1855[c]	++	++	+	±
Chlorobium luteolum	262[c]	–	–	–	–
Chlorobium luteolum	273[c]	–	–	–	–
Deltaproteobacteria					
Desulfomicrobium baculatum	4028	–	–	–	–

a. DSM identification numbers of investigated species (J. Imhoff laboratory-internal numbers are in italic type); cultures received from the culture collection of J. Imhoff are marked with c.
b. Quality of hybridization results summarized with the following abbreviations: (–) no hybridization (+) hybridization signal (++) strong hybridization signal.

path of *soxB* genes among SOB. The overall tree topology was congruent with the previous one based on a limited dataset of 13 validated SOB species (Petri *et al.*, 2001). However, with respect to the improved species coverage, the enlarged database refined the resolution of the inter- and intrafamily relationships in the major SoxB lineages. Comparative analysis of the SoxB- and the 16S rRNA-based phylogenetic tree (Fig. 2; see also references Imhoff, 1999; 2001a,b,c; 2003; Kelly and Wood, 2000; Kuever *et al.*, 2002; Cavanaugh *et al.*, 2004; Buchan *et al.*, 2005; Takai *et al.*, 2006) revealed several topological discrepancies indicative for incorrect taxonomical classifications and even lateral *soxB* gene transfers among SOB (marked by letters in the trees). According to the SoxB phylogeny, the alphaproteobacterial *Rhodobacteraceae* and *Bradyrhizobiaceae* (Imhoff, 2001b) are not monophyletic (see distinct branching position of *Rhodobacteraceae* representatives *Stappia aggregata* and *Rhodothalassium salexigens* and the cluster formation of *Bradyrhizobiaceae* members), and *Rhodospirillum photometricum* (*Rhodospirillaceae*) is affiliated with *Rhodopseudomonas* spp. (*Bradyrhizobiaceae*). Indeed, the current taxonomical classification of *R. salexigens* and *S. aggregata* is also not well supported by the 16S rRNA gene-based phylogeny. Potential LGT events involving *Alphaproteobacteria* are indicated by the 16S rRNA gene-incongruent close relationships of (i) *Spirochaeta* sp. strain M-6 (Dubinina *et al.*, 2004) to *Sulfitobacter* spp. (LGT a), and (ii) *Acidiphilium cryptum*, *Nitrobacter hamburgensis* and *Bradyrhizobium* spp. (*Alphaproteobacteria* II) to the *Gammaproteobacteria* (LGTs b and c). Interestingly, the latter xenologous cluster comprises species which harbour a second, non-LGT-affected *soxB* gene in their genomes (*Bradyrhizobium* spp.). The 16S rRNA gene-discordant affiliation of *Anaeromyxobacter dehalogenans* (*Deltaproteobacteria*) and *Thiovirga sulfuroxydans* strain A7 (*Gammaproteobacteria*) with the *Betaproteobacteria* points to further lateral transfers of *soxB* genes with the previous species as recipients (LGTs d and e). According to the SoxB tree, the *Gammaproteobacteria* were not monophyletic but formed at least four distinct SOB groups consisting of the *Thiotrichaceae*, '*Thiobacillus prosperus*', *Halothiobacillaceae*, free-living relatives of invertebrate symbionts and *Ectothiorhodospira* spp. (cluster I), the *Piscirickettsiaceae*, *Oceanospirillum* sp., *Beggiatoa alba*, invertebrate symbionts and *Chromatiaceae* (cluster II), the newly described *Congregibacter litoralis* (cluster III), and *Halorhodospira halophila* (cluster IV). The SoxB-proposed separate branching positions of *Thiothrix*/*Leucothrix* and *Beggiatoa* members are supported by the 16S rRNA gene-based phylogeny (Fig. 2) and point to their incorrect classification at the family level (*Thiotrichaceae*). According to the SoxB phylogeny, the *Chromatiaceae* and affiliated invertebrate symbionts are closest related to members of the *Piscirickettsiaceae* and *Oceanospirillum* (cluster II). The affiliation of the *Ectothiorhodospira* spp. with the *Halothiobacillaceae* (cluster I) while *H. halophila* formed a distinct lineage (cluster IV) is discordant to their close relationship based on the 16S rRNA phylogeny (*Ectothiorhodospiraceae*) and indicates independent lateral transfers of *soxB* genes to the anaerobic anoxygenic phototrophic lineages (including the symbionts) (LGTs f to h). The 16S rRNA gene-incongruent affiliation of the *Chlorobiaceae* with the *Gammaproteobacteria* cluster II points also to a lateral *soxB* acquisition of the green sulphur bacteria (LGT i). The detailed comparison of the relative branching order within the *Chlorobiaceae*

© 2007 The Authors
Journal compilation © 2007 Society for Applied Microbiology and Blackwell Publishing Ltd,

Table 4. Presence of *sox*, *sor*, *apr* and *dsr* homologues coding for the Sox enzyme system (SoxXAYZBCD), sulfite dehydrogenase (SorAB, *Starkeya novella*), dissimilatory APS reductase (AprBA) and sulfite reductase (DsrAB) including its functionally associated transmembrane complex (DsrMKJOP) in genome sequences of *Bacteria* (the genomic arrangement is indicated by the GenBank accession numbers of the encoded proteins).

		Homologues present in genome sequences of *Bacteria*[b]								
		Sox				Sor	Apr	Dsr		
Species[a]		SoxXA	SoxYZ	SoxB	SoxCD	SorAB	AprBA	DsrAB	DsrMKJOP
Bacteria										
Aquificae phylum, *Aquificae*										
Aquificaceae										
Aquifex aeolicus str. VF5[c]		NP_214238; NP_214239	NP_214241; NP_214240	NP_214237	–	–	–	–	–	
Deinococcus–Thermus phylum, *Deinococci*										
Thermaceae										
Thermus thermophilus str. HB8[c]		YP_144682/ YP_144684; YP_144681/ YP_144685	YP_144687; YP_144686	YP_144683	YP_144677; YP_144676	–	–	–	–	
Thermus thermophilus str. HB27[c]		YP_005020/ YP_005022; YP_005019/ YP_005023	YP_005025; YP_005024	YP_005021	YP_005015; YP_005014	–	–	–	–	
Chloroflexi phylum, *Chloroflexi*										
Chloroflexaceae										
Chloroflexus aggregans DSM 9485		–	–	–	–	–	–	–	–	
Chloroflexus aurantiacus str. J-10-fl		–	–	–	–	–	–	–	–	
Chlorobi phylum, *Chlorobia*										
Chlorobiaceae										
1a	*Prosthecochloris aestuarii* str. DSM 271	–	–	–	–	–	–	+	+	
2a	*Chlorobium luteolum* str. DSM 273	–	–	–	–	–	–	+	+	
2b	Chlorobium phaeovibrioides str. DSM 265	ZP_00661606; ZP_00661604	ZP_00661605; ZP_00661603	ZP_00661601	–	–	–	+	+	
3a	*Chlorobium phaeobacteroides* str. DSM 266	–	–	–	–	–	–	+	+	
	Chlorobium phaeobacteroides str. BS1	–	–	–	–	–	+	+	+	
	Chlorobium clathratiforme str. DSM 5477	ZP_00588637; ZP_00588640	ZP_00588638; ZP_00588639	ZP_00588642	–	–	+	+	+	
	Chlorobium chlorochromatii str. CaD3	YP_380213; ZP_380216	YP_380214; ZP_380215	YP_380218	–	–	+	+	+	
3b	*Chlorobium limicola* strain DSM 245	–	–	–	–	–	–	+	+	
4b	*Chlorobaculum tepidum* str. ATCC 49652	NP_661908; NP_661911	NP_661909; NP_661910	NP_661913	–	–	+	+	+	
	Chlorobaculum thiosulfatophilum str. DSM 249	AAL68883; AAL68886[d]	AAL68884; AAL68885[d]	AAL68888[d]	–[d]	n.a.[d]	n.a.[d]	n.a.[d]	n.a.[d]	
Proteobacteria phylum, *Alphaproteobacteria*										
SAR11-cluster										
Pelagibacter ubique str. HTCC1002		–	–	–	–	–	+	–	–	
Pelagibacter ubique str. HTCC1062		–	–	–	–	–	+	–	–	

© 2007 The Authors
Journal compilation © 2007 Society for Applied Microbiology and Blackwell Publishing Ltd, *Environmental Microbiology*, **9**, 2957–2977

Table 4. *cont.*

Species[a]	Homologues present in genome sequences of *Bacteria*[b]								
	Sox				Sor	Apr	Dsr		
	SoxXA	SoxYZ	SoxB	SoxCD	SorAB	AprBA	DsrAB	DsrMKJOP
SAR116-cluster Uncultured Alphaproteobacterium EBAC2C11	n.a.	n.a.	n.a.	n.a.	n.a.	+	n.a.	n.a.
Rhodospirillaceae								
Magnetospirillum magneticum str. AMB-1	–	–	–	–	–	–	+	+
Magnetospirillum magnetotacticum str. MS-1[c]	–; ZP_00051298	ZP_00048026; ZP_00056090	ZP_00051299	ZP_00050505; –	ZP_00051098; ZP_00051120	–	+	+
Acetobacteraceae								
Acidiphilium cryptum str. JF-5[c]	ZP_01144910; ZP_01144907	ZP_01144909; ZP_01144908	ZP_01144905	ZP_01144912; ZP_01144911	ZP_01144296; ZP_01144295	–	–	–
Rhodobacteraceae						–	–	–
Dinoroseobacter shibae str. DFL 12[c]	ZP_01583271; ZP_01583268	ZP_01583270; ZP_01583269	ZP_01583267	ZP_01583266; ZP_01583265	–	–	–	–
Paracoccus denitrificans str. GB17	CAB94379; CAA55827[d]	CAB94380; CAB94381[d]	CAA55824[d]	CAA55829; CAA55825[d]	n.a.[d]	n.a.[d]	n.a.[d]	n.a.[d]
Paracoccus denitrificans str. PD1222	ZP_00628734; ZP_00628737	ZP_00628735; ZP_00628736	ZP_00628738	ZP_00628739; ZP_00628740	–	–	–	–
Rhodobacter sphaeroides str. 2.4.1	–	–	–	–	–	–	–	–
Rhodobacter sphaeroides str. ATCC 17025	ZP_00912867; ZP_00912864	ZP_00912866; ZP_00912865	ZP_00912863	ZP_00912862; ZP_00912861	–	–	–	–
Rhodobacter sphaeroides str. ATCC 17029	–	–	–	–	–	–	–	–
Roseobacter sp. str. MED193[c]	ZP_01055916; ZP_01055913	ZP_01055915; ZP_01055914	ZP_01055912	ZP_01055911; ZP_01055910	–	–	–	–
Roseobacter denitrificans str. Och 114[c]	YP_681830; YP_681833	YP_681831; YP_681832	YP_681834	YP_681835; YP_681836	–	–	–	–
Roseovarius nubinhibens str. ISM	ZP_00961298; ZP_00961295	ZP_00961297; ZP_00961296	ZP_00961294	ZP_00961293; ZP_00961292	–	–	–	–
Roseovarius sp. str. 217[c]	ZP_01037120; ZP_01037117	ZP_01037119; ZP_01037118	ZP_01037116	ZP_01037115; ZP_01037114	–	–	–	–
Rhodovulum sulfidophilum str. DSM 1374	AAF99431; AAF99434	AAF99432; AAF99433	AAF99435	AAF99436; AAF99437	–	–	–	–
Sagittula stellata str. E-37	ZP_01748363; ZP_01748360	ZP_01748362; ZP_01748361	ZP_01748359	ZP_01748358; ZP_01748357	–	–	–	–
Silicibacter pomeroyi str. DSS-3	YP_166245; YP_166248	YP_166246; YP_166247	YP_166249	YP_166250; YP_166251	–	–	–	–
Silicibacter sp. str. TM1040	–	–	–	–	–	–	–	–
Stappia aggregata str. IAM 12614[c]	ZP_01549051; ZP_01549054	ZP_01549052; ZP_01549053	ZP_01549055	ZP_01549056; ZP_01549057	–	–	–	–
Sulfitobacter sp. str. NAS-14.1	ZP_00963533; ZP_00963530/ ZP_00963374	ZP_00963532/ ZP_00963372; ZP_00963531/ ZP_00963373	ZP_00963529/ ZP_00963375	–/ ZP_00963377; ZP_00963526/ ZP_00963378	–	–	–	–
Sulfitobacter sp. str. EE-36	ZP_00956135; ZP_00956138	ZP_00956136; ZP_00956137	ZP_00956139	ZP_00956140; ZP_00956141	–	–	–	–

© 2007 The Authors
Journal compilation © 2007 Society for Applied Microbiology and Blackwell Publishing Ltd, *Environmental Microbiology*, **9**, 2957–2977

Uncertain phylogenetic affiliation								
Rhodobacterales bacterium str. HTCC 2654[c]	ZP_01014855; ZP_01014858	ZP_01014856; ZP_01014857	ZP_01014859	ZP_01014860; ZP_01014861	–	–	–	–
Rhodobacterales bacterium str. HTCC 2150[c]	ZP_01743249; ZP_01743246	ZP_01743248; ZP_01743247	ZP_01743245	ZP_01743243; ZP_01743242	–	–	–	–
Aurantimonadaceae								
Aurantimonas sp. str. SI85-9A1[c]	ZP_01225769; ZP_01225766	ZP_01225768; ZP_01225767	ZP_01225765	ZP_01225764; ZP_01225763	–	–	–	–
Fluvimarina pelagi str. HTCC 2506[c]	ZP_01439477; ZP_01439480	ZP_01439479; ZP_01439478	ZP_01439476	ZP_01439476; ZP_01439474	–	–	–	–
Phyllobacteriaceae								
Pseudoaminobacter salicylatoxidans str. KTC001	CAH59732; CAB94219[d]	CAH59733; CAC39169[d]	CAC39170[d]	CAH59734; CAH59735[d]	n.a.[d]	n.a.[d]	n.a.[d]	n.a.[d]
Bradyrhizobiaceae								
Bradyrhizobium japonicum str. USDA 110[c]	NP_770151/ NP_767654; NP_770154/ NP_767651/ NP_769372	NP_770152/ NP_769374; NP_770153/ NP_769373	NP_770155/ NP_767649	NP_770156/ NP_772761; NP_770157/ NP_772760	NP_773897; NP_773898	–	–	–
Bradyrizobium sp. str. BTAi1[c]	ZP_00857396/ ZP_00857569; ZP_00857393/ ZP_00863131	ZP_00857395/ ZP_00857570; ZP_00857394/ ZP_00857571	ZP_00857392/ ZP_00863133	ZP_00857391/ ZP_00862549; ZP_00857390/ ZP_00862550	–	–	–	–
Nitrobacter hamburgensis str. X14[c]	YP_578864; YP_578861	YP_578863; YP_578862	YP_578859	YP_576401; YP_576402	YP_578584; YP_578585	–	–	–
Nitrobacter sp. strain Nb-311A	–	–	–	–	ZP_01044876; ZP_01044877	–	–	–
Nitrobacter winogradskyi str. Nb-255	–	–	–	–	YP_319624; YP_319625	–	–	–
Rhodopseudomonas palustris str. BisA53	ZP_00810280; ZP_00810279	ZP_00810278; ZP_00810277	ZP_00810276	ZP_00810275; ZP_00810274	–	–	–	–
Rhodopseudomonas palustris str. BisB5	YP_571375; YP_571374	YP_571373; YP_571372	YP_571371	YP_571370; YP_571369	–	–	–	–
Rhodopseudomonas palustris str. BisB18	–	–	–	–	–	–	–	–
Rhodopseudomonas palustris str. HaA2	YP_487971; YP_487970	YP_487969; YP_487968	YP_487967	YP_487966; YP_487965	–	–	–	–
Rhodopseudomonas palustris str. CGA009	NP_949805; NP_949804	NP_949803; NP_949802	NP_949801	NP_949800; NP_949799	–	–	–	–
Hyphomicrobiaceae								
Starkeya novella	AAR98728; AAR98727[d]	AAR98726; AAR98725[d]	AAF61448[d]	AAF61449; AAF61450[d]	AAF64400; AAF64401[d]	n.a.[d]	n.a.[d]	n.a.[d]
Xanthobacter autotrophicus str. Py2	ZP_01196269; ZP_01196270	ZP_01196271; ZP_01196272	ZP_01196273	ZP_01196274; ZP_01196275	ZP_01199037/ ZP_01196335; ZP_01199083/ ZP_01196336	–	–	–

© 2007 The Authors
Journal compilation © 2007 Society for Applied Microbiology and Blackwell Publishing Ltd, *Environmental Microbiology*, **9**, 2957–2977

Table 4. *cont.*

Species[a]	Homologues present in genome sequences of *Bacteria*[b]							
	Sox				Sor	Apr	Dsr	
	SoxXA	SoxYZ	SoxB	SoxCD	SorAB	AprBA	DsrAB	DsrMKJOP
Proteobacteria phylum, *Betaproteobacteria*								
Burkholderiaceae								
Cupriavidus metallidurans str. CH34[c]	ZP_00593662; –	ZP_00593853; ZP_00593852	ZP_00593847	–	ZP_00595461; ZP_00595460	–	–	–
Polynucleobacter sp. str. QLW-P1DMWA-1[c]	ZP_01494652; ZP_01494653	ZP_01494655; ZP_01494654	ZP_01494651	ZP_01493496; ZP_01494656	ZP_01493045; ZP_01493143	–	–	–
Ralstonia eutrophica str. JMP134[c]	YP_297454; YP_297455	YP_297458; YP_297457	YP_297452	YP_297461; YP_297460	YP_297287; YP_297286	–	–	–
Ralstonia pickettii str. 12J[c]	ZP_01661485; ZP_01661484	ZP_01661481; ZP_01661482	ZP_01661487	–	YP_297287; YP_297286	–	–	–
Ralstonia solanacearum str. GMI1000[c]	NP_521374; NP_521375	NP_521378; NP_521377	NP_521372	–	NP_518934–3; NP_518932	–	–	–
Ralstonia solanacearum str. UW551[c]	ZP_00944484; ZP_00944483	ZP_00944482; ZP_00944481	ZP_00944480	–	ZP_00944736; ZP_00944735			
Comamonadaceae								
Comamonas testosteroni str. KF-1[c]	ZP_01521177; ZP_01521176	ZP_01521174; ZP_01521175	ZP_01521178	ZP_01521172; ZP_01521173	–	–	–	–
Polaromonas naphtalenivorans str. CJ2[c]	–	YP_981902; YP_981903	–	–	YP_982913; YP_982914	–	–	–
Polaromonas sp. str. JS666[c]	YP_549440; YP_549441	YP_549443; YP_549442	YP_549439	YP_549445; YP_549444	–	–	–	–
Oxalobacteraceae								
Herminiimonas arsenicoxydans str. KF-1[c]	CAL61371; CAL61370	CAL61368; CAL61369	CAL61372	CAL61365; CAL61376	CAL62480; CAL62479	–	–	–
Uncertain phylogenetic affiliation								
Methylibium petroleiphilum str. PM1[c]	YP_001021623; YP_001021624	YP_001021626; YP_001021625	YP_001021622	YP_001021628; YP_001021627	–	–	–	–
Hydrogenophilaceae								
Hydrogenophilus thermoluteolus str. TH-1	BAF34124; BAF34123[d]	BAF34121; BAF34122[d]	BAF34125[d]	BAF34119; BAF34120[d]	n.a.[d]	n.a.[d]	n.a.[d]	n.a.[d]
Thiobacillus denitrificans str. ATCC 25259	YP_314325/ YP_314675; YP_314322/ YP_314676	YP_314324; YP_314323	YP_314321	–	–	+	+	+
Rhodocyclaceae								
Dechloromonas aromatica str. RCB[c]	YP_286329; YP_286330	YP_286332; YP_286331	YP_286328	YP_286334; YP_286333	–	–	–	–
Proteobacteria phylum, *Gammaproteobacteria*								
Chromatiaceae								
Allochromatium vinosum str. DSM 180	ABE01360; ABE01361[d]	ABE01369; n.a.[d]	ABE01359[d]	n.a.[d]	n.a.[d]	+[d]	+[d]	+[d]

© 2007 The Authors
Journal compilation © 2007 Society for Applied Microbiology and Blackwell Publishing Ltd, *Environmental Microbiology*, **9**, 2957–2977

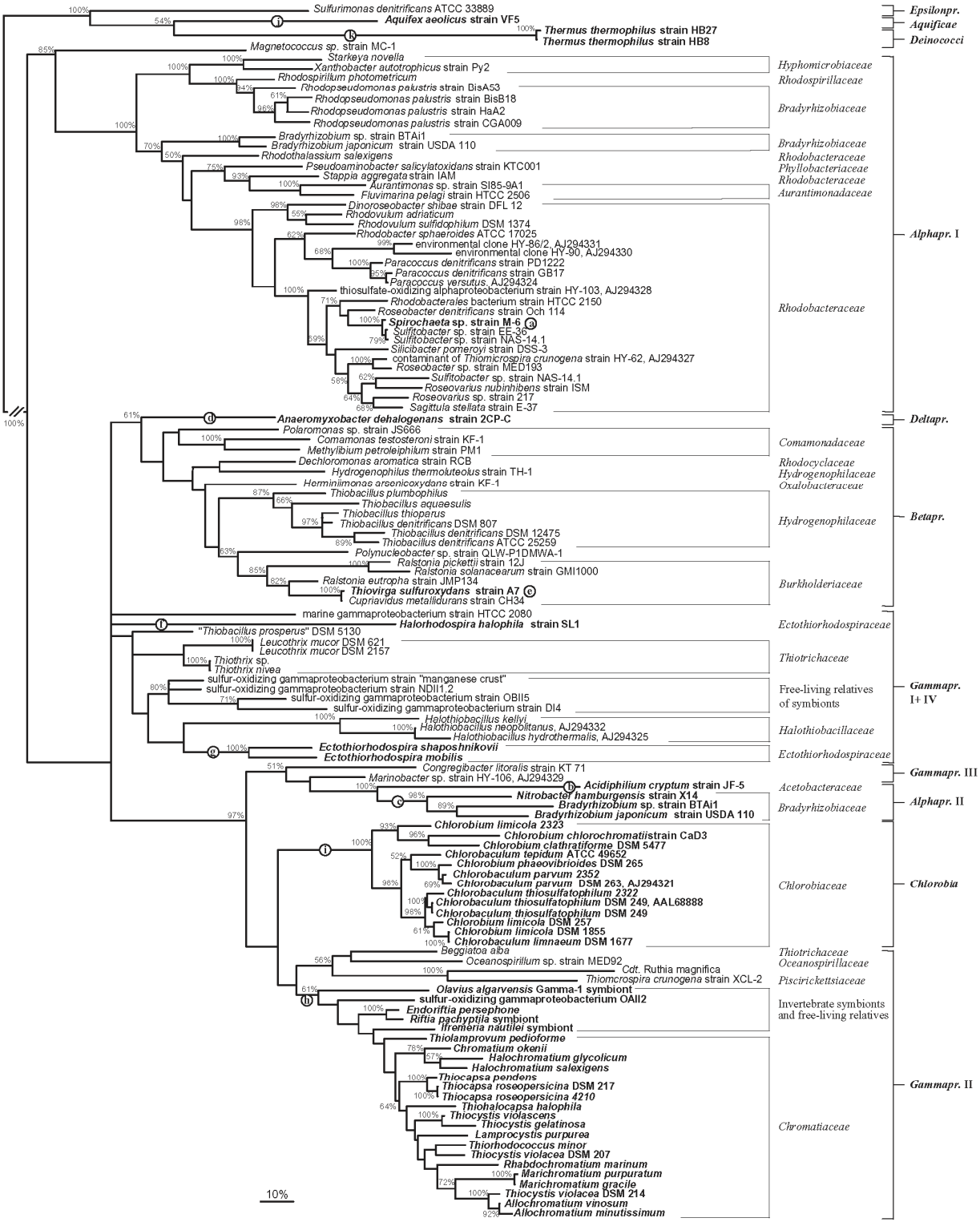

© 2007 The Authors
Journal compilation © 2007 Society for Applied Microbiology and Blackwell Publishing Ltd, *Environmental Microbiology*, **9**, 2957–2977

Fig. 1. SoxB consensus tree based on 124 SoxB sequences from the investigated SOB including the full-length SoxB sequences retrieved from the public databases. Polytomic nodes connect branches for which a relative order could not be determined unambiguously by applying distance matrix-based, maximum parsimony and maximum likelihood methods. Maximum likelihood bootstrap re-sampling values greater than 50% (100 re-samplings) are indicated near the nodes. The SoxB sequences of *Sulfurimonas denitrificans*, *Aquifex aeolicus* and *Thermus thermophilus* ssp. were used as outgroup references. Sulfur-oxidizing bacteria (SOB) with putative laterally transferred *soxB* genes are in boldface; proposed LGT events are indicated by letters (a–k). The 16S rRNA gene-based taxonomical classification of SOB species is indicated. The scale bar corresponds to 10% estimated sequence divergence.

and *Chromatiaceae* revealed that the 16S rRNA gene-based species relationships are not reflected in the SoxB tree topology. Interestingly, the latter is consistent to the AprBA-based tree topology (B. Meyer and J. Kuever, 2007b); both protein phylogenies point to an incorrect classification of SOB strain DSM 214 as *Thiocystis violacea* subspecies (see also Fig. 2). The 16S rRNA gene-discordant affiliation of the epsilonproteobacterial *S. denitrificans* (Takai *et al.*, 2006) with the hyperthermophilic *Aquifex aeolicus* and *Thermus thermophilus* ssp. near the root of the SoxB tree indicates their involvement in LGT events (LGTs j and k).

Additional evidence for lateral transfer of soxB *genes*

Additional evidence for the inferred phylogenetic position of the SOB taxa in the SoxB tree is given by the presence of insertions and deletions (indels) at identical sequence positions (see Table S1). The comparison of the aligned SoxB sequences supports the distinct branching position from *S. denitrificans* and representatives of the *Aquificae* and *Thermaceae* by the presence of several unique indels. The xenology of the SoxB from *Spirochaeta* sp. strain M-6, *T. sulfuroxydans* strain A7, *A. dehalogenans* and members of *Alphaproteobacteria* II is confirmed by the presence of *Roseobacter*-, *Betaproteobacteria*- and *Gammaproteobacteria* cluster III-specific indels respectively. In addition, the 16S rRNA gene-discordant affiliations of the anaerobic anoxygenic phototrophic SOB lineages with the *Gammaproteobacteria* clusters I to III are supported by shared, distinctive indels, while the separate branching position of *H. halophila* (cluster IV) is confirmed by *Beta*- and *Gammaproteobacteria* cluster I-specific as well as two unique indels.

Atypical sequence characteristics, e.g. significant deviations in G + C content and codon usage between the proposed LGT-derived *soxB* gene and the recipient genome, are useful as signposts for recent events of LGT. In general, no indications for recent LGT events were identified among the presumed LGT-affected SOB with the exception of the *T. sulfuroxydans* strain A7. This strain has a genome G + C content of 47.1%, while its *soxB* G + C content (64.2%) and codon usage are nearly identical to those of the putative donor strain *Cupriavidus metallidurans* strain CH34 (G + C content of *soxB* and genome, 65.9% and 63.7%, respectively).

Correlation between the sox *gene cluster composition and the occurrence of* dsr *genes in genomes of sulfur-storing SOB*

Genome data concerning the *sox* gene cluster, *soxXAYZBCD*, were available from 61 different *Proteobacteria* and *Chlorobiaceae* species, *A. aeolicus* and two *T. thermophilus* strains. The comparison of the genomic gene content revealed that the presence of the *dsrAB*/*dsrMKJOP* correlated with the absence of *soxCD* genes: all thiosulfate-oxidizing species that are known to intermediately deposit elemental sulfur lack the sulfur dehydrogenase encoding genes of the periplasmic Sox enzyme system but possess the genetic ability to oxidize the stored sulfur via the cytoplasmic dissimilatory sulfite reductase (DsrAB), e.g. (i) the *Chlorobiaceae,* (ii) *Allochromatium vinosum* and *H. halophila* (as representatives of the *Chromatiaceae* and *Ectothiorhodospiraceae*, respectively), (iii) *Thiobacillus denitrificans*, and (iv) '*Cdt.* R. magnifica'. In contrast, the majority of *sox* gene-containing *Alpha*-, *Beta*- and *Gammaproteobacteria*, *S. denitrificans* and *T. thermophilus* ssp. harboured a complete, *Paracoccus pantotrophus*-/*Rhodovulum sulfidophilum*-homologous *sox* gene cluster (Appia-Ayme *et al.*, 2001; Friedrich *et al.*, 2001) in their genomes and lacked the *dsrAB*/*dsrMKJOP* genes. Notably, the presence of the *sox* gene cluster differed at the species (*Chlorobium*, *Silicibacter*, *Nitrobacter* and *Polaromonas*) and subspecies (*Rhodobacter sphaeroides* and *Rhodopseudomonas palustris*) level.

Discussion

Distribution of soxB *genes among photo- and chemotrophic SOB*

The members of the anaerobic anoxygenic phototrophic *Chlorobiaceae*, *Chromatiaceae* and *Ectothiorhodospiraceae* and aerobic chemotrophic *Beggiatoa*, *Thiothrix*, *Thiobacillus*, *Thiomicrospira* and free-living relatives of invertebrate symbionts form intra- and extracellularly stored sulfur globules as obligate intermediate during thiosulfate oxidation (Nelson and Fisher, 1995; Howarth *et al.*, 1999; Imhoff, 1999; 2001a; 2003; Kuever *et al.*, 2002; Robertson and Kuenen, 2002; Teske and Nelson, 2004). Based on recent experimental results on sulfur-storing *Chlorobaculum tepidum* (Hanson and Tabita, 2003),

© 2007 The Authors
Journal compilation © 2007 Society for Applied Microbiology and Blackwell Publishing Ltd,

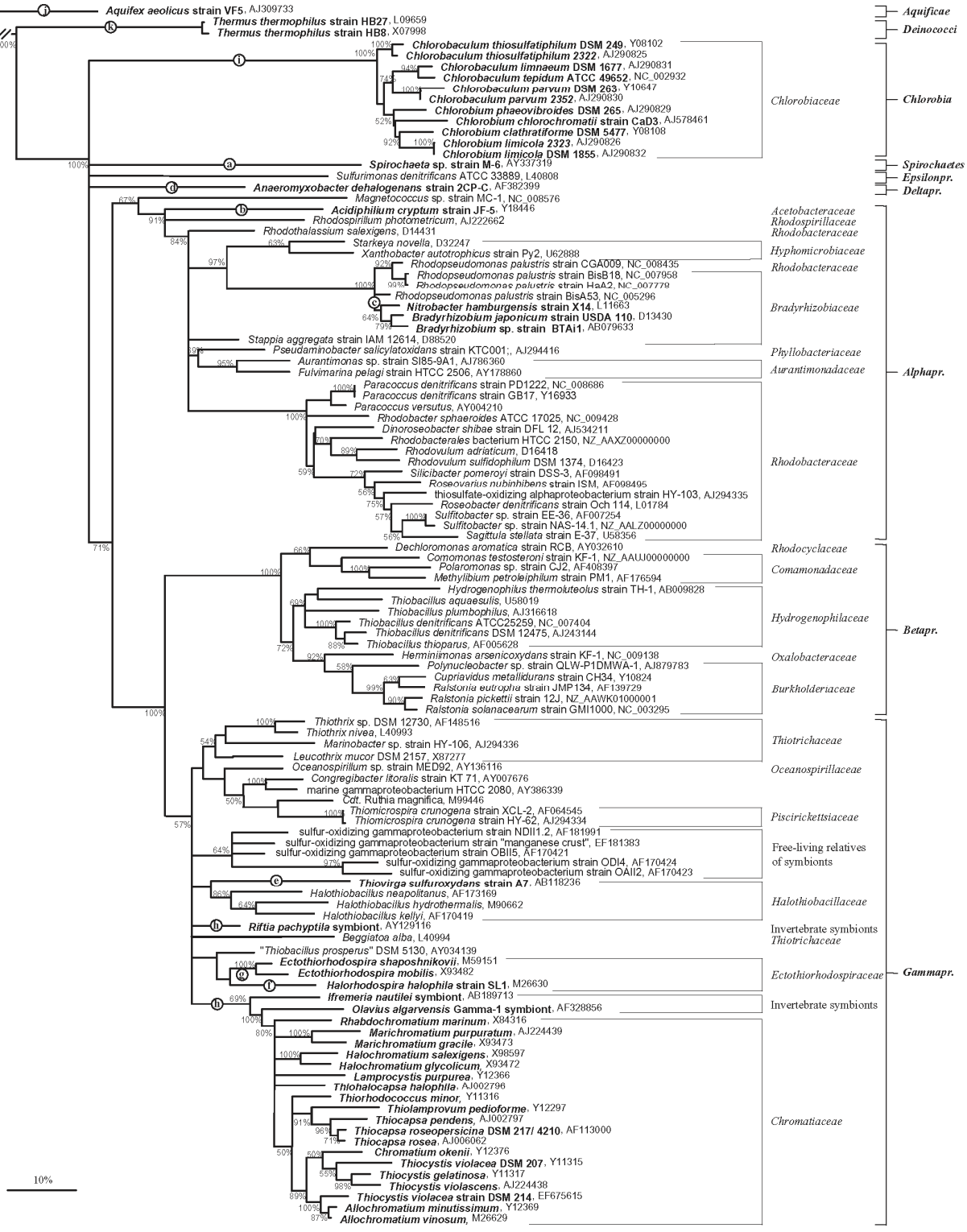

© 2007 The Authors
Journal compilation © 2007 Society for Applied Microbiology and Blackwell Publishing Ltd, *Environmental Microbiology*, **9**, 2957–2977

Fig. 2. Consensus tree based on the 16S rRNA gene sequences of the *soxB* gene-containing SOB species as indicated by the genetic and genomic analyses of this study. Polytomic nodes connect branches for which a relative order could not be determined unambiguously by applying distance matrix-based, maximum parsimony and maximum likelihood methods. Maximum likelihood bootstrap re-sampling values greater than 50% (100 re-samplings) are indicated near the nodes. The 16S rRNA gene sequence of *Aquifex aeolicus* was used as an outgroup reference. Sulfur-oxidizing bacteria (SOB) with putative laterally transferred *soxB* genes are in boldface; proposed LGT events are indicated by letters (a–k, see Fig. 1). The scale bar corresponds to 10% estimated sequence divergence.

A. vinosum (Hensen *et al.*, 2006) and *T. denitrificans* (Beller *et al.* 2006), the truncated Sox enzyme system, SoxXAYZB, was postulated to be functionally linked to the reverse-acting enzymes of the cytoplasmic sulfate-reduction pathway (Friedrich *et al.*, 2005; Hensen *et al.*, 2006): in analogy to the *P. pantotrophus*-based mechanism (Friedrich *et al.*, 2001), the SoxXA would oxidatively couple thiosulfate to a cysteine-sulfhydryl group of the SoxYZ complex from which sulfate would be hydrolysed off by SoxB. Due to the lack of the sulfur dehydrogenase $Sox(CD)_2$ component, the sulfane sulfur of thiosulfate would be transferred to the sulfur globules and subsequently oxidized to sulfate via the reverse dissimilatory sulfite reductase, APS reductase, ATP sulfurylase and sulfite:acceptor oxidoreductase. Indeed, the previous proteins have been identified in several members of the anaerobic anoxygenic phototrophic SOB lineages as well as chemolithotrophic *T. denitrificans*, marine *Beggiatoa*, invertebrate symbionts and their free-living relatives (Brune, 1995; Nelson and Fisher, 1995; Pott and Dahl, 1998; Dahl *et al.*, 1999; 2005; Kappler and Dahl, 2001; Sanchez *et al.*, 2001; Kuever *et al.*, 2002; Teske and Nelson, 2004), whereas the general presence of Sox proteins was unconfirmed for most sulfur-storing species. The present study confirmed the ubiquitous presence of the *soxB* gene in all known thiosulfate-oxidizing, sulfur-storing chemo- and phototrophic SOB species but also for species that have not yet been reported to use this sulfur compounds as electron donor (e.g. *C. limicola* DSM 1855, *Thiocystis gelatinosa*, *Ectothiorhodospira marismortui*, *Leucothrix mucor*, *Spirochaeta* sp.) (see Table 1). As the *soxB* is generally a part of the *sox* gene cluster (see Table 4), its PCR-based detection in the respective SOB species might be used as a first indication for the putative presence of components of the Sox enzyme system. In context with the absence of *soxCD* genes and the presence of genes coding for the reverse dissimilatory sulfate-reduction pathway in the accessible genomes of *Chlorobiaceae*, *A. vinosum*, *H. halophila*, *T. denitrificans* and '*Cdt.* R. magnifica' (Table 4), the recently postulated model for a general involvement of the Sox enzyme system in the thiosulfate oxidation in sulfur-storing bacteria is therefore supported by the results of our study (Friedrich *et al.*, 2005; Hensen *et al.*, 2006).

The PCR amplification results are most likely false-negative for the examined *Thiomicrospira* spp. and related symbionts of Mytilid mussels as well as Vesicomyid clams as *T. crunogena* and '*Cdt.* R. magnifica' harbour *soxB* genes with non-complementary primer target sites. Indeed, the investigated *Thiomicrospira* spp. have been demonstrated to oxidize thiosulfate to sulfate (Brinkhoff *et al.*, 1999) (note: *T. crunogena* deposits sulfur globules despite the presence of a *P. pantotrophus*-homologous *sox* gene cluster and the absence of *dsr* and *apr* genes). In contrast, the thiosulfate-oxidizing abilities of the symbiotic bacteria have not been investigated in detail (Nelson and Fisher, 1995; Cavanaugh *et al.*, 2004). The *soxB* target site of *Endoriftia persephone* and *Olavius algarvensis* Gamma-1/-3 symbionts are complementary to the primers used in the PCR assays; thus, the absence of the *soxB* in certain symbiotic bacteria might be correct and reflect the preferred utilization of sulfide as energy source, as it is generally proposed for invertebrate symbionts (Cavanaugh *et al.*, 2004). Direct supply of thiosulfate to their symbionts has only been reported for *Bathymodiolus thermophilus* and *Calyptogena magnifica* that detoxify sulfide by conversion to this less reduced sulfur compound (Nelson and Fisher, 1995; Cavanaugh *et al.*, 2004).

In support of the postulated wide distribution of the Sox enzyme system-mediated pathway as a common mechanism for bacterial thiosulfate oxidation (Friedrich *et al.*, 2001; 2005), the collected genomic data demonstrated the complete *sox* gene cluster to be present in various photo- and chemotrophic representatives of the *Proteobacteria* as well as hyperthermophilic *T. thermophilus* ssp.; however, for most of these species the ability to utilize thiosulfate has not been experimentally confirmed (see Table 4), and thus the presence of an operative, *P. pantotrophus*-/*R. sulfidophilum*-homologous Sox enzyme system is speculative until experimentally proven. Nevertheless, the abundance of *sox* genes in aerobic photo- and non-phototrophic species of the marine *Roseobacter* clade points to the energetical benefit of the Sox enzyme system-mediated oxidation of inorganic sulfur compounds for members of the latter group that generally dominate the degradation of organic sulfur compounds in the bacterioplankton community (Buchan *et al.*, 2005). In contrast, the capability to use reduced inorganic sulfur compounds as photosynthetic electron donors is restricted among anaerobic anoxygenic phototrophic members of the *Alphaproteobacteria* to certain genera (Brune, 1995; Imhoff, 2001b). This is reflected by the limited detection of the *soxB* gene in *Rhodothalassium*, *Rhodospirillum* and *Rhodovulum*

© 2007 The Authors
Journal compilation © 2007 Society for Applied Microbiology and Blackwell Publishing Ltd,

species in the PCR assays of this study (Table 1), although false-negative amplification results cannot be completely ruled out, e.g. for thiosulfate-oxidizing *R. acidophilus* as *R. palustris*-relative (Imhoff, 2001b).

In SOB living in extreme habitats, such as *Acidithiobacillus*, *Halothiobacillus* and *Thermothiobacillus*, the complete oxidation of thiosulfate to sulfate has been suggested to be performed via polythionates (Pronk *et al.*, 1990; Meulenberg *et al.*, 1993; Kelly *et al.*, 1997). For acidophiles such a pathway makes perfect sense, allowing rapid conversion of thiosulfate, which is chemically unstable under acidic conditions, into an acid-stable intermediate (tetrathionate). Interestingly, the *soxB* gene was identified in the acidophilic '*T. prosperus*' (Huber and Stetter, 1989), which might be a first indication that the Sox enzyme system is also present in some acidophilic SOB; however, further experimental investigation is needed for verification (note: *Acidithiobacillus ferrooxidans* harbours no *sox* homologues in its genome). The ability to use more than one thiosulfate-oxidizing enzymatic system/enzyme, e.g. the incomplete Sox system plus Dsr and a thiosulfate dehydrogenase as reported for *A. vinosum* (Hensen *et al.*, 2006), allows an adaptation of the energy conservation to the varying physico-chemical conditions in environment.

Phylogeny of SoxB: evidence for LGT among SOB

Multiple events of lateral *soxB* gene transfer among the SOB are the most reasonable explanation for (i) the inferred close relationships of SoxB from SOB species that are distantly related on the basis of the 16S rRNA gene phylogeny, e.g. *S. denitrificans*, *A. aeolicus* and *T. thermophilus* ssp., and (ii) the presence of two distantly related *soxB* genes in the genome of the same organism, e.g. *Bradyrhizobium* species (Figs 1 and 2). The betaproteobacterial and the gammaproteobacterial strains that served as donors for the LGT-affected *Bradyrhizobiaceae, Acetobacteraceae* (*Alphaproteobacteria* lineage II) and *A. dehalogenans* respectively, are not apparent. The *Bradyrhizobium* spp. and related *N. hamburgensis* strain X14 might have acquired their *soxB* gene by independent LGT events. Alternatively, a single LGT might have affected their ancestor prior to the diversification of *Bradyrhizobium* and *Nitrobacter*, which was followed by a replacement of the authentic *soxB* gene by the xenolog in the ancestor of *Nitrobacter* (the xenolog will have later been lost by most *Nitrobacter* spp. except *N. hamburgensis* strain X14, see Table 4). The high sequence identity values of the partial SoxB sequences from *Spirochaeta* sp. strain M-6 and *T. sulfuroxydans* strain A7 to those of their putative donor strains, *Sulfitobacter* and *Ralstonia* spp. (98.3% and 99.5%, respectively), are indicative for recent lateral transfers. However, genome data of *Spirochaeta* sp. strain M-6 are needed for verification. The coexistence of recipient and potential donor strains have been reported, e.g. in '*Thiodendron*' sulfur bacterial mats and sulfur-containing microaerobic wastewaters and sludge (Qureshi *et al.*, 2003; Dubinina *et al.*, 2004; Ito *et al.*, 2004) that would have enabled interspecies gene exchange.

According to the SoxB tree, the *Gammaproteobacteria* are not monophyletic. The anaerobic anoxygenic phototrophic lineages are 16S rRNA-discordantly affiliated to the different chemotrophic SOB lineages (*Gammaproteobacteria* I or II). Therefore, the genera of the *Ectothiorhodospiraceae* (*Ectothio-* and *Halorhodospira*) and the *Chromatiaceae* (and affiliated invertebrate symbionts), as well as the *Chlorobiaceae*, are proposed to have received their *soxB* genes by four independent LGT events with different chemotrophic SOB of the *Gammaproteobacteria* having served as donors, e.g. moderate halophilic *Ectothiorhodospiraceae* and habitat-sharing Halothiobacilli (Imhoff, 1999; Kelly and Wood, 2000). These transfers most likely occurred before their diversification, which was followed by a *sox* gene loss in those genera that are described as metabolically less versatile, e.g. *Thiococcus* and *Prosthecochloris* spp. (Imhoff, 1999; 2001a; 2003). All proteobacterial SoxB lineages comprise chemotrophic SOB with *P. pantotrophus*-/*R. sulfidophilum*-homologous *sox* gene clusters in their genomes, whereas the xenologous anaerobic anoxygenic phototrophic SOB lineages (including invertebrate symbionts) harbour truncated gene loci. This might indicate that initially the ancestors of the latter groups acquired the complete *soxXAYZBCD* gene cluster from their chemotrophic donors [note: the *sox* gene cluster is located on a endogenous plasmid in certain green sulfur bacteria, and its successful lateral transfer to non-thiosulfate-utilizing strains was demonstrated (Mendez-Alvarez *et al.*, 1994)]. In adaptation, the Sox enzyme pathway could have been functionally linked to the pre-existing cytoplasmic sulfide/elemental sulfur oxidation pathway (DsrAB/DsrMKJOP) and the *soxCD* genes were subsequently lost, which resulted in the recognized thiosulfate oxidation pathway via sulfur-globule formation. Alternatively, this process could have happened in the potential sulfur-storing chemotrophic donors of *Chromatiaceae* and *Chlorobiaceae* prior to the LGTs.

With regard to the 16S rRNA gene-discordant relationship of *S. denitrificans*, *A. aeolicus* and *T. thermophilus* ssp. at the root of the SoxB tree, there are two possible scenarios for the direction of LGT and the origin of the SoxB protein. First, if the *soxB* of the hyperthermophilic species is assumed to be xenologous, a (epsilon-)proteobacterial origin of the SoxB protein would be consistent with the tree topology. In support, all currently available sequences of other non-proteobacterial SOB species (*Chlorobiaceae*, *Spirochaeta* sp. strain M-6)

© 2007 The Authors
Journal compilation © 2007 Society for Applied Microbiology and Blackwell Publishing Ltd,

seem to be laterally acquired from *Proteobacteria*. Indeed, recent phylogenomic studies disputed the 16S rRNA gene-based basal branching of *Aquifex* but placed it next to the *Epsilon-/Deltaproteobacteria* (Dutilh *et al.* 2004). Second, if the SoxB of *S. denitrificans* is assumed to be xenologous, the tree topology would indicate a *soxB* origin within the *Aquificales* or the *Thermus* lineage followed by a LGT to the evolving proteobacterial lineages. Irrespective of scenario, exchange of genetic material between these phylogenetic groups would have been possible, as various molecular studies confirmed their coexistence and dominance at hydrothermal vents (Reysenbach *et al.*, 2000; Takai *et al.*, 2005; Campbell *et al.*, 2006).

Potential evolutionary scenario for the Sox enzyme pathway in SOB

During the Proterozoic era, the ocean was proposed to have been globally anoxic and sulfidic (Shen *et al.*, 2003; Canfield, 2005) with a widespread occurrence and predominance of planktonic ancestors of the *Chromatiaceae* and *Chlorobiaceae* lineages as demonstrated by molecular fossils (Brocks *et al.*, 2005). The anoxic formation of thiosulfate via (i) chemical FeS_2 oxidation with MnO_2 and (ii) biogenic FeS oxidation by denitrifying bacteria (Schippers, 2004) would have been absent. As the dissimilatory sulfite and APS reductase phylogenies point to an ancient origin of the sulfate reduction/sulfide oxidation pathway in SRP and SOB (Boucher *et al.*, 2003; Meyer and Kuever, 2007a) as early as 3.47 giga annum (Ga) (Shen and Buick, 2004), the anaerobic anoxygenic phototrophs most likely converted the abundant compounds sulfide/sulfur by the reverse-operating enzymes of the sulfate reduction pathway. During the Neoproterozoic, the atmospheric oxygen increased to > 10% of the present levels until 1.05 Ga that resulted in (i) the deepening of the oxic/anoxic interface in the ocean, (ii) the oxygenation of coastal marine sediments, and (iii) decreased levels of sulfide while less reduced inorganic sulfur compounds like thiosulfate became more abundant (Canfield and Teske, 1996; Canfield, 2005). This change in the oxidation state of Earth promoted the evolution and diversification of non-photosynthetic, facultative aerobic or even strict aerobic SOB with a wide-scale initiation of the oxidative sulfur cycle postulated to have occurred lately in the Proterozoic at 0.75–0.62 Ga (Canfield and Teske, 1996). Novel pathways that allowed the usage of the less reduced inorganic sulfur compounds as respiratory electron donor evolved simultaneously in the non-photosynthetic SOB. With regard to the SoxB phylogeny, the Sox enzyme system might have originated in an aerobic, chemotrophic proteobacterial SOB that lacked the reverse sulfate reduction pathway and became widespread among the thiosulfate-utilizing *Proteobacteria*. The reverse sulfate reduction pathway persisted in some facultative anaerobic, chemolithoautotrophic SOB groups (e.g. in *Thiobacillus*, *Thiothrix*, invertebrate symbionts and their free-living relatives) that employed the branched oxidation pathway for thiosulfate oxidation. In adaptation to the changing environmental conditions, the members of the anaerobic anoxygenic phototrophic SOB lineages acquired novel pathways that allowed thiosulfate utilization, e.g. the *sox* gene cluster by lateral transfer from chemotrophic SOB.

Experimental procedures

Microorganisms

The investigated reference strains of photo- and chemotrophic SOB (listed in Table 1) were obtained from the DSMZ (Braunschweig, Germany) as actively growing cultures. Genomic DNA of green sulfur bacteria and several purple sulfur bacteria were received from the culture collection of J. Imhoff, University of Kiel. Extracted genomic DNA of tissue material was provided by N. Dubilier (*Inanidrilus* spp., *B. azoricus*, *B. brevior*), A. D. Nussbauer (*R. pachyptila*, *B. thermophilus*, *C. magnifica*, *Oasisia* sp.) and C. Borowski (*I. nautilei*). Harvested cells of *Beggiatoa* spp., *Aquaspirillum* spp., *Macromonas bipunctata* strain D-408 and *Spirochaeta* spp. were received from G. Dubinina. The SOB strain 'manganese crust' was isolated from enrichment cultures of sediment and seawater samples of the Caribbean Sea (Caribflux project, SO-154).

DNA isolation

Genomic DNA from the investigated reference strains was obtained by applying the DNAeasy Kit (Qiagen, Hilden, Germany) or the NUCLEOBOND® Kit (MACHEREY-NAGEL, Düren, Germany) according to the manufacturer's instructions. The DNA concentration and quality was estimated spectrophotometrically, while its integrity was examined visually by gel electrophoresis on 0.8% (w/v) agarose gels run in 1× Tris-borate-EDTA (TBE) buffer and followed by ethidium bromide staining (0.5 μg ml^{-1}).

Polymerase chain reaction (PCR) amplification of soxB *and 16S rRNA genes*

Amplification of the *soxB* gene fragments was performed using the primer sets (Table 2) and PCR protocols according to Petri *et al.* (2001). Reaction mixtures (total volume of 50 μl) contained 5 μl 10× RED*Taq* PCR reaction buffer, 5 μl 10× BSA solution (3 mg ml^{-1}), 200 μM (dNTPs) mixture, 1 μM of each primer, 2.5 U RED*Taq* DNA polymerase and 10–100 ng genomic DNA from the reference strains as template. 16S rRNA gene fragments were amplified using the primer sets GM3F/GM4R and GM5F-GC clamp/907R [for subsequent denaturing gradient gel electrophoresis (DGGE) analysis] with the PCR conditions as described elsewhere (Muyzer *et al.*, 1995).

© 2007 The Authors
Journal compilation © 2007 Society for Applied Microbiology and Blackwell Publishing Ltd,

Cloning of PCR products

Cloning assays of 16S rDNA amplicons and subsequent ARDRA analyses of the recombinant plasmids were performed as described elsewhere (Meyer and Kuever, 2007a).

Double gradient (DG)-DGGE analysis of PCR-amplified 16S rRNA gene fragments

For DG-DGGE analysis, an acrylamide gradient from 6% to 8% acrylamide/bis-acrylamide stock solution, 37.5:1 (v/v) (Bio-Rad), was superimposed over a co-linear denaturant gradient from 20% to 70% of denaturant [100% denaturant corresponds to 7 M urea and 40% formamide (v/v), deionized with AG501-X8 mixed bed resin (Bio-Rad)]. Gradients were formed using a Bio-Rad Gradient Former Model 385. polymerase chain reaction (PCR) samples were applied to the gels in aliquots of 20 µl per lane. Further analysis was performed using the D-CODE™ and D-GENE™ systems (Bio-Rad) for electrophoresis runs in 1× Tris-acetate-EDTA (TAE) buffer at 60°C for 3.5 h at 200 V as previously described by Muyzer *et al.* (1995). After staining with ethidium bromide (0.5 µg ml^{-1}), DNA bands were visualized on a UV transillumination table (Biometra, Göttingen, Germany), excised from the polyacrylamide gel, eluted in 50 µl Tris-HCl, pH 8.0, and re-amplified using the original PCR conditions and primer pair without GC-clamp.

Nucleotide sequencing

The *soxB* and 16S rDNA amplicons of expected size were purified using either the QIAquick PCR purification, the QIAquick gel extraction kit (Qiagen, Hilden, Germany) or the Perfectprep gel cleanup sample kit (Eppendorf, Hamburg, Germany) following the supplier's recommendations. The PCR products were directly sequenced in both directions using the respective amplification primers and the ABI BigDye terminator cycle sequencing kit (Applied Biosystems, Foster City, USA). Sequencing reactions were run on an ABI PRISM® 3100 Genetic Analyzer (Applied Biosystems).

Sequence analysis tools and phylogeny inference

The DNA sequence data of the *soxB* amplicons from each SOB reference strain were assembled with subsequent manual correction using the sequence alignment editor program Bioedit (http://www.mbio.ncsu.edu/BioEdit/bioedit.html). BLAST searches for homologous sequences of SoxB in the public databases were performed at the NCBI website (http://www.ncbi.nlm.nih.gov/BLAST/). Searches on the preliminary sequence data of accessible SOB genomes were performed at The Institute for Genomic Research website (http://www.tigr.org) and at the DOE Joint Genome Institute website (http://img.jgi.doe.gov/cgi-bin/pub/main.cgi). The SoxB partial sequences obtained in this study and the complete sequences of the public databases were automatically aligned using the web server Tcoffee@igs (http://igs-server.cnrs-mrs.fr/Tcoffee/). The corresponding nucleic acid sequences of the *soxB* gene fragments were aligned based on the manually corrected amino acids alignment.

The phylogenetic analyses were based on a dataset of (i) 67 full-length SoxB sequences from publicly available genome data of SOB (Table 4), (ii) 7 partial sequences of chemotrophic SOB retrieved from the study of Petri and coworkers (2001), and (iii) 50 novel partial sequences obtained in this study (Table 1). Alignment regions of ambiguous homology as well as indels not present in all investigated sequences were omitted. Unrooted phylogenetic trees were constructed using the tree inference methods included in the ARB software package (http://www.arb-home.de) (distance matrix, neighbour-joining, Fitch; maximum parsimony, ProPars; maximum likelihood, ProML) on the basis of 118 SoxB sequences with 203 compared amino acid positions respectively. The trees were calculated using the global rearrangement, randomized species input order options and JTT matrix as amino-acid replacement model. The robustness of phylogenetic trees was tested by bootstrap analysis with 100 re-samplings. Short partial sequences were individually added to the initial trees using the QUICK_ADD parsimony tool of ARB without allowing changes in the overall tree topology. Finally, a SoxB-based consensus tree was constructed after comparing the topologies of the phylogenetic trees calculated by distance matrix, maximum parsimony and maximum likelihood analyses. The 16S rRNA gene-based consensus tree was generated as described for the SoxB phylogeny inference (16S rRNA gene sequences were obtained from the public databases).

Southern blot analysis

Identical amounts of genomic DNA (5 µg) from sulfur-oxidizing and sulfate-reducing bacteria (Table 3) were digested at 37°C with HindIII and EcoRI overnight, precipitated by ethanol, electrophoresed on 0.8% 1× TAE buffer at 100 V for 3 h, transferred to positively charged nylon membranes (Hybond N + filter, Amersham) by capillary neutral transfer and immobilized by UV cross-linking (Transilluminator, Biometra). The DNA probes for *soxB* genes (0.7 kb in length) were radioactively labelled with [α-^{32}P]dCTP by the random priming method using the HexaLabel™ DNA Labeling Kit (MBI Fermentas) according to the manufacturer's directions. The membranes were placed into glass hybridization bottles and prehybridized in 5× SSC (1× SSC is 0.15 M NaCl, 0.015 M Na-citrate, pH 8.0), 50% formamide, 0.1% sarcosyl, 7% SDS, 50 mM phosphate buffer, pH 7.0 and 2% casein ('Church' hybridization solution) at 50°C for 1 h in a hybridization oven (Biometra). Subsequently, a freshly denaturated, labelled DNA probe was added to the prehybridization solution followed by incubation for 12–16 h at 50°C under slow-speed rotation. The membranes were washed twice at 50°C for 30 min in 0.1× SSC-0.1% SDS, exposed to PhosphorImaging screen cassettes (Molecular Dynamics, Krefeld, Germany), scanned with a Typhoon Variable Mode Imager and processed with Image Quant software (Amersham). The membranes were stripped by two incubations for 15 min in probe-stripping solution (consisting of 0.4 M NaOH and 0.1% SDS) at 37°C under permanent agitation and re-probed, starting from the prehybridization step of the hybridization procedure.

© 2007 The Authors

GenBank accession numbers

The nucleotide sequence data reported in this study have been submitted to GenBank and are available under accession number EF618568-EF618617.

Acknowledgements

This study was supported by grants of the BMBF (project 'Caribflux' under contract number 03G0154C), the DFG (under contract number KU 916/8–1) and the Max-Planck-Society, Munich.

References

Appia-Ayme, C., Little, P.J., Matsumoto, Y., Leech, A.P., and Berks, B.C. (2001) Cytochrome complex essential for photosynthetic oxidation of both thiosulfate and sulfide in *Rhodovulum sulfidophilum*. *J Bacteriol* **183:** 6107–6118.

Beller, H.R., Letain, T.E., Chakicherla, A., Kane, S.R., Legler, T.C., and Coleman, M.A. (2006) Whole-genome transcriptional analysis of chemolithoautotrophic thiosulfate oxidation by *Thiobacillus denitrificans* under aerobic versus denitrifying conditions. *J Bacteriol* **188:** 7005–7015.

Boucher, Y., Douady, C.J., Papke, R.T., Walsh, D.A., Boudreau, M.E.R., Nesbo, C.L., *et al.* (2003) Lateral gene transfer and the origins of prokaryotic groups. *Annu Rev Genet* **37:** 283–328.

Brinkhoff, T., Muyzer, G., Wirsen, C.O., and Kuever, J. (1999) *Thiomicrospira kuenenii* sp. nov. & *Thiomicrospira frisia* sp. nov., two mesophilic obligately chemolithoautotrophic sulfur-oxidizing bacteria isolated from an intertidal mud flat. *Int J Syst Bacteriol* **49:** 385–392.

Brocks, J.J., Love, G.D., Summons, R.E., Knoll, A.H., Logan, G.A., and Bowden, S.A. (2005) Biomarker evidence for green and purple sulphur bacteria in a stratified Palaeoproterozoic sea. *Nature* **437:** 866–870.

Brune, D.C. (1995) Sulfur compounds as photosynthetic electron donors. In *Anoxygenic Photosynthetic Bacteria*. Blankenship, R.E., Madigan, M.T., and Bauer, C.E. (eds). Dordrecht, The Netherlands: Kluwer Academic Publishers, pp. 847–870.

Brüser, T., Lens, P.N.L., and Trüper, H.G. (2000) The biological sulfur cycle. In *Environmental Technologies to Treat Sulfur Pollution*. Lens, P.N.L., and Pol, L.H. (eds). London, UK: IWA Publishing, pp. 47–86.

Buchan, A., Gonzalez, J.M., and Moran, M.A. (2005) Overview of the marine Roseobacter lineage. *Appl Environ Microbiol* **71:** 5665–5677.

Campbell, B.J., Engel, A.S., Porter, M.L., and Takai, K. (2006) The versatile epsilon-proteobacteria: key players in sulphidic habitats. *Nat Rev Genet* **4:** 458–468.

Canfield, D.E. (2005) The early history of atmospheric oxygen: Homage to Robert A. Garrels. *Annu Rev Earth Planet Sci* **33:** 1–36.

Canfield, D.E., and Teske, A. (1996) Late Proterozoic rise in atmospheric oxygen concentration inferred from phylogenetic and sulphur-isotope studies. *Nature* **382:** 127–132.

Cavanaugh, C.M., McKiness, Z.P., Newton, I.L.G., and Stewart, F.J. (2004) Marine chemosynthetic symbioses. In *The Prokaryotes: An Evolving Electronic Resource for the Microbial Community*. Dworkin, M., Falkow, E., Rosenberg, E., Schleifer, K.-H., and Stackebrandt, E. (eds). [WWW document]. URL http://link.springer-ny.com/link/service/books/10125/index.htm.

Dahl, C., Rakhely, G., Pott-Sperling, A.S., Fodor, B., Takacs, M., Toth, A., *et al.* (1999) Genes involved in hydrogen and sulfur metabolism in phototrophic sulfur bacteria. *FEMS Microbiol Lett* **180:** 317–324.

Dahl, C., Engels, S., Pott-Sperling, A.S., Schulte, A., Sander, J., Lubbe, Y., *et al.* (2005) Novel genes of the dsr gene cluster and evidence for close interaction of Dsr proteins during sulfur oxidation in the phototrophic sulfur bacterium *Allochromatium vinosum*. *J Bacteriol* **187:** 1392–1404.

Dubinina, G.A., Grabovich, M.Y., and Chernyshova, Y.Y. (2004) The role of oxygen in the regulation of the metabolism of aerotolerant Spirochetes, a major component of '*Thiodendron*' bacterial sulfur mats. *Microbiology* **73:** 725–733.

Dutilh, B.E., Huynen, M.A., Bruno, W.J., and Snel, B. (2004) The consistent phylogenetic signal in genome trees revealed by reducing the impact of noise. *J Mol Evol* **58:** 527–539.

Epel, B., Schafer, K.O., Quentmeier, A., Friedrich, C., and Lubitz, W. (2005) Multifrequency EPR analysis of the dimanganese cluster of the putative sulfate thiohydrolase SoxB of *Paracoccus pantotrophus*. *J Biol Inorg Chem* **10:** 636–642.

Friedrich, C.G., Rother, D., Bardischewsky, F., Quentmeier, A., and Fischer, J. (2001) Oxidation of reduced inorganic sulfur compounds by bacteria: emergence of a common mechanism? *Appl Environ Microbiol* **67:** 2873–2882.

Friedrich, C.G., Bardischewsky, F., Rother, D., Quentmeier, A., and Fischer, J. (2005) Prokaryotic sulfur oxidation. *Curr Opin Microbiol* **8:** 253–259.

Hanson, T.E., and Tabita, F.R. (2003) Insights into the stress response and sulfur metabolism revealed by proteome analysis of a *Chlorobium tepidum* mutant lacking the Rubisco-like protein. *Photosynthesis Res* **78:** 231–248.

Hensen, D., Sperling, D., Trüper, H.G., Brune, D.C., and Dahl, C. (2006) Thiosulphate oxidation in the phototrophic sulphur bacterium *Allochromatium vinosum*. *Mol Microbiol* **62:** 794–810.

Howarth, R., Unz, R.F., Seviour, E.M., Seviour, R.J., Blackall, L.L., Pickup, R.W., *et al.* (1999) Phylogenetic relationships of filamentous sulfur bacteria (*Thiothrix* spp. & Eikelboom type 021N bacteria) isolated from wastewater-treatment plants and description of *Thiothrix eikelboomii* sp. nov., *Thiothrix unzii* sp. nov., *Thiothrix fructosivorans* sp. nov. and *Thiothrix defluvii* sp. nov. *Int J Syst Bacteriol* **49:** 1817–1827.

Huber, H., and Stetter, K.O. (1989) *Thiobacillus prosperus* sp. nov., represents a new group of halotolerant metal-mobilizing bacteria isolated from a marine geothermal field. *Arch Microbiol* **151:** 479–485.

Imhoff, J.F. (1999) The family *Ectothiorhodospiraceae*. In *The Prokaryotes: An Evolving Electronic Resource for the Microbial Community*. Dworkin, M., Falkow, E., Rosenberg, E., Schleifer, K.-H., and Stackebrandt, E. (eds). [WWW document]. URL http://link.springer-ny.com/link/service/books/10125/index.htm.

© 2007 The Authors
Journal compilation © 2007 Society for Applied Microbiology and Blackwell Publishing Ltd,

Imhoff, J.F. (2001a) The *Chromatiaceae*. In *The Prokaryotes: An Evolving Electronic Resource for the Microbial Community*. Dworkin, M., Falkow, E., Rosenberg, E., Schleifer, K.-H., and Stackebrandt, E. (eds). [WWW document]. URL http://link.springer-ny.com/link/service/books/10125/index.htm.

Imhoff, J.F. (2001b) The phototrophic alpha-Proteobacteria. In *The Prokaryotes: An Evolving Electronic Resource for the Microbial Community*. Dworkin, M., Falkow, E., Rosenberg, E., Schleifer, K.-H., and Stackebrandt, E. (eds). [WWW document]. URL http://link.springer-ny.com/link/service/books/10125/index.htm.

Imhoff, J.F. (2001c) The phototrophic beta-Proteobacteria. In *The Prokaryotes: An Evolving Electronic Resource for the Microbial Community*. Dworkin, M., Falkow, E., Rosenberg, E., Schleifer, K.-H., and Stackebrandt, E. (eds). [WWW document]. URL http://link.springer-ny.com/link/service/books/10125/index.htm.

Imhoff, J.F. (2003) Phylogenetic taxonomy of the family *Chlorobiaceae* on the basis of 16S rRNA and *fmo* (Fenna Matthews-Olson protein) gene sequences. *Int J Syst Evol Microbiol* **53:** 941–951.

Ito, T., Sugita, K., and Okabe, S. (2004) Isolation, characterization, and in situ detection of a novel chemolithoautotrophic sulfur-oxidizing bacterium in wastewater biofilms growing under microaerophilic conditions. *Appl Environ Microbiol* **70:** 3122–3129.

Joergensen, B.B., and Nelson, D.C. (2004) Sulfide oxidation in marine sediments: geochemistry meets microbiology. In *Sulfur Biogeochemistry – Past and Present*. Amend, J.P., Edwards, K.J., and Lyons, T.W. (eds). Boulder, Colorado, USA: Geological Society of America, pp. 63–81.

Kappler, U., and Dahl, C. (2001) Enzymology and molecular biology of prokaryotic sulfite oxidation. *FEMS Microbiol Lett* **203:** 1–9.

Kappler, U., Friedrich, C.G., Truper, H.G., and Dahl, C. (2001) Evidence for two pathways of thiosulfate oxidation in *Starkeya novella* (formerly *Thiobacillus novellus*). *Arch Microbiol* **175:** 102–111.

Kelly, D.P., and Wood, A.P. (2000) Reclassification of some species of *Thiobacillus* to the newly designated genera *Acidithiobacillus* gen. nov., *Halothiobacillus* gen. nov. and *Thermithiobacillus* gen. nov. *Int J Syst Evol Microbiol* **50:** 511–516.

Kelly, D.P., Shergill, J.K., Lu, W.P., and Wood, A.P. (1997) Oxidative metabolism of inorganic sulfur compounds by bacteria. *Antonie Van Leeuwenhoek* **71:** 95–107.

Kletzin, A., Urich, T., Muller, F., Bandeiras, T.M., and Gomes, C.M. (2004) Dissimilatory oxidation and reduction of elemental sulfur in thermophilic archaea. *J Bioenerg Biomembr* **36:** 77–91.

Kuever, J., Sievert, S.M., Stevens, H., Brinkhoff, T., and Muyzer, G. (2002) Microorganisms of the oxidative and reductive part of the sulfur cycle at a shallow-water hydrothermal vent in the Aegean Sea (Milos, Greece). *Cah Biol Mar* **43:** 413–416.

Kwok, S., Kellogg, D.E., McKinney, N., Spasic, D., Goda, L., Levenson, C., and Sninsky, J.J. (1990) Effects of primer-template mismatches on the polymerase chain reaction. *Nucleic Acids Res* **18:** 999–1005.

Mendez-Alvarez, S., Pavon, V., Esteve, I., Guerrero, R., and Gaju, N. (1994) Transformation of *Chlorobium limicola* by a plasmid that confers the ability to utilize thiosulfate. *J Bacteriol* **176:** 7395–7397.

Meulenberg, R., Scheer, E.J., Pronk, J.T., Hazeu, W., Bos, P., and Kuenen, J.G. (1993) Metabolism of tetrathionate in *Thiobacillus acidophilus*. *FEMS Microbiol Lett* **112:** 167–172.

Meyer, B., and Kuever, J. (2007a) Phylogeny of the alpha and beta subunits of the dissimilatory adenosine-5′-phosphosulfate (APS) reductase from sulfate-reducing prokaryotes – origin and evolution of the dissimilatory sulfate-reduction pathway. *Microbiology* **153:** 2026–2044.

Meyer, B., and Kuever, J. (2007b) Molecular analysis of the distribution and phylogeny of dissimilatory adenosine-5′-phosphosulfate reductase encoding genes (*aprBA*) among sulfur-oxidizing prokaryotes. *Microbiology*: in press.

Mukhopadhyaya, P.N., Deb, C., Lahiri, C., and Roy, P. (2000) A *soxA* gene, encoding a diheme cytochrome c, and a sox locus, essential for sulfur oxidation in a new sulfur lithotrophic bacterium. *J Bacteriol* **182:** 4278–4287.

Muyzer, G., Teske, A., Wirsen, C.O., and Jannasch, H.W. (1995) Phylogenetic relationships of *Thiomicrospira* species and their identification in deep-sea hydrothermal vent samples by denaturing gradient gel electrophoresis of 16S rDNA fragments. *Arch Microbiol* **164:** 165–172.

Nelson, D.C., and Fisher, C.R. (1995) Chemoautotrophic and methanoautotrophic endosymbiontic bacteria at deep-sea vents and seeps. In *Deep Sea Hydrothermal Vents*. Karl, D.M. (ed.). Boca Raton, Florida, USA: CRC Press, pp. 125–167.

Petri, R., Podgorsek, L., and Imhoff, J.F. (2001) Phylogeny and distribution of the *soxB* gene among thiosulfate-oxidizing bacteria. *FEMS Microbiol Lett* **197:** 171–178.

Pott, A.S., and Dahl, C. (1998) Sirohaem sulfite reductase and other proteins encoded by genes at the dsr locus of *Chromatium vinosum* are involved in the oxidation of intracellular sulfur. *Microbiol* **144:** 1881–1894.

Pronk, J.T., Meulenberg, R., Hazeu, W., Bos, P., and Kuenen, J.G. (1990) Oxidation of reduced anorganic sulphur compounds by acidophilic thiobacilli. *FEMS Microbiol Rev* **75:** 293–306.

Qureshi, S., Richards, B.K., Hay, A.G., Tsai, C.C., McBride, M.B., Baveye, P., and Steenhuis, T.S. (2003) Effect of microbial activity on trace element release from sewage sludge. *Environ Sci Technol* **37:** 3361–3366.

Reysenbach, A.L., Banta, A.B., Boone, D.R., Cary, S.C., and Luther, G.W. (2000) Biogeochemistry – microbial essentials at hydrothermal vents. *Nature* **404:** 835–835.

Robertson, L.A., and Kuenen, G.J. (2002) The genus *Thiobacillus*. In *The Prokaryotes: An Evolving Electronic Resource for the Microbial Community*. Dworkin, M., Falkow, E., Rosenberg, E., Schleifer, K.-H., and Stackebrandt, E. (eds). [WWW document]. URL http://link.springer-ny.com/link/service/books/10125/index.htm.

Rohwerder, T., and Sand, W. (2003) The sulfane sulfur of persulfides is the actual substrate of the sulfur-oxidizing enzymes from *Acidithiobacillus* and *Acidiphilium* spp. *Microbiology* **149:** 1688–1709.

Sanchez, O., Ferrera, I., Dahl, C., and Mas, J. (2001) In vivo role of adenosine-5′-phosphosulfate reductase in the

© 2007 The Authors
Journal compilation © 2007 Society for Applied Microbiology and Blackwell Publishing Ltd,

purple sulfur bacterium *Allochromatium vinosum*. *Arch Microbiol* **176:** 301–305.
Schippers, A. (2004) Biogeochemistry of metal sulfide oxidation in mining environments, sediments and soils. In *Sulfur Biogeochemistry – Past and Present*. Amend, J.P., Edwards, K.J., and Lyons, T.W. (eds). Boulder, Colorado, USA: Geological Society of America, pp. 49–62.
Shen, Y., Knoll, A.H., and Walter, M.R. (2003) Evidence for low sulphate and anoxia in a mid-Proterozoic marine basin. *Nature* **423:** 632–635.
Shen, Y.N., and Buick, R. (2004) The antiquity of microbial sulfate reduction. *Earth Sci Rev* **64:** 243–272.
Simsek, M., and Adnan, H. (2000) Effect of single mismatches at 3′-end of primers on polymerase chain reaction. *Med Sci* **2:** 11–14.
Sorokin, D.Y. (2003) Oxidation of inorganic sulfur compounds by obligately organotrophic bacteria. *Microbiology* **72:** 641–653.
Takai, K., Campbell, B.J., Cary, S.C., Suzuki, M., Oida, H., Nunoura, T., *et al.* (2005) Enzymatic and genetic characterization of carbon and energy metabolisms by deep-sea hydrothermal chemolithoautotrophic isolates of *Epsilonproteobacteria*. *Appl Environ Microbiol* **71:** 7310–7320.
Takai, K., Suzuki, M., Nakagawa, S., Miyazaki, M., Suzuki, Y., Inagaki, F., and Horikoshi, K. (2006) *Sulfurimonas paravinellae* sp. nov., a novel mesophilic, hydrogen- and sulfur-oxidizing chemolithoautotroph within the *Epsilonproteobacteria* isolated from a deep-sea hydrothermal vent polychaete nest, reclassification of *Thiomicrospira denitrificans* as *Sulfurimonas denitrificans* comb. nov. and emended description of the genus *Sulfurimonas*. *Int J Syst Evol Microbiol* **56:** 1725–1733.
Teske, A., and Nelson, D.C. (2004) The genera *Beggiatoa* and *Thioploca*. In *The Prokaryotes: An Evolving Electronic Resource for the Microbial Community*. Dworkin, M., Falkow, E., Rosenberg, E., Schleifer, K.-H., and Stackebrandt, E. (eds). [WWW document]. URL http://link.springer-ny.com/link/service/books/10125/index.htm.
Zopfi, J., Ferdelman, T.G., and Fossing, H. (2004) Distribution and fate of sulfur intermediates– sulfite, tetrathionate, thiosulfate, and elemental sulfur – in marine sediments. In *Sulfur Biogeochemistry – Past and Present*. Amend, J.P., Edwards, K.J., and Lyons, T.W. (eds). Boulder, Colorado, USA: Geological Society of America, pp. 97–116.

Supplementary material

The following supplementary material is available for this article online:

Table S1. SoxB alignment showing indels among selected representatives of the major phylogenetic SOB lineages, supporting the inferred relationships including the postulated LGTs of *soxB* among the investigated SOB species. Amino acid positions according to the enumeration of *Paracoccus denitrificans* str. GB17 proteins. Identical indel positions in SoxB sequences are indicated by boxes.

This material is available as part of the online article from http://www.blackwell-synergy.com

© 2007 The Authors
Journal compilation © 2007 Society for Applied Microbiology and Blackwell Publishing Ltd,

Supplementary Material

Supplementary Table S1. SoxB alignment showing indels among selected representatives of the major phylogenetic SOB lineages supporting the inferred relationships including the postulated LGTs of *soxB* among the investigated SOB species. Amino acid positions according to the enumeration of *Paracoccus denitrificans* str. GB17 proteins. Identical indel positions in SoxB sequences are indicated by boxes.

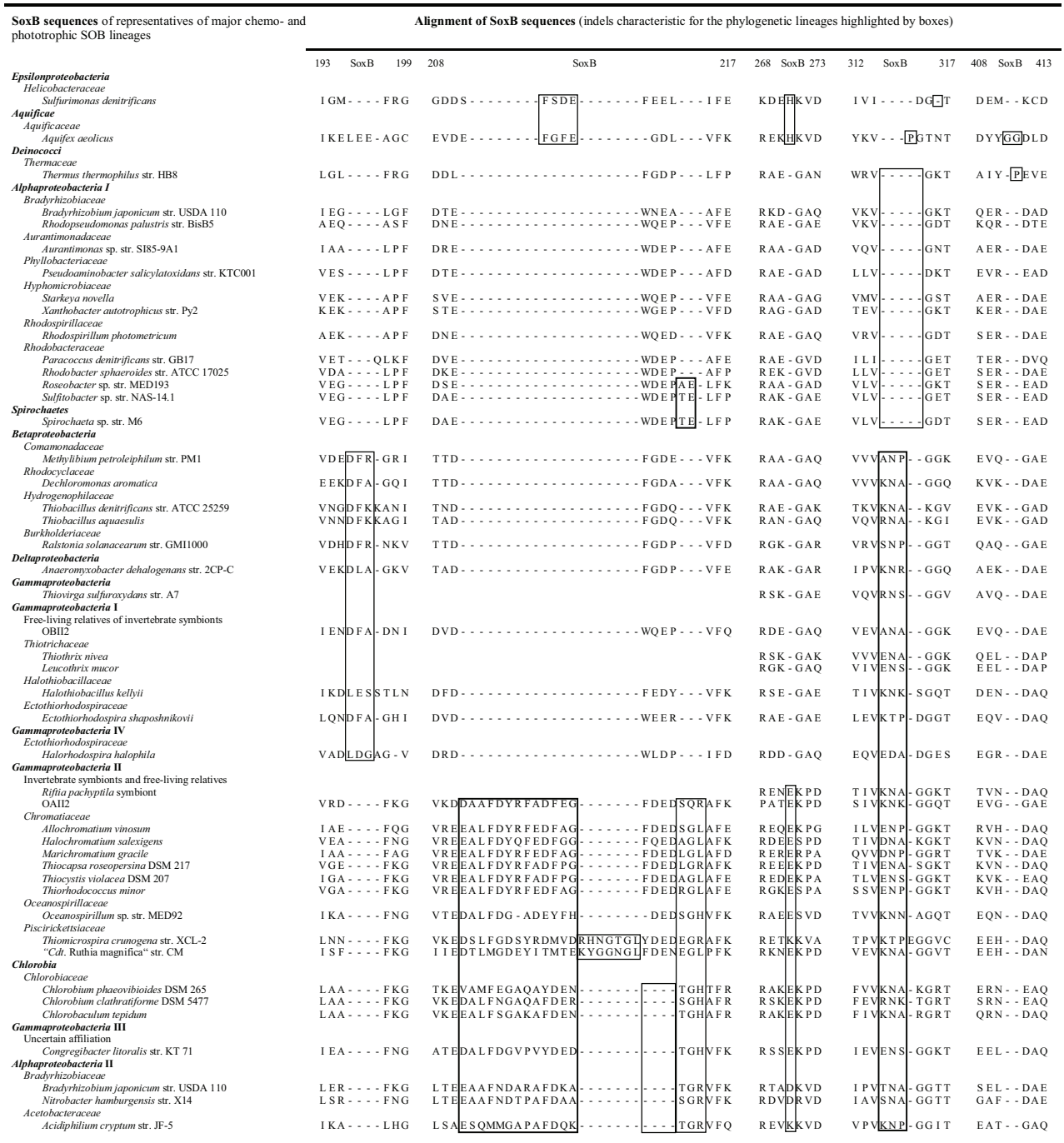

4.2.5 Publikation 5

Molecular analysis of the diversity of sulfate-reducing and sulfur-oxidizing prokaryotes in the environment, using *aprA* as functional marker gene

Birte Meyer und Jan Küver

Applied and Environmental Microbiology (2007). 73 (23), 7664-7679

APPLIED AND ENVIRONMENTAL MICROBIOLOGY, Dec. 2007, p. 7664–7679 Vol. 73, No. 23
0099-2240/07/$08.00+0 doi:10.1128/AEM.01272-07
Copyright © 2007, American Society for Microbiology. All Rights Reserved.

Molecular Analysis of the Diversity of Sulfate-Reducing and Sulfur-Oxidizing Prokaryotes in the Environment, Using *aprA* as Functional Marker Gene▽†

Birte Meyer and Jan Kuever*

Max Planck Institute for Marine Microbiology, Celsiusstrasse 1, D-28359 Bremen, Germany

Received 8 June 2007/Accepted 26 September 2007

The dissimilatory adenosine-5′-phosposulfate reductase is a key enzyme of the microbial sulfate reduction and sulfur oxidation processes. Because the alpha- and beta-subunit-encoding genes, *aprBA*, are highly conserved among sulfate-reducing and sulfur-oxidizing prokaryotes, they are most suitable for molecular profiling of the microbial community structure of the sulfur cycle in environment. In this study, a new *aprA* gene-targeting assay using a combination of PCR and denaturing gradient gel electrophoresis is presented. The screening of sulfate-reducing and sulfur-oxidizing reference strains as well as the analyses of environmental DNA from diverse habitats (e.g., microbial mats, invertebrate tissue, marine and estuarine sediments, and filtered hydrothermal water) by the new primer pair revealed an improved microbial diversity coverage and less-pronounced template-to-PCR product bias in direct comparison to those of the previously published primer set (B. Deplancke, K. R. Hristova, H. A. Oakley, V. J. McCracken, R. Aminov, R. I. Mackie, and H. R. Gaskins, Appl. Environ. Microbiol. 66:2166–2174, 2000). The concomitant molecular detection of sulfate-reducing and sulfur-oxidizing prokaryotes was confirmed. The new assay was applied in comparison with the 16S rRNA gene-based analysis to investigate the microbial diversity of the sulfur cycle in sediment, seawater, and manganese crust samples from four study sites in the area of the Lesser Antilles volcanic arc, Caribbean Sea (Caribflux project). The *aprA* gene-based approach revealed putative sulfur-oxidizing *Alphaproteobacteria* of chemolithoheterotrophic lifestyle to have been abundant in the nonhydrothermal sediment and water column. In contrast, the sulfur-based microbial community that inhabited the surface of the volcanic manganese crust was more complex, consisting predominantly of putative chemolithoautotrophic sulfur oxidizers of the *Betaproteobacteria* and *Gammaproteobacteria*.

The sulfur cycle is predominated by reductive and oxidative processes of microorganisms: the dissimilatory sulfate reduction is considered as the main anaerobic process in the biomineralization of organic matter in the environment, accounting for up to 50% of its degradation in marine sediments (29), while dissimilatory sulfur oxidation processes occur wherever reduced inorganic sulfur compounds are available from the activity of the sulfate-reducing prokaryotes or from geological sources (5, 16). The sulfate-reducing and sulfur-oxidizing prokaryotes (SRP and SOP, respectively) are phylogenetically and physiologically diverse groups (5, 16, 25, 40, 47). Their polyphyletic nature restricts the concomitant detection of all recognized members by the use of a single 16S rRNA gene-targeting probe or primer pair in environmental analyses and limits the identification of novel lineages. In addition, the 16S rRNA gene-based analysis cannot provide an unambiguous link between the genetic identity of an uncultured microorganism and its physiological or metabolic capacity. Alternative molecular approaches circumvent these limitations by using functional genes that encode key enzymes of the dissimilatory sulfate reduction and sulfur oxidation pathways (ATP sulfurylase, Sat; adenosine-5′-phosphosulfate [APS] reductase, AprBA; sulfite reductase, DsrAB) and thus are much more suited to analyze and determine the phylogenetic complexity of the microbial sulfur cycle in nature.

Indeed, PCR assays have been developed for the amplification of *dsrAB* genes, but up to now these approaches are restricted to diversity analyses of the SRP community (2, 3, 15, 42, 43, 57). Although multiple events of lateral gene transfer (LGT) have affected the Dsr phylogeny of certain SRP lineages, the usefulness of *dsrAB* as functional gene markers for environmental analysis was confirmed (32, 62, 67). Recently, new PCR assays have been developed for the amplification of the *aprBA* gene locus from SRP and sulfur-oxidizing bacteria (SOB). The ubiquitous presence of *aprBA* genes in SRP was confirmed (38); however, the PCR-based screening among SOB reference strains revealed its restricted distribution to photo- and chemotrophs with strict anaerobic or at least facultative anaerobic lifestyles, e.g., several *Chlorobiaceae* and most *Chromatiaceae* species, *Thiobacillus*, *Thiothrix*, as well as invertebrate symbionts and their free-living relatives (37). The functional role of a reverse-acting APS reductase in *apr*-possessing, aerobic members of the alphaproteobacterial SAR11 and SAR116 cluster (19) is unresolved. Phylogenetic studies revealed the occurrence of LGT events with the results showing some anoxygenic photo- and chemolithotrophic representatives (e.g., *Thiocapsa roseopersicina*, *Thiobacillus* spp.) harboring a second, SRP-related *apr* gene locus in addition to a LGT-unaffected gene locus. In some SOB species (e.g., *Thio-*

* Corresponding author. Present address: Bremen Institute for Materials Testing, Paul-Feller-Strasse 1, D-28199 Bremen, Germany. Phone: 49-(0)421-5370870. Fax: 49-(0)421-5370810. E-mail: kuever@mpa-bremen.de.

† Supplemental material for this article may be found at http://aem.asm.org/.

▽ Published ahead of print on 5 October 2007.

TABLE 1. Location and characteristics of environmental samples from habitats investigated in this study by *aprA* and 16S rRNA gene fragment analyses

Analysis type and sample name(s) from habitat	Sampling site	Position	Depth (m)	Characteristics of the habitat	Sample type(s)
Comparative *aprA* gene fragment analysis					
Spkg	Spiekeroog Island, German Wadden Sea (Germany)	Janssand region, 53°43.45′N, 7°41.80′E		Marine	Sediment surface layer
Ec2, Ec4, Ec9	Wimereux, Pas-de-Calais (France)			Marine	*Echinocardium cordatum* tissue, digestive tract
MatA, MatB, MatD	Cu-Pb-Zn Toyoha underground mine, Hokkaido (Japan)		500, 550, 550	Freshwater (53–73°C)	Terrestrial, thermophilic subsurface microbial mats
Vail	Hobo Springs, Vail, CO			Freshwater (50°C)	Terrestrial hot spring, surface water
Vilm	Vilm Island, Baltic Sea (Germany)	54°21′N, 13°28′E		Brackish water, estuarine	Sediment surface layer
HR28Begg	Hydrate Ridge, Cascadia margin, OR	44°34.19′N, 125°08.81′W	777	Marine	*Beggiatoa* field, microbial mats
HS2, HS3, HS7, HS8	Mono Lake, CA		17.5–28	Hypersaline (84–95 g liter^{-1}), alkaline	Sulfidogenic and methanogenic enrichment cultures from water column
Comparative *aprA* and 16S rRNA gene fragment analysis					
KB-Sed	Kahouanne Basin, Lesser Antilles, Caribbean Sea	Station 15MC, 16°28.83′N, 61°58.81′W	1,133	Marine	Sediment surface layer, enrichment cultures
MR-Sed	Montserrat Ridge, Lesser Antilles, Caribbean Sea	Station 49MC, 16°39.51′N, 62°20.22′W	978	Marine	Sediment surface layer, enrichment cultures
MR-MnCr	Montserrat Ridge, Lesser Antilles, Caribbean Sea	Station 52CD, 16°38.85′N, 62°19.97′W begin; 16°37.40′N, 62°19.69′W end	619–950	Marine	Manganese crust surface, enrichment cultures
SLB-W	St. Lucia Bay, Lesser Antilles, Caribbean Sea	Station 99CTD, 13°51.16′N, 61°04.15′W	82	Marine	Filtered seawater (15 liters), enrichment cultures

cystis violascens), only the LGT-derived gene copy is present due to loss of the authentic gene (37). The previous analyses allowed the establishment of a comprehensive AprBA database covering most of the genus level diversity of SRP and *apr*-harboring SOB which provides a high-resolution framework for the assignment of environmentally retrieved gene sequences in molecular ecological studies. Comparative sequence analyses confirmed the reductive- and oxidative-type APS reductases to be highly conserved among SRP and SOB. Although affected by several LGT events involving representatives of SRP and SOB lineages, the *aprBA* genes have in general been transmitted vertically during evolution, which supports their usage as functional gene markers in microbial diversity surveys (37, 38). Astonishingly, the genes have only been employed by two medical studies to assess the SRP biodiversity in human tissue (13, 65).

In this study, we present a new assay for the functional *aprA* gene analysis using a combination of PCR and double-gradient denaturing gradient gel electrophoresis (DG-DGGE). The species diversity coverage of the new *aprA* gene-targeting primer set is evaluated in comparison with a previously published one (13) by phylogenetic investigation of SRP and SOB reference strains as well as several environmental samples derived from distinct habitats (sediment, filtered seawater, microbial mats, and invertebrate tissue). The *aprA* gene analysis allowed the simultaneous determination of the environmental SRP and SOB diversity, in contrast to the published *dsrAB*-based assays (32, 62). Finally, the assay was applied to investigate the sulfate-reducing and sulfur-oxidizing microbial communities inhabiting deep-sea sediment, seawater, and manganese crust samples of the volcanic arc of the Lesser Antilles, Caribbean Sea (Caribflux project); the work is complemented with 16S rRNA gene analyses and SRP and SOB cultivation studies.

MATERIALS AND METHODS

Microorganisms. The investigated SRP and SOB reference strains were either obtained from the Deutsche Sammlung von Mikroorganismen und Zellkulturen (DSMZ) or provided by others as described in Table S1 in the supplemental material.

Study sites and sampling from the Caribbean Sea. Sediment, seawater, and manganese crusts samples were collected from the volcanic arc of the Lesser Antilles, Caribbean Sea, during the RV Sonne cruise SO-154 (15 January to 8 February 2001) (Table 1). The deep-sea sediment cores and manganese crusts of the Kahouanne Basin (KB) and Montserrat Ridge (MR) were obtained by a multiple corer and a chain bag dredge, respectively. The cores were immediately subsampled by slicing the extruded sediment at 2-cm intervals. Fifteen liters of surface seawater was sampled from the photic water zone near St. Lucia Bay (SLB) by a rosette water sampler and subsequently filtered with Sterivex (pore size, 0.2 μm; Millipore) to collect the pelagic microbial community. For further molecular analyses, the sample material was immediately frozen and stored at −20°C until DNA extraction.

MPN counts. Most probable number (MPN) counts were performed for SRP and SOB by preparing liquid MPN dilution series with media defined for sulfate-reducing and aerobic, thiosulfate-oxidizing bacteria with 1:10 steps as described elsewhere (49). The MPN dilution series were inoculated in parallel with 1 ml of suspended sediment and filtered seawater samples of the Caribbean Sea. Lactate (10 mM), butyrate (5 mM), and propionate (5 mM) were added as carbon sources to the SRP-defined medium.

DNA isolation. Genomic DNAs from the SRP and SOB reference strains and the enrichment cultures of the MPN series were obtained by using a DNAeasy kit (Qiagen, Hilden, Germany) according to the manufacturer's instructions. Total

TABLE 2. *aprA* gene-targeting primers and thermocycling conditions[a] used in the PCR assays

Primer	Sequence (in 5′→3′ direction)	Primer binding site[b]
New primer set		
AprA-1-FW	TGG CAG ATC ATG ATY MAY GG	1236–1256
AprA-5-RV	GCG CCA ACY GGR CCR TA	1615–1631
Modified Deplancke primer set		
AprA-3-FW	TGG CAG ATM ATG ATY MAC GG[c]	1236–1256
APS-RV	GGG CCG TAA CCG TCC TTG AA	1602–1623
GC clamp	CGC CCG CCG CGC CCC GCG CCC GGC CCG CCG CCC CCG CCC G	

[a] PCR thermocycling conditions: initial denaturation step for 5 min at 95°C; followed by 20 cycles of denaturing for 60 s at 95°C, annealing for 60 s at 60 to 50°C ("touchdown" PCR, −0.5°C every new cycle), and elongation for 90 s at 72°C; followed by 15 cycles of 60 s at 94°C, 60 s at 50°C, and 90 s at 72°C; followed by a 10-min final extension step.

[b] Corresponding nucleotide positions of the *aprBA* operon of *Desulfovibrio vulgaris* subsp. *vulgaris* strain Hildenborough (GenBank accession no. Z69372).

[c] AprA-3-FW lacks the false third G at the 3′ end of the primer APS-FW published by Deplancke et al. (13).

environmental DNAs from (i) filtered seawater (SLB), (ii) the 0- to 2- and 4- to 6-cm horizons of the sediments (KB and MR), and (iii) the manganese crust (MR) were extracted in duplicate using a modified version of the original protocol of Zhou et al. (64) (five cycles of freezing [liquid nitrogen] and thawing [at 30°C] of either 2 g of sediment/manganese crust or one filter [in 5.4 ml of the extraction buffer] were included before starting the extraction procedure). Environmental DNAs from (i) the surface sediments of an intertidal sand flat from "Janssand" on Spiekeroog Island, German Wadden Sea, and of a coastal (reed-covered) area from Vilm Island, Baltic Sea, (ii) microbial mats collected from the thermophilic subsurface environment of the Toyoha Mine, Japan, (iii) filtered water of a hydrothermal spring from Vail, CO, (iv) sulfido- and methanogenic enrichment cultures of anoxic bottom waters of Mono Lake, CA, (v) microbial mats of cold-seep *Beggiatoa* fields at the Hydrate Ridge, Cascadia margin, OR, and (vi) tissue material of *Echinocardium cordatum* (Table 1) were kindly provided by M. Mussmann, J. Kuever, M. Fukui, J. C. M. Scholten, T. Treude, and S. Gomes da Silva, respectively (see references 20, 28, 34, 42, 48, and 58 for descriptions of sample collection and the DNA extraction procedures). The quality of the isolated DNAs was verified by PCR amplification of the 16S rRNA gene using the primer set GM3F/GM4R and PCR protocol as described by Muyzer et al. (41). The extracted DNAs (dissolved in 10 mM Tris-HCl, 1 mM EDTA, pH 7.5) were stored at −20°C until further molecular analysis.

PCR amplification of partial *aprA* and 16S rRNA genes for DGGE analysis. A modified version of the primer set AprA-3-FW/APS-RV, published by Deplancke et al. (13), and a new primer set, AprA-1-FW/AprA-5-RV, were used to amplify an approximately 0.4-kb *aprA* gene fragment for subsequent DGGE analysis (GC clamp added to the reverse primers) (Table 2). PCR assays were performed with a RED*Taq* DNA polymerase kit from Sigma-Aldrich (St. Louis, MO). Reaction mixtures (50 μl total volume) contained 5 μl 10× RED*Taq* PCR buffer (with 11 mM $MgCl_2$), 5 μl 10× bovine serum albumin solution (3 mg/ml), 200 μM deoxynucleoside triphosphates mixture, 1 μM each primer, and 100 ng genomic DNA as template (10 and 100 ng environmental DNA were used in the assays). "Hot start" PCR was performed in a thermocycler (Eppendorf, Hamburg, Germany) followed by a "touchdown" PCR protocol as described in Table 2.

Partial 16S rRNA gene amplification from environmental DNAs for subsequent DGGE analysis was performed using the primer sets (i) GM5F (341F) with a GC clamp and 907R for *Bacteria* (41) and (ii) Arch516F with a GC clamp (K. Knittel, unpublished data) and Arch958R for *Archaea* (11), following the respective PCR protocols of the former authors.

The PCR products were visually analyzed by electrophoresis of aliquots (10% of the reaction volume) on a 2% (wt/vol) agarose gels run in 1× Tris-borate-EDTA buffer stained with ethidium bromide (0.5 mg $liter^{-1}$) to verify correct amplicon size. Prior to further analysis, the amplicons of the expected gene fragment size were purified using either a QIAquick gel extraction kit (Qiagen, Hilden, Germany) or a Perfectprep gel cleanup sample kit (Eppendorf, Hamburg, Germany) following the supplier's recommendations.

DG-DGGE analysis of PCR-amplified *aprA* and 16S rRNA gene fragments. DG-DGGE analyses (10) of the mixed-template *aprA* and 16S rRNA gene PCR products were performed using the D-GENE and D-CODE systems (Bio-Rad, München, Germany). For *aprA* gene fragment analysis, DG-DGGE gels (1.0-mm thick) were poured with an acrylamide gradient from 6 to 8% acrylamide/bis-acrylamide stock solution, 37.5:1 (vol/vol) (Bio-Rad), superimposed over a co-linear denaturant gradient from 30 to 60% of denaturant (100% denaturant corresponds to 7 M urea and 40% formamide [vol/vol], deionized with AG501-X8 mixed bed resin [Bio-Rad]). For 16S rRNA gene analysis, DG-DGGE gels (1.0 mm thick) consisted of a 6 to 8% acrylamide gradient superimposed over a colinear 20 to 70% denaturant gradient. Gradients were formed using a Bio-Rad gradient former model 385. Twenty microliters of PCR product was mixed with 6 μl of dye solution (0.1% bromphenol blue [wt/vol], 70% [vol/vol] glycerol) and applied to the gels. The DG-DGGE electrophoresis runs were performed (i) for 2 h at 150 V and subsequently for 2 h at 200 V (*aprA* gene fragment) and (ii) for 3.5 h at a constant voltage of 200 V (16S rRNA gene fragment) using 1× Tris-acetate-EDTA as buffer and a constant temperature of 60°C. After gel electrophoresis, the gels were stained for 15 min with ethidium bromide (0.5 mg $liter^{-1}$) and rinsed for 10 min in Milli Q water. The DNA bands were visualized on a UV transillumination table (Biometra, Göttingen, Germany); persisting and dominant bands were excised from the polyacrylamide gel by a scalpel, eluted in 50 μl Tris-HCl, pH 8.0, and reamplified using 1 μl of the eluate as template and PCR conditions as described above. The purity and migration behavior of the reamplification products of the DGGE bands were checked by DG-DGGE. The reamplification products were purified from free PCR primers using either a QIAquick gel extraction kit (Qiagen) or a Perfectprep gel cleanup sample kit (Eppendorf) following the suppliers' recommendations.

Nucleotide sequencing. The reamplification products of the DG-DGGE bands were sequenced directly in both directions using the respective *aprA* and 16S rRNA gene amplification primers and an ABI Prism BigDye terminator cycle sequencing ready reaction kit (Applied Biosystems, Foster City, CA) according to the manufacturer's instructions. Sequencing reactions were run on an ABI PRISM 3100 genetic analyzer (Applied Biosystems).

Comparative analysis of the environmentally derived, partial *aprA* and 16S rRNA sequences. The partial 16S rRNA sequences obtained from DGGE analysis were checked using the program CHECK_CHIMERA from the Ribosomal Database Project for detection of chimeric artifacts. The sequence data of each DGGE band were then added into the 16S rRNA sequence database of the Technical University Munich, Germany, using the software program package ARB (http://www.arb-home.de), and the data were assembled and first aligned automatically with the ARB_Align tool; the alignment was then manually corrected. The operational taxonomic units (OTUs) were compared to the GenBank database by the BLAST analysis tools of the National Centre for Biotechnology Information (www.ncbi.nlm.nih.gov/BLAST/) in order to determine their phylogenetic affiliation and to identify their closest phylogenetic relatives.

The *aprA* sequence data obtained from DGGE analysis were assembled and manually corrected using the BioEdit sequence alignment editor (version 7.0.5) (http://www.mbio.ncsu.edu/BioEdit/bioedit.html). The deduced, partial AprA sequences of the environmental samples were implemented into the persisting AprBA alignment of SRP and SOB references strains (see the introduction), including all full-length Apr sequences available from the public databases. The AprA data sets were phylogenetically analyzed with the tree inference methods included in the ARB software package and PHYLIP. Regions of ambiguous homology as well as insertions and deletions (indels) were excluded, yielding a final data set of 110 compared amino acid positions. Unrooted phylogenetic trees were calculated based on 411 sequences by performing distance matrix (neighbor-joining), maximum-parsimony, and maximum-likelihood analyses. The global rearrangement and randomized species input order options as well as the JTT matrix as an amino acid replacement model were used in the phylogenetic analysis.

GenBank accession numbers. The nucleotide sequence data are available under the GenBank accession numbers EF614307 to EF614329 (archaeal 16S rRNA), EF614394 to EF614449 (bacterial 16S rRNA), and EF618618 to EF618673 and EF633037 to EF633105 (*aprA*).

RESULTS

In this study, the application of a new *aprA* gene-targeting primer pair (AprA-1-FW/AprA-5-RV) is described for SRP and SOB biodiversity surveys. Prior to environmental analysis, the species coverage and amplification behavior were evaluated and compared to the modified (corrected) version (AprA-3-FW/APS-RV) of a previous primer set published by Deplancke et al. (13); both primer pairs target nearly the same conserved gene region.

Species coverage: PCR amplification results of the new *aprA* gene-targeting primer pair from reference strains. By using DNA templates from single SRP and SOB reference strains in the PCR assays, no 0.4-kb *aprA* amplicon was obtained with AprA-3-FW/APS-RV (with a GC clamp) from the thermophilic sulfate reducer lineages, from several members of the *Desulfobulbaceae*, *Desulfobacteraceae*, *Syntrophobacteraceae*, and the *Desulfobacterium anilini*-related groups, nor from some *Desulfotomaculum* and *Desulfosporosinus* spp., *Desulfobacca acetoxidans*, *Caldivirga maquilingensis*, and some *aprBA* gene-containing, sulfur oxidizer lineages of the *Gammaproteobacteria*. In contrast, the new primer pair allowed the amplification of correct-sized PCR products from SRP and SOB of a wider phylogenetic range (amplification results are summarized in Table S1 and Fig. S1 in the supplemental material), reflecting its improved species coverage compared to the previous set. Nevertheless, we were still unable to yield amplicons from the *Desulfosporosinus* spp. tested, which might have been caused by inhibited primer annealing (caused by differential codon usage and/or unusual amino acid substitutions in the target sequence). Indeed, the comparison of the primer sequences to the novel *apr* database revealed the presence of single mismatches of AprA-1-FW and AprA-5-RV with *apr* sequences of, e.g., *Desulfotomaculum* spp. (subcluster Ia), *Desulfobacteraceae*, and some representatives of sulfur-oxidizing *Alphaproteobacteria* and *Gammaproteobacteria*. However, the presence of single mismatches at internal or 5′-end sequence positions in the new PCR primers did not affect their PCR efficiency, as it has been demonstrated for 16S rRNA gene-targeting primers (35, 50). In contrast, the presence of several mismatches at the 3′ ends of AprA-3-FW and APS-RV inhibited an efficient annealing and elongation in the PCR assays and thus caused the limited species coverage of this primer set.

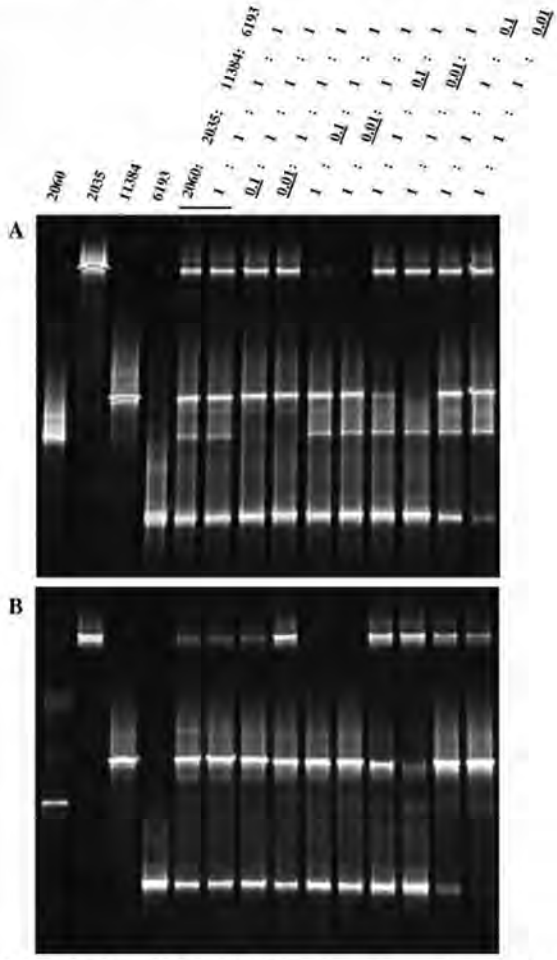

FIG. 1. Preferential amplification of *aprA* gene fragments from defined genomic DNA ratio mixtures of the four SRP species *Desulfosarcina variabilis* (DSM 2060), *Desulfobacter* sp. (DSM 2035), *Desulfovibrio profundus* (DSM 11384), and *Desulfotomaculum thermobenzoicum* (6193) by the primer sets used for DGGE analysis. (A) Primer set AprA-1-FW/AprA-5-RV (GC clamp). (B) Primer set AprA-3-FW/APS-RV (GC clamp). In the PCR assays, the DNA concentration of each SRB species was varied to mixing ratios of 1:1, 1:0.1, or 1:0.01.

Preferential amplification: PCR amplification results of the new *aprA* gene-targeting primer from defined DNA template ratio mixtures by DG-DGGE analysis. The *aprA* gene-based approach may suffer from the same methodical constraints as reported for the 16S rRNA gene amplification of mixed-template PCR assays (46, 61), which bias the coverage of phylotypes relative to the original microbial communities they were derived from. To evaluate the template-to-PCR product bias introduced by preferential amplification of certain target sequences, assays were performed using defined template mixtures of genomic DNA from four different SRP reference strains (*Desulfosarcina variabilis*, *Desulfobacter* sp. strain DSM 2035, *Desulfovibrio profundus*, and *Desulfotomaculum thermobenzoicum*). The DNA concentration of each SRP species was varied to yield relative template mixing ratios of 1:1:1:1, 1:1:1:0.1, or 1:1:1:0.01 in the PCR assays. The denaturing gradient analysis of the obtained mixed-template amplicons indicated that although the AprA-1-FW/AprA-5-RV(GC) primer set appeared to preferentially amplify *D. thermobenzoicum* (see band intensities on the DGGE gels, Fig. 1), the *aprA* gene fragments of the remaining SRP species were amplified and detectable in the gels even when the DNA template ratio of one species is only 1:10 relative to the other ones (Fig. 1A). In contrast, the primer pair AprA-3-FW/APS-RV(GC) preferentially amplified *D. profundus*, leaving only the amplicon of *D. thermobenzoicum* detectable when the DNA template ratio declined to 1:10 (relative to *D. profundus*) in the defined mixtures (Fig. 1B). The *aprA* gene fragment of *D. variabilis* was only amplified when its template ratio was above 100:1 relative to *D. profundus*. Thus, the bias introduced by preferential amplification of certain *aprA* phylotypes appears to be less pronounced with the new primer pair of this study, which is demonstrated by the

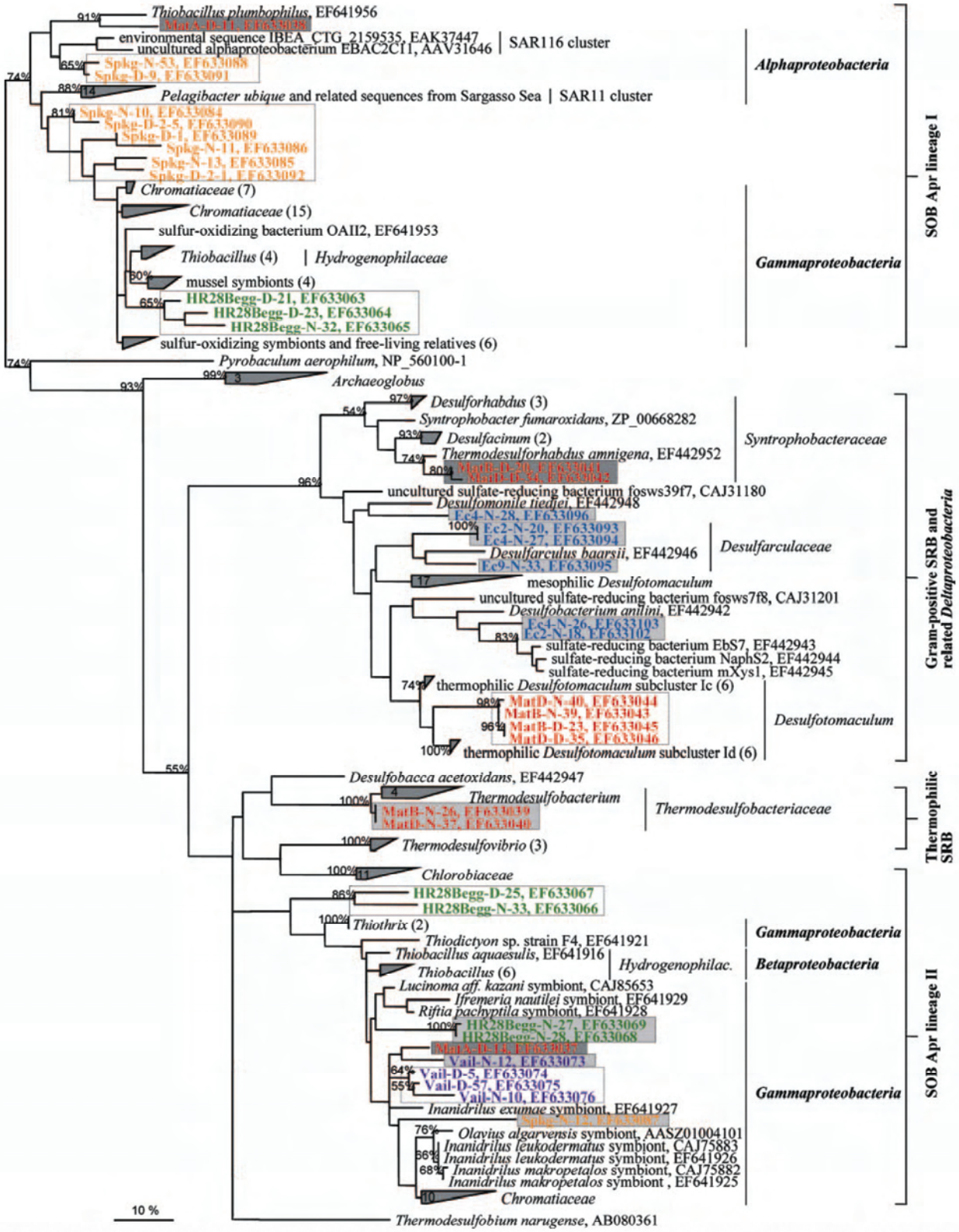

FIG. 2. Phylogenetic tree based on 411 SRP/SOB reference strain and environmentally derived partial AprA sequences. The tree was inferred using the maximum-likelihood method. Sequences of the SOB Apr lineage I and *Pyrobaculum aerophilum* were used as outgroup references. The 16S rRNA gene-based taxonomic classification of SOB and SRP reference strains is indicated. The environmental AprA sequences are highlighted in boldface type and colored according to the habitat they were retrieved from (Spiekeroog Island, orange [Spkg]; Toyoha Mine, red [MatA/B/D]; Hydrate Ridge, green [HR28Begg]; *Echinodermata cordatum*, blue [Ec2, -4, -9]; Mono Lake, yellow [HS2, -3, -7, -8]; Vilm Island, brown; Vail, violet). The environmental AprA sequences received with primer set AprA-3-FW/APS-RV are termed with a "D" while those obtained with the new primer set AprA-1-FW/AprA-5-RV are termed with a "N" in the sequence name. For comparison of the microbial diversity coverage of both

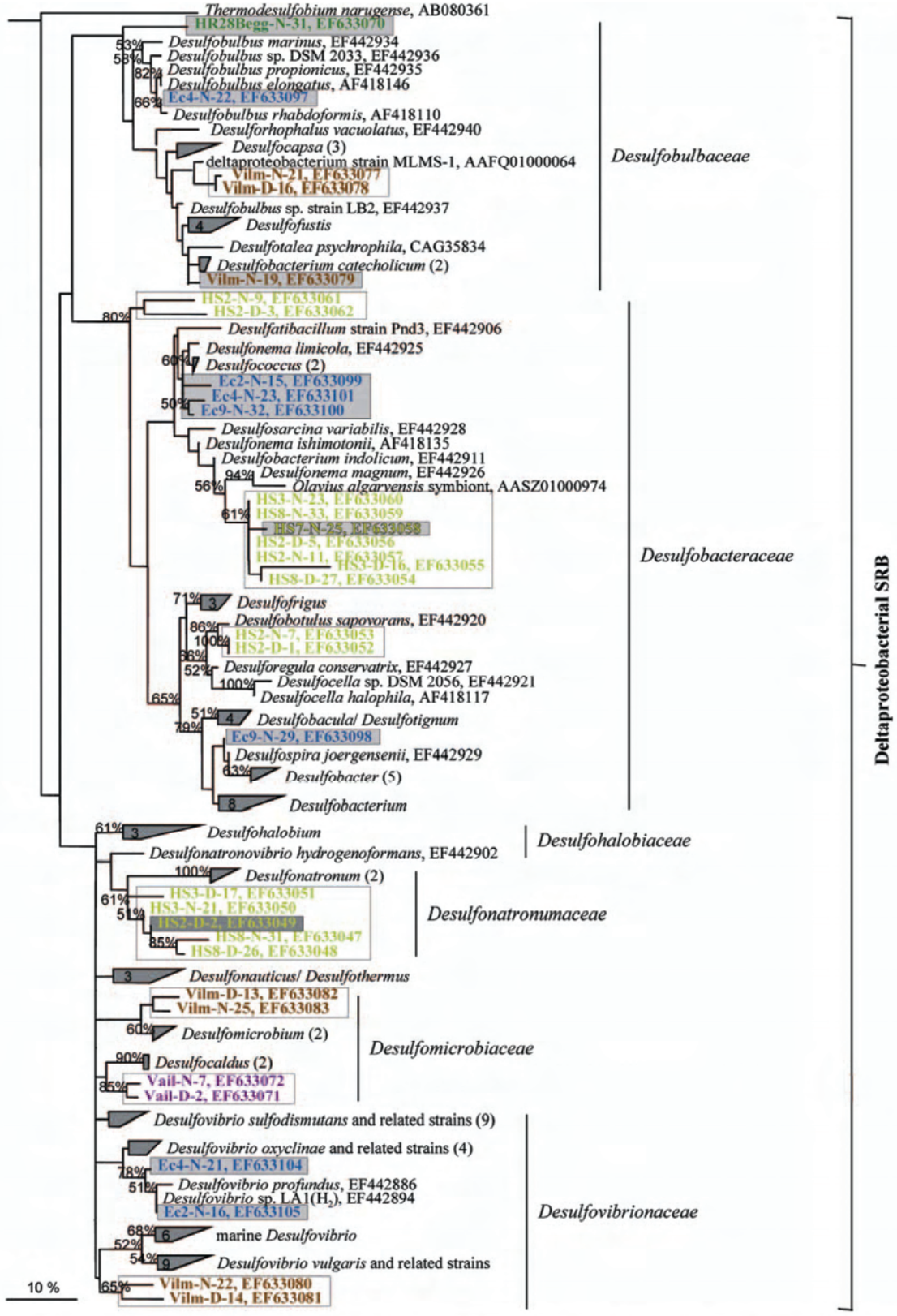

aprA gene-targeting primer pairs, identical phylotypes detected with both primer pairs are marked with open boxes, whereas those phylotypes that were obtained with only one primer pair are highlighted by dark gray (AprA-3-FW/APS-RV) and light gray (AprA-1-FW/AprA-5-RV) shaded boxes. The scale bar corresponds to 10% estimated sequence divergence.

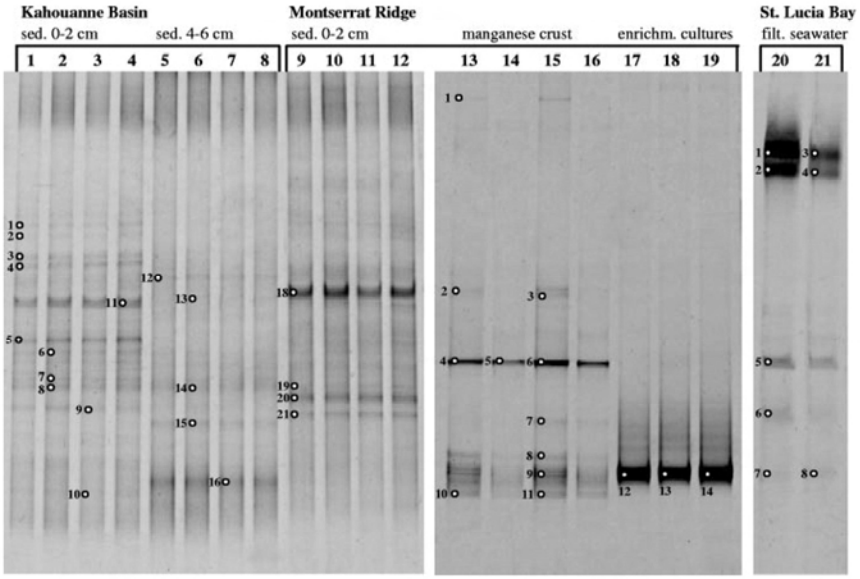

FIG. 3. DGGE analysis of *aprA* gene fragments (amplified with primer pair AprA-1-FW/AprA-5-RV) using DNA samples from sediment (sed.), manganese crust, and seawater of the Caribbean Sea as templates. Lanes 1 to 8, DNA samples from Kahouanne Basin sediment (horizon 0 to 2 cm, lanes 1 to 4; horizon 4 to 6 cm, lanes 5 to 8); lanes 9 to 12, DNA samples from Montserrat Ridge sediment (horizon 0 to 2 cm); lanes 13 to 16, DNA samples from Montserrat Ridge manganese crust; lanes 17 to 19, DNA samples from aerobic sulfur oxidizer enrichment (enrichm.) cultures inoculated with manganese crust; lanes 20 and 21, DNA samples from St. Lucia Bay filtered (filt.) seawater. Bands indicated with numbers were excised from the gels and sequences.

improved congruence between PCR-detected diversity coverage and actual genetic diversity of SRP in the defined multitemplate mixtures as an example for environmentally derived DNA.

Evaluation of the microbial diversity coverage of the new *aprA* gene-targeting primer by comparative phylogenetic analysis of different habitats. The microbial diversity coverage of the new *aprA* gene-targeting primer pair was evaluated and compared to that of the modified Deplancke primer set by exploring the environmental community composition of seven divergent habitats (listed in Table 1). The phylogenetic analysis of the received AprA phylotypes revealed congruent results obtained with both primer pairs (marked by open boxes in Fig. 2) for most investigated environmental samples. However, the new primer pair appeared to be generally superior with regard to the environmental SRP and SOB diversity coverage, since several additional phylotypes were only identified by applying AprA-1-FW/AprA-5-RV(GC) in the PCR assays (highlighted by light-gray shaded boxes in Fig. 2). These encompass OTUs related to, e.g., (i) thiotrophic gammaproteobacterial symbionts of *Oligochaeta*, e.g., *Inanidrilus* (Spiekeroog Island, oxic sediment surface layer), (ii) *Desulfobacterium catecholicum* (estuarine area on Vilm Island, anoxic sediment surface layer), (iii) *Desulfonema magnum* (water column of the hypersaline, alkaliphilic Mono Lake, methanogenic enrichment culture HS7), (iv) thiotrophic gammaproteobacterial symbionts of invertebrates and *Desulfobulbaceae* (Hydrate Ridge, Cascadia margin, microbial mats of cold-seep *Beggiatoa* fields), and (v) *Desulfonema limicola*, *Desulfarculus baarsii*, "*Desulfobacterium anilini*," *Desulfomonile tiedjei*, *Desulfospira joergensenii*, *Desulfobulbus rhabdoformis*, and *Desulfovibrio* subspecies (*Echinocardium cordatum* specimen, nodules of the digestive tract). From the latter tissue samples, no *aprA* amplicon was even obtained using the modified Deplancke primer pair. The received AprA phylotype diversity from the subsurface microbial mats of Toyoha Mine was different for both primer sets, despite generally low microbial diversity present (42). Besides their consistent detection of thermophilic *Desulfotomaculum* (subclusters Ic/d) in MatB and MatD, the *Thermodesulforhabdus*- and *Thermodesulfobacterium*-related OTUs were obtained when applying either the modified or the new primer pair. The *Thiobacillus plumbophilus* (Apr lineage I) and thiotrophic *Oligochaeta* symbiont (Apr lineage II) relatives were only identified in mat A with the modified Deplancke primer set (highlighted by dark-gray shaded boxes in Fig. 2).

Irrespective of the inference method used, the tree topologies calculated on the basis of the partial AprA sequences and the entire AprBA data set of SRP and SOB reference strains (see the introduction) were highly similar. This confirms that the smaller data set is applicable for the calculation of AprA-based trees and the phylogenetic assignment of environmental AprA sequences. However, as indicated by the low bootstrap values and multifurcations within, e.g., the gamma- and betaproteobacterial SOB group of Apr lineage I or the *Desulfovibrionales*, the limited capacity of phylogenetic information of the partial AprA sequence is insufficient for higher-level resolutions in certain major phylogenetic groups.

16S rRNA and *aprA* gene-based analysis: microbial communities of the sulfur cycle from sediment, manganese crust, and seawater samples of the Caribbean Sea. The microbial communities of the sulfur cycle at four study sites in the area of the Lesser Antilles volcanic arc (Table 1) was explored by molecular and cultivation approaches. Because of its improved coverage of environmental species diversity, only the new *aprA*

TABLE 3. List of phylogenetic affiliations of 16S rRNA partial sequences obtained from DGGE bands of environmental samples and enrichment cultures from the Caribbean Sea (collected in January 2001)[a]

Investigated study site and environmental sample names	Major phylogenetic group	DGGE band(s) (ID no.)	Closest phylotype/species (acc. no.)	Sim. (%)	Remarks on closest phylotype/relative
Kahouanne Basin					
Sediment 0–2 cm	*Crenarchaeota*	KB-Sed-A3	Uncultured archaeon clone Napoli-2A-11 (AY592231)	98	Environmental sample from sediments of Napoli mud volcano, Eastern Mediterranean, 1,910 m depth
		KB-Sed-A4	"*Candidatus* Nitrosopumilus maritimus" (DQ085097)	98	Isolated from a tropical seawater tank, ammonia-oxidizing marine archaeon
		KB-Sed-A33	Uncultured archaeon clone Urania-1A-36 (AY627460)	98	Environmental sample from sediments of a mound near Urania brine lake, Eastern Mediterranean, 3,442 m depth
	Gammaproteobacteria	KB-Sed-B15	Uncultured bacterium isolate JH12_C30 (AY568871)	89	Environmental marine sample
		KB-Sed-B14, KB-Sed-B16, KB-Sed-B21	Uncultured gammaproteobacterium clone BNT-33–01 (AY240721)	90	Environmental marine sample from cold-seep sediment, Nankai Trough
	Deltaproteobacteria	KB-Sed-B4	Uncultured deltaproteobacterium Artic95c95C-5 (AF355039)	99	Environmental marine sample from Artic Ocean, SAR324 cluster
	Bacteroidetes	KB-Sed-B13	Uncultured *Bacteroidetes* bacterium clone PLY-P3–5 (AY354804)	90	Environmental sample from coastal seawater (*Bacteroidetes* "AGG58 cluster")
Sediment 4–6 cm	*Crenarchaeota*	KB-Sed-A5, KB-Sed-A6, KB-Sed-A11	Uncultured archaeon clone Urania-1A-01 (AY627426)	98	Environmental sample from sediments of a mound near Urania brine lake, Eastern Mediterranean, 3,442 m depth
		KB-Sed-A7	Uncultured archaeon clone Urania-1A-36 (AY627460)	99	Environmental sample from sediments of a mound near Urania brine lake, Eastern Mediterranean, 3,442 m depth
	Gammaproteobacteria	KB-Sed-B24	Uncultured bacterium clone A59 (AY373414)	94	Environmental sample from deep-sea sediments of Western Pacific
	Low G+C gram positive	KB-Sed-B25	Uncultured low G+C gram-positive bacterium clone AT-s30 (AY225657)	90	Environmental marine sample from hydrothermal sediment of Mid-Atlantic Ridge
Enrichment culture					
Aerobic SOB	*Alphaproteobacteria*	KB-Sed-B11	*Pelagibaca bermudensis* (DQ178660)	99	Isolated from the Bermuda Atlantic Time Series Station, Sargasso Sea
		KB-Sed-B12	Uncultured *Sphingomonas* sp. clone JL-ECS-C44	99	Environmental marine sample, East China Sea
	Gammaproteobacteria	KB-Sed-B9, KB-Sed-B10	Uncultured gammaproteobacte- rium clone BNT-33–01 (AY240721)	90	Environmental marine sample from cold-seep sediment, Nankai Trough
SRB Lactat	*Deltaproteobacteria*	KB-Sed-B30	*Desulfovibrio* sp. strain M2 (AY786352)	97	Marine SRB strain
Montserrat Ridge					
Sediment 0–2 cm	*Crenarchaeota*	MR-Sed-A8, MR-Sed-A9	"*Candidatus* Nitrosopumilus maritimus" (DQ085097)	99	Isolated from a tropical seawater tank, ammonia-oxidizing marine archaeon
		MR-Sed-A10	Uncultured archaeon 19a-5 (AJ294876)	94	Environmental sample from sediments of Milos, Aegean Sea
		MR-Sed-A12	Uncultured archaeon 42-AB6 (AJ867792)	95	Environmental sample from sediments of Peru margin, ODP Leg 201, site 1229
		MR-Sed-A36	Uncultured archaeon clone ODP1227A17.06 (AB177004)	97	Environmental sample from sediments of Peru margin, ODP Leg 201, site 1227
	Gammaproteobacteria	MR-Sed-B40	Uncultured bacterium isolate JH10_C50 (AY568804)	96	Environmental marine sample

Continued on following page

TABLE 3—*Continued*

Investigated study site and environmental sample names	Major phylogenetic group	DGGE band(s) (ID no.)	Closest phylotype/species (acc. no.)	Sim. (%)	Remarks on closest phylotype/relative
	Deltaproteobacteria	MR-Sed-B36	Uncultured deltaproteobacterium clone Therm30-D12	92	Environmental sample from oxic surface sediments of Eastern Mediterranean Sea
	Bacteroidetes	MR-Sed-B35	Uncultured bacterium clone FEMidBac47 (AY769022)	91	Environmental sample from sulfide- and methane-rich cold seep, Florida
	Acidobacteria	MR-Sed-B39	Uncultured *Acidobacteriaceae* bacterium clon VHS-B5–22 (DQ395041)	99	Environmental sample from sediment, Victoria Harbor, China
Enrichment culture SRB Lactat	*Deltaproteobacteria*	MR-Sed-B49	*Desulfovibrio* sp. strain M2 (AY786352)	99	Marine SRB strain
Montserrat Ridge Manganese crust	*Crenarchaeota*	MR-MnCr-A26, MR-MnCr-A27, MR-MnCr-A28	Uncultured archaeon clone Urania-2A-31 (AY627509)	97, 96, 98	Environmental sample from sediments of a mound near Urania brine lake, Eastern Mediterranean, 3,442 m depth
		MR-MnCr-A29	Uncultured archaeon clone 43mENZ.2 (AY661820)	93	Environmental sample from metal-rich sediments of Peru margin, ODP Leg 201, site 1231
	Alphaproteobacteria	MR-MnCr-B7	Uncultured bacterium (AY753387)	89	Environmental sample from biofilms grown on metal surfaces
		MR-MnCr-B9	Uncultured alphaproteobacterium clone 131637 (AY922203)	92	Environmental sample from Santa Cruz Basin, Pacific Ocean, 1,674 m depth
		MR-MnCr-B13	Uncultured alphaproteobacterium clone JTB131 (AB015245)	94	Environmental sample from cold-seep area of the Japan Trench
	Gammaproteobacteria	MR-MnCr-B4, MR-MnCr-B6	Uncultured gammaproteobacterium clone APe4_38 (AB074619)	91, 92	Environmental sample
		MR-MnCr-B1	*Thiohalomonas nitratireducens* (DQ836238)	93	Isolated from hypersaline lakes
		MR-MnCr-B5	Uncultured organism clone ctg_NISA060 (DQ396147)	99	Environmental sample from deep-sea octacoral
	Bacteroidetes	MR-MnCr-B2, MR-MnCr-B8	Uncultured bacterium clone WLB16–200 (DQ015862)	92, 94	Environmental sample from water of Lake Bonney, Antarctica, 16 m depth
Enrichment culture Aerobic SOB	*Alphaproteobacteria*	MR-MnCr-B13, MR-MnCr-B17	Uncultured alphaproteobacterium JL-ECS_C25 (AY663896)	98, 97	Environmental marine sample, East China Sea
	Gammaproteobacteria	MR-MnCr-B15, MR-MnCr-B16	Sulfur-oxidizing bacterium ODIII6 (AF170422)	93	Environmental sample from shallow-water hydrothermal vent, Milos, Aegean Sea
St. Lucia Bay Filtered seawater	*Euryarchaeota*	SLB-W-A13	Uncultured archaeon clone Sd- EA05 (AB194001)	95	Environmental sample from hydrothermal vent water, Suiyo Seamount
		SLB-W-A14, SLB-W-A21	uncultured marine group II euryarchaeote HF70_97E04 (DQ156478)	92	Environmental sample from North Pacific subtropical gyre water (Hawaii), 70 m below sea surface
		SLB-W-A15	HF70_25A12 (DQ156469)	91	
		SLB-W-A20	HF70_106D07 (DQ156467)	91	
		SLB-W-A16	Uncultured marine group II euryarchaeote clone A_08 (DQ299289)	98	Environmental marine sample from sponge *Reinochalina stalagmites*
		SLB-W-A17	Uncultured marine group II euryarchaeote clone A9D1 (DQ299286)	96	Environmental marine sample from sponge *Axechina raspailoides*
	Alphaproteobacteria	SLB-W-B9	Uncultured organism ctg_CGOAB89 (DQ395477)	93	Environmental marine sample from deep-sea octacoral
	Cyanobacteria	SLB-W-B7	Uncultured *Synechococcus* sp. strain JL-WNPG-T40 (AY664136)	98	Environmental marine sample, West Pacific Gyre

Continued on following page

TABLE 3—*Continued*

Investigated study site and environmental sample names	Major phylogenetic group	DGGE band(s) (ID no.)	Closest phylotype/species (acc. no.)	Sim. (%)	Remarks on closest phylotype/relative
		SLB-W-B8	Uncultured *Synechococcus* sp. strain JL-ECS-X16 (AY663962)	97	Environmental marine sample, East China Sea
		SLB-W-B11	Uncultured *Prochlorococcus* sp. strain JL-WNPG-T37 (AY664133)	97	Environmental marine sample, West Pacific Gyre
	Bacteroidetes	SLB-W-B1, SLB-W-B4	*Gramella portivictoriae* (DQ002871)	97, 95	Isolated from marine sediment, Victoria Harbor, East China Sea
Enrichment culture					
Aerobic SOB LC1	*Alphaproteobacteria*	SLB-W-B22	*Erythrobacter* sp. strain JL-316 (AY646157)	99	Environmental marine sample
		SLB-W-B23	*Pelagibaca bermudensis* (DQ178660)	99	Isolated from the Bermuda Atlantic Time Series Station, Sargasso Sea
		SLB-W-B24	Alphaproteobacterium MBIC3923 (AB016848)	94	Environmental marine sample
Aerobic SOB LA5	*Alphaproteobacteria*	SLB-W-B25, SLB-W-B26, SLB-W-B27	*Rhodobacter* group bacterium LA5 (AF513437)	97, 98, 97	Environmental sample from Hawaiian Archipelago
Phototroph 1	*Chlorobia*	SLB-W-B9	*Chlorobium bathyomarinum* (AY627756)	99	Marine isolate from deep-sea hydrothermal vent
	Bacteroidetes	SLB-W-B48	*Gramella portivictoriae* (DQ002871)	95	Isolated from marine sediment
	Deltaproteobacteria	SLB-W-B12	*Desulfovibrionaceae* bacterium MSL79 (AB110541)	96	Environmental sample from harbor sediment in Japan
Phototroph 2	*Chlorobia*	SLB-W-B13	*Prosthecochloris* sp. strain Vk (AJ888467)	99	Marine isolate from fishing harbor of Visakhapatnam, India
	Deltaproteobacteria	SLB-W-B14	*Desulfovibrionaceae* bacterium MSL79 (AB110541)	96	Environmental sample from harbor sediment in Japan
Phototroph 3	*Chlorobia*	SLB-W-B18	*Chlorobium vibrioforme* f. sp. *thios*, NCIB 8346 (AJ290830)	99	
	Deltaproteobacteria	SLB-W-B26	*Desulfovibrionaceae* bacterium MSL79 (AB110541)	97	Environmental sample from harbor sediment in Japan
SRB H_2 LA1	*Deltaproteobacteria*	SLB-W-B19	*Desulfovibrionaceae* bacterium MSL79 (AB110541)	98	Environmental sample from harbor sediment in Japan
SRB Lactat-1 LB2	*Deltaproteobacteria*	SLB-W-B31	*Desulfovibrio caledonenis* (U53465)	94	
SRB Lactat-2 LA2	*Deltaproteobacteria*	SLB-W-B33	*Desulfovibrio brasiliensis* (AJ544687)	98	
SRB Lactat-3 LB1	*Deltaproteobacteria*	SLB-W-B30	*Desulfovibrio* sp. strain M2 (AY786352)	97	Marine SRB strain
SRB Propion. LC1	*Deltaproteobacteria*	SLB-W-B29	*Desulfobulbus rhabdoformis* (U12253)	100	
SRB Butyrat. LB2	*Deltaproteobacteria*	SLB-W-B35	Uncultured *Desulfocapsa* sp. clone CBII115 (U12253)	96	Environmental sample from marine sediment

[a] The DGGE band identification number (ID no.) of each received 16S rRNA sequence and the accession number (acc. no.) of its closest phylotype/described species (including their sequence similarity [Sim.]) are given as retrieved by BLAST analysis.

gene-targeting primer pair was used to investigate the sediment, manganese crust, and filtered seawater samples (Fig. 3) in comparison with the 16S rRNA gene-based DG-DGGE analysis. The 16S rRNA analysis (summarized in Table 3) revealed a homogenous microbial community structure within the oxic sediment surface layers of the KB and MR (temperature, 4.5 to 4.8°C), comprising members of the *Crenarchaeota*, *Gammaproteobacteria* and *Deltaproteobacteria*, *Bacteroidetes*, low G+C gram-positive organisms, and *Acidobacteria*. The OTUs were affiliated with environmental sequences derived from various deep-sea sediments (1, 4, 23, 27, 45, 55) but only distantly with validated SOB and SRP. According to the MPN counting technique, the number of SRP increased in the surface sediments of KB and MR with depth from 4.3×10^5 to 2.4×10^6 cells/g, whereas the number of aerobic SOB remained constant between 4.3×10^6 to 7.5×10^6 cells/g. A single thiosulfate-oxidizing isolate revealed distantly related free-living relatives of thiotrophic mussel symbionts (1), whereas most strains belonged to the commonly culturable alphaproteobacterial lineages, e.g., *Sphingomonadaceae* and *Roseobacter* (14, 18). Sulfate-reducing relatives of *Desulfovibrio acrylicus* were isolated from both study sites. Similar to the 16S rRNA analysis, the *aprA* gene-based results (Fig. 4) demonstrated a homogenous microbial diversity in the sediments of KB and MR; however, all identified environmental AprA phylotypes belonged to novel alphaproteobacterial SOB clusters (AprA lineage I) that lack reference sequences of cultured SOB species. AprA sequences related to further SOB lineages


Thiobacillus plumbophilus, EF641956
SLB-W-7, EF618659
SLB-W-8, EF618660
MR-Sed-0/2cm-19, EF618636 , MR-Sed-0/2cm-20, EF618637, MR-Sed-0/2cm-21, EF618638
KB-Sed-4/6cm-16, EF618634 *
KB-Sed-0/2cm-10, EF618625, KB-Sed-0/2cm-9, EF618624, KB-Sed-0/2cm-11, EF618626
Environmental sequence IBEA_CTG_2159535, EAK37447
uncultured alphaproteobacterium EBAC2C11, AAV31646
SAR116 cluster
KB-Sed-4/6cm-14, EF618632
KB-Sed-0/2cm-2, EF618618 **
MR-Sed-0/2cm-18, EF618635
KB-Sed-0/2cm-11, EF618626
MR-MnCr-11, EF618650
MR-MnCr-7, EF618646
MR-MnCr-1, EF618640
MR-MnCr-10, EF618649
Pelagibacter ubique and related environmental sequences from Sargasso Sea
SAR11 cluster
SLB-W-6, EF618661
SLB-W-5, EF618658
SLB-W-1, EF618654; SLB-W-3, EF618655
SLB-W-2, EF618656; SLB-W-4, EF618657
Chromatiaceae (7)
Chromatiaceae (15)
Caribflux isolate "manganese crust", EF641930
MR-MnCr-12 SOB enrichment culture 1, EF618651
MR-MnCr-9, EF618648
MR-MnCr-14 SOB enrichment culture 3, EF618653
MR-MnCr-13 SOB enrichment culture 2, EF618652
Olavius algarvensis symbiont, AASZ_01000200
sulfur-oxidizing bacterium ODIII5, EF641951
Oasisia sp. symbiont, EF641962
sulfur-oxidizing bacterium OAII2, EF641953
Mussel symbionts
MR-MnCr-2, EF618641; MR-MnCr-3, EF618642
Thiobacillus denitrificans ATCC 25259, YP_316040
MR-MnCr-8, EF618647
Thiobacillus denitrificans DSM 12475, EF641952
Thiobacillus thioparus, EF641954
Thiobacillus denitrificans DSM 739, EF641955
Inanidrilus exumae symbiont
Pyrobaculum aerophilum, NP_560100-1
Archaeoglobus
Gram-positive SRB and related deltaproteobacterial sequences
Desulfobacca acetoxidans, EF442947
Thermodesulfobacterium
Thermodesulfovibrio (3)
Chlorobium clathratiforme, EF641906
Chlorobium clathratiforme, ZP_00589418
SLB-W-10 phototrophic enrichment culture 1, EF618662
SLB-W-13 phototrophic enrichment culture 2, EF618663
Chlorobiaceae (7)
MR-MnCr-4, EF618643
MR-MnCr-5, EF618644
MR-MnCr-6, EF618645
Chemotrophic and phototrophic sulfur-oxidizing bacteria
Thermodesulfobium narugense, AB080361
Desulfobulbus marinus, EF442934
Desulfobulbus sp. DSM 2033, EF442936
Desulfobulbus propionicus, EF442935
Desulfobulbus elongatus, AF418146
SLB-W-29 enrichment culture SRB Prop LC1, EF618673
Desulfobulbus rhabdoformis, AF418110
Desulforhopalus vacuolatus, EF442940
Desulforhopalus sp., AF418160
Desulfocapsa thiozymogenes, EF442938
Desulfocapsa sulfexigens, AF418131
deltaproteobacterium strain MLMS-1, AAFQ01000064
SLB-W-31 enrichment culture SRB But LB2, EF618672
Desulfobulbus sp. strain LB2, EF442937
Desulfofustis/ Desulfotalea/ Desulfobacterium catecholicum
Desulfobacteraceae
Desulfohalobium
Desulfonatronum/ Desulfonatronovibrio
Desulfonauticus/ Desulfothermus
Desulfomicrobium
Desulfocaldus (2)
Desulfovibrio sulfodismutans and related strains
SLB-W-28 enrichment culture SRB Lact-2 LA2, EF618671
Desulfovibrio oxyclinae, EF442883
Desulfovibrio sp. strain HRS-LA4, EF442889
Desulfovibrio salexigens, EF442887
Desulfovibrio sp. strain X, EF442890
SLB-W-27 enrichment culture SRB Lact-1 LB2, EF618667
SLB-W-12 phototrophic enrichment culture 1, EF618668
SLB-W-18 phototrophic enrichment culture 2, EF618669
SLB-W-9 phototrophic enrichment culture 3, EF618670
Desulfovibrio profundus, EF442886
uncultured sulfate-reducing bacterium, ABF72459
Desulfovibrio sp. strain LA1(H2), EF442894
SLB-W-23 enrichment culture SRB H2 LA1, EF618664
SLB-W-24 enrichment culture SRB H2 LA1, EF618665
Desulfovibrio giganteus, AF 418141
Desulfovibrio sp. DSM 9953, EF442888
Desulfovibrio desulfuricans strain G20, ABB37910
Desulfovibrio acrylicus, EF442882
Desulfovibrio sp. strain LB1, EF442892
KB-Sed-0/2cm-17 enrichment culture SRB Lact, EF618629
SLB-W-26 enrichment culture SRB Lact-3 LB1, EF618669
Desulfovibrio sp. strain 49MC, EF442893
MR-Sed-0/2cm-22 enrichment culture SRB Lact, EF618639
Desulfovibrio sp. strain sponge tissue 85CD, EF442896
Desulfovibrio vulgaris and related strains
10 %
Alphaproteobacteria
Gammaproteobacteria
Betaproteobacteria
Chlorobia
Beta-/Gamma-proteobacteria
Desulfobulbaceae
Desulfovibrionaceae
SOB Apr lineage I
SOB Apr lineage II
SRB

or SRP were not obtained from the sediment samples. Since *aprA* genes were absent from the thiosulfate-oxidizing isolates, the *aprA* gene-detected *Alphaproteobacteria* are not identical to the cultivated ones but represent yet-unrecognized alphaproteobacterial SOB. Consistent with the 16S rRNA analysis, the AprA sequences derived from the sulfidogenic cultures are closely related to the sequence of *Desulfovibrio acrylicus*.

The crenarchaeotic 16S rRNA sequences identified from the manganese crust surface were closely related to the phylotypes of KB and MR sediments. In contrast, the 16S rRNA analysis revealed a higher diversity of OTUs affiliated to *Alphaproteobacteria* and *Gammaproteobacteria* that are putatively involved in sulfur oxidation processes within the crust surface. Indeed, several gammaproteobacterial OTUs were related to a newly described nitrate-reducing SOB strain (52) (detected directly in the crust surface) and free-living, thiodenitrifying relatives of marine invertebrate symbionts (34, 44) (thiotrophic cultures). The *aprA* gene analysis reflected the proposed higher phylogenetic diversity of putative sulfur-oxidizing strains in this habitat in comparison with the sediments (Fig. 4). The identified phylotypes diverged within the SOB-AprA lineage I into sequence clusters of (i) novel alphaproteobacterial SOB (also found in the KB and MR sediments), (ii) *Thiobacillus* spp. (*Betaproteobacteria*), and (iii) free-living relatives of thiotrophic invertebrate symbionts (*Gammaproteobacteria*). The detected phylotypes of AprA lineage II form a basal-branching sequence cluster that is only distantly related to the group of gamma- and betaproteobacterial SOB reference strains. The AprA sequences of the cultivated thiotrophic gammaproteobacterial strains are identical to an OTU directly detected in the manganese crust samples (Fig. 4). These AprA sequences most likely correspond to the 16S rRNA-identified SOB strain ODIII6 (Table 3). As in the sediments, no reductive-type AprA phylotype was detected in the manganese crusts; indeed, no SRP was obtained in enrichment cultures inoculated with sample material from this study site.

The 16S rRNA-based microbial diversity from seawater of SLB (collected from the thermocline zone; temperature, 22°C) was characteristic for bacterioplankton of photic zones in temperate oceanic waters (12, 18, 30) with OTUs related to marine group II euryarchaeota (12, 17) as well as *Prochlorococcus* and *Synechococcus* spp. (66), dominating the archaeal and bacterial community; no phylotypes affiliated with validated SOB and SRP were detected. The MPN counting technique, however, pointed to the presence of 2.4×10^9 aerobic SOB cells/ml and 3.9×10^5 SRP cells/ml in the oxic SLB water column. Thiosulfate-oxidizing members of the commonly cultured *Alphaproteobacteria*, e.g., *Erythrobacter*, *Roseobacter* lineage, and *Rhodobacter* spp. (7, 14, 18), were predominantly cultivated, whereas no gammaproteobacterial SOB were isolated. Besides the *Desulfovibrio*-, *Desulfobulbus*- and *Desulfocapsa*-related SRB strains isolated, three marine green sulfur bacteria (related to *Chlorobium vibrioforme* f. sp. *thios* NCBI 8346, *Chlorobium bathyomarinum*, and *Prosthecochloris* sp. strain Vk) could be enriched in coculture with a *Desulfovibrio* species. Consistent with the 16S rRNA, the *aprA* gene analysis demonstrated the absence of SAR11 or SAR116 cluster-like AprA phylotypes in the SLB water column. The three environmentally derived AprA phylotypes form a separate planktonic sequence cluster within the *Alphaproteobacteria* (SOB-Apr lineage I) and a novel Apr lineage of yet-uncertain phylogenetic affiliation (distant relationship to the gamma/betaproteobacterial SOB reference strains). Since *aprA* genes were absent from the cultivated *Alphaproteobacteria*, the environmental AprA sequences originated from a yet-undiscovered group of planktonic SOB. No *aprA* gene fragment could be obtained from the *C. vibrioforme* f. sp. *thios* relative, whereas the AprA sequences of the *C. bathyomarinum* and *Prosthecochloris* sp. cultures represented a novel Apr lineage of marine *Chlorobiaceae*. No AprA sequences related to SRP were identified from the oxygenated water column, although the results of the MPN cultures pointed to their presence. However, the phylogenetic placements of these cultured sulfate-reducing strains by AprA and 16S rRNA analysis were consistent.

DISCUSSION

In this study, a new PCR- and DGGE-based assay for functional *aprA* gene analysis is presented which allowed the concomitant molecular determination of the diversity of SRP and SOB in the environment. By screening taxonomically divergent SRP and SOB reference strains in PCR assays, the new primer pair showed an improved species coverage compared to the modified (corrected) version of a previously published primer set (13). In addition, the new primer set presented a higher detection sensitivity in multitemplate PCR assays with defined DNA concentrations; the *aprA* gene template-to-PCR product bias (generally caused by preferential amplification of certain target sequences [46, 61]) was less pronounced. Finally, comparative phylogenetic analyses of different environmental samples applying both primer pairs demonstrated that the phylotype diversity coverage of the new primer set was superior for most of the investigated habitats (see Results and Fig. 2). Overall, the detected environmental community structures of SRP and SOB based on the identified AprA phylotypes are consistent with previous cultivation and 16S rRNA gene analysis studies of the same or similar study sites/samples (20, 28, 34, 42, 48, 58).

***aprA* as a functional marker gene for SRP and SOB diversity surveys in comparison with 16S rRNA and *dsrAB* gene-based studies.** A direct comparison of the diversity analysis results for the *aprA* and 16S rRNA (and *dsrAB*) gene approaches is possible in the cases of the subsurface microbial mats of Toyoha

FIG. 4. Phylogenetic tree based on 411 SRP/SOB reference strain and environmentally derived partial AprA sequences. The tree was inferred using the maximum-likelihood method. Sequences of the Apr lineage I and *Pyrobaculum aerophilum* were used as outgroup references. The environmental AprA sequences of sediment, seawater, and manganese crust samples of the Caribbean Sea are highlighted in boldface type (for abbreviations used for study sites and enrichment cultures, see Table 1 and Table 3). The 16S rRNA gene-based taxonomic classification of SOB and SRP reference strains is indicated. The scale bar corresponds to 10% estimated sequence divergence.

Mine (42) and digestive tissue of *E. cordatum* specimens (20). The *aprA* gene-based analysis of the microbial mats provided a more complete picture of the dissimilatory microbial sulfur cycle: the *Thermodesulforhabdus*, *Thermodesulfobacterium*, and *Desulfotomaculum*, as well as the (sulfur-oxidizing) *Thiobacillus plumbophilus*, and free-living invertebrate symbiont relatives remained unidentified by the 16S rRNA gene approaches when applying universal primers (42). According to *aprA* gene analysis, the symbiotic SRP community of the nodules of *E. cordatum* is less diverse as it has been suggested by the 16S rRNA data (20). The *aprA* gene-undetected, putative sulfate-reducing strains were affiliated with sequence clusters of uncultured *Deltaproteobacteria*, which lack a closely related validated SRP species (only moderate relationships to *Desulfobacterium catecholicum*, *Desulfobacula toluolica*, and *Desulfotomaculum acetoxidans*). This reflects the above-mentioned limitations of the rRNA gene analysis in unambiguously linking the genetic identity of an unknown microorganism to its physiology.

Based on the *dsrAB* gene analysis of the Toyoha Mine microbial mats, the existence of two novel gram-positive SRP lineages was proposed by Nakagawa and coworkers (42). Indeed, newly discovered Dsr lineages of environmental sequences that lack sequences of cultured reference strains have frequently been found in various ecological studies and used to propose the presence of yet-unrecognized sulfate-respiring representatives (2, 3, 15, 42, 43, 57). However, many sulfite-reducing strains that are incapable of sulfate respiration are closely related to validated SRP, e.g., members of *Desulfitobacterium* (affiliated with *Desulfosporosinus*) (53), *Sporotomaculum* and *Pelotomaculum* (affiliated with *Desulfotomaculum* subclusters Ib and Ih) (26), *Bilophila* and *Lawsonia* (affiliated with *Desulfovibrio*), as well as the gram-positive genera *Moorella*, *Carboxydothermus* (24, 26), and archaeal *Pyrobaculum* (25). Since the *dsrAB* genes of these sulfite reducers have target sites that are fully complementary to the published primer sets (26, 67), the usage of the latter does not allow a differentiation between physiological groups of sulfite and sulfate reducers in PCR amplification. Therefore, the proposal of novel SRP lineages based on Dsr sequences that belong to environmental clusters is ambiguous. In contrast, an identified Apr lineage that lacks a close relationship to SRP reference sequences is a straightforward indication for the presence of an unrecognized phylogenetic lineage of SRP. Thus, our failure to detect additional *Desulfotomaculum*-related AprA phylotypes in MatB and MatD of Toyoha Mine, besides those affiliated to the thermophilic *Desulfotomaculum* (the *dsrAB*-consistent result), might be explained by the presence of gram-positive sulfite respirers.

All published *dsr* gene-targeting PCR assays are currently restricted to the investigation of SRP diversity because of the low sequence similarity between Dsr in SRP and SOB (32, 62); no universal or SOB-specific amplification primers and no comprehensive DsrAB database of sulfur-oxidizing reference strains exist. The *aprA* gene-targeting primers of this study, however, allowed the identification of the divergent SOB lineages and even the concomitant investigation of the SRP and SOB species diversity, as demonstrated for some environmental samples e.g., in hydrothermal water (Vail, CO) and microbial mats of *Beggiatoa* fields (Hydrate Ridge, OR) (Fig. 2). In the latter, the existence of a basal-branching *Desulfobulbaceae* representative was demonstrated within a microbial community that was otherwise predominated by different chemotrophic SOB species. (Note: a *Desulfobulbus* relative was identified in these sediment samples by 16S rRNA cloning analysis [T. Losekann, unpublished data]). Nevertheless, the *aprA* gene-based analysis will underestimate the microbial diversity involved in the oxidative processes of inorganic sulfur compounds in nature as a result of the restricted distribution of the *apr* genes among the SOB species (see the introduction). As a drawback, this molecular approach will allow their selected detection in environmental samples. However, the low bootstrap values in the SOB lineages show that the partial AprA sequences have only limited phylogenetic information which renders the direct assignment of the oxidative-type environmental AprA sequences to distinct SOB genera/species often difficult. This is also complicated by the LGT-affected evolutionary history of these genes in SOB with the result of some SOB species harboring a second, SRP-related *apr* gene locus besides an authentic one or only the LGT-derived gene copy (37). Concerning the phylogenetic complexity of SOB in the *Beggiatoa* field microbial mats, the identified AprA phylotypes pointed to the presence of (at least) one chemolithotrophic sulfur-oxidizing gammaproteobacterium (free-living relative of invertebrate symbionts) and one chemolithotrophic SOB forming a novel lineage of currently uncertain affiliation.

Comparison of 16S rRNA and *aprA* gene-based analyses: the sulfur-cycling microbial community in the area of the Lesser Antilles volcanic arc (Caribbean Sea). The results of the 16S rRNA analyses revealed that the microbial community compositions from the aerated deep-sea sediment surfaces of KB and MR and the SLB photic water zone are similar to those of other nonhydrothermal, subtropical study sites in the Mediterranean and East China Seas as well as in the Western Pacific (12, 18, 23, 27, 45, 55). Most identified sediment-associated bacteria might have been involved in the decomposition of detritus-derived organic matter, e.g., the *Bacteroidetes* comprising chemoorganoheterotrophic degraders of various biopolymers (31), while the archaeal community appeared to be dominated by potential chemolithoautotrophic, nitrifying crenarchaeota (33, 63). In contrast, the SLB bacterioplankton consisted predominantly of phototrophic microorganisms, e.g., (putative) proteorhodopsin-containing euryarchaeota (17) and diverse unicellular cyanobacteria (66). However, no environmental 16S rRNA sequence was closely related to a validated SRP or SOB species; thus, the analyses provided no insights into the microbial community of the sulfur cycle at the investigated study sites. Their presence could only be demonstrated by selective cultivation techniques, with the highest taxa diversity apparent in the SLB photic water zone. The collected geochemical data collected during sampling indicated the absence of a direct, external input of reduced inorganic sulfur compounds at these study sites (Caribflux project final report). Interestingly, the *aprA* gene analysis revealed the bacterioplankton assemblages and the deep-sea sediments of the Caribbean Sea to be dominated by chemotrophic sulfur oxidizers that belong to four distinct and habitat-specific phylotype clusters within the alphaproteobacterial lineage (closest relatives are the SAR116 group members) and at least one separately branching lineage of yet-uncertain taxonomic affiliation. No

phylotypes corresponding to SRP and beta/gammaproteobacterial chemolithoautotrophic SOB were detected at the study sites. The wide distribution of *apr* genes among members of the *Alphaproteobacteria* was unexpected because previous studies (37) demonstrated their absence in reference strains of this lineage, with the exceptions of *Pelagibacter ubique* of the SAR11 group (19) and an uncultivated representative of the SAR116 group. The alphaproteobacterial SAR11 cluster and *Roseobacter* clade members are the numerically dominant bacterioplankton groups in the decomposition of abundant organic sulfur compounds, e.g., dimethylsulfoniopropionate (DMSP) (21, 22, 36), and thus are implicated in sulfur cycling. Several representatives of the *Roseobacter* clade have also been reported to harbor the ability to oxidize inorganic sulfur intermediates, e.g., sulfite or thiosulfate to facilitate sulfur-based lithoheterotrophy (6, 21, 39), since reduced inorganic sulfur compounds are produced during the degradation of DMSP (21) or organosulfonates (8, 9). Indeed, thiosulfate-oxidizing, sulfate-producing members of this marine heterotrophic SOB group (e.g., *Sulfitobacter* spp.) have frequently been identified and isolated from various nonhydrothermal (deep-sea) sediments (51, 56, 59). Based on the results of the *aprA* gene analysis, we postulate that these chemolithoheterotrophic, sulfur-oxidizing members of the *Roseobacter* clade are also present in the investigated deep-sea sediment and photic water zone samples from the Caribbean Sea. Indeed, thiotrophic *Pelagibaca bermudensis* relatives were isolated from both habitats. However, no *aprA* partial sequence was obtained from the latter; this indicates that the culturable members do not represent the abundant species in these habitats. The functional role of the enzyme "dissimilatory APS reductase" in the alphaproteobacterial strains is unclear: a reverse-acting APS reductase might primarily be used for intracellular detoxification of sulfite as an accumulating product of the organic sulfur compound degradation; the oxidation product APS will be incorporated into the assimilatory sulfur metabolism or converted to sulfate (by the activity of a dissimilatory ATP sulfurylase), allowing additional energy conservation as previously proposed for species of SAR11 and SAR116 (37). The dominant role of chemolithoheterotrophic alphaproteobacterial instead of chemolithoautotrophic gammaproteobacterial SOB in the microbial sulfur transformation processes might be realistic for the investigated nonhydrothermal sediment and water column samples that lack a direct input of inorganic sulfur compounds. Nevertheless, the recognized limitations of PCR amplification (46, 61) and the DGGE method (41) might probably have biased the analysis towards the abundant groups in the microbial community, the SOB, with the consequence of the nondetection of minor present sulfate reducers. The 16S rRNA and *aprA* gene analyses of the sulfidogenic enrichment cultures point consistently to the presence of *Desulfovibrio acrylicus*-related strains. Interestingly, this SRB species is capable of DMSP cleavage for subsequent reduction of the acrylate moiety to propionate (60).

In contrast to the previous habitats, the geochemical data pointed to a (at least) subrecent, external (hydrothermal) input of inorganic sulfur compounds at the MR manganese crust collection site, reflected in the sulfur-based, resident microbial community structure. Indeed, OTUs affiliated with validated chemolithoautotrophic SOB species (52) were detected directly from the environmental samples by 16S rRNA gene analysis, while close relatives of SOB derived from hydrothermal systems in the Aegean Sea and Mid-Atlantic Ridge (34, 44) could even be isolated. Nevertheless, sulfur-oxidizing members of phylogenetic lineages recognized to be generally dominant at active deep-sea hydrothermal vents, e.g., *Epsilonproteobacteria* (44, 54), were not identified. The *aprA* gene analysis revealed the high phylogenetic complexity of SOB in the crust surface which was not discovered by 16S rRNA analysis. The sulfur-cycling microbial community is suggested to consist of (i) putative chemolithoautotrophic SOB strains of the *Betaproteobacteria* and *Gammaproteobacteria*, (ii) sulfur-oxidizing representatives of an uncertain-affiliated, novel SOB lineage, and (iii) members of the previously mentioned chemolithoheterotrophic alphaproteobacterial SOB. The betaproteobacterium appeared to be a marine representative of the genus *Thiobacillus*; however, a clear assignment of the other phylotypes to certain SOB genera/species is not possible with the amount of sequence information of the partial AprAs and the current database because Apr reference sequences of *Beggiatoa* and chemolithoautotrophic *Epsilonproteobacteria* (54) are missing. Previous work on *Thiomicrospira* spp. indicated the general absence of *apr* genes in this genus (see also Table S1 in the supplemental material), whereas the APS pathway seemed to be restricted to a few chemolithoautotrophic, marine members of *Beggiatoa*.

ACKNOWLEDGMENTS

This study was supported by grants of the BMBF (project "Caribflux" under contract number 03G0154C), the DFG (under contract number KU 916/8-1), and the Max Planck Society, Munich, Germany.

REFERENCES

1. **Arakawa, S., T. Sato, Y. Yoshida, R. Usami, and C. Kato.** 2006. Comparison of the microbial diversity in cold-seep sediments from different depths in the Nankai Trough. J. Gen. Appl. Microbiol. **52:**47–54.
2. **Bagwell, C. E., X. Liu, L. Wu, and J. Zhou.** 2006. Effects of legacy nuclear waste on the compositional diversity and distributions of sulfate-reducing bacteria in a terrestrial subsurface aquifer. FEMS Microbiol. Ecol. **55:**424–431.
3. **Bahr, M., B. C. Crump, V. Klepac-Ceraj, A. Teske, M. L. Sogin, and J. E. Hobbie.** 2005. Molecular characterization of sulfate-reducing bacteria in a New England salt marsh. Environ. Microbiol. **7:**1175–1185.
4. **Bano, N., and J. T. Hollibaugh.** 2002. Phylogenetic composition of bacterioplankton assemblages from the Artic Ocean. Appl. Environ. Microbiol. **68:** 505–518.
5. **Brüser, T., P. N. L. Lens, and H. G. Trüper.** 2000. The biological sulfur cycle, p. 47–86. *In* P. N. L. Lens and L. H. Pol (ed.), Environmental technologies to treat sulfur pollution. IWA Publishing, London, United Kingdom.
6. **Buchan, A., J. M. Gonzalez, and M. A. Moran.** 2005. Overview of the marine *Roseobacter* lineage. Appl. Environ. Microbiol. **71:**5665–5677.
7. **Cho, J.-C., and S. J. Giovannoni.** 2006. *Pelagibaca bermudensis* gen. nov., sp. nov., a novel marine bacterium within the *Roseobacter* clade in the order *Rhodobacterales*. Int. J. Syst. Evol. Microbiol. **56:**855–859.
8. **Cook, A. M., and K. Denger.** 2002. Dissimilation of the C_2 sulfonates. Arch. Microbiol. **179:**1–6.
9. **Cook, A. M., K. Denger, and T. H. M. Smits.** 2006. Dissimilation of C_3 sulfonates. Arch. Microbiol. **185:**83–90.
10. **Cremonesi, L., S. Firpo, M. Ferrari, P. G. Righetti, and C. Gelfi.** 1997. Double-gradient DGGE for optimized detection of DNA point mutations. BioTechniques **22:**326–330.
11. **DeLong, E.** 1992. Archaea in coastal marine environments. Proc. Natl. Acad. Sci. USA **89:**5685–5689.
12. **DeLong, E. F., C. M. Preston, T. Mincer, V. Rich, S. J. Hallam, N. U. Frigaard, A. Martinez, M. B. Sullivan, R. Edwards, B. R. Brito, S. W. Chilsholm, and D. M. Karl.** 2006. Community genomics among stratified microbial assemblages in the ocean's interior. Nature **311:**496–503.
13. **Deplancke, B., K. R. Hristova, H. A. Oakley, V. J. McCracken, R. Aminov, R. I. Mackie, and H. R. Gaskins.** 2000. Molecular ecological analysis of the succession and diversity of sulfate-reducing bacteria in the mouse gastrointestinal tract. Appl. Environ. Microbiol. **66:**2166–2174.

14. **Eilers, H., J. Pernthaler, F. O. Gloeckner, and R. Amann.** 2000. Culturability and in situ abundance of pelagic bacteria from the North Sea. Appl. Environ. Microbiol. **66:**3044–3051.
15. **Fishbain, S., J. G. Dillon, H. L. Gough, and D. A. Stahl.** 2003. Linkage of high rates of sulfate reduction in Yellowstone hot springs to unique sequence types in the dissimilatory sulfate respiration pathway. Appl. Environ. Microbiol. **69:**3663–3667.
16. **Friedrich, C. G.** 1998. Physiology and genetics of sulfur-oxidizing bacteria, p. 235–289. *In* R. K. Poole (ed.), Advances in microbial physiology, vol. 39. Academic Press, San Diego, CA.
17. **Frigaard, N. U., A. Martinez, T. J. Mincer, and E. F. DeLong.** 2006. Proteorhodopsin lateral gene transfer between marine planktonic Bacteria and Archaea. Nature **439:**847–850.
18. **Giovannoni, S. J., and M. S. Rappe.** 2000. Evolution, diversity and molecular ecology of marine prokaryotes, p. 47–84. *In* D. L. Kirchman (ed.), Microbial ecology of the oceans. Wiley, New York, NY.
19. **Giovannoni, S. J., H. J. Tripp, S. Givan, M. Podar, K. L. Vergin, D. Baptista, L. Bibbs, J. Eads, T. H. Richardson, M. Noordewier, M. S. Rappe, J. M. Short, J. C. Carrington, and E. J. Mathur.** 2005. Genome streamlining in a cosmopolitan oceanic bacterium. Science **309:**1242–1245.
20. **Gomes da Silva, S., D. C. Gillan, N. Dubilier, and C. De Ridder.** 2006. Characterization by 16S rRNA gene analysis and in situ hybridization of bacteria living in the hindgut of a deposit-feeding echinoid (Echinodermata). J. Mar. Biol. Assoc. U.K. **86:**1209–1213.
21. **Gonzalez, J. M., R. P. Kiene, and M. A. Moran.** 1999. Transformation of sulfur compounds by an abundant lineage of marine bacteria in the α-subclass of the class *Proteobacteria*. Appl. Environ. Microbiol. **65:**3810–3819.
22. **Gonzalez, J. M., R. Simo, R. Massana, J. S. Covert, E. O. Casamayor, C. Pedros-Alio, and M. A. Moran.** 2000. Bacterial community structure associated with a dimethylsulfoniopropionate-producing North Atlantic algal bloom. Appl. Environ. Microbiol. **66:**4237–4246.
23. **Heijs, S. K., G. Aloisi, I. Bouloubassi, R. D. Pancost, C. Pierre, J. S. Sinninghe Damste, J. C. Gottschal, J. D. van Elsas, and L. J. Forney.** 2006. Microbial community structure in three deep-sea carbonate crusts. Microb. Ecol. **52:**451–462.
24. **Henstra, A. M., and A. J. M. Stams.** 2004. Novel physiological features of *Carboxydothermus hydrogenoformans* and *Thermoterrabacterium ferrireducens*. Appl. Environ. Microbiol. **70:**7236–7240.
25. **Huber, H., R. Huber, and K. O. Stetter.** 2002. *Thermoproteales*. *In* M. Dworkin, E. Falkow, E. Rosenberg, K.-H. Schleifer, and E. Stackebrandt (ed.), The prokaryotes. An evolving electronic resource for the microbial community. Springer, New York, NY.
26. **Imachi, H., Y. Sekiguchi, Y. Kamagata, A. Loy, Y. L. Qiu, P. Hugenholtz, N. Kimura, M. Wagner, A. Ohashi, and H. Harada.** 2006. Non-sulfate-reducing, syntrophic bacteria affiliated with *Desulfotomaculum* cluster I are widely distributed in methanogenic environments. Appl. Environ. Microbiol. **72:**2080–2091.
27. **Inagaki, F., T. Nunoura, S. Nakagawa, A. Teske, M. Lever, A. Lauer, M. Suzuki, K. Takai, M. Delwiche, F. S. Colwell, K. H. Nealson, K. Horikoshi, S. D'Hondt, and B. B. Joergensen.** 2006. Biogeographical distribution and diversity of microbes in methane hydrate-bearing deep marine sediments on the Pacific Ocean Margin. Proc. Natl. Acad. Sci. USA **103:**2815–2820.
28. **Ishii, K., M. Mussmann, M. B. J. MacGregor, and R. Amann.** 2004. An improved fluorescence in situ hybridization protocol for the identification of bacteria and archaea in marine sediments. FEMS Microbiol. Ecol. **50:**203–212.
29. **Joergensen, B. B.** 1982. Mineralization of organic matter in the sea bed—the role of sulphate reduction. Nature **296:**643–645.
30. **Karner, M. B., E. F. DeLong, and D. M. Karl.** 2001. Archaeal dominance in the mesopelagic zone of the Pacific Ocean. Nature **409:**507–510.
31. **Kirchman, D. L.** 2002. The ecology of *Cytophaga-Flavobacteria* in aquatic environments. FEMS Microbiol. Ecol. **39:**91–100.
32. **Klein, M., M. Friedrich, A. J. Roger, P. Hugenholtz, S. Fishbain, H. Abicht, L. L. Blackall, D. A. Stahl, and M. Wagner.** 2001. Multiple lateral transfers of dissimilatory sulfite reductase genes between major lineages of sulfate-reducing prokaryotes. J. Bacteriol. **183:**6028–6035.
33. **Koennecke, M., A. E. Bernhard, J. R. de la Torre, C. B. Walker, J. B. Waterbury, and D. A. Stahl.** 2005. Isolation of an autotrophic ammonia-oxidizing marine archaeon. Nature **437:**543–546.
34. **Kuever, J., S. M. Sievert, H. Stevens, T. Brinkhoff, and G. Muyzer.** 2002. Microorganisms of the oxidative and reductive part of the sulfur cycle at a shallow-water hydrothermal vent in the Aegean Sea (Milos, Greece). Cah. Biol. Mar. **43:**413–416.
35. **Kwok, S., D. E. Kellogg, N. McKinney, D. Spasic, L. Goda, C. Levenson, and J. J. Sninsky.** 1990. Effects of primer-template mismatches on the polymerase chain reaction. Nucleic Acids Res. **18:**999–1005.
36. **Malmstom, R. R., R. P. Kiene, M. T. Cottrell, and D. L. Kirchman.** 2004. Contribution of SAR11 bacteria to dissolved dimethylsulfoniopropionate and amino acid uptake in the North Atlantic Ocean. Appl. Environ. Microbiol. **70:**4129–4135.
37. **Meyer, B., and J. Kuever.** 2007. Molecular analysis of the distribution and phylogeny of dissimilatory adenosine-5′-phosphosulfate reductase-encoding genes (*aprBA*) among sulfur-oxidizing prokaryotes. Microbiology **153:**3478–3498.
38. **Meyer, B., and J. Kuever.** 2007. Phylogeny of the alpha and beta subunits of the dissimilatory adenosine-5′-phosphosulfate (APS) reductase from sulfate-reducing prokaryotes—origin and evolution of the dissimilatory sulfate-reduction pathway. Microbiology **153:**2026–2044.
39. **Moran, M. A., J. M. Gonzalez, and R. P. Kiene.** 2003. Linking a bacterial taxon to sulfur cycling in the sea: studies of the marine *Roseobacter* group. Geomicrobiol. J. **20:**375–388.
40. **Mori, K., H. Kim, T. Kakegawa, and S. Hanada.** 2003. A novel lineage of sulfate-reducing microorganisms: *Thermodesulfobiaceae* fam. nov., *Thermodesulfobium narugense*, gen. nov., sp nov., a new thermophilic isolate from a hot spring. Extremophiles **7:**283–290.
41. **Muyzer, G., A. Teske, C. O. Wirsen, and H. W. Jannasch.** 1995. Phylogenetic relationships of *Thiomicrospira* species and their identification in deep-sea hydrothermal vent samples by denaturing gradient gel electrophoresis of 16S rDNA fragments. Arch. Microbiol. **164:**165–172.
42. **Nakagawa, T., S. Hanada, A. Maruyama, K. Marumo, T. Urabe, and M. Fukui.** 2002. Distribution and diversity of thermophilic sulfate-reducing bacteria within a Cu-Pb-Zn mine. FEMS Microbiol. Ecol. **41:**199–209.
43. **Nercessian, O., N. Bienvenu, D. Moreira, D. Prieur, and C. Jeanthon.** 2005. Diversity of functional genes of methanogens, methanotrophs and sulfate reducers in deep-sea hydrothermal environments. Environ. Microbiol. **7:**118–132.
44. **Nercessian, O., Y. Fouquet, C. Pierre, D. Prieur, and C. Jeanthon.** 2005. Diversity of *Bacteria* and *Archaea* associated with a carbonate-rich metalliferous sediment sample from the Rainbow vent field on the Mid-Atlantic Ridge. Environ. Microbiol. **7:**698–714.
45. **Polymenakou, P. N., S. Bertilsson, A. Tselepides, and E. G. Stephanou.** 2005. Bacterial community composition in different sediments from the Eastern Mediterranean Sea: a comparison of four 16S ribosomal DNA clone libraries. Microb Ecol. **50:**447–462.
46. **Polz, M. F., and C. M. Cavanaugh.** 1998. Bias in template-to-product ratios in multitemplate PCR. Appl. Environ. Microbiol. **64:**3724–3730.
47. **Rabus, R., T. A. Hansen, and F. Widdel.** 1999. Dissimilatory sulfate- and sulfur-reducing prokaryotes, p. 1–87. *In* M. Dworkin, E. Falkow, E. Rosenberg, K.-H. Schleifer, and E. Stackebrandt (ed.), The prokaryotes. An evolving electronic database for the microbiological community. Springer, New York, NY.
48. **Scholten, J. C. M., S. B. Joye, J. T. Hollibaugh, and J. C. Murrell.** 2005. Molecular analysis of the sulfate reducing and archaeal community in a meromictic soda lake (Mono Lake, California) by targeting 16S rRNA, *mcrA*, *apsA*, and *dsrAB* genes. Microb. Ecol. **50:**29–39.
49. **Sievert, S. M., T. Brinkhoff, G. Muyzer, V. Ziebis, and J. Kuever.** 1999. Spatial heterogeneity of bacterial populations along an environmental gradient at a shallow submarine hydrothermal vent near Milos Island (Greece). Appl. Environ. Microbiol. **65:**3834–3842.
50. **Simsek, M., and H. Adnan.** 2000. Effect of single mismatches at 3′-end of primers on polymerase chain reaction. Med. Sci. **2:**11–14.
51. **Sorokin, D. Y.** 2003. Oxidation of inorganic sulfur compounds by obligately organotrophic bacteria. Microbiology **72:**641–653.
52. **Sorokin, D. Y., T. P. Tourova, A. M. Lysenko, and G. Muyzer.** 2006. Diversity of culturable halophilic sulfur-oxidizing bacteria in hypersaline habitats. Microbiology **152:**3013–3023.
53. **Spring, S., and F. Rosenzweig.** 2003. The genera *Desulfitobacterium* and *Desulfosporosinus*: taxonomy. *In* M. Dworkin, E. Falkow, E. Rosenberg, K.-H. Schleifer, and E. Stackebrandt (ed.), The prokaryotes. An evolving electronic resource for the microbial community. Springer, New York, NY.
54. **Takai, K., B. J. Campbell, S. C. Cary, M. Suzuki, H. Oida, T. Nunoura, H. Hirayama, S. Nakagawa, Y. Suzuki, F. Inagaki, and K. Horikoshi.** 2005. Enzymatic and genetic characterization of carbon and energy metabolisms by deep-sea hydrothermal chemolithoautotrophic isolates of *Epsilonproteobacteria*. Appl. Environ. Microbiol. **71:**7310–7320.
55. **Teske, A.** 2006. Microbial communities of deep marine subsurface sediments: molecular and cultivation surveys. Geomicrobiol. J. **23:**357–368.
56. **Teske, A., T. Brinkhoff, G. Muyzer, D. P. Moser, J. Rethmeier, and H. W. Jannasch.** 2000. Diversity of thiosulfate-oxidizing bacteria from marine sediments and hydrothermal vents. Appl. Environ. Microbiol. **66:**3125–3133.
57. **Thomsen, T. R., K. Finster, and N. B. Ramsing.** 2001. Biogeochemical and molecular signatures of anaerobic methane oxidation in a marine sediment. Appl. Environ. Microbiol. **67:**1646–1656.
58. **Treude, T., A. Boetius, K. Knittel, K. Wallmann, and B. B. Joergensen.** 2003. Anaerobic oxidation of methane above gas hydrates at Hydrate Ridge, NE Pacific Ocean. Mar. Ecol. Prog. Ser. **264:**1–14.
59. **Tuttle, J. H., and H. W. Jannasch.** 1976. Microbial utilization of thiosulfate in the deep sea. Limnol. Oceanogr. **21:**697–701.
60. **van der Maarel, M. J. E. C., S. van Bergeijk, A. F. van Werkhoven, A. M. Laverman, W. G. Meijer, W. T. Stam, and T. Hansen.** 1996. Cleavage of

dimethylsulfoniopropionate and reduction of acrylate by *Desulfovibrio acrylicus*. Arch. Microbiol. **166:**109–115.

61. **von Wintzingerode, F., U. B. Gobel, and E. Stackebrandt.** 1997. Determination of microbial diversity in environmental samples: pitfalls of PCR-based rRNA analysis. FEMS Microbiol. Rev. **21:**213–229.
62. **Wagner, M., A. J. Roger, J. L. Flax, G. A. Brusseau, and D. A. Stahl.** 1998. Phylogeny of dissimilatory sulfite reductases supports an early origin of sulfate respiration. J. Bacteriol. **180:**2975–2982.
63. **Wuchter, C., B. Abbas, M. J. L. Coolen, L. Herfort, J. van Bleijswijk, P. Timmers, M. Strous, E. Teira, G. J. Herndl, J. J. Middleburg, S. Schouten, and J. S. Sinninghe Damste.** 2006. Archaeal nitrification in the ocean. Proc. Natl. Acad. Sci. USA **103:**12317–12322.
64. **Zhou, J. Z., M. A. Bruns, and J. M. Tiedje.** 1996. DNA recovery from soils of diverse composition. Appl. Environ. Microbiol. **62:**316–322.
65. **Zinkevich, V., and I. B. Beech.** 2000. Screening of sulfate-reducing bacteria in colonoscopy samples from healthy and colitic human gut mucosa. FEMS Microbiol. Ecol. **34:**147–155.
66. **Zinser, E. R., A. Coe, Z. I. Johnson, A. C. Martiny, N. J. Fuller, D. J. Scalan, and S. W. Chilsholm.** 2006. *Prochlorococcus* ecotype abundances in the North Atlantic Ocean as revealed by an improved quantitative PCR method. Appl. Environ. Microbiol. **72:**723–732.
67. **Zverlov, V., M. Klein, S. Lücker, M. W. Friedrich, J. Kellermann, D. A. Stahl, A. Loy, and M. Wagner.** 2005. Lateral gene transfer of dissimilatory (bi)sulfite reductase revisited. J. Bacteriol. **187:**2203–2208.

Supplementary Material

Supplementary Table S1. PCR amplification results of new *aprA* gene targeting primer pair AprA-1-FW/ AprA-5-RV-GC from genomic DNA of sulfate-reducing and sulfur-oxidizing reference strains

Species[a]	Strain[b]	PCR product obtained with primer AprB-1-FW/ AprA-5-RV-GC[q]	GenBank accession no. *aprBA*
Sulfate-reducing prokaryotes			
Archaea			
Crenarchaeota phylum, Thermoprotei			
Thermoproteaceae			
Caldivirga maquilingensis	13496^T	± (54)	NA
Euryarchaeota phylum, Archaeoglobi			
Archaeaglobaceae			
Archaeoglobus fulgidus	4304^T	+	NC_000917
Archaeoglobus profundus	5631^T	+	**EF442876**
Archaeoglobus veneficus	11195^T	+	**EF442877**
Bacteria			
Thermodesulfobacteria phylum, *Thermodesulfobacteria*			
Thermodesulfobacteriaceae			
Thermodesulfobacterium commune	2178^T	+	**EF442878**
Thermodesulfobacterium hveragardense	12571^T	+	**EF442879**
Thermodesulfatator indicus	15286^T	+	**EF442880**
Nitrospira phylum, *Nitrospira*			
Nitrospiraceae			
Thermodesulfovibrio yellowstonii	11347^T	+	**EF442881**
Proteobacteria phylum, *Deltaproteobacteria*			
Desulfovibrionaceae			
Desulfovibrio acrylicus	10141^T	+	**EF442882**
Desulfovibrio oxyclinae	11498^T	+	**EF442883**
„Desulfovibrio ferrophilus" strain IS5[c]	15579	+	**EF442884**
Desulfovibrio piger	749^T	+	**EF442885**
Desulfovibrio profundus	11384^T	+	**EF442886**
Desulfovibrio salexigens	2638^T	+	**EF442887**
Desulfovibrio sp.	9953	+	**EF442888**
Desulfovibrio sp. strain HRS-LA4[d]	-	+	**EF442889**
Desulfovibrio sp. strain X	-	+	**EF442890**
Desulfovibrio sp. strain JD-160[e]	-	+	**EF442891**
Desulfovibrio sulfodismutans	3969^T	+	**EF442897**
Desulfomicrobiaceae			
Desulfocaldus sp. strain Hobo	-	+	**EF442898**
Desulfomicrobium baculatum	4028^T	+	**EF442899**
Desulfohalobiaceae			
Desulfohalobium retbaense	5692^T	+	**EF442900**
Desulfonatronovibrio hydrogenovorans	9292^T	+	**EF442902**
Desulfonauticus submarinus	15269^T	+	**EF442903**
Desulfothermus naphtae strain TD3	13418^T	+	**EF442901**
sulfate-reducing bacterium strain 4206	4206	+	**EF442904**
Desulfonatronumaceae			
Desulfonatronum lacustre	10312^T	+	**EF442905**
Desulfobacteraceae			
Desulfatibacillum sp. strain Pnd3	-	+	**EF442906**
Desulfobacter postgatei	2034^T	±	**EF442907**
Desulfobacter sp.	2035	+	**EF442908**
Desulfobacter sp.	2057	+	**EF442909**
Desulfobacterium autotrophicum	3382^T	+	**EF442910**
Desulfobacterium indolicum	3883^T	+	**EF442911**
Desulfobacterium niacini	2650^T	+	**EF442912**
Desulfobacterium niacini strain PM4[f]	-	±	**EF442913**
"Desulfobacterium oleovorans" strain Hxd3	6200^T	±	**EF442914**
sulfate-reducing bacterium strain JHA1[g]	-	+	**EF442915**
Desulfobacterium sp.	7120^T	+	**EF442916**
Desulfobacterium zeppelinii	9120	+	**EF442917**
Desulfobacula phenolica	3384^T	+	**EF442918**
Desulfobacula toluolica	7467^T	+	**EF442919**
Desulfobotulus sapovorans	2055^T	+	**EF442920**
Desulfocella sp.	2056^T	±	**EF442921**
Desulfococcus multivorans	2059^T	+	**EF442922**
Desulfococcus sp.	8541	+	**EF442923**
Desulfofrigus sp. strain HRS-LA3X[d]	-	+	**EF442924**
Desulfonema limicola	2076^T	+	**EF442925**
Desulfonema magnum	2077^T	+	**EF442926**
Desulforegula conservatrix	13587^T	+	**EF442927**
Desulfosarcina variabilis	2060^T	+	**EF442928**
Desulfospira joergensenii	10085^T	±	**EF442929**
Desulfotignum balticum	7044^T	+	**EF442930**
Desulfobulbaceae			
Desulfobacterium catecholicum	3882^T	+	**EF442931**
Desulfobacterium catecholicum strain Kette	-	+	**EF442932**
„Desulfobacterium corrodens" strain IS4[e]	15630	+	**EF442933**
Desulfobulbus marinus	2058^T	+	**EF442934**
Desulfobulbus propionicus	2032^T	+	**EF442935**

	Desulfobulbus sp.	2033	+	**EF442936**
	Desulfocapsa thiozymogenes	7269^{T}	±	**EF442938**
	Desulfofustis glycolicus	9705^{T}	+	**EF442939**
	Desulforhopalus vacuolatus	9700^{T}	+	**EF442940**
	Desulfotalea psychrophila	12343^{T}	+	NC_006138
	sulfate-reducing bacterium strain QLNR1[c]	-	±	**EF442941**
	Uncertain affiliation			
	Desulfobacterium anilini	4660^{T}	+	**EF442942**
	sulfate-reducing bacterium strain EbS7[h]	15769	±	**EF442943**
	sulfate-reducing bacterium strain NaphS2[i]	14454	±	**EF442944**
	sulfate-reducing bacterium strain mXyS1[j]	12567	+	**EF442945**
	Desulfarculaceae			
	Desulfarculus baarsii	2075^{T}	+	**EF442946**
	Syntrophaceae			
	Desulfobacca acetoxidans	11109^{T}	±	**EF442947**
	Desulfomonile tiedjei	6799^{T}	±	**EF442948**
	Syntrophobacteraceae			
	Desulforhabdus amnigena	10338^{T}	±	**EF442949**
	Desulforhabdus sp. strain BKA11	-	+	**EF442950**
	Desulforhabdus sp. strain DDT	-	+	**EF442951**
	Thermodesulforhabdus norvegica	9990^{T}	±	**EF442952**
	Firmicutes phylum, *Clostridia*			
	Peptococcaceae			
	Desulfosporosinus orientis	765^{T}	- (54)	**EF442953**
	Desulfosporosinus meridei	13257^{T}	- (54)	**EF442954**
	Desulfotomaculum acetoxidans	771^{T}	+	**EF442955**
	Desulfotomaculum australicum	11792^{T}	+	**EF442956**
	Desulfotomaculum geothermicum	3669^{T}	+	**EF442957**
	Desulfotomaculum gibsoniae	7213^{T}	+	**EF442958**
	Desulfotomaculum halophilum	11559^{T}	±	**EF442959**
	Desulfotomaculum luciae	12396^{T}	+	**EF442960**
	Desulfotomaculum ruminis	2154^{T}	±	**EF442961**
	Desulfotomaculum sapomandens	3223^{T}	+	**EF442962**
	Desulfotomaculum solfataricum[k]	14956^{T}	+	**EF442963**
	Desulfotomaculum sp.	7440	±	**EF442964**
	Desulfotomaculum sp.	7474	+	**EF442965**
	Desulfotomaculum sp.	7475	+	**EF442966**
	Desulfotomaculum sp.	7476	+	**EF442967**
	Desulfotomaculum sp.	8775	+	**EF442968**
	Desulfotomaculum thermoacetoxidans	5813^{T}	+	**EF442969**
	Desulfotomaculum thermobenzoicum ssp. *thermobenzoicum*	6193^{T}	+	**EF442970**
	Desulfotomaculum thermobenzoicum ssp. *thermosyntrophicum*	14055^{T}	+	**EF442971**
	Desulfotomaculum thermocisternum	10259^{T}	+	**EF442972**
	Desulfotomaculum thermosapovorans	6562^{T}	+	**EF442973**
	Desulfotomaculum sp. strain JD-175[e]	-	+	**EF442975**
	Desulfotomaculum sp. strain JD-176[e]	-	+	**EF442976**
	Thermoanaerobacteriaceae			
	Thermacetogenium phaeum	12270^{T}	+	**EF442974**
	Sulfur-oxidizing prokaryotes			
	Archaea			
	Crenarchaeota phylum, *Thermoprotei*			
	Sulfolobaceae			
	Acidianus ambivalens	3772^{T}	- (52)*	-
	Metallosphaera sedulae	5348^{T}	- (52)*	-
	Metallosphaera prunae	10039^{T}	- (52)*	-
	Sulfolobus metallicus	6482^{T}	- (52)*	-
	Bacteria			
	Chloroflexi phylum, *Chloroflexi*			
	Chloroflexaceae			
	Chloroflexus aggregans	9485	- (52)*	-
	Chlorobi phylum, Chlorobia			
	Chlorobiaceae			
1	*Prosthecochloris aestuarii*[l]	271^{T}	- (52)*	-
	Prosthecochloris sp.[l]	*2K*	- (52)*	-
	Prosthecochloris vibrioforme[l]	260	- (52)*	-
	Prosthecochloris vibrioforme[l]	1678	- (52)*	-
2a	*Chlorobium luteolum*[l]	273^{T}	- (52)*	-
	Chlorobium luteolum[l]	262	- (52)*	-
2b	*Chlorobium phaeovibrioides*[l]	269^{T}	- (52)*	-
	Chlorobium phaeovibrioides[l]	265	- (52)*	-
	Chlorobium phaeovibrioides[l]	261	- (52)*	-
	Chlorobium phaeovibrioides[l]	270	- (52)*	-
3a	*Chlorobium phaeobacteroides*[l]	266^{T}	- (52)*	-
	Chlorobium clathratiforme[l]	5477^{T}	+ (55)	EF641906
	"Chlorobium ferrooxidans"	13031^{T}	- (52)*	-
3b	*Chlorobium limicola*[l]	245^{T}	- (52)*	-
	Chlorobium limicola[l]	246	- (52)*	-
	Chlorobium limicola[l]	*2323*	- (52)*	-
	Chlorobium limicola[l]	1855	+	EF641905
	Chlorobium limicola[l]	257	+	EF641903
	Chlorobium limicola[l]	247	- (52)*	-
	Chlorobium limicola[l]	248	- (52)*	-
4a	*Chlorobaculum parvum*[l]	263^{T}	- (52)*	-
	Chlorobaculum parvum[l]	*2352*	- (52)*	-

4b	*Chlorobaculum limnaeum*[l]	1677	+	EF641904
	Chlorobaculum thiosulfatiphilum[l]	249[T]	+	NA
	Chlorobaculum thiosulfatiphilum[l]	*2322*	+	EF641902
Proteobacteria phylum, *Alphaproteobacteria*				
Rhodospirillaceae				
	Rhodospirillum photometricum	122[T]	- (52)*	-
Rhodobacteraceae				
	Rhodothalassium salexigens	2132[T]	- (52)*	-
	Rhodovulum adriaticum	2781	- (52)*	-
	Rhodovulum sulfidophilum	1374[T]	- (52)*	-
Bradyrhizobiaceae				
	Rhodoblastus acidophilus	137[T]	- (52)*	-
Hyphomicrobiaceae				
	Blastochloris viridis	133[T]	- (52)*	-
Rhodobiaceae				
	Rhodobium marinum	2698[T]	- (52)*	-
Proteobacteria phylum, *Betaproteobacteria*				
Hydrogenophilaceae				
	Thiobacillus aquaesulis	4255[T]	+	EF641916
	Thiobacillus denitrificans	12475[T]	+	EF641952, EF641924
	Thiobacillus denitrificans	739	+	EF641955, EF641923
	Thiobacillus denitrificans	807	+	EF641922
	Thiobacillus plumbophilus	6690[T]	+	EF641956, EF641917
	Thiobacillus thioparus	505[T]	+	EF641954, EF641920
Proteobacteria phylum, *Gammaproteobacteria*				
Chromatiaceae				
	Allochromatium minutissimum	1376[T]	+	EF641963
	Allochromatium vinosum	180[T]	+	-
	Allochromatium warmingii	173[T]	+	EF641931
	Chromatium okenii[l]	*6010*	+	EF641935
	Halochromatium glycolicum	11080[T]	+	EF641934
	Halochromatium salexigens	4395[T]	+	EF641933
	Isochromatium buderi	176[T]	- (52)*	-
	Isochromatium buderi[l]	*5612*	- (52)*	-
	Lamprocystis purpurea[l]	4197[T]	+	EF641909
	Lamprocystis roseopersicina[l]	*4510*	+	EF641939
	Marichromatium gracile	203[T]	- (52)*	-
	Marichromatium purpuratum	1591[T]	- (52)*	-
	Rhabdochomatium marinum	5261[T]	+	EF641947
	Thermochromatium tepidum	3771[T]	+	EF641936
	Thiocapsa pendens	236[T]	± (55)	EF641914
	Thiocapsa rosea[l]	235[T]	± (55)	EF641961
	Thiocapsa roseopersicina	217[T]	+	EF641937, EF641907
	Thiocapsa roseopersicina[l]	*4210*	+	EF641938, EF641908
	Thiococcus pfennigii[l]	226[T]	+	EF641942
	Thiococcus pfennigii	227	+	EF641943
	Thiococcus pfennigii	228	+	EF641944
	Thiocystis gelatinosa	215[T]	+	EF641911
	Thiocystis violacea	207[T]	+	EF641948, EF641912
	Thiocystis violacea	214	+	EF641949
	Thiocystis violascens	198[T]	+	EF641910
	Thiodictyon bacillosum[l]	234[T]	±	EF641915
	Thiodictyon sp. strain F4	-	+	EF641921
	Thiohalocapsa halophila	6210[T]	+	EF641932
	Thiolamprovum pedioforme	3802[T]	+	EF641941
	Thiorhodococcus minor	11518[T]	+	EF641950, EF641913
	Thiorhodovibrio winogradskyi	6702[T]	±	EF641946
Ectothiorhodospiraceae				
	Ectothiorhodospira mobilis	4180	- (52)*	-
	Ectothiorhodospira shaposhnikovii	243[T]	- (52)*	-
Halothiobacillaceae				
	Halothiobacillus kellyi	13162[T]	- (52)*	-
	Halothiobacillus neapolitanus	581[T]	- (52)*	-
	Thiovirga sulfuroxydans sp. strain A7	-	- (52)*	-
Uncertain affiliation				
	"Thiobacillus prosperus"	5130[T]	- (52)*	-
Thiotrichaceae				
	Beggiatoa alba	1416[T]	- (52)*	-
	Beggiatoa leptomitiformis strain D-401[m]	-	- (52)*	-
	Beggiatoa leptomitiformis strain D-402[m]	-	- (52)*	-
	Leucothrix mucor	2157[T]	- (52)*	-
	Leucothrix mucor	621	- (52)*	-
	Macromonas bipunctata strain D-408[m]	-	- (52)*	-
	Thiothrix nivea	5205[T]	+	EF641919
	Thiothrix sp.	12730	+	EF641918
Piscirickettsiaceae				
	Thiomicrospira frisia	12351[T]	- (52)*	-
	Thiomicrospira kuenenii	12350[T]	- (52)*	-
	Thiomicrospira sp.	13163	- (52)*	-
	Thiomicrospira sp.	13164	- (52)*	-
	Thiomicrospira sp.	13189	- (52)*	-
	Thiomicrospira sp.	13190	- (52)*	-
Invertebrate symbionts and free-living relatives				
	Bathymodiolus azoricus symbiont[n]	-	+	EF641959
	Bathymodiolus brevior symbiont[n]	-	+	EF641958
	Bathymodiolus thermophilus symbiont[o]	-	+	EF641960
	Calyptogena magnifica symbiont[o]	-	+	NA

Ifremeria nautilei symbiont[p]	-	+	EF641929
Inanidrilus exumae symbiont[n]	-	+	EF641957, EF641927
Inanidrilus leukodermatus symbiont[n]	-	+	EF641926
Inanidrilus makropetalos symbiont[n]	-	+	EF641925
Oasisia sp. symbiont[o]	-	+	EF641962
Riftia pachyptila symbiont[o]	-	+	EF641928
sulfur-oxidizing bacterium OAII2	-	+	EF641953
sulfur-oxidizing bacterium OBII5	-	+	-
sulfur-oxidizing bacterium ODIII5	-	+	EF641951
sulfur-oxidizing bacterium ODI4	-	- (52)*	-
sulfur-oxidizing bacterium NDII1.2	-	- (52)*	-
Proteobacteria phylum, *Epsilonproteobacteria* *Helicobacteraceae*			
Sulfurimonas denitrificans	1251[T]	- (52)*	-

[a] taxonomic classification of investigated SRP species according to the Taxonomic outline of the prokaryotes, Bergey`s Manual of Systematic Bacteriology, 2nd edition, release 5.0 May 2004 (http://dx.doi.org/10.1007/bergeysoutline) and Kuever *et al*. (1996)

[b] DSMZ strain numbers: (-) strain not deposited in a culture collection; T, type strain; J. Imhoff laboratory (Kiel, University) -internal strain numbers are in italic type

[c] SRB reference strain provided by H. T. Dinh (MPI Bremen, Germany)

[d] SRB reference strain provided by K. Nauhaus (MPI Bremen, Germany)

[e] SRB reference strain provided by J. Detmers (MPI Bremen, Germany)

[f] SRB reference strain provided by T. A. Hansen (University Groningen, Netherlands)

[g] SRB reference strain provided by M. Könnecke (MPI Bremen, Germany)

[h] SRB reference strain provided by O. Kniemeyer (MPI Bremen, Germany)

[i] SRB reference strain provided by A. Galushko (MPI Bremen, Germany)

[j] SRB reference strain provided by G. Harms (MPI Bremen, Germany)

[k] SRB reference strain provided by H. P. Goorissen (University Groningen, Netherlands)

[l] SOB reference strain provided by J. Imhoff laboratory (Kiel, Germany)

[m] SOB reference strain provided by G. Dubinina (Winogradsky Institute of Microbiology, Russia)

[n] invertebrate tissue DNA provided by N. Dubilier (MPI Bremen, Germany)

[o] invertebrate tissue DNA provided by A. D. Nussbauer (University Vienna, Austria)

[p] invertebrate tissue DNA provided by C. Borowski (MPI Bremen, Germany)

[q] PCR amplification results with primer pair AprA-1-FW/ AprA-5-RV-GC (a "touchdown PCR" with an initial annealing temperature of 58°C was generally performed; lower initial annealing temperatures additionally tested in PCR assays are in parentheses): (+) correct-sized PCR amplicon without byproducts, (±) correct-sized PCR amplicon with byproducts, (-) no PCR amplicon obtained; (*) the absence of *aprBA* genes has been verified for respective SOB reference strain by additional molecular analysis (37)

Supplementary Fig. S1. PCR amplification results with new DGGE primer pair AprA-1-FW/ AprA-5-RV (with added GC-clamp) from selected sulfate-reducing and sulfur-oxidizing reference strains (indicated by their DSMZ numbers) as representatives of the major lineages of SRP and SOB

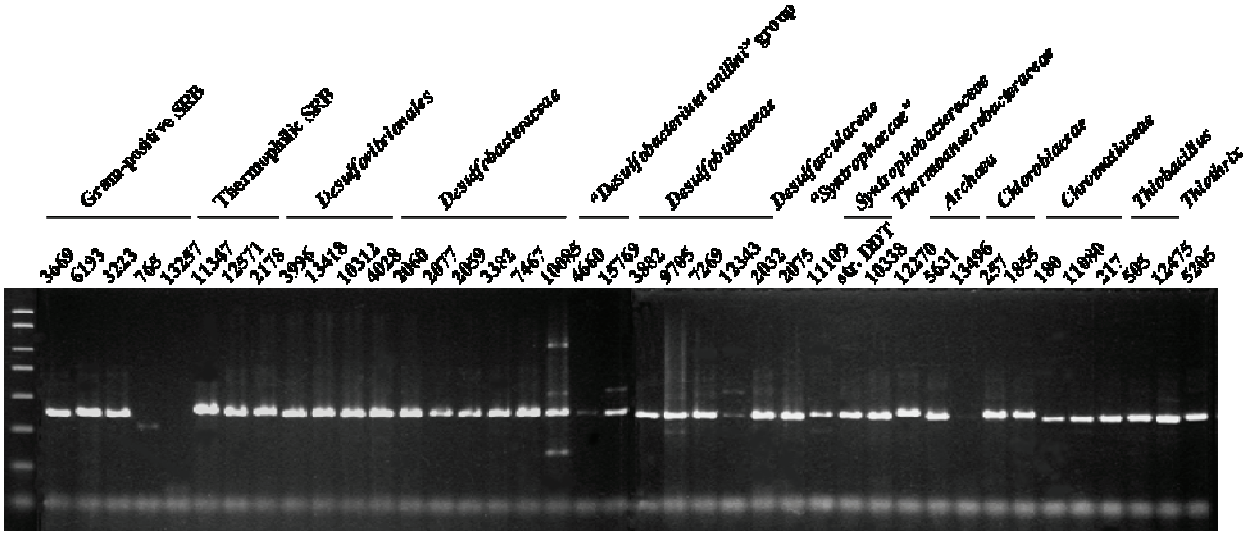

4.2.6 Publikation 6

Phylogenetic diversity and spatial distribution of the microbial community associated with the Caribbean deep-water sponge *Polymastia* cf. *corticata* by 16S rRNA, *aprA*, and *amoA* gene analysis

Birte Meyer und Jan Küver

Microbial Ecology (2008). 56, 306-321

Microb Ecol (2008) 56:306–321
DOI 10.1007/s00248-007-9348-5

ORIGINAL ARTICLE

Phylogenetic Diversity and Spatial Distribution of the Microbial Community Associated with the Caribbean Deep-water Sponge *Polymastia* cf. *corticata* by 16S rRNA, *aprA*, and *amoA* Gene Analysis

Birte Meyer · Jan Kuever

Received: 9 July 2007 / Accepted: 12 November 2007 / Published online: 10 January 2008
© Springer Science + Business Media, LLC 2007

Abstract Denaturing gradient gel electrophoresis (DGGE)-based analyses of 16S rRNA, *aprA*, and *amoA* genes demonstrated that a phylogenetically diverse and complex microbial community was associated with the Caribbean deep-water sponge *Polymastia* cf. *corticata* Ridley and Dendy, 1887. From the 38 archaeal and bacterial 16S rRNA phylotypes identified, 53% branched into the sponge-specific, monophyletic sequence clusters determined by previous studies (considering predominantly shallow-water sponge species), whereas 26% appeared to be *P.* cf. *corticata* specifically associated microorganisms ("specialists"); 21% of the phylotypes were confirmed to represent seawater- and sediment-derived proteobacterial species ("contaminants") acquired by filtration processes from the host environment. Consistently, the *aprA* and *amoA* gene-based analyses indicated the presence of environmentally derived sulfur- and ammonia-oxidizers besides putative sponge-specific sulfur-oxidizing *Gammaproteobacteria* and *Alphaproteobacteria* and a sulfate-reducing archaeon. A sponge-specific, endosymbiotic sulfur cycle as described for marine oligochaetes is proposed to be also present in *P.* cf. *corticata*. Overall, the results of this work support the recent studies that demonstrated the sponge species specificity of the associated microbial community while the biogeography of the host collection site has only a minor influence on the composition. In *P.* cf. *corticata*, the specificity of the sponge–microbe associations is even extended to the spatial distribution of the microorganisms within the sponge body; distinct bacterial populations were associated with the different tissue sections, papillae, outer and inner cortex, and choanosome. The local distribution of a phylotype within *P.* cf. *corticata* correlated with its (1) phylogenetic affiliation, (2) classification as sponge-specific or nonspecifically associated microorganism, and (3) potential ecological role in the host sponge.

Electronic supplementary material The online version of this article (doi:10.1007/s00248-007-9348-5) contains supplementary material, which is available to authorized users.

B. Meyer · J. Kuever
Max-Planck-Institute for Marine Microbiology,
Celsiusstrasse 1,
28359 Bremen, Germany

Present address:
J. Kuever (✉)
Bremen Institute for Materials Testing,
Paul-Feller-Strasse 1,
28199 Bremen, Germany
e-mail: kuever@mpa-bremen.de

Introduction

Sponges constitute the phylum *Porifera*, which is taxonomically divided into the three classes: *Calcarea*, *Hexactinellida*, and *Demospongiae* with the latter encompassing approximately 85% of the recognized species [23]. They are benthic, sessile filter feeders that depend on (dissolved) organic particle uptake from a continuous stream of water passing through their aquiferous canal system of channels and chambers. Particles including bacteria and single-celled eukaryotes can be captured by epithelial pinacocytes (forming the ectosome) at the sponge surface but are predominantly trapped from the filtered water within the choanocyte chambers-containing region of the sponge, the choanosome (or endosome). The food particles are transferred via transcytosis to the sponge cells of the interior mesohyl matrix. In some sponge species, a specialized area of the mesohyl that lacks choanocyte chambers but contains mineral deposits or collagen fibrils is located immediately below the exopinacoderm, the cortex. As part of the ectosome, the cortex has

been presumed to act as a special supportive device for the openings of the canal system and as a protective layer of the endosome against superficial injury or strong currents [1, 56]. The genus *Polymastia* Bowerbank, 1864 (*Demospongiae*, *Tetractinomorpha*, *Hadromerida*, *Polymastiidae*) with approximately 50 described species is characterized by their encrusting, spherical- or cushion-shaped sponges always with pore-bearing, inhalant and exhalant papillae and a cortex of the ectosomal skeleton that is composed of at least two layers [4, 43]. The species *Polymastia* cf. *corticata* Ridley and Dendy, 1887, is distinctive by its dense and leathery cortex (2 mm thickness; two distinct layers; intermediary layer collagenous), 100 inhalant and 4 to 5 exhalant papillae of approximately 8 mm height, and choanosomal bundles of spicules that stop below the cortex (the latter can be easily detached from the endosome). The species has been collected off the coast of Brazil and east of the Azores in a bathymetric range from 200 to 1,385 m [4, 43].

Early microscopic and culture-based examinations demonstrated that large numbers of microbes populate the mesohyl matrix of many demosponges (termed "bacteriosponges") forming up to 40% of the sponge volume with densities of 10^8 to 10^{10} bacteria per gram of sponge wet weight [64, 72]. The hypothesis of a widespread, sponge-specific microbial community that is distinctly different from the marine bacterioplankton that was postulated by Hentschel *et al.* [15, 16] and has been supported by others (for recent reviews, see [17, 19, 59, 67]). In contrast, the results of several recent diversity surveys contradict the existence of a general uniform sponge-associated microbial community regardless of sponge species and location. Instead, they provided evidence that the composition of the sponge-inhabiting microbial consortium depends on the host species [18, 22, 33, 60–63, 68]. A correlation between the presence of certain major bacterial taxonomic groups in the sponge microbiota and the geographical location of the host sponge was proposed by Hill *et al.* [18]. However, the presence of distinct microbial consortia in different sponge species sharing the same habitat indicated a low impact of the surrounding marine plankton for the sponge–bacteria associations [60, 62, 63, 68]. As recently demonstrated by Thiel *et al.* [63], the specificity of sponge–microbe associations extends to the spatial distribution of microbial populations within the sponge body: Distinct bacterial communities were found to inhabit the endosome and cortex of marine sponge *Tethya aurantium*; specifically associated phylotypes (e.g., cortex-associated members of the *Bacteroidetes* and *Alphaproteobacteria*) were identified for both regions.

The current knowledge about sponge–microbe associations is restricted to investigations of shallow-water species with the only exception of the bacterial 16S rRNA gene-based analysis published by Olson and McCarthy [48]. The aim of the present study was to examine the phylogenetic composition and spatial distribution of the archaeal and bacterial community associated with a deep-water sponge *P.* cf. *corticata* by DGGE-based 16S rRNA and functional gene analyses. The analyses of functional genes that encode key enzymes of the dissimilatory sulfate reduction, sulfur oxidation, and ammonia oxidation pathway, e.g., *aprA* and *amoA* (coding for the alpha subunits of the dissimilatory APS reductase, AprA, and ammonia monooxygenase, AmoA), allow diversity surveys of certain physiological groups, e.g., sulfate-reducing, sulfur-oxidizing, and ammonia-oxidizing prokaryotes. The polyphyly of these physiological groups (see [5, 11, 13, 24, 28, 29, 50, 73] and references therein) restricts the concomitant detection of all recognized members by the use of single 16S rRNA gene-targeting probes or primer pairs and limits the identification of novel lineages in environmental analyses. In addition, the analysis of 16S rRNA genes cannot provide an unambiguous link between the genetic identity of an uncultured microorganism and its physiological or metabolic capacity. Analyses of functional genes like *aprA* and *amoA* circumvent these limitations and (although complicated by lateral gene transfer events of *aprA* [39, 40]) have been successfully applied for biodiversity studies [2, 14, 31, 41, 46, 47]. They were used to determine the phylogenetic complexity of the *P.* cf. *corticata*-associated microbial communities putatively involved in sulfur and nitrogen cycling within the sponge.

Materials and Methods

Sampling

The deep-water sponge was collected by a chain bag dredge from a depth of 1,127 m at the Kahouanne Basin (Lesser Antilles, Caribbean Sea) (16°28.80′ N, 61°58.66′ W) in January 2001 (RV Sonne cruise SO-154). Ambient seawater (temperature 5°C) was sampled from the surface of undisturbed sediment cores with a sterile syringe; all samples were immediately frozen and stored at −20°C until further molecular investigation. In the laboratory, the sponge was washed carefully three times in autoclaved artificial seawater before cutting. Small subsamples (2–3 cm^3 tissue cubes) were fixed in 4% formaldehyde, placed in 70% ethanol, and sent to the Senckenberg Museum, Frankfurt am Main, Germany, for sponge identification. Examination of its general morphological features including spicules geometry of the tissue sample (deposited under the registration number SMF 9633) classified this deep-water specimen as *P.* cf. *corticata* Ridley and Dendy, 1887, a member of the *Polymastiidae* (*Demospongiae*, *Hadromerida*) (D. Janussen, pers. comm.). For molecular analy-

sis, two sponge tissue subsamples were separated into papillae, outer cortex (including ectopinacoderm), inner cortex, and endosome (choanosome) sections (Fig. 1) with a sterile scalpel. The tissue sections were gently rinsed in autoclaved artificial seawater to remove loosely attached bacteria from the surfaces and cut into small pieces before DNA extraction. Two seawater samples (each 200 ml) were filtered through a Sterivex filter (0.2 μM pore size, Millipore).

Genomic DNA Extraction

Total genomic DNA were extracted from the four different sponge tissue sections in duplicate and purified using the DNeasy® Tissue Kit (Qiagen, Hilden, Germany) following the manufacturer's protocol for Gram-positive bacteria and animal tissue. Genomic DNA from both filtered seawater samples was extracted after five cycles of thawing at 30°C and freezing in liquid nitrogen using the protocol of Zhou *et al.* [74]. The DNA concentrations were estimated spectrophotometrically, whereas its integrity was examined visually by gel electrophoresis on 0.8% (*w*/*v*) agarose gels run in 1x Tris–borate–EDTA (TBE) buffer followed by ethidium bromide staining (0.5 mg l^{-1}). The extracted DNA (dissolved in 10 mM Tris–HCl, 1 mM EDTA, pH 7.5) was stored at −20°C until further analysis.

PCR Amplification of Partial 28S rRNA Gene

Besides its morphological identification, 28S rRNA gene fragments (C1, D1, C2, and D2 domains at the 5′-end) were amplified from the sponge-derived genomic DNA using the primers and polymerase chain reaction (PCR) protocol of Chombard *et al.* [6] to confirm the former morphological classification by molecular systematics (for PCR primer sequences and detailed thermocycling conditions see Table S1 of the Electronic Supplementary Material).

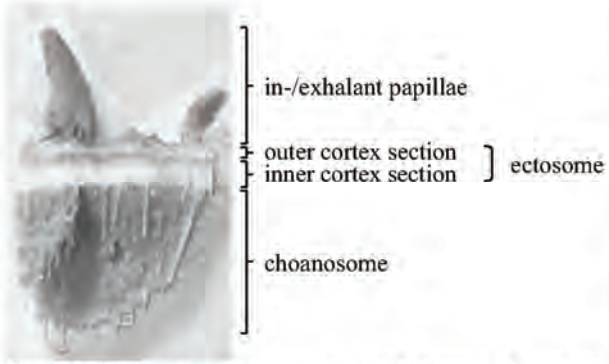

Figure 1 Photograph of a cross-section of *Polymastia* cf. *corticata* showing the examined morphologically different tissue regions, (1) papillae, (2) outer section of the cortex including the exopinacoderm and (3) inner (collagenous) section of the cortex (comprising the ectosome), and (4) the choanosome (endosome)

PCR Amplification of Partial 16S rRNA, *aprA*, and *amoA* genes for Subsequent Double Gradient Denaturing Gradient Gel Electrophoresis Analysis

In general, PCR mixtures (50 μl total volume) contained 1x RED*Taq* PCR reaction buffer (Sigma-Aldrich, St. Louis, Missouri, USA), 0.3 mg ml^{-1} bovine serum albumin (BSA), 200 μM deoxynucleoside triphosphates (dNTPs) mixture, 1 μM of each primer, 0.05 U μl^{-1} RED*Taq* DNA Polymerase, and 100 ng genomic DNA as template (negative controls with water). Partial 16S rRNA gene amplification for subsequent double gradient denaturing gradient gel electrophoresis (DG-DGGE) analysis was performed using the primer sets (1) GM5F-GC clamp (341F) and 907R for *Bacteria* [45], (2) Arch516F-GC clamp (K. Knittel, unpublished) and Arch958R [7] for *Archaea*, and (3) CTO189f-GC clamp and CTO654r specific for betaproteobacterial ammonia-oxidizers [30]. An approximately 0.4-kb *aprA* gene fragment was amplified using the primer set AprA-1-FW and AprA-5-RV with GC clamp [41]. An approximately 0.5-kb *amoA* gene fragment was yielded applying the primer pair AmoA-1F and AmoA-2R-TC [46] (for details see Table S1 of the Electronic Supplementary Material). Duplicate amplifications were performed from each sponge tissue section and seawater DNA sample. The PCR products were visually analyzed by electrophoresis of aliquots (10% of the reaction volume) on 2% agarose gels (*w*/*v*) run in 1x TBE buffer stained with ethidium bromide (0.5 mg l^{-1}) to verify correct amplicon size. If necessary, amplicons of the expected gene fragment size were purified before further analysis using either the QIAquick gel extraction kit (Qiagen, Hilden, Germany) or the Perfectprep gel cleanup sample kit (Eppendorf, Hamburg, Germany) following the supplier's recommendations.

DG-DGGE Analysis

The DG-DGGE analyses of the aforementioned duplicate 16S rRNA, *aprA*, and *amoA* amplicons from each sponge tissue type and seawater DNA sample were performed using the D-GENE™ and D-CODE™ system (Bio-Rad, Munich, Germany). DG-DGGE gels (1.0 mm thick) were poured with an polyacrylamide gradient from 6% to 8% of acrylamide/bis-acrylamide stock solution, 37.5:1 (*v*/*v*) (Bio-Rad) superimposed over a colinear denaturant gradient [100% denaturant corresponds to 7 M urea and 40% (*v*/*v*) formamide, deionized with AG501-X8 mixed bed resin (Bio-Rad)], which varied for the different genes analyzed in this study (see Table S2 of the Electronic Supplementary Material). Gradients were formed using a Bio-Rad Gradient

Former Model 385. Twenty microliters of the PCR samples were mixed with 6 µl of dye solution [0.1% bromphenol blue (*w*/*v*), 70% glycerol (*v*/*v*)] and applied to the gels. Triplicate gel runs were carried out as reported elsewhere (for references see Table S2 of the Electronic Supplementary Material) followed by ethidium bromide staining (0.5 mg l^{-1}) for 15 min and subsequent destaining in double-distilled water for 10 min. The DNA bands were visualized on a UV transillumination table (Biometra, Göttingen, Germany); persisting and dominant bands were excised from multiple lanes of the polyacrylamide gels with ethyl alcohol-sterilized scalpel, incubated in 50 µl Tris–HCl, pH 8.0, overnight at 4°C, and reamplified using 1 µl of the eluate as template and PCR conditions as described above. The purity and migration behavior of the reamplification products of the bands were checked by DG-DGGE. The reamplification products were purified from free PCR primers using either the QIAquick gel extraction kit (Qiagen) or the Perfectprep gel cleanup sample kit (Eppendorf) following the supplier's recommendations.

Nucleotide Sequencing

All reamplification products of the DG-DGGE bands were sequenced directly in both directions using the respective amplification primers and the ABI Prism BigDye terminator cycle sequencing ready reaction kit (Applied Biosystems, Foster City, USA) according to the manufacturer's instructions. Sequencing reactions were run on an ABI PRISM® 3100 Genetic Analyzer (Applied Biosystems).

Phylogenetic Analysis

The partial 16S rRNA sequences obtained from DGGE analysis were checked for chimeras with the program CHECK_CHIMERA of the Ribosomal Database Project, added to the 16S rRNA sequence database of the Technical University Munich (Germany) using the automatic alignment function ARB_Align implemented in the ARB software program package (http://www.arb-home.de), and manually corrected. The sequences were maintained separately according to their source (sponge tissue type, seawater); each set of sequences was grouped into phylotypes, i.e., operational taxonomic units (OTUs), based on a >99% identity cutoff. Only one sequence per OTU and tissue type/seawater was used for further analysis. The closest phylogenetic relatives of each phylotype were identified by comparison to the National Center for Biotechnology Information (NCBI) GenBank database using the Basic Local Alignment Search Tool (BLAST) analysis tools (www.ncbi.nlm.nih.gov/BLAST/). For phylogenetic analysis, the online version of PhyML (http://atgc.lirmm.fr/phyml) was used. Maximum-likelihood trees were calculated based on the near full-length 16S rRNA reference sequences received from the database; their robustness was tested by bootstrap analysis with 100 resamplings. Subsequently, these trees were imported into ARB and the DGGE analysis-derived short sequences were individually added by using the QUICK_ADD parsimony tool of ARB without allowing changes in the overall tree topology. The phylogenetic positions of the short sequences were additionally verified by bootstrap analysis with 100 resamplings (maximum-likelihood method). To determine the specificity of the microbial associations, the detected phylotypes from *P.* cf. *corticata* were classified as (1) "specialists", (2) "sponge associates", or (3) "generalists" depending on their presence in (1) this host species only, (2) several sponge species but absent from seawater, or (3) several sponge species and seawater in accordance to Taylor *et al.* [60]; the enumeration of the sponge-associated bacterial (SAB) and archaeal (SAA) phylogenetic clusters is based on the previous studies of Hentschel *et al.* [16], Thiel *et al.* [63], Holmes and Blanch [22], and Lee *et al.* [32].

The *aprA* and *amoA* nucleotide sequence data obtained from DGGE analysis were assembled and manually corrected using the Bioedit (version 7.0.5) sequence alignment editor (http://www.mbio.ncsu.edu/BioEdit/bioedit.html). The sequences were maintained separately according to their source (sponge tissue type, seawater); each set of sequences was grouped into phylotypes based on a >99% identity cutoff. Only one sequence per OTU and tissue type/seawater was used for further analysis. BLAST searches in the public databases for homologous sequences of the partial AmoA sequences were performed. The partial and complete AmoA sequences were automatically aligned using the Web server Tcoffee@igs (http://igs-server.cnrs-mrs.fr/Tcoffee/); the initial alignment was refined manually. The partial AprA sequences were integrated into the persisting Apr alignment of sulfate-reducing and sulfur-oxidizing reference strains [39, 40] including all full-length Apr sequences available from the public databases. The AmoA and AprA data sets were phylogenetically analyzed using PhyML. Regions of insertions and deletions (indels) were omitted. The maximum-likelihood method-based phylogenetic trees were constructed using the global rearrangement and randomized species input order options and the JTT matrix as amino acid replacement model. Statistical support is given by bootstrap analysis with 100 resamplings.

GenBank Accession Numbers

The nucleotide sequence data reported in this article are available under the GenBank accession numbers EU005552 (28S rRNA gene), EU005553-EU005595 and EU005641-EU005648 (16S rRNA gene), EU005596-EU005620 (*aprA* gene), and EU005621-EU005640 (*amoA* gene).

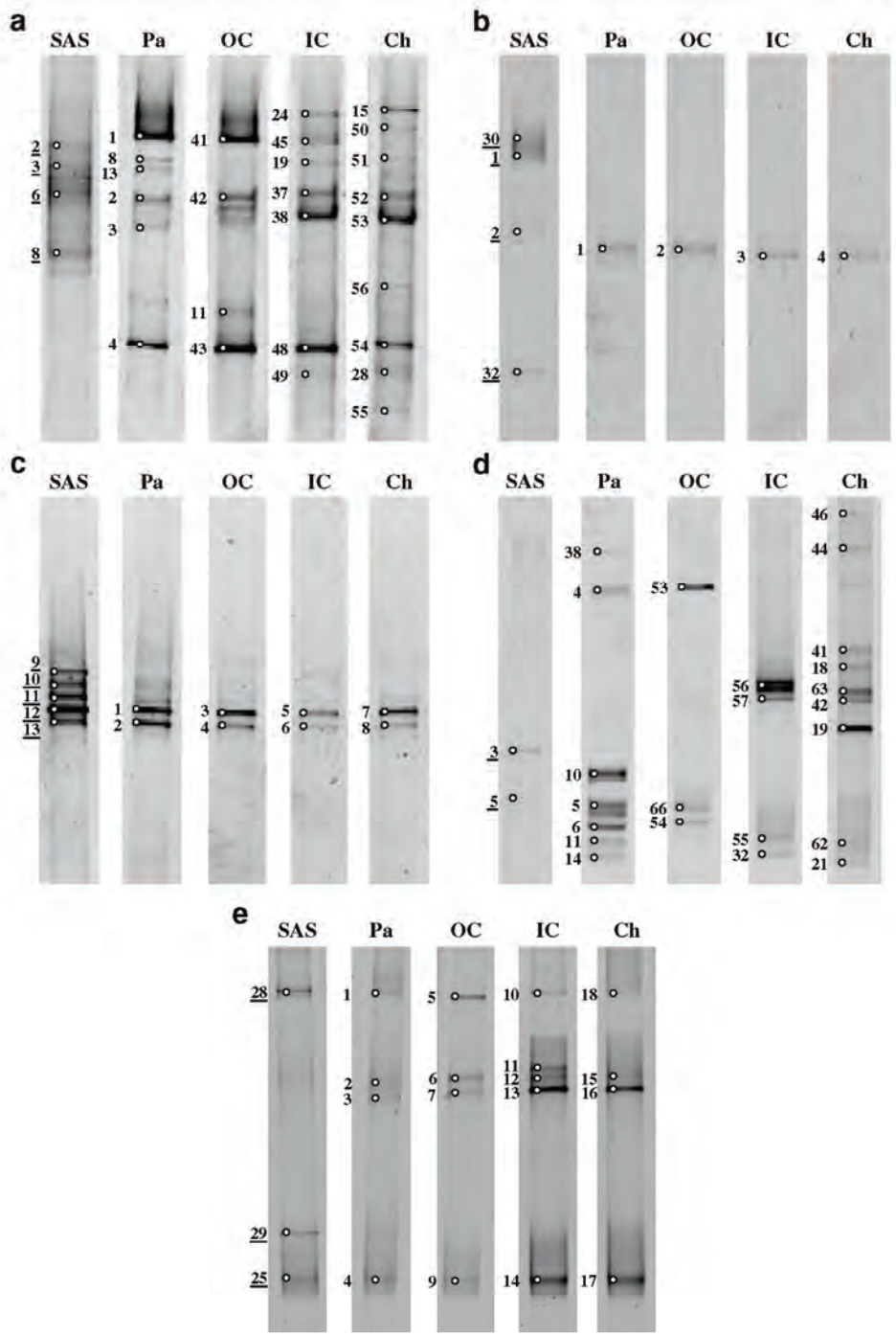

Figure 2 DGGE banding patterns of amplified 16S rRNA, *aprA*, and *amoA* gene fragments using DNA samples from sponge tissue sections, papillae (*Pa*), outer cortex (*OC*), inner cortex (*IC*), and choanosome (*Ch*) of Caribbean *P.* cf. *corticata* and sponge ambient seawater (SAS) collected at the Kahouanne Basin (see Fig. 1). 16S rRNA gene-specific diversity analysis was performed applying universal bacterial (**a**), universal archaeal (**b**), and betaproteobacterial ammonia-oxidizer-specific (**b**) gene-targeting primer pairs in PCR. Diversity analysis of functional genes was performed using SRP- and SOB-specific *aprA* gene-targeting primers (**d**) and betaproteobacterial ammonia-oxidizer-specific *amoA* gene-targeting primers (**e**). *Numbered* DGGE bands were excised from replicate gels and successfully sequenced (phylogenetic analyses of retrieved sequences, see Figs. 3, 4, and 5)

Results

DGGE

DGGE was used to fingerprint the microbial community in *P.* cf. *corticata* (Fig. 1). The banding patterns of the same tissue type were identical, indicating no genomic DNA extraction and PCR amplification bias. The banding patterns of DGGE analyses using universal archaeal, bacterial, and *aprA* gene-targeting primers showed the presence of different microbial communities in the inner and outer regions of *P.* cf. *corticata* (Fig. 2a, b, d). In addition, all tissue

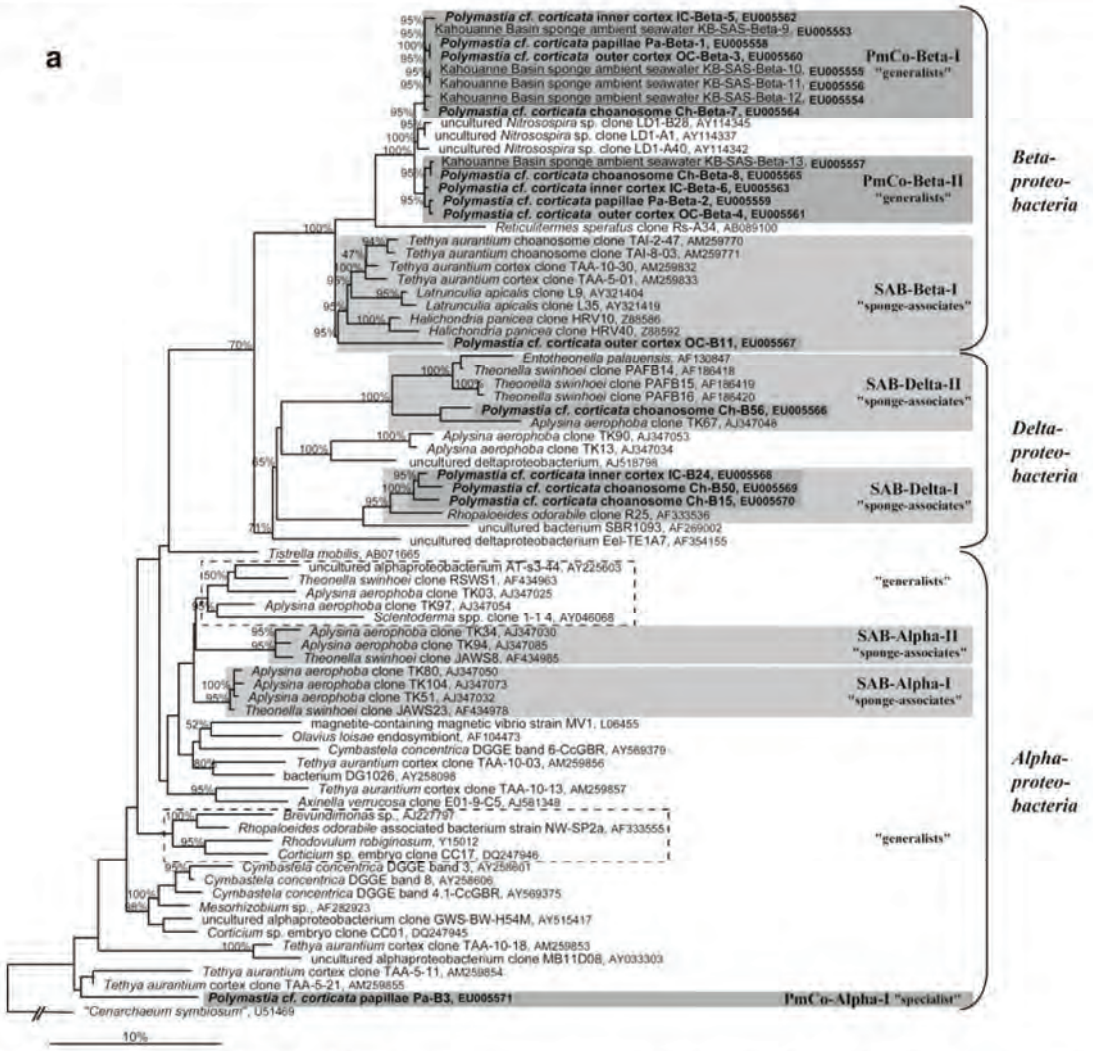

Figure 3 Phylogenetic trees based on the 16S rRNA sequences obtained from the *P.* cf. *corticata*-associated microbial community and host sponge surrounding seawater with the three 16S rRNA gene-targeting primer sets used in this study and related sequences belonging to the *Alphaproteobacteria*, *Betaproteobacteria*, and *Deltaproteobacteria* (**a**); *Gammaproteobacteria* (**b**); *Acidobacteria* and *Nitrospira* (**c**); and *Actinobacteria* and *Archaea* (**d**). Sequences obtained from *P.* cf. *corticata* are shown in *bold type* and highlighted by *dark-gray boxes*, whereas those obtained from the host sponge ambient seawater are *underlined*. The monophyletic, sponge-associated bacterial and archaeal 16S rRNA clusters are highlighted by *light-gray boxes*. The *P.* cf. *corticata*-derived sequences are classified into clusters of *P.* cf. *corticata* specialists ("PmCo specialist"), general "sponge-associated" *Bacteria* and *Archaea* (SAB, SAA) and "generalists" ("generalist" groups formed by other sponge species-derived sequences are framed by *dashed lines*) according to Taylor *et al.* [60]. Maximum-likelihood bootstrap resampling values greater than 50% (100 resamplings) are indicated near the nodes. The 16S rRNA gene sequence of *Cenarchaeum symbiosum* was used as outgroup reference. The scale bar corresponds to 10% estimated sequence divergence

sections of the sponge differed in their DGGE banding pattern from the sponge ambient seawater (SAS) samples. Archaeal and bacterial phylotypes specifically associated with the distinct sponge regions were represented by DGGE bands that were exclusively present in all papillae, outer cortex, inner cortex, or choanosome samples, respectively, but absent in seawater (Fig. 2a, b, d). Other bands were found in all sponge tissue samples. Contrarily, the DGGE banding patterns of the betaproteobacterial ammonia-oxidizer-specific 16S rRNA and *amoA* gene-based analyses were highly similar (1) between the distinct sponge tissue types and (2) between sponge and ambient seawater (Fig. 2c and e). Phylotypes specifically associated with *P.* cf. *corticata* that were represented by DGGE bands exclusively found in the sponge samples (but not in seawater) were only detected by the *amoA* gene-based analysis (Fig. 2e).

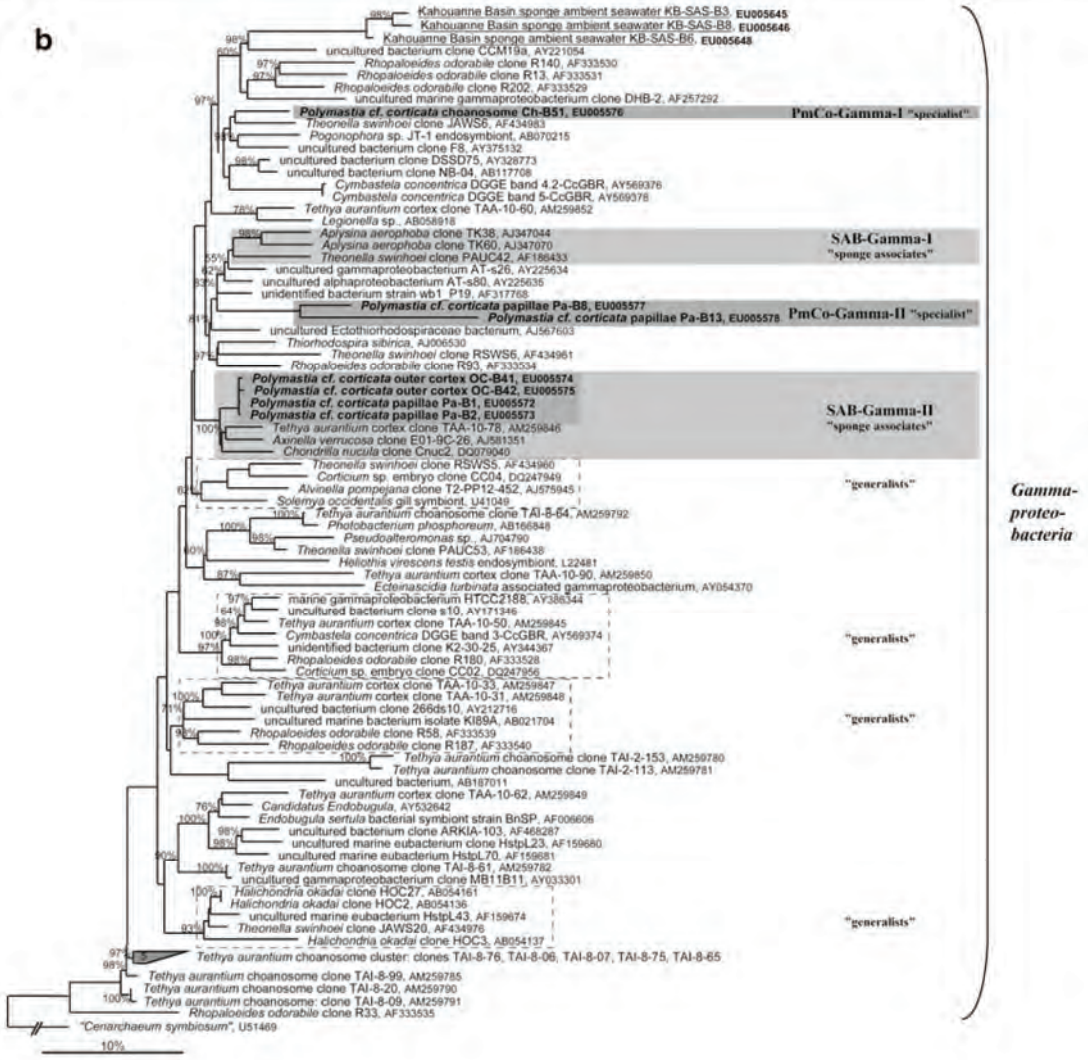

Figure 3 (continued)

Phylogenetic Analysis of Partial 16S rRNA Gene Sequences

A total of 38 OTUs was identified in *P.* cf. *corticata* forming 18 distinct sequence clusters. The sequences fell into eight different archaeal and bacterial divisions, the *Crenarchaeota*, *Alphaproteobacteria*, *Betaproteobacteria*, *Gammaproteobacteria*, *Deltaproteobacteria*, *Acidobacteria*, *Actinobacteria*, and *Nitrospira* (Fig. 3). In agreement with microbial communities associated with other examined deep-water sponges [48], no phylotype related to the cyanobacterial lineage was identified in the deep-water specimen of *P.* cf. *corticata*. Members of the latter phototrophic group are abundant in shallow-water sponges [16, 18, 51, 60, 61, 63]. Twenty of the aforementioned 38 phylotypes (53%) were most closely affiliated with other sponge-derived sequences previously found in *Tethya aurantium*, *Rhopaloides odorabile*, *Theonella swinhoei*, *Latrunculia apicalis*, *Halichondria panicea*, *Aplysina aerophoba*, *Sclerotiderma* sp., *Chondrilla nucula*, *Petrosia* sp., *Suberites* sp., and *Axinella verucosa* from different geographical locations (predominantly shallow-water habitats). These phylotypes comprised the eight sponge-specific, monophyletic clusters SAB-Beta-I [63], SAB-Gamma-II, SAB-Delta-I and SAB-Delta-II, SAB-Acido-III, SAB-Actino-III, SAB-Nitrospira-I [16], and SAA-Cren-I (sponge group C) [22, 32] (classified as "sponge associates"). It is interesting to note that the detected alphaproteobacterial, most gammaproteobacterial, actinobacterial, and crenarchaeal phylotypes appeared to represent *P.* cf. *corticata* host-

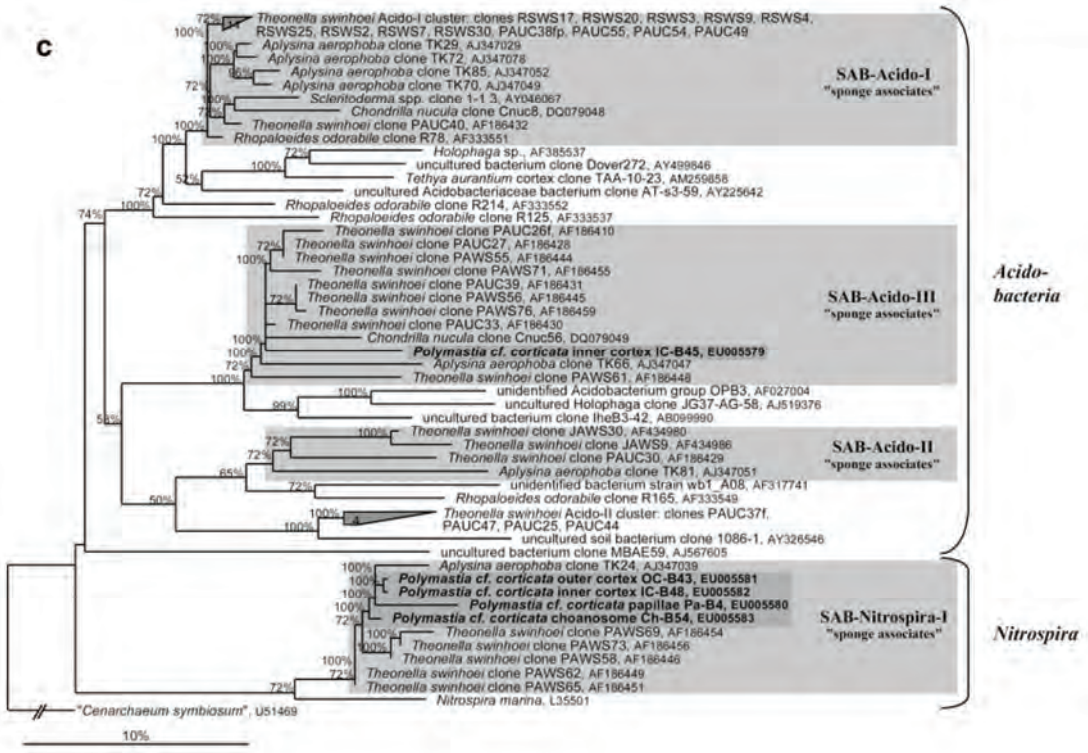

Figure 3 (continued)

specific microorganisms ("specialists" PmCo-Alpha-I, PmCo-Gamma-I/-II, PmCo-Actino-I/-II/-III, and PmCo-Cren-I) not present in the ambient seawater and other sponge species. Based on the current database, these 10 phylotypes (26%) were only moderately related to other sponge-derived sequences but affiliated to environmental sequences received from other marine macroorganisms (*Pogonophora* endosymbionts; PmCo-Gamma-II), aquatic microbial formations in Nullarbor caves [21] (PmCo-Gamma-I, PmCo-Actino-I), inactive deep-sea hydrothermal vent chimneys [57] (PmCo-Actino-II), and deep-sea sediments [65] (PmCo-Cren-I). Indeed, by the use of betaproteobacterial ammonia-oxidizer-specific primers [30], close relatives of uncultured marine *Nitrosospira* [10] were detected in the sponge tissue and in the host surrounding seawater (classified as "generalists" PmCo-Beta-I and PmCo-Beta-II).

The bacterioplankton assemblage of the sponge ambient seawater at the Kahouanne Basin (1,127 m depth) was phylogenetically less diverse with respect to the complex microbial community associated with *P.* cf. *corticata* (Fig. 3). The detected phylotypes were most closely affiliated with seawater- and deep-sea sediment-derived sequences of uncultured members of the marine group-I *Crenarchaeota* (MG-I, group C1a-α) [65], *Euryarchaeota* [38], *Nitrosospira* [10], uncultured *Gammaproteobacteria* and *Bacteroidetes* (respective SAS-B2 16S rRNA sequence is not shown in Fig. 3; closest relative is AJ567605; M.X. Xu, P. Wang, F.P. Wang, and X. Xiao, unpublished results).

Phylogenetic Analysis of Partial AprA and AmoA Sequences

The *aprA* gene-based analysis allowed the detection of six phylotypes that are indicative for the presence of five sulfur-oxidizing alphaproteobacterial and gammaproteobacterial species and one sulfate-reducing archaeon in the tissue of *P.* cf. *corticata* (Fig. 4). The alphaproteobacterial SOB-phylotypes were most closely related to AprA sequences of cultured members of the SAR11 clade [12] (PmCo-sulfur-oxidizer-I to PmCo-sulfur-oxidizer-III) and the LGT-affected *Thiobacillus plumbophilus* (PmCo-sulfur-oxidizer-IV). Because representatives of the alphaproteobacterial clusters I to III have also been found to be abundant in deep-sea sediments of the Kahouanne Basin and the sponge ambient seawater (Fig. 4), the corresponding SOB species were classified as "generalists". The gammaproteobacterial SOB-phylotype (PmCo-sulfur-oxidizer-V) was moderately affiliated to AprA sequences of uncultured *Thiothrix* species, which have been found in cold seep *Beggiatoa*-mats at the Hydrate Ridge, Oregon [41]. All identified SOB-phylotypes could not be assigned to any detected 16S rRNA gene-

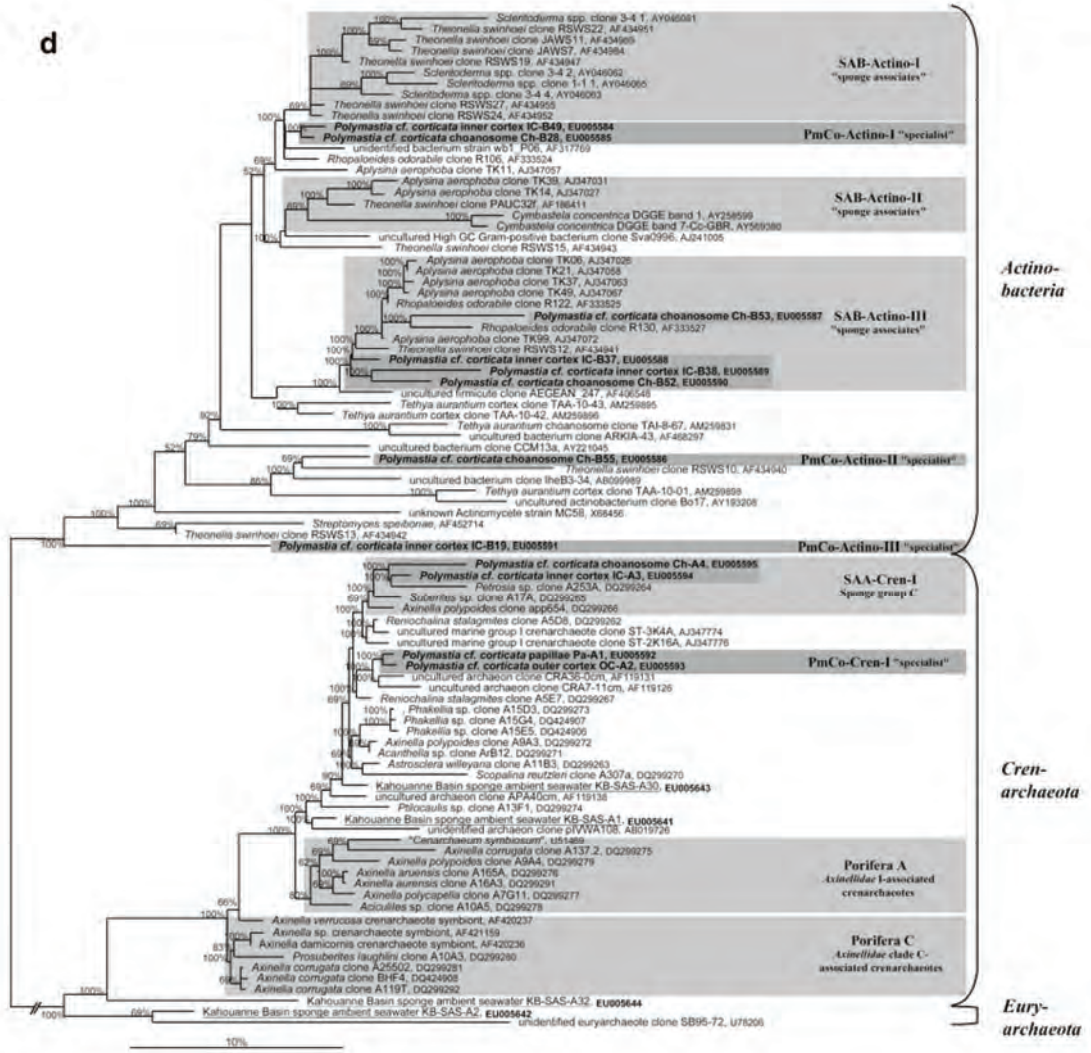

Figure 3 (continued)

based OTU. Besides, a SRP-phylotype was detected that is most closely related to the AprA sequences of *Archaeoglobus* members; a corresponding euryarchaeal species was not identified by the 16S rRNA gene-based analysis.

The *amoA* gene-based analysis (*Betaproteobacteria*-specific primers) allowed the detection of nearly identical phylotypes (PmCo-ammonia-oxidizer-I and PmCo-ammonia-oxidizer-II) in the sponge tissue and the host surrounding seawater (Fig. 5); closely related environmental sequences have also been reported from diverse sediment or seawater–sediment interface samples of other habitats [2, 14, 31]. The AmoA sequence clusters corresponded to the uncultured *Nitrosospira* sequence clusters that have been identified by the group-specific 16S rRNA gene analysis (Fig. 3).

Spatial Distribution of the Sponge-Associated Microbial Community

The phylogenetic investigations of different tissue regions from *P.* cf. *corticata* (Fig. 1) demonstrated high variability in the microbial communities associated with the sponge papillae/outer cortex and the inner cortex/choanosome (Figs. 3, 4, and 5, summarized in Table 1). The 16S rRNA gene-based analysis indicated that the highest phylogenetic diversity is present in the inner region of the sponge, the choanosome. From the total of 38 different 16S rRNA gene-based phylotypes, 12 and 10 OTUs were detected in the choanosome and the inner cortex, respectively, whereas only 7 and 9 OTUs were found in the outer cortex and in the papillae tissue sections, respectively. The members of

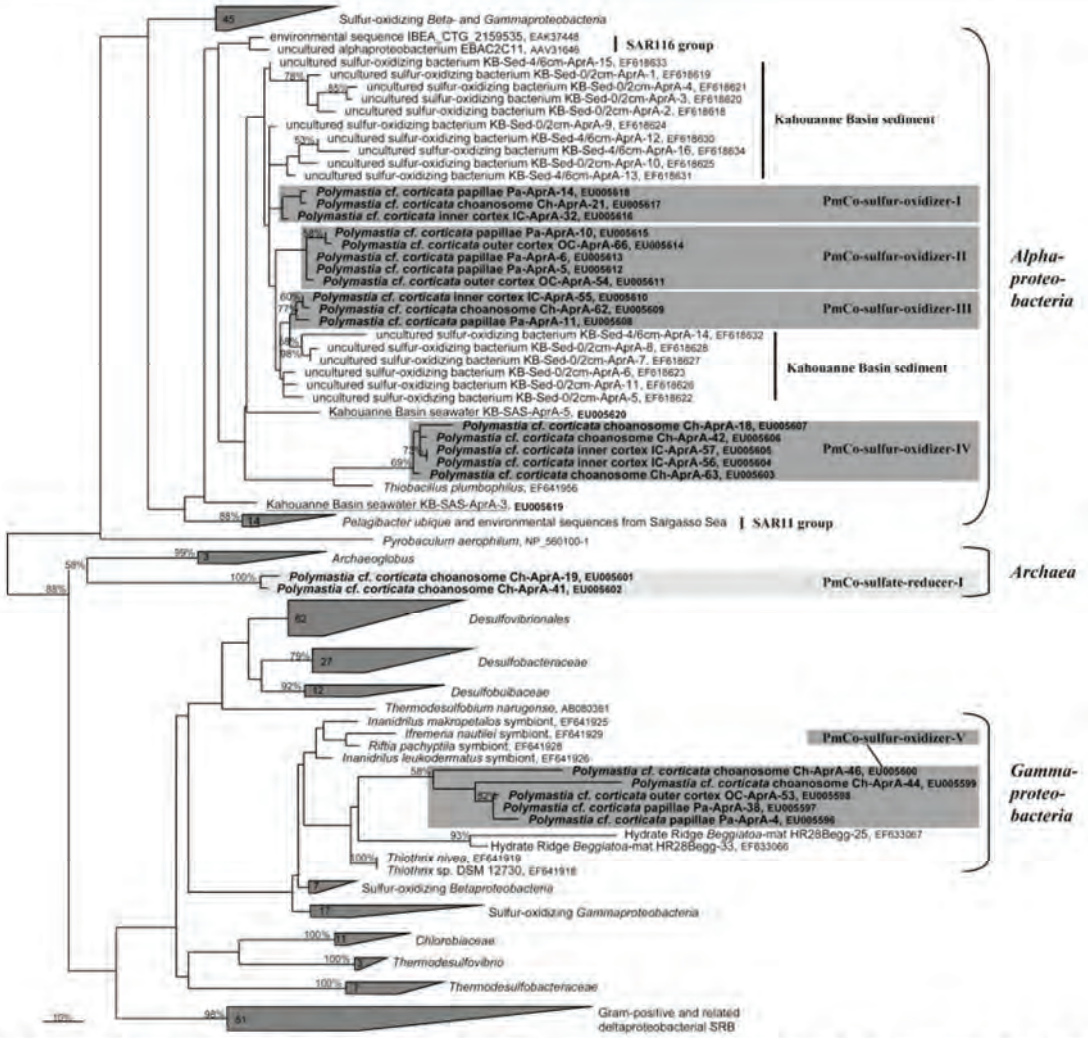

Figure 4 Phylogenetic tree based on the AprA sequences obtained from the *P.* cf. *corticata*-associated microbial community, the host sponge surrounding seawater, and adjacent sediment samples from the Kahouanne Basin. SRP- and SOB-type sequences received from *P.* cf. *corticata* are shown in *bold type* and highlighted by *light-gray* and *dark-gray boxes*, respectively; those obtained from the host sponge ambient seawater are *underlined*. The taxonomic classification of the SRP and SOB reference strains and affiliated sponge-derived sequences is indicated. Maximum likelihood bootstrap resampling values greater than 50% (100 resamplings) are indicated near the nodes. The scale bar corresponds to 10% estimated sequence divergence

the different archaeal and bacterial divisions were not evenly distributed within the sponge body but appeared to be associated with distinct parts of the host tissue. Five of the eight general sponge-specific clusters (SAB-Delta-I and SAB-Delta-II, SAB-Acido-III, SAB-Actino-III, SAA-Cren-I, 11 phylotypes) and all *P.* cf. *corticata*-specifically associated actinobacterial phylotypes (PmCo-Actino-I, PmCo-Actino-II, and PmCo-Actino-III, 4 phylotypes) were exclusively present in the inner cortex and the choanosome. Thus, the members of the *Deltaproteobacteria*, *Acidobacteria*, and *Actinobacteria* were restricted to the inner parts of this sponge. In contrast, four of the five *P.* cf. *corticata*-derived sequence clusters that were exclusively identified in the sponge surface regions belonged to the *Alphaproteobacteria*, *Betaproteobacteria*, and *Gammaproteobacteria* (8 phylotypes). The OTUs comprised only two general sponge-specific clusters (SAB-Beta-I, SAB-Gamma-II) besides four putative "specialists" clusters (PmCo-Alpha-I, PmCo-Gamma-II, PmCo-Cren-I) whose phylotypes were affiliated with nonsponge-derived sequences received from diverse habitats. The *Crenarchaeota* associated with the papillae and outer cortex sections were distinct to those found in the inner cortex and choanosome. Notably, with the exception of PmCo-Gamma-I, no phylotype obtained from the choanosome or the inner cortex section was closely related to environmental sequences found in seawater and sediment samples.

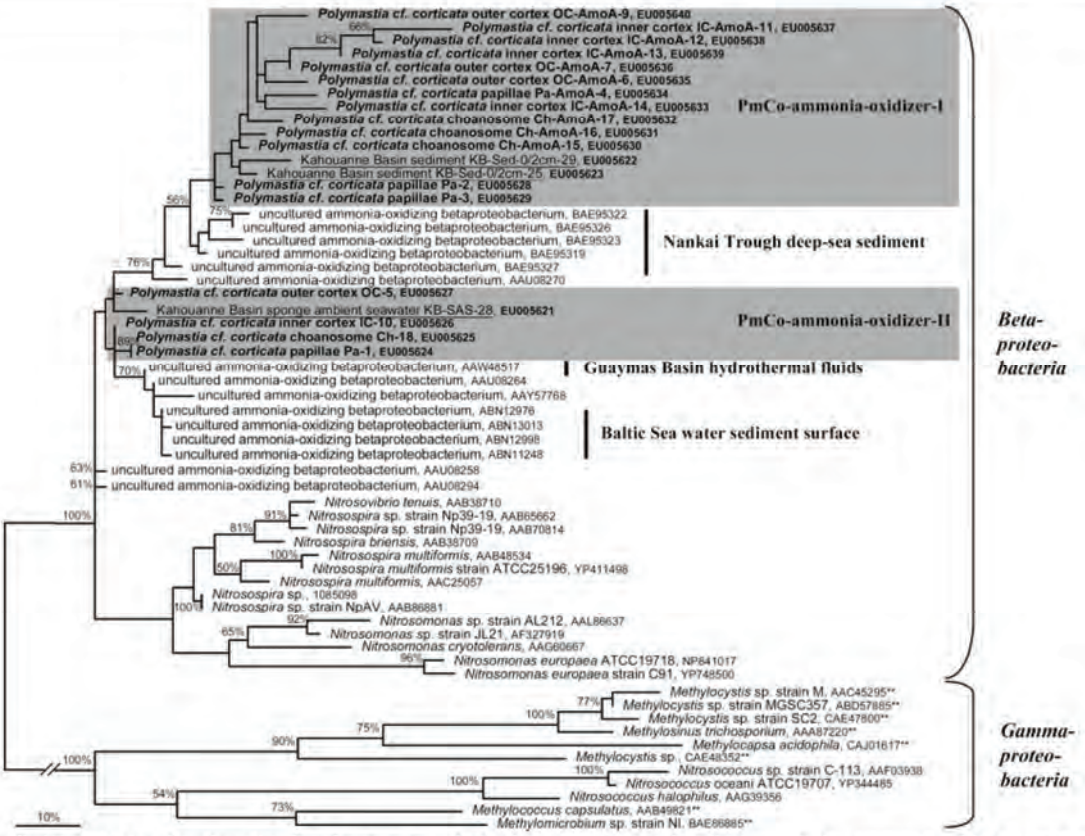

Figure 5 Phylogenetic tree based on the AmoA sequences obtained from the *P.* cf. *corticata*-associated microbial community and host sponge surrounding seawater including related (reference strain and environmental) sequences belonging to the *Betaproteobacteria* and *Gammaproteobacteria*. Sequences received from *P.* cf. *corticata* are shown in *bold type* and highlighted by *dark-gray boxes*, whereas those obtained from the host sponge ambient seawater are *underlined*. The taxonomic classification of the ammonia-oxidizing proteobacterial reference strains and affiliated sponge-derived sequences is indicated. Maximum-likelihood bootstrap resampling values greater than 50% (100 resamplings) are indicated near the nodes. The AmoA sequences of the *Gammaproteobacteria* were used as outgroup reference. The scale bar corresponds to 10% estimated sequence divergence

Table 1 Spatial distribution of phylotypes from the major microbial taxonomic/physiological groups identified in different tissue sections of *P.* cf. *corticata* by DGGE analysis of PCR-amplified 16S rRNA, *aprA*, and *amoA* gene fragments

Taxonomic/physiological group	Papillae	Outer cortex	Inner cortex	Choanosome
16S rRNA gene-based analysis				
Crenarchaeota	+	+	+	+
Alphaproteobacteria	+	+	−	−
Betaproteobacteria[a]	+	++	++	++
Gammaproteobacteria	++	++		+
Deltaproteobacteria	−	−	++	++
Actinobacteria	−	−	++	++
Acidobacteria	−	−	+	+
Nitrospira	+	+	+	+
aprA gene-based analysis				
Sulfate-reducing prokaryotes	−	−	−	+
Sulfur-oxidizing bacteria	++	++	++	++
amoA gene-based analysis				
Ammonia-oxidizing *Betaproteobacteria*	+	+	+	+

−: no phylotype affiliated with this major taxonomic/physiological group identified, +: phylotype affiliated with this major taxonomic/physiological group identified, ++: two or more distinct phylotypes affiliated with this major taxonomic/physiological group identified
[a] Phylotypes retrieved from universal bacterial and betaproteobacterial-specific 16S rRNA gene analysis

Consistent with the 16S rRNA analysis, the *aprA* gene-based analysis revealed that the highest phylogenetic complexity was present in the choanosome of *P.* cf. *corticata*. In accordance to the 16S rRNA gene-observed local variability of the microbial community structure, the members of the six identified sulfur-oxidizing and sulfate-reducing lineages differed significantly in their distribution within the host sponge. Whereas the gammaproteobacterial SOB (*Thiothrix* spp.-affiliated cluster V) and most alphaproteobacterial SOB species (potential "generalist" clusters PmCo-sulfur-oxidizer-I to PmCo-sulfur-oxidizer-III) were present in the entire sponge body, the putative sponge-specific alphaproteobacterial sulfur-oxidizers (*Thiobacillus plumbophilus*-affiliated cluster IV) and the archaeal sulfate-reducing strains (PmCo-sulfate-reducer-I) were restricted to the inner tissue sections. In support of the 16S rRNA analysis results obtained with the group-specific primers, the *amoA* gene-based analysis showed the ubiquitous presence of two potential ammonia-oxidizing betaproteobacterial species in the sponge body.

Discussion

Microbial Diversity in the Caribbean Deep-water Sponge *Polymastia* cf. *corticata* in Comparison to Other Sponge Species

The 16S rRNA gene-based diversity analysis of the deep-water sponge *P.* cf. *corticata* collected at the Kahouanne Basin in the Caribbean Sea revealed its associated microbial community to be as phylogenetically complex and diverse as reported for the shallow-water sponge species [16, 18, 33, 60–63, 68]. Of the *P.* cf. *corticata*-associated phylotypes, 53% belonged to 16S rRNA sequence clusters that were strictly confined to sponges ("sponge associates" groups SAB-Beta-I, SAB-Gamma-II, SAB-Delta-I and SAB-Delta-II, SAB-Acido-III, SAB-Actino-III, SAB-Nitrospira-I, and SAA-Cren-I; see Fig. 3). The residual 47% of the detected OTUs, however, did not branch into any of the recognized sponge-specific, monophyletic clusters [15, 16, 19, 22, 59, 67]. Whereas the PmCo-Beta-I and PmCo-Beta-II members have been confirmed to be sponge-unspecific, the PmCo-Gamma-I, PmCo-Gamma-II, PmCo-Alpha-I, PmCo-Actino-I, PmCo-Actino-II, PmCo-Actino-III, and PmCo-Cren-I phylotypes might represent *P.* cf. *corticata*-specifically associated microorganisms ("specialists"). By the increasing number of environmental sequences available in the databases, identical free-living relatives of these currently designated "specialists" might be identified in the future and change their classification status into "generalists." Indeed, most sponge-derived alphaproteobacterial and gammaproteobacterial OTUs share low sequence similarity but are more closely affiliated with 16S rRNA sequences received from other marine organisms, sediment, or the water column [16, 18, 33, 60–63, 68, 71]. In addition, the *aprA* gene-based diversity analysis indicated the presence of one sulfate-reducing archaeal species and two *Thiothrix* spp.- and *Thiobacillus plumbophilus*-related potential SOB strains that might be general sponge-specific microorganisms; however, with respect to the limited sequence information available concerning sponge–SRP/SOB associations, their specificity might also be restricted to a certain group of sponges (e.g., genus or family) or possibly only to the species *P.* cf. *corticata* itself.

Overall, the bacterial community resident in *P.* cf. *corticata* was significantly distinct to those of the examined deep-water specimens of *Sclerotiderma* spp. [48], which were also collected from the Lesser Antilles area of the Caribbean Sea (coast of Curaçao and Bonnaire; 242–255 m depth). The phylotypes of *Sclerotiderma* spp. comprised representatives of the *Alphaproteobacteria*, *Actinobacteria*, *Acidobacteria*, *Spirochaeta*, and *Chloroflexaceae*, while members of the latter two groups were not present in *P.* cf. *corticata*. The identified OTUs of the three deep-water sponge species were only distantly related: The acidobacterial and actinobacterial phylotypes belonged to different sponge-specific clusters (SAB-Acido-I and SAB-Actino-I in *Sclerotiderma*, SAB-Acido-III and SAB-Actino-III in *P.* cf. *corticata*, see Fig. 3c and d), whereas the alphaproteobacterial OTUs represented unrelated bacteria classified as "generalist" and *P.* cf. *corticata*-"specialist" (PmCo-Alpha-I, see Fig. 3a). Nevertheless, as both studies were based on DGGE analysis of PCR products obtained with different primers, the nonoverlapping in their associated bacterial diversity might also be caused by primer-introduced different amplification bias [58, 66] and the sensitivity limitation of the DGGE method detecting only populations that comprise 1% or more of a sampled community [44]. The archaeal community of the *Sclerotiderma* spp. has not been assessed by Olson and McCarthy [48]. In *P.* cf. *corticata*, four crenarchaeotic phylotypes (SAA-Cren-I, PmCo-Cren-I) were detected that belonged to the cosmopolitan group C1a-α of MG-I [27, 38]; only two of them branched into the sponge-specific, monophyletic "sponge C group" [22, 32] (SAA-Cren-I, Fig. 3d). It is interesting to note that all sponge-derived C1a-α sequences were recently disputed to represent sponge-specific phylotypes because of the absence of significant host-clade specificity in clones of this group. Truly specific (potential mutualistic) associations between sponges and *Archaea* were postulated to exist only for *Cenarchaeum symbiosum* relatives (group C1a, *Porifera* A and C cluster) and axinellid sponges based on their parallel evolution (cospeciation) [22, 35]. Besides the aforementioned *P.* cf. *corticata*-associated *Crenarchaeota*, a putative sponge-

specific sulfate-reducing euryarchaeon was identified by the *aprA* gene analysis (Fig. 4). Euryarchaeal 16S rRNA clones have so far only been reported from *Axechina raspailoides*, *Reniochalina stalagmites*, *Ptilocaulis* sp. [22], and *Rhopaloides odorabile* (*Methanomicrobiales* relative) [69]. In contrast to our results, Holmes and Blanch reported the general absence of *Archaea* in *Polymastia invaginata* [22], which is a close relative of *P.* cf. *corticata*.

The 16S rRNA gene analysis with the universal primer sets demonstrated that the microbial consortium of *P.* cf. *corticata* and the ambient bacterioplankton were distinctly different, indicative for the low impact of the surrounding seawater on the sponge–microbe associations. In contrast, the usage of group-specific 16S rRNA, *aprA*, and *amoA* gene-targeting primers confirmed that seawater- and sediment-derived "generalist" phylotypes were present in *P.* cf. *corticata* (PmCo-Beta-I and PmCo-Beta-II; PmCo-ammonia-oxidizer-I and PmCo-ammonia-oxidizer-II; PmCo-sulfur-oxidizer-I, PmCo-sulfur-oxidizer-II, and PmCo-sulfur-oxidizer-III). These phylotypes most likely corresponded to ammonia-oxidizing *Nitrosospira* relatives and putative sulfur (or sulfite)-oxidizing, yet uncultivated *Alphaproteobacteria*. The nondetection of the *Nitrosospira* relatives with the universal 16S rRNA gene-targeting primer pair might indicate that the abundance of the respective populations was below the detection limit of approximately 1% to 5% [44]. Vice versa, the failure to amplify the 16S rRNA genes of the sponge-specific SAB-Beta-I members with the group-specific primer pair (CTO) [46] might indicate that these *Betaproteobacteria* were no chemolithoautrophic ammonia-oxidizers. Nevertheless, the CTO primer set [30] has been documented to bias the PCR-based analysis toward *Nitrosospira* relatives [36]. Because sponges are powerful filter-feeders (see [17, 19, 59, 67] and references therein) and are not able to discriminate between different types of food bacteria [70], even less abundant seawater- or sediment-derived microorganisms might be enriched by the stable and nutritionally rich microhabitat "sponge" ("microbial fermenter" [17]) and become part of the sponge-associated microbiota. As close relatives of the *P.* cf. *corticata*-associated *Nitrosospira* and *Alphaproteobacteria* were demonstrated to be abundant in the seawater–sediment interface [2, 10, 14, 41, 47], they might have represented transient bacterial populations that either served as "food bacteria" or resisted the phagocytosis process. In consequence, although a subset of the *P.* cf. *corticata*-associated microbial community (comprising especially the "sponge associates") will be transferred vertically as documented for several other sponges [9, 54, 55], the ambient seawater had an influence on the composition of its associated microbial community (see presence of proven "generalists").

A correlation between the geographical location of sponges and the presence of major bacterial taxonomic groups in their associated microbiota was proposed by Hill *et al.* [18]. However, this postulated geographical impact appears to be of minor importance with respect to the results obtained from the Caribbean sponges ([18, 48] and this study). *Acidobacteria*, *Deltaproteobacteria*, and *Nitrospira* relatives that were proposed to be characteristic for warm-water sponges were also present in the *P.* cf. *corticata* specimen collected from 5°C cold deep-sea habitat. However, representatives of *Bacteroidetes* and *Planctomycetes*, which were suggested to be typical for microbial consortia of cold/temperate sponge, were absent. Indeed, several phylogenetic surveys demonstrated that the microbial consortia associated with different sponge species are highly diverse even if the hosts share one habitat [33, 51, 60, 62, 63, 68]. In contradiction to the hypothesis of a uniform microbial signature of sponges across spatial and temporal scales [15, 16], the abundance, phylogenetic composition, and diversity of the host-associated microbial community mainly depends on the sponge-species and host state-depending interior factors as demonstrated by results of previous studies [18, 22, 33, 60–63, 68] and confirmed by this work. The proportion of the "sponge associates," "specialists," and "generalists" populations appears to be a sponge-specific feature.

Spatial Differences in the *Polymastia* cf. *corticata*-associated Microbial Community

The 16S rRNA, *aprA*, and *amoA* gene-based phylogenetic investigation of the tissue sections, papillae, inner and outer cortex, and choanosome revealed that distinct bacterial and archaeal populations are associated with the different tissue regions of the deep-water specimen of *P.* cf. *corticata*. In accordance, spatial differences in the microbial community have recently been documented for the shallow-water sponge *Tethya aurantium* [63]. However, in contrast to the latter work, our study indicated that the local distribution of a phylotype in the host tissue depended on its phylogenetic affiliation (bacterial/archaeal division) and correlated with its classification as "sponge associate," "specialist," and "generalist," and its potential ecological role in the sponge. Indeed, compartmented sponges might provide distinct microenvironments as ecological niches for the different bacterial and archaeal populations. Nutrient-rich conditions within the mesohyl of *P.* cf. *corticata* (extensive phagocytosis by archaeocytes) might explain that the choanosome- and inner cortex-associated microbiota was the most complex. Notably, all identified *Acidobacteria*, *Actinobacteria*, and *Deltaproteobacteria* were (1) general sponge-specific members or at least specifically associated with *P.* cf. *corticata* and (2) restricted in their distribution to the choanosome. Sponge-associated *Actinobacteria* and *Deltaproteobacteria* (e.g., *Entotheonella paulensis*) have been reported to be prolific secondary metabolite producers

[34, 42, 52, 53] and suggested to attribute largely to the chemical defense mechanisms of their host sponges against predators with biologically active compounds (repellents) and biofouling (see [15, 25] and references therein). Thus, their association with *P.* cf. *corticata* could have represented true mutualistic sponge–symbiont interactions. The functional role of the sponge-specific *Acidobacteria* is still unresolved because information concerning the physiology and metabolism of the marine acidobacterial members are not yet available and even limited for the abundant terrestrial species [26, 49]. In further support of a correlation between spatial distribution, sponge specificity, and the ecological role of the associated microorganisms, the *aprA* gene analysis demonstrated that the presumed general sponge-specific archaeal SRP and SOB strains (PmCo-sulfate-reducer-I, PmCo-sulfur-oxidizer-IV; Fig. 4) were also restricted to the host inner tissue regions. Consistently, potential sulfate-reducing strains (relatives of *Desulfovibrionaceae* and the *Desulfarculus/Desulfomonile/Syntrophus* cluster) were only present in the choanosome sections of two shallow-water sponge species [20, 37]. As postulated for *Geodia barretti* [20], the associations of sponges with sulfate-reducing microorganisms might generally be synergistic. Most sponges alternate between periods of high water-pumping velocity and periods of low water circulation [1, 56]; during the latter periods, oxygen becomes limited by the ongoing active respiration of sponge cells and aerobic microorganisms with the consequence of intermittent tissue anoxia. It was postulated that the anaerobic SRPs might benefit from the metabolic end products of sponge cells that switch to fermentation in these anoxic zones of the mesohyl; in turn, the microbial biomass might be consumed by the sponge cells ("bacterial farming") [20]. If oxygen is present again, the SRP-derived reduced sulfur compounds could be reoxidized by the activity of sulfur-oxidizing chemolithoautotrophs. Because potential members of both physiological groups were identified in the choanosome of *P.* cf. *corticata* by functional gene analysis, a sponge-specific, endosymbiotic sulfur cycle as described for marine oligochaetes [3, 8] may also be present in *P.* cf. *corticata*. As their closest related and cultivated species, *Pelagibacter ubique* (SAR11 clade) [12], the ubiquitous *Alphaproteobacteria* (cluster I to III; Fig. 4) might not rely on a sulfur-based chemolithoautotrophic lifestyle. As "generalists," they most likely represented opportunistic, transient bacterial populations obtained from the seawater and sediment.

In contrast to the aforementioned choanosome/inner cortex-associated bacteria, most microbes that were exclusively present in the outer tissue regions of *P.* cf. *corticata* were not general sponge-specific (exception SAB-Gamma-II representatives) but presented putative host-specific members of the *Alphaproteobacteria*, *Gammaproteobacteria*, and *Crenarchaeota*. These "specialists" might have been acquired by the settlement of free-living, opportunistic populations at the sponge surface with no benefit for the host. Indeed, the papillae- and outer cortex-associated microbial communities reflected the phylum level structure of the planktonic and surface sediment-associated microbiota at the Kahouanne Basin (Fig. 3).

The ubiquitous presence of potential ammonia- and nitrite-oxidizing bacteria and archaea in the entire sponge tissue probably reflected the overall availability of nitrogenous host waste products (e.g., ammonia, urea) in the sponge body. The coordinated metabolism of *Nitrosospira* and *Cenarchaeum symbiosum/Nitrosopumilus maritimus* relatives as ammonia-oxidizing bacteria/archaea [13, 28, 73] together with members of the genus *Nitrospira* as nitrite-oxidizing bacteria [29] (PmCo-Beta-I and PmCo-Beta-II and corresponding PmCo-ammonia-oxidizer-I and PmCo-ammonia-oxidizer-II; SAA-Cren-I and PmCo-Cren-I; SAB-Nitrospira-I) might be responsible for the process of nitrification in *P.* cf. *corticata* as it has been proposed for other sponge species (see [17, 59] and references therein). In analogy to the mutualistic sponge–SRP/SOB interactions ("bacterial farming"), the chemolithoautotrophic CO_2 fixation by the nitrifying microbial community could provide new carbohydrates for the host cells via microbe–sponge exchange. The members of the *Nitrospira* and inner cortex/choanosome-associated SAA-Cren-I-*Crenarchaeota* belong to sponge-specific clusters, which might be indicative for long-term mutualistic interactions, whereas the *P.* cf. *corticata*-associated *Nitrosospira* relatives were most likely colonizers acquired by filtration processes from free-living populations that are generally abundant in marine habitats [10, 47].

Acknowledgements This study was supported by grants from the BMBF (project "Caribflux" under contract number 03G0154C), the DFG (under contract number KU 916/8–1), and the Max-Planck-Society, Munich.

References

1. Bergquist PR (1978) Sponges. Hutchinson, London
2. Bernhard AE, Donn T, Giblin AE, Stahl DA (2005) Loss of diversity of ammonia-oxidizing bacteria correlates with increasing salinity in an estuary system. Environ Microbiol 7:1289–1297
3. Blazejak A, Erseus C, Amann R, Dubilier N (2005) Coexistence of bacterial sulfide oxidizers, sulfate reducers, and spirochetes in a gutless worm (Oligochaeta) from the Peru margin. Appl Environ Microbiol 71:1553–1561
4. Boury-Esnault N (2002) Family *Polymastiidae* Gray, 1867. In: Hooper NJA, van Soest RWM (eds) Systema Porifera: a guide to the classification of sponges. Kluwer, New York, NY, pp 201–219

5. Brüser T, Lens PNL, Trüper HG (2000) The biological sulfur cycle. In: Lens PNL, Pol LH (eds) Environmental technologies to treat sulfur pollution. IWA Publishing, London, pp 47–86
6. Chombard C, Boury-Esnault N, Tillier S (1998) Reassessment of homology of morphological characters in tetractinellid sponges based on molecular data. Syst Biol 47:351–366
7. DeLong E (1992) Archaea in coastal marine environments. Proc Natl Acad Sci USA 89:5685–5689
8. Dubilier N, Mulders C, Ferdelman T et al (2001) Endosymbiotic sulphate-reducing and sulphide-oxidizing bacteria in an oligochaete worm. Nature 411:298–302
9. Enticknap JJ, Kelly M, Peraud O, Hill RT (2006) Characterization of a culturable alphaproteobacterial symbiont common to many sponges and evidence for vertical transmission via sponge larvae. Appl Environ Microbiol 72:3724–3732
10. Freitag TE, Prosser JI (2004) Differences between betaproteobacterial ammonia-oxidizing communities in marine sediments and those in overlying water. Appl Environ Microbiol 70: 3789–3793
11. Friedrich CG (1998) Physiology and genetics of sulfur-oxidizing bacteria. Adv Microb Physiol 39:235–289
12. Giovannoni SJ, Tripp HJ, Givan S et al (2005) Genome streamlining in a cosmopolitan oceanic bacterium. Science 309:1242–1245
13. Hallam SJ, Konstantinidis KT, Putnam N et al (2006) Genomic analysis of the uncultivated marine crenarchaeote *Cenarchaeum symbiosum*. Proc Natl Acad Sci USA 103:18296–18301
14. Hayashi T, Tanahashi M, Naganuma T (2007) Molecular diversity of the genes encoding ammonia monooxygenase and particulate methane monooxygenase from deep-sea sediments. Res Microbiol 2:530–537
15. Hentschel U, Fieseler L, Wehrl M et al (2003) Microbial diversity of marine sponges. In: Müller WEG (ed) Marine molecular biotechnology. Springer, Berlin, pp 59–88
16. Hentschel U, Hopke J, Horn M et al (2002) Molecular evidence for a uniform microbial community in sponges from different oceans. Appl Environ Microbiol 68:4431–4440
17. Hentschel U, Usher KM, Taylor MW (2006) Marine sponges as microbial fermenters. FEMS Microbiol Ecol 55:167–177
18. Hill M, Hill A, Lopez N, Harriott O (2006) Sponge-specific bacterial symbionts in the Caribbean sponge, *Chondrilla nucula* (*Demospongiae*, *Chondrosida*). Mar Biol 148:1221–1230
19. Hill RT (2004) Microbes from marine sponges: a treasure of biodiversity for natural products discovery. In: Bull AT (ed) Microbial diversity and bioprospecting. ASM, Washington, DC, pp 177–190
20. Hoffmann F, Larsen O, Thiel V et al (2005) An anaerobic world in sponges. Geomicrobiol J 22:1–10
21. Holmes AJ, Tujula NA, Holley M et al (2001) Phylogenetic structure of unusual aquatic microbial formations in Nullarbor caves, Australia. Environ Microbiol 3:256–264
22. Holmes B, Blanch H (2007) Genus-specific associations of marine sponges with group I crenarchaeotes. Mar Biol 150:759–772
23. Hooper NJA, van Soest RWM (2002) Systema *Porifera*: a guide to the classification of sponges. Kluwer, New York, NY
24. Huber H, Huber R, Stetter KO (2002) *Thermoproteales*. In: Dworkin M, Falkow E, Rosenberg E, Schleifer K-H, Stackebrandt E (eds) The prokaryotes. An evolving electronic resource for the microbial community. Fischer, New York, NY
25. Imhoff JF, Stöhr R (2003) Sponge-associated bacteria: general overview and special aspects of bacteria associated with *Halichondria panicea*. In: Müller WEG (ed) Marine molecular biotechnology. Springer, Berlin, pp 35–56
26. Janssen PH (2006) Identifying the dominant soil bacterial taxa in libraries of 16S rRNA and 16S rRNA genes. Appl Environ Microbiol 72:1719–1728
27. Karner MB, DeLong EF, Karl DM (2001) Archaeal dominance in the mesopelagic zone of the Pacific Ocean. Nature 409:507–510
28. Koennecke M, Bernhard AE, de la Torre JR et al (2005) Isolation of an autotrophic ammonia-oxidizing marine archaeon. Nature 437:543–546
29. Koops H-P, Pommerening-Röser A (2001) Distribution and ecophysiology of the nitrifying bacteria emphasizing cultured species. FEMS Microbiol Ecol 37:1–9
30. Kowalchuk GA, Stephen JR, De Boer W et al (1997) Analysis of ammonia-oxidizing bacteria of the beta subdivision of the class Proteobacteria in coastal sand dunes by denaturing gradient gel electrophoresis and sequencing of PCR-amplified 16S ribosomal DNA fragments. Appl Environ Microbiol 63:1489–1497
31. Lam P, Cowen JP, Jones RD (2004) Autotrophic ammonia oxidation in a deep-sea hydrothermal plume. FEMS Microbiol Ecol 47:191–206
32. Lee EY, Lee HK, Lee YK, Sim CJ, Lee JH (2003) Diversity of symbiotic archaeal communities in marine sponges from Korea. Biomolecular Engineering 20:299–304
33. Li Z, Hu Y, Liu Y et al (2007) 16S rDNA clone library-based bacterial phylogenetic diversity associated with three South China Sea sponges. World J Microbiol Biotechnol 23:1265–1272
34. Li Z-Y, Liu Y (2006) Marine sponge *Craniella australiensis*-associated bacterial diversity revelation based on 16S rDNA library and biologically active Actinomycetes screening, phylogenetic analysis. Lett Appl Microbiol 43:410–416
35. Magot H, Acebal C, Toril E, Amils R, Fernandez PJL (2002) Consistent associations of crenarchaeal *Archaea* with sponges of the genus *Axinella*. Mar Biol 140:739–745
36. Mahmood S, Freitag TE, Prosser JI (2006) Comparison of PCR primer-based strategies for characterization of ammonia oxidizer communities in environmental samples. FEMS Microbiol Ecol 56:482–493
37. Manz W, Arp G, Schumann-Kindel G, Szewzyk U, Reitner J (2000) Widefield deconvolution epifluorescence microscopy combined with fluorescence *in situ* hybridization reveals the spatial arrangement of bacteria in sponge tissue. J Microbiol Methods 40:125–134
38. Massana R, Murray A, Preston C, DeLong E (1997) Vertical distribution and phylogenetic characterization of marine planktonic *Archaea* in the Santa Barbara Channel. Appl Environ Microbiol 63:50–56
39. Meyer B, Kuever J (2007) Molecular analysis of the distribution and phylogeny of dissimilatory adenosine-5′-phosphosulfate reductase-encoding genes (*aprBA*) among sulfur-oxidizing prokaryotes. Microbiology 153:3478–3498
40. Meyer B, Kuever J (2007) Phylogeny of the alpha and beta subunits of the dissimilatory adenosine-5′-phosphosulfate (APS) reductase from sulfate-reducing prokaryotes – origin and evolution of the dissimilatory sulfate-reduction pathway. Microbiology 153:2026–2044
41. Meyer B, Kuever J (2007) Molecular analysis of the diversity of sulfate-reducing and sulfur-oxidizing prokaryotes in the environment using *aprA* as functional marker gene. Appl Environ Microbiol 73:7664–7679
42. Montalvo NF, Mohamed NM, Enticknap JJ, Hill RT (2005) Novel actinobacteria from marine sponges. Antonie van Leeuwenhoek 87:29–36
43. Morrow C, Boury-Esnault N (2000) Redescription of the type species of the genus *Polymastia* Bowerbank, 1864 (*Porifera*, *Demospongiae*, *Hadromerida*). Zoosystema 22:327–335
44. Muyzer G, de Waal EC, Uitterlinden AG (1993) Profiling of complex microbial populations by denaturing gradient gel electrophoresis analysis of polymerase chain reaction-amplified genes coding for 16S rRNA. Appl Environ Microbiol 59:695–700
45. Muyzer G, Teske A, Wirsen CO, Jannasch HW (1995) Phylogenetic relationships of *Thiomicrospira* species and their identification in deep-sea hydrothermal vent samples by denaturing

gradient gel electrophoresis of 16S rDNA fragments. Arch Microbiol 164:165–172
46. Nicolaisen MH, Ramsing NB (2002) Denaturing gradient gel electrophoresis (DGGE) approaches to study the diversity of ammonia-oxidizing bacteria. J Microbiol Methods 50:189–203
47. O'Mullan GD, Ward BB (2005) Relationship of temporal and spatial variabilities of ammonia-oxidizing bacteria to nitrification rates in Monterey Bay, California. Appl Environ Microbiol 71:697–705
48. Olson JB, McCarthy PJ (2005) Associated bacterial communities of two deep-water sponges. Aquat Microb Ecol 39:47–55
49. Quaiser A, Ochsenreiter T, Lanz C et al (2003) *Acidobacteria* form a coherent but highly diverse group within the bacterial domain: evidence from environmental genomics. Mol Microbiol 50:563–575
50. Rabus R, Hansen TA, Widdel F (1999) Dissimilatory sulfate- and sulfur-reducing prokaryotes. In: Dworkin M, Schleifer K-H, Stackebrandt E (eds) The prokaryotes: an evolving electronic database for the microbiological community. Springer, New York, NY, pp 1–87
51. Ridley CP, Faulkner DJ, Haygood MG (2005) Investigation of *Oscillatoria spongeliae*-dominated bacterial communities in four dictyoceratid sponges. Appl Environ Microbiol 71:7366–7375
52. Schirmer A, Gadkari R, Reeves CD et al (2005) Metagenomic analysis reveals diverse polyketide synthase gene clusters in microorganisms associated with the marine sponge *Discodermia dissoluta*. Appl Environ Microbiol 71:4840–4849
53. Schmidt EW, Obraztsova AY, Davidson SK, Faulkner DJ, Haygood MG (2000) Identification of the antifungal peptide-containing symbiont of the marine sponge *Theonella swinhoei* as a novel deltaproteobacterium, "*Candidatus* Entotheonella palauensis". Mar Biol 136:969–977
54. Schmitt S, Weisz JB, Lindquist N, Hentschel U (2007) Vertical transmission of a phylogenetically complex microbial consortium in the viviparous sponge *Ircinia felix*. Appl Environ Microbiol 73:2067–2078
55. Sharp KH, Eam B, Faulkner DJ, Haygood MG (2007) Vertical transmission of diverse microbes in the tropical sponge *Corticium* sp. Appl Environ Microbiol 73:622–629
56. Simpson TL (1984) The cell biology of sponges. Springer, New York, NY
57. Suzuki F, Inagaki K, Takai K, Nealson KH, Horikoshi K (2004) Microbial diversity in inactive chimney structures from deep-sea hydrothermal systems. Microb Ecol 47:186–196
58. Suzuki MT, Giovannoni SJ (1996) Bias caused by template annealing in the amplification of mixtures of 16S rRNA genes by PCR. Appl Environ Microbiol 62:625–630
59. Taylor MW, Radax R, Steger D, Wagner M (2007) Sponge-associated microorganisms: evolution, ecology, and biotechnological potential. Microbiol Mol Biol Rev 71:295–347
60. Taylor MW, Schupp PJ, Dahllof I, Kjelleberg S, Steinberg PD (2004) Host specificity in marine sponge-associated bacteria, and potential implications for marine microbial ecology. Environ Microbiol 6:121–130
61. Taylor MW, Schupp PJ, de Nys R, Kjelleberg S, Steinberg PD (2005) Biogeography of bacteria associated with the marine sponge *Cymbastela concentrica*. Environ Microbiol 7:419–433
62. Thiel V, Leininger S, Schmaljohann R, Brümmer F, Imhoff JF (2007) Sponge-specific bacterial associations of the Mediterranean sponge *Chondrilla nucula* (*Demospongiae*, *Tetractinomorpha*). Microb Ecol 54:101–111
63. Thiel V, Neulinger SC, Staufenberger T, Schmaljohann R, Imhoff JF (2007) Spatial distribution of sponge-associated bacteria in the Mediterranean sponge *Tethya aurantium*. FEMS Microbiol Ecol 59:47–63
64. Vacelet J, Donadey C (1977) Electron microscope study of the association between some sponges and bacteria. J Exp Mar Biol Ecol 30:301–314
65. Vetriani C, Jannasch HW, MacGregor BJ, Stahl DA, Reysenbach A-L (1999) Population structure and phylogenetic characterization of marine benthic archaea in deep-sea sediments. Appl Environ Microbiol 65:4375–4384
66. von Wintzingerode F, Gobel UB, Stackebrandt E (1997) Determination of microbial diversity in environmental samples: pitfalls of PCR-based rRNA analysis. FEMS Microbiol Rev 21:213–229
67. Wang G (2006) Diversity and biotechnological potential of the sponge-associated microbial consortia. J Ind Microbiol Biotech 33:545–551
68. Webster NS, Negri AP, Munro M, Battershill CN (2004) Diverse microbial communities inhabit Antarctic sponges. Environ Microbiol 6:288–300
69. Webster NS, Watts JEM, Hill RT (2001) Detection and phylogenetic analysis of novel crenarchaeote and euryarchaeote 16S ribosomal gene sequences from a Great Barrier Reef sponge. Mar Biotechnol 3:600–608
70. Wehrl M, Steinert M, Hentschel U (2007) Bacterial uptake by the marine sponge *Aplysina aerophoba*. Microb Ecol 53:355–366
71. Wichels A, Wurtz S, Dopke H, Schutt C, Gerdts G (2006) Bacterial diversity in the breadcrumb sponge *Halichondria panicea* (Pallas). FEMS Microbiol Ecol 56:102–118
72. Wilkinson CR (1978) Microbial associations in sponges. III. Ultrastructure of the *in situ* association in coral reef sponges. Mar Biol 49:177–185
73. Wuchter C, Abbas B, Coolen MJL et al (2006) Archaeal nitrification in the ocean. Proc Natl Acad Sci USA 103:12317–12322
74. Zhou JZ, Bruns MA, Tiedje JM (1996) DNA recovery from soils of diverse composition. Appl Environ Microbiol 62:316–322

Supplementary Material

Supplementary Table S1. PCR primers and thermocycling conditions used in this study for amplification of the 28S rRNA, 16S rRNA, *aprA* and *amoA* gene fragments

Primer	Sequence (in 5`→3` direction)	Target gene of primer	PCR thermocycling conditions	Reference
C1	ACCCGCTGAATTTAAGCAT	28S rRNA	first cycle of 4 min at 94°C, 120 sec at 57°C and 120 sec at 72°C is followed by 30 cycles of 60 sec at 94°C, 60 sec at 57°C and 60 sec at 72°C, followed by a 4-min final extension step	[6]
C2	GAAAAGAACTTTGRARAGAGAGT			
D2	TCCGTGTTTCAAGACGGG			
GM5F(-GC)	(CGCCCGCCGCGCCCCGCGCCCGTCCCGCCGCCCCCGCCCG-) CCTACGGGAGGCAGCAG	16S rRNA[a]	5 min at 94°C is followed by 20 cycles of 60 sec at 94°C, 60 sec at 65°C ("touchdown" PCR, -0,5°C every new cycle) and 60 sec at 72°C, followed by 15 cycles of 60 sec at 94°C, 60 sec at 55°C and 60 sec at 72°C, followed by a 3-min final extension step	[45]
907R	CCGTCAATTCCTTTRAGTTT			
Arch516F(-GC)	K. Knittel, unpublished results	16S rRNA[b]	5 min at 94°C is followed by 30 cycles of 60 sec at 94°C, 45 sec at 59°C and 45 sec at 72°C, followed by a 3-min final extension step	K.Knittel, unpubl. [7]
Arch958R	YCCGGCGTTGAMTCCAATT			
CTO189f(-GC)	(CGCCGCGCGGCGGGCGGGGCGGGGGC-) GGAGRAAAGYAGGGGATCG	16S rRNA[c]	PCR-I (primer without GC-clamp): 15 min at 95°C is followed by 35 cycles of 30 sec at 92°C, 30 sec 57°C and 45 sec 72°C, followed by 5-min final extension step PCR-II (primer with GC-clamp): 15 min at 95°C is followed by 18 cycles of 30 sec at 92°C, 30 sec 57°C and 45 sec 72°C, followed by a 5-min final extension step	[30, 46]
CTO654r	CTAGCYTTGTAGTTTCAAACGC			
AprA-1-FW	TGGCAGATMATGATYMACGG	*aprA*[d]	5 min at 95°C is followed by 20 cycles of 60 sec at 95°C, 60 sec at 60 - 50°C ("touchdown" PCR, -0,5°C every new cycle) and 90 sec at 72°C, followed by 15 cycles of 60 sec at 94°C, 60 sec at 50°C and 90 sec at 72°C, followed by a 10-min final extension step	[41]
AprA-5-RV(-GC)	(CGCCCGCCGCGCCCCGCGCCCGGCCCGCCGCCCCCGCCCG-) GCGCCAACYGGRCCRTA			
AmoA-1F(-GC)	(CGCCGCGCGGCGGGCGGGGCGGGGGC-) GGGGTTTCTACTGGTGGT	*amoA*[e]	PCR-I (primer without GC-clamp): 15 min at 95°C is followed by 35 cycles of 30 sec at 92°C, 30 sec 57°C and 45 sec 72°C, followed by 5-min final extension step PCR-II (primer with GC-clamp): 15 min at 95°C is followed by 18 cycles of 30 sec at 92°C, 30 sec 57°C and 45 sec 72°C, followed by a 5-min final extension step	[46]
AmoA-2R-TC	CCCCTCTGCAAAGCCTTCTTC			

[a] universal bacterial primer pair
[b] universal archaeal primer pair
[c] betaproteobacterial ammonia-oxidizer 16S rRNA gene-targeting primer pair
[d] universal SRP and SOB *aprA* gene-targeting primer pair
[e] betaproteobacterial ammonia-oxidizer *amoA* gene-targeting primer pair

Supplementary Table S2. Double gradient-DGGE analysis of PCR-amplified 16S rRNA, *aprA* and *amoA* gene fragments

Gene	Primer pair	Denaturant gradient[a]	Acrylamide gradient	DG-DGGE analysis	Reference
16S rRNA	GM5F-GC/ 907R	20 - 70%	6 - 8 %	3.5 h at 200 Volt in 1× TAE at 60°C	[45]
	Arch516F-GC/ Arch958R	20 - 70%	6 - 8 %	3.5 h at 200 Volt in 1× TAE at 60°C	K. Knittel, unpublished
	CTO189f-GC/ CTO654r	30 - 60%	6 - 8 %	6 h at 200 Volt in 1× TAE at 60°C	[46]
aprA	AprA-1-FW/ AprA-5-RV-GC	30 - 60%	6 – 8%	2 h at 150 Volt followed by 2 h at 200 Volt in 1× TAE at 60°C	[41]
amoA	AmoA-1F-GC/ AmoA-2R-TC	38 - 50%	6 - 8 %	6 h at 200 Volt in 1× TAE at 60°C	[46]

[a] denaturing solution strength of 100% is defined as 7 M urea and 40% (v/v) formamide according to Muyzer *et al.* (1995)

5 Anhang

Tabelle 1. Schwefelmetabolisierende Fähigkeiten der anaeroben anoxygenen phototrophen Grünen Schwefelbakterien und Schwefel-Purpurbakterien

Gattung oder Spezies	dissimilatorisch genutzte reduzierte anorganische Schwefelverbindungen	Intermediate bei der Sulfidoxidation	Endprodukt	Sulfatassimilation	Chemolithoautotrophes Wachstum
Grüne Schwefelbakterien					
Chlorobiaceae					
Ancalochloris perfilievii [a b]	Sulfid	S^0, EZ	Sulfat	-	-
Chlorobaculum chlorovibrioides	Sulfid, el. Schwefel	S^0, EZ	Sulfat	-	-
Chlorobaculum limnaeum	Sulfid, el. Schwefel	S^0, EZ	Sulfat	-	-
Chlorobaculum parvum	Sulfid, el. Schwefel, Thiosulfat (Tetrathionat in Stamm NCIB 8346)	S^0, EZ	Sulfat	-	-
Chlorobaculum tepidum	Sulfid, el. Schwefel, Thiosulfat	S^0, EZ	Sulfat	-	-
Chlorobaculum thiosulfatiphilum	Sulfid, el. Schwefel, Thiosulfat	S^0, EZ	Sulfat	-	-
"*Chlorobium bathyomarinum*"	Sulfid, el. Schwefel	n. b.	n. b.	n. b.	n. b.
Chlorobium chlorochromatii	Sulfid	n. b.	n. b.	-	-
Chlorobium clathratiforme	Sulfid, el. Schwefel, Thiosulfat in Stamm DSM 5477^T	S^0, EZ	Sulfat	-	-
Chlorobium ferrooxidans	-	-		+	-
Chlorobium limicola	Sulfid, el. Schwefel, Thiosulfat in Stamm 1630, 9330 und DSM 257	S^0, EZ	Sulfat	-	-
Chlorobium luteolum	Sulfid, el. Schwefel	S^0, EZ	Sulfat	-	-
Chlorobium phaeobacteroides	Sulfid, el. Schwefel	S^0, EZ	Sulfat	-	-
Chlorobium phaeovibrioides	Sulfid, el. Schwefel	S^0, EZ	Sulfat	-	-
Chloroherpeton thalassium	Sulfid	S^0, EZ	S^0 (Sulfat)	-	-
Prosthecochloris aestuarii	Sulfid, el. Schwefel	S^0, EZ	Sulfat	-	-
Prosthecochloris vibrioformis	Sulfid, el. Schwefel	S^0, EZ	Sulfat	-	-
Schwefel-Purpurbakterien					
Chromatiaceae					
Allochromatium	Sulfid, el. Schwefel, Thiosulfat, Sulfit (letztere zwei Verbindungen nicht in *A. warmingii*)	S^0, IZ	Sulfat	+ (nicht in *A. warmingi*)	+ (in einigen Stämmen)
Chromatium	Sulfid, el. Schwefel	S^0, IZ	Sulfat	-	-
Halochromatium	Sulfid, el. Schwefel (nicht in *H. roseum*), Thiosulfat, Sulfit	S^0, IZ	Sulfat	-	+ (Sulfid, Thiosulfat)
Isochromatium	Sulfid, el. Schwefel	S^0, IZ	Sulfat	-	-
Lamprobacter [b]	Sulfid, el. Schwefel, Thiosulfat	S^0, IZ	S^0 oder Sulfat	-	+
Lamprocystis	Sulfid, el. Schwefel, Thiosulfat	S^0, IZ	Sulfat	-/n. b.	+/-
Marichromatium	Sulfid, el. Schwefel, Thiosulfat, Sulfit (nur in *M. gracile*, *M. bheemlicum*)	S^0, IZ	Sulfat	+/-	+/-
Rhabdochromatium	Sulfid, el. Schwefel, Thiosulfat	S^0, IZ	Sulfat	n. b.	-
Thermochromatium	Sulfid, el. Schwefel	S^0, IZ	Sulfat	n. b.	-
Thioalkalicoccus	Sulfid, el. Schwefel	S^0, IZ	Sulfat	n. b.	-
Thiobaca	Sulfid	S^0, IZ	Sulfat	n. b.	n. b.
Thiocapsa	Sulfid, el. Schwefel, Thiosulfat, Sulfit (nur in *T. litoralis* and *T. pendens*)	S^0, IZ	Sulfat	+/-	+/-
Thiococcus	Sulfid, el. Schwefel	S^0, IZ	Sulfat	-	-
Thiocystis	Sulfid, el. Schwefel, Thiosulfat (nicht in *T. gelatinosa*), Sulfit in einigen Stämmen	S^0, IZ	Sulfat	+ (in einigen Stämmen)	+
Thiodictyon	Sulfid, el. Schwefel	S^0, IZ	Sulfat	n. b.	-
Thioflaviococcus	Sulfid, el. Schwefel	S^0, IZ	Sulfat	n. b.	-
Thiohalocapsa	Sulfid, el. Schwefel, Thiosulfat, Sulfit	S^0, IZ	Sulfat	-	+
Thiolamprovum	Sulfid, el. Schwefel, Thiosulfat	S^0, IZ	Sulfat	-	+
Thiopedia [a]	Sulfid, el. Schwefel	S^0, IZ	Sulfat	-	-
Thiorhodococcus	Sulfid, el. Schwefel, Thiosulfat (nicht in *T. kakinadensis*)	S^0, IZ	Sulfat	-	+/-
Thiorhodovibrio	Sulfid, el. Schwefel	S^0, IZ	Sulfat	n. b.	+
Thiospirillum [a b]	Sulfid, el. Schwefel	S^0, IZ	Sulfat	n. b.	-
Ectothiorhodospiraceae					
Ectothiorhodosinus	Sulfid, Thiosulfat	S^0, EZ	Sulfat	n. b.	n. b.
Ectothiorhodospira	Sulfid, el. Schwefel (nicht in *E. halochloris*), Thiosulfat (nicht in *E. marismortui*), Sulfit in einigen	S^0, EZ	Sulfat	+/-	+/-

	Stämmen				
Halorhodospira	Sulfid, Thiosulfat, el. Schwefel nur in *H. halophila*	S^0, EZ	S^0 oder Sulfat	+ (in *H. halo-chloris)*	-
Thiorhodospira	Sulfid, el. Schwefel	S^0, EZ u. IZ	Sulfat	n. b.	-

Daten wurden tabellarisch zusammengefasst aus Publikationen von (Arunasri *et al.*, 2005; Asao *et al.*, 2007; Beatty *et al.*, 2005; Gorlenko *et al.*, 2004; Imhoff, 1999; Imhoff, 2001b; Imhoff, 2003; Kumar *et al.*, 2007a; Kumar *et al.*, 2007b; Kumar *et al.*, 2007c; Vogl *et al.*, 2006; Zaar *et al.*, 2003)

Abkürzungen: +, Fähigkeit vorhanden; -, Fähigkeit nicht vorhanden, +/-, Fähigkeit in einigen Spezies vorhanden; el. Schwefel, elementarer Schwefel; S^0, gespeicherter Schwefel der Oxidationsstufe 0; IZ, intrazellulär; EZ, extrazellulär; n. b., nicht bekannt

[a] Typenstamm nicht hinterlegt

[b] keine 16S rRNA Sequenzdaten zur phylogenetischen Einordnung der Spezies/Gattung vorhanden

Tabelle 2: Schwefelmetabolisierende Fähigkeiten der nicht-phototrophen sulfid-/thiosulfatoxidierenden Gattungen bzw. Spezies

Gattung oder Spezies	Auto-trophie	Nitrat/ Nitrit-reduk-tion	dissimilatorisch genutzte reduzierte anorganische Schwefelverbindungen	Intermediate bei der Thiosulfat-oxidation	End-pro-dukt
Bacteria					
Alphaproteobacteria					
Acidicaldus organivorans	-	n. b.	el. Schwefel	n. b.	Sulfat
Acidiphilium acidophilum	f	-	el. Schwefel, Thiosulfat, Tetrathionat	$S_4O_6^{4-}$	Sulfat
Albidovulum inexpectatum	-	-	Sulfid, Thiosulfat	-	Sulfat
Ancylobacter spp.	o/f	-	Thiosulfat	n. b.	n. b.
Bosea thiooxidans	-	-	Thiosulfat	-	Sulfat
Methylobacterium spp.	-	-	Thiosulfat	-	Sulfat
Paracoccus spp.	f, C	+/-	Sulfid, el. Schwefel, Thiosulfat, Tetrathionat (in Stamm SST)	- (SO_3^{2-})	Sulfat
Pseudaminobacter salicylatoxidans Stamm KCT001	-	-	Sulfid, el. Schwefel, Thiosulfat, Tetrathionat	-	Sulfat
Starkeya novella	f, C	-	Sulfid, Thiosulfat, Tetrathionat	- (SO_3^{2-})	Sulfat
„*Roseobacter*“ spp. Stamm DSS-8, NF18, TB66, AG33, DI4* etc.	-	n. b.	Thiosulfat, Sulfit	n. b.	Sulfat
Xanthobacter spp.	f	-	Sulfid, el. Schwefel, Thiosulfat, Tetrathionat	n. b.	Sulfat
Silicibacter pomeroyi	-	-	Thiosulfat, Sulfit	-	Sulfat
Sulfitobacter spp.	-	-	Thiosulfat (nicht in *Sbt. mediterraneus*), Sulfit	-	Sulfat
Thioclava pacifica	f, C	-	Sulfid, Thiosulfat	- (SO_3^{2-})	Sulfat
Betaproteobacteria					
Burholderia norimbergensis	-	-	Sulfid, el. Schwefel, Thiosulfat, Tetrathionat	n. b.	Sulfat
Catenococcus spp.	-	-	Sulfid, el. Schwefel, Thiosulfat	$S_4O_6^{4-}$	$S_4O_6^{4-}$
Hydrogenophilus thermo-luteolus	o	n. b.	Thiosulfat	-	Sulfat
Limnobacter thiooxidans	-	-	Thiosulfat	-	Sulfat
Macromonas bipunctata	-	-	Sulfid, el. Schwefel, Thiosulfat	$S_4O_6^{4-}$	$S_4O_6^{4-}$
Tepidimonas spp.	-	-	Thiosulfat	-	Sulfat
Tetrathiobacter kashmirensis	f	-	Thiosulfat, Tetrathionat	$S_4O_6^{4-}$	Sulfat
Thermothrix spp.	o/f	-	Sulfid, el. Schwefel, Thiosulfat, Tetrathionat	S^0, $S_4O_6^{4-}$, SO_3^{2-}	Sulfat
Thiobacillus spp.	o, C	+/-	Sulfid, el. Schwefel, Thiosulfat, Tetrathionat (letzte drei Verbindungen nicht in *T. plumbophilus*), Sulfit (in *T. denitrificans*)	S^0 (in einigen Spezies)	Sulfat
Thiobacter subterraneus	o	-	Sulfid, el. Schwefel, Thiosulfat	S^0	Sulfat
Thiomonas spp.	f, C	+/-	Sulfid (nicht in *T. perometabolis*), el. Schwefel, Thiosulfat, Tetrathionat (letztere zwei Verbindungen nicht in *T. cuprina*)	S^0, $S_4O_6^{4-}$ (in *T. intermedia* K12)	Sulfat
Gammaproteobacteria					
Acidithiobacillus spp.	o, C	-	Sulfid, el. Schwefel, Thiosulfat, Tetrathionat	$S_4O_6^{4-}$	Sulfat
Achromatium spp.	n. b.	n. b.	Sulfid	k. $S_2O_3^{2-}$-Ox.	n.b.
Alkalilimnicola ehrlichei	f, C	+	Sulfid, Thiosulfat (nur anaerob)	n. b.	Sulfat
Beggiatoa spp.	o/f/-, C	+/-	Sulfid, el. Schwefel, Thiosulfat (in einigen Stämmen)	S^0	Sulfat
„*Halomonas*“ spp. Stamm ChG 7-3 etc.	-	+	Thiosulfat	$S_4O_6^{4-}$	$S_4O_6^{4-}$
Halothiobacillus spp.	o, C	-	Thiosulfat, el. Schwefel, Sulfid, Tetrathionat	S^0, $S_4O_6^{4-}$ (in *H. neopolitanus*)	Sulfat
Hydrogenovibrio spp.	o, C	-	Sulfid, el. Schwefel, Thiosulfat, Tetrathionat	S^0	Sulfat
Leucothrix spp.	-	-	Sulfid, Thiosulfat	S^0	Sulfat
„*Pseudomonas stutzeri*“ ssp. Stamm ChG 5-3, BG 2 etc.	-	+	Thiosulfat	$S_4O_6^{4-}$	$S_4O_6^{4-}$
Thermithiobacillus tepidarius	o	-	Sulfid, el. Schwefel, Thiosulfat, Tetrathionat	$S_4O_6^{4-}$	Sulfat
Thioalkalimicrobium spp.	o, C	-	Sulfid, Thiosulfat	- (SO_3^{2-})	Sulfat
Thioalkalispira microaerophila	o, C	-	Sulfid, Thiosulfat	S^0	Sulfat
Thioalkalivibrio spp.	o, C	+/-	Sulfid, el. Schwefel, Thiosulfat, Tetrathionat, Sulfit	S^0	Sulfat
„*Thiobacillus prosperus*“ Stamm DSM 5130	o	-	Sulfid, el. Schwefel		Sulfat
Thiohalopilus thiocyano-oxidans	o	+	Thiosulfat	S^0	Sulfat
„*Thiohalorhabdus*“ spp.	o	+	Thiosulfat, Tetrathionat	$S_4O_6^{4-}$	Sulfat
„*Thiohalospira*“ spp.	o	-	Sulfid, Thiosulfat, Tetrathionat	$S_4O_6^{4-}$	Sulfat

Thiohalomonas spp.	o	+	Sulfid, Thiosulfat (nicht in *T. nitratireducens*)	S^0	Sulfat
Thiomargarita namibiensis	n. b.	+	Sulfid	k. $S_2O_3^{2-}$-Ox.	Sulfat
Thiomicrospira spp.	o, C	-	Sulfid, el. Schwefel, Thiosulfat	S^0 (nicht in *T. kuenenii*, *T. frisia*)	Sulfat
Thioploca spp.	o	+	Sulfid	k. $S_2O_3^{2-}$-Ox.	Sulfat
Thiospira spp.	-	-	Sulfid, Thiosulfat	$S_4O_6^{4-}$	$S_4O_6^{4-}$
Thiothrix spp.	o/f/-	+/-	Sulfid, Thiosulfat	S^0	Sulfat
Thiovirga sulfuroxydans	o	-	Sulfid, el. Schwefel, Thiosulfat	S^0	Sulfat
Symbionten von marinen Invertebraten (z. B. *Riftia*, *Bathymodiolus*, *Inanidrilus* etc.)	o, C/T	+/-	Sulfid, Thiosulfat (in einigen Spezies, z. B. *Candidatus* Ruthia magnifica und *Bathymodiolus thermophilus* Symbiont)	n. b.	Sulfat
Epsilonproteobacteria					
Candidatus Arcobacter sulfidicus	o, T	-	Sulfid	k. $S_2O_3^{2-}$-Ox.	S^0 (Sulfat)
Sulfuricurvum kujiense	o	+	Sulfid, el. Schwefel, Thiosulfat	-	Sulfat
Sulfurimonas spp.	o, T	+/-	Sulfid (nicht in *S. paralvinella* und *S. autotrophica*), el. Schwefel (nicht in *S. denitrificans*), Thiosulfat	-	Sulfat
Sulfurovum lithotrophicum	o, T	+	el. Schwefel, Thiosulfat	-	Sulfat
Thiovulum spp.	o	n. b.	Sulfid	k. $S_2O_3^{2-}$-Ox.	Sulfat
Firmicutes					
Alicylcobacillus spp.	-	-	Sulfid, el. Schwefel, Thiosulfat	$S_4O_6^{4-}$	Sulfat
Bacillus schlegeli	f, C	-	Thiosulfat	n.b.	Sulfat
Sulfobacillus thermosulfidooxidans	f, C	-	Sulfid, el. Schwefel, Thiosulfat	$S_4O_6^{4-}$	Sulfat
Deinococci					
Thermus spp.	-	+	el. Schwefel, Thiosulfat	-	Sulfat
Aquificae					
Aquifex spp.	o, T	+/-	el. Schwefel, Thiosulfat	S^0	Sulfat
Hydrogenobacter spp.	o, T	+/-	el. Schwefel, Thiosulfat (beide Verbindungen nicht in *H. thermophilus*)	n. b.	Sulfat
Persephonella spp.	o, T	+	el. Schwefel, Thiosulfat	n. b.	Sulfat
Sulfurihydrogenibium spp.	o/f, T	+/-	el. Schwefel, Thiosulfat, Sulfit (in *S. azorense*)	n. b.	Sulfat
Archaea					
Crenarchaeota					
Acidianus spp.	o/f	-	Sulfid, el. Schwefel, Tetrathionat	k. $S_2O_3^{2-}$-Ox.	Sulfat
Metallosphaera spp.	f, H	-	el. Schwefel	k. $S_2O_3^{2-}$-Ox.	Sulfat
Sulfolobus spp.	o/f/-	-	Sulfid, el. Schwefel, Tetrathionat	k. $S_2O_3^{2-}$-Ox.	Sulfat

Daten wurden tabellarisch zusammengefasst aus Publikationen von (Albuquerque *et al.*, 2002; Albuquerque *et al.*, 2006; Anandham *et al.*, 2007; Brüser *et al.*, 2000a; Campbell *et al.*, 2006; Cavanaugh *et al.*, 2004; Dam *et al.*, 2007; Deb *et al.*, 2004; Friedrich, 1998; Ghosh *et al.*, 2005; Ghosh & Roy, 2007; Gonzalez *et al.*, 1999; Gonzalez *et al.*, 2003; Grabovich *et al.*, 2002; Hirayama *et al.*, 2005; Hoeft *et al.*, 2007; Howarth *et al.*, 1999; Huber & Prangishvili, 2000; Johnson *et al.*, 2006; Karavaiko *et al.*, 2005; Kelly *et al.*, 2007; Krasil'nikova *et al.*, 1998; Lahiri *et al.*, 2006; Miyake *et al.*, 2007; Nakagawa *et al.*, 2005; Newton *et al.*, 2007; Odintsova *et al.*, 1996; Sievert *et al.*, 2000; Sievert *et al.*, 2008; Skirnisdottir *et al.*, 2001; Sorokin, 2003; Sorokin & Kuenen, 2005; Sorokin *et al.*, 2006; Sorokin, 2008; Spring *et al.*, 2001; Takai *et al.*, 2005; Takai *et al.*, 2006; Teske *et al.*, 2000; Teske & Nelson, 2004; Wirsen *et al.*, 2002)

Abkürzungen: +, vorhanden; -, nicht vorhanden, +/-, in einigen Spezies vorhanden; o, obligat autotroph; f, fakultativ autotroph; C, Calvin-Zyklus; T, reduktiver Tricarbonsäure-Zyklus; H, 3-Hydroxypropionat-Weg; el. Schwefel, elementarer Schwefel; S^0, gespeicherter Schwefel der Oxidationsstufe 0; n. b., nicht bekannt; k. $S_2O_3^{2-}$-Ox., Fähigkeit zur Thiosulfatoxidation zu Sulfat in SOP Spezies nicht nachgewiesen

Tabelle 3. Homologe ORFs, die für die dissimilatorische APS-Reduktase und deren funktionell-assoziierte Proteine (AprM, QmoABC/HdrCB) kodieren, in (meta-)genomischen Sequenzen von SRP und SOP

SRP und SOP Spezies	GenBank Genom-Zugangsnummer	Homologe ORFs in (Meta-)Genomsequenzen*								
		sat	***aprM***	***aprB***	***aprA***	***qmoA***	***qmoB***	***qmoC***	***hdrC***	***hdrB***
Chlorobia										
Chlorobium clathratiforme BU-1	AAIK01000013	ZP_00589416	-	ZP_00589417	ZP_00589418	ZP_00589419	ZP_00589420	ZP_00589421	-	-
Chlorobium chlorochromatii CaD3	NC_07514	YP_379885	-	YP_379884	YP_379883	YP_379882	YP_379881	YP_379880	-	-
Chlorobium phaeobacteroides BS1	NZ_AAIC01000057, NZ_AAIC01000606, NZ_AAIC01000002	ZP_00532500	-	ZP_00532499	inkompletter ORF: *aprA*-NTKS in ZP_00532499 nachfolgender Sequenz‡	inkompletter ORF: *qmoA*-CTKS in Sequenz vor ZP_005333969 ‡	inkompletter ORF: *qmoB*- NTKS in ZP_005333969 nachfolgender Sequenz ‡	ZP_00530754	-	-
Chlorobaculum tepidum TLS	NC_002932	NP_661756	-	NP_661758	NP_661759	NP_661760	NP_661761	NP_661762	-	-
Proteobacteria										
Alphaproteobacteria **SAR11**										
Cdt. Pelagibacter ubique HTCC1002	NZ_AAPV01000001	-	ZP_01264008	ZP_01264007†	ZP_01264006	-	-	-	-	-
Cdt. Pelagibacter ubique HTCC1062	NC_007205	-	YP_266255	YP_266256	YP_266257	-	-	-	-	-
Metagenomseq. IBEA_CTG_2004608	AACY01002870	-	inkompletter ORF: *aprM*-CTKS in EAK63329 preceding sequence‡	EAK63329	EAK63328	n. b.	n. b.	n. b.	n. b.	n. b.
Metagenomseq. IBEA_CTG_2148592	AACY01050991	-	inkompletter ORF: *aprM*-CTKS in EAJ52712 preceding sequence‡	EAJ52712	EAJ52711	n. b.	n. b.	n. b.	n. b.	n. b.
Metagenomseq. IBEA_CTG_1977812	AACY01000596	-	inkompletter ORF: *aprM*-CTKS in EAK69056 preceding sequence‡	EAK69056	inkompletter ORF: *aprA*-NTKS in EAK69055	n. b.	n. b.	n. b.	n. b.	n. b.
Metagenomseq. IBEA_CTG_2104149	AACY01023675	-	inkompletter ORF: *aprM*-CTKS in EAK12872 preceding sequence‡	EAK12872	EAK12873	n. b.	n. b.	n. b.	n. b.	n. b.
Metagenomseq. IBEA_CTG_2157860	AACY01055405	-	-	EAJ42062	EAJ42063	n. b.	n. b.	n. b.	n. b.	n. b.
Metagenomseq. IBEA_CTG_2023371	AACY01021098	EAK19071	EAK19072	EAK19073	EAK19074	n. b.	n. b.	n. b.	n. b.	n. b.
Metagenomseq. IBEA_CTG_2151824	AACY01077644	-	EAI88884	EAI88883	EAI88882	n. b.	n. b.	n. b.	n. b.	n. b.
Metagenomseq. IBEA_CTG_2037797	AACY01013231	-	EAK37254	EAK37255	EAK37256	n. b.	n. b.	n. b.	n. b.	n. b.
Metagenomseq. IBEA_CTG_2149712	AACY01043919	-	EAJ68379	EAJ68380	EAJ68381	n. b.	n. b.	n. b.	n. b.	n. b.
Metagenomseq. IBEA_CTG_2157518	AACY01120224	-	EAH91106	EAH91107	EAH91108	n. b.	n. b.	n. b.	n. b.	n. b.
Metagenomseq. IBEA_CTG_2150375	AACY01003082	-	EAK62842	EAK62843	EAK62844	n. b.	n. b.	n. b.	n. b.	n. b.
Metagenomseq. IBEA_CTG_2126577	AACY01037195	-	EAJ82119	EAJ82118	EAJ82117	n. b.	n. b.	n. b.	n. b.	n. b.
Metagenomseq. IBEA_CTG_2151480	AACY01061995	-	EAJ26240†	EAJ26241	EAJ26242	n. b.	n. b.	n. b.	n. b.	n. b.
Metagenomseq. GOS JCVI_SCAF_1096627290886	AACY020462498	-	ECY16402	ECY16403†	ECY16404	n. b.	n. b.	n. b.	n. b.	n. b.
Metagenomseq. GOS JCVI_SCAF_1096627382238	AACY020554205	-	ECV44750	ECV44747†	ECV44749	n. b.	n. b.	n. b.	n. b.	n. b.
Metagenomseq. GOS JCVI_SCAF_1096627298037	AACY020469649	-	ECX95787	ECX95782†	ECX95783	n. b.	n. b.	n. b.	n. b.	n. b.
Metagenomseq. GOS JCVI_SCAF_1096627101521	AACY020261343	-	EDC13639	EDC13633†	EDC13634	n. b.	n. b.	n. b.	n. b.	n. b.
Metagenomseq. GOS JCVI_SCAF_1096626908659	AACY020064518	-	EDH22559	EDH22558	EDH22562	n. b.	n. b.	n. b.	n. b.	n. b.
Metagenomseq. GOS JCVI_SCAF_1096627182140	AACY020342646	-	EDA97723	EDA97724†	EDA97726	n. b.	n. b.	n. b.	n. b.	n. b.
Metagenomseq. GOS JCVI_SCAF_1096627385852	AACY020557910	ECV24839	ECV24840	ECV24842†	ECV24843†	n. b.	n. b.	n. b.	n. b.	n. b.
Metagenomseq. GOS JCVI_SCAF_1096627381860	AACY020553819	-	ECV46560	ECV46557†	ECV46564†	n. b.	n. b.	n. b.	n. b.	n. b.
Metagenomseq. GOS JCVI_SCAF_1096626971466	AACY020129089	-	EDF56792	EDF56791†	EDF56790†	n. b.	n. b.	n. b.	n. b.	n. b.

Metagenomseq. ALOHA Station HOTS_Contig54195	ABEF01054195	-	CTKS: +‡	+	+	n. b.	n. b.	n. b.	n. b.	n. b.
SAR116										
Metagenomseq. EBAC2C11	AY744399	AAV31643	AAV31644	AAV31645	AAV31646	n. b.	n. b.	n. b.	n. b.	n. b.
Metagenomseq. IBEA_CTG_2159535	AACY01013150	-	EAK37449	EAK37448	inkompletter ORF: *aprA*-NTKS in EAK37447	n. b.	n. b.	n. b.	n. b.	n. b.
Metagenomseq. ALOHA Station HOTS_Contig53595	ABEF01053595	-	+	+	NTKS: +‡	n. b.	n. b.	n. b.	n. b.	n. b.
Betaproteobacteria										
Thiobacillus denitrificans ATCC 25259	NC_007404	YP_314632	YP_316042	YP_314631/ YP_316041	YP_314630/ YP_316040	YP_315406	YP_315405	-	YP_315404	YP_315403
Gammaproteobacteria										
Allochromatium vinosum	U84759	AAC23622	AAK16200	AAC23620	AAC23621	-	-	-	-	-
Olavius algarvensis Symbiont Gamma-3	AASZ_01000166, AASZ_01000200	Inkompletter ORF: *sat*-NTKS:+	+	+	+	-	-	-	-	-
Olavius algarvensis Symbiont Gamma-1	AASZ_01002870, AASZ_01004101, AASZ_01004100, AASZ_01000461	+	-	Inkompletter ORF: *aprB*-CTKS: +	Inkompletter ORF: *aprA*-NTKS, CTKS: +	+	+	-	+	+
Cdt. Ruthia magnifica CM	NC_008610	YP_903355	YP_903356	YP_903357	YP_903358	-	-	-	-	-
Cdt. Vesicomyosocius okutanii HA	NC_009465	YP_001218949	YP_001218950	YP_001218951	YP_001218952	-	-	-	-	-
Endoriftia persephone	NZ_AASF01001200, NZ_AASF01001506, NZ_AASF01002113, NZ_AASF01001775, NZ_AASF01001739, NZ_AASF01002107	ZP_02534131	-	ZP_02534969 + ZP_02534970†	Inkompletter ORF: *aprA*-NTKS in ZP_02534986†, *aprA*-CTKS in ZP_02537883†‡	Inkompletter ORF: *qmoA*-NTKS in ZP_02535934 + 5†, *qmoA*-CTKS in Sequenz vor ZP_02535795†‡	Inkompletter ORF: *qmoB*-NTKS in ZP_02535795, *qmoB*-CTKS in ZP_02537825	-	ZP_02537826	ZP_02537827
Beggiatoa sp. PS	NZ_ABBZ01001314, NZ_ABBZ01002733, NZ_ABBZ01000201	ZP_0200455	-	ZP_02004148†	Inkompletter ORF: *aprA*-NTKS: in ZP_02004148 nachfolgender Sequenz, *aprA*-CTKS in ZP_02002482†‡	ZP_01999993	ZP_01999994†	-	ZP_01999690	ZP_01999691
Metagenomseq. GOS JCVI_SCAF_1101668652715	AACY023845364	n. b.	n. b.	CTKS: EBF11654‡	NTKS: EBF11655‡	n. b.	n. b.	n. b.	n. b.	n. b.
Deltaproteobacteria										
Desulfovibrio vulgaris DP4	NC_008751	YP_967215	-	YP_967580	YP_967579	YP_967578	YP_967577	YP_967576	-	-
Desulfovibrio vulgaris Hildenborough	NC_002937	YP_010514	-	YP_010067	YP_010068	YP_010069	YP_010070	YP_010071	-	-
Desulfovibrio desulfuricans ATCC 29577	AAF226708	n. b.	-	AAF36689	AAF36690	n. b.	n. b.	n. b.	n. b.	n. b.
Desulfovibrio desulfuricans ATCC 27774	AY227146	n. b.	n. b.	n. b.	n. b.	AAO46097	AAO46098	AAO46099	n. b.	n. b.
Desulfovibrio desulfuricans G20	NC_007519	YP_388757	-	YP_387605	YP_387606	YP_387607	YP_387608	YP_387609	-	-
Desulfotalea psychrophila LSv54	NC_006138	YP_065208	-	YP_064840	YP_064841†	YP_064842†	YP_064843	YP_064844	-	-
Desulfobulbus sp. MLMS-1	NZ_AAQF01000064, NZ_AAQF01000037, NZ_AAQF01000113	ZP_01289077	-	ZP_01288426	ZP_01288427	ZP_01288428	inkompletter ORF: *qmoB*-NTKS in ZP_01288428 nachfolgender Sequenz, *qmoB*-CTKS in ZP_01289964‡	ZP_01289963	-	-
Desulfatibacillum alkenivorans AK-01	NZ_ABII01000004, NZ_ABII01000008	ZP_02131628	-	ZP_02130770	ZP_02130771	ZP_02130772	ZP_02130773	ZP_02130774	-	-
Cdt. Desulfococcus oleovorans Hxd3	NC_009943	YP_001528889	-	YP_001528884	YP_001528885	YP_001528886	YP_001528887	YP_00152888		
Olavius algarvensis Delta-1 Symbiont *Desulfosarcina/-nema*	AASZ_01000974	+	-	+	+	+	+	+	-	-
Olavius algarvensis Delta-4 Symbiont *Desulfosarcina/-nema*	AASZ_01002308, AASZ_01002996	n. b.	-	+	CTKS: +	+	+	+	-	-
Syntrophobacter fumaroxidans	NC_008554	YP_845175	-	YP_845176	YP_845177	YP_845178 YP_845414	YP_845179 YP_845413	- YP_845412	*hdrD*-homologe Sequenz YP_845180	
Thermodesulfobacteria										
Thermodesulfobacterium commune	TIGR Datenbank	+	-	+	+	+	+	+	-	-

Nitrospira										
Thermodesulfovibrio yellowstonii	TIGR Datenbank	+	-	+	+	+	+	+	-	-
Firmicutes										
Desulfotomaculum reducens MI-1	NC_009253	YP_001112000	-	YP_001112001	YP_001112002	YP_001112003	YP_001112004	-	YP_001111998	YP_001111999
Cdt. Desulforudis audaxviator MP104C	NC_010424	YP_001717220	-	YP_001718011	YP_001718010	YP_001718009	YP_001718008	-	YP_001718007	YP_001718006
Ungeklärte phylogenetische Zuordnung										
Metagenomseq. fosws39f7	CT025835	CAJ31178	-	CAJ31179	CAJ31180	CAJ31160	CAJ31161	CAJ31177	n. b.	n. b.
Metagenomseq. fosws7f8	CT025836	CAJ31203	-	CAJ31202	CAJ31201	-	-	CAJ31196	n. b.	n. b.
Metagenomseq. ALOHA Station HOTS_Contig54143	ABEF01054143	n. b.	-	+	+	n. b.	n. b.	n. b.	n. b.	n. b.
Euryarchaeota										
Archaeoglobus fulgidus	NC_000917	NP_070495	-	NP_070497	NP_070498	NP_069497	NP_069496	NP_069495	-	-
Crenarchaeota										
Pyrobaculum aerophilum IM-2	NC_003364	NP_560134	-	NP_560098/ NP_560099§	NP_560100/ NP_560101§	-	-	-	-	-
Pyrobaculum arsenaticum	NC_009376	YP_001153458	-	YP_001153453	YP_001153454	-	-	-	-	-
Pyrobaculum calidifontis JCM	NC_009073	YP_001056310	-	YP_001056315	YP_001056314	-	-	-	-	-
Pyrobaculum islandicum	NC_008701	YP_931010	-	-	-	-	-	-	-	-
Caldivirga maquilingensis IC-167	NZ_AAXQ01000001	ZP_01711817	-	ZP_01711819	ZP_01711818	-	-	-	-	-

* die GenBank Protein-Zugangsnummern der homologen ORFs sind angegeben; für Genome ohne Protein Annotationen wurden folgende Abkürzungen verwendet: (+) homologer ORF in (Meta-)Genom vorhanden, (-) homologer ORF nicht in (Meta-)Genom vorhanden, (n. b.) Vorkommen/Fehlen einer homologen Sequenz nicht bestimmbar/bekannt, da Sequenzen aus Genlocus-Klonierung stammen bzw. Shotgun-Sequenzierungen von Metagenomen sind

‡ verwendete Abkürzungen für inkomplette Gensequenzen von noch nicht abgeschlossenen Genomsequenzierungsprojekten und Metagenomprojekten: (NTKS/ CTKS) N- bzw. C-terminale proteinkodierende Sequenz

† fehlerhafte ORF Annotation in Genomsequenz durch Automatische Proteinbestimmungs-Programme

§ ORF-Sequenz mit frameshift

Tabelle 4. Homologe ORFs, die für die dissimilatorische Sulfitreduktase und deren funktionell-assoziierten Transmembrankomplex (DsrMKJOP/HmeABCDE) kodieren, in genomischen Sequenzen von sulfat- und sulfitreduzierenden Prokaryonten sowie SOP

SRP und SOP Spezies	GenBank Genom-Zugangsnummer	Homologe ORFs in (Meta-)Genomsequenzen*					
		dsrAB	*dsrM*	*dsrK*	*dsrJ*	*dsrO*	*dsrP*
Chlorobia							
Chlorobium clathratiforme BU-1	AAIK01000042	ZP_00509517, ZP_00509516	ZP_00509509	ZP_00509508	ZP_00509529	ZP_00509507	ZP_00509506
Chlorobium chlorochromatii CaD3	NC_007514	YP_380247, YP_380246	YP_380239	YP_380238	YP_380237	YP_380236	YP_380235
Chlorobium phaeobacteroides BS1	NZ_AAIC01000057, NZ_AAIC01000113	ZP_00532849, ZP_00532850	ZP_00532509	ZP_00532508	ZP_00532511	ZP_00532507	ZP_00532506
Chlorobaculum tepidum TLS	NC_002932	NP_661746, NP_661747	NP_663118	NP_663117	NP_663116	NP_663115	NP_663114
Chlorobium phaeobacteroides DSM 266	NC_008639	YP_910622, YP_910623	YP_910630	YP_910631	YP_910632	YP_910633	YP_910634
Prosthecochloris aestuarii DSM 271	NZ_AAIJ01000019	ZP_00592685, ZP_00592686	ZP_00592693	ZP_00592694	ZP_00592695	ZP_00592696	ZP_00592697
Prosthecochloris vibrioformis DSM 265	NZ_AAJD01000006	ZP_00661491, ZP_00661490	ZP_00661483	ZP_00661482	ZP_00661481	ZP_00661480	ZP_00661479
Pelodictyon luteolum DSM 273	NC_007512	YP_373969, YP_373970	YP_373977	YP_373978	YP_373979	YP_373980	YP_373981
Chlorobium limicola DSM 245	NZ_AAHJ01000040	ZP_00513264, ZP_00513265	ZP_00513272	ZP_00513273	ZP_00513274	ZP_00513275	ZP_00513276
Proteobacteria							
Alphaproteobacteria							
Magnetococcus sp. MC-1	NC_008576	YP_866063, YP_866064	YP_863984	YP_863985	YP_865622	YP_865623	YP_865624
Magnetospirillum magneticum AMB-1	NC_007626	YP_422730, YP_422731	YP_422736	YP_422737	YP_422739	YP_422740	YP_422741
Magnetospirillum gryphiswaldense MSR-1	CU459003*	CAM75808	CAM75802		CAM75799		CAM75797
Magnetospirillum magnetotacticum MS-1	NZ_AAAP01003703, NZ_AAAP01003586, NZ_AAAP01003833	ZP_00053119, ZP_00053120	ZP_00052646	ZP_00052647+ ZP_00054611	ZP_00208198	ZP_00208197	ZP_00208196+ ZP_00208195
Betaproteobacteria							
Thiobacillus denitrificans ATCC 25259	NC_007404	YP_316243, YP_316242	YP_316237	YP_316236	YP_316234	YP_316233	YP_316232
Gammaproteobacteria							
Allochromatium vinosum	U84759, U84760*	AAC35394, AAC35395	AAC35400	AAC35401	AAG13083	AAG13084	AAG13085
Olavius algarvensis Gamma-3 Symbiont	NZ_AASZ_01000200, NZ_AASZ_01000111, NZ_AASZ_01004984	+, +	+	+	+	+	+
Olavius algarvensis Gamma-1 Symbiont	NZ_AASZ_01004101, NZ_AASZ_01004100, NZ_AASZ_01000461, NZ_AASZ_01001690	+, +	+	+	+	+	+
Cdt. Ruthia magnifica CM	NC_008610	YP_904057, YP_904056	YP_904051	YP_904050	YP_904048	YP_904047	YP_904046
Cdt. Vesicomyosocius okutanii HA	NC_ 009465	YP_001219625, YP_001219624	YP_001219619	YP_001219618	YP_001219616	YP_001219615	YP_001219614
Endoriftia persephone	NZ_AASF01001644, NZ_AASF01001547, NZ_AASF01001341	+, +	+	+	+	+	+
Beggiatoa sp. PS und SS	NZ_ABBY01000136, NZ_ABBZ01000830	ZP_02004886, ZP_02004264	ZP_02001527, ZP_01997347 (SS)	ZP_01998573, ZP_01997348 (SS)	ZP_01998575	ZP_01998577	ZP_01998578, ZP_01997356 (SS)
Alkalilimnicola ehrlichei MLHE-1	NC_008340	YP_742489, YP_742490	YP_742495	YP_742496	YP_742498	YP_742499	YP_742500
Halorhodospira halophila SL1	NC_008789	YP_001003517, YP_001003518	YP_001003523	YP_001003524	YP_001003526	YP_001003527	YP_001003528
SAR86							
Metagenomseq. BAC13K9BAC	DQ068067	AAY89969, AAY89968	AAY89963	AAY89962	AAY89960	AAY89959	AAY89958
Deltaproteobacteria							
Desulfotalea psychrophila LSv54	NC_006138	YP_064533, YP_064534	YP_066811	YP_066810	YP_066809	YP_066808+ YP_066807†	YP_066806
Desulfovibrio vulgaris Hildenborough	NC_002937	YP_009626, YP_009627	YP_010509	YP_010508	YP_010507	YP_010506	YP_010505
Desulfovibrio vulgaris DP4	NC_008751	YP_967975, YP_967974					
Desulfovibrio desulfuricans G20	NC_007519	YP_387022, YP_387023	YP_388763	YP_388764	YP_388765	YP_388766	YP_388767
Desulfobulbus sp. MLMS-1	NZ_AAQ01000532, NZ_AAQ01000051	ZP_01292188, ZP_01288799	ZP_01291344	ZP_01291345	ZP_01291346	ZP_01291347	ZP_01291348
Desulfobulbus rhabdoformis	AJ250473*	CAB95038, CAB95039	n. b.	n. b.	n. b.	n. b.	n. b.
Desulfobacula toluolica	AJ457136*	CAD29754, CAD29755	n. b.	n. b.	n. b.	n. b.	n. b.
Cdt. Desulfococcus oleovorans Hxd3	NC_009943	YP_001530549, ZP_01674168	ZP_01673988	ZP_01673987	ZP_01673986	ZP_01673985	ZP_01673984

Desulfatibacillum alkenivorans AK-01	NZ_ABII01000006; NZ_ABII01000010	ZP_02131243, ZP_02131244	ZP_02132051	ZP_02132050	ZP_02132049	ZP_02132048	ZP_02132047
Thermodesulforhabdus norvegica	AJ277293*	CAC36212, CAC36213	n. b.	n. b.	n. b.	n. b.	n. b.
Syntrophobacter fumaroxidans MPOB	NC_008554	YP_848143, YP_848144	YP_845274	YP_845275	YP_845276	YP_845277	YP_845278
Ungeklärte phylogenetische Zuordnung							
Metagenomseq. fosws39f7	CT025835	CAJ31162, CAJ31163	CAJ31169	CAJ31170	CAJ31171	CAJ31172	CAJ31173
Metagenomseq. fosws7f8	CT025836	CAJ31214, CAJ31215	CAJ31207	CAJ31206	CAJ31205		CAJ31217
Metagenomseq. fosws42c90003	CT025834	CAJ31124, CAJ31123	CAJ31133	CAJ31134	CAJ31135	CAJ31136	CAJ31137
Thermodesulfobacteria							
Thermodesulfobacterium commune	TIGR Datenbank	+, +	+	+	+	+	+
Nitrospira							
Thermodesulfovibrio yellowstonii	TIGR Datenbank	+, +	+	+	+	+	+
Firmicutes							
Desulfotomaculum reducens MI-1		YP_001114514	YP_001114526	YP_001114525	-	-	-
Desulfotomaculum thermocisternum	AF074396*	AAC96107, AAC96108	n. b.	n. b.	n. b.	n. b.	n. b.
Desulfitobacterium hafniense Y51	NC_007907	YP_516542, YP_516543	YP_516545	YP_516546	YP_516547	YP_516548	YP_516549
Desulfitobacterium hafniense DCB-2	NZ_AAAW04000003	ZP_01371540, ZP_01371539	ZP_01371536	ZP_01371535	ZP_01371534	ZP_01371533	ZP_01371532
Pelotomaculum thermopropionicum SI	NC_009454	YP_001211240	YP_001211240	YP_001211241	-	-	-
Thermosinus carboxydivorans Nor1	NZ_AAWL01000006	ZP_01666265, ZP_01666264	ZP_01666263	ZP_01666262	-	-	-
Carboxydothermus hydrogenoformans Z-2901	NC_007503	YP_361207, YP_361206	YP_361201	YP_361200	-	YP_360900?	YP_360899?
Moorella thermoacetica ATCC 39073	NC_007644	YP_430450, YP_430449	YP_430451	YP_430455	YP_430454	YP_430453	YP_430452
Cdt. Desulforudis audaxviator MP104C	NC_010424	YP_001718320, YP_001718319	YP_001718311	YP_001718310	-	-	-
Euryarchaeota							
Archaeoglobus fulgidus	NC_000917	NP_069259, NP_069260	NP_069337	NP_069338	NP_069339	NP_069335	NP_069336
Archaeoglobus profundus	AF071499*	AAC78309, AAC78310	n. b.	n. b.	n. b.	n. b.	n. b.
Crenarchaeota							
Pyrobaculum aerophilum IM-2		NP_560123, NP_560124; NP_560107, NP_560106	NP_560136	NP_560138	-	-	-
Pyrobaculum islandicum	NC_008701	YP_929696, YP_929695	YP_929697	YP_929699	-	-	-
Pyrobaculum arsenaticum	NC_009376	YP_001153433, YP_001153432; YP_001153140, YP_001153141, YP_001153143	YP_001153447, YP_001153139	YP_001153439, YP_001153148	-	-	-
Pyrobaculum calidifontis JCM	NC_009073	YP_001056332, YP_001056331; YP_001056343, YP_001056342	YP_001056322	YP_001056325	-	-	-
Thermoproteus neutrophilus V24Sta	NC_010525	YP_001793740, YP_001793741	YP_001793739	YP_001793737	-	-	-
Caldivirga maquilingensis IC-167	NZ_AAXQ01000001	ZP_01711194, ZP_01711192	ZP_01711195	ZP_01711197	-	-	-

* die GenBank Protein-Zugangsnummern der homologen ORFs sind angegeben; für Genome ohne Protein Annotationen wurden folgende Abkürzungen verwendet: (+) homologer ORF in Genom vorhanden, (-) homologer ORF nicht in Genom vorhanden, (n. b.) Vorkommen/Fehlen einer homologen Sequenz nicht bestimmbar/bekannt, da Sequenzen aus Genlocus-Klonierung stammen bzw. Shotgun-Sequenzierungen von Metagenomen sind

Publikation 3: Supplementary Material

Supplementary data material Table S1. AprB secondary structure element succession

SOB Apr lineage I

Secondary structure element succession AprB *Allochromatium vinosum*

AprB segments	No	*Archaeoglobus fulgidus* sequence	AA position	Sec. str. element	*Allochromatium vinosum* sequence	AA position	Sec. str. element
Ferredoxin	1	P S F V N	2-6	beta-sheet	P T F V Y (Loop: missing)	2-6	beta-sheet
(2-68 AA)	2	A C E Y I	20-24	alpha-helix	C V D I **shortened**	16-19	alpha-helix
	3	L M T L D	29-33	beta-sheet	I M H I D	24-28	beta-sheet
	4	K A Y N R	38-42	beta-sheet	R A Y N I	33-37	beta-sheet
	5	S C V K M	52-56	alpha-helix	S C V K A	47-51	alpha-helix
	6	A I D V R	61-65	beta-sheet	A I D V R	56-60	beta-sheet
3 antiparallel	7	A C V P M R G	76-82	beta-sheet	S V R V R D	71-76	beta-sheet
Beta-sheet	8	S D I M W T V K Y	84-92	beta-sheet	G V I A W R I I F (EK-Insert: 7 AA Loop, 5	81-89	beta-sheet
(69-104 AA)					charged AA)		
	9	K V L R F K F A I	96-104	beta-sheet	K D M N L L A P I	94-102	beta-sheet
Tail	10	E E A L	123-126	alpha-helix	N E M R	122-125	alpha-helix
(105-148 AA)	11	E I	136-137	alpha-helix	**missing**		

Structural differences: 12-14 loop
77-80 loop
91-93 loop
112-114 loop
133-142 loop

156 AA total

identical AA	**67**	43,0%
similar AA**	**91**	58,3%
1.0Å RMSD backbone	**134**	**85,9%**

** incl. identical AA

Protein problems:

backbone
Pro2, Gln15, Asn132, His145

sidechain
Gln15, Met25, Met41, Cys42, Arg76,

Ramachandran Plot
Gly14, Gln15, Gly12, Gly142, Gly69, Asn132, His145

AA Accessibility: **Trp43**, Asp64, Thr104

Secondary structure element succession AprB *Thiobacillus denitrificans* ATCC25259

AprB segments	No	*Archaeoglobus fulgidus* sequence	AA position	Sec. str. element	*Thiobacillus denitrificans* sequence	AA position	Sec. str. element
Ferredoxin	1	P S F V N	2-6	beta-sheet	P T F V Y (Loop: missing)	2-6	beta-sheet
(2-68 AA)	2	A C E Y I	20-24	alpha-helix	C V D I **shortened**	16-19	alpha-helix
	3	L M T L D	29-33	beta-sheet	I M H I D	24-28	beta-sheet
	4	K A Y N R	38-42	beta-sheet	R A Y N I	33-37	beta-sheet
	5	S C V K M	52-56	alpha-helix	S C V K A	47-51	alpha-helix
	6	A I D V R	61-65	beta-sheet	A I D V R	56-60	beta-sheet
3 antiparallel	7	A C V P M R G	76-82	beta-sheet	S V R V R R D	71-77	beta-sheet

beta-sheet (69-104 AA)	8	S D I M W T V K Y	84-92	beta-sheet	G V I A W R I K F (EK-Insert: 7 AA Loop, 5 charged AA)	81-89	beta-sheet
	9	K V L R F K F A I	96-104	beta-sheet	K D M E L L A P I	94-102	beta-sheet
Tail	10	E E A L	123-126	alpha-helix	Q A M R	122-125	alpha-helix
(105-148 AA)	11	E I	136-137	alpha-helix	**missing**		

Structural deviations: 12-14 loop
77-80 loop
91-93 loop
111-114 loop
135-144 loop

156 AA total

identical AA	**65**	41,7%
similar AA**	**89**	57,1%
1.0Å RMSD backbone	**133**	**85,3%**

** incl. identical AA

Protein problems: **backbone**
Pro2, Tyr15, Lys94, Leu114, Ala115, Asp116, Asn132, Pro134, Asp143, Arg138, His145
sidechain
Met25, Met41, Arg76, Lys109, Thr146

Ramachandran Plot
Gly14, Tyr15, Gly69, Gly12, Leu114, Ala115, Asn132, Arg138, Asp143, His145

AA Accessibility: **Glu64, Trp43**

Secondary structure element succession AprB *Cdt.* Ruthia magnifica

AprB segments	**No**	***Archaeoglobus fulgidus* sequence**	**AA position**	**Sec. str. element**	***Cdt.* Ruthia magnifica sequence**	**AA position**	**Sec. str. element**
Ferredoxin	1	P S F V N	2-6	beta-sheet	P T F V Y (Loop : missing)	2-6	beta-sheet
(2-68 AA)	2	A C E Y I	20-24	alpha-helix	→C V D I **shortened**	16-19	alpha-helix
	3	L M T L D	29-33	beta-sheet	I M H I D	24-28	beta-sheet
	4	K A Y N R	38-42	beta-sheet	R A Y N I	33-37	beta-sheet
	5	S C V K M	52-56	alpha-helix	S C V K A	47-51	alpha-helix
	6	A I D V R	61-65	beta-sheet	A I D V R	56-60	beta-sheet
3 antiparallel	7	A C V P M R G	76-82	beta-sheet	S V R V I R D	71-77	beta-sheet
beta-sheet (69-104 AA)	8	S D I M W T V K Y	84-92	beta-sheet	G T I A W R V K F (EK-Insert: 7 AA Loop, 5 charged AA)	81-89	beta-sheet
	9	K V L R F K F A I	96-104	beta-sheet	R V K N F L S P I	93-101	beta-sheet
Tail	10	E E A L	123-126	alpha-helix	D D M R	121-124	alpha-helix
(105-148 AA)	11	E I	136-137	alpha-helix	**missing**		

Abweichungen: 12-14 loop
77-80 loop
131-141 loop
107-112 loop

155 AA total

identical AA	**71**	45,8%
similar AA**	**96**	62,0%
1.0Å RMSD backbone	**136**	**87,7%**

** incl. identical AA

Protein problems: **backbone**
Pro2, His15, His141
sidechain
His15, Met25, Tyr31, Met41, Cys42, Arg76, Arg114

Ramachandran Plot
Gly12, Gly14, His15, Gly69, Gly92, Gly107, His144, Gly141

AA Accessibility: Lys30, **Trp43**, Asp64, Thr103

Secondary structure element succession AprB *Cdt.* Pelagibacter ubique HTCC1062

AprB segments	No	*Archaeoglobus fulgidus* sequence	AA position	Sec. str. element	*Cdt.* Pelagibacter ubique sequence	AA position	Sec. str. element
Ferredoxin	1	P S F V N	2-6	beta-sheet	S T F V Y (Loop : missing)	2-6	beta-sheet
(2-68 AA)	2	A C E Y I	20-24	alpha-helix	→C V D I **shortened**	16-19	alpha-helix
	3	L M T L D	29-33	beta-sheet	I M H I D	24-28	beta-sheet
	4	K A Y N R	38-42	beta-sheet	R A V N I	33-37	beta-sheet
	5	S C V K M	52-56	alpha-helix	S C V K A	47-51	alpha-helix
	6	A I D V R	61-65	beta-sheet	A I D V R	56-60	beta-sheet
3 antiparallel	7	A C V P M R G	76-82	beta-sheet	S V R V R R E	71-77	beta-sheet
beta-sheet	8	S D I M W T V K Y	84-92	beta-sheet	G T I S W K I K F (EK-Insert: 7 AA Loop, 5 charged AA)	81-89	beta-sheet
(69-104 AA)							
	9	K V L R F K F A I	96-104	beta-sheet	T T K D F V S P I	93-101	beta-sheet
Tail	10	E E A L	123-126	alpha-helix	Q G E I	121-124	alpha-helix
(105-148 AA)	11	E I	136-137	alpha-helix	**missing**		

Structural deviations: 12-14 loop
77-80 loop
132-141 loop
109-113 loop

identical AA **59** 38,6%
similar AA** **86** 56,2%
1.0Å RMSD backbone **133** **87,0%**
** incl. identical AA

153 AA total

Protein problems: **backbone**
His15, Leu113, Glu115, Thr131, Lys141, Leu142
sidechain
His15, Met25, Cys42, Lys108

Ramachandran Plot
Gly12, Gly14, His15, Gly69, Leu113, Lys141, Gly92, Leu142, Glu115, Thr131, Gly81

AA Accessibility: Asn30, **Trp43**, Asp64

Secondary structure element succession AprB environmental sequence EBAC2C11

AprB segments	No	*Archaeoglobus fulgidus* sequence	AA position	Sec. str. element	EBAC2C11 sequence	AA position	Sec. str. element
Ferredoxin	1	P S F V N	2-6	beta-sheet	P T F V Y (Loop : missing)	2-6	beta-sheet
(2-68 AA)	2	A C E Y I	20-24	alpha-helix	→C V D I **shortened**	16-19	alpha-helix
	3	L M T L D	29-33	beta-sheet	I M H I D	24-28	beta-sheet
	4	K A Y N R	38-42	beta-sheet	R A V N I	33-37	beta-sheet
	5	S C V K M	52-56	alpha-helix	S C V K A	47-51	alpha-helix
	6	A I D V R	61-65	beta-sheet	A I D A R	56-60	beta-sheet
3 antiparallel	7	A C V P M R G	76-82	beta-sheet	S V R V L R E	71-77	beta-sheet
beta-sheet	8	S D I M W T V K Y	84-92	beta-sheet	G T I S W R L K F (DK-Insert: 7 AA Loop, 5 charged AA)	81-89	beta-sheet
(69-104 AA)							
	9	K V L R F K F A I	96-104	beta-sheet	R E K H F E S P I	93-101	beta-sheet
Tail	10	E E A L	123-126	alpha-helix	L D D M	120-123	alpha-helix
(105-148 AA)	11	E I	136-137	alpha-helix	**missing**		

Structural deviations: 12-14 loop

153 AA

Protein problems: **backbone**

77-80	loop	**identical AA**	**61**	40,0%		Pro2, His15, His130, Leu141, Pro142
131-140	loop	**similar AA****	**90**	58,8%		**sidechain**
		1.0Å RMSD backbone	**137**	**89,5%**		His15, Met25, Cys42, Arg76, Lys110, Tyr115
		** incl. identical AA				
						Ramachandran Plot
						Gly12, Gly14, His15, Gly69, Gly81, Gly92, His130, Leu141, Ser143
					AA Accessibility:	**Trp43**, Asp64, Thr103

Crenarchaeal SRP

Secondary structure element succession AprB *Pyrobaculum aerophilum*

AprB segments	**No**	***Archaeoglobus fulgidus* sequence**	**AA position**	**Sec. str. element**	***Pyrobaculum aerophilum* sequence**		**AA position**	**Sec. str. element**
Ferredoxin	1	P S F V N	2-6	beta-sheet	P T F V Y	(Loop : missing)	2-6	beta-sheet
(2-68 AA)	2	A C E Y I	20-24	alpha-helix	C V D I **shortened**		16-19	alpha-helix
	3	L M T L D	29-33	beta-sheet	N M Q Y N		24-28	beta-sheet
	4	K A Y N R	38-42	beta-sheet	K G Y N A		33-37	beta-sheet
	5	S C V K M	52-56	alpha-helix	N C V K Y		47-51	alpha-helix
	6	A I D V R	61-65	beta-sheet	A V D V R		56-60	beta-sheet
3 antiparallel	7	A C V P M R G	76-82	beta-sheet	E M V R D T K		71-77	beta-sheet
beta-sheet	8	S D I M W T V K Y	84-92	beta-sheet	N I I Y W R I V Y		79-87	beta-sheet
(69-104 AA)								
	9	K V L R F K F A I	96-104	beta-sheet	T V Y D F A S P I		91-99	beta-sheet
Tail	10	E E A L	123-126	alpha-helix	R Q D L		116-119	alpha-helix
(105-148 AA)	11	E I	136-137	alpha-helix	**Insert: K D E**		129-131	**beta-sheet**
					Insert: G F P		134-136	**beta-sheet**

Structural deviations:	12-14	loop	**150 AA total**		**Protein problems:**	**backbone**
	106-110	loop	**identical AA**	**58**	38,7%	Pro2, Lys15, Lys77, Ala110, Ala125, Pro130, Pro136, Arg140
	128-129	loop-beta	**similar AA****	**81**	54,0%	**sidechain**
	132-137	loop-beta-loop	**1.0Å RMSD backbone**	**129**	**86,0%**	Lys15, Met25, Tyr87
			** incl. identical AA			
						Ramachandran Plot
						Gly14, Gly12, Ala110, Lys77, Lys15, Gly69, Gly90, Arg140, Ala125
					AA Accessibility:	**Ile40**, Lys30, Asp64, Thr101

Secondary structure element succession AprB *Pyrobaculum calidifontis*

AprB segments	**No**	***Archaeoglobus fulgidus* sequence**	**AA position**	**Sec. str. element**	***Pyrobaculum calidifontis* sequence**		**AA position**	**Sec. str. element**
Ferredoxin	1	P S F V N	2-6	beta-sheet	P T F V Y	(Loop : missing)	2-6	beta-sheet
(2-68 AA)	2	A C E Y I	20-24	alpha-helix	C V D I **shortened**		16-19	alpha-helix
	3	L M T L D	29-33	beta-sheet	N M H Y N		24-28	beta-sheet

	4	K A Y N R	38-42	beta-sheet	K A Y N A	33-37	beta-sheet
	5	S C V K M	52-56	alpha-helix	N C V K Y	47-51	alpha-helix
	6	A I D V R	61-65	beta-sheet	A V E V R	56-60	beta-sheet
3 antiparallel	7	A C V P M R G	76-82	beta-sheet	R I G V V R D	71-77	beta-sheet
beta-sheet	8	S D I M W T V K Y	84-92	beta-sheet	N I I Y W R V M Y	81-89	beta-sheet
(69-104 AA)							
	9	K V L R F K F A I	96-104	beta-sheet	T V Y E F A S P I	93-101	beta-sheet
Tail	10	E E A L	123-126	alpha-helix	R P D L	118-121	alpha-helix
(105-148 AA)	11	E I	136-137	alpha-helix	**Insert: N P E**	131-133	**beta-sheet**
					Insert: G F K	136-138	**beta-sheet**

Structural deviations: 12-14 loop
108-112 loop
130-131 loop-beta
134-148 loop-beta-loop
77-80 loop

identical AA **151 AA total**
similar AA** **64** 42,4%
1.0Å RMS backbone **86** 57,0%
** incl. identical AA **119** **78,8%**

Protein problems: **backbone**
Pro2, Lys15, Asn81, Ala112, Glu139
sidechain
Lys15, Met25, Cys42, Arg76, Tyr8**9**

Ramachandran Plot
Gly14, Gly12, Ala112, Glu139, Lys15, Gly69, Gly92

AA Accessibility: Lys30, Asp64, Thr103

Secondary structure element succession AprB *Caldivirga maquilingensis*

AprB segments	**No**	***Archaeoglobus fulgidus* sequence**	**AA position**	**Sec. str. element**	***Caldivirga maquilingensis* sequence**	**AA position**	**Sec. str. element**
Ferredoxin	1	P S F V N	2-6	beta-sheet	P S Y V I (Loop : missing)	2-6	beta-sheet
(2-68 AA)	2	A C E Y I	20-24	alpha-helix	C V N I **shortened**	16-19	alpha-helix
	3	L M T L D	29-33	beta-sheet	I M R F T K S **elongated** (3 AA Insert)	24-30	beta-sheet
					Insert: V L G new	32-34	**beta-sheet**
	4	K A Y N R	38-42	beta-sheet	K A V N I	36-40	beta-sheet
	5	S C V K M	52-56	alpha-helix	N C V K H	50-54	alpha-helix
3 antiparallel	6	A I D V R	61-65	beta-sheet	A V Q I R	59-63	beta-sheet
beta-sheet	7	A C V P M R G	76-82	beta-sheet	S V E V Y R D	74-80	beta-sheet
(69-104 AA)							
	8	S D I M W T V K Y	84-92	beta-sheet	N R V Y W T R I Y	84-92	beta-sheet
	9	K V L R F K F A I	96-104	beta-sheet	S V K H F V F P I	96-104	beta-sheet
Tail	10	E E A L	123-126	alpha-helix	R E L L	123-126	alpha-helix
(105-148 AA)	11	E I	136-137	alpha-helix	**missing**		

Structural deviations: 12-14 loop
29-33 loop-beta-loop
80-85 loop
134-145 loop

identical AA **154 AA total**
similar AA** **70** 45,5%
1.0Å RMSD backbone **95** 61,7%
** incl. identical AA **130** **84,4%**

Protein problems: **backbone**
Pro2, Asp15, Asn84, Pro115, Pro122, Phe133
sidechain
Met25, Ser44, Cys45, Arg79, Tyr92, Lys113, Tyr118, Tyr130

Ramachandran Plot
Gly14, Gly12, Gly31, Asp15, Gly72, Gly95, Phe133, Asn84
Gly144

AA Accessibility: Gly31, **Trp46**, Asp67, Thr106

SRB and affiliated SOB Apr lineage II

Secondary structure element succession AprB *Desulfotomaculum reducens*

AprB segments	No	*Archaeoglobus fulgidus* sequence	AA position	Sec. str. element	*Desulfotomaculum reducens* sequence		AA position	Sec. str. element
Ferredoxin	1	P S F V N	2-6	beta-sheet	P S F V I	(Loop: KGQDK)	2-6	beta-sheet
(2-68 AA)	2	A C E Y I	20-24	alpha-helix	A C M Y I		20-24	alpha-helix
	3	L M T L D	29-33	beta-sheet	L M V L D		29-33	beta-sheet
	4	K A Y N R	38-42	beta-sheet	K A Y N R		38-42	beta-sheet
	5	S C V K M	52-56	alpha-helix	C C V K I		52-56	alpha-helix
	6	A I D V R	61-65	beta-sheet	A I D V R		61-65	beta-sheet
3 antiparallel	7	A C V P M RG	76-82	beta-sheet	S C V P L R S		76-82	beta-sheet
beta-sheet	8	S D I M W T V K Y	84-92	beta-sheet	D S I M W T V K F		84-92	beta-sheet
(69-104 AA)	9	K V L R F K F A I	96-104	beta-sheet	M L K R F K F P I		96-104	beta-sheet
Tail	10	E E A L	123-126	alpha-helix	**missing**			
(105-148 AA)	11	E I	136-137	alpha-helix	**missing**			

Structural deviations: 123-125 loop
135-136 loop

147 AA total

identical AA	**91**	61,9%
similar AA**	**115**	78,2%
1.0Å RMSD backbone	**135**	**91,8%**

** incl. identical AA

Protein problems:
backbone
Pro2, Lys14, Pro79, Ser82, Asn126, Thr132 Pro134, Pro143
sidechain
Lys18, Thr19, Met22, Met30, Lys36, Gln46, Cys47, Tyr118, Thr137

Ramachandran Plot
Lys14, Ser82, Asn126, Gly74, Gly95, Thr132

AA Accessibility: **Trp48, Glu8, Asp17**, Asp69, Thr106

Secondary structure element succession AprB *Syntrophobacter fumaroxidans*

AprB segments	No	*Archaeoglobus fulgidus* sequence	AA position	Sec. str. element	*Syntrophobacter fumaroxidans* sequence		AA position	Sec. str. element
Ferredoxin	1	P S F V N	2-6	beta-sheet	P S Y V L	(Loop: KGQDK)	2-6	beta-sheet
(2-68 AA)	2	A C E Y I	20-24	alpha-helix	A C M Y I		20-24	alpha-helix
	3	L M T L D	29-33	beta-sheet	L M V L D		29-33	beta-sheet
	4	K A Y N R	38-42	beta-sheet	K A F N R		38-42	beta-sheet
	5	S C V K M	52-56	alpha-helix	N C V K I		52-56	alpha-helix
	6	A I D V R	61-65	beta-sheet	A I D V R		61-65	beta-sheet
3 antiparallel	7	A C V P M RG	76-82	beta-sheet	S V V P L R G		76-82	beta-sheet
beta-sheet	8	S D I M W T V K Y	84-92	beta-sheet	E D I M W T V K F		84-92	beta-sheet
(69-104 AA)	9	K V L R F K F A I	96-104	beta-sheet	M V K R F K F P I		96-104	beta-sheet
Tail	10	E E A L	123-126	alpha-helix	**missing**			
(105-148 AA)	11	E I	136-137	alpha-helix	A S		135-136	alpha-helix

Structural deviations: 123-125 loop

	147 AA total	
identical AA	**92**	62,6%
similar AA**	**120**	81,6%
1.0Å RMSD backbone	**140**	**95,2%**

** incl. identical AA

Protein problems: **backbone**
Pro2, Lys14, Pro79, Thr132, Trp138
sidechain
Lys18, Thr19, Met22, Met30, Lys36, Met46, Cys47, Arg81, Thr122, Ser127, Thr132, Ser136
Ramachandran Plot
Lys14, Gly82, Thr132, Gly74, Gly95, Trp138

AA Accessibility: **Trp48, Glu8, Asp17**, Asp69, Thr106

Secondary structure element succession AprB environmental sequence fosws39f7

AprB segments	No	*Archaeoglobus fulgidus* sequence	AA position	Sec. str. element	fosws39f7 sequence		AA position	Sec. str. element
Ferredoxin	1	P S F V N	2-6	beta-sheet	P S F V L	(Loop: KALDK)	2-6	beta-sheet
(2-68 AA)	2	A C E Y I	20-24	alpha-helix	A C Q Y V		20-24	alpha-helix
	3	L M T L D	29-33	beta-sheet	L M V L D		29-33	beta-sheet
	4	K A Y N R	38-42	beta-sheet	M A F N R		38-42	beta-sheet
	5	S C V K M	52-56	alpha-helix	S C V K I		52-56	alpha-helix
	6	A I D V R	61-65	beta-sheet	A I E V R		61-65	beta-sheet
3 antiparallel	7	A C V P M R G	76-82	beta-sheet	T V T P L R A		76-82	beta-sheet
beta-sheet	8	S D I M W T V K Y	84-92	beta-sheet	D S I M W T V K F		84-92	beta-sheet
(69-104 AA)	9	K V L R F K F A I	96-104	beta-sheet	M L K R F K F P I		96-104	beta-sheet
Tail	10	E E A L	123-126	alpha-helix	**missing**			
(105-148 AA)	11	E I	136-137	alpha-helix	E A		135-136	alpha-helix

Structural deviations: 121-123 loop

	146 AA total	
identical AA	**87**	59,6%
similar AA**	**115**	78,8%
1.0Å RMSD backbone	**145**	**99,3%**

** incl. identical AA

Protein problems: **backbone**
Pro2, Lys14, Pro17, Ala82, Pro114, Glu132, Arg138
sidechain
Lys18, Thr19, Glu22, Met30, Lys36, Met46, Arg81, Lys111, Asp124, Leu125

Ramachandran Plot
Lys14, Ala82, Leu125, Gly74, Gly95, Arg138

AA Accessibility: **Trp48, Asp8, Asp17**, Phe70, Thr106

Secondary structure element succession AprB environmental sequence fosws7f8

AprB segments	No	*Archaeoglobus fulgidus* sequence	AA position	Sec. str. element	fosws7f8 sequence		AA position	Sec. str. element
Ferredoxin	1	P S F V N	2-6	beta-sheet	P S Y V I	(Loop: KALDK)	2-6	beta-sheet
(2-68 AA)	2	A C E Y I	20-24	alpha-helix	A C Q Y V		20-24	alpha-helix
	3	L M T L D	29-33	beta-sheet	L M V L D		29-33	beta-sheet
	4	K A Y N R	38-42	beta-sheet	K A F N Q		38-42	beta-sheet
	5	S C V K M	52-56	alpha-helix	C C V K I		52-56	alpha-helix
	6	A I D V R	61-65	beta-sheet	A I E V R		61-65	beta-sheet

3 antiparallel	7	A C V P M R G	76-82	beta-sheet	L V T P L R A		76-82	beta-sheet
beta-sheet	8	S D I M W T V K Y	84-92	beta-sheet	D S I M W T L K F		84-92	beta-sheet
(69-104 AA)	9	K V L R F K F A I	96-104	beta-sheet	M L K R F K F P I		96-104	beta-sheet
Tail	10	E E A L	123-126	alpha-helix	**missing**			
(105-148 AA)	11	E I	136-137	alpha-helix	A G		135-136	alpha-helix

Structural deviations: 122-125 loop

	149 AA total	
identical AA	**85**	57,0%
similar AA**	**111**	74,5%
1.0Å RMSD backbone	**145**	**97,3%**

** incl. identical AA

Protein problems:
backbone
Pro2, Lys14, Pro79, Ala82, Asp124, Ser132, Pro134, Asn138
sidechain
Arg18, Thr19, Gln22, Met30, Met46, Cys47

Ramachandran Plot
Lys14, Ala82, Asp124, Gly74, Gly95, Asn138, Ser132

AA Accessibility: **Trp48, Glu8, Asp17**, Asp69, Thr106

Secondary structure element succession AprB *Thermodesulfobacterium commune*

AprB segments	**No**	***Archaeoglobus fulgidus* sequence**	**AA position**	**Sec. str. element**	***Thermodesulfobacterium commune* sequence**		**AA position**	**Sec. str. element**
Ferredoxin	1	P S F V N	2-6	beta-sheet	P S Y V N	(Loop: KGGDR)	2-6	beta-sheet
(2-68 AA)	2	A C E Y I	20-24	alpha-helix	V C M Y I		20-24	alpha-helix
	3	L M T L D	29-33	beta-sheet	L M I L D		29-33	beta-sheet
	4	K A Y N R	38-42	beta-sheet	K A Y N Q		38-42	beta-sheet
	5	S C V K M	52-56	alpha-helix	S C V K S		52-56	alpha-helix
	6	A I D V R	61-65	beta-sheet	A I A I R		61-65	beta-sheet
3 antiparallel	7	A C V P M R G	76-82	beta-sheet	T C Q P M R G		76-82	beta-sheet
beta-sheet	8	S D I M W T V K Y	84-92	beta-sheet	T D I M W T I K F		84-92	beta-sheet
(69-104 AA)	9	K V L R F K F A I	96-104	beta-sheet	Y V L R F K F P I		96-104	beta-sheet
Tail	10	E E A L	123-126	alpha-helix	P S K L		123-126	alpha-helix
(105-148 AA)	11	E I	136-137	alpha-helix	A D		136-137	alpha-helix

Structural deviations: 144-147 loop

	152 AA total	
identical AA	**92**	60,5%
similar AA**	**113**	74,3%
1.0Å RMSD backbone	**148**	**97,4%**

** incl. identical AA

Protein problems:
backbone
Pro2, Lys14, His74, Pro79, Thr133, Ile139, Leu148
sidechain
Arg18, Thr19, Met22, Met30, Gln46, Cys47, His66, His 74, Arg81, Lys118 Thr133, Asp137
Ramachandran Plot
Gly82, Lys14, His74, Glu142, Gly95, Ile139, Thr133, Leu148

AA Accessibility: **Glu8**, **Trp48, Asp17**, Glu35, Lys14, Asp69, Thr106

Secondary structure element succession AprB *Desulfovibrio desulfuricans*

AprB segments	No	*Archaeoglobus fulgidus* sequence	AA position	Sec. str. element	*Desulfovibrio desulfuricans* sequence		AA position	Sec. str. element
Ferredoxin	1	P S F V N	2-6	beta-sheet	P T F V D	(Loop: KGGEK)	2-6	beta-sheet
(2-68 AA)	2	A C E Y I	20-24	alpha-helix	A C M Y I		20-24	alpha-helix
	3	L M T L D	29-33	beta-sheet	L M I L D		29-33	beta-sheet
	4	K A Y N R	38-42	beta-sheet	K A Y N Q		38-42	beta-sheet
	5	S C V K M	52-56	alpha-helix	S C V K I		52-56	alpha-helix
	6	A I D V R	61-65	beta-sheet	A I T A R		61-65	beta-sheet
3 antiparallel	7	A C V P M R G	76-82	beta-sheet	T C I P M R S		76-82	beta-sheet
beta-sheet	8	S D I M W T V K Y	84-92	beta-sheet	D S I M W T V K F		84-92	beta-sheet
(69-104 AA)	9	K V L R F K F A I	96-104	beta-sheet	N V K R F K F P I		96-104	beta-sheet
Tail	10	E E A L	123-126	alpha-helix	**missing**			
(105-148 AA)	11	E I	136-137	alpha-helix	A L		134-135	alpha-helix

Structural deviations: 119-120 loop

	148 AA total	
identical AA	**91**	61,5%
similar AA**	**111**	75,0%
1.0Å RMSD backbone	**145**	**98,0%**

** incl. identical AA

Protein problems: **backbone**
Pro2, Lys14, Pro79, Ser82, Ala122, Asn123, Thr131, Ala137
sidechain
Lys18, Thr19, Met22, Met30, Cys47, Lys113, Thr131, Thr133

Ramachandran Plot
Ser82, Lys14, Asn123, Gly74, Gly95, Ala137, Thr131, Ala122

AA Accessibility: **Trp48, Lys14, Glu17**, Asp69, Thr106

Secondary structure element succession AprB *Desulfovibrio vulgaris*

AprB segments	No	*Archaeoglobus fulgidus* sequence	AA position	Sec. str. element	*Desulfovibrio vulgaris* sequence		AA position	Sec. str. element
Ferredoxin	1	P S F V N	2-6	beta-sheet	P T Y V D	(Loop: KGGEK)	2-6	beta-sheet
(2-68 AA)	2	A C E Y I	20-24	alpha-helix	A C M Y I		20-24	alpha-helix
	3	L M T L D	29-33	beta-sheet	L M I L D		29-33	beta-sheet
	4	K A Y N R	38-42	beta-sheet	R A Y N Q		38-42	beta-sheet
	5	S C V K M	52-56	alpha-helix	S C V K I		52-56	alpha-helix
	6	A I D V R	61-65	beta-sheet	A I T A R		61-65	beta-sheet
3 antiparallel	7	A C V P M R G	76-82	beta-sheet	T C I P M R S		76-82	beta-sheet
beta-sheet	8	S D I M W T V K Y	84-92	beta-sheet	D S I M W T V K F		84-92	beta-sheet
(69-104 AA)	9	K V L R F K F A I	96-104	beta-sheet	N V K R F K F P I		96-104	beta-sheet
Tail	10	E E A L	123-126	alpha-helix	**missing**			
(105-148 AA)	11	E I	136-137	alpha-helix	A L		134-135	alpha-helix

Structural deviations: 119-120 loop

	148 AA total	
identical AA	**91**	61,5%
similar AA**	**113**	76,4%

Protein problem: **backbone**
Pro2, Lys14, Pro79, Ser82, Asp123, Thr131, Ala137
sidechain

1.0Å RMSD backbone	**145**	**98,0%**	
** incl. identical AA			

Lys18, Thr19, Met22, Met30, Cys47, Lys113, Lys118, Thr131, Thr133 Thr136

Ramachandran Plot
Ser82, Lys14, Asp123, Gly74, Gly95, Ala137, Thr131, Ala122

AA Accessibility: **Trp48, Lys14, Glu17**, Asp69, Thr106

Secondary structure element succession AprB *Desulfobulbus* sp. str. MLMS-1

AprB segments	No	*Archaeoglobus fulgidus* sequence	AA position	Sec. str. element	*Desulfobulbus* sp. sequence		AA position	Sec. str. element
Ferredoxin	1	P S F V N	2-6	beta-sheet	P S Y V E	(Loop: KGGDK)	2-6	beta-sheet
(2-68 AA)	2	A C E Y I	20-24	alpha-helix	A C M Y I		20-24	alpha-helix
	3	L M T L D	29-33	beta-sheet	L M V L N		29-33	beta-sheet
	4	K A Y N R	38-42	beta-sheet	K A Y N Q		38-42	beta-sheet
	5	S C V K M	52-56	alpha-helix	S C V K I		52-56	alpha-helix
	6	A I D V R	61-65	beta-sheet	A I A V R		61-65	beta-sheet
3 antiparallel	7	A C V P M R G	76-82	beta-sheet	V V H P M R S		76-82	beta-sheet
beta-sheet	8	S D I M W T V K Y	84-92	beta-sheet	D S I M W T V K F		84-92	beta-sheet
(69-104 AA)	9	K V L R F K F A I	96-104	beta-sheet	N M K R F K F P I		96-104	beta-sheet
Tail	10	E E A L	123-126	alpha-helix	**missing**			
(105-148 AA)	11	E I	136-137	alpha-helix	D L		133-134	alpha-helix

Structural deviations: 114-120 loop

	139 AA total	
identical AA	**79**	56,9%
similar AA**	**103**	74,1%
1.0Å RMSD backbone	**131**	**92,2%**
** incl. identical AA		

Protein problems: **backbone**
Pro2, Lys14, Pro79, Ser82, Asp121, Gln136
sidechain
Glu6, Lys18, Thr19, Met22, Met30, Glu36, Cys47, Asn122

Ramachandran Plot
Ser82, Lys14, Asp121, Gly74, Gly95, Gln136

AA Accessibility: **Trp48,** Lys14**, Asp17**, Glu8, **Lys34**, Thr106

Secondary structure element succession AprB *Desulfotalea psychrophila*

AprB segments	No	*Archaeoglobus fulgidus* sequence	AA position	Sec. str. element	*Desulfotalea psychrophila* sequence		AA position	Sec. str. element
Ferredoxin	1	P S F V N	2-6	beta-sheet	P S Y V D	(Loop: KGGDK)	2-6	beta-sheet
(2-68 AA)	2	A C E Y I	20-24	alpha-helix	A C M Y I		20-24	alpha-helix
	3	L M T L D	29-33	beta-sheet	L M V L D		29-33	beta-sheet
	4	K A Y N R	38-42	beta-sheet	K A Y N Q		38-42	beta-sheet
	5	S C V K M	52-56	alpha-helix	S C V K I		52-56	alpha-helix
	6	A I D V R	61-65	beta-sheet	A I R V R		61-65	beta-sheet
3 antiparallel	7	A C V P M R G	76-82	beta-sheet	Q V H P M R S		76-82	beta-sheet
beta-sheet	8	S D I M W T V K Y	84-92	beta-sheet	D S I M W T V K F		84-92	beta-sheet
(69-104 AA)	9	K V L R F K F A I	96-104	beta-sheet	A L K R F K F P I		96-104	beta-sheet
Tail	10	E E A L	123-126	alpha-helix	**missing**			

(105-148 AA)	11	E I	136-137	alpha-helix	E L		133-134	alpha-helix

Structural deviations: 118-122 loop

	138 AA total	
identical AA	**82**	59,4%
similar AA**	**103**	74,6%
1.0Å RMSD backbone	**133**	**96,4%**

** incl. identical AA

Protein problem: **backbone**
Pro2, Lys14, Pro79, Ser82, Thr136
sidechain
Lys18, Thr19, Met22, Met30, Cys47, Asp33, Ser36

Ramachandran Plot
Ser82, Lys14, Gly120, Gly74, Gly95, Thr136

AA Accessibility: **Trp48, Lys14, Asp17**, Lys34, Thr106

Secondary structure element succession AprB *Olavius algarvensis* Delta 1 symbiont

AprB segments	**No**	***Archaeoglobus fulgidus* sequence**	**AA position**	**Sec. str. element**	***O. algarvensis* Delta 1 symbiont sequence**		**AA position**	**Sec. str. element**
Ferredoxin	1	P S F V N	2-6	beta-sheet	P S F V D	(Loop: KGGDK)	2-6	beta-sheet
(2-68 AA)	2	A C E Y I	20-24	alpha-helix	A C Q Y I		20-24	alpha-helix
	3	L M T L D	29-33	beta-sheet	L M V L E		29-33	beta-sheet
	4	K A Y N R	38-42	beta-sheet	K A Y N Q		38-42	beta-sheet
	5	S C V K M	52-56	alpha-helix	S C V K I		52-56	alpha-helix
	6	A I D V R	61-65	beta-sheet	A I E V R		61-65	beta-sheet
3 antiparallel	7	A C V P M R G	76-82	beta-sheet	S V M P M L G		76-82	beta-sheet
beta-sheet	8	S D I M W T V K Y	84-92	beta-sheet	E D V M W T C K F		84-92	beta-sheet
(69-104 AA)	9	K V L R F K F A I	96-104	beta-sheet	T I K R F K F P I		96-104	beta-sheet
Tail	10	E E A L	123-126	alpha-helix	**missing**			
(105-148 AA)	11	E I	136-137	alpha-helix	A D		133-134	alpha-helix

Structural deviations: 118-122 loop

	147 AA total	
identical AA	**78**	53,1%
similar AA**	**102**	69,4%
1.0Å RMSD backbone	**142**	**96,6%**

** incl. identical AA

Protein problems: **backbone**
Pro2, Lys14, Pro79, Thr130, Thr136
sidechain
Lys18, Thr19, Gln22, Met30, Glu33, Glu36, Gln46, Cys47, Gln111, Ser125, Thr130, Asp134
Ramachandran Plot
Gly82, Lys14, Gly120, Gly74, Gly95, Thr130, Thr136

AA Accessibility: **Glu8, Trp48,** Lys14, **Asp17**, Asp69, Thr106

Secondary structure element succession AprB *Thermodesulfovibrio yellowstonii*

AprB segments	**No**	***Archaeoglobus fulgidus* sequence**	**AA position**	**Sec. str. element**	***Thermodesulfovibrio yellowstonii* sequence**		**AA position**	**Sec. str. element**
Ferredoxin	1	P S F V N	2-6	beta-sheet	P S F V I	(Loop: KAQDK)	2-6	beta-sheet
(2-68 AA)	2	A C E Y I	20-24	alpha-helix	A C Q Y I		20-24	alpha-helix
	3	L M T L D	29-33	beta-sheet	L M T L D		29-33	beta-sheet

	4	K A Y N R	38-42	beta-sheet	K A F N Q	38-42	beta-sheet
	5	S C V K M	52-56	alpha-helix	N C V K I	52-56	alpha-helix
	6	A I D V R	61-65	beta-sheet	A I E V R	61-65	beta-sheet
3 antiparallel	7	A C V P M R G	76-82	beta-sheet	S V I P M R G	76-82	beta-sheet
beta-sheet	8	S D I M W T V K Y	84-92	beta-sheet	D A I M W T I K F	84-92	beta-sheet
(69-104 AA)	9	K V L R F K F A I	96-104	beta-sheet	S I K R F K F P I	96-104	beta-sheet
Tail	10	E E A L	123-126	alpha-helix	Y G K I	126-129	alpha-helix
(105-148 AA)	11	E I	136-137	alpha-helix	A R	139-140	alpha-helix

Structural deviations: 111-116 loop

	142 AA total	
identical AA	**81**	57,0%
similar AA**	**104**	73,2%
1.0Å RMSD backbone	**136**	**95,8%**

** incl. identical AA

Protein problems:

backbone
Pro2, Lys14, Pro79, Tyr118, Asn136, Glu142
sidechain
Lys18, Thr19, Gln22, Met30, Lys36, Gln46, Cys47, Cys71, Tyr111, Tyr118, Tyr137, Lys141
Ramachandran Plot
Gly82, Lys14, Glu142, Gly74, Gly95, Asn136, Tyr118

AA Accessibility: **Glu8**, **Trp48, Asp17**, **Arg34**, Asp69, Leu106

Secondary structure element succession AprB *Chlorobaculum tepidum*

AprB segments	**No**	***Archaeoglobus fulgidus* sequence**	**AA position**	**Sec. str. element**	***Chlorobaculum tepidum* sequence**	**AA position**	**Sec. str. element**
Ferredoxin	1	P S F V N	2-6	beta-sheet	P S F V I (Loop : KGQER)	2-6	beta-sheet
(2-68 AA)	2	A C E Y I	20-24	alpha-helix	A C M Y I	20-24	alpha-helix
	3	L M T L D	29-33	beta-sheet	L M K L D	29-33	beta-sheet
	4	K A Y N R	38-42	beta-sheet	K A W N Q	38-42	beta-sheet
	5	S C V K M	52-56	alpha-helix	N C V K I	52-56	alpha-helix
	6	A I D V R	61-65	beta-sheet	A I E V R	61-65	beta-sheet
3 antiparallel	7	A C V P M R G	76-82	beta-sheet	N V I P L R G	76-82	beta-sheet
beta-sheet	8	S D I M W T V K Y	84-92	beta-sheet	D A I M W T I K F	84-92	beta-sheet
(69-104 AA)	9	K V L R F K F A I	96-104	beta-sheet	I L K R Y K F P I	96-104	beta-sheet
Tail	10	E E A L	123-126	alpha-helix	Y A N L	123-126	alpha-helix
(105-148 AA)	11	E I	136-137	alpha-helix	E Y	136-137	alpha-helix

Structural deviations: -

	140 AA total	
identical AA	**86**	61,4%
similar AA**	**104**	74,3%
1.0Å RMS AA	**139**	**99,3%**

** incl. identical AA

Protein problems:

backbone
nicht vorhanden
sidechain
Arg18, Thr19, Met30, Glu46, Cys47, Asp13, Lys118, Met134, Tyr137

Ramachandran Plot
Gly82, Lys14, Gly74, Gly95, Asn133, Thr139

AA Accessibility: **Trp48, Glu8, Glu17**, Lys14, Asp69, Thr106

Secondary structure element succession AprB *Thiobacillus denitrificans* ATCC25259

AprB segments	No	*Archaeoglobus fulgidus* sequence	AA position	Sec. str. element	*Thiobacillus denitrificans* sequence		AA position	Sec. str. element
Ferredoxin	1	P S F V N	2-6	beta-sheet	P T Y V R	(Loop: KGQDK)	2-6	beta-sheet
(2-68 AA)	2	A C E Y I	20-24	alpha-helix	A C M Y I		20-24	alpha-helix
	3	L M T L D	29-33	beta-sheet	L M K L D	**(additional loop: 36-41 AA)**	29-33	beta-sheet
	4	K A Y N R	38-42	beta-sheet	R A F N Q		44-48	beta-sheet
	5	S C V K M	52-56	alpha-helix	S C V K I		58-62	alpha-helix
	6	A I D V R	61-65	beta-sheet	A I E A R		67-71	beta-sheet
3 antiparallel	7	A C V P M R G	76-82	beta-sheet	M V Q P L R G		82-89	beta-sheet
beta-sheet	8	S D I M W T V K Y	84-92	beta-sheet	D S I M W T I K F		90-98	beta-sheet
(69-104 AA)	9	K V L R F K F A I	96-104	beta-sheet	T L K R F K F P I		102-110	beta-sheet
Tail	10	E E A L	123-126	alpha-helix	L A D L		129-132	alpha-helix
(105-148 AA)	11	E I	136-137	alpha-helix	**missing**			

Structural deviations: 34-41 loop
142-150 loop
155-157 loop

	157 AA total	
identical AA	**77**	49,0%
similar AA**	**106**	67,5%
1.0Å RMSD backbone	**140**	**89,2%**

** incl. identical AA

Protein problems: **backbone**
Pro2, Lys14, Ala42, Pro85, Thr139, Pro155
sidechain
Lys18, Thr19, Met22, Met30, His72, Ser141, Asp143
Ramachandran Plot
Lys14, Ala42, Gly88, Gly80, Gly101, Thr139, Gly145, Glu157

AA Accessibility: **Lys14, Asp17, Glu38, Glu51, Trp54**, Asp75, Thr112

Supplementary data material Figure S1. AprB comparative models of SRP and SOB

Reference structure *Archaeoglobus fulgidus*

Structure of AprB from *A. fulgidus*. (A, B) Ribbon structure colored by secondary structure elements shown from front and back view (positions of [4Fe-4S] clusters indicated); (C-F) protein molecular surface colored by calculated electrostatic potential shown from front and back view (electric charge at the molecular surface is colored with a red (negative), white (neutral, and blue (positive) color gradient; electric field extending into the solvent is shown), in (E) and (F) Trp-B48 and negatively charged loop (Cys-B13 to Arg-B18 are marked by yellow color; (G, H) protein molecular surface colored by calculated solvent accessibility shown from front and back view

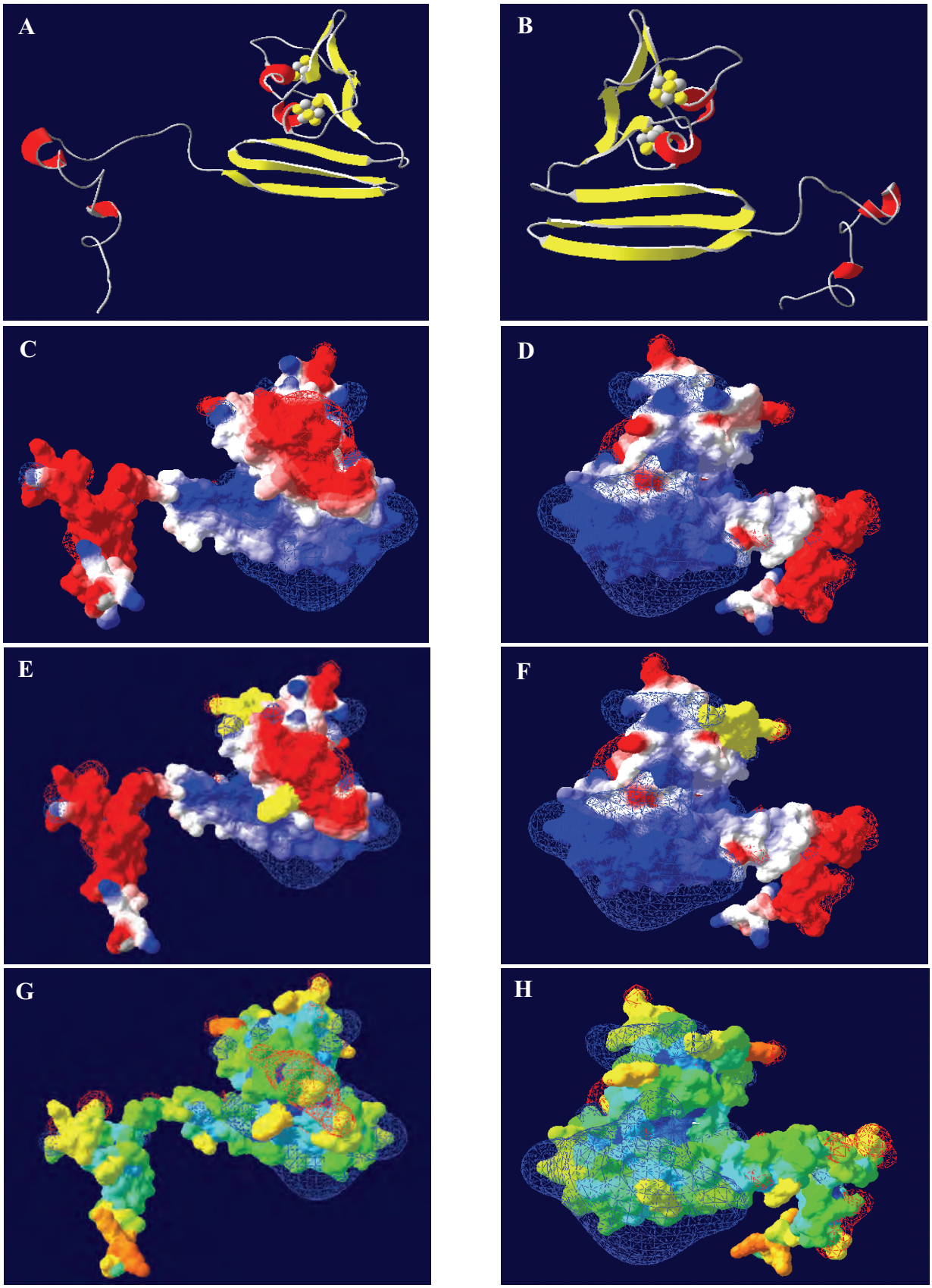

SOB Apr lineage I

Allochromatium vinosum

AprB model: front view (side towards AprA)

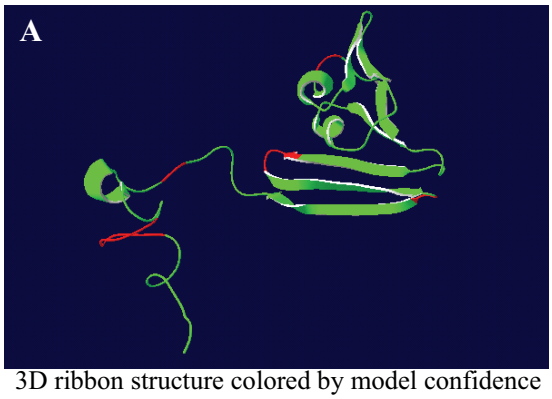

3D ribbon structure colored by model confidence

AprB model: back view

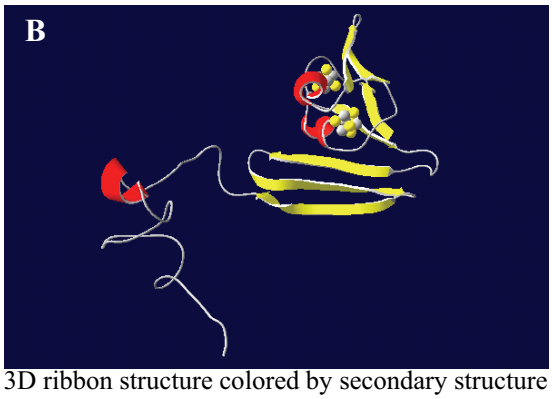

3D ribbon structure colored by secondary structure elements (positions of [4Fe-4S] cluster indicated)

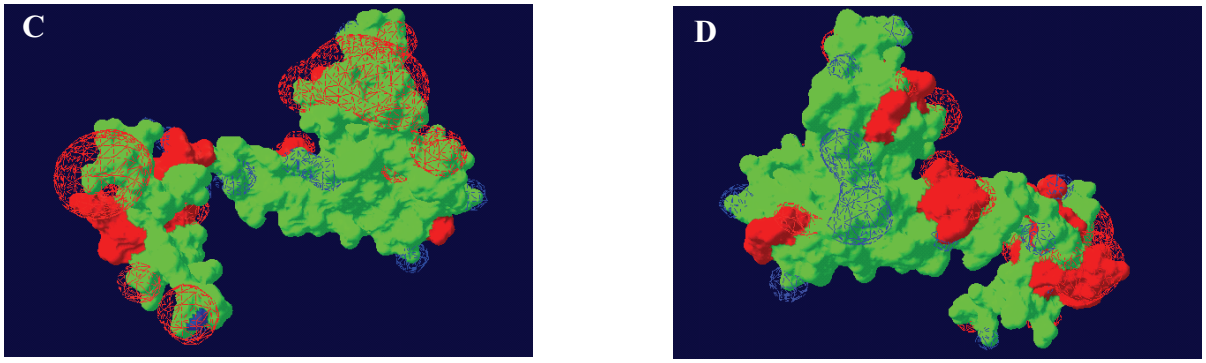

Protein molecular surface colored by model confidence

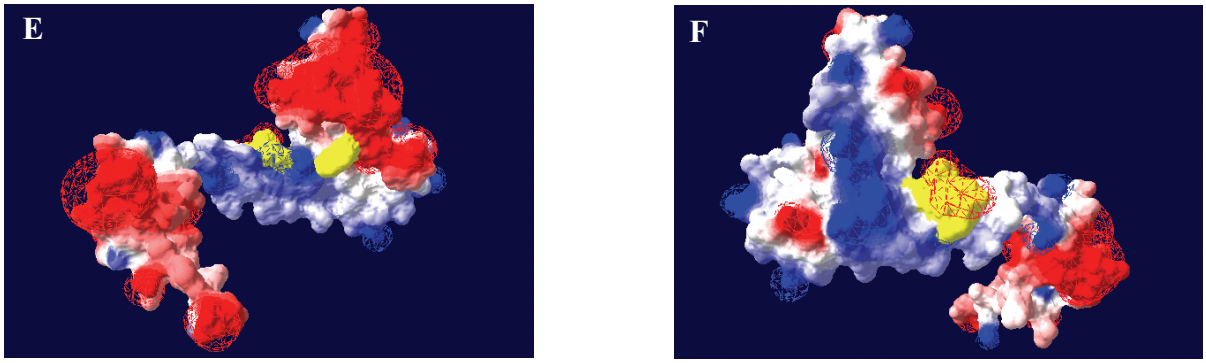

Protein molecular surface colored by calculated electrostatic potential (electric charge at the molecular surface is colored with a red (negative), white (neutral, and blue (positive) color gradient; electric field extending into the solvent is shown); Trp-B43 and negatively charged loop are marked by yellow color)

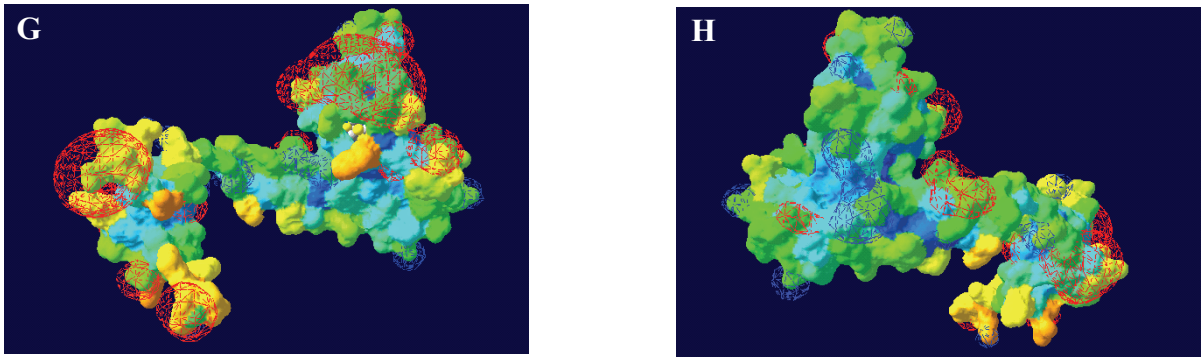

Protein molecular surface colored by calculated solvent accessibility

Thiobacillus denitrificans

AprB model: front view (side towards AprA)

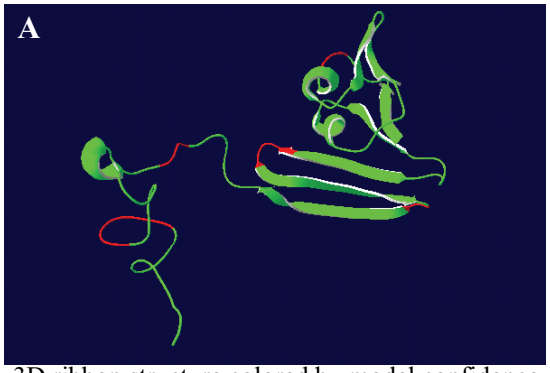

3D ribbon structure colored by model confidence

AprB model: back view

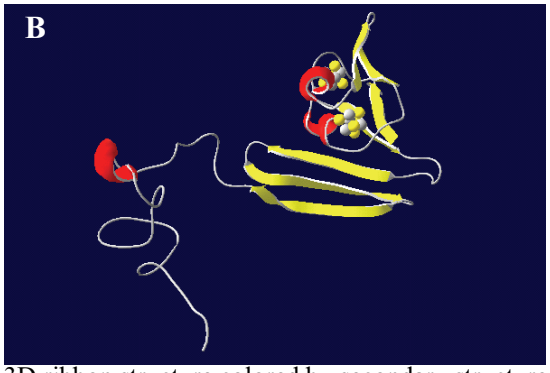

3D ribbon structure colored by secondary structure elements (positions of [4Fe-4S] cluster indicated)

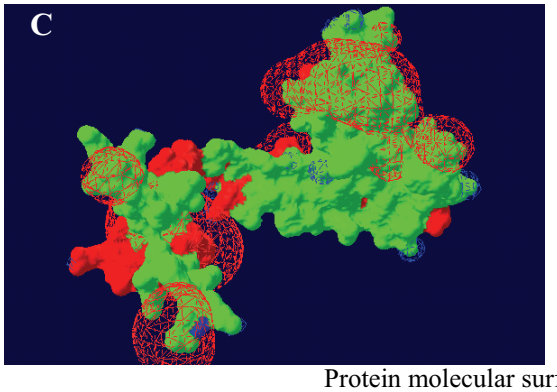

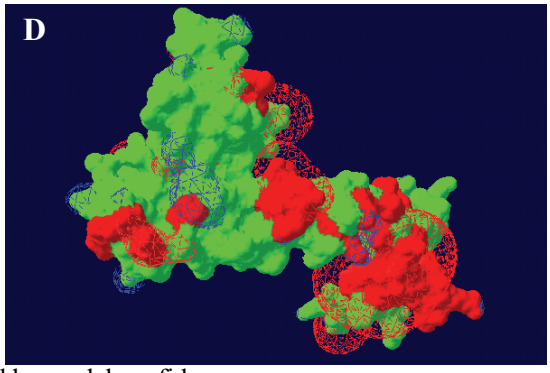

Protein molecular surface colored by model confidence

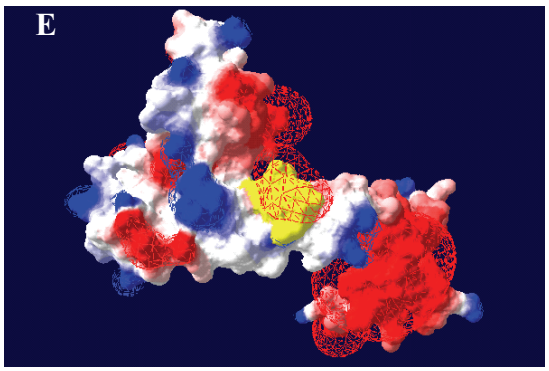

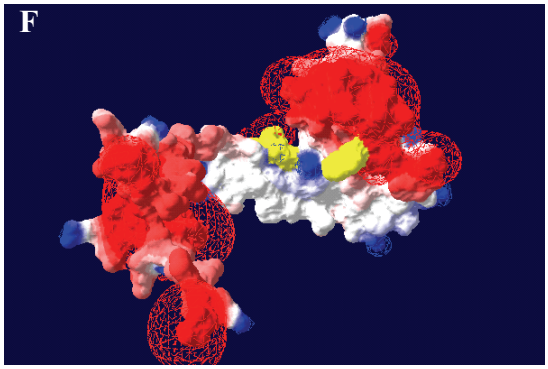

Protein molecular surface colored by calculated electrostatic potential (electric charge at the molecular surface is colored with a red (negative), white (neutral, and blue (positive) color gradient; electric field extending into the solvent is shown); Trp-B43 and negatively charged loop are marked by yellow color)

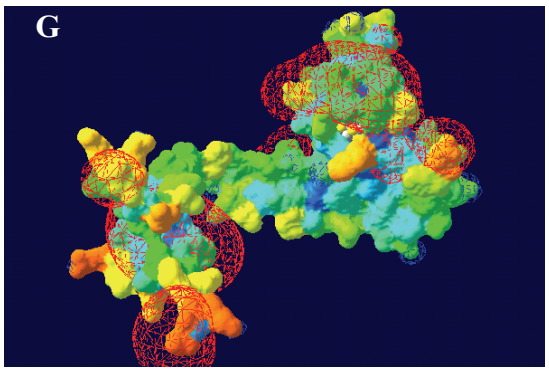

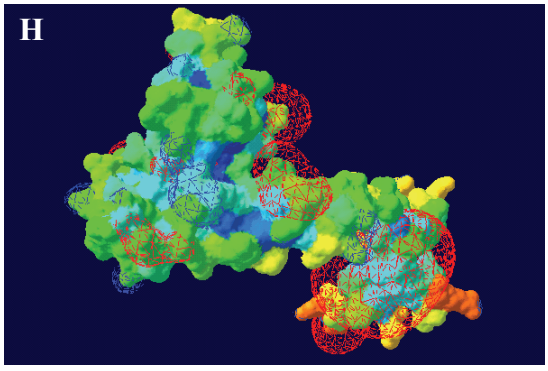

Protein molecular surface colored by calculated solvent accessibility

Cdt. Ruthia magnifica

AprB model: front view (side towards AprA)

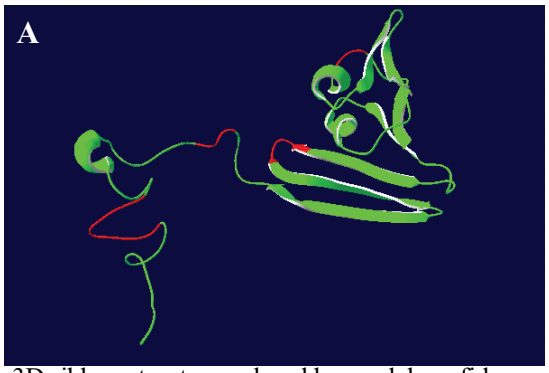

3D ribbon structure colored by model confidence

AprB model: back view

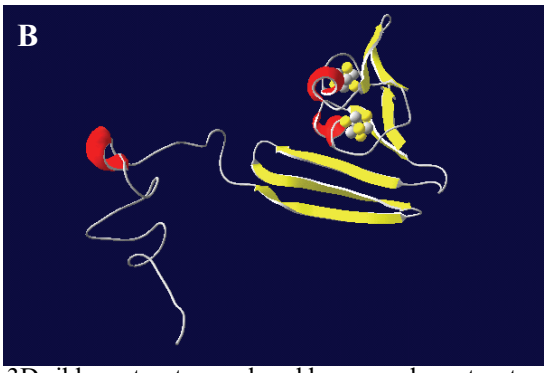

3D ribbon structure colored by secondary structure elements (positions of [4Fe-4S] cluster indicated)

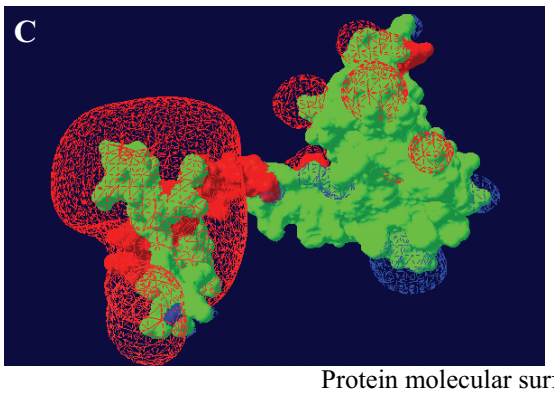

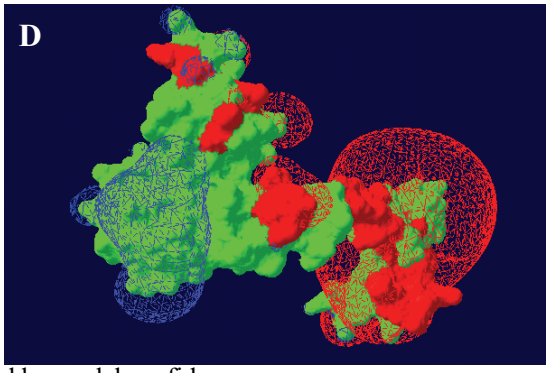

Protein molecular surface colored by model confidence

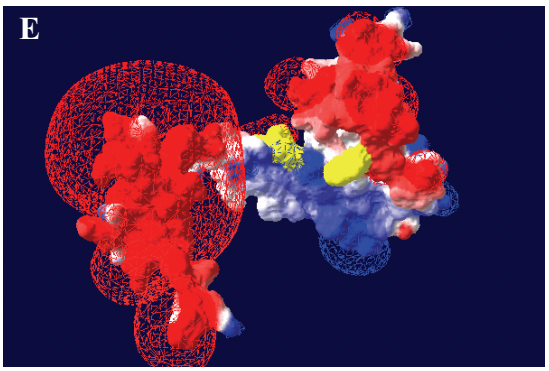

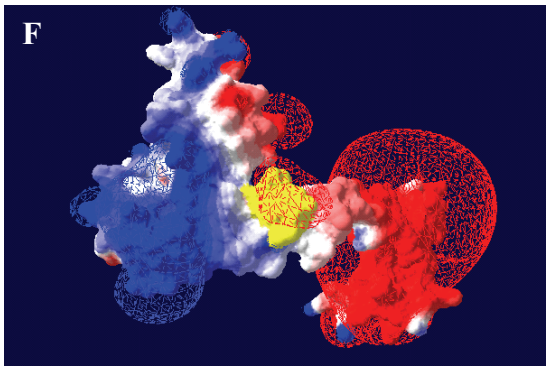

Protein molecular surface colored by calculated electrostatic potential (electric charge at the molecular surface is colored with a red (negative), white (neutral, and blue (positive) color gradient; electric field extending into the solvent is shown); Trp-B43 and negatively charged loop are marked by yellow color)

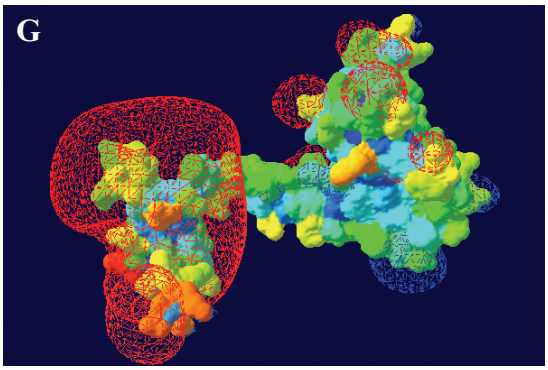

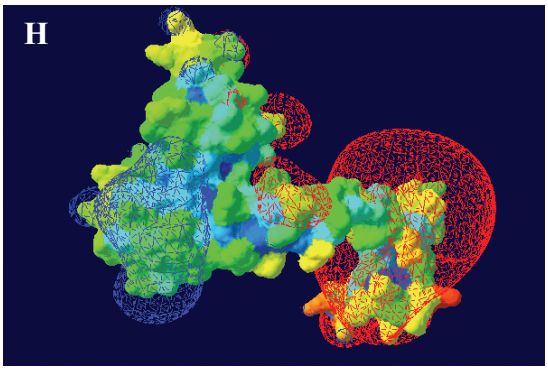

Protein molecular surface colored by calculated solvent accessibility

Cdt. Pelagibacter ubique

AprB model: front view (side towards AprA)

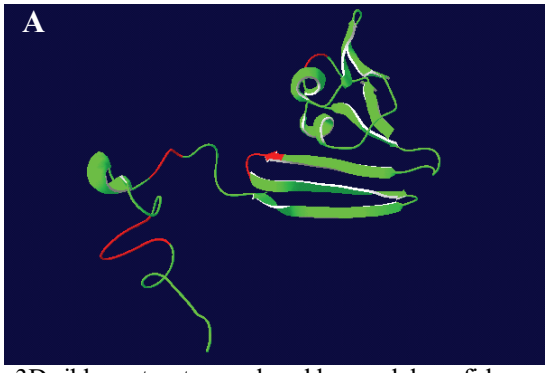

3D ribbon structure colored by model confidence

AprB model: back view

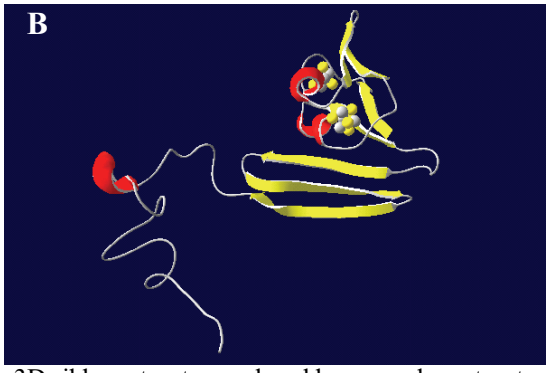

3D ribbon structure colored by secondary structure elements (positions of [4Fe-4S] cluster indicated)

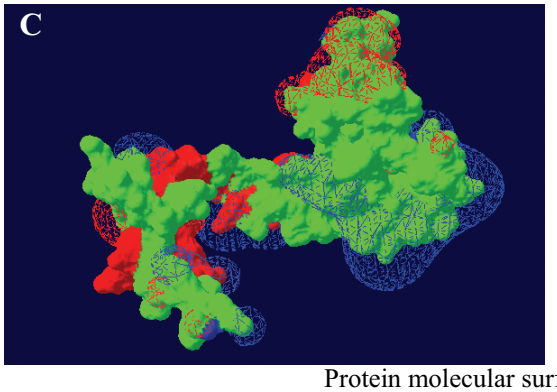

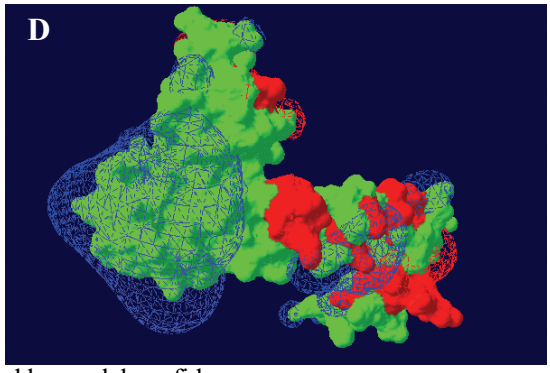

Protein molecular surface colored by model confidence

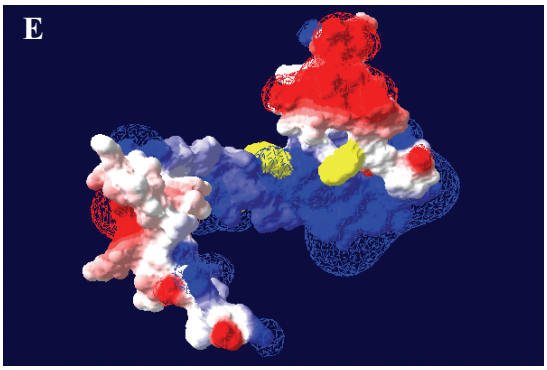

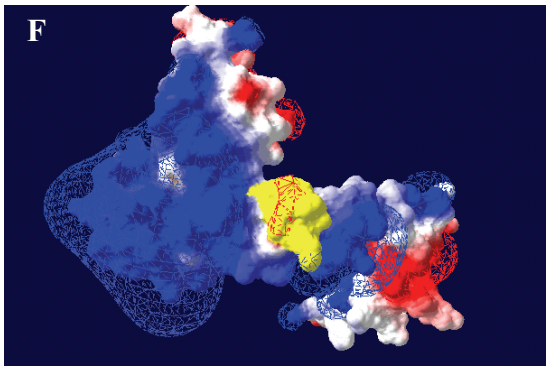

Protein molecular surface colored by calculated electrostatic potential (electric charge at the molecular surface is colored with a red (negative), white (neutral, and blue (positive) color gradient; electric field extending into the solvent is shown); Trp-B43 and negatively charged loop are marked by yellow color)

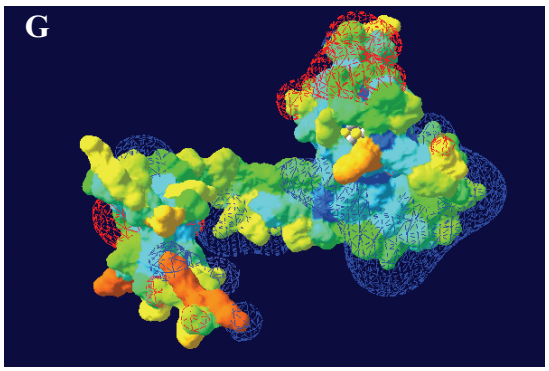

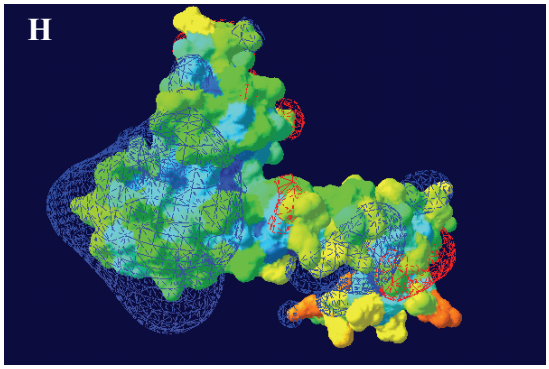

Protein molecular surface colored by calculated solvent accessibility

EBAC2C11

AprB model: front view (side towards AprA)

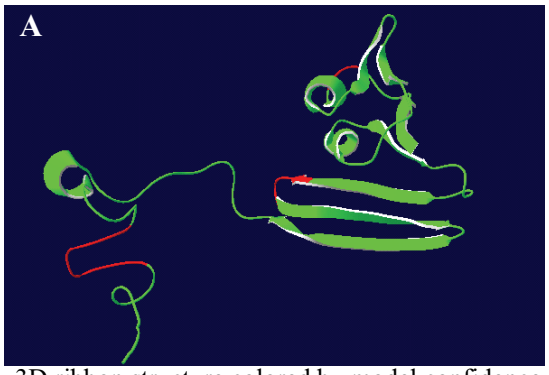

3D ribbon structure colored by model confidence

AprB model: back view

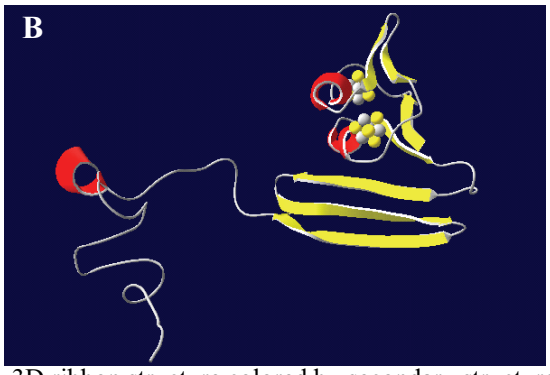

3D ribbon structure colored by secondary structure elements (positions of [4Fe-4S] cluster indicated)

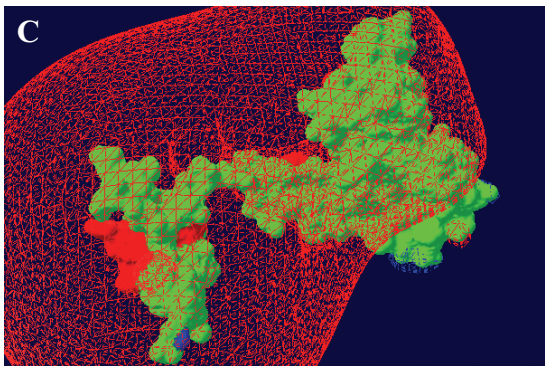

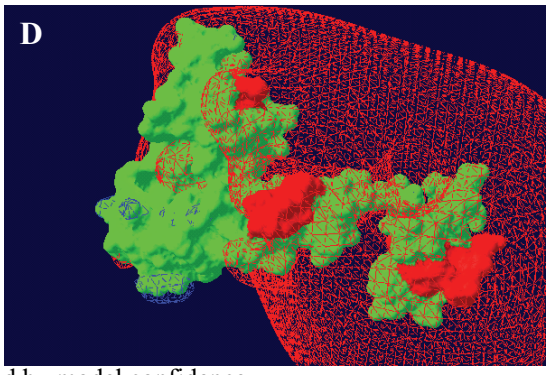

Protein molecular surface colored by model confidence

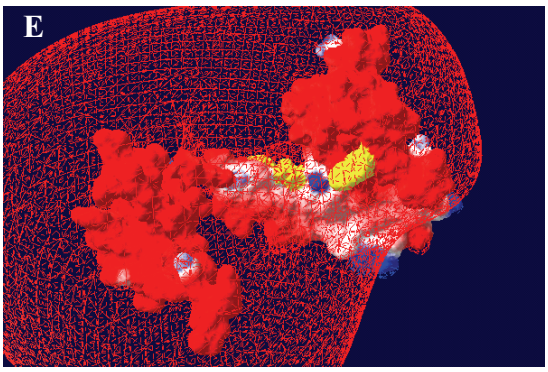

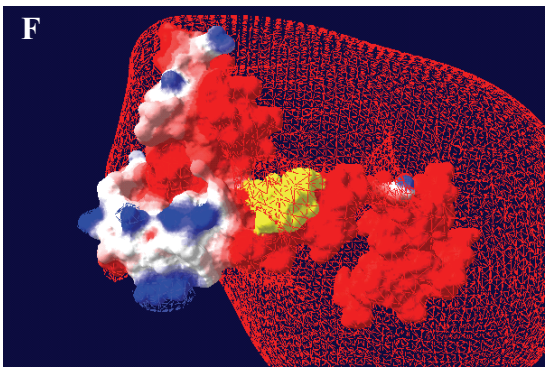

Protein molecular surface colored by calculated electrostatic potential (electric charge at the molecular surface is colored with a red (negative), white (neutral, and blue (positive) color gradient; electric field extending into the solvent is shown); Trp-B43 and negatively charged loop are marked by yellow color)

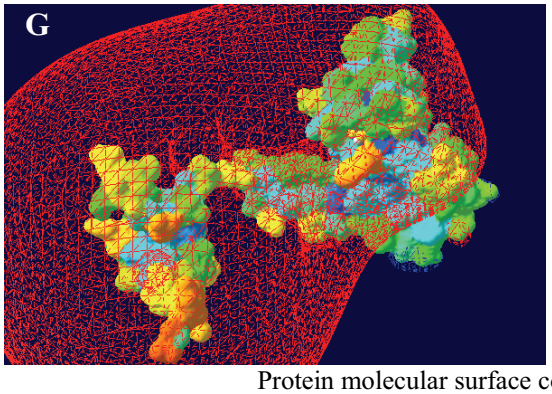

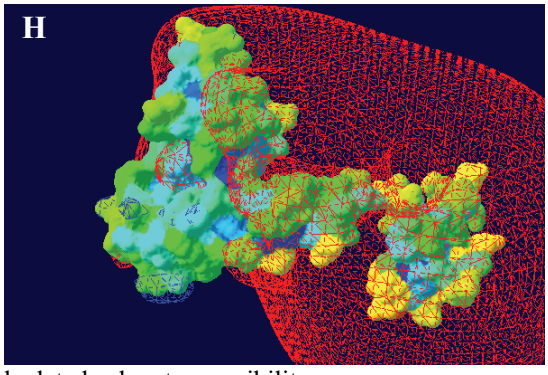

Protein molecular surface colored by calculated solvent accessibility

Crenarchaeal SRP

Pyrobaculum calidifontis

AprB model: front view (side towards AprA)

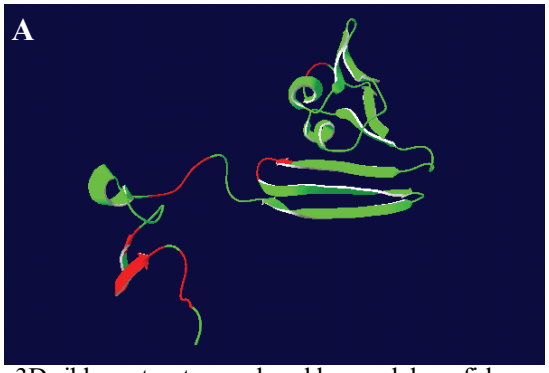

3D ribbon structure colored by model confidence

AprB model: back view

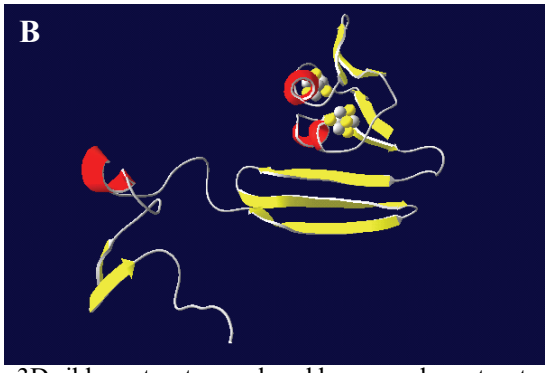

3D ribbon structure colored by secondary structure elements (positions of [4Fe-4S] cluster indicated)

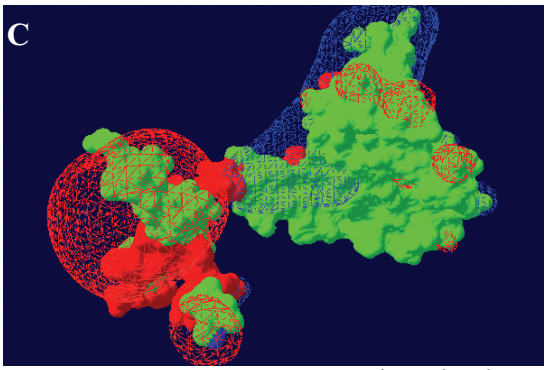

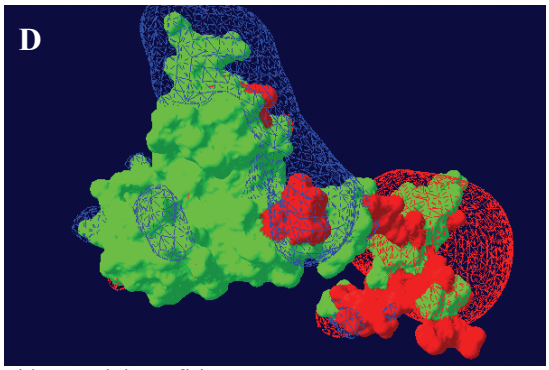

Protein molecular surface colored by model confidence

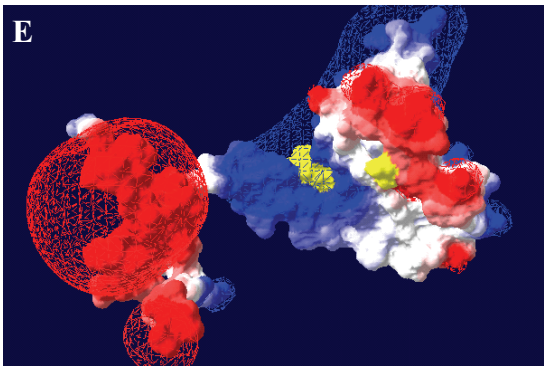

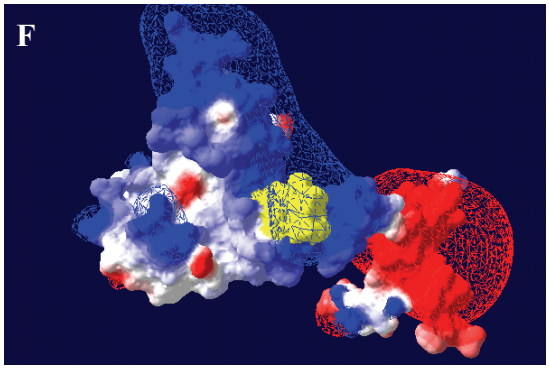

Protein molecular surface colored by calculated electrostatic potential (electric charge at the molecular surface is colored with a red (negative), white (neutral, and blue (positive) color gradient; electric field extending into the solvent is shown); Ala-B43 and charged loop are marked by yellow color)

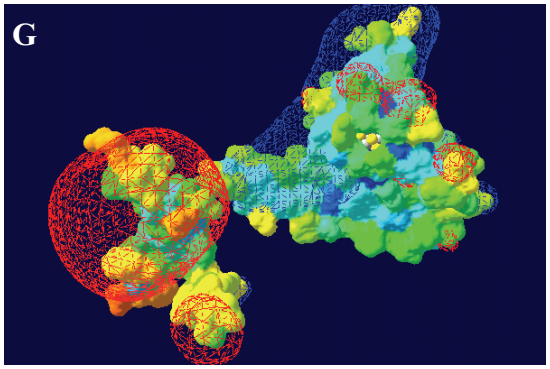

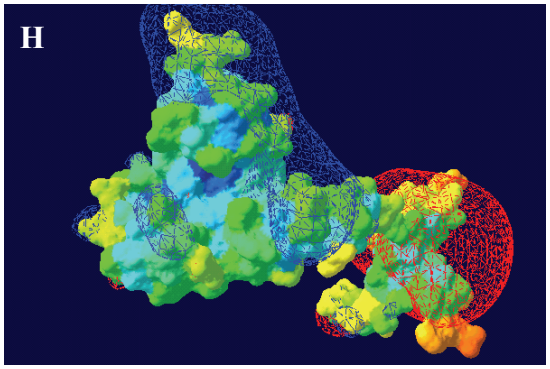

Protein molecular surface colored by calculated solvent accessibility

Caldivirga maquilingensis

AprB model: front view (side towards AprA)

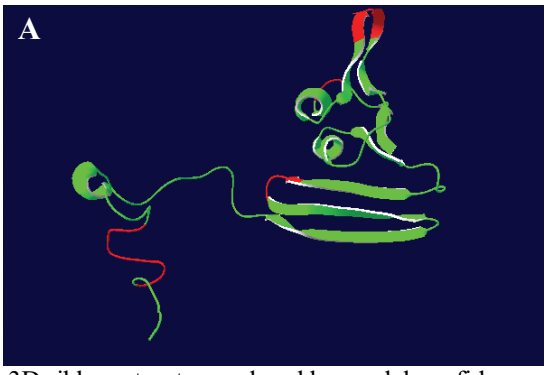

3D ribbon structure colored by model confidence

AprB model: back view

3D ribbon structure colored by secondary structure elements (positions of [4Fe-4S] cluster indicated)

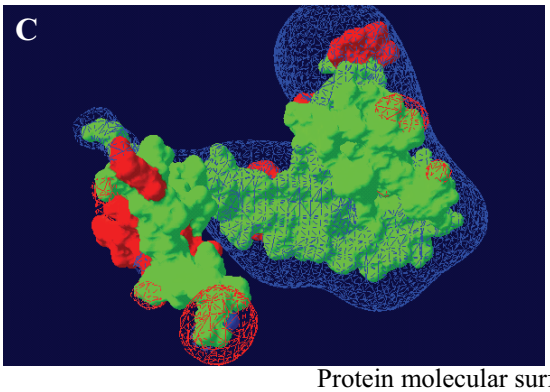

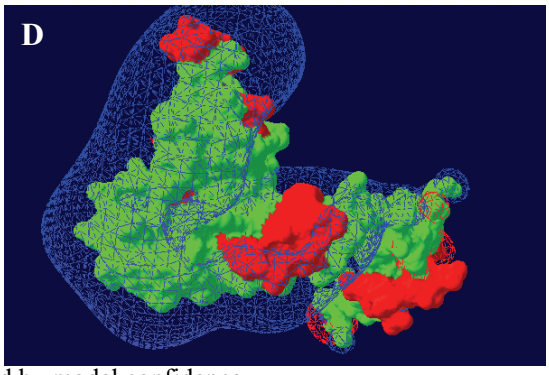

Protein molecular surface colored by model confidence

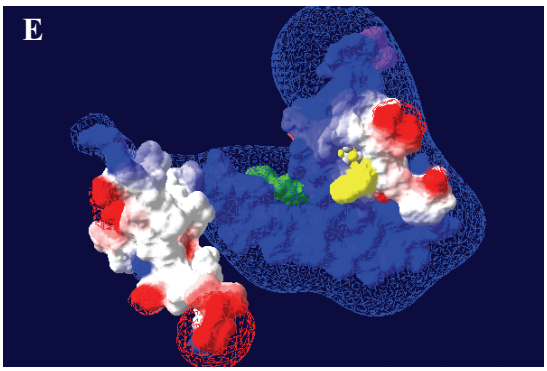

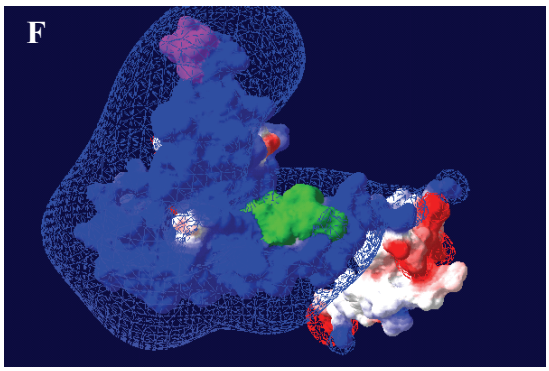

Protein molecular surface colored by calculated electrostatic potential (electric charge at the molecular surface is colored with a red (negative), white (neutral, and blue (positive) color gradient; electric field extending into the solvent is shown); Trp-B43 and charged loop are marked by green color; additional loop is colored in violett)

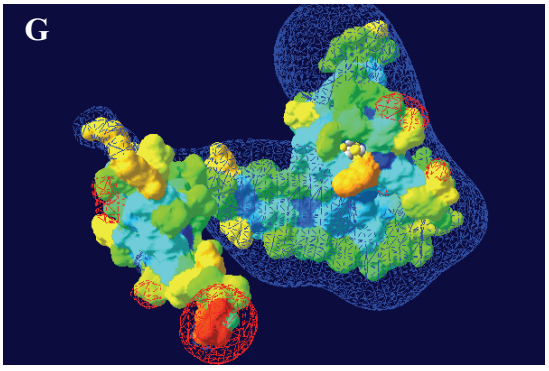

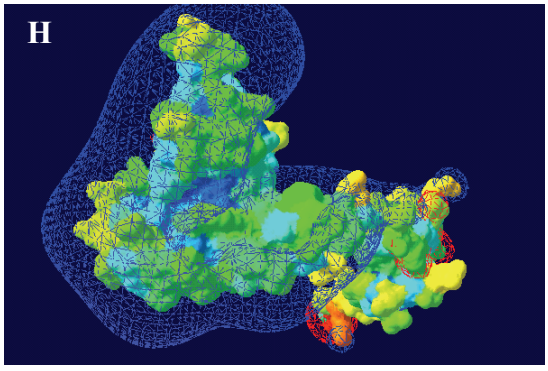

Protein molecular surface colored by calculated solvent accessibility

SRB and related SOB Apr lineage II

Desulfotomaculum reducens

AprB model: front view (side towards AprA)

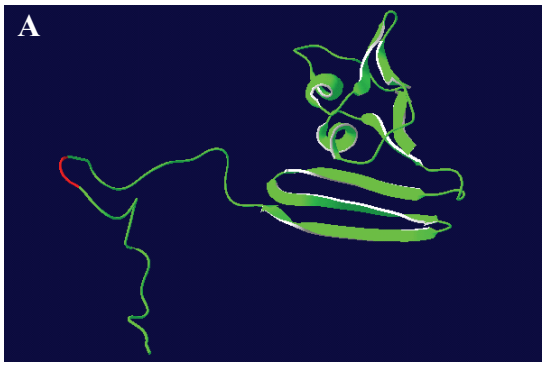

3D ribbon structure colored by model confidence

AprB model: back view

3D ribbon structure colored by secondary structure elements (positions of [4Fe-4S] cluster indicated)

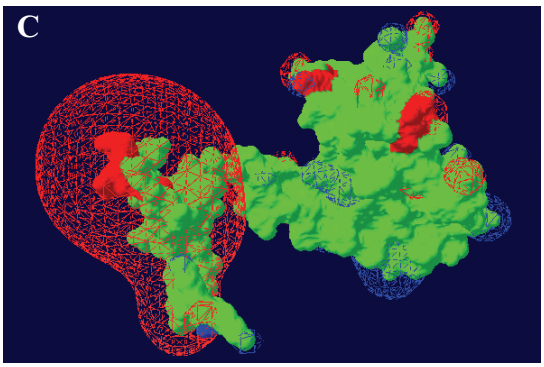

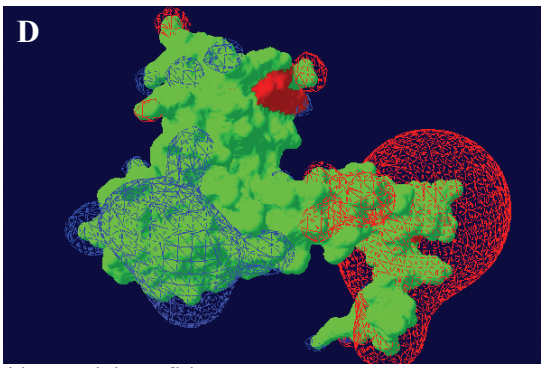

Protein molecular surface colored by model confidence

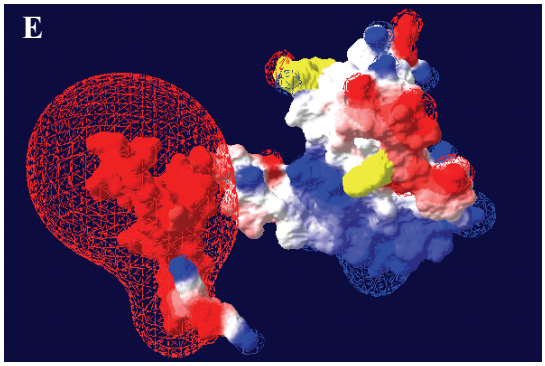

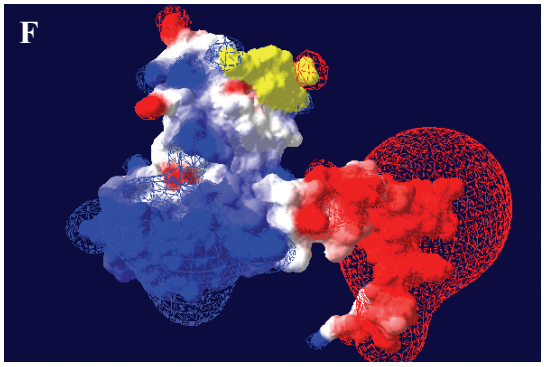

Protein molecular surface colored by calculated electrostatic potential (electric charge at the molecular surface is colored with a red (negative), white (neutral, and blue (positive) color gradient; electric field extending into the solvent is shown); Trp-B48 and exposed, potential Qmo-docking loop are marked by yellow color)

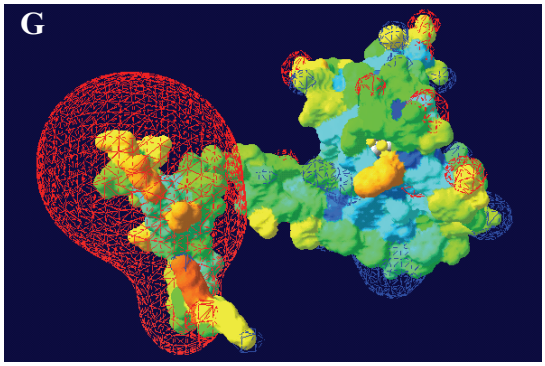

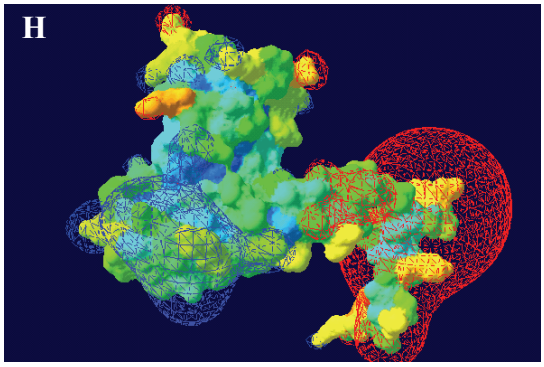

Protein molecular surface colored by calculated solvent accessibility

Syntrophobacter fumaroxidans

AprB model: front view (side towards AprA)

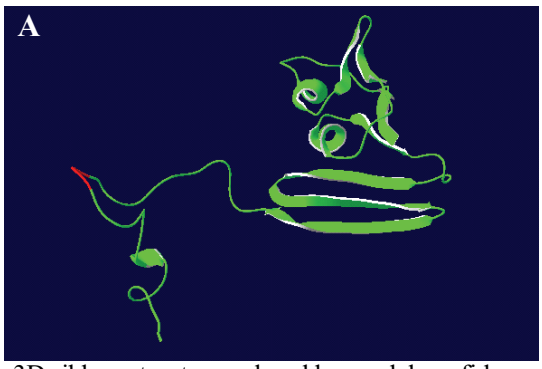

3D ribbon structure colored by model confidence

AprB model: back view

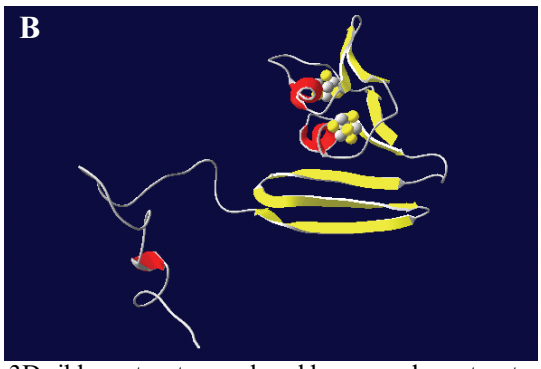

3D ribbon structure colored by secondary structure elements (positions of [4Fe-4S] cluster indicated)

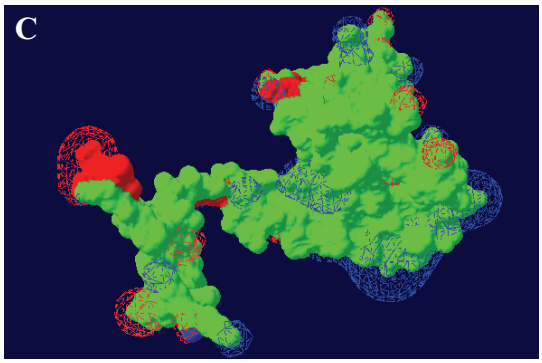

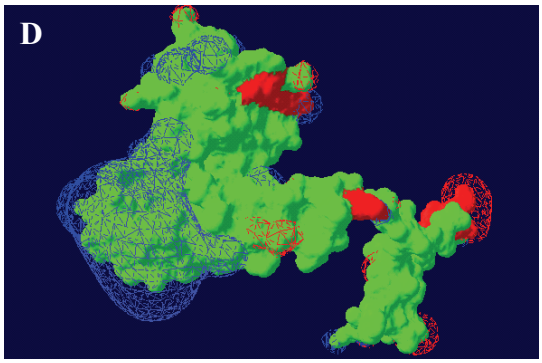

Protein molecular surface colored by model confidence

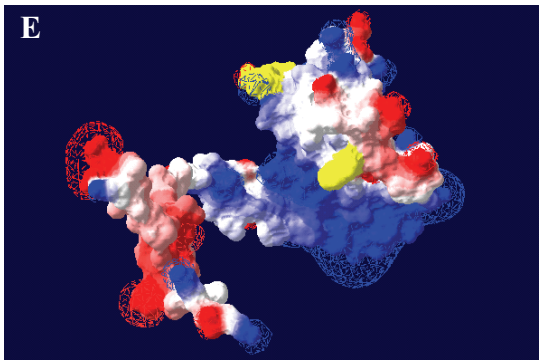

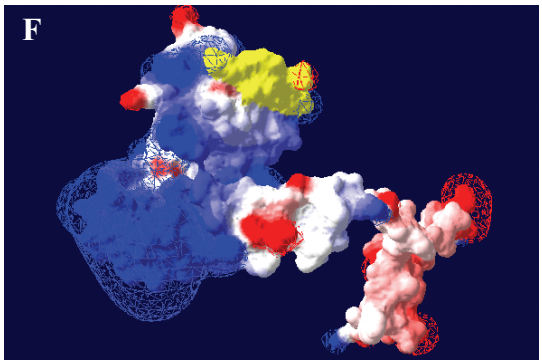

Protein molecular surface colored by calculated electrostatic potential (electric charge at the molecular surface is colored with a red (negative), white (neutral, and blue (positive) color gradient; electric field extending into the solvent is shown); Trp-B48 and exposed, potential Qmo-docking loop are marked by yellow color)

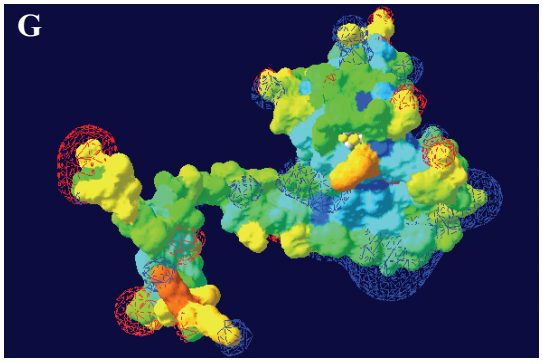

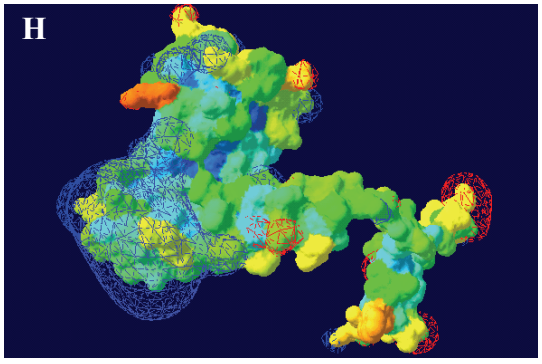

Protein molecular surface colored by calculated solvent accessibility

fosws39f8

AprB model: front view (side towards AprA)

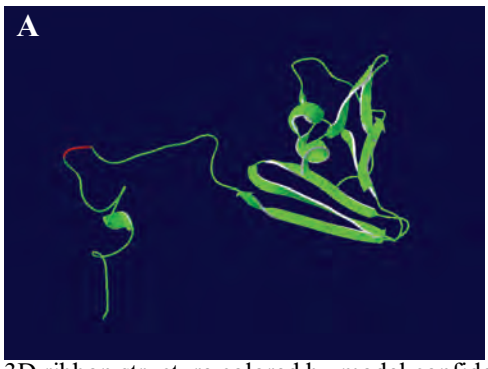

3D ribbon structure colored by model confidence

AprB model: back view

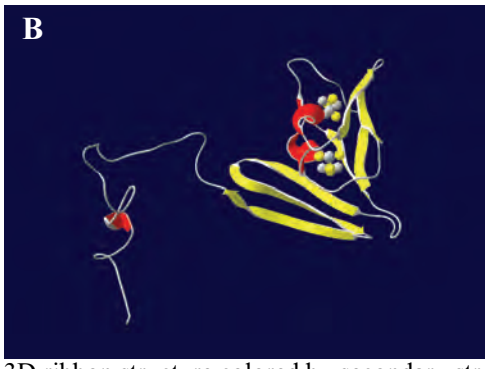

3D ribbon structure colored by secondary structure elements (positions of [4Fe-4S] cluster indicated)

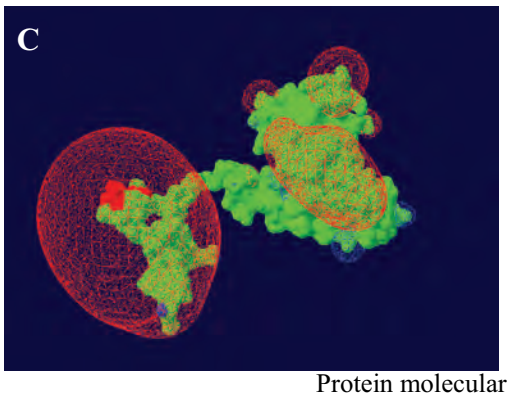

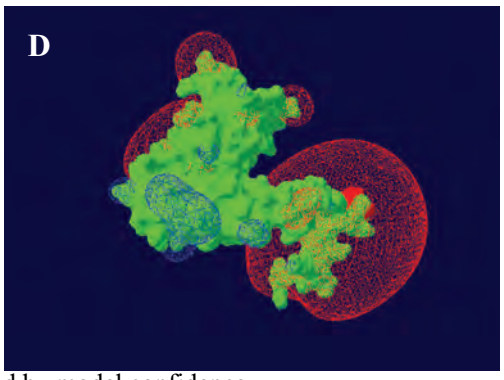

Protein molecular surface colored by model confidence

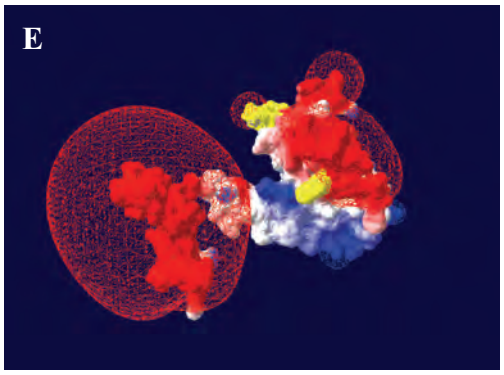

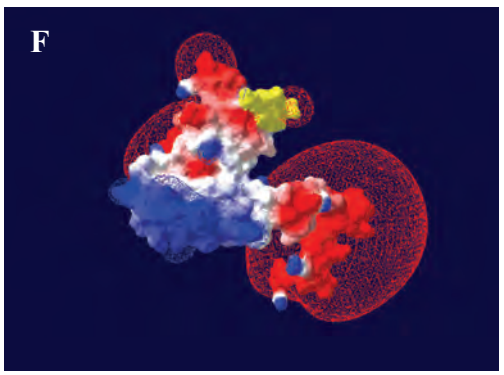

Protein molecular surface colored by calculated electrostatic potential (electric charge at the molecular surface is colored with a red (negative), white (neutral, and blue (positive) color gradient; electric field extending into the solvent is shown); Trp-B48 and exposed, potential Qmo-docking loop are marked by yellow color)

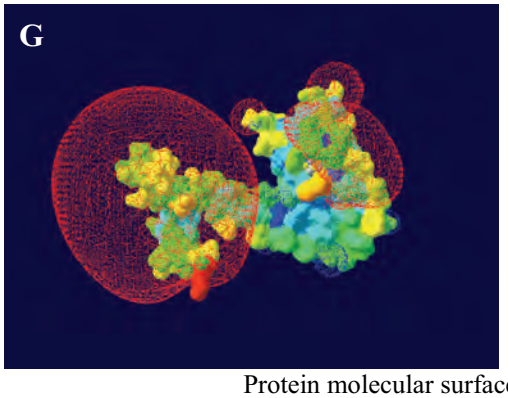

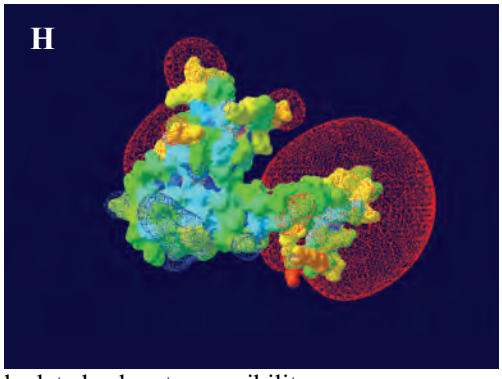

Protein molecular surface colored by calculated solvent accessibility

fosws7f8

AprB model: front view (side towards AprA)

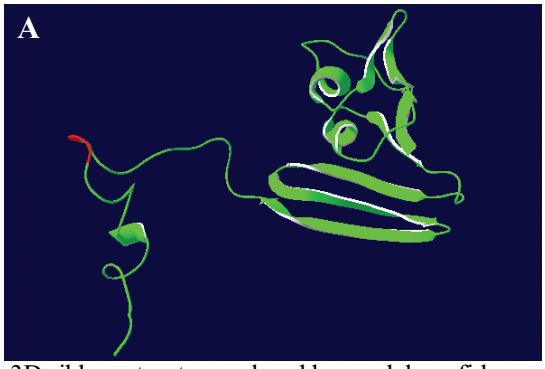

3D ribbon structure colored by model confidence

AprB model: back view

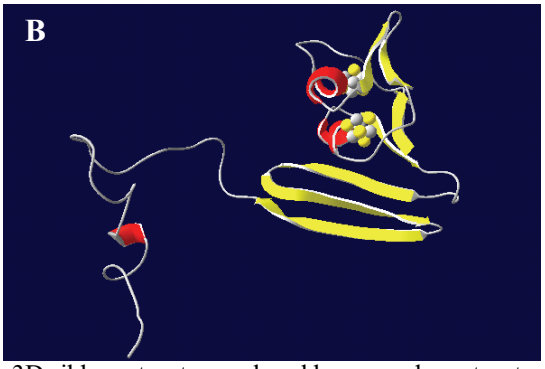

3D ribbon structure colored by secondary structure elements (positions of [4Fe-4S] cluster indicated)

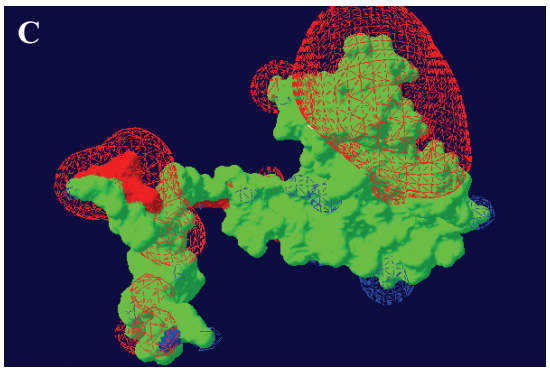

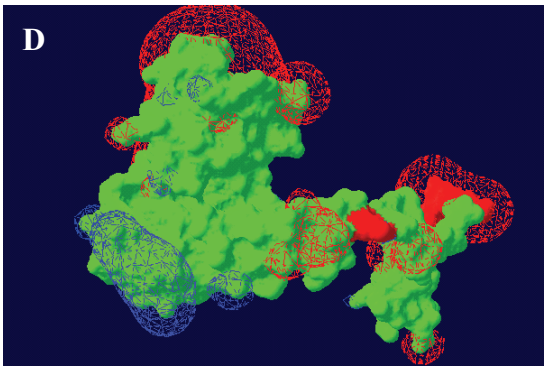

Protein molecular surface colored by model confidence

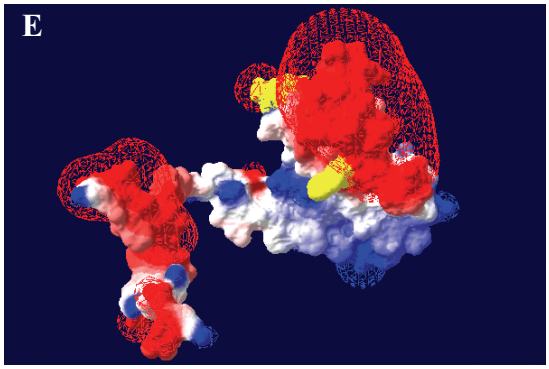

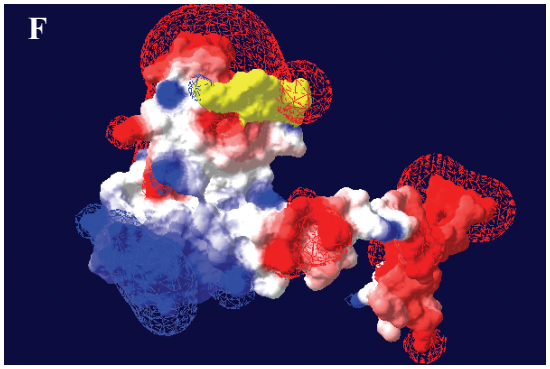

Protein molecular surface colored by calculated electrostatic potential (electric charge at the molecular surface is colored with a red (negative), white (neutral, and blue (positive) color gradient; electric field extending into the solvent is shown); Trp-B48 and exposed, potential Qmo-docking loop are marked by yellow color)

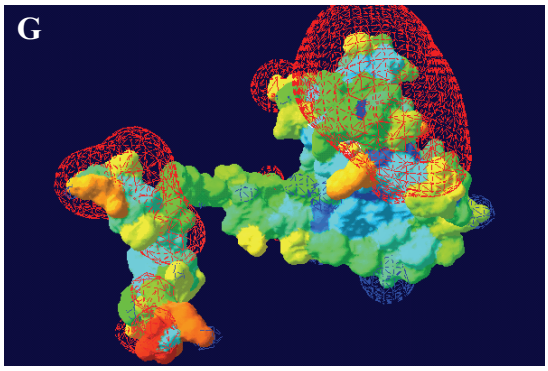

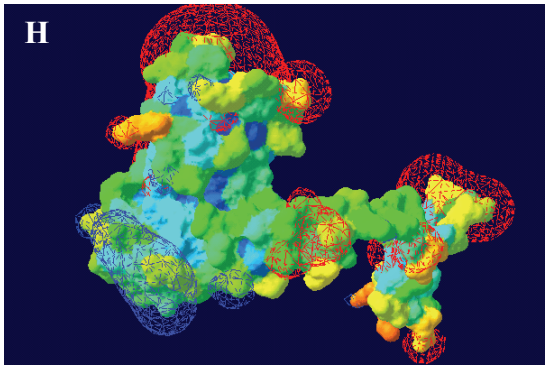

Protein molecular surface colored by calculated solvent accessibility

Thermodesulfobacterium commune

AprB model: front view (side towards AprA)

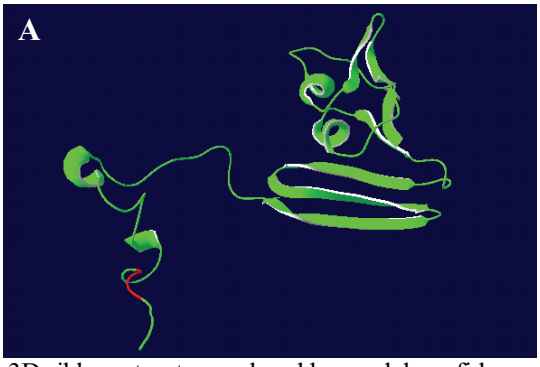

3D ribbon structure colored by model confidence

AprB model: back view

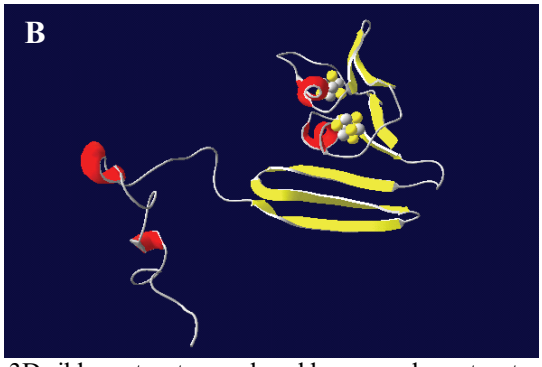

3D ribbon structure colored by secondary structure elements (positions of [4Fe-4S] cluster indicated)

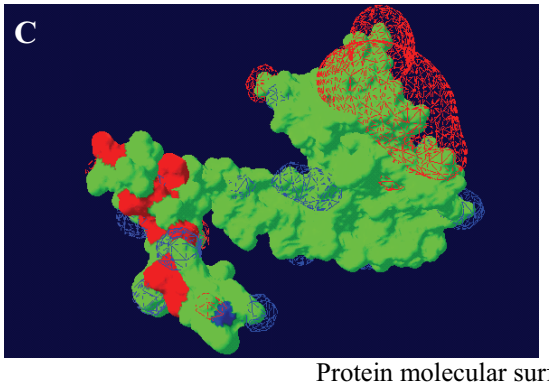

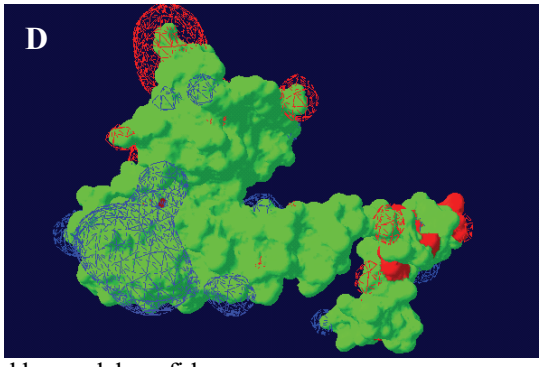

Protein molecular surface colored by model confidence

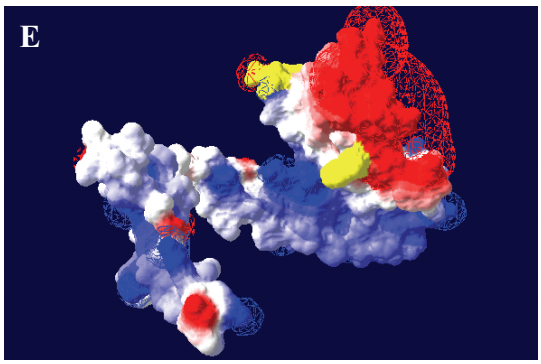

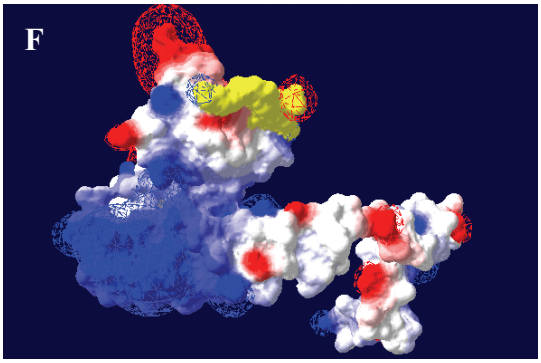

Protein molecular surface colored by calculated electrostatic potential (electric charge at the molecular surface is colored with a red (negative), white (neutral, and blue (positive) color gradient; electric field extending into the solvent is shown); Trp-B48 and exposed, potential Qmo-docking loop are marked by yellow color)

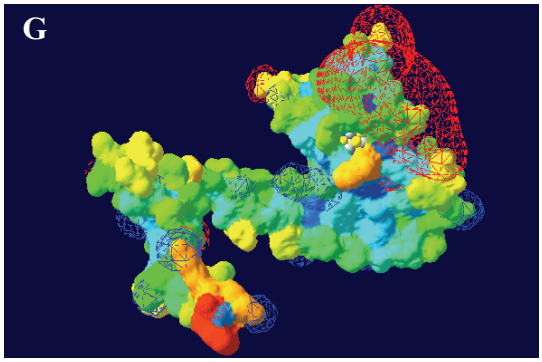

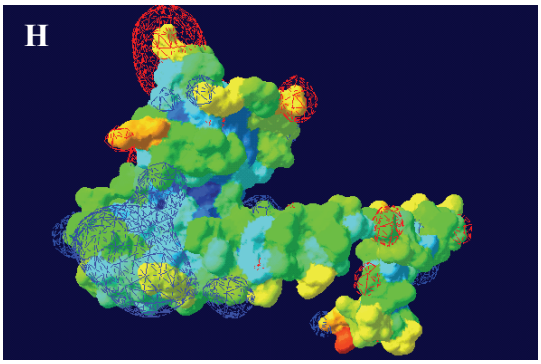

Protein molecular surface colored by calculated solvent accessibility

Desulfovibrio vulgaris

AprB model: front view (side towards AprA)

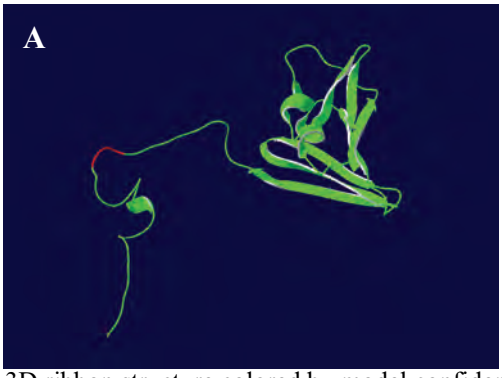

3D ribbon structure colored by model confidence

AprB model: back view

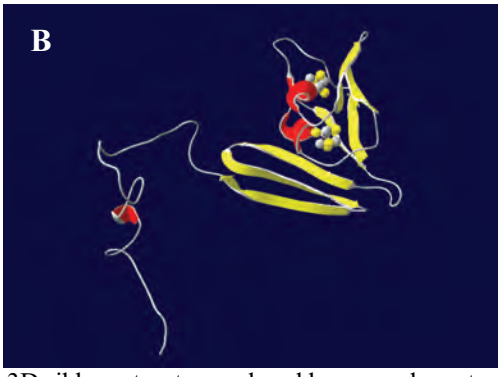

3D ribbon structure colored by secondary structure elements (positions of [4Fe-4S] cluster indicated)

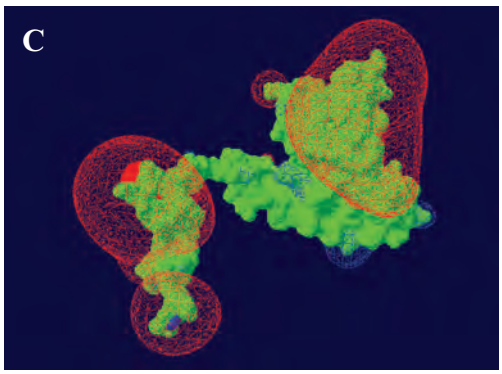

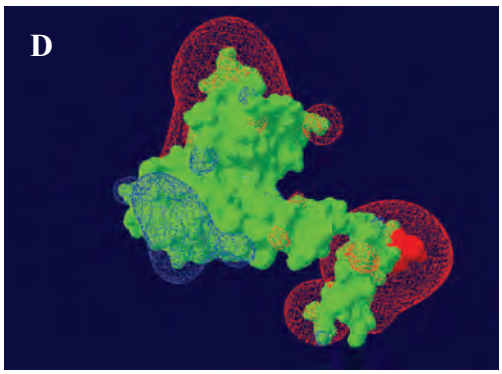

Protein molecular surface colored by model confidence

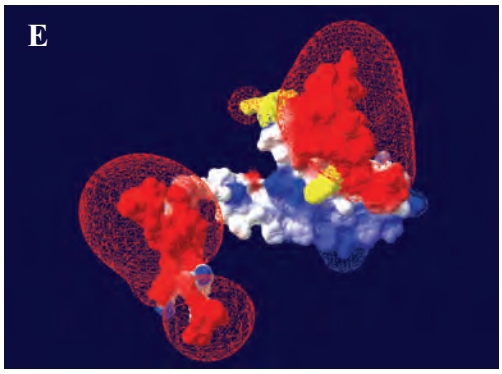

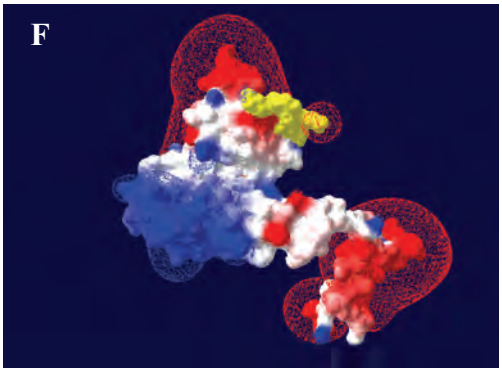

Protein molecular surface colored by calculated electrostatic potential (electric charge at the molecular surface is colored with a red (negative), white (neutral, and blue (positive) color gradient; electric field extending into the solvent is shown); Trp-B48 and exposed, potential Qmo-docking loop are marked by yellow color)

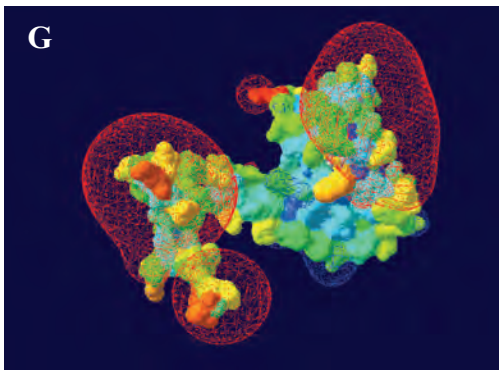

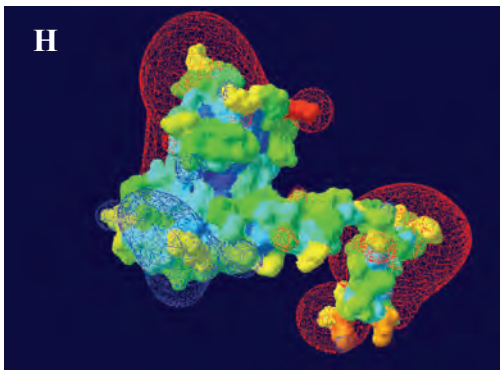

Protein molecular surface colored by calculated solvent accessibility

Desulfovibrio desulfuricans

AprB model: front view (side towards AprA)

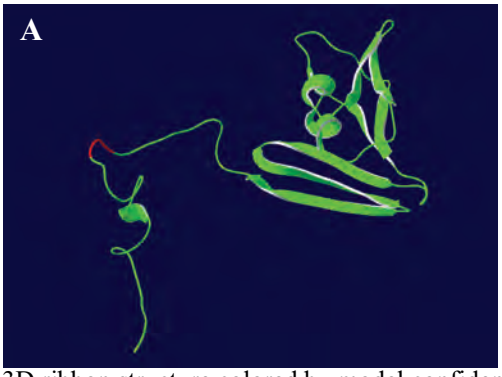

3D ribbon structure colored by model confidence

AprB model: back view

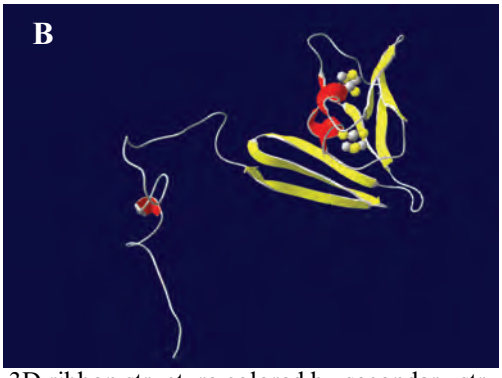

3D ribbon structure colored by secondary structure elements (positions of [4Fe-4S] cluster indicated)

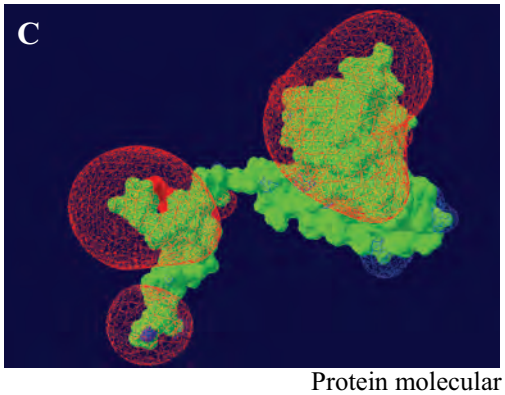

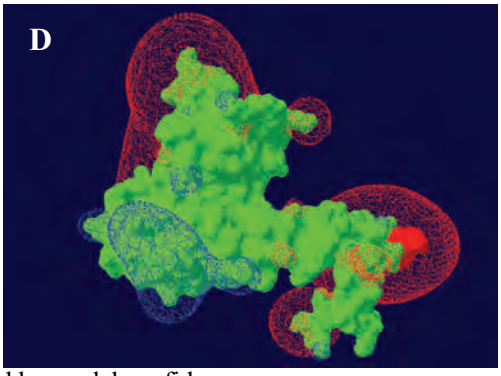

Protein molecular surface colored by model confidence

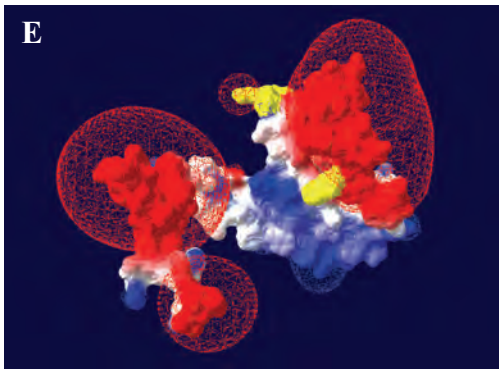

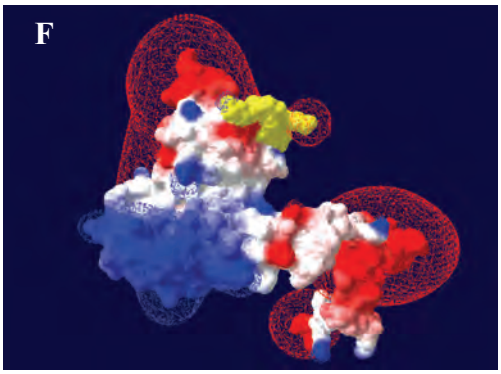

Protein molecular surface colored by calculated electrostatic potential (electric charge at the molecular surface is colored with a red (negative), white (neutral, and blue (positive) color gradient; electric field extending into the solvent is shown); Trp-B48 and exposed, potential Qmo-docking loop are marked by yellow color)

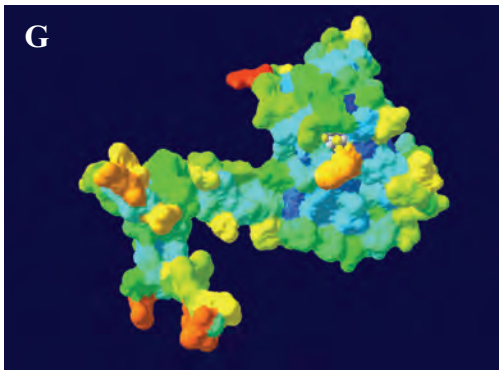

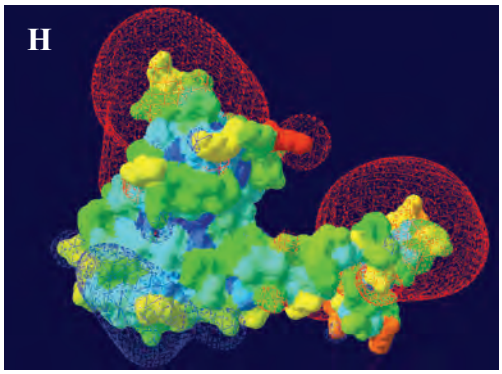

Protein molecular surface colored by calculated solvent accessibility

Desulfobulbus sp. str. MLMS-1

AprB model: front view (side towards AprA)

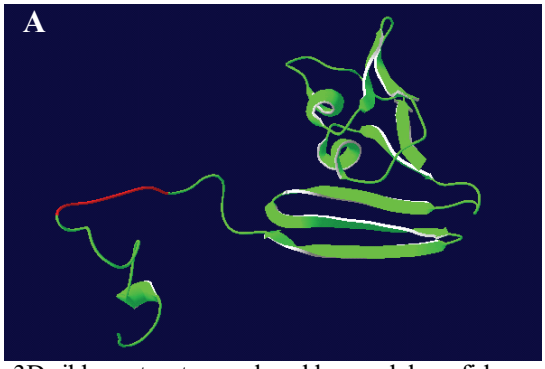

3D ribbon structure colored by model confidence

AprB model: back view

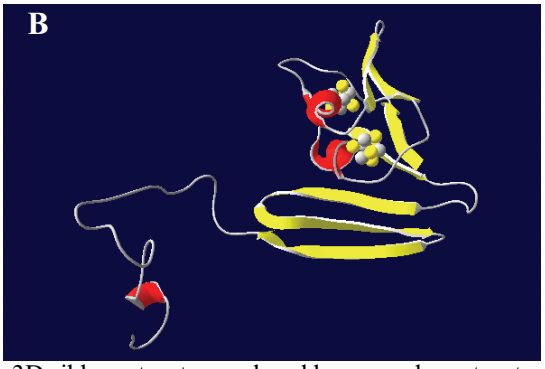

3D ribbon structure colored by secondary structure elements (positions of [4Fe-4S] cluster indicated)

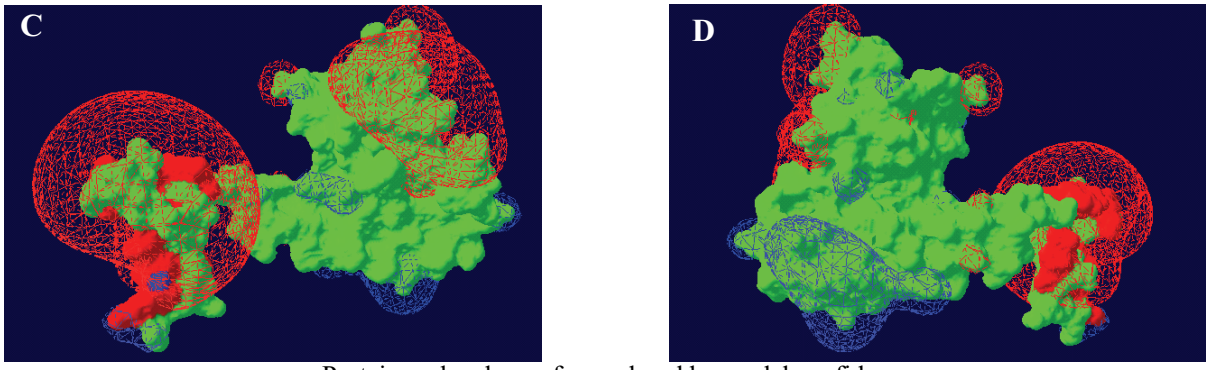

Protein molecular surface colored by model confidence

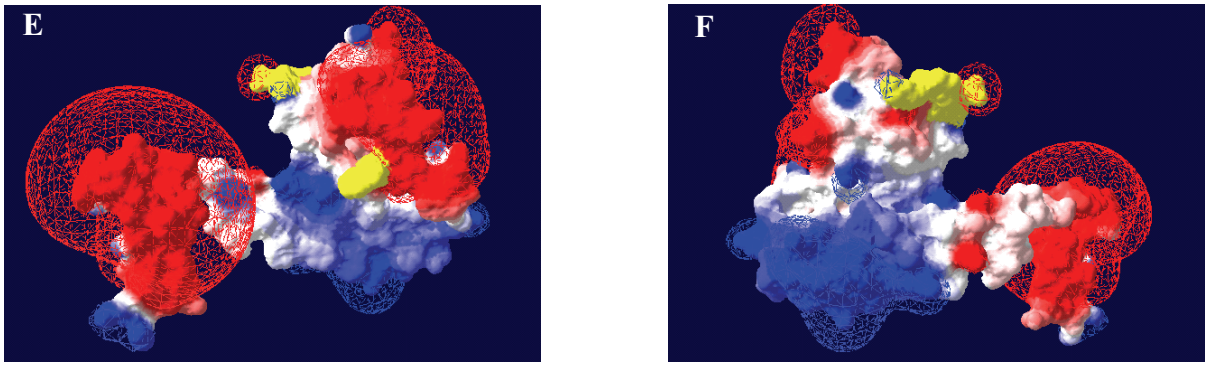

Protein molecular surface colored by calculated electrostatic potential (electric charge at the molecular surface is colored with a red (negative), white (neutral, and blue (positive) color gradient; electric field extending into the solvent is shown); Trp-B48 and exposed, potential Qmo-docking loop are marked by yellow color)

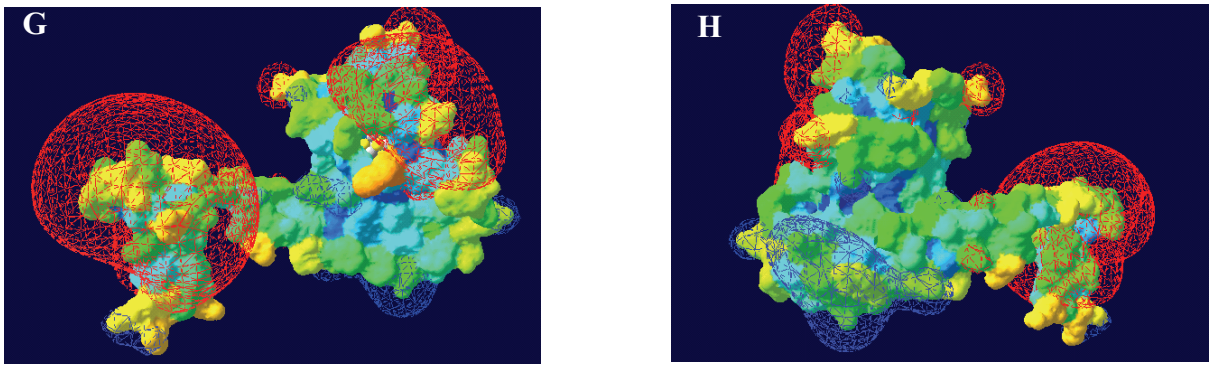

Protein molecular surface colored by calculated solvent accessibility

Desulfotalea psychrophila

AprB model: front view (side towards AprA)

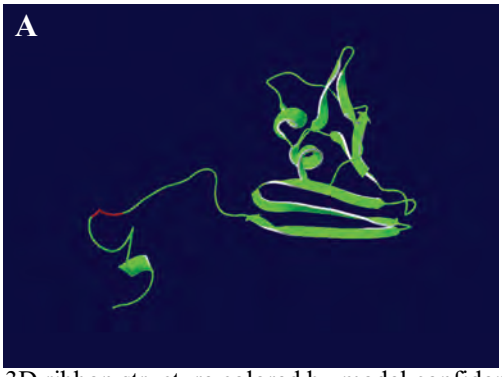

3D ribbon structure colored by model confidence

AprB model: back view

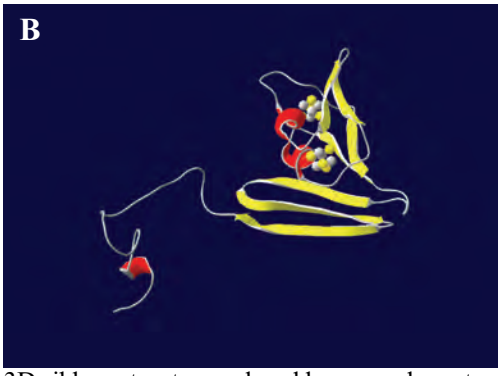

3D ribbon structure colored by secondary structure elements (positions of [4Fe-4S] cluster indicated)

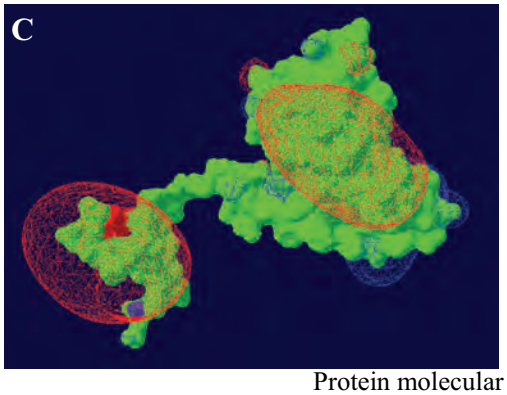

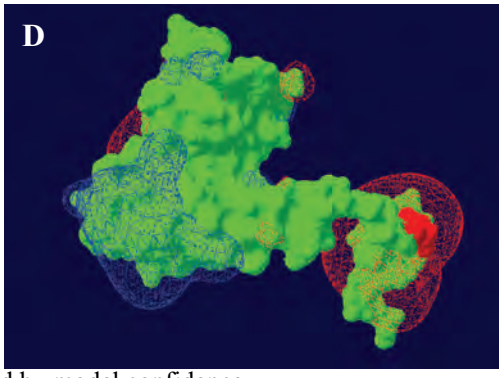

Protein molecular surface colored by model confidence

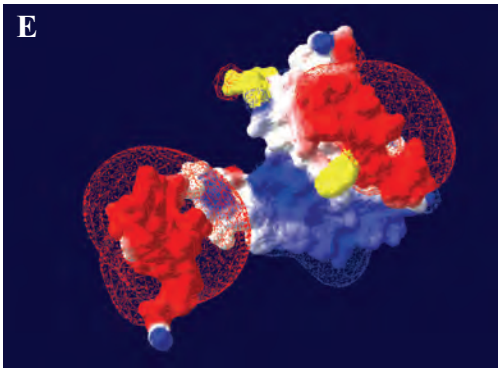

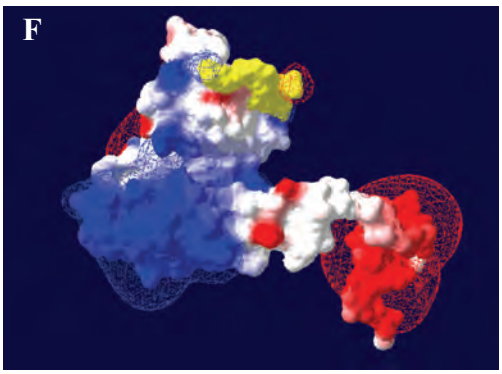

Protein molecular surface colored by calculated electrostatic potential (electric charge at the molecular surface is colored with a red (negative), white (neutral, and blue (positive) color gradient; electric field extending into the solvent is shown); Trp-B48 and exposed, potential Qmo-docking loop are marked by yellow color)

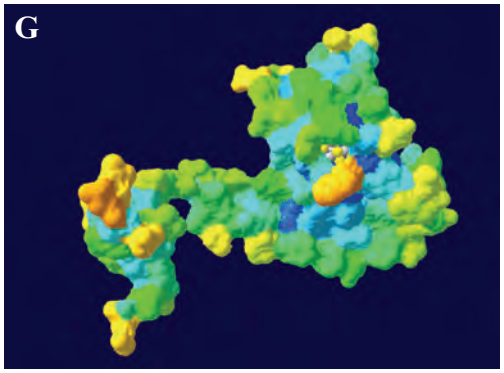

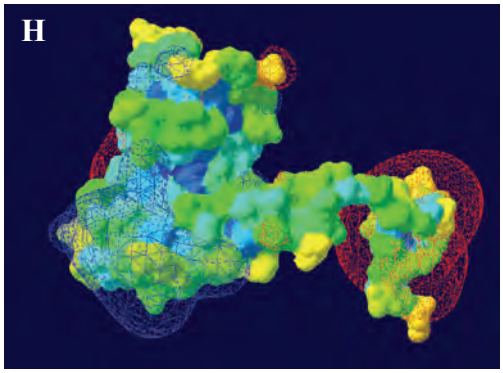

Protein molecular surface colored by calculated solvent accessibility

Olavius algarvensis Delta 1 symbiont

AprB model: front view (side towards AprA)

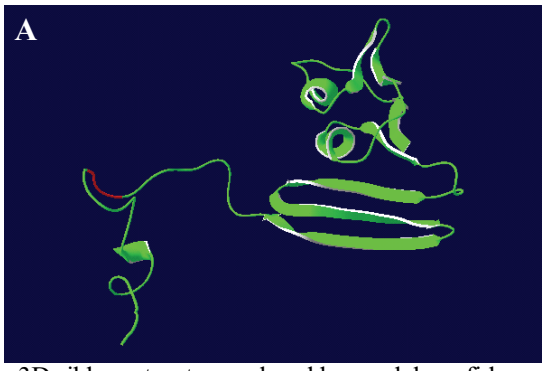

3D ribbon structure colored by model confidence

AprB model: back view

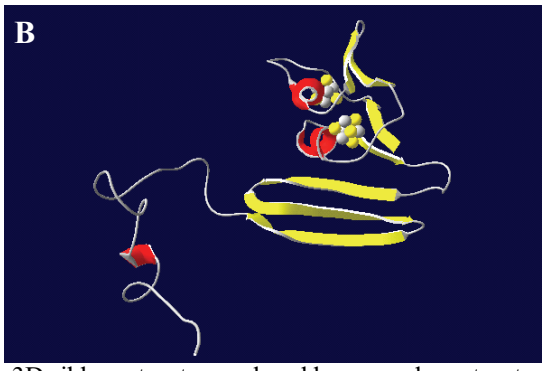

3D ribbon structure colored by secondary structure elements (positions of [4Fe-4S] cluster indicated)

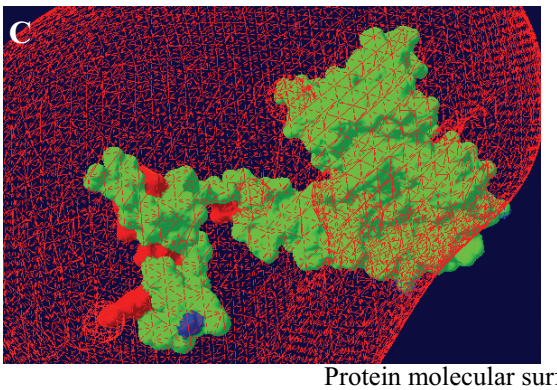

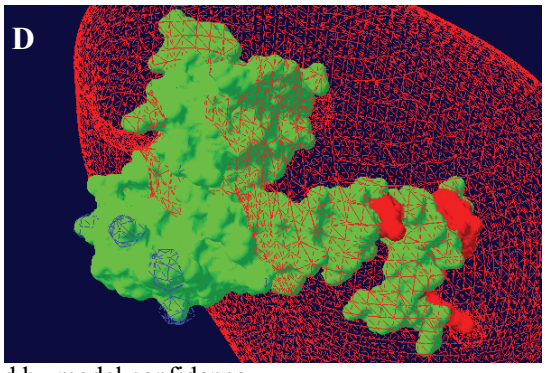

Protein molecular surface colored by model confidence

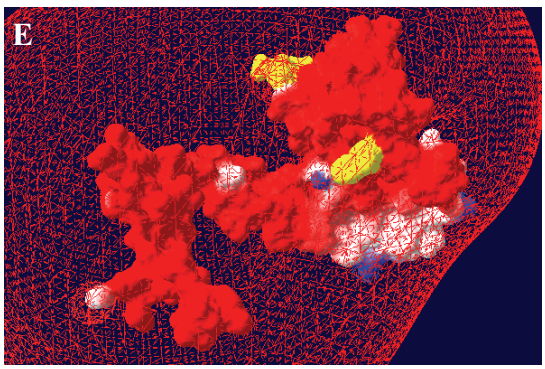

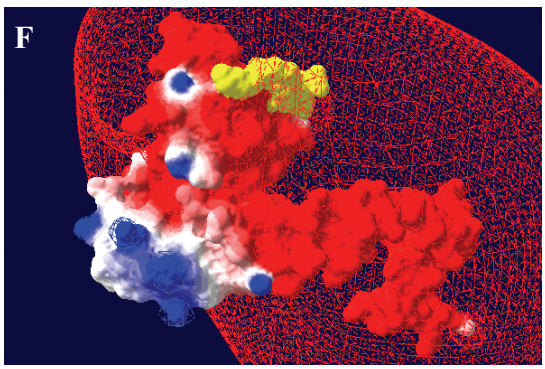

Protein molecular surface colored by calculated electrostatic potential (electric charge at the molecular surface is colored with a red (negative), white (neutral, and blue (positive) color gradient; electric field extending into the solvent is shown); Trp-B48 and exposed, potential Qmo-docking loop are marked by yellow color)

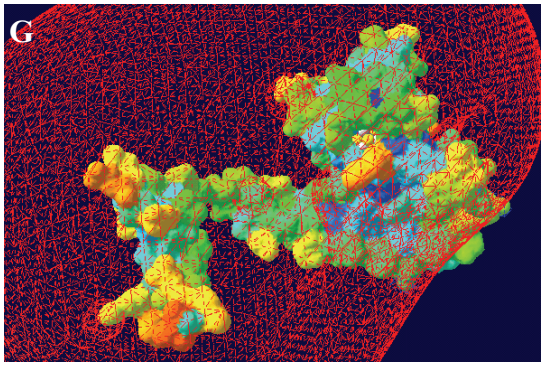

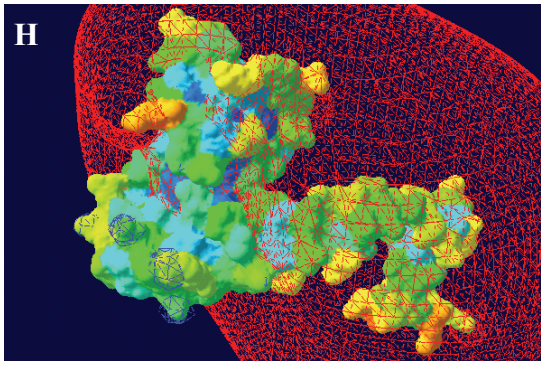

Protein molecular surface colored by calculated solvent accessibility

Thermodesulfovibrio yellowstonii

AprB model: front view (side towards AprA)

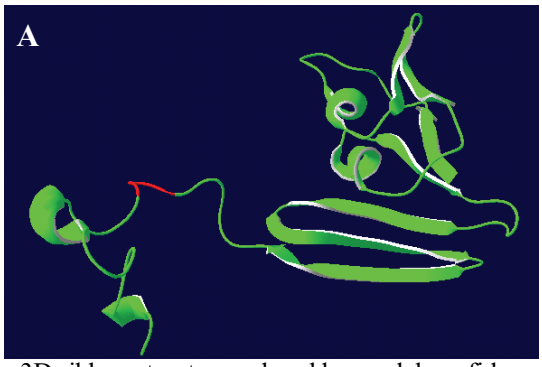

3D ribbon structure colored by model confidence

AprB model: back view

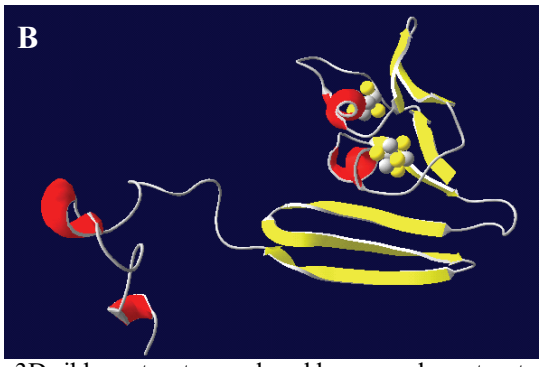

3D ribbon structure colored by secondary structure elements (positions of [4Fe-4S] cluster indicated)

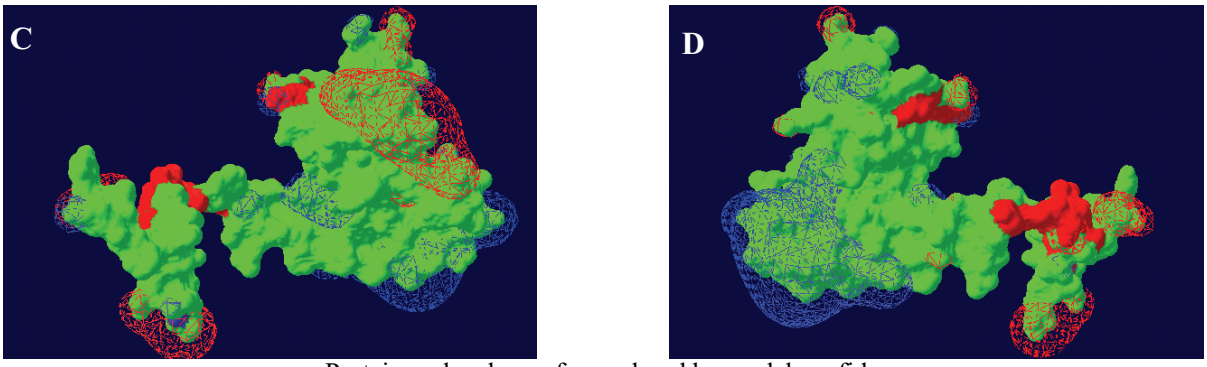

Protein molecular surface colored by model confidence

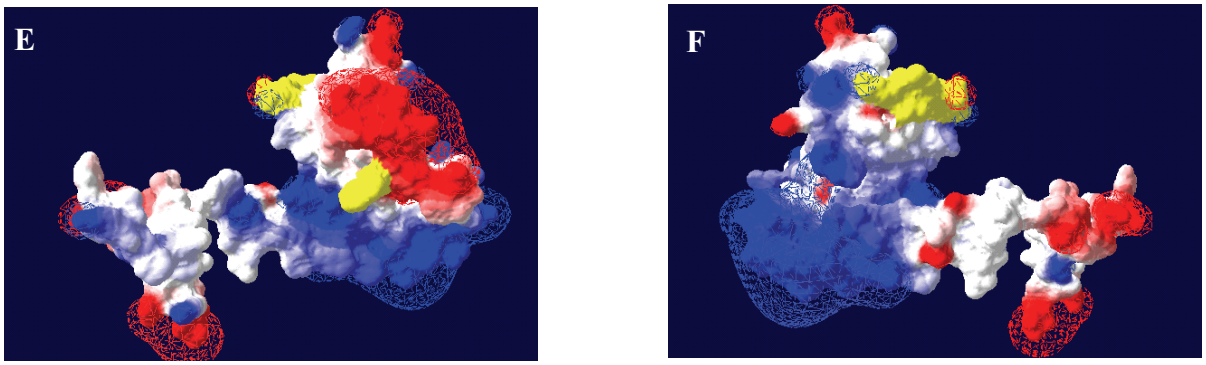

Protein molecular surface colored by calculated electrostatic potential (electric charge at the molecular surface is colored with a red (negative), white (neutral, and blue (positive) color gradient; electric field extending into the solvent is shown); Trp-B48 and exposed, potential Qmo-docking loop are marked by yellow color)

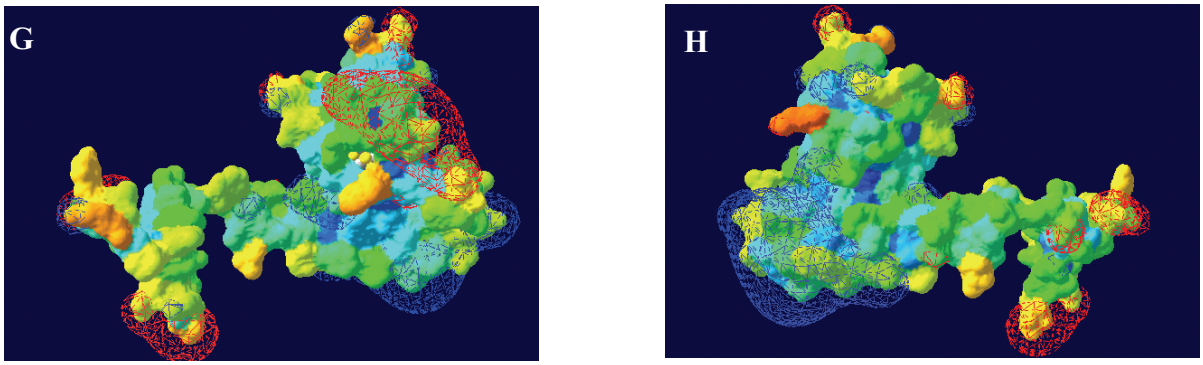

Protein molecular surface colored by calculated solvent accessibility

Chlorobaculum tepidum

AprB model: front view (side towards AprA)

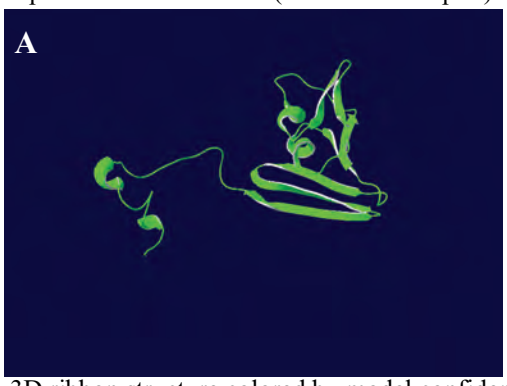

3D ribbon structure colored by model confidence

AprB model: back view

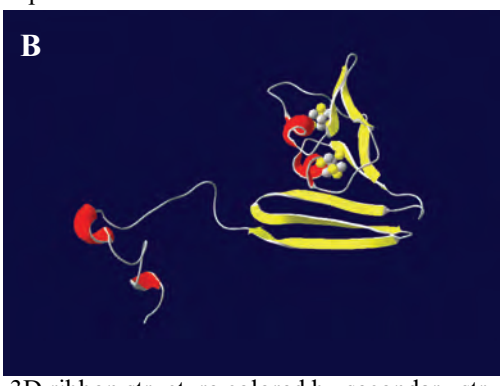

3D ribbon structure colored by secondary structure elements (positions of [4Fe-4S] cluster indicated)

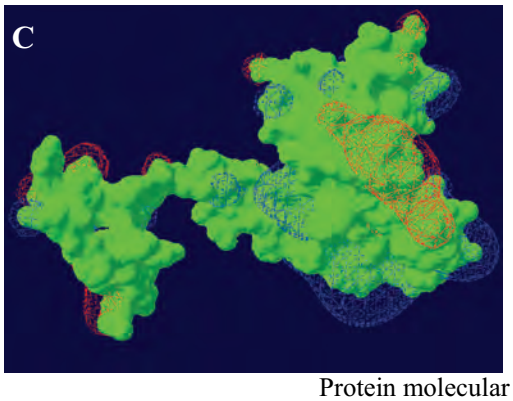

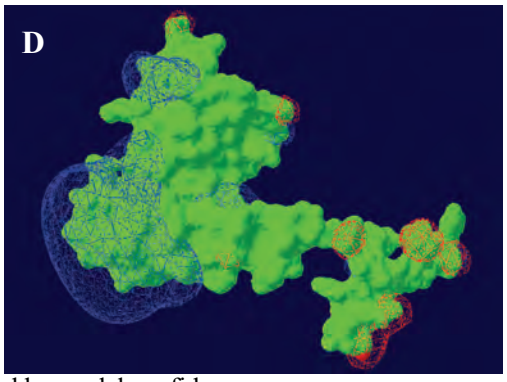

Protein molecular surface colored by model confidence

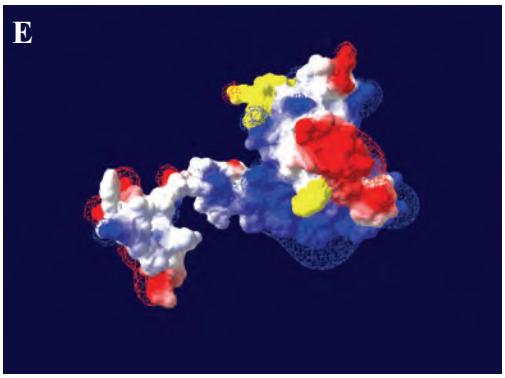

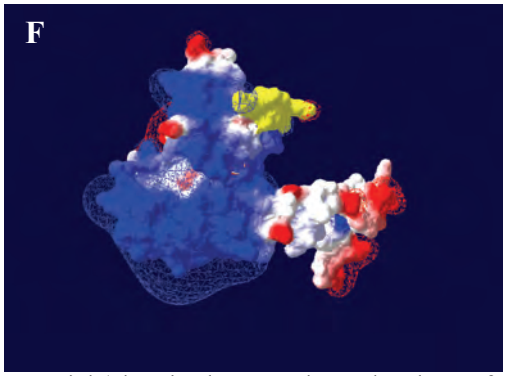

Protein molecular surface colored by calculated electrostatic potential (electric charge at the molecular surface is colored with a red (negative), white (neutral, and blue (positive) color gradient; electric field extending into the solvent is shown); Trp-B48 and exposed, potential Qmo-docking loop are marked by yellow color)

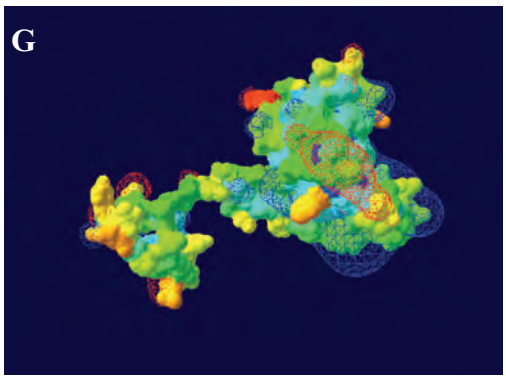

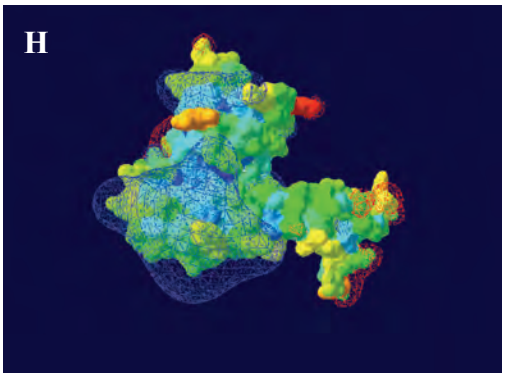

Protein molecular surface colored by calculated solvent accessibility

Thiobacillus denitrificans

AprB model: front view (side towards AprA)

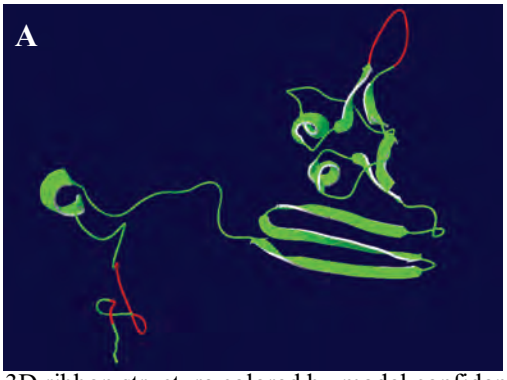

3D ribbon structure colored by model confidence

AprB model: back view

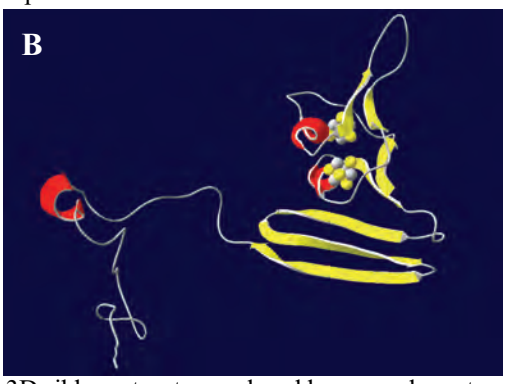

3D ribbon structure colored by secondary structure elements (positions of [4Fe-4S] cluster indicated)

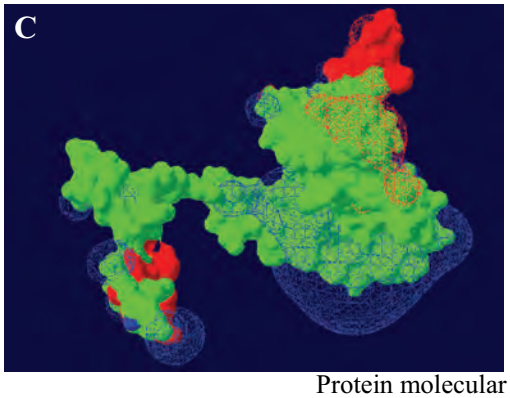

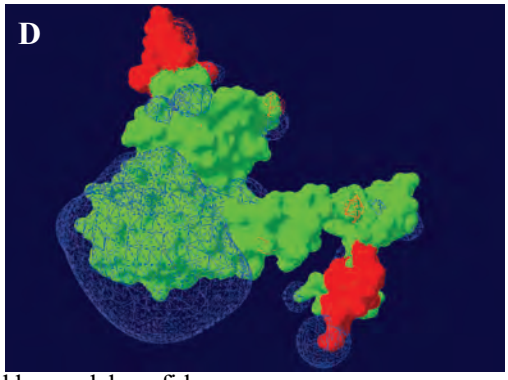

Protein molecular surface colored by model confidence

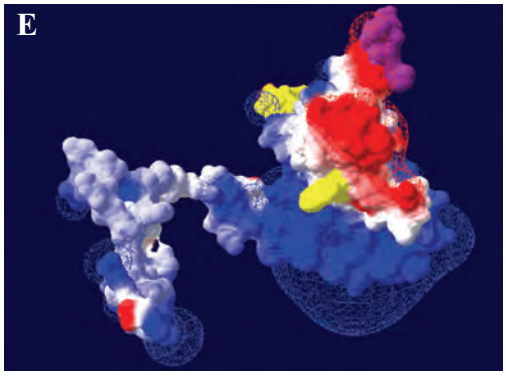

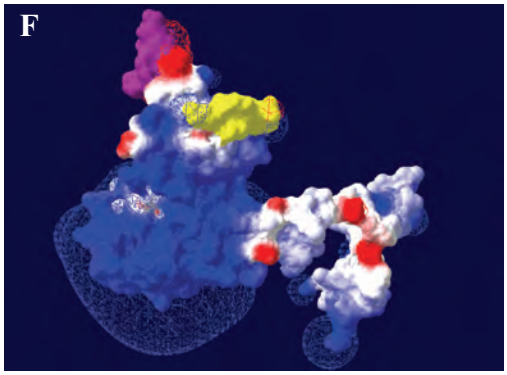

Protein molecular surface colored by calculated electrostatic potential (electric charge at the molecular surface is colored with a red (negative), white (neutral, and blue (positive) color gradient; electric field extending into the solvent is shown); Trp-B54 and exposed, potential Qmo-docking loop are marked by yellow color; additional loop is colored violett

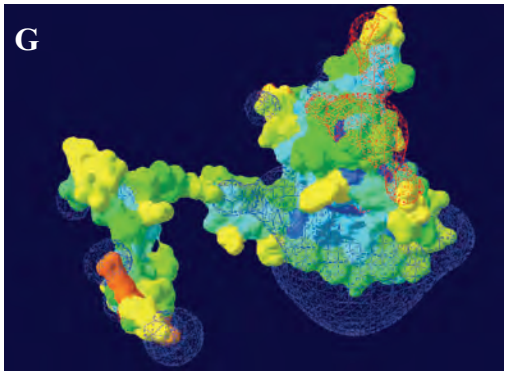

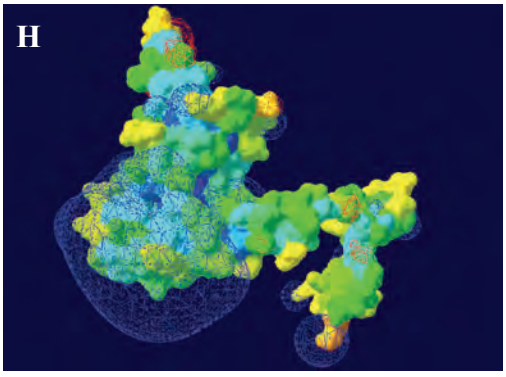

Protein molecular surface colored by calculated solvent accessibility

Supplementary data material Figure S2. AprB protein matrix surrounding the [4Fe-4S] clusters

Reference structure	Residues in a distance <5.0Å to the [4Fe-4S] clusters I and II	Charged and polar residues marked	Cysteine and tryptophane marked
Archaeoglobus fulgidus	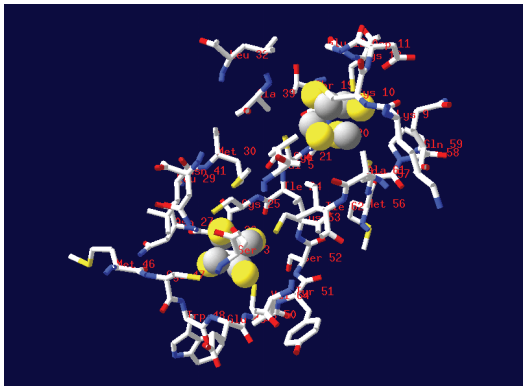	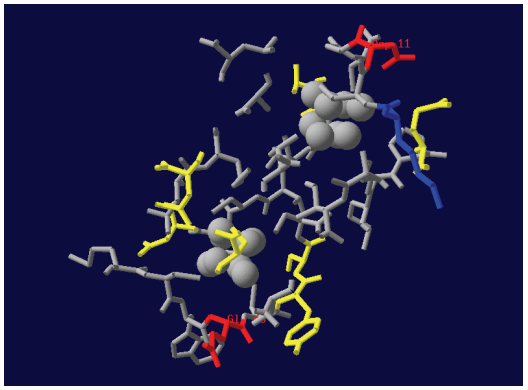	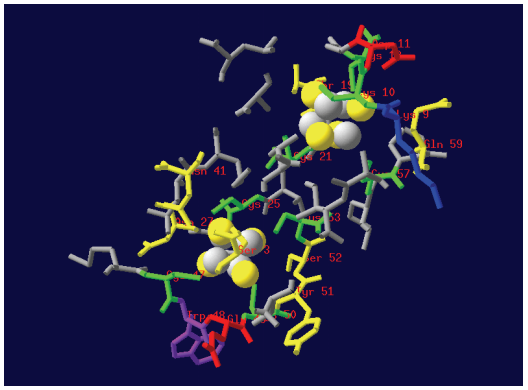
SOB lineage I *Allochromatium vinosum*	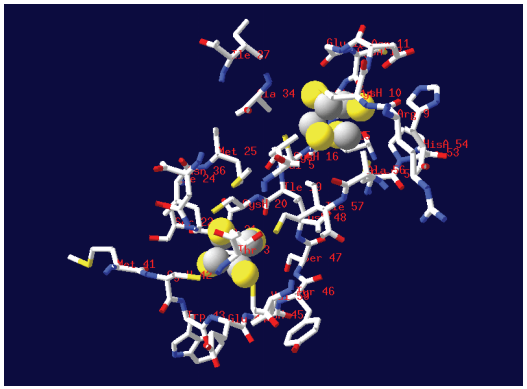	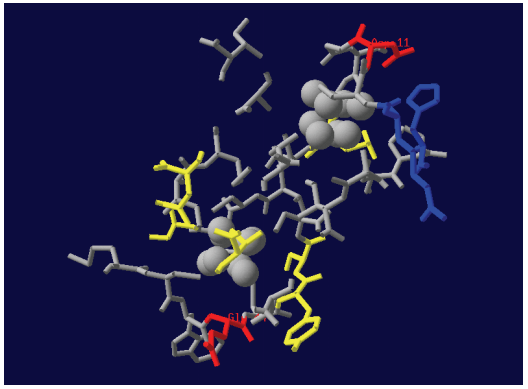	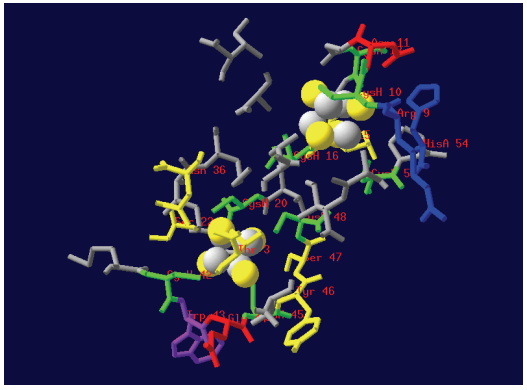
Thiobacillus denitrificans	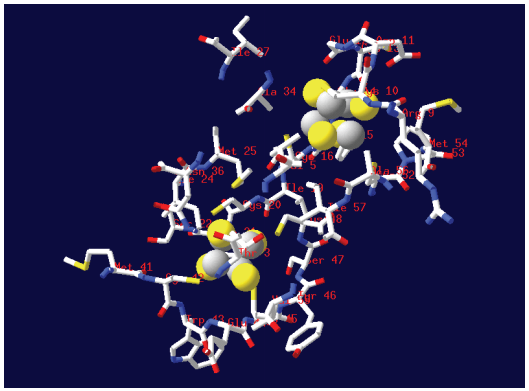	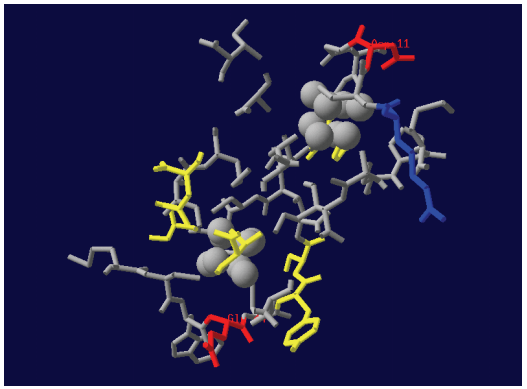	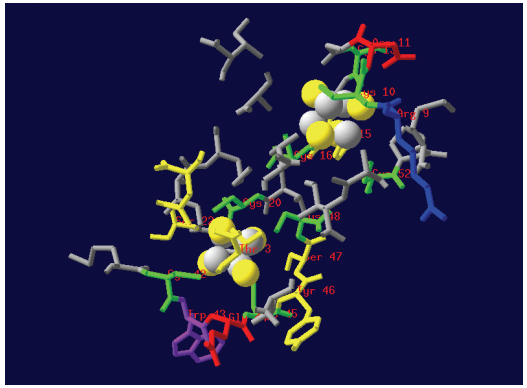

SOB lineage I	Residues in a distance <5.0Å to the [4Fe-4S] clusters	Charged and polar residues marked	Cysteine and tryptophan marked
Cdt. Ruthia magnifica	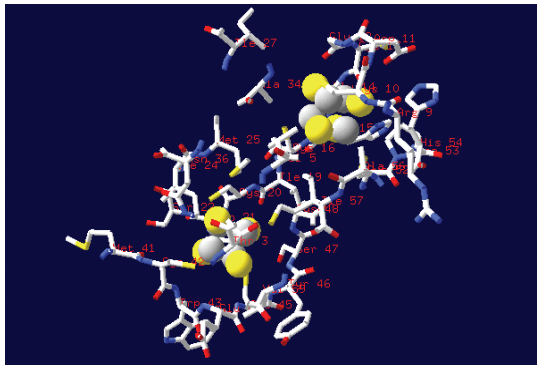	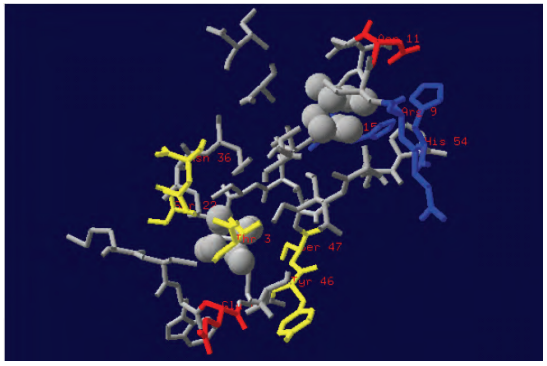	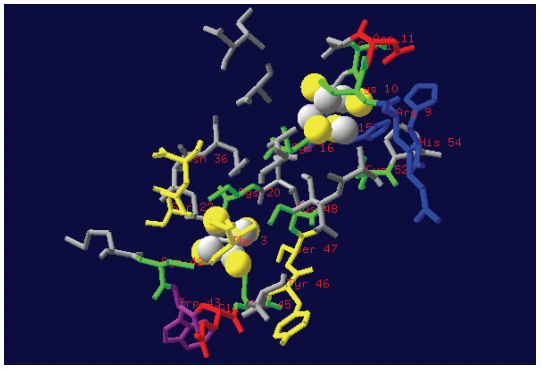
Cdt. Pelagibacter ubique	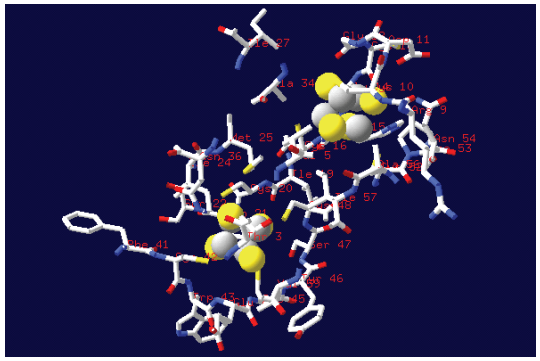	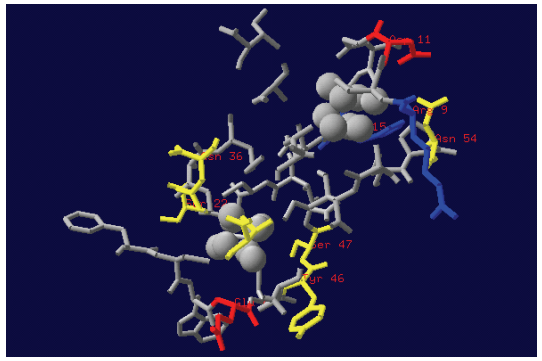	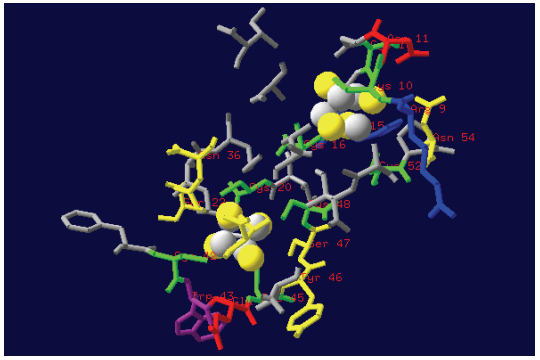
EBAC2C11	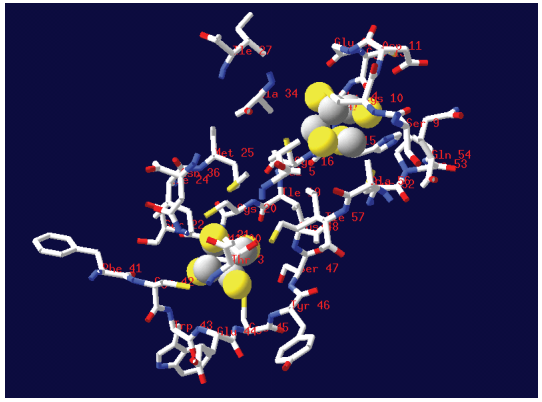	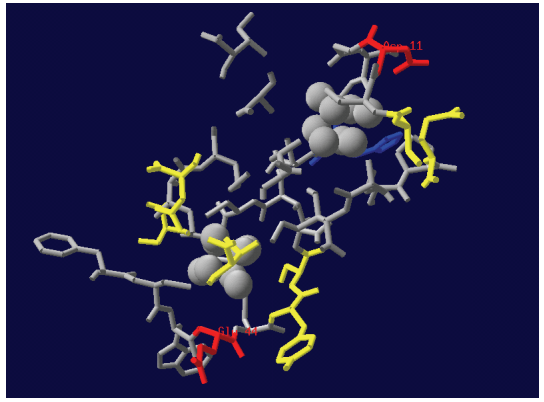	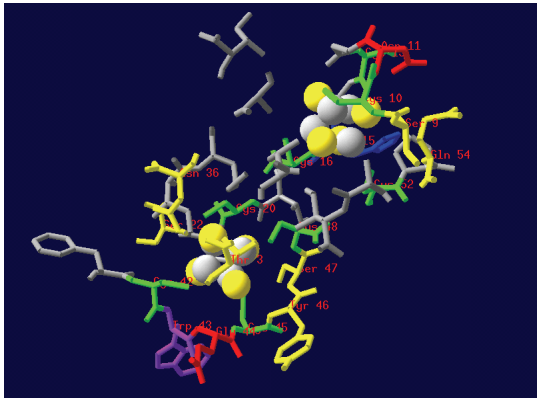

Crenarchaeal SRP	Residues in a distance <5.0Å to the [4Fe-4S] clusters	Charged and polar residues marked	Cysteine and tryptophan marked
Pyrobaculum calidifontis	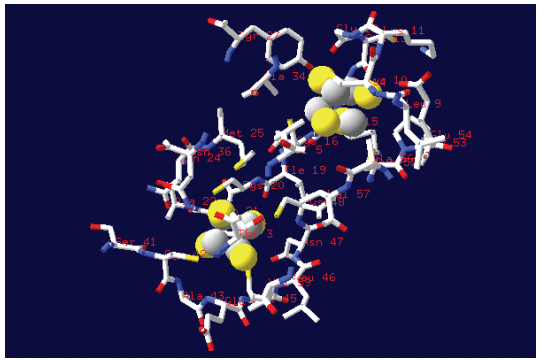	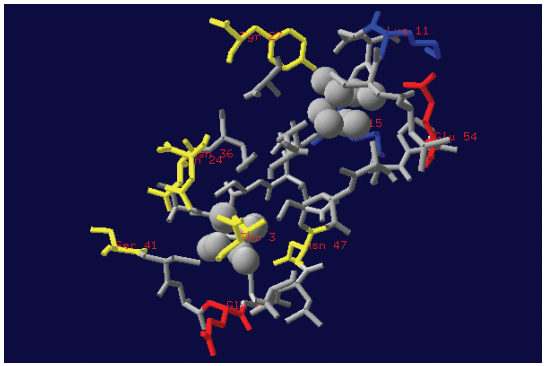	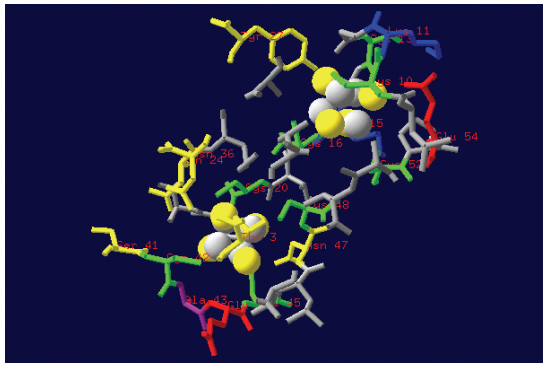
Pyrobaculum aerophilum	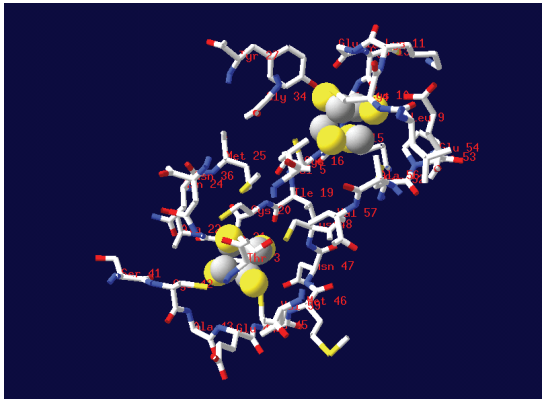	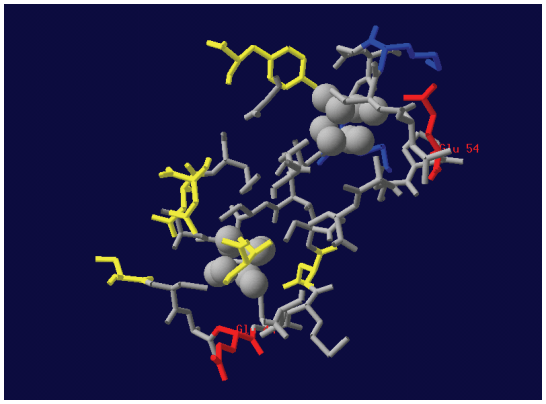	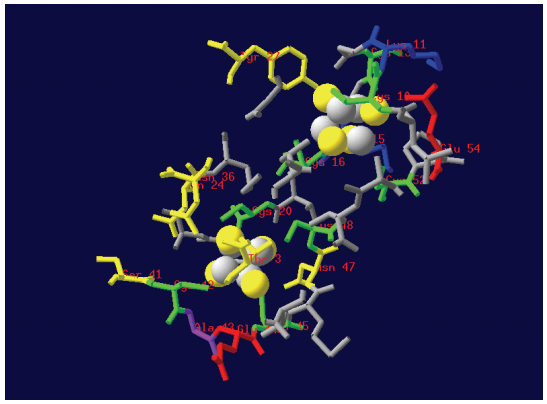
Caldivirga maquilingensis	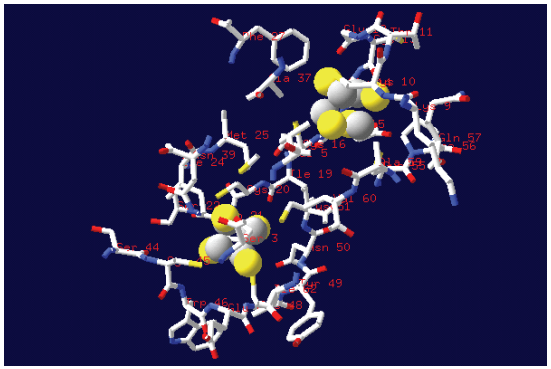	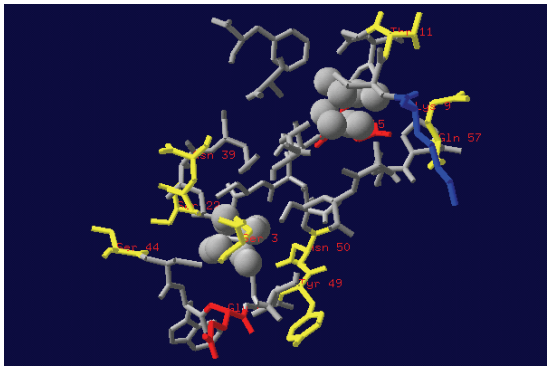	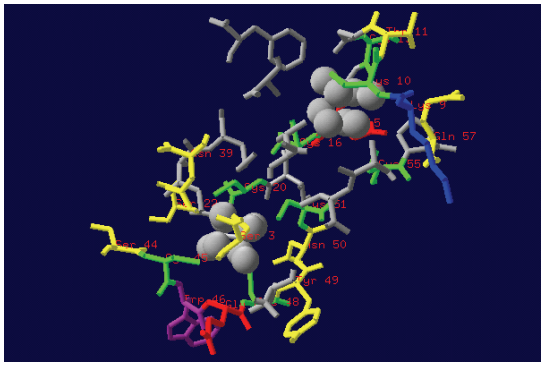

SRB and related SOB lineage II	Residues in a distance <5.0Å to the [4Fe-4S] clusters	Charged and polar residues marked	Cysteine and tryptophan marked
Desulfotomaculum reducens	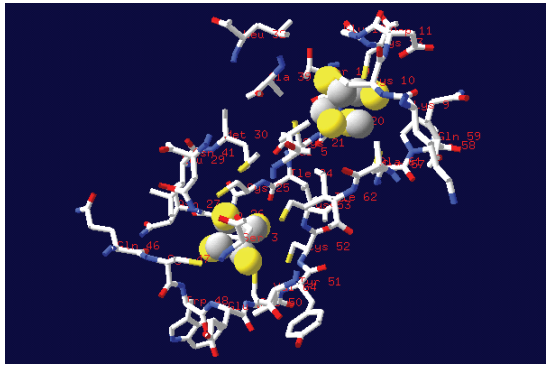	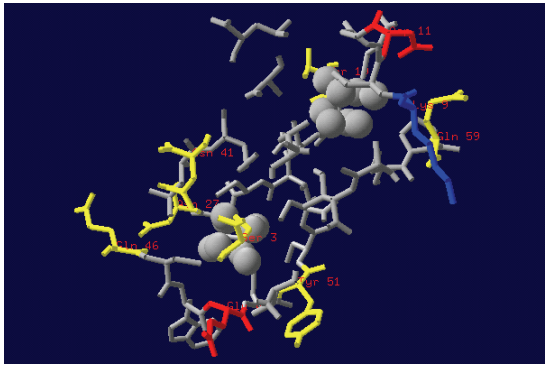	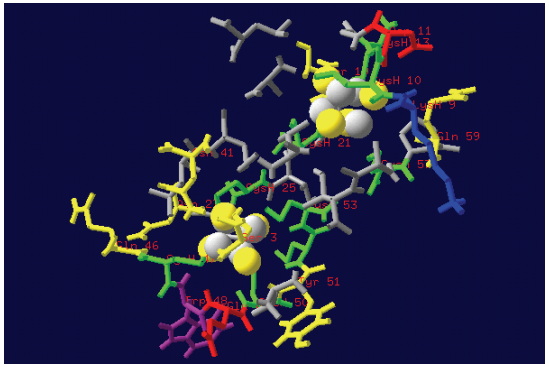
Syntrophobacter fumaroxidans	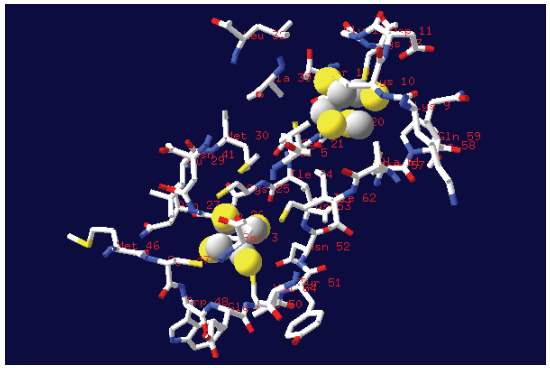	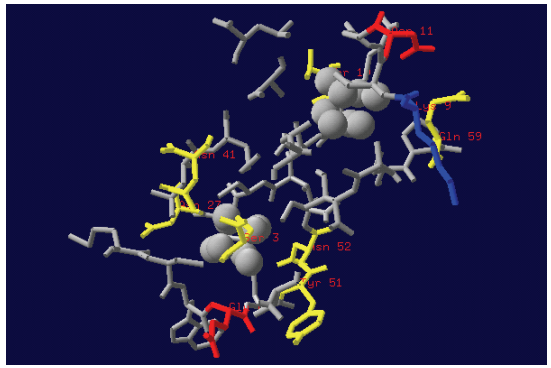	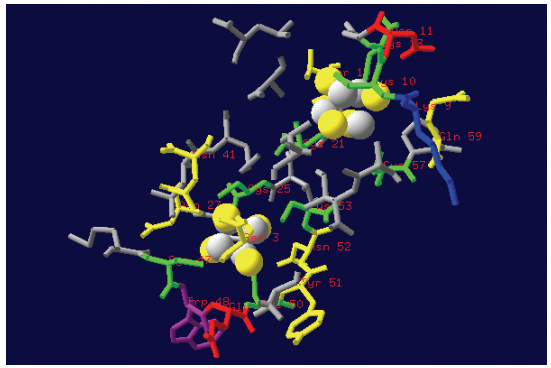
fosws39f7	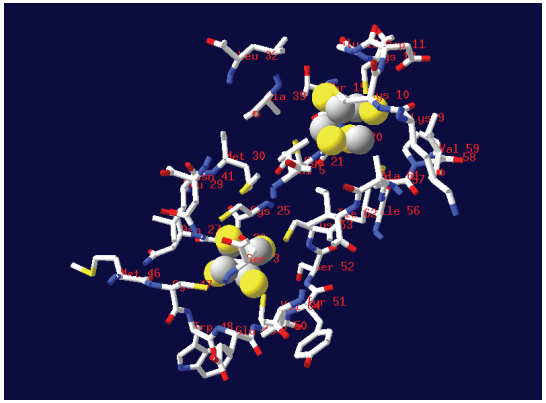	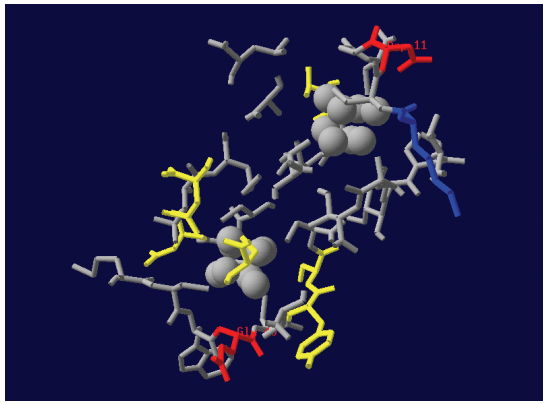	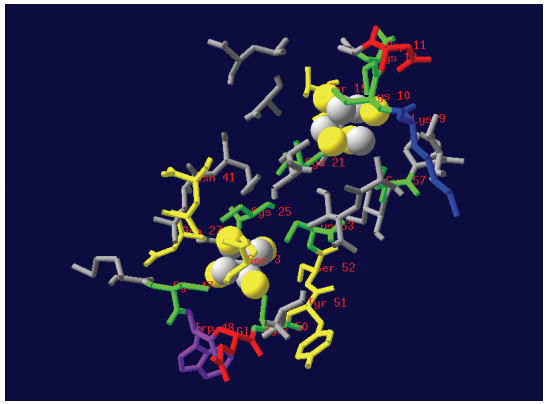

	Residues in a distance <5.0Å to the [4Fe-4S] clusters	Charged and polar residues marked	Cysteine and tryptophan marked
fosws7f8	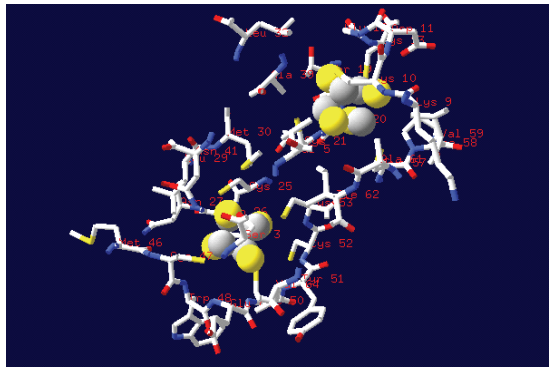	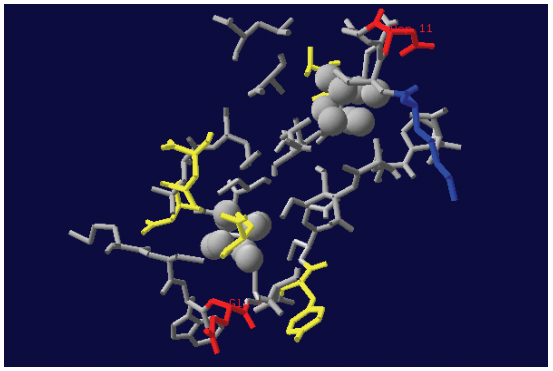	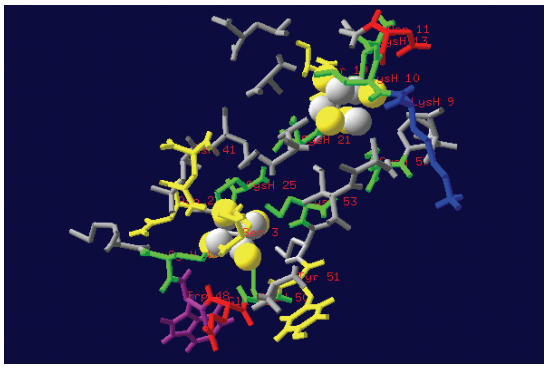
Thermodesulfo-bacterium commune	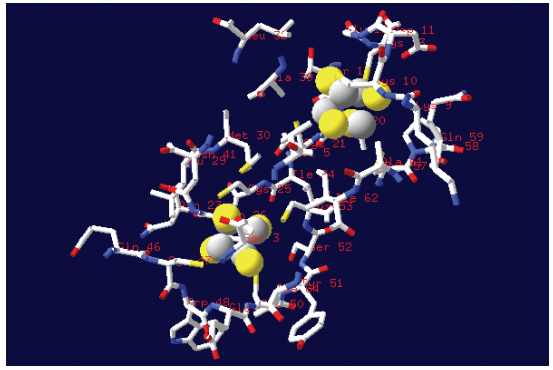	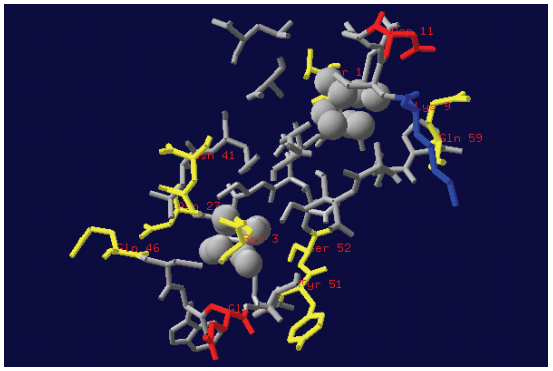	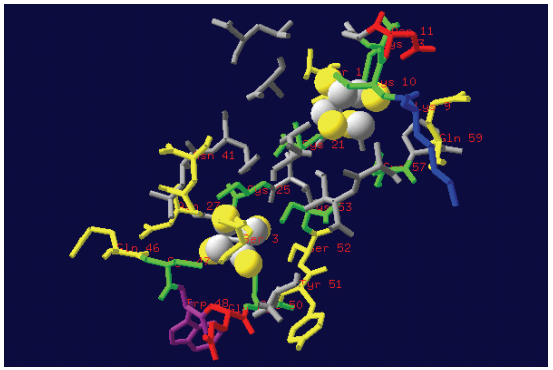
Desulfovibrio desulfuricans	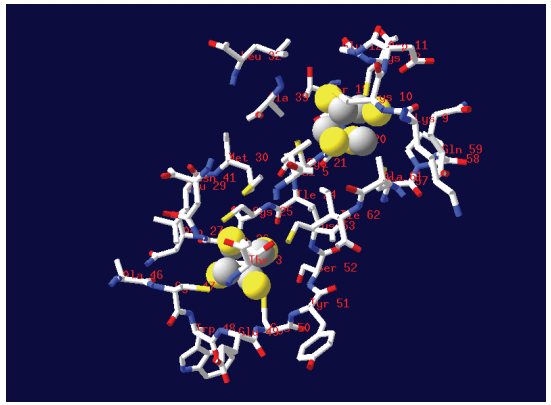	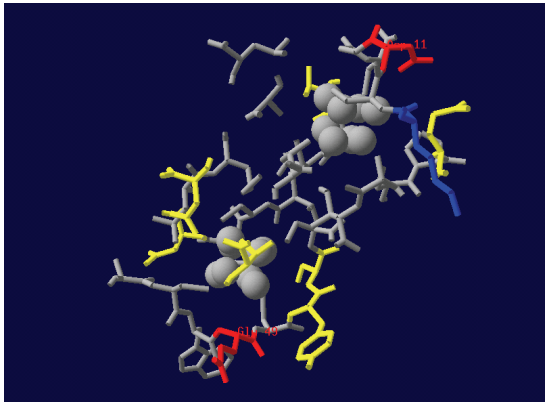	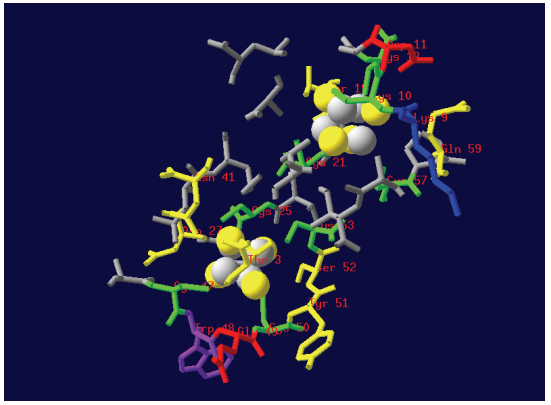

	Residues in a distance <5.0Å to the [4Fe-4S] clusters	Charged and polar residues marked	Cysteine and tryptophan marked
Desulfovibrio vulgaris	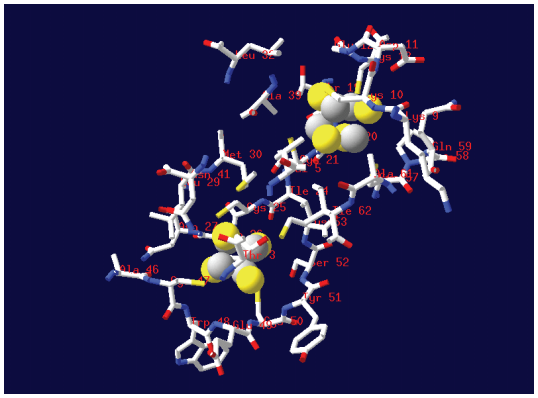	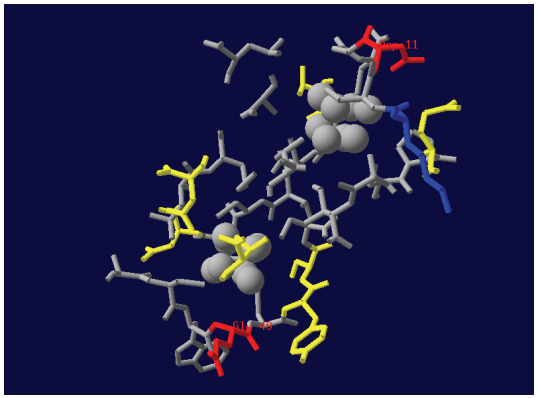	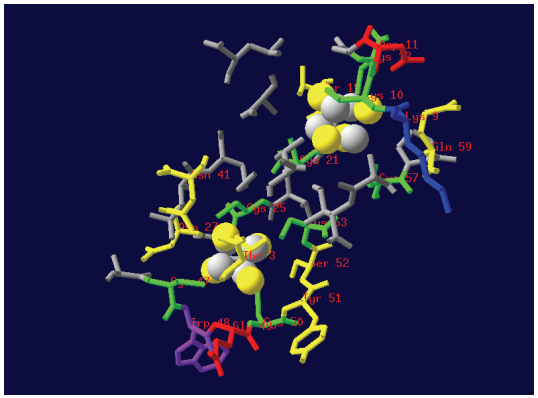
Desulfobulbus sp.	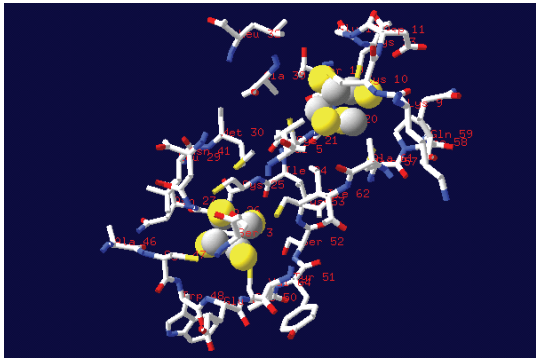	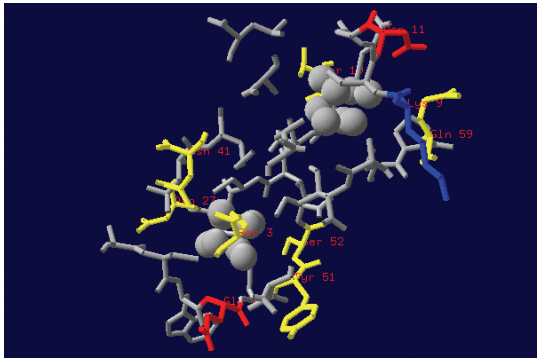	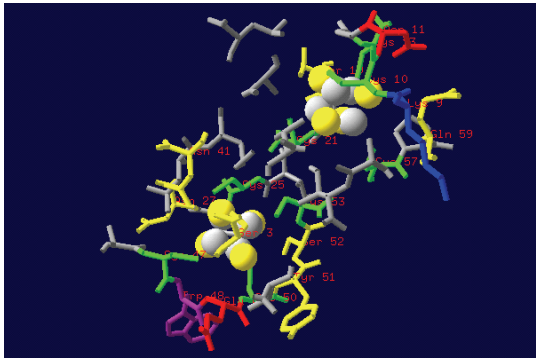
Desulfotalea psychrophila	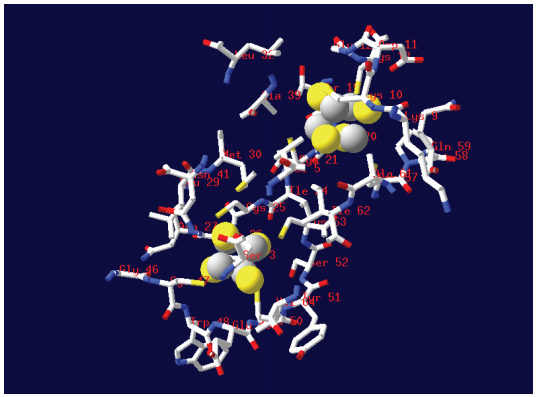	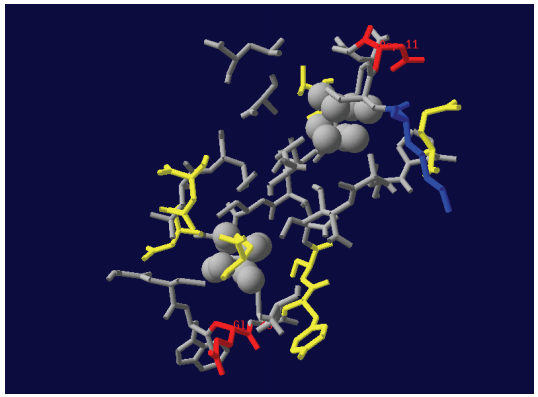	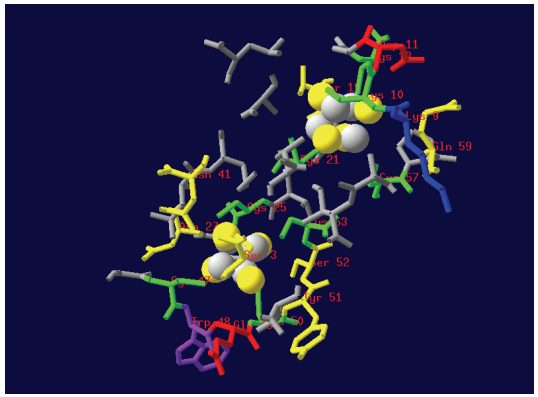

	Residues in a distance <5.0Å to the [4Fe-4S] clusters	Charged and polar residues marked	Cysteine and tryptophan marked
O. algarvensis Delta 1 symbiont	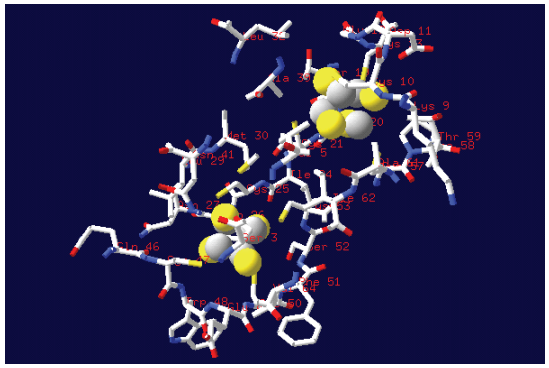	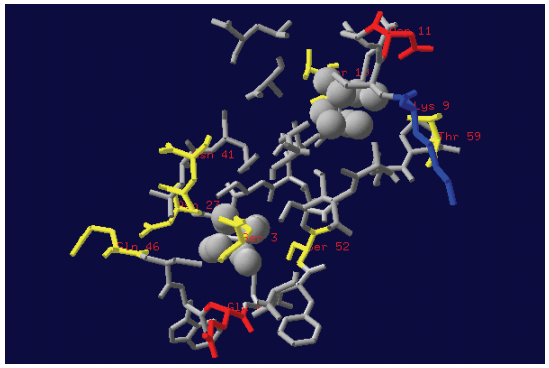	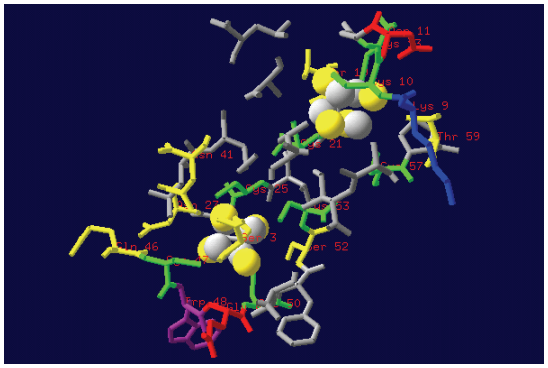
Thermodesulfo-vibrio yellowstonii	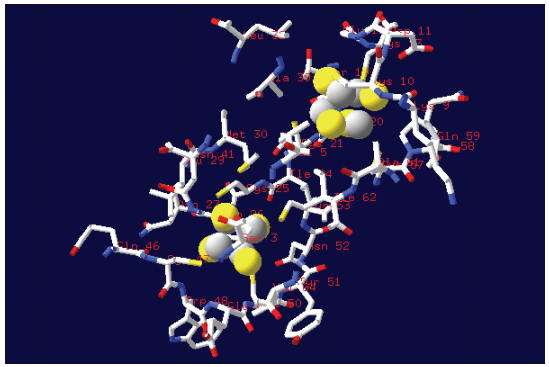	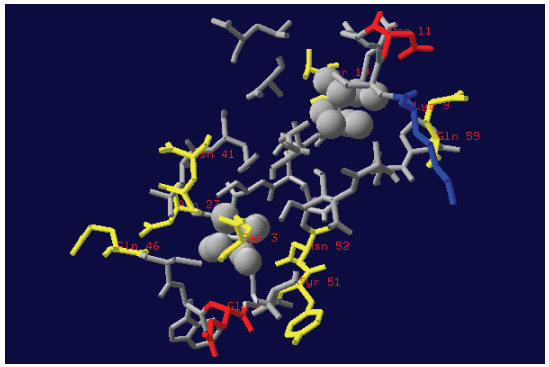	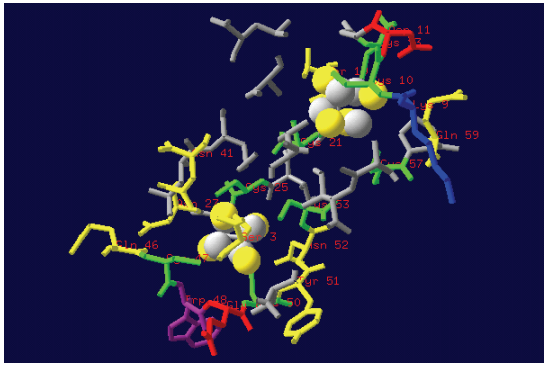
Chlorobaculum tepidum	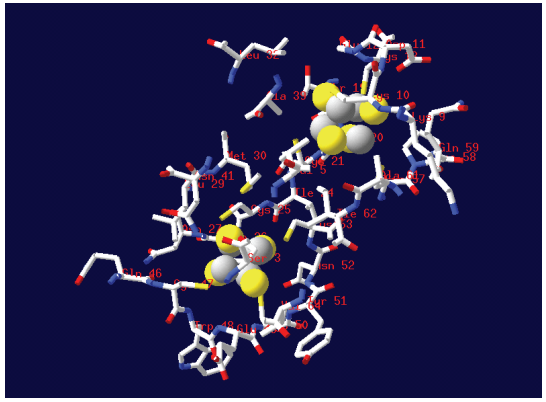	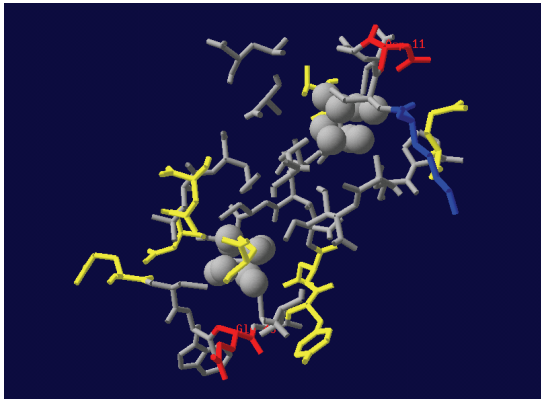	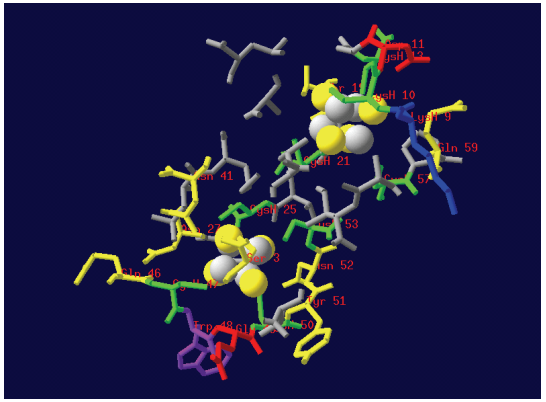

	Residues in a distance <5.0Å to the [4Fe-4S] clusters	Charged and polar residues marked	Cysteine and tryptophan marked
Thiobacillus denitrificans	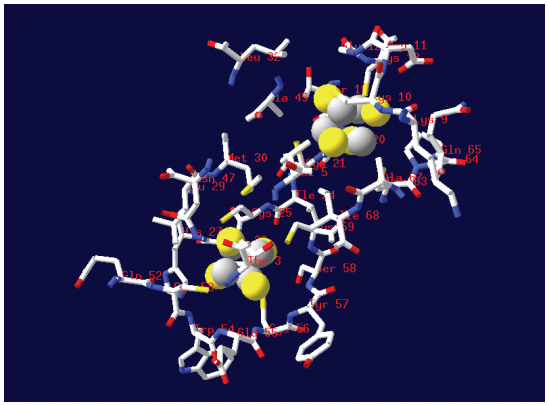	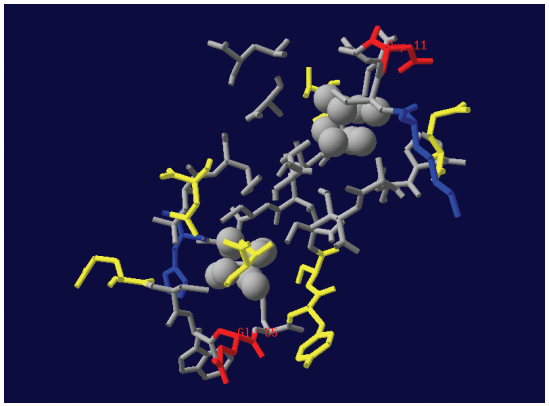	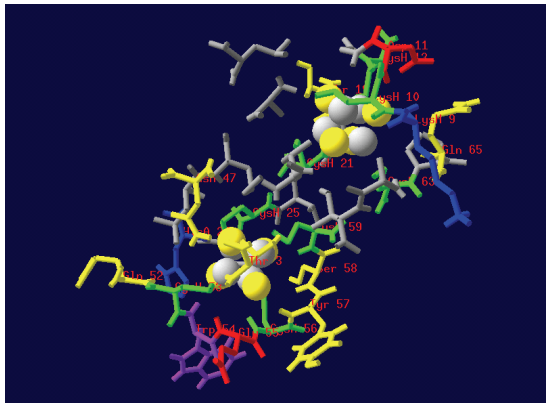

Supplementary data material Table S2. AprB protein matrix surrounding the [4Fe-4S] clusters I and II: appearance of residues in a [4Fe-4S] cluster distance range from 2.0 to 5.0Å

[4Fe-4S] cluster	Distance in Å	*Archaeoglobus fulgidus*	*Allochromatium vinosum*	*Thiobacillus denitrificans*	*Cdt.* Ruthia magnifica	*Cdt.* Pelagi-bacter ubique	EBAC2C11	*Pyrobaculum calidifontis*	*Pyrobaculum aerophilum*	*Caldivirga maquilingensis*	*Chlorobaculum tepidum*	*Thermodesulfovibrio yellowstonii*	*Thiobacillus denitrificans*
Cluster I	2.0	-	Ile24	Ile24	Ile24	Ile24	Ile24	-	-	Ile24	-	-	-
	2.5	Cys25, Cys47, Cys50, Cys53	Cys20, Cys42, Cys45, Cys48	Cys20, Cys42, Cys45, Cys48	Cys20, Cys42, Cys45, Cys48	Cys20, Cys42, Cys45, Cys48	Cys20, Cys42, Cys45, Cys48	Cys20, Cys42, Cys45, Cys48	Cys20, Cys42, Cys45, Cys48	Cys20, Cys45, Cys48, Cys51	Cys25, Cys47, Cys50, Cys53	Cys25, Cys47, Cys50, Cys53	Cys25, Cys53, Cys56, Cys59
	3.0	-	Thr3	Thr3	Thr3	Thr3	Thr3	Thr3	Thr3		-	-	Thr3
	3.5	Ser3, Asn41, Tyr51	Tyr46	Tyr46	Tyr46	Tyr46	Tyr46	Leu46	Met46	Ser3, Tyr49	Ser3, Tyr51	Ser3, Tyr51	Tyr57
	4.0	Pro26, Leu29, Met30, Trp48, Glu49, Ser52	Pro21, Met25, Asn36, Glu44, Trp43, Ser47	Pro21, Met25, Asn36, Glu44, Trp43, Ser47	Pro21, Met25, Asn36, Glu44, Trp43, Ser47	Pro21, Met25, Asn36, Glu44, Trp43, Ser47	Pro21, Met25, Asn36, Glu44, Trp43, Ser47	Pro21, Met25, Asn36, Glu44, Ala43, Asn47	Pro21, Met25, Asn36, Glu44, Ala43, Asn47	Pro21, Met25, Asn39, Glu47, Trp46, Asn50, Ile62	Pro26, Leu29, Met30, Asn41, Trp48, Glu49, Asn52	Pro26, Leu29, Met30, Asn41, Trp48, Glu49, Asn52	Pro26, His27, Leu29, Met30, Asn47, Trp54, Glu55,Ser58
	4.5	-	-	-	-	-	-	Asn24	Asn24	-	-	-	-
	5.0	Asn27, Val64, Ile24, Met46	Ile19, Ser22, Met41, Val59	Ile19, Ser22, Met41, Val59	Ile19, Ser22, Met41, Val59	Ile19, Ser22, Phe41, Val59	Ile19, Ser22, Phe41	Ile19, Ala22, Ser41, Val59	Ile19, Ala22, Ser41, Val59	Ile19, Ser22, Ser44	Ile24, Asn27, Gln46, Val64	Ile24, Asn27, Gln46, Val64	Ile24, Gln52
Cluster II	2.0	-	Cys13	Cys13, Tyr15	Cys13	Cys13	Cys13	Cys13	Cys13	Cys13	-	-	-
	2.5	Cys10, Cys21, Cys57	Cys10, Gly12, Cys16, Cys52	Cys10, Gly12, Cys16	Cys10, Gly12, Cys16, Cys52	Cys10, Gly12, Cys16, Cys52	Cys10, Gly12, Cys16, Cys52	Cys10, Gly12, Cys16, Cys52	Cys10, Gly12, Cys16, Cys52	Cys10, Gly12, Cys16, Cys55	Cys10, Cys13, Cys21, Cys57	Cys10, Cys13, Cys21, Cys57	Cys10, Cys13, Cys21, Cys63
	3.0	Cys13	Gly14	Cys52, Gly14	Gly14	Gly14	Gly14	Gly14, Glu54	Gly14, Glu54	Gly14	-	-	-
	3.5	Asp11	Asp11, His54, Ile57	Asp11, Ile57	Asp11, His15, Ile57	Asp11, Asn54, Ile57	Asp11, Ile57	Tyr27	Tyr27	Phe27	Asp11, Ala20	Asp11, Ala20	Asp11, Ala20
	4.0	Val5, Gly12, Thr19, Ala20, Ala39, Pro58, Gln59, Ile62	Val5, Gln15, Ala34, Pro53,	Val5, Ala34, Met54, Pro53	Val5, Ala34, His54, Pro53	Val5, His15, Ala34, Pro53	Val5, His15, Ala34, Pro53, Gln54	Val5, Lys11, Lys15, Ala34, Pro53	Val5, Lys11, Lys15, Pro53	Val5, Thr11, Asp15, Ala37, Pro56, Gln57	Val5, Gly12, Thr19, Ala39, Pro58, Gln59, Ile62	Val5, Gly12, Thr19, Ala39, Pro58, Gln59, Ile62	Gly12, Thr19, Ala45, Pro64, Gln65, Ile68
	4.5	Leu32, Ala61	Ala56	Ala56	Ala56	Ala56	Ala56	Ala56	Gly34, Ala56	Ala59	Leu32, Ala61	Leu32, Ala61	Val5, Leu32, Ala67
	5.0	Lys9	Arg9, Ile27	Arg9	Arg9, Ile27	Arg9, Ile27	Ser9, Ile27	Leu9, Val57	Leu9, Val57	Lys9, Val60	Lys9	Lys9	Lys9

[4Fe-4S] cluster	Distance in Å	*Archaeoglobus fulgidus*	*Desulfotomaculum reducens*	*Syntrophobacter fumaroxidans*	fosws39f7	fosws7f8	*Thermodesulfobac-terium commune*	*Desulfovibrio desulfuricans*	*Desulfovibrio vulgaris*	*Desulfobulbus* sp.	*Desulfotalea psychrophila*	*O. algarvensis* Delta 1 symbiont
Cluster I	2.0	-	-	-	-	-	-	-	-	-	-	-
	2.5	Cys25, Cys47, Cys50, Cys53	Cys25, Cys47, Cys50, Cys53	Cys25, Cys47, Cys50, Cys53	Cys25, Cys47, Cys50, Cys53	Cys25, Cys47, Cys50, Cys53	Cys25, Cys47, Cys50, Cys53	Cys25, Cys47, Cys50, Cys53	Cys25, Cys47, Cys50, Cys53	Cys25, Cys47, Cys50, Cys53	Cys25, Cys47, Cys50, Cys53	Cys25, Cys47, Cys50, Cys53
	3.0	-	-	-	-	-	-	Thr3	Thr3			
	3.5	Ser3, Asn41, Tyr51	Ser3, Tyr51	Ser3, Tyr51	Ser3, Asn41, Tyr51	Ser3, Tyr51	Ser3, Tyr51	Tyr51	Tyr51	Ser3, Tyr51	Ser3, Tyr51	Ser3, Phe51
	4.0	Pro26, Leu29, Met30, Trp48, Glu49, Ser52	Pro26, Leu29, Met30, Asn41, Trp48, Glu49, Cys52	Pro26, Leu29, Met30, Asn41, Trp48, Glu49, Asn52	Pro26, Leu29, Met30, Trp48, Glu49, Ser52	Pro26, Leu29, Met30, Asn41, Trp48, Glu49, Cys52	Pro26, Leu29, Met30, Asn41, Trp48, Glu49, Ser52	Pro26, Leu29, Met30, Asn41, Trp48, Glu49, Ser52	Pro26, Leu29, Met30, Asn41, Trp48, Glu49, Ser52	Pro26, Leu29, Met30, Asn41, Trp48, Glu49, Ser52	Pro26, Leu29, Met30, Asn41, Trp48, Glu49, Ser52	Pro26, Leu29, Met30, Asn41, Trp48, Glu49, Ser52
	4.5	-	-	-	-	-	-	-	-	-	-	-
	5.0	Asn27, Val64, Ile24, Met46	Ile24, Asn27, Val64, Gln46	Ile24, Asn27, Val64, Met46	Asn27, Val54, Met46	Asn27, Val64, Met46	Ile24, Asn27, Ile64, Gln46	Ile24, Asn27, Ala46	Ile24, Asn27, Ala46	Ile24, Asn27, Ala46, Val64	Ile24, Asn27, Gly46, Val64	Ile24, Asn27, Gln46, Val64
Cluster II	2.0	-	-	-	-	-	-	-	-	-	-	-
	2.5	Cys10, Cys21, Cys57	Cys10, Cys13, Cys21, Cys57	Cys10, Cys13, Cys21, Cys57	Cys10, Cys21, Cys57	Cys10, Cys13, Cys21, Cys57	Cys10, Cys13, Cys21, Cys57, Val20	Cys10, Cys13, Cys21, Cys57	Cys10, Cys13, Cys21, Cys57	Cys10, Cys13, Cys21, Cys57	Cys10, Cys13, Cys21, Cys57	Cys10, Cys13, Cys21, Cys57
	3.0	Cys13	-	-	Cys13	-	-	-	-	-	-	Thr59
	3.5	Asp11	Asp11, Ala20, Ile62	Asp11, Ala20	Asp11	Asp11, Ala20, Val59	Asp11	Asp11, Ala20, Ile62	Asp11, Ala20, Ile62	Asp11, Ala20	Asp11, Ala20, Ile62	Asp11, Ala20, Ile62
	4.0	Val5, Gly12, Thr19, Ala20, Ala39, Pro58, Gln59, Ile62	Val5, Gly12, Thr19, Ala39, Pro58, Gln59	Val5, Gly12, Thr19, Ala39, Pro58, Gln59, Ile62	Val5, Gly12, Thr19, Ala20, Ala39, Pro58, Ile62	Val5, Gly12, Thr19, Ala39, Pro58, Gln59, Ile62	Val5, Gly12, Thr19, Ala39, Pro58, Gln59, Ile62	Val5, Gly12, Thr19, Ala39, Pro58, Gln59	Val5, Gly12, Thr19, Ala39, Pro58, Gln59	Val5, Gly12, Thr19, Ala39, Pro58, Gln59, Ile62	Val5, Gly12, Thr19, Ala39, Pro58, Gln59	Val5, Gly12, Thr19, Ala39, Pro58, Thr59
	4.5	Leu32, Ala61	Leu32, Ala61	Leu32, Ala61	Leu32, Val59, Ala61	Leu32, Ala61	Leu32, Ala61	Leu32, Ala61	Leu32, Ala61	Leu32, Ala61	Leu32, Ala61	Leu32, Ala61
	5.0	Lys9	Lys9	Lys9	Lys9, Ile56	Lys9	Lys9	Lys9	Lys9	Lys9	Lys9	Lys9

Supplementary data material Table S3. AprA secondary structure element succession

SOB Apr lineage I

Secondary structure element succession AprA *Allochromatium vinosum*

AprA domains	No	*Archaeoglobus fulgidus* sequence	AA position	Sec. str. element	*Allochromatium vinosum* sequence	AA position	Sec. str. element
FAD-Binding site I (2-261 AA)	1	P T E V V E T D I L I I G	17-29	beta-sheet	T I I E D G I D V L V V G	5-17	beta-sheet
	2	F S G C G G A A Y E A A Y W A K	32-44	alpha-helix	L G G T G A A F E A R Y W→ **shortened**	20-32	alpha-helix
	3	K V T L V E	51-56	beta-sheet	K I V I A E	37-42	beta-sheet
	4	S A I	71-73	beta-sheet	Y A I **loop shortended**	57-59	beta-sheet
	5	L E D Y V R Y V T L D M	89-100	alpha-helix	P E D H V R Y A R I D L	72-83	alpha-helix
	6	E D L V A D Y A R H V D G T V H L F E K	106-125	alpha-helix	E D L L F D M A R H V D S A V H Q F E E W	89-109	alpha-helix
	7	P I W K T	129-133	beta-sheet	P L M R N **loop elongated**	112-116	beta-sheet
	8	K Y V R E	137-141	beta-sheet	A Y Q R E	121-125	beta-sheet
	9	Q I M I H	145-149	beta-sheet	Q I M I H	128-133	beta-sheet
	10	Y K P I I A E A A K M A V	153-165	alpha-helix	Y K P I V A E A A K K S→ **shortened**	137-148	alpha-helix
	11	N I Y E R V F I F E L L K D	169-182	beta-sheet	→F N R I C V T H L L M D **shortened**	153-164	beta-sheet
	12	A V A G A V G F S V	188-197	beta-sheet	R I A G A V G F N V	170-179	beta-sheet
	13	K F Y V F K A	201-207	beta-sheet	N Y H V F K S	183-189	beta-sheet
	14	A V I L A	209-213	beta-sheet	T V I V A	191-195	beta-sheet
	15	G A T	216-218	beta-sheet	G A S	198-200	beta-sheet
	16	A A	229-230	alpha-helix	G A	211-212	alpha-helix
	17	D T G	239-241	beta- sheet	S S G	221-223	beta- sheet
	18	S G Y Y M G L K A	242-250	alpha-helix	S A Y G L L I G A	224-232	alpha-helix
	19	M L T Q	253-256	beta-sheet	K M T Q	235-238	beta-sheet
Capping (262-393 AA)	20	P F R F K	263-267	beta-sheet	L A R F K	245-249	beta-sheet
	21	G A W F L F	274-279	alpha-helix	G A Y F L H	256-261	alpha-helix
	22	K A K N A	283-287	beta-sheet	Y T Q N G	265-269	beta-sheet
	23	I K	293-294	alpha-helix	missing		alpha-helix
	24	A	298	alpha-helix	**K E Y L D elongated alpha-helix**	288-292	alpha-helix
	25	Y G	306-307	alpha-helix	H R	297-298	alpha-helix
	26	T P L R N H Q V M L E I M D	314-327	alpha-helix	T C L R N H A L I S E V N A	305-318	alpha-helix
	27	P I M Y M H	331-335	beta-sheet	P I H M V	322-326	beta-sheet
	28	T E E A L A E L A	336-344	alpha-helix	T M E A→ **shortened**	327-330	alpha-helix
	29	K K K L K H I Y E E A F E D F L	348-363	alpha-helix	→L E E I G W H N F L **shortened**	336-344	alpha-helix
	30	S Q A L L W A C Q	368-375	alpha-helix	G Q A V L W A A T	350-358	alpha-helix
	31	S E A A P A	385-390	beta-sheet	P E L T T S	367-372	beta-sheet
FAD Binding site II (393-487 AA)	32	G F W	403-405	beta-sheet	G A W	385-387	beta-sheet
	33	K	419	alpha-helix	**missing**		alpha-helix
	34	R M T	427-429	beta-sheet	R M T	405-407	beta-sheet
	35	G L F A I	433-437	beta-sheet	G L F G A	411-415	beta-sheet
	36	S S G S F T E G R I A A K A A V R F I L E Q	449-470	alpha-helix	S S G S F T E G R L A A K A A C K Y I D D G **loop elongated**	427-448	alpha-helix
	37	D A V V E E L K K K	478-487	alpha-helix	D A Q I E R R R Q E	457-466	alpha-helix
Helical	38	P M E R F M Q	491-497	alpha-helix	P M E H Y R V	470-476	alpha-helix

(488-643 AA)	39	P W Q G L V R L Q K I M D E	514-527	alpha-helix	P R Q G L D R L Q K L M D E	493-506	alpha-helix
	40	Y K T	536-538	beta-sheet	Y M T	515-517	beta-sheet
	41	E K M L L Q R A L E L L A F L K E D L	540-557	alpha-helix	E N L L N I G L K K M K L L E E D L	519-536	alpha-helix
	42	L H E L M R A W E L V H R V W T A E A H V R H M L F	565-590	alpha-helix	I H E L L R A W E L K H R Q L T S E A V L H H T L F	544-569	alpha-helix
	43	Y R T	601-603	beta-sheet	Y R G	580-582	beta-sheet
	44	K C F V C S K Y D	614-622	beta-sheet	H V L T V S R R D	593-601	beta-sheet
	45	E W T F E K V P Y	627-635	beta-sheet	E Y T M E K A P C	606-614	beta-sheet

Structural deviations:

33-35	loop	
66-69	loop	**identical AA**
116-119	loop	**similar AA****
148-151	loop	**1.0Å RMSD backbone**
278-286	loop	** incl. identical AA
331-334	loop	
396-402	alpha-Helix missing	
452-454	loop	

620 AA total	
306	49,4%
437	70,5%
583	**94,0%**

Protein problems: **backbone**
Ala44, Asp250, Glu275, His335, Pro367, His380, Tyr407, Phe426, Val455

Secondary structure element succession AprA *Thiobacillus denitrificans* ATCC25259

AprA domains	No	*Archaeoglobus fulgidus* sequence	AA position	Sec. str. element	*Thiobacillus denitrificans* sequence	AA position	Sec. str. element
FAD-Binding	1	P T E V V E T D I L I I G	17-29	beta-sheet	T V V E D N I D I L V V G	5-17	beta-sheet
site I	2	F S G C G G A A Y E A A Y W A K	32-44	alpha-helix	L G G T G A A W E A R Y W→ **shortened**	20-32	alpha-helix
(2-261 AA)	3	K V T L V E	51-56	beta-sheet	K I V I A E	39-42	beta-sheet
	4	S A I	71-73	beta-sheet	Y A I **loop elongated**	57-59	beta-sheet
					M G T (new)	63-65	**beta-sheet**
					G E N (new)	68-70	**beta-sheet**
	5	L E D Y V R Y V T L D M	89-100	alpha-helix	P E D H V R Y A R M D L	72-83	alpha-helix
	6	E D L V A D Y A R H V D G T V H L F E K	106-125	alpha-helix	E D L L F D M A R H V D S A V H Q F E E **W** verlängert	89-109	alpha-helix
	7	P I W K T	129-133	beta-sheet	P I M R D **loop elongated**	112-116	beta-sheet
	8	K Y V R E	137-141	beta-sheet	H Y Q R E	121-125	beta-sheet
	9	Q I M I H	145-149	beta-sheet	Q I M I H	129-133	beta-sheet
	10	Y K P I I A E A A K M A V	153-165	alpha-helix	Y K P I V A E A A K K S A→ **shortened**	137-149	alpha-helix
	11	N I Y E R V F I F E L L K D	169-182	beta-sheet	→Y N R I C V T H L L M D **shortened**	153-164	beta-sheet
	12	A V A G A V G F S V	188-197	beta-sheet	R V A G A V G F N V	170-179	beta-sheet
	13	K F Y V F K A	201-207	beta-sheet	D Y H V F K S	183-189	beta-sheet
	14	A V I L A	209-213	beta-sheet	T V I L G	191-195	beta-sheet
	15	G A T	216-218	beta-sheet	G A S	198-200	beta-sheet
	16	A A	229-230	alpha-helix	G A	211-212	alpha-helix
	17	D T G	239-241	beta- sheet	S S G	221-223	beta- sheet
	18	S G Y Y M G L K A	242-250	alpha-helix	S A Y G L M I Q A	224-232	alpha-helix
	19	M L T Q	253-256	beta-sheet	K M T Q	235-238	beta-sheet
Capping	20	P F R F K	263-267	beta-sheet	L A R F K	245-249	beta-sheet
(262-393 AA)	21	G A W F L F	274-279	alpha-helix	G A Y F L H	256-261	alpha-helix

	22	K A K N A	283-287	beta-sheet	Y T Q N C	265-269	beta-sheet
	23	I K	293-294	alpha-helix	P A L T E alpha-helix elongated	280-284	alpha-helix
	24	A	298	alpha-helix	E	289	alpha-helix
	25	Y G	306-307	alpha-helix	H L	297-298	alpha-helix
	26	T P L R N H Q V M L E I M D	314-327	alpha-helix	T C L R N H A F I S E V N A	305-318	alpha-helix
	27	P I M Y M H	331-335	beta-sheet	P I H M V	322-326	beta-sheet
	28	T E E A L A E L A	336-344	alpha-helix	T M E A→ shortened	327-330	alpha-helix
	29	K K K L K H I Y E E A F E D F L	348-363	alpha-helix	→L E E I G W H N F L shortened	336-345	alpha-helix
	30	S Q A L L W A C Q	368-375	alpha-helix	G Q A V L W A A T	350-358	alpha-helix
	31	S E A A P A	385-390	beta-sheet	P E L T T S	367-372	beta-sheet
FAD Binding	32	G F W	403-405	beta-sheet	G A W	385-387	beta-sheet
site II	33	K	419	alpha-helix	missing		
(393-487 AA)	34	R M T	427-429	beta-sheet	R M T	405-407	beta-sheet
	35	G L F A I	433-437	beta-sheet	G L F G A	411-415	beta-sheet
	36	S S G S F T E G R I A A K A A V R F I L E Q	449-470	alpha-helix	S S G S F T E G R L A A C K Y I D D G loop elongated.	427-448	alpha-helix
	37	D A V V E E L K K K	478-487	alpha-helix	D E Q I Q R R E E	457-466	alpha-helix
Helical	38	P M E R F M Q	491-497	alpha-helix	P M E H Y R I	470-476	alpha-helix
(488-643 AA)	39	P W Q G L V R L Q K I M D E	514-527	alpha-helix	P R Q G L D R L Q K L M D E	493-506	alpha-helix
	40	Y K T	536-538	beta-sheet	Y M T	515-517	beta-sheet
	41	E K M L L Q R A L E L L A F L K E D L	540-557	alpha-helix	D K L L Q I G L K K L K L M E E D L	519-536	alpha-helix
	42	L H E L M R A W E L V H R V W T A E A H V R H M L F	565-590	alpha-helix	I H E L L R A W E L K H R H L T S E A V M Q H T L F	544-569	alpha-helix
	43	Y R T	601-603	beta-sheet	Y R G	580-582	beta-sheet
	44	K C F V C S K Y D	614-622	beta-sheet	H V L T V S R R D	593-601	beta-sheet
	45	E W T F E K V P Y	627-635	beta-sheet	E Y M E K A P C	606-614	beta-sheet

Structural deviations:

33-35	loop
66-69	loop-beta
116-119	loop
148-151	loop
278-286	loop-helix-loop
331-334	loop
396-402	alpha-helix missing
452-454	loop

identical AA	**307**	49,4%
similar AA**	**424**	68,2%
1.0Å RMSD backbone	**584**	**93,7%**

** incl. identical AA

622 AA total

Protein problems: **backbone**
Asn35, Ala44, Asp250, Glu275, Val 286, Pro367, His380, Phe426, Val455

Secondary structure element succession AprA *Cdt.* Ruthia magnifica

AprA domains	No	*Archaeoglobus fulgidus* sequence	AA position	Sec. str. element	*Cdt. Ruthia magnifica* sequence	AA position	Sec. str. element
FAD-Binding	1	P T E V V E T D I L I I G	17-29	beta-sheet	T I V E D N I D I L V V G	5-17	beta-sheet
site I	2	F S G C G G A A Y E A A Y W A K	32-44	alpha-helix	L G G T G A A Y E A R → shortened	20-30	alpha-helix
(2-261 AA)	3	K V T L V E	51-56	beta-sheet	K I I I A E	39-42	beta-sheet
	4	S A I	71-73	beta-sheet	Y A I loop shortened	57-59	beta-sheet
	5	L E D Y V R Y V T L D M	89-100	alpha-helix	P E D H V R Y A R M D L	72-83	alpha-helix
	6	E D L V A D Y A R H V D G T V H L F E K	106-125	alpha-helix	E D L L F D M A R H V D S A V H K F E E W	89-109	alpha-helix

	7	P I W K T	129-133	beta-sheet	P L M K D loop elongated	112-116	beta-sheet
	8	K Y V R E	137-141	beta-sheet	A Y M R E	124-128	beta-sheet
	9	Q I M I H	145-149	beta-sheet	Q I M I H	132-136	beta-sheet
	10	Y K P I I A E A A K M A V	153-165	alpha-helix	Y K P I V A E A A T K Q → shortened	140-152	alpha-helix
	11	N I Y E R V F I F E L L K D	169-182	beta-sheet	→Y N R I M V T H L L M D shortened	156-167	beta-sheet
	12	A V A G A V G F S V	188-197	beta-sheet	R I A G A V G F N V	173-182	beta-sheet
	13	K F Y V F K A	201-207	beta-sheet	N Y H V F K S	186-192	beta-sheet
	14	A V I L A	209-213	beta-sheet	T T I V G	194-198	beta-sheet
	15	G A T	216-218	beta-sheet	G A S	201-203	beta-sheet
	16	A A	229-230	alpha-helix	G M	214-215	alpha-helix
	17	D T G	239-241	beta- sheet	S S G	224-226	beta- sheet
	18	S G Y Y M G L K A	242-250	alpha-helix	S A Y G L L I E A	227-235	alpha-helix
	19	M L T Q	253-256	beta-sheet	K M T Q	238-241	beta-sheet
Capping	20	P F R F K	263-267	beta-sheet	L A R F K	248-252	beta-sheet
(262-393 AA)	21	G A W F L F	274-279	alpha-helix	G A Y F L H	259-264	alpha-helix
	22	K A K N A	283-287	beta-sheet	Y T Q N G	268-272	beta-sheet
	23	I K	293-294	alpha-helix	W F P (new)	281-283	**beta-sheet**
					K M V (new)	287-289	**beta-sheet**
	24	A	298	alpha-helix	K E	291-292	alpha-helix
	25	Y G	306-307	alpha-helix	H L	300-301	alpha-helix
	26	T P L R N H Q V M L E I M D	314-327	alpha-helix	T C L R N H A F I S E V N A	308-321	alpha-helix
	27	P I M Y M H	331-335	beta-sheet	P I H M V	325-329	beta-sheet
	28	T E E A L A E L A	336-344	alpha-helix	T M E A→ shortened	330-333	alpha-helix
	29	K K K L K H I Y E E A F E D F L	348-363	alpha-helix	→L E E V G W E N F L shortened	339-348	alpha-helix
	30	S Q A L L W A C Q	368-375	alpha-helix	G Q A V L W A A T	353-361	alpha-helix
	31	S E A A P A	385-390	beta-sheet	P E L T T S	370-375	beta-sheet
FAD Binding	32	G F W	403-405	beta-sheet	G A W	388-390	beta-sheet
site II	33	K	419	alpha-helix	missing		
(393-487 AA)	34	R M T	427-429	beta-sheet	R M T	408-410	beta-sheet
	35	G L F A I	433-437	beta-sheet	G L F G A	411-415	beta-sheet
	36	S S G S F T E G R I A A K A A V R F I L E Q	449-470	alpha-helix	S S G S F T E G R L A A K A A C K Y I D D G loop elongated	430-451	alpha-helix
	37	D A V V E E L K K K	478-487	alpha-helix	D K Q I A E R K E Q	460-469	alpha-helix
Helical	38	P M E R F M Q	491-497	alpha-helix	P L E N Y T I	473-479	alpha-helix
(488-643 AA)	39	P W Q G L V R L Q K I M D E	514-527	alpha-helix	P M S G L Q R L Q K L M D E	496-509	alpha-helix
	40	Y K T	536-538	beta-sheet	Y V T	518-520	beta-sheet
	41	E K M L L Q R A L E L L A F L K E D L	540-557	alpha-helix	D K L L N I G L K K L A I L E E D L	522-539	alpha-helix
	42	L H E L M R A W E L V H R V W T A E A H V R H M L F	565-590	alpha-helix	F H Q L M R G W E L R H R H R T S E C V T Q H T L F	547-572	alpha-helix
	43	Y R T	601-603	beta-sheet	Y R G	583-585	beta-sheet
	44	K C F V C S K Y D	614-622	beta-sheet	H V L T V S H R D	593-601	beta-sheet
	45	E W T F E K V P Y	627-635	beta-sheet	K Y T L E K A P C	609-617	beta-sheet

Structural deviations:
32-35 loop
66-69 loop-beta
117-123 loop

identical AA **298** 47,7%
similar AA** **419** 67,0%
625 AA total

Protein problems: **backbone**
Asn35, Ala44, Ala124, Lys154, Val155, Asp253, Glu278, Ser286, Val289, His338, Pro370, His383*, Phe429*, Val458

151-154	loop	**1.0Å RMSD Bb**	**583**	**93,3%**
281-289	beta-loop-beta	** incl. identical AA		
334-337	loop			
399-405	alpha-helix missing			
455-457	loop			

Secondary structure element succession AprA *Cdt.* Pelagibacter ubique

AprA domains	No	*Archaeoglobus fulgidus* sequence	AA position	Sec. str. element	*Cdt.* Pelagibacter ubique sequence	AA position	Sec. str. element
FAD-Binding	1	P T E V V E T D I L I I G	17-29	beta-sheet	K T H F E D C D V L V V G	5-17	beta-sheet
site I	2	F S G C G G A A Y E A A Y W A K	32-44	alpha-helix	M A G T G A T F E A R H W→ **shortened**	20-32	alpha-helix
(2-261 AA)	3	K V T L V E	51-56	beta-sheet	K I I C V E	39-42	beta-sheet
	4	S A I	71-73	beta-sheet	Y A I **loop shortened**	57-59	beta-sheet
	5	L E D Y V R Y V T L D M	89-100	alpha-helix	P E D H V R Y A R N D L	72-83	alpha-helix
	6	E D L V A D Y A R H V D G T V H L F E K	106-125	alpha-helix	E D L G Y D M A R H V D S T V H M F D E W	89-109	alpha-helix
	7	P I W K T	129-133	beta-sheet	P M M K N **loop elongated**	112-116	beta-sheet
	8	K Y V R E	137-141	beta-sheet	R Y L R E	121-125	beta-sheet
	9	Q I M I H	145-149	beta-sheet	Q I M I H	129-134	beta-sheet
	10	Y K P I I A E A A K M A V	153-165	alpha-helix	Y K P I V A E A A K K A→ **shortened**	137-148	alpha-helix
	11	N I Y E R V F I F E L L K D	169-182	beta-sheet	→Y N R I M I T H L L M D **shortened**	151-164	beta-sheet
	12	A V A G A V G F S V	188-197	beta-sheet	R V G G A V G F N M	170-179	beta-sheet
	13	K F Y V F K A	201-207	beta-sheet	D F H V F R A	183-189	beta-sheet
	14	A V I L A	209-213	beta-sheet	T V I V A	191-195	beta-sheet
	15	G A T	216-218	beta-sheet	G A S	198-200	beta-sheet
	16	A A	229-230	alpha-helix	G M	211-212	alpha-helix
	17	D T G	239-241	beta- sheet	S N G	221-223	beta- sheet
	18	S G Y Y M G L K A	242-250	alpha-helix	S A Y A L P I A V	224-232	alpha-helix
	19	M L T Q	253-256	beta-sheet	K M T Q	235-238	beta-sheet
Capping	20	P F R F K	263-267	beta-sheet	L C R F K	245-249	beta-sheet
(262-393 AA)	21	G A W F L F	274-279	alpha-helix	G A Y F L H	256-261	alpha-helix
	22	K A K N A	283-287	beta-sheet	Y T Q N A	265-269	beta-sheet
	23	I K	293-294	alpha-helix	**missing**		
	24	A	298	alpha-helix	**missing**		
	25	Y G	306-307	alpha-helix	**missing**		
	26	T P L R N H Q V M L E I M D	314-327	alpha-helix	T C L R N H A F I Q E T I A	297-310	alpha-helix
	27	P I M Y M H	331-335	beta-sheet	P I H M V	314-318	beta-sheet
	28	T E E A L A E L A	336-344	alpha-helix	T T E A→ **shortened**	319-322	alpha-helix
	29	K K K L K H I Y E E A F E D F L	348-363	alpha-helix	→L E T V G W E N F L **shortened**	328-337	alpha-helix
	30	S Q A L L W A C Q	368-375	alpha-helix	G Q A V V W A S Q	342-350	alpha-helix
	31	S E A A P A	385-390	beta-sheet	P E L T T S	359-364	beta-sheet
FAD Binding	32	G F W	403-405	beta-sheet	G A W	377-379	beta-sheet
site II	33	K	419	alpha-helix	**missing**		
(393-487 AA)	34	R M T	427-429	beta-sheet	R M L	397-399	beta-sheet
	35	G L F A I	433-437	beta-sheet	G L F G A	403-407	beta-sheet
	36	S S G S F T E G R I A A K A A V R F I L E Q	449-470	alpha-helix	S S G S F T E G R L A A K A A V K Y I Q D K **loop elongated**	419-440	alpha-helix
	37	D A V V E E L K K K	478-487	alpha-helix	D K Q C E D F K T A	449-458	alpha-helix

Helical	38	P M E R F M Q	491-497	alpha-helix	P L E T Y Q V	462-468	alpha-helix
(488-643 AA)	39	P W Q G L V R L Q K I M D E	514-527	alpha-helix	P I Q G L Q R L Q R I M D E	485-498	alpha-helix
	40	Y K T	536-538	beta-sheet	Y M V	507-509	beta-sheet
	41	E K M L L Q R A L E L L A F L K E D L	540-557	alpha-helix	G N M L K R G L E L L A W L E E D L	511-528	alpha-helix
	42	L H E L M R A W E L V H R V W T A E A H V R H M L F	565-590	alpha-helix	L H Q L M R A W E L K H R A L T S Q C V T E H T M F	536-561	alpha-helix
	43	Y R T	601-603	beta-sheet	Y R G	572-574	beta-sheet
	44	K C F V C S K Y D	614-622	beta-sheet	H C L T V S R R D	585-593	beta-sheet
	45	E W T F E K V P Y	627-635	beta-sheet	K F S L E K V P V	598-606	beta-sheet

Structural deviations:

32-35	loop
66-69	loop
117-119	loop
148-151	loop
278-286	loop
323-326	loop
388-394	alpha-helix missing
444-446	loop

	614 AA total	
identical AA	**309**	50,3%
similar AA**	**431**	70,2%
1.0Å RMSD Bb	**572**	**93,2%**

** incl. identical AA

Protein problems: **backbone**
Met36, Ala44, Asp250, Glu288, Pro359, His372*, Phe418*

Secondary structure element succession AprA environmental sequence EBAC2C11

AprA domains	No	*Archaeoglobus fulgidus* sequence	AA position	Sec. str. element	Environmental sequence EBAC2C11 sequence	AA position	Sec. str. element
FAD-Binding	1	P T E V V E T D I L I I G	17-29	beta-sheet	K T V F V D S D I L V I G	5-17	beta-sheet
site I	2	F S G C G G A A Y E A A Y W A K	32-44	alpha-helix	F G G C G A A Y E S R Y W→ **shortened**	20-32	alpha-helix
(2-261 AA)	3	K V T L V E	51-56	beta-sheet	K V V V V E	39-42	beta-sheet
	4	S A I	71-73	beta-sheet	Y A I **loop shortened**	57-59	beta-sheet
	5	L E D Y V R Y V T L D M	89-100	alpha-helix	P E D Y V R Y Q R N D L	72-83	alpha-helix
	6	E D L V A D Y A R H V D G T V H L F E K	106-125	alpha-helix	E D L G Y D I G R H V D S T V H K F E E **W verlängert**	89-109	alpha-helix
	7	P I W K T	129-133	beta-sheet	P I M T D **loop elongated**	112-116	beta-sheet
	8	K Y V R E	137-141	beta-sheet	R Y Q R E	121-125	beta-sheet
	9	Q I M I H	145-149	beta-sheet	Q I M I H	129-134	beta-sheet
	10	Y K P I I A E A A K M A V	153-165	alpha-helix	Y K P I V A E A A R K A→ **shortened**	137-148	alpha-helix
	11	N I Y E R V F I F E L L K D	169-182	beta-sheet	→A V Y N R I M V T H L L M D **shortened**	151-164	beta-sheet
	12	A V A G A V G F S V	188-197	beta-sheet	R V A G A V G F N V	170-179	beta-sheet
	13	K F Y V F K A	201-207	beta-sheet	D F Y V F Q S	183-189	beta-sheet
	14	A V I L A	209-213	beta-sheet	A V I V A	191-195	beta-sheet
	15	G A T	216-218	beta-sheet	G A S	198-200	beta-sheet
	16	A A	229-230	alpha-helix	G M	211-212	alpha-helix
	17	D T G	239-241	beta- sheet	S S A	221-223	beta- sheet
	18	S G Y Y M G L K A	242-250	alpha-helix	S A Y A L P I R V	224-232	alpha-helix
	19	M L T Q	253-256	beta-sheet	K M T Q	235-238	beta-sheet
Capping	20	P F R F K	263-267	beta-sheet	L T R F K	245-249	beta-sheet
(262-393 AA)	21	G A W F L F	274-279	alpha-helix	G A Y F L H	256-261	alpha-helix
	22	K A K N A	283-287	beta-sheet	Y T Q N G	265-269	beta-sheet

	23	I K	293-294	alpha-helix	missing		
	24	A	298	alpha-helix	M V G D Y V N H alpha-helix elongated	285-292	alpha-helix
	25	Y G	306-307	alpha-helix	**missing**		
	26	T P L R N H Q V M L E I M D	314-327	alpha-helix	T C L R N H A F L K E V E A	297-310	alpha-helix
	27	P I M Y M H	331-335	beta-sheet	P I R M V	314-318	beta-sheet
	28	T E E A L A E L A	336-344	alpha-helix	T K E A→ **shortened**	319-322	alpha-helix
	29	K K K L K H I Y E E A F E D F L	348-363	alpha-helix	→K E E V G W E N F L **shortened**	328-337	alpha-helix
	30	S Q A L L W A C Q	368-375	alpha-helix	G Q A V V W A A N	342-350	alpha-helix
	31	S E A A P A	385-390	beta-sheet	P E L V M S	359-364	beta-sheet
FAD Binding	32	G F W	403-405	beta-sheet	G A W	377-379	beta-sheet
site II	33	K	419	alpha-helix	missing		alpha-helix
(393-487 AA)	34	R M T	427-429	beta-sheet	R M M	397-399	beta-sheet
	35	G L F A I	433-437	beta-sheet	G L F G A	403-407	beta-sheet
	36	S S G S F T E G R I A A K A A V R F I L E Q	449-470	alpha-helix	S S G S F T E G R L A G K A A N K Y V D D→ **shortened, loop elongated**	419-439	alpha-helix
	37	D A V V E E L K K K	478-487	alpha-helix	E E E Y L E L K E Q	449-458	alpha-helix
Helical	38	P M E R F M Q	491-497	alpha-helix	P L E T Y R V	462-468	alpha-helix
(488-643 AA)	39	P W Q G L V R L Q K I M D E	514-527	alpha-helix	P L S G L Q R L E K I M D E	485-498	alpha-helix
	40	Y K T	536-538	beta-sheet	Y M V	507-509	beta-sheet
	41	E K M L L Q R A L E L L A F L K E D L	540-557	alpha-helix	E P L M T R G I E L L K M L K E D L	511-528	alpha-helix
	42	L H E L M R A W E L V H R V W T A E A H V R H M L F	565-590	alpha-helix	L H Q L Q R A W E L H H R V L A S E C V T A H T M F	536-561	alpha-helix
	43	Y R T	601-603	beta-sheet	Y R G	572-574	beta-sheet
	44	K C F V C S K Y D	614-622	beta-sheet	H C F T L S Q Y D	585-593	beta-sheet
	45	E W T F E K V P Y	627-635	beta-sheet	E F E M E K A P V	598-606	beta-sheet

Structural deviations:

32-35	loop
66-69	loop
117-119	loop
148-151	loop
278-286	loop
323-326	loop
388-394	alpha-helix missing
440-442	loop

	613 AA total	
identical AA	**316**	51,5%
similar AA**	**426**	69,5%
1.0Å RMSD Bb	**570**	**93,0%**

** incl. identical AA

Protein problems: **backbone**
Ala44, Thr119, Asp250, Val295, Pro326, His327, Pro359, His372, Phe418, Thr442, Asn443

Crenarchaeal SRP

Secondary structure element succession AprA *Pyrobaculum calidifontis*

AprA domains	No	*Archaeoglobus fulgidus* sequence	AA position	Sec. str. element	*Pyrobaculum calidifontis* sequence	AA position	Sec. str. element
FAD-Binding	1	P T E V V E T D I L I I G	17-29	beta-sheet	P T K V V E T D I L V V G	7-19	beta-sheet
site I	2	F S G C G G A A Y E A A Y W A K	32-44	alpha-helix	M A G C G A V F E A K Y→ **shortened**	22-33	alpha-helix
(2-261 AA)	3	K V T L V E	51-56	beta-sheet	K V T L V E	30-45	beta-sheet
	4	S A I	71-73	beta-sheet	S A T **loop shortened**	60-62	beta-sheet
	5	L E D Y V R Y V T L D M	89-100	alpha-helix	P E E F V R Y V R N D→ shortened	76-86	alpha-helix

	6	E D L V A D Y A R H V D G T V H L F E K	106-125	alpha-helix	E D L V Y D I A R H M T S T I K L F D M **W** **verlängert**	93-113	alpha-helix
	7	P I W K T	129-133	beta-sheet	P I W R D **loop elongated**	116-120	beta-sheet
	8	K Y V R E	137-141	beta-sheet	K Y L R T	125-129	beta-sheet
	9	Q I M I H	145-149	beta-sheet	Q H P I H	133-137	beta-sheet
	10	Y K P I I A E A A K M A V	153-165	alpha-helix	Y K A I I A E P C R K → **shortened.**	141-151	alpha-helix
	11	N I Y E R V F I F E L L K D	169-182	beta-sheet	→Y E R V F V T H P L L D **shortened**	157-168	beta-sheet
	12	A V A G A V G F S V	188-197	beta-sheet	R I A G V V G F H V	174-183	beta-sheet
	13	K F Y V F K A	201-207	beta-sheet	T F Y V F K A	187-193	beta-sheet
	14	A V I L A	209-213	beta-sheet	A V I V A	195-199	beta-sheet
	15	G A T	216-218	beta-sheet	G T S	202-204	beta-sheet
	16	A A	229-230	alpha-helix	G L	215-216	alpha-helix
	17	D T G	239-241	beta- sheet	A S G	225-227	beta- sheet
	18	S G Y Y M G L K A	242-250	alpha-helix	S A Y A I P L L A	228-236	alpha-helix
	19	M L T Q	253-256	beta-sheet	E T V N	239-242	beta-sheet
Capping	20	P F R F K	263-267	beta-sheet	V V R F K	249-253	beta-sheet
(262-393 AA)	21	G A W F L F	274-279	alpha-helix	G F P Y L L	260-265	alpha-helix
	22	K A K N A	283-287	beta-sheet	R S T D V	269-273	beta-sheet
	23	I K	293-294	alpha-helix	**missing**		
	24	A	298	alpha-helix	E	288	alpha-helix
	25	Y G	306-307	alpha-helix	Y A	296-297	alpha-helix
	26	T P L R N H Q V M L E I M D	314-327	alpha-helix	T P I R T W V T I Q N L K E	304-317	alpha-helix
	27	P I M Y M H	331-335	beta-sheet	P D I M Q	321-325	beta-sheet
	28	T E E A L A E L A	336-344	alpha-helix	**missing**		
	29	K K K L K H I Y E E A F E D F L	348-363	alpha-helix	**missing**		
	30	S Q A L L W A C Q	368-375	alpha-helix	T Q V I Y W A S Q	349-357	alpha-helix
	31	S E A A P A	385-390	beta-sheet	S E L L P T	366-371	beta-sheet
FAD Binding	32	G F W	403-405	beta-sheet	G M W	384-386	beta-sheet
site II	33	K	419	alpha-helix	**missing**		
(393-487 AA)	34	R M T	427-429	beta-sheet	R M L	404-406	beta-sheet
	35	G L F A I	433-437	beta-sheet	G L F G A	410-414	beta-sheet
	36	S S G S F T E G R I A A K A A V R F I L E Q	449-470	alpha-helix	S S G S F T E G R I A G K S A A R Y V L T Q	426-447	alpha-helix
	37	D A V V E E L K K K	478-487	alpha-helix	N D T I E R Y K E I	457-466	alpha-helix
Helical	38	P M E R F M Q	491-497	alpha-helix	P L E W Y H K	470-476	alpha-helix
(488-643 AA)					**T P (new)**	483-484	**alpha-Helix**
	39	P W Q G L V R L Q K I M D E	514-527	alpha-helix	W Y Q L L T R L Q K I M D E	503-516	alpha-helix
	40	Y K T	536-538	beta-sheet	Y T T	525-527	beta-sheet
	41	E K M L L Q R A L E L L A F L K E D L	540-557	alpha-helix	M Y M L G R A W E L L K M L E E D F	529-546	alpha-helix
	42	L H E L M R A W E L V H R V W T A E A H V R H M L F	565-590	alpha-helix	L H E L L R V W E V Y H R L I V G Q A V V F S M M N	553-579	alpha-helix
	43	Y R T	601-603	beta-sheet	F N A	588-590	beta-sheet
	44	K C F V C S K Y D	614-622	beta-sheet	H V F T H V R R D	601-609	beta-sheet
	45	E W T F E K V P Y	627-635	beta-sheet	Q W S F R T S P V	614-622	beta-sheet

Str. deviations:

35-37	loop
62-66	loop
121-124	loop
152-155	loop

	628 AA total	
identical AA	**299**	47,6%
similar AA**	**425**	67,7%
1.0Å RMSD Bb	**562**	**89,5%**

Protein problems: **backbone**
Ala47, Phe67, Ser68, Pro94, Glu155, Asp254, His379, Phe425, Asp450, Pro453, Val454, Pro487, Leu490, Ile496

277-284 loop
327-341 loop
395-402 alpha-helix missing
449-453 loop
485-494 alpha-loop
581-586 loop

** incl. identical AA

Secondary structure element succession AprA *Caldivirga maquilingensis*

AprA domains	No	*Archaeoglobus fulgidus* sequence	AA position	Sec. str. element	*Caldivirga maquilingensis* sequence	AA position	Sec. str. element
FAD-Binding	1	P T E V V E T D I L I I G	17-29	beta-sheet	R V K Q V D S D I L I I G	5-17	beta-sheet
site I	2	F S G C G G A A Y E A A Y W A K	32-44	alpha-helix	M A G T G A A W E A K Y W → **shortened**	20-32	alpha-helix
(2-261 AA)	3	K V T L V E	51-56	beta-sheet	R I V L A E	37-42	beta-sheet
	4	S A I	71-73	beta-sheet	S A I **loop shortened**	57-59	beta-sheet
	5	L E D Y V R Y V T L D M	89-100	alpha-helix	V E D Y V K Y V R G D L	72-83	alpha-helix
	6	E D L V A D Y A R H V D G T V H L F E K	106-125	alpha-helix	E D L V Y D Y A R H V D S T V H L F D E W	89-109	alpha-helix
	7	P I W K T	129-133	beta-sheet	P I W P A	112-116	beta-sheet
	8	K Y V R E	137-141	beta-sheet	C Y V R E	120-124	beta-sheet
	9	Q I M I H	145-149	beta-sheet	Q I M I H	128-132	beta-sheet
	10	Y K P I I A E A A K M A V	153-165	alpha-helix	Y K A I V A E A A R K A I	136-148	alpha-helix
	11	N I Y E R V F I F E L L K D	169-182	beta-sheet	N I M N R V M V T H L L K S	152-165	beta-sheet
	12	A V A G A V G F S V	188-197	beta-sheet	R V A G A L G F N V	171-180	beta-sheet
	13	K F Y V F K A	201-207	beta-sheet	T I Y V F K A	184-190	beta-sheet
	14	A V I L A	209-213	beta-sheet	A I I M A	192-196	beta-sheet
	15	G A T	216-218	beta-sheet	G G S	199-201	beta-sheet
	16	A A	229-230	alpha-helix	G L	212-213	alpha-helix
	17	D T G	239-241	beta- sheet	S S A	222-224	beta- sheet
	18	S G Y Y M G L K A	242-250	alpha-helix	S S Y G M M I E S	225-233	alpha-helix
	19	M L T Q	253-256	beta-sheet	V M T M	236-239	beta-sheet
Capping	20	P F R F K	263-267	beta-sheet	V P R F K	246-250	beta-sheet
(262-393 AA)	21	G A W F L F	274-279	alpha-helix	G A Y Q L M	257-262	alpha-helix
	22	K A K N A	283-287	beta-sheet	R I S N V	266-270	beta-sheet
	23	I K	293-294	alpha-helix	missing		
	24	A	298	alpha-helix	**missing**		
	25	Y G	306-307	alpha-helix	**missing**		
	26	T P L R N H Q V M L E I M D	314-327	alpha-helix	→T L R V Y A Q R L E W I N **shortened**	302-314	alpha-helix
	27	P I M Y M H	331-335	beta-sheet	P S L M R	318-322	beta-sheet
	28	T E E A L A E L A	336-344	alpha-helix	T D E T V K K G → **shortened**	323-330	alpha-helix
	29	K K K L K H I Y E E A F E D F L	348-363	alpha-helix	→ E D F L **shortened**	339-342	alpha-helix
	30	S Q A L L W A C Q	368-375	alpha-helix	S Q V A I W A G Q	347-352	alpha-helix
	31	S E A A P A	385-390	beta-sheet	Y E V I T T	364-369	beta-sheet
FAD Binding	32	G F W	403-405	beta-sheet	G A W	382-384	beta-sheet
site II	33	K	419	alpha-helix	**missing**		
(393-487 AA)	34	R M T	427-429	beta-sheet	R M T	413-415	beta-sheet
	35	G L F A I	433-437	beta-sheet	G L F C A	419-423	beta-sheet
	36	S S G S F T E G R I A A K A A V R F I L E Q	449-470	alpha-helix	S S G S F T E G R L A A K S A V L Y L M D H	435-456	alpha-helix
	37	D A V V E E L K K K	478-487	alpha-helix	K G Q V D S M I S K	465-474	alpha-helix

Helical	38	P M E R F M Q	491-497	alpha-helix	P L E R W E E **loop elongated**	478-484	alpha-helix
(488-643 AA)	39	P W Q G L V R L Q K I M D E	514-527	alpha-helix	W K Q G L F R L Q K I M D E	506-519	alpha-helix
	40	Y K T	536-538	beta-sheet	Y T T	528-530	beta-sheet
	41	E K M L L Q R A L E L L A F L K E D L	540-557	alpha-helix	E W M L N R A I E L L Q F L K E D F	532-549	alpha-helix
	42	L H E L M R A W E L V H R V W T A E A H V R H M L F	565-590	alpha-helix	W H E L M R T W E L W H R I L T A E A V V R H M L F	558-583	alpha-helix
	43	Y R T	601-603	beta-sheet	V R A	594-596	beta-sheet
	44	K C F V C S K Y D	614-622	beta-sheet	H V F V N S R Y D	607-615	beta-sheet
	45	E W T F E K V P Y	627-635	beta-sheet	R W E L W K V P V	620-628	beta-sheet

Str. deviations:

33-35	loop
66-69	loop
276-282	loop
298-300	loop
331-337	loop
394-410	alpha helix missing
460-462	loop
490-497	loop
554-556	loop

	635 AA	
identical AA	**336**	52,9
similar AA**	**444**	70,0
1.0Å RMSD Bb	**587**	**92,4%**

** incl. identical AA

Protein problems: **backbone**
Ala44, Pro115, Asp251, Glu281, Ile283, Thr301, Phe338, His377, Phe434, Arg403, Asp462, Ile463, Pro498, Asp557

SRB and affiliated SOB Apr lineage II

Secondary structure element succession AprA *Desulfotomaculum reducens*

AprA domains	No	*Archaeoglobus fulgidus* sequence	AA position	Sec. str. element	*Desulfotomaculum reducens* sequence	AA position	Sec. str. element
FAD-Binding	1	P T E V V E T D I L I I G	17-29	beta-sheet	E T V V V N T D I L I L G	6-18	beta-sheet
site I	2	F S G C G G A A Y E A A Y W A K	32-44	alpha-helix	M A A C G A A V E A A Y W A K	21-35	alpha-helix
(2-261 AA)	3	K V T L V E	51-56	beta-sheet	K I T L V D	40-45	beta-sheet
	4	S A I	71-73	beta-sheet	S A I **loop shortened**	60-62	beta-sheet
	5	L E D Y V R Y V T L D M	89-100	alpha-helix	V E D Y V K Y V K N D L	74-85	alpha-helix
	6	E D L V A D Y A R H V D G T V H L F E K	106-125	alpha-helix	D D Q V A D I A R H V D S S V H L F E K **W** **verlängert**	91-111	alpha-helix
	7	P I W K T	129-133	beta-sheet	P I W T N	114-118	beta-sheet
	8	K Y V R E	137-141	beta-sheet	N Y V R G	122-126	beta-sheet
	9	Q I M I H	145-149	beta-sheet	Q I M L N	130-134	beta-sheet
	10	Y K P I I A E A A K M A V	153-165	alpha-helix	Y K I I V A E A A K N A L	138-150	alpha-helix
	11	N I Y E R V F I F E L L K D	169-182	beta-sheet	N I Y E R V Y I C E P I M D **loop shortened**	154-167	beta-sheet
	12	A V A G A V G F S V	188-197	beta-sheet	R I A G A I G F S T	170-179	beta-sheet
	13	K F Y V F K A	201-207	beta-sheet	K V Y V F K A	183-189	beta-sheet
	14	A V I L A	209-213	beta-sheet	A V L A S	191-195	beta-sheet
	15	G A T	216-218	beta-sheet	G A V	198-200	beta-sheet
	16	A A	229-230	alpha-helix	G L	211-212	alpha-helix
	17	D T G	239-241	beta- sheet	S S G	221-223	beta- sheet
	18	S G Y Y M G L K A	242-250	alpha-helix	S S A Y F T M V A	224-232	alpha-helix
	19	M L T Q	253-256	beta-sheet	E M T C	235-238	beta-sheet

Capping	20	P F R F K	263-267	beta-sheet	P V R F K	245-249	beta-sheet
(262-393 AA)	21	G A W F L F	274-279	alpha-helix	G A W F L L	256-261	alpha-helix
	22	K A K N A	283-287	beta-sheet	R A V N G	265-269	beta-sheet
	23	I K	293-294	alpha-helix	**Y** M V alpha-helix elongated	274-276	alpha-helix
	24	A	298	alpha-helix	P	280	alpha-helix
	25	Y G	306-307	alpha-helix	Y G	288-289	alpha-helix
	26	T P L R N H Q V M L E I M D	314-327	alpha-helix	A N L R N Y L G M L D V S D	296-309	alpha-helix
	27	P I M Y M H	331-335	beta-sheet	P L F M E	313-317	beta-sheet
	28	T E E A L A E L A	336-344	alpha-helix	T D E A I A N L A **loop elongated**	318-326	alpha-helix
	29	K K K L K H I Y E E A F E D F L	348-363	alpha-helix	K K K M K E L E N E A W E D F L	337-352	alpha-helix
	30	S Q A L L W A C Q	368-375	alpha-helix	A Q A I L W A A S	357-365	alpha-helix
	31	S E A A P A	385-390	beta-sheet	S E I A A A	374-379	beta-sheet
FAD Binding	32	G F W	403-405	beta-sheet	G A W	392-394	beta-sheet
site II	33	K	419	alpha-helix	**missing**		
(393-487 AA)	34	R M T	427-429	beta-sheet	N M T	412-414	beta-sheet
	35	G L F A I	433-437	beta-sheet	G L F A A	418-422	beta-sheet
	36	S S G S F T E G R I A A K A A V R F I L E Q	449-470	alpha-helix	S S G S H A E G R I A G K S M V R F V V E N	434-455	alpha-helix
	37	D A V V E E L K K K	478-487	alpha-helix	D A K V E E L K A K	463-472	alpha-helix
Helical	38	P M E R F M Q	491-497	alpha-helix	P L A V W E E	476-482	alpha-helix
(488-643 AA)	39	P W Q Q G L V R L Q K I M D E	514-527	alpha-helix	P K M Y M F R L Q K M M D E	499-512	alpha-helix
	40	Y K T	536-538	beta-sheet	F T T	521-523	beta-sheet
	41	E K M L L Q R A L E L L A F L K E D L	540-557	alpha-helix	K T L L E V G L E L L T M L K E D S	525-542	alpha-helix
	42	L H E L M R A W E L V H R V W T A E A H V R H M L F	565-590	alpha-helix	L H E L M R A W E N I H R T L Q A E S H I R T V L F	550-575	alpha-helix
	43	Y R T	601-603	beta-sheet	F R A	586-588	beta-sheet
	44	K C F V C S K Y D	614-622	beta-sheet	E V F C N C K Y D	698-606	beta-sheet
	45	E W T F E K V P Y	627-635	beta-sheet	E W E M I K R P I	611-619	beta-sheet

Str. deviations:

68-71	loop		**624 AA**	
166-171	loop	**identical AA**	**359**	57,5%
328-336	loop	**similar AA****	**478**	76,6%
403-409	alpha-helix missing	**1.0Å RMSD Bb**	**598**	**95,8%**
593-595	loop	** incl. identical AA		

Protein problems: **backbone**
Pro2, Ala46, Pro114, Pro164, Asp250, Pro287, His387, Phe433, Pro596, Asp596

Secondary structure element succession AprA *Syntrophobacter fumarooxidans*

AprA domains	**No**	***Archaeoglobus fulgidus* sequence**	**AA position**	**Sec. str. element**	***Syntrophobacter fumarooxidans* sequence**	**AA position**	**Sec. str. element**
FAD-Binding	1	P T E V V E T D I L I I G	17-29	beta-sheet	E T V V V E T D L L I I G	5-17	beta-sheet
site I	2	F S G C G G A A Y E A A Y W A K	32-44	alpha-helix	M S A C G A A F E A A Y W A K	20-34	alpha-helix
(2-261 AA)	3	K V T L V E	51-56	beta-sheet	K V T V V D	39-44	beta-sheet
	4	S A I	71-73	beta-sheet	S A I	59-61	beta-sheet
					I G Y (new)	65-67	**beta-sheet**
					G E N (new)	70-72	**beta-sheet**
	5	L E D Y V R Y V T L D M	89-100	alpha-helix	L E D Y V K Y V R Q D L	74-85	alpha-helix
	6	E D L V A D Y A R H V D G T V H L F E K	106-125	alpha-helix	E D L V Y N I A R H V D S S V H L F E K W	91-111	alpha-helix
	7	P I W K T	129-133	beta-sheet	P I W K D	115-119	beta-sheet

	8	K Y V R E	137-141	beta-sheet	K Y V H E	122-126	beta-sheet
	9	Q I M I H	145-149	beta-sheet	Q I M I N	130-134	beta-sheet
	10	Y K P I I A E A A K M A V	153-165	alpha-helix	Y K V L V A E A A K N A → shortened	138-149	alpha-helix
	11	N I Y E R V F I F E L L K D	169-182	beta-sheet	E L L E R V F I V E P L → shortened	158-169	beta-sheet
	12	A V A G A V G F S V	188-197	beta-sheet	→V G G V G F S V shortened	176-183	beta-sheet
	13	K F Y V F K A	201-207	beta-sheet	K F Y V I K A	187-193	beta-sheet
	14	A V I L A	209-213	beta-sheet	A T I A A	195-199	beta-sheet
	15	G A T	216-218	beta-sheet	G A V	202-204	beta-sheet
	16	A A	229-230	alpha-helix	G L	215-216	alpha-helix
	17	D T G	239-241	beta- sheet	N A G	225-227	beta- sheet
	18	S G Y Y M G L K A	242-250	alpha-helix	S T A Y F T I R A	228-236	alpha-helix
	19	M L T Q	253-256	beta-sheet	E M T C	239-242	beta-sheet
Capping	20	P F R F K	263-267	beta-sheet	P V R F K	249-253	beta-sheet
(262-393 AA)	21	G A W F L F	274-279	alpha-helix	G A W F L L	260-265	alpha-helix
	22	K A K N A	283-287	beta-sheet	R A V N A	269-273	beta-sheet
	23	I K	293-294	alpha-helix	**Y** M V alpha-helix elongated	278-280	alpha-helix
	24	A	298	alpha-helix	P	287	alpha-helix
	25	Y G	306-307	alpha-helix	Y G	292-293	alpha-helix
	26	T P L R N H Q V M L E I M D	314-327	alpha-helix	A N L R N W L G M E D V M A	300-313	alpha-helix
	27	P I M Y M H	331-335	beta-sheet	P I Y M K	317-321	beta-sheet
	28	T E E A L A E L A	336-344	alpha-helix	T E E A I A N L A **loop elongated**	322-330	alpha-helix
	29	K K K L K H I Y E E A F E D F L	348-363	alpha-helix	→K K M K E L E S E A W E D F L **shortened**	342-356	alpha-helix
	30	S Q A L L W A C Q	368-375	alpha-helix	S Q A L L W A G S	361-369	alpha-helix
	31	S E A A P A	385-390	beta-sheet	S E I A A A	378-383	beta-sheet
FAD Binding	32	G F W	403-405	beta-sheet	G A W	396-398	beta-sheet
site II	33	K	419	alpha-helix	K **loop elongated**	412	alpha-helix
(393-487 AA)	34	R M T	427-429	beta-sheet	N M T	422-424	beta-sheet
	35	G L F A I	433-437	beta-sheet	A L F T C	428-432	beta-sheet
	36	S S G S F T E G R I A A K A A V R F I L E Q	449-470	alpha-helix	S S G S H A E G R V A A K G A I A Y I L D N	444-465	alpha-helix
	37	D A V V E E L K K K	478-487	alpha-helix	D A K V E A L K K I	473-482	alpha-helix
Helical	38	P M E R F M Q	491-497	alpha-helix	P M D R F E E	486-492	alpha-helix
(488-643 AA)	39	P W Q Q G L V R L Q K I M D E	514-527	alpha-helix	P K M F M F R L Q K I M D E	509-522	alpha-helix
	40	Y K T	536-538	beta-sheet	F T T	531-533	beta-sheet
	41	E K M L L Q R A L E L L A F L K E D L	540-557	alpha-helix	K S L L T R G L E L L T M L K E D S	535-552	alpha-helix
	42	L H E L M R A W E L V H R V W T A E A H V R H M L F	565-590	alpha-helix	L H E L L R A W E N T H R L W I A E S H L R H V M F	560-585	alpha-helix
	43	Y R T	601-603	beta-sheet	Y R A	596-598	beta-sheet
	44	K C F V C S K Y D	614-622	beta-sheet	K C F V N S V Y N	609-617	beta-sheet
	45	E W T F E K V P Y	627-635	beta-sheet	E W T M K K V P V	622-630	beta-sheet

Str. deviations:

68-71	beta-loop-beta	
150-155	loop	**identical AA**
171-174	loop-beta	**similarAA****
332-340	loop	**1.0Å RMSD Bb**
416-419	loop	** incl. identical AA

634 AA		
385	60,7%	
490	77,3%	
608	**95,9%**	

Protein problems: **backbone**
Pro2, Ala46, Pro114, Asp155, Lys156, Pro168, Cys175, Asp254, Pro291, Phe340, Lys341, His391, Val419, Phe443

Secondary structure element succession AprA environmental sequence fosws39f7

AprA domains	No	*Archaeoglobus fulgidus* sequence	AA position	Sec. str. element	fosws39f7 sequence	AA position	Sec. str. element
FAD-Binding	1	P T E V V E T D I L I I G	17-29	beta-sheet	E T V E V T T D L L I L G	6-18	beta-sheet
site I	2	F S G C G G A A Y E A A Y W A K	32-44	alpha-helix	M S A C G A A V E A S Y W A K	21-35	alpha-helix
(2-261 AA)	3	K V T L V E	51-56	beta-sheet	K V T L V D	40-45	beta-sheet
	4	S A I	71-73	beta-sheet	S A L **loop shortened**	60-62	beta-sheet
	5	L E D Y V R Y V T L D M	89-100	alpha-helix	I K D Y V D Y V R M D	75-85	alpha-helix
	6	E D L V A D Y A R H V D G T V H L F E K	106-125	alpha-helix	E D L V A N I A R H V D S S V H L F E K W	92-112	alpha-helix
	7	P I W K T	129-133	beta-sheet	P I W T D	115-119	beta-sheet
	8	K Y V R E	137-141	beta-sheet	R Y V H E	123-127	beta-sheet
	9	Q I M I H	145-149	beta-sheet	Q L M I N	131-135	beta-sheet
	10	Y K P I I A E A A K M A V	153-165	alpha-helix	Y K V V V A E A A K N A L A → **elongated**	139-152	alpha-helix
	11	N I Y E R V F I F E L L K D	169-182	beta-sheet	E Y L E R I F I T E P L → **shortened**	157-168	beta-sheet
	12	A V A G A V G F S V	188-197	beta-sheet	→A G A V G F S V **shortened**	175-182	beta-sheet
	13	K F Y V F K A	201-207	beta-sheet	K F Y V F K A	186-192	beta-sheet
	14	A V I L A	209-213	beta-sheet	A T I V A	194-198	beta-sheet
	15	G A T	216-218	beta-sheet	G A V	201-203	beta-sheet
	16	A A	229-230	alpha-helix	G L	214-215	alpha-helix
	17	D T G	239-241	beta- sheet	N S G	224-226	beta- sheet
	18	S G Y Y M G L K A	242-250	alpha-helix	S S A Y F T L R A	227-235	alpha-helix
	19	M L T Q	253-256	beta-sheet	E M T S	238-241	beta-sheet
Capping	20	P F R F K	263-267	beta-sheet	P V R F K	248-252	beta-sheet
(262-393 AA)	21	G A W F L F	274-279	alpha-helix	G A W F L L	259-264	alpha-helix
	22	K A K N A	283-287	beta-sheet	A A T N A	268-272	beta-sheet
	23	I K	293-294	alpha-helix	**Y** M V **alpha-helix elongated**	277-279	alpha-helix
	24	A	298	alpha-helix	E	286	alpha-helix
	25	Y G	306-307	alpha-helix	Y G	291-292	alpha-helix
	26	T P L R N H Q V M L E I M D	314-327	alpha-helix	A N L R N W L G M L D I M D	299-312	alpha-helix
	27	P I M Y M H	331-335	beta-sheet	P I S M R	316-320	beta-sheet
	28	T E E A L A E L A	336-344	alpha-helix	T E Q A I Q K I A **loop elongated**	321-329	alpha-helix
	29	K K K L K H I Y E E A F E D F L	348-363	alpha-helix	→K K L K E L E S E A W E D F L **shortened**	340-354	alpha-helix
	30	S Q A L L W A C Q	368-375	alpha-helix	S Q A I L W A A S	359-367	alpha-helix
	31	S E A A P A	385-390	beta-sheet	S E I A A A	376-381	beta-sheet
FAD Binding	32	G F W	403-405	beta-sheet	G A W	394-396	beta-sheet
site II	33	K	419	alpha-helix	K	410	alpha-helix
(393-487 AA)	34	R M T	427-429	beta-sheet	H M A	418-420	beta-sheet
	35	G L F A I	433-437	beta-sheet	G M F C A	424-428	beta-sheet
	36	S S G S F T E G R I A A K A A V R F I L E Q	449-470	alpha-helix	S S G S H A E G R I V G K A A V K Y I T E N	440-461	alpha-helix
	37	D A V V E E L K K K	478-487	alpha-helix	G G Q V E E I K G R	469-478	alpha-helix
Helical	38	P M E R F M Q	491-497	alpha-helix	P L E T F E T	482-488	alpha-helix
(488-643 AA)	39	P W Q G L V R L Q K I M D E	514-527	alpha-helix	P K M F M F R L Q K I M D E	505-518	alpha-helix
	40	Y K T	536-538	beta-sheet	F S T	527-529	beta-sheet
	41	E K M L L Q R A L E L L A F L K E D L	540-557	alpha-helix	K A C L D R A L E L L T M L S E D S	531-548	alpha-helix
	42	L H E L M R A W E L V H R V W T A E A H V R H M L F	565-590	alpha-helix	L H E L M R C W E N V Q R M W Q A E A H T R T I L F	556-581	alpha-helix

	43	Y R T	601-603	beta-sheet	R R A	592-594	beta-sheet
	44	K C F V C S K Y D	614-622	beta-sheet	H A F A N C R W D	605-613	beta-sheet
	45	E W T F E K V P Y	627-635	beta-sheet	D W E M I K R P M	618-626	beta-sheet

Str. deviations:

69-72	loop
151-156	helix-loop
169-175	loop-beta
331-338	loop
411-415	loop

	634 AA	
identical AA	**361**	56,9
similar AA**	**480**	75,7
1.0Å RMSD Bb	**607**	**95,7%**
** incl. identical AA		

Protein problems: **backbone**
Pro2, Ala59, Pro115, Glu157, Pro167, Asp253, Pro290, Lys339, His389, Phe439, Pro465, Pro633

Secondary structure element succession AprA environmental sequence fosws7f8

AprA domains	**No**	***Archaeoglobus fulgidus* sequence**	**AA position**	**Sec. str. element**	**fosws7f8 sequence**	**AA position**	**Sec. str. element**
FAD-Binding	1	P T E V V E T D I L I I G	17-29	beta-sheet	E T V T V E T D L L L A G	5-17	beta-sheet
site I	2	F S G C G G A A Y E A A Y W A K	32-44	alpha-helix	M A A C G A A V E A S Y W A K	20-34	alpha-helix
(2-261 AA)	3	K V T L V E	51-56	beta-sheet	K V T L V D	39-44	beta-sheet
	4	S A I	71-73	beta-sheet	S A I **loop shortened**	59-61	beta-sheet
	5	L E D Y V R Y V T L D M	89-100	alpha-helix	L K D Y C D Y V R N D L	74-85	alpha-helix
	6	E D L V A D Y A R H V D G T V H L F E K	106-125	alpha-helix	E D Q V A N I A R H V D S T V H L F E K W	91-111	alpha-helix
	7	P I W K T	129-133	beta-sheet	P I W T D	114-118	beta-sheet
	8	K Y V R E	137-141	beta-sheet	N Y V H E	122-126	beta-sheet
	9	Q I M I H	145-149	beta-sheet	Q L M I N	130-134	beta-sheet
	10	Y K P I I A E A A K M A V	153-165	alpha-helix	Y K I I V A E A A K N A→ **shortened**	138-150	alpha-helix
	11	N I Y E R V F I F E L L K D	169-182	beta-sheet	E Y F E R V F L T H P L **loop shortened**	156-167	beta-sheet
	12	A V A G A V G F S V	188-197	beta-sheet	→V G A I G F S V **shortened**	174-181	beta-sheet
	13	K F Y V F K A	201-207	beta-sheet	K F Y V F K A	185-191	beta-sheet
	14	A V I L A	209-213	beta-sheet	A V L C A	193-197	beta-sheet
	15	G A T	216-218	beta-sheet	G A V	200-202	beta-sheet
	16	A A	229-230	alpha-helix	G F	213-214	alpha-helix
	17	D T G	239-241	beta- sheet	N S G	222-225	beta- sheet
	18	S G Y Y M G L K A	242-250	alpha-helix	A S A F F T L Y A	226-234	alpha-helix
	19	M L T Q	253-256	beta-sheet	E M T C	237-240	beta-sheet
Capping	20	P F R F K	263-267	beta-sheet	P V R F K	247-251	beta-sheet
(262-393 AA)	21	G A W F L F	274-279	alpha-helix	G A W F L L	258-263	alpha-helix
	22	K A K N A	283-287	beta-sheet	V A T N A	267-271	beta-sheet
	23	I K	293-294	alpha-helix	**Y** M Q **alpha-helix elongated**	276-278	alpha-helix
	24	A	298	alpha-helix	D	285	alpha-helix
	25	Y G	306-307	alpha-helix	Y G	290-291	alpha-helix
	26	T P L R N H Q V M L E I M D	314-327	alpha-helix	A N L R N R W M M L D V M E	298-311	alpha-helix
	27	P I M Y M H	331-335	beta-sheet	P I Y M Q	315-319	beta-sheet
	28	T E E A L A E L A	336-344	alpha-helix	T A E A I Q R I A **loop elongated**	320-328	alpha-helix
	29	K K K L K H I Y E E A F E D F L	348-363	alpha-helix	→R K L K E L E A E A W E D F L **shortened**	339-353	alpha-helix
	30	S Q A L L W A C Q	368-375	alpha-helix	S Q A I L W A A S	358-366	alpha-helix
	31	S E A A P A	385-390	beta-sheet	S E I M A C	375-380	beta-sheet
FAD Binding	32	G F W	403-405	beta-sheet	G A W	393-395	beta-sheet

site II	33	K	419	alpha-helix	**D T K G elongated**	406-409	alpha-helix
(393-487 AA)	34	R M T	427-429	beta-sheet	Q M T	417-419	beta-sheet
	35	G L F A I	433-437	beta-sheet	G L F A A	423-427	beta-sheet
	36	S S G S F T E G R I A A K A A V R F I L E Q	449-470	alpha-helix	S S G S H A E G R I A G K A A I S Y I V D N	439-459	alpha-helix
	37	D A V V E E L K K K	478-487	alpha-helix	Q G Q I D A L T A E	468-477	alpha-helix
Helical	38	P M E R F M Q	491-497	alpha-helix	P L D T Y E E	481-487	alpha-helix
(488-643 AA)	39	P W Q G L V R L Q K I M D E	514-527	alpha-helix	A K Q F M F R L Q K I M D E	504-517	alpha-helix
	40	Y K T	536-538	beta-sheet	F K T	526-528	beta-sheet
	41	E K M L L Q R A L E L L A F L K E D L	540-557	alpha-helix	D K L I E K G L E L M A F L K E D A	530-547	alpha-helix
	42	L H E L M R A W E L V H R V W T A E A H V R H M L F	565-590	alpha-helix	L H D L M R C W E A Y H R M F Q G E A H M R S I L F	555-580	alpha-helix
	43	Y R T	601-603	beta-sheet	F R S	591-593	beta-sheet
	44	K C F V C S K Y D	614-622	beta-sheet	L A F C N C K Y D	604-612	beta-sheet
	45	E W T F E K V P Y	627-635	beta-sheet	E W E M M K K P V	617-625	beta-sheet

Str. deviations:

68-71	loop	
150-156	loop	
169-173	loop	
330-337	loop	
406-409	alpha-helix elongated	

	630 AA total	
identical AA	**342**	54,3%
similar AA**	**463**	73,5%
1.0Å RMSD Bb	**610**	**96,8%**

** incl. identical AA

Protein problems: **backbone**
Ala47, Cys173, Asp252, Ala337, Lys338, His388*, Phe438*

Secondary structure element succession AprA *Thermodesulfobacterium commune*

AprA domains	No	*Archaeoglobus fulgidus* sequence	AA position	Sec. str. element	*Thermodesulfobacterium commune* sequence	AA position	Sec. str. element
FAD-Binding	1	P T E V V E T D I L I I G	17-29	beta-sheet	E I V E K E T D I L I V G	17-29	beta-sheet
site I	2	F S G C G G A A Y E A A Y W A K	32-44	alpha-helix	M A A C G A A V E A V Q W A K	32-46	alpha-helix
(2-261 AA)	3	K V T L V E	51-56	beta-sheet	R I L L C D	51-56	beta-sheet
	4	S A I	71-73	beta-sheet	S A I **loop shortened**	71-73	beta-sheet
	5	L E D Y V R Y V T L D M	89-100	alpha-helix	P D D Y V R M V R C D L	82-93	alpha-helix
	6	E D L V A D Y A R H V D G T V H L F E K	106-125	alpha-helix	E D L V F D V G R H V D D T V H C F E E W	99-119	alpha-helix
	7	P I W K T	129-133	beta-sheet	P I W K K D P→ **beta-sheet elongated**	122-128	beta-sheet
					N G A (new)	148-150	**alpha-helix**
	8	K Y V R E	137-141	beta-sheet	→Q P V R S **beta-sheet elongated**	151-155	beta-sheet
	9	Q I M I H	145-149	beta-sheet	Q I M I N	159-163	beta-sheet
	10	Y K P I I A E A A K M A V	153-165	alpha-helix	Y K V I V A E A A K N A L **loop elongated**	167-179	alpha-helix
	11	N I Y E R V F I F E L L K D	169-182	beta-sheet	E I I E R C F I V R P L L D	186-199	beta-sheet
	12	A V A G A V G F S V	188-197	beta-sheet	R C A G A V G F S V	205-214	beta-sheet
	13	K F Y V F K A	201-207	beta-sheet	K I Y I I K A	218-224	beta-sheet
	14	A V I L A	209-213	beta-sheet	A T L L A	226-230	beta-sheet
	15	G A T	216-218	beta-sheet	G A V	233-235	beta-sheet
	16	A A	229-230	alpha-helix	G K	246-247	alpha-helix
	17	D T G	239-241	beta- sheet	N P G	256-258	beta- sheet
	18	S G Y Y M G L K A	242-250	alpha-helix	T G Y A M C A M S	259-267	alpha-helix
	19	M L T Q	253-256	beta-sheet	K L V L	270-273	beta-sheet
Capping	20	P F R F K	263-267	beta-sheet	P A R F K	280-284	beta-sheet

(262-393 AA)	21	G A W F L F	274-279	alpha-helix	G A W F L L	291-296	alpha-helix
	22	K A K N A	283-287	beta-sheet	R A T N A	300-304	beta-sheet
	23	I K	293-294	alpha-helix	V A	310-311	alpha-helix
	24	A	298	alpha-helix	K	318	alpha-helix
	25	Y G	306-307	alpha-helix	Y G	323-324	alpha-helix
	26	T P L R N H Q V M L E I M D	314-327	alpha-helix	T C L R N H A M L I E M E Q	332-345	alpha-helix
	27	P I M Y M H	331-335	beta-sheet	P I Y M H	349-353	beta-sheet
	28	T E E A L A E L A	336-344	alpha-helix	T E W A L Q E E A	354-362	alpha-helix
	29	K K K L K H I Y E E A F E D F L	348-363	alpha-helix	→K E F K H L I A E A W E D F L **shortened**	367-381	alpha-helix
	30	S Q A L L W A C Q	368-375	alpha-helix	T Q A G L W A C L	386-394	alpha-helix
	31	S E A A P A	385-390	beta-sheet	S E I M P T	403-408	beta-sheet
FAD Binding	32	G F W	403-405	beta-sheet	G A W **loop elongated**	421-423	beta-sheet
site II	33	K	419	alpha-helix	**missing**		alpha-helix
(393-487 AA)	34	R M T	427-429	beta-sheet	R M T	448-450	beta-sheet
	35	G L F A I	433-437	beta-sheet	G L F C A	454-458	beta-sheet
	36	S S G S F T E G R I A A K A A V R F I L E Q	449-470	alpha-helix	S S G S H V E G R I A A K A M V Q Y C L D N	470-491	alpha-helix
	37	D A V V E E L K K K	478-487	alpha-helix	→ T A E E L K K E **shortened**	501-508	alpha-helix
Helical	38	P M E R F M Q	491-497	alpha-helix	P W Y R F E E	512-518	alpha-helix
(488-643 AA)	39	P W Q G L V R L Q K I M D E	514-527	alpha-helix	P R H I Q A R L M K L M D E	535-548	alpha-helix
	40	Y K T	536-538	beta-sheet	Y K T	557-559	beta-sheet
	41	E K M L L Q R A L E L L A F L K E D L	540-557	alpha-helix	K V M L E R G L D L L R M L K E D M	561-578	alpha-helix
	42	L H E L M R A W E L V H R V W T A E A H V R H M L F	565-590	alpha-helix	L H E L M R A W E N R H R V W T A E A H L L H I L F	586-611	alpha-helix
	43	Y R T	601-603	beta-sheet	Y R T	621-623	beta-sheet
	44	K C F V C S K Y D	614-622	beta-sheet	R C F T L S S W D	635-643	beta-sheet
	45	E W T F E K V P Y	627-635	beta-sheet	E W T L E T Y P Y	648-656	beta-sheet

Str. deviations:

8-15	loop	
77-79	loop	
363-365	loop	
128-150	alpha	
180-184	loop	
429-431	loop	
442-446	loop	

	664 AA total	
identical AA	**369**	55,6%
similar AA**	**463**	70,0%
1.0Å RMSD Bb	**610**	**91,9%**

** incl. identical AA

Protein problems: **backbone**
Pro2, Pro16, Ala58, Pro122, Pro128, Gln151, Ala185, Pro196, Asp244, Pro257, Asp285, Pro322, Lys363, Asp365, Lys366, His416, Asp430, Pro439, Asn447, Phe469, Lys499, Pro663

Secondary structure element succession AprA *Desulfovibrio vulgaris*

AprA domains	No	*Archaeoglobus fulgidus* sequence	AA position	Sec. str. element	*Desulfovibrio vulgaris* sequence	AA position	Sec. str. element
FAD-Binding	1	P T E V V E T D I L I I G	17-29	beta-sheet	T V K E H D V D L L I V G	19-31	beta-sheet
site I	2	F S G C G G A A Y E A A Y W A K	32-44	alpha-helix	M G A C G T A F E A V R W →**shortened.**	34-46	alpha-helix
(2-261 AA)	3	K V T L V E	51-56	beta-sheet	K I L L I D	55-60	beta-sheet
	4	S A I	71-73	beta-sheet	S A I **loop shortened**	75-77	beta-sheet
	5	L E D Y V R Y V T L D M	89-100	alpha-helix	A D D Y V R M V R T D L	86-97	alpha-helix
	6	E D L V A D Y A R H V D G T V H L F E K	106-125	alpha-helix	E D L I F D L G R H V D D S V H L F E E W	103-123	alpha-helix
	7	P I W K T	129-133	beta-sheet	P C W I K → **elongated**	126-130	beta-sheet

					D E H G H N L D G A (new)	131-140	**beta-sheet**
					K A A G K S L R N G D (new)	143-153	**beta-sheet**
	8	K Y V R E	137-141	beta-sheet	→ D P V R S **elongated**	154-158	beta-sheet
	9	Q I M I H	145-149	beta-sheet	Q I M I N	162-166	beta-sheet
	10	Y K P I I A E A A K M A V	153-165	alpha-helix	Y K C I V A E A A K N A L	170-182	alpha-helix
	11	N I Y E R V F I F E L L K D	169-182	beta-sheet	R I M E R I F I V K L L L D	186-199	beta-sheet
	12	A V A G A V G F S V	188-197	beta-sheet	R V A G A V G F N L	205-214	beta-sheet
	13	K F Y V F K A	201-207	beta-sheet	E V H I F R S	218-224	beta-sheet
	14	A V I L A	209-213	beta-sheet	A M L V A	226-230	beta-sheet
	15	G A T	216-218	beta-sheet	G A V	223-225	beta-sheet
	16	A A	229-230	alpha-helix	G M	246-247	alpha-helix
	17	D T G	239-241	beta- sheet	N A G	256-258	beta- sheet
	18	S G Y Y M G L K A	242-250	alpha-helix	S T Y T M C A Q V	259-267	alpha-helix
	19	M L T Q	253-256	beta-sheet	E M T M	270-273	beta-sheet
Capping	20	P F R F K	263-267	beta-sheet	P A R F K	280-284	beta-sheet
(262-393 AA)	21	G A W F L F	274-279	alpha-helix	G A W F L L	291-296	alpha-helix
	22	K A K N A	283-287	beta-sheet	K A T N Y	300-304	beta-sheet
	23	I K	293-294	alpha-helix	C A	310-311	alpha-helix
	24	A	298	alpha-helix	A	315	alpha-helix
	25	Y G	306-307	alpha-helix	R G **loop elongated**	323-324	alpha-helix
	26	T P L R N H Q V M L E I M D	314-327	alpha-helix	T C L R N H M M L R E M R E	333-346	alpha-helix
	27	P I M Y M H	331-335	beta-sheet	P I Y M D	350-354	beta-sheet
	28	T E E A L A E L A	336-344	alpha-helix	T K T A L Q S T F	355-362	alpha-helix
	29	K K K L K H I Y E E A F E D F L	348-363	alpha-helix	→E Q Q K H L E S E A W E D F L **shortened**	369-383	alpha-helix
	30	S Q A L L W A C Q	368-375	alpha-helix	G Q A N L W A S M	388-396	alpha-helix
	31	S E A A P A	385-390	beta-sheet	S E I M P T	405-410	beta-sheet
FAD Binding	32	G F W	403-405	beta-sheet	G I W **loop elongated**	423-425	beta-sheet
site II	33	K	419	alpha-helix	S N **alpha-helix elongated**	443-444	alpha-helix
(393-487 AA)	34	R M T	427-429	beta-sheet	R M T	450-452	beta-sheet
	35	G L F A I	433-437	beta-sheet	G L W T C	456-460	beta-sheet
	36	S S G S F T E G R I A A K A A V R F I L E Q	449-470	alpha-helix	S S G S H A E G R I C G K Q M V R W C L D H	472-493	alpha-helix
	37	D A V V E E L K K K	478-487	alpha-helix	→ S A D E L V K L **shortened**	503-510	alpha-helix
Helical	38	P M E R F M Q	491-497	alpha-helix	P Y Y N Y M E	514-520	alpha-helix
(488-643 AA)	39	P W Q G L V R L Q K I M D E	514-527	alpha-helix	P K N F M M R L V K C T D E	537-550	alpha-helix
	40	Y K T	536-538	beta-sheet	Y T T	559-561	beta-sheet
	41	E K M L L Q R A L E L L A F L K E D L	540-557	alpha-helix	A A A L D T G F S L L G M L E E D S	563-580	alpha-helix
	42	L H E L M R A W E L V H R V W T A E A H V R H M L F	565-590	alpha-helix	L H E L L R C W E N Y H R L W T V R L H M Q H I R F	588-613	alpha-helix
	43	Y R T	601-603	beta-sheet	Y R A	624-626	beta-sheet
	44	K C F V C S K Y D	614-622	beta-sheet	K C F V N S K Y D	637-645	beta-sheet
	45	E W T F E K V P Y	627-635	beta-sheet	E T K I F K K A Y	650-658	beta-sheet

Str. deviations:	12-14	loop	**664 AA**		
	81-83	loop	**identical AA**	**329**	49,5
	48-53	loop	**similar AA****	**432**	65,1
	132-153	beta-loop-beta	**1.0Å RMSD Bb**	**595**	**89,6%**

Protein problems: **backbone**
Pro2, Glu17, Pro18, Glu53, Leu54, Ala62, Pro126, Gln141, Asp285, Trp433, Ile331, Pro368, His418, Lys439, Ile447, Arg450, Ala461, Phe471

327-330 loop ** incl. identical AA
364-367 loop
430-433 loop verlängert d. +1 As Insertion
436-447 alpha-helix
495-501 loop

Secondary structure element succession AprA *Desulfovibrio desulfuricans*

AprA domains	No	*Archaeoglobus fulgidus* sequence	AA position	Sec. str. element	*Desulfovibrio desulfuricans* sequence	AA position	Sec. str. element
FAD-Binding site I (2-261 AA)	1	P T E V V E T D I L I I G	17-29	beta-sheet	E V K E H A V D L L I V G	19-31	beta-sheet
	2	F S G C G G A A Y E A A Y W A K	32-44	alpha-helix	M G S C G T A F E A V R W G D	34-48	alpha-helix
	3	K V T L V E	51-56	beta-sheet	K I M L V D	53-58	beta-sheet
	4	S A I	71-73	beta-sheet	S A I **loop shortened**	73-75	beta-sheet
	5	L E D Y V R Y V T L D M	89-100	alpha-helix	A D D Y V R M V R T D L	84-95	alpha-helix
	6	E D L V A D Y A R H V D G T V H L F E K	106-125	alpha-helix	E D L I F D V G R H V D D S V H L F E D W	101-121	alpha-helix
	7	P I W K T	129-133	beta-sheet	P C W I K	126-130	beta-sheet
					D G P H L E G A A (new)	131-139	**beta-sheet**
					V A G K S L R K G D (new)	142-150	**beta-sheet**
	8	K Y V R E	137-141	beta-sheet	A P V R S	154-156	beta-sheet
	9	Q I M I H	145-149	beta-sheet	Q I M I N	160-164	beta-sheet
	10	Y K P I I A E A A K M A V	153-165	alpha-helix	Y K C I V A E A A K N A L	168-180	alpha-helix
	11	N I Y E R V F I F E L L K D	169-182	beta-sheet	R I M E R I F I V K L L L D	184-197	beta-sheet
	12	A V A G A V G F S V	188-197	beta-sheet	R I A G A V G F N L	203-212	beta-sheet
	13	K F Y V F K A	201-207	beta-sheet	E V H I F K A	216-222	beta-sheet
	14	A V I L A	209-213	beta-sheet	T I M V A	224-228	beta-sheet
	15	G A T	216-218	beta-sheet	G A V	231-233	beta-sheet
	16	A A	229-230	alpha-helix	G M	244-245	alpha-helix
	17	D T G	239-241	beta- sheet	N A G	254-256	beta- sheet
	18	S G Y Y M G L K A	242-250	alpha-helix	S T Y T M C A Q V	257-265	alpha-helix
	19	M L T Q	253-256	beta-sheet	E M T M	268-271	beta-sheet
Capping (262-393 AA)	20	P F R F K	263-267	beta-sheet	P A R F K	278-282	beta-sheet
	21	G A W F L F	274-279	alpha-helix	G A W F L L	289-294	alpha-helix
	22	K A K N A	283-287	beta-sheet	K A T N S	298-302	beta-sheet
	23	I K	293-294	alpha-helix	C A	308-309	alpha-helix
	24	A	298	alpha-helix	A	313	alpha-helix
	25	Y G	306-307	alpha-helix	R G **loop elongated**	321-322	alpha-helix
	26	T P L R N H Q V M L E I M D	314-327	alpha-helix	T C L R N H M M L R E M R E	331-344	alpha-helix
	27	P I M Y M H	331-335	beta-sheet	P I Y M D	347-352	beta-sheet
	28	T E E A L A E L A	336-344	alpha-helix	T K S A L Q N T F	353-361	alpha-helix
	29	K K K L K H I Y E E A F E D F L	348-363	alpha-helix	→E Q Q K D L E S E A W E D F L **shortened**	367-381	alpha-helix
	30	S Q A L L W A C Q	368-375	alpha-helix	G Q A N L W A C T	386-394	alpha-helix
	31	S E A A P A	385-390	beta-sheet	S E I M P T	403-408	beta-sheet
FAD Binding site II (393-487 AA)	32	G F W	403-405	beta-sheet	G I W **loop elongated**	421-423	beta-sheet
	33	K	419	alpha-helix	**missing**		
	34	R M T	427-429	beta-sheet	R M T	448-450	beta-sheet
	35	G L F A I	433-437	beta-sheet	G L F T C	454-458	beta-sheet
	36	S S G S F T E G R I A A K A A V R F I L E Q	449-470	alpha-helix	S S G S H A E G R M A G K Q M V R W C L D H	470-491	alpha-helix

	37	D A V V E E L K K K	478-487	alpha-helix	→ T A E E L K K A **shortened**	501-508	alpha-helix
Helical	38	P M E R F M Q	491-497	alpha-helix	P F Y N F E E	512-518	alpha-helix
(488-643 AA)	39	P W Q G L V R L Q K I M D E	514-527	alpha-helix	P K N F M M R L V K C T D E	535-548	alpha-helix
	40	Y K T	536-538	beta-sheet	Y T T	557-559	beta-sheet
	41	E K M L L Q R A L E L L A F L K E D L	540-557	alpha-helix	K A L L D T G F N L L A M M E E D S	561-578	alpha-helix
	42	L H E L M R A W E L V H R V W T A E A H V R H M L F	565-590	alpha-helix	L H E L L R C W E N Y H R L W T V R L H M Q H I S F	586-611	alpha-helix
	43	Y R T	601-603	beta-sheet	Y R A	622-624	beta-sheet
	44	K C F V C S K Y D	614-622	beta-sheet	K C F V N S K Y N	634-643	beta-sheet
	45	E W T F E K V P Y	627-635	beta-sheet	E T K I F K K P Y	648-656	beta-sheet

Str. deviations:

12-15	loop
79-81	loop
131-151	beta-loop-beta
325-328	loop
362-365	loop
430-432	loop
434-445	alpha-helix missing
493-499	loop

identical AA	**332**	50,2
similar AA**	**444**	67,1
1.0Å RMSD Bb	**601**	**90,8%**

** incl. identical AA

662 AA total

Protein problems: **backbone**
Pro2, Ala16, Glu17, Ala60, Pro124, Pro133, Val142, Asp283, Asn365, Glu366, His416, Val432, Pro433, Ala459, Phe469, Lys437, Val445

Secondary structure element succession AprA *Desulfobulbus* sp. str. MLMS-1

AprA domains	No	*Archaeoglobus fulgidus* sequence	AA position	Sec. str. element	*Desulfobulbus* sp. sequence	AA position	Sec. str. element
FAD-Binding	1	P T E V V E T D I L I I G	17-29	beta-sheet	E V V E H D V D V L I I G	18-30	beta-sheet
site I	2	F S G C G G A A Y E A A Y W A K	32-44	alpha-helix	M A A C G T A F E I K K W→ **shortened**	33-45	alpha-helix
(2-261 AA)	3	K V T L V E	51-56	beta-sheet	K I K L V D	51-56	beta-sheet
	4	S A I	71-73	beta-sheet	S A I **loop shortened**	71-73	beta-sheet
	5	L E D Y V R Y V T L D M	89-100	alpha-helix	I E N Y V K M V R N D L	82-93	alpha-helix
	6	E D L V A D Y A R H V D G T V H L F E K	106-125	alpha-helix	E D L I Y D L G R H V D E S V K L F E E W	99-119	alpha-helix
	7	P I W K T	129-133	beta-sheet	P I W K K	122-126	beta-sheet
					G D N (new)	130-132	**beta-sheet**
					R E G (new)	143-145	**beta-sheet**
	8	K Y V R E	137-141	beta-sheet	T P V R T	147-151	beta-sheet
	9	Q I M I H	145-149	beta-sheet	Q I M I N	155-159	beta-sheet
	10	Y K P I I A E A A K M A V	153-165	alpha-helix	Y K C I V A E P A K T A L	163-175	alpha-helix
	11	N I Y E R V F I F E L L K D	169-182	beta-sheet	N I L E R V F I V K L I L D	179-192	beta-sheet
	12	A V A G A V G F S V	188-197	beta-sheet	Q I A G A V G F S T	198-207	beta-sheet
	13	K F Y V F K A	201-207	beta-sheet	K V H V F R C	211-217	beta-sheet
	14	A V I L A	209-213	beta-sheet	T A L C A	219-223	beta-sheet
	15	G A T	216-218	beta-sheet	G A V	226-228	beta-sheet
	16	A A	229-230	alpha-helix	G K	239-240	alpha-helix
	17	D T G	239-241	beta- sheet	N A G	249-251	beta- sheet
	18	S G Y Y M G L K A	242-250	alpha-helix	S T Y T M C A Q V	252-260	alpha-helix
	19	M L T Q	253-256	beta-sheet	T L T M	263-266	beta-sheet
Capping	20	P F R F K	263-267	beta-sheet	P A R F K	273-277	beta-sheet

(262-393 AA)	21	G A W F L F	274-279	alpha-helix	G A W F L L	284-289	alpha-helix
	22	K A K N A	283-287	beta-sheet	K V Q N G	293-297	beta-sheet
	23	I K	293-294	alpha-helix	missing		
	24	A	298	alpha-helix	**missing**		
	25	Y G	306-307	alpha-helix	**missing**		
	26	T P L R N H Q V M L E I M D	314-327	alpha-helix	T C L R N H L L L N E L K A	326-339	alpha-helix
	27	P I M Y M H	331-335	beta-sheet	P I Y M A	343-347	beta-sheet
	28	T E E A L A E L A	336-344	alpha-helix	T D V A L N A F L→ **shortened**	348-355	alpha-helix
					R R E A G M (new)	359-364	**alpha-helix**
	29	K K K L K H I Y E E A F E D F L	348-363	alpha-helix	→K F W K H L E S E A W E D F L **shortened**	371-385	alpha-helix
	30	S Q A L L W A C Q	368-375	alpha-helix	G Q A G L W A G M	390-398	alpha-helix
	31	S E A A P A	385-390	beta-sheet	S E I M P T	407-412	beta-sheet
FAD Binding	32	G F W	403-405	beta-sheet	G I W **loop elongated**	425-427	beta-sheet
site II	33	K	419	alpha-helix	**missing**		
(393-487 AA)	34	R M T	427-429	beta-sheet	R M T	453-455	beta-sheet
	35	G L F A I	433-437	beta-sheet	G L F T A	459-463	beta-sheet
	36	S S G S F T E G R I A A K A A V R F I L E Q	449-470	alpha-helix	S S G S H A E G R I V A K M M V R F C R D N	475-496	alpha-helix
	37	D A V V E E L K K K	478-487	alpha-helix	→S A Q E Y A D E **shortened**	506-513	alpha-helix
Helical	38	P M E R F M Q	491-497	alpha-helix	P V K R Y L E	517-523	alpha-helix
(488-643 AA)	39	P W Q G L V R L Q K I M D E	514-527	alpha-helix	P A G L M M R L M K A T D E	540-553	alpha-helix
	40	Y K T	536-538	beta-sheet	Y M T	562-564	beta-sheet
	41	E K M L L Q R A L E L L A F L K E D L	540-557	alpha-helix	G K L L N I C L D L L K M M R E D A	566-583	alpha-helix
	42	L H E L M R A W E L V H R V W T A E A H V R H M L F	565-590	alpha-helix	L H E L M R A W E N Y H R I W C V E T H I R H I E F	591-616	alpha-helix
	43	Y R T	601-603	beta-sheet	Y R S	627-629	beta-sheet
	44	K C F V C S K Y D	614-622	beta-sheet	K A F V N S T F D	640-648	beta-sheet
	45	E W T F E K V P Y	627-635	beta-sheet	E W K C E K V E C	653-661	beta-sheet

Str. deviations:

5-14	loop	
46-48	loop	
77-79	loop	
129-146	beta-loop-beta	
305-308	loop	
320-324	loop	
361-371	helix-loop	
359-369	loop-helix-loop	
433-435	loop	
447-451	alpha-helix missing	
498-504	loop	

	669AA total	
identical AA	**334**	49,9%
similar AA**	**446**	66,7%
1.0Å RMSD Bb	**600**	**89,7%**

** incl. identical AA

Protein problems: **backbone**
Ala15, Pro81, Asp127, Pro134, Ala139, Thr147, Asp278, Gln309, Pro317, Lys370, His420, Asp434, Pro442, Asn452, Pro504, Lys505, Phe474

Secondary structure element succession AprA *Desulfotalea psychrophila*

AprA domains	**No**	***Archaeoglobus fulgidus* sequence**	**AA position**	**Sec. str. element**	***Desulfotalea psychrophila* sequence**	**AA position**	**Sec. str. element**
FAD-Binding	1	P T E V V E T D I L I I G	17-29	beta-sheet	E I V E H D I D V L I V G	20-32	beta-sheet
site I	2	F S G C G G A A Y E A A Y W A K	32-44	alpha-helix	M A A C G T A F E I K K W→ **shortened**	35-47	alpha-helix
(2-261 AA)	3	K V T L V E	51-56	beta-sheet	K I M L V D	55-59	beta-sheet

	4	S A I	71-73	beta-sheet	S A I **loop shortened**	73-75	beta-sheet
	5	L E D Y V R Y V T L D M	89-100	alpha-helix	I E D Y V K M V R N D L	84-95	alpha-helix
	6	E D L V A D Y A R H V D G T V H L F E K	106-125	alpha-helix	E D L I V D C G R H V D E S V K L F E E W	101-121	alpha-helix
	7	P I W K T	129-133	beta-sheet	P V W K K **→ elongated**	124-128	beta-sheet
					D A A G D N L D (new)	129-136	**beta-sheet**
					P A A S L R E G G (new)	140-148	**beta-sheet**
	8	K Y V R E	137-141	beta-sheet	**→** T P V R T **elongated**	149-153	beta-sheet
	9	Q I M I H	145-149	beta-sheet	Q I M I N	157-161	beta-sheet
	10	Y K P I I A E A A K M A V	153-165	alpha-helix	Y K P I V A E P A A T A L	165-177	alpha-helix
	11	N I Y E R V F I F E L L K D	169-182	beta-sheet	N I E R V F I V K L L L D	181-194	beta-sheet
	12	A V A G A V G F S V	188-197	beta-sheet	Q I A G A A G F S T	200-209	beta-sheet
	13	K F Y V F K A	201-207	beta-sheet	T V H I F R C	213-219	beta-sheet
	14	A V I L A	209-213	beta-sheet	A A M V A	221-225	beta-sheet
	15	G A T	216-218	beta-sheet	G A V	228-230	beta-sheet
	16	A A	229-230	alpha-helix	G K	241-242	alpha-helix
	17	D T G	239-241	beta- sheet	N A G	251-253	beta- sheet
	18	S G Y Y M G L K A	242-250	alpha-helix	S T Y T M C A Q V	254-262	alpha-helix
	19	M L T Q	253-256	beta-sheet	T L T M	265-268	beta-sheet
Capping	20	P F R F K	263-267	beta-sheet	P A R F K	275-279	beta-sheet
(262-393 AA)	21	G A W F L F	274-279	alpha-helix	G A W F L L	286-291	alpha-helix
	22	K A K N A	283-287	beta-sheet	K V A N G	295-299	beta-sheet
	23	I K	293-294	alpha-helix	**missing**		
	24	A	298	alpha-helix	**K** E **elongated**	311-312	alpha-helix
	25	Y G	306-307	alpha-helix	Y G **loop elongated**	320-321	alpha-helix
	26	T P L R N H Q V M L E I M D	314-327	alpha-helix	T C L R N H L M I K E L K E	328-341	alpha-helix
	27	P I M Y M H	331-335	beta-sheet	P I Y M A	345-349	beta-sheet
	28	T E E A L A E L A	336-344	alpha-helix	T D V A L N A F L**→ shortened**	350-358	alpha-helix
					R K E A G L (new)	361-366	**alpha-helix**
	29	K K K L K H I Y E E A F E D F L	348-363	alpha-helix	**→**K F W K H L E S E A W E D F L **shortened**	373-387	alpha-helix
	30	S Q A L L W A C Q	368-375	alpha-helix	G Q A G L W A G N	392-400	alpha-helix
	31	S E A A P A	385-390	beta-sheet	S E I M P T	409-414	beta-sheet
FAD Binding	32	G F W	403-405	beta-sheet	G I W **loop elongated**	427-429	beta-sheet
site II	33	K	419	alpha-helix	E **loop elongated**	444	alpha-helix
(393-487 AA)	34	R M T	427-429	beta-sheet	R M T	456-458	beta-sheet
	35	G L F A I	433-437	beta-sheet	G L F T A	462-466	beta-sheet
	36	S S G S F T E G R I A A K A A V R F I L E Q	449-470	alpha-helix	S S G S H A E G R I A A K Q M V K F C R**→shortened**	478-497	alpha-helix
	37	D A V V E E L K K K	478-487	alpha-helix	**→**P Q E I A D E **shortened**	509-515	alpha-helix
Helical	38	P M E R F M Q	491-497	alpha-helix	P V R L Y N E	519-525	alpha-helix
(488-643 AA)	39	P W Q G L V R L Q K I M D E	514-527	alpha-helix	P A G L M M R L M K A T D E	542-555	alpha-helix
	40	Y K T	536-538	beta-sheet	Y M T	564-566	beta-sheet
	41	E K M L L Q R A L E L L A F L K E D L	540-557	alpha-helix	G K L L N I C L D L L L L L R E D A	568-585	alpha-helix
	42	L H E L M R A W E L V H R V W T A E A H V R H M L F	565-590	alpha-helix	L H E L L R C W E N Y H R I W C V E T H I R H I E F	593-618	alpha-helix
	43	Y R T	601-603	beta-sheet	Y R S	629-631	beta-sheet
	44	K C F V C S K Y D	614-622	beta-sheet	K C F V N S T F N	642-650	beta-sheet
	45	E W T F E K V P Y	627-635	beta-sheet	E W L C E K V E C	655-663	beta-sheet

Str. deviations:	7-16	loop
	48-50	loop
	79-81	loop
	130-148	beta-loop-beta
	306-310	loop
	322-325	loop
	361-371	helix-loop
	435-437	loop
	448-454	loop
	498-507	loop

	670AA total	
identical AA	**332**	49,6%
similar AA**	**446**	66,6%
1.0Å RMSD Bb	**598**	**89,3%**

** incl. identical AA

Protein problems: **backbone**
Val16, Val17, Ala60, Asp136, Asp280,
Ala310, Pro319, Thr326, Lys372, His422, Phe477, Thr508

Secondary structure element succession AprA *Olavius algarvensis* Delta 1 symbiont

AprA domains	No	*Archaeoglobus fulgidus* sequence	AA position	Sec. str. element	*O. algarvensis* Delta 1 symbiont sequence	AA position	Sec. str. element
FAD-Binding	1	P T E V V E T D I L I I G	17-29	beta-sheet	E V E E R E V D I L I V G	18-30	beta-sheet
site I	2	F S G C G G A A Y E A A Y W A K	32-44	alpha-helix	M A A C G A A F E V K K W → **shortened**	33-45	alpha-helix
(2-261 AA)	3	K V T L V E	51-56	beta-sheet	S V L L V D	51-55	beta-sheet
	4	S A I	71-73	beta-sheet	S A I **loop shortened**	71-73	beta-sheet
	5	L E D Y V R Y V T L D M	89-100	alpha-helix	P E D Y V R M V R N D L	82-93	alpha-helix
	6	E D L V A D Y A R H V D G T V H L F E K	106-125	alpha-helix	E D L I F D L G C H V D D S V H L F E E W	99-119	alpha-helix
	7	P I W K T	129-133	beta-sheet	P V W K K	122-126	beta-sheet
					G Q K M G T L K S (new)	138-146	**alpha-helix**
	8	K Y V R E	137-141	beta-sheet	S P V R T	149-153	beta-sheet
	9	Q I M I H	145-149	beta-sheet	Q I M I N	157-161	beta-sheet
	10	Y K P I I A E A A K M A V	153-165	alpha-helix	Y K R I V A E A G K L A L	165-177	alpha-helix
	11	N I Y E R V F I F E L L K D	169-182	beta-sheet	N I L E R V F I V E L L L D	181-194	beta-sheet
	12	A V A G A V G F S V	188-197	beta-sheet	Q I A G A V G F S V	200-209	beta-sheet
	13	K F Y V F K A	201-207	beta-sheet	K V I I F K C	213-219	beta-sheet
	14	A V I L A	209-213	beta-sheet	T M M V A	221-225	beta-sheet
	15	G A T	216-218	beta-sheet	G A V	228-230	beta-sheet
	16	A A	229-230	alpha-helix	G K	241-242	alpha-helix
	17	D T G	239-241	beta- sheet	N S G	251-253	beta- sheet
	18	S G Y Y M G L K A	242-250	alpha-helix	S T Y T L C M K V	254-262	alpha-helix
	19	M L T Q	253-256	beta-sheet	E L S M	265-268	beta-sheet
Capping	20	P F R F K	263-267	beta-sheet	P A R F K	275-279	beta-sheet
(262-393 AA)	21	G A W F L F	274-279	alpha-helix	G A W F L L	286-291	alpha-helix
	22	K A K N A	283-287	beta-sheet	K T L N G	295-299	beta-sheet
	23	I K	293-294	alpha-helix	**missing**		
	24	A	298	alpha-helix	A	312	alpha-helix
	25	Y G	306-307	alpha-helix	Y G **loop elongated**	320-321	alpha-helix
	26	T P L R N H Q V M L E I M D	314-327	alpha-helix	T C L R N H L M L F E M K E	328-341	alpha-helix
	27	P I M Y M H	331-335	beta-sheet	P I I M D	345-349	beta-sheet
	28	T E E A L A E L A	336-344	alpha-helix	T V S A L A A L G	350-358	alpha-helix
	29	K K K L K H I Y E E A F E D F L	348-363	alpha-helix	→K E L K H L E S E A W E D F L **shortened**	364-378	alpha-helix
	30	S Q A L L W A C Q	368-375	alpha-helix	G Q A N L W C A T	383-391	alpha-helix
	31	S E A A P A	385-390	beta-sheet	S E V M P T	400-405	beta-sheet
FAD Binding	32	G F W	403-405	beta-sheet	G L W **loop elongated**	418-420	beta-sheet

site II	33	K	419	alpha-helix	**missing**		
(393-487 AA)	34	R M T	427-429	beta-sheet	R M T	445-447	beta-sheet
	35	G L F A I	433-437	beta-sheet	G L F T A	451-455	beta-sheet
	36	S S G S F T E G R I A A K A A V R F I L E Q	449-470	alpha-helix	S S G S H A E G R M A V K Q M V R Y A K D H	467-488	alpha-helix
	37	D A V V E E L K K K	478-487	alpha-helix	→ Q S N E E L V D M **shortened**	497-505	alpha-helix
Helical	38	P M E R F M Q	491-497	alpha-helix	P V R T Y L D	509-515	alpha-helix
(488-643 AA)	39	P W Q G L V R L Q K I M D E	514-527	alpha-helix	P N G M M Y R M M K A G H E	532-545	alpha-helix
	40	Y K T	536-538	beta-sheet	Y Q T	554-556	beta-sheet
	41	E K M L L Q R A L E L L A F L K E D L	540-557	alpha-helix	S K N L E I A M D L L E T M R E D N	558-575	alpha-helix
	42	L H E L M R A W E L V H R V W T A E A H V R H M L F	565-590	alpha-helix	L H E L M R A W E I Q H R I W T L E S H L R H I Q Y	583-608	alpha-helix
	43	Y R T	601-603	beta-sheet	Y Q A	619-621	beta-sheet
	44	K C F V C S K Y D	614-622	beta-sheet	F C F V N S K Y D	631-640	beta-sheet
	45	E W T F E K V P Y	627-635	beta-sheet	K W D I F K K D Y	645-653	beta-sheet

Str. deviations:

5-14	loop	
47-50	loop	
77-79	loop	
128-148	alpha	
305-310	loop	
322-326	loop	
359-362	loop	
426-428	loop	
431-443	alpha-helix missing	
490-496	loop	

	659 AA total	
identical AA	**339**	51,4%
similar AA**	**451**	68,4%
1.0Å RMSD Bb	**589**	**89,4%**

** incl. identical AA

Protein problems: **backbone**
Val14, Arg15, Gln50, Ala58, Asn132, Asp280, Ala310, Pro319, Pro327, Glu359, Lys363, His413, Asp427, Ile435, Tyr443, Phe466

Secondary structure element succession AprA *Thermodesulfovibrio yellowstonii*

AprA domains	No	*Archaeoglobus fulgidus* sequence	AA position	Sec. str. element	*Thermodesulfovibrio yellowstonii* sequence	AA position	Sec. str. element
FAD-Binding	1	P T E V V E T D I L I I G	17-29	beta-sheet	D V V E V E T D F L I I G	15-27	beta-sheet
site I	2	F S G C G G A A Y E A A Y W A K	32-44	alpha-helix	M S A C G A A Y E A A R W A T	30-44	alpha-helix
(2-261 AA)	3	K V T L V E	51-56	beta-sheet	K V T L V D	49-54	beta-sheet
	4	S A I	71-73	beta-sheet	S A I **loop shortened**	69-71	beta-sheet
	5	L E D Y V R Y V T L D M	89-100	alpha-helix	V V D Y V K Y V R A D L	80-91	alpha-helix
	6	E D L V A D Y A R H V D G T V H L F E K	106-125	alpha-helix	E D L V Y D L G R H V D N S V H L F E E W	97-117	alpha-helix
	7	P I W K T	129-133	beta-sheet	P I W K K	120-124	beta-sheet
					L D G F Q A R D A G K P A L (new)	131-144	**alpha-helix**
	8	K Y V R E	137-141	beta-sheet	V P C R S	149-153	beta-sheet
	9	Q I M I H	145-149	beta-sheet	Q I M I N	157-161	beta-sheet
	10	Y K P I I A E A A K M A V	153-165	alpha-helix	Y K V I V A E A A K A →**shortened**	165-175	alpha-helix
					L E F (new)	177-179	**beta-sheet**
					T G Q (new)	184-186	**beta-sheet**
	11	N I Y E R V F I F E L L K D	169-182	beta-sheet	N I Y E R V F I V K L L K D	189-202	beta-sheet
	12	A V A G A V G F S V	188-197	beta-sheet	R V A G A I G F S V	208-217	beta-sheet
	13	K F Y V F K A	201-207	beta-sheet	K I Y L F K A	221-227	beta-sheet
	14	A V I L A	209-213	beta-sheet	A I L A G	229-233	beta-sheet

	15	G A T	216-218	beta-sheet	G A V	236-238	beta-sheet
	16	A A	229-230	alpha-helix	G Q	249-250	alpha-helix
	17	D T G	239-241	beta- sheet	N S G	259-261	beta- sheet
	18	S G Y Y M G L K A	242-250	alpha-helix	S G Y Y L G M T V	262-270	alpha-helix
	19	M L T Q	253-256	beta-sheet	E M T M	273-276	beta-sheet
Capping	20	P F R F K	263-267	beta-sheet	P A R F K	283-287	beta-sheet
(262-393 AA)	21	G A W F L F	274-279	alpha-helix	G A W F L F	294-299	alpha-helix
	22	K A K N A	283-287	beta-sheet	K A T N A	303-307	beta-sheet
	23	I K	293-294	alpha-helix	**Y C** A K **alpha-helix elongated**	312-315	alpha-helix
	24	A	298	alpha-helix	K **E** **elongated**	321-322	alpha-helix
	25	Y G	306-307	alpha-helix	Y G	327-328	alpha-helix
	26	T P L R N H Q V M L E I M D	314-327	alpha-helix	T A I R N H L M M Q S M K Q	336-349	alpha-helix
	27	P I M Y M H	331-335	beta-sheet	P I L M N	353-357	beta-sheet
	28	T E E A L A E L A	336-344	alpha-helix	T H T A M Q E L A	358-366	alpha-helix
	29	K K K L K H I Y E E A F E D F L	348-363	alpha-helix	→K R L K H L E A E A W E D F L **shortened**	372-386	alpha-helix
	30	S Q A L L W A C Q	368-375	alpha-helix	G Q A G L W A A Q	391-399	alpha-helix
	31	S E A A P A	385-390	beta-sheet	S E I M P T	408-413	beta-sheet
FAD-Binding	32	G F W	403-405	beta-sheet	G F W **loop elongated**	426-428	beta-sheet
site II	33	K	419	alpha-helix	**missing**		
(393-487 AA)	34	R M T	427-429	beta-sheet	R M S	448-450	beta-sheet
	35	G L F A I	433-437	beta-sheet	G L F M S	454-458	beta-sheet
	36	S S G S F T E G R I A A K A A V R F I L E Q	449-470	alpha-helix	S S G S H A E G R I A A K A A I A F I L D N	470-491	alpha-helix
	37	D A V V E E L K K K	478-487	alpha-helix	→ D I N A L A A E **shortened**	501-508	alpha-helix
Helical	38	P M E R F M Q	491-497	alpha-helix	P F E L Y E K	512-518	alpha-helix
(488-643 AA)	39	P W Q G L V R L Q K I M D E	514-527	alpha-helix	P D M Y Q A R L Q K I A D E	535-548	alpha-helix
	40	Y K T	536-538	beta-sheet	Y M T	557-559	beta-sheet
	41	E K M L L Q R A L E L L A F L K E D L	540-557	alpha-helix	K T M I E E G L N K L Q L L K E D A	561-578	alpha-helix
	42	L H E L M R A W E L V H R V W T A E A H V R H M L F	565-590	alpha-helix	L H E L L R C W E N V H R T L S L E A H A R H I L F	586-611	alpha-helix
	43	Y R T	601-603	beta-sheet	Y R G	621-623	beta-sheet
	44	K C F V C S K Y D	614-622	beta-sheet	R A F V N S V Y D	635-643	beta-sheet
	45	E W T F E K V P Y	627-635	beta-sheet	T F T L K K V P Y	648-656	beta-sheet

Str. deviations:

6-12	loop
75-77	loop
126-148	alpha-helix
176-186	beta-loop-beta
316-319	loop
330-334	loop
367-370	loop
434-438	loop
441-445	alpha-helix missing
493-499	loop

	661 AA total	
identical AA	**352**	53,3%
similar AA**	**450**	68,1%
1.0Å RMSD Bb	**595**	**90,0%**

** incl. identical AA

Protein problems: **backbone**
Cys11, Ala56, Gln186, Ala187, Arg247, Asp288, Ala333, Leu334, Ala371, His421, Pro439, Phe469, Glu500

Secondary structure element succession AprA *Chlorobaculum tepidum*

AprA domains	No	*Archaeoglobus fulgidus* sequence	AA position	Sec. str. element	*Chlorobaculum tepidum* sequence	AA position	Sec. str. element
FAD-Binding	1	P T E V V E T D I L I I G	17-29	beta-sheet	E V V Y V D T D I L L I G	15-27	beta-sheet
site I	2	F S G C G G A A Y E A A Y W A K	32-44	alpha-helix	M A C C G A A Y E A A K W A T	30-44	alpha-helix
(2-261 AA)	3	K V T L V E	51-56	beta-sheet	R I T M V D	49-52	beta-sheet
	4	S A I	71-73	beta-sheet	S A I **loop shortened**	69-71	beta-sheet
	5	L E D Y V R Y V T L D M	89-100	alpha-helix	P A D Y V K Y V R A D L	80-91	alpha-helix
	6	E D L V A D Y A R H V D G T V H L F E K	106-125	alpha-helix	E D L V Y D L G R H V D N S V H L F E E W	97-117	alpha-helix
	7	P I W K T	129-133	beta-sheet	P I W K R **→ elongated**	120-124	beta-sheet
					D E D G S (new)	125-129	**beta-sheet**
					L T E G G (new)	140-144	**beta-sheet**
	8	K Y V R E	137-141	beta-sheet	**→** K P V R S **elongated**	145-149	beta-sheet
	9	Q I M I H	145-149	beta-sheet	Q I M I N	153-157	beta-sheet
	10	Y K P I I A E A A K M A V	153-165	alpha-helix	Y K V I V A E A A K K **→shortened**	161-171	alpha-helix
					L E Y (new)	173-175	**beta-sheet**
					T G V (new)	180-182	**beta-sheet**
	11	N I Y E R V F I F E L L K D	169-182	beta-sheet	N L Y E R V F I S E L I H D	184-198	beta-sheet
	12	A V A G A V G F S V	188-197	beta-sheet	K V A G A I G F S V	204-213	beta-sheet
	13	K F Y V F K A	201-207	beta-sheet	K A Y V F T A	217-223	beta-sheet
	14	A V I L A	209-213	beta-sheet	T M L L A	225-229	beta-sheet
	15	G A T	216-218	beta-sheet	G A V	232-234	beta-sheet
	16	A A	229-230	alpha-helix	G Q	245-246	alpha-helix
	17	D T G	239-241	beta- sheet	N A G	255-257	beta- sheet
	18	S G Y Y M G L K A	242-250	alpha-helix	T T Y A L A A Q A	258-266	alpha-helix
	19	M L T Q	253-256	beta-sheet	E L V L	269-272	beta-sheet
Capping	20	P F R F K	263-267	beta-sheet	P A R F K	279-283	beta-sheet
(262-393 AA)	21	G A W F L F	274-279	alpha-helix	G A W F L F	290-295	alpha-helix
	22	K A K N A	283-287	beta-sheet	K A T N S	299-303	beta-sheet
	23	I K	293-294	alpha-helix	C A	309-310	alpha-helix
	24	A	298	alpha-helix	A	314	alpha-helix
	25	Y G	306-307	alpha-helix	**missing**		
	26	T P L R N H Q V M L E I M D	314-327	alpha-helix	T A M R N H M M M I D M K A	332-345	alpha-helix
	27	P I M Y M H	331-335	beta-sheet	P I L M R	349-353	beta-sheet
	28	T E E A L A E L A	336-344	alpha-helix	T H E A M A A L A **loop elongated**	354-362	alpha-helix
	29	K K K L K H I Y E E A F E D F L	348-363	alpha-helix	**→**K Q I K H L E A E A W E D F L **shortened**	368-382	alpha-helix
	30	S Q A L L W A C Q	368-375	alpha-helix	G Q A V V W A G N	387-395	alpha-helix
	31	S E A A P A	385-390	beta-sheet	S E L M P T	404-409	beta-sheet
FAD-Binding	32	G F W	403-405	beta-sheet	G I W **loop elongated**	422-424	beta-sheet
site II	33	K	419	alpha-helix	**missing**		
(393-487 AA)	34	R M T	427-429	beta-sheet	R M T	444-446	beta-sheet
	35	G L F A I	433-437	beta-sheet	G L F T A	450-454	beta-sheet
	36	S S G S F T E G R I A A K A A V R F I L E Q	449-470	alpha-helix	S S G S H A E G R I A G K S M T A Y C L D H	466-487	alpha-helix
	37	D A V V E E L K K K	478-487	alpha-helix	**→**R D V D E V I A E **shortened**	495-504	alpha-helix
Helical	38	P M E R F M Q	491-497	alpha-helix	P M E T F A K	508-514	alpha-helix
(488-643 AA)	39	P W Q G L V R L Q K I M D E	514-527	alpha-helix	P K M F Q A R L Q K I M D E	531-544	alpha-helix
	40	Y K T	536-538	beta-sheet	Y T T	553-555	beta-sheet
	41	E K M L L Q R A L E L L A F L K E D L	540-557	alpha-helix	K T M L E K G L E H L S L L K E D A	557-574	alpha-helix

	42	L H E L M R A W E L V H R V W T A E A H V R H M L F	565-590	alpha-helix	L H E L M R A W E N Y H R L M A G E A H A R H I L F	581-607	alpha-helix
	43	Y R T	601-603	beta-sheet	F R A	618-620	beta-sheet
	44	K C F V C S K Y D	614-622	beta-sheet	K C F T I S K Y D	631-639	beta-sheet
	45	E W T F E K V P Y	627-635	beta-sheet	E W T L S K R D Y	644-652	beta-sheet

Str. deviations:

6-10	loop
75-77	loop
126-144	beta-loop-beta
174-182	beta-loop-beta
324-330	loop
363-366	loop
430-434	loop
436-441	alpha-helix missing
490-495	loop

identical AA	**355**	54,0%
similar AA**	**466**	70,8%
1.0Å RMSD Bb	**598**	**91,0%**

** incl. identical AA

658 AA total

Protein problems: **backbone**
Phe10, Ala56, Ala134, Glu142, Val182, Glu183, Ala243, Asp284, Leu330, Glu363, Pro367, His417, Asp430, Pro435 Phe 465

Secondary structure element succession AprA *Thiobacillus denitrificans* ATCC25259

AprA domains	No	*Archaeoglobus fulgidus* sequence	AA position	Sec. str. element	*Thiobacillus denitrificans* sequence	AA position	Sec. str. element
FAD-Binding	1	P T E V V E T D I L I I G	17-29	beta-sheet	E V V Q E D V D V L L I G	9-21	beta-sheet
site I	2	F S G C G G A A Y E A A Y W A K	32-44	alpha-helix	M A C C G A G Y E I M R W A D **loop elongated**	24-38	alpha-helix
(2-261 AA)	3	K V T L V E	51-56	beta-sheet	K I K L V D	49-54	beta-sheet
	4	S A I	71-73	beta-sheet	S A I **loop shortened**	69-71	beta-sheet
	5	L E D Y V R Y V T L D M	89-100	alpha-helix	P A D Y A R M V S N D L → **shortened**	81-91	alpha-helix
	6	E D L V A D Y A R H V D G T V H L F E K	106-125	alpha-helix	D D L A Y D L G D D S V H L F E E W	98-105	alpha-helix
	7	P I W K T	129-133	beta-sheet	P I W K T	121-125	beta-sheet
					N G E (new)	128-130	**beta-sheet**
					L K D (new)	141-143	**beta-sheet**
	8	K Y V R E	137-141	beta-sheet	K P V R S	146-150	beta-sheet
	9	Q I M I H	145-149	beta-sheet	Q I M I N	154-158	beta-sheet
	10	Y K P I I A E A A K M A V	153-165	alpha-helix	Y K W I V A E T K K A L	162-174	alpha-helix
	11	N I Y E R V F I F E L L K D	169-182	beta-sheet	R I E E R I F I V K L V N D	178-191	beta-sheet
	12	A V A G A V G F S V	188-197	beta-sheet	R I A G A V G F S T	197-206	beta-sheet
	13	K F Y V F K A	201-207	beta-sheet	K V V V Y K A	210-216	beta-sheet
	14	A V I L A	209-213	beta-sheet	A I L L A	218-222	beta-sheet
	15	G A T	216-218	beta-sheet	G C V	225-227	beta-sheet
	16	A A	229-230	alpha-helix	G T	238-239	alpha-helix
	17	D T G	239-241	beta- sheet	N A G	248-250	beta- sheet
	18	S G Y Y M G L K A	242-250	alpha-helix	S T Y A M A A E A	251-259	alpha-helix
	19	M L T Q	253-256	beta-sheet	E L T M	262-265	beta-sheet
Capping	20	P F R F K	263-267	beta-sheet	P A R F K	272-276	beta-sheet
(262-393 AA)	21	G A W F L F	274-279	alpha-helix	G A W F L L	283-288	alpha-helix
	22	K A K N A	283-287	beta-sheet	Q A V N A	292-296	beta-sheet
	23	I K	293-294	alpha-helix	**Y** M Q **elongated**	301-303	alpha-helix
	24	A	298	alpha-helix	E	307	alpha-helix

	25	Y G	306-307	alpha-helix	Y G	321-322	alpha-helix
	26	T P L R N H Q V M L E I M D	314-327	alpha-helix	→C L R N H L M L K E M Q E **shortened**	324-336	alpha-helix
	27	P I M Y M H	331-335	beta-sheet	P I Y M D	340-344	beta-sheet
	28	T E E A L A E L A	336-344	alpha-helix	T V T A L A K L R **loop elongated**	345-353	alpha-helix
	29	K K K L K H I Y E E A F E D F L	348-363	alpha-helix	→R E V K H L E A E A W E D F L **shortened**	359-373	alpha-helix
	30	S Q A L L W A C Q	368-375	alpha-helix	G Q C G I W V G E	378-386	alpha-helix
	31	S E A A P A	385-390	beta-sheet	S E L M P T	395-400	beta-sheet
FAD-Binding	32	G F W	403-405	beta-sheet	G I W **loop elongated**	413-415	beta-sheet
site II	33	K	419	alpha-helix	A **H** **elongated, loop elongated**	438-439	alpha-helix
(393-487 AA)	34	R M T	427-429	beta-sheet	S M T	450-452	beta-sheet
	35	G L F A I	433-437	beta-sheet	G L F T A	456-460	beta-sheet
	36	S S G S F T E G R I A A K A A V R F I L E Q	449-470	alpha-helix	S S G S H A E G R M C A K S M V K Y C I D N	472-493	alpha-helix
	37	D A V V E E L K K K	478-487	alpha-helix	→T P V E Q L V E E **shortened**	502-510	alpha-helix
Helical	38	P M E R F M Q	491-497	alpha-helix	P V R T F L E	514-520	alpha-helix
(488-643 AA)	39	P W Q G L V R L Q K I M D E	514-527	alpha-helix	P K M L Q F R L Q K I M D E	537-550	alpha-helix
	40	Y K T	536-538	beta-sheet	Y K T	559-561	beta-sheet
	41	E K M L L Q R A L E L L A F L K E D L	540-557	alpha-helix	A N M L A V A E D K L G M L K E D A	563-580	alpha-helix
	42	L H E L M R A W E L V H R V W T A E A H V R H M L F	565-590	alpha-helix	L H E L L R A W E N Y H R I L T A E A H M K H I Q F	589-613	alpha-helix
	43	Y R T	601-603	beta-sheet	Y R M	624-626	beta-sheet
	44	K C F V C S K Y D	614-622	beta-sheet	H C F V N S V Y D	637-647	beta-sheet
	45	E W T F E K V P Y	627-635	beta-sheet	Q W N C F K R A H		beta-sheet

Str. deviations:

3-7	loop
40-47	loop
75-77	loop
127-145	beta-loop-beta
318-322	loop
354-357	loop
421-424	loop
428-436	loop-alpha-loop
443-447	loop
496-501	loop

	666 AA total	
identical AA	**334**	50,2%
similar AA**	**448**	67,3%
1.0Å RMSD Bb	**596**	**89,5%**

** incl. identical AA

Protein problems: **backbone**
Pro8, Asp47, Ala56, Gln136, Pro139, Asp277, Pro314, Glu354, Pro358, His408, Ala429, Lys435, Ile436, Tyr448, Phe471

Supplementary data material Figure S3. AprA comparative models of SRP and SOB

Reference structure *Archaeoglobus fulgidus*

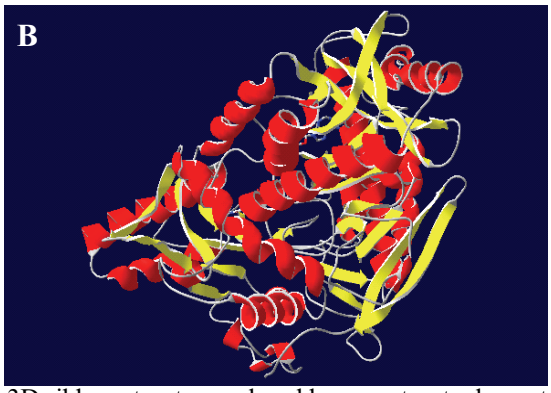

3D ribbon structure colored by sec. struct. elements

AprA model shown from front side

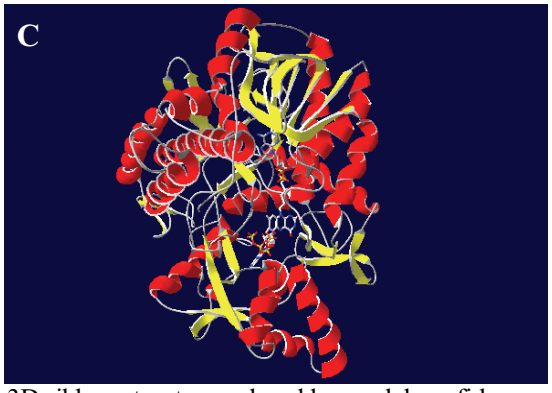

3D ribbon structure colored by model confidence

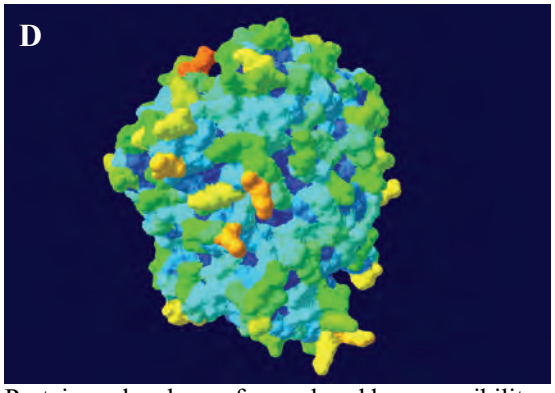

Protein molecular surface colored by accessibility

AprA model shown from top view

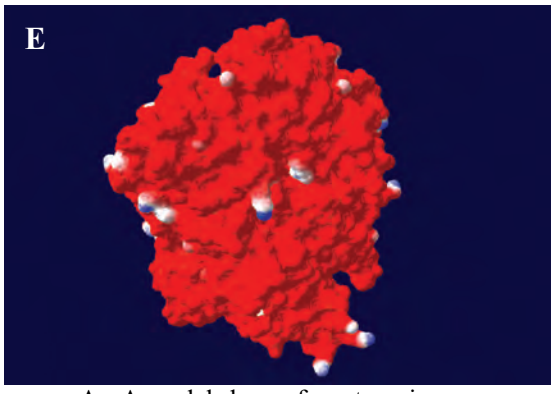

AprA model shown from top view

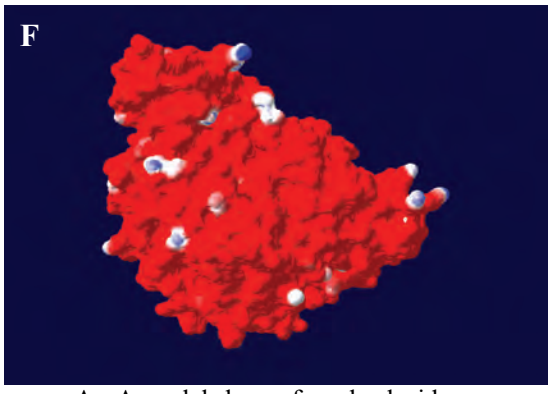

AprA model shown from back side

Protein molecular surface colored by calculated electrostatic potential (electric charge at the molecular surface is colored with a red (negative), white (neutral, and blue (positive) color gradient)

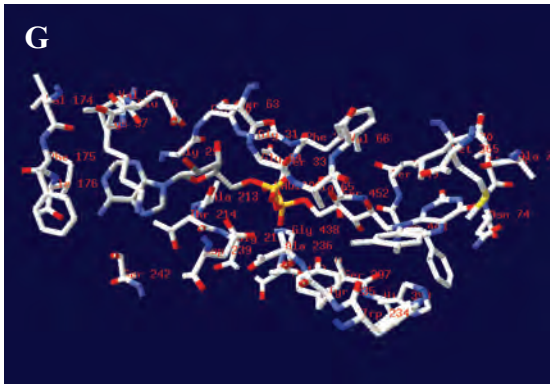

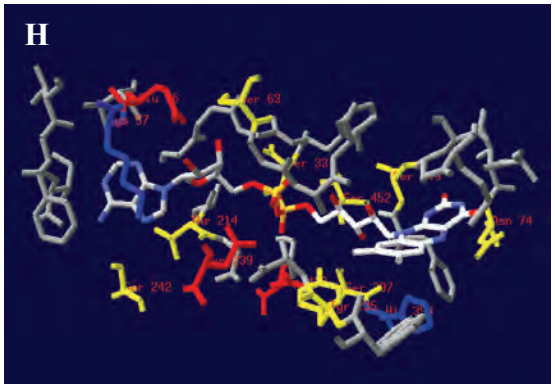

FAD surrounding protein matrix: residues present in a distance of < 4.1Å are shown (amino acids are coloured as follows: positively charged, basic AA, blue; negatively charged, acidic AA, red; polar AA, yellow; and unpolar, uncharged AA, grey

SOB Apr lineage I

Allochromatium vinosum

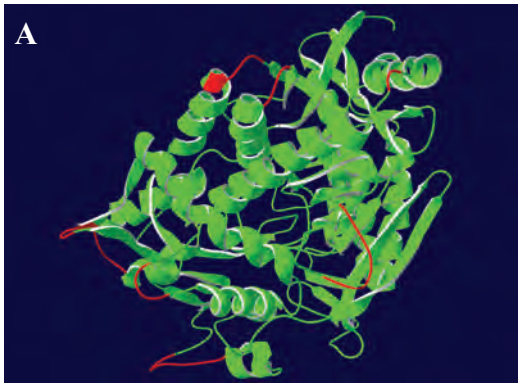

3D ribbon structure colored by model confidence

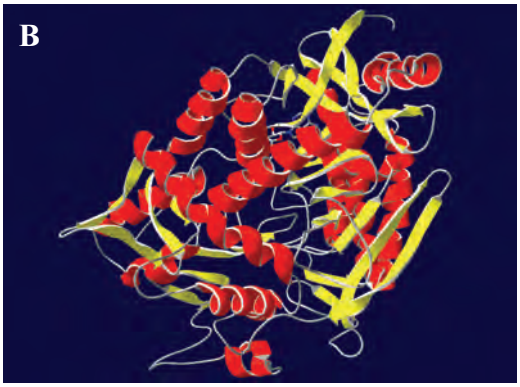

3D ribbon structure colored by sec. struct. elements

AprA model shown from front side

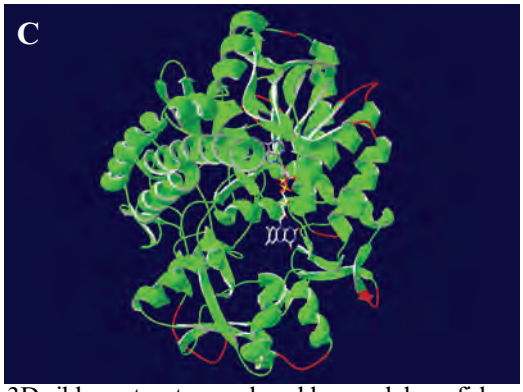

3D ribbon structure colored by model confidence

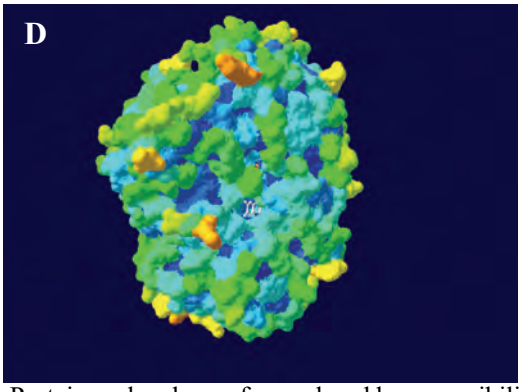

Protein molecular surface colored by accessibility

AprA model shown from top view

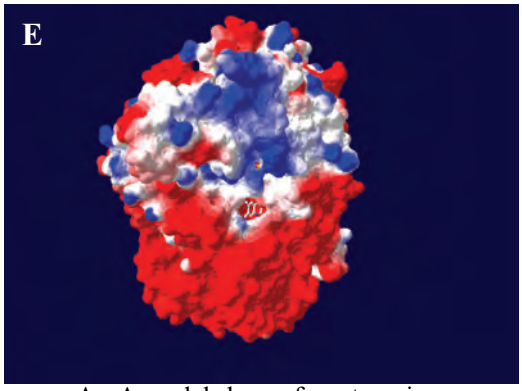

AprA model shown from top view

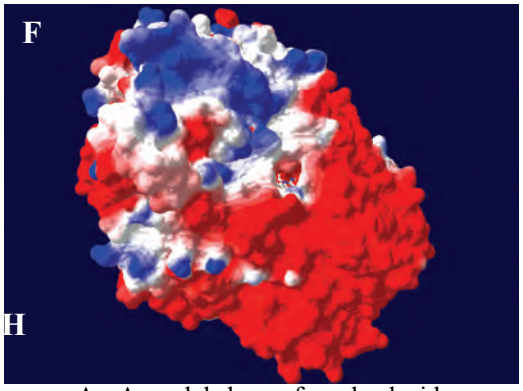

AprA model shown from back side

Protein molecular surface colored by calculated electrostatic potential (electric charge at the molecular surface is colored with a red (negative), white (neutral, and blue (positive) color gradient)

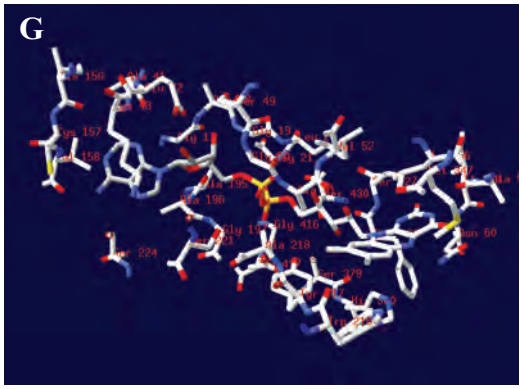

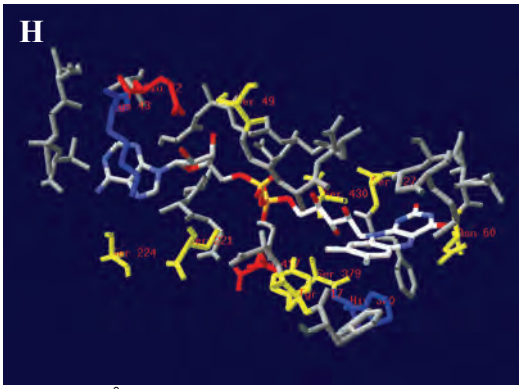

FAD surrounding protein matrix: residues present in a distance of < 4.1Å are shown (amino acids are coloured as follows: positively charged, basic AA, blue; negatively charged, acidic AA, red; polar AA, yellow; and unpolar, uncharged AA, grey)

Thiobacillus denitrificans

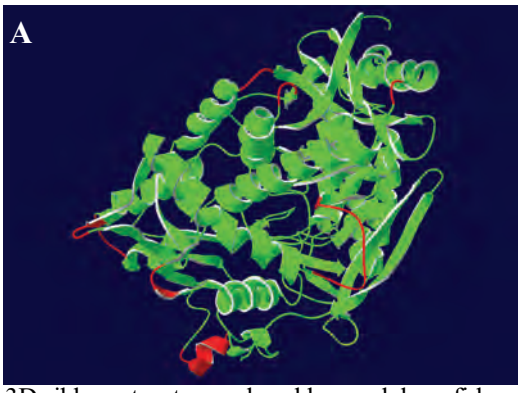

3D ribbon structure colored by model confidence

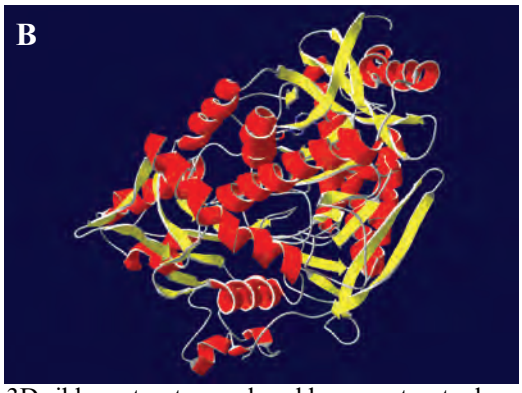

3D ribbon structure colored by sec. struct. elements

AprA model shown from front side

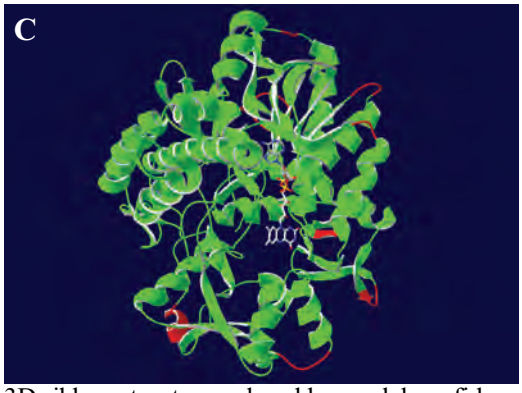

3D ribbon structure colored by model confidence

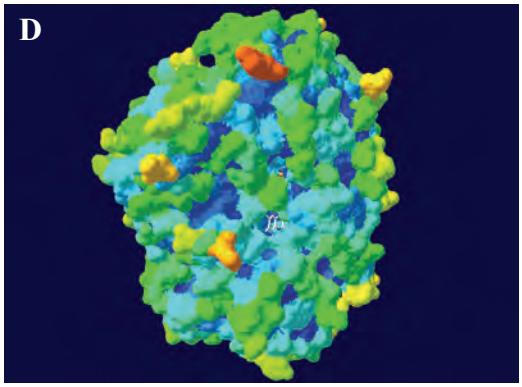

Protein molecular surface colored by accessibility

AprA model shown from top view

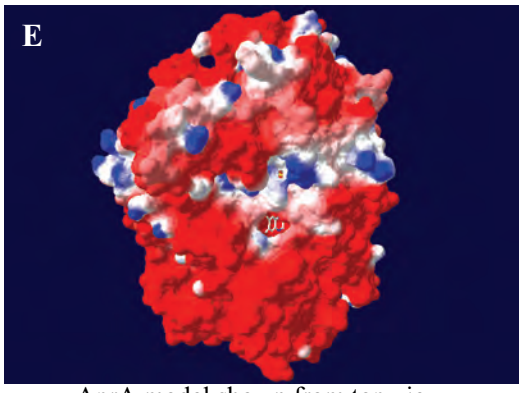

AprA model shown from top view

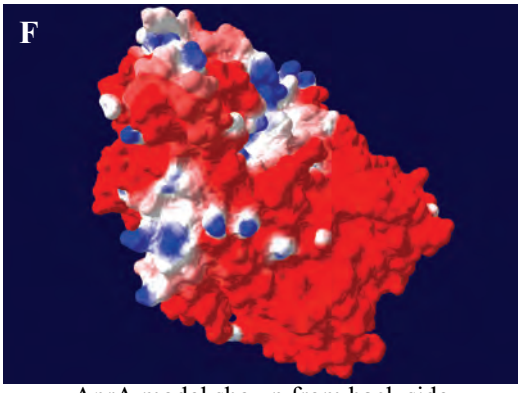

AprA model shown from back side

Protein molecular surface colored by calculated electrostatic potential (electric charge at the molecular surface is colored with a red (negative), white (neutral, and blue (positive) color gradient)

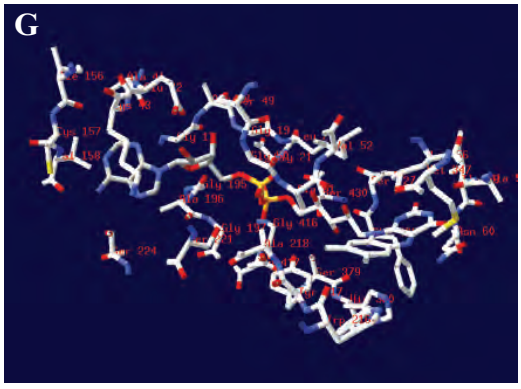

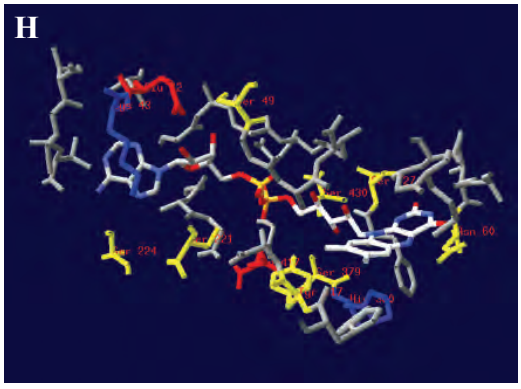

FAD surrounding protein matrix: residues present in a distance of < 4.1Å are shown (amino acids are coloured as follows: positively charged, basic AA, blue; negatively charged, acidic AA, red; polar AA, yellow; and unpolar, uncharged AA, grey)

Cdt. Ruthia magnifica

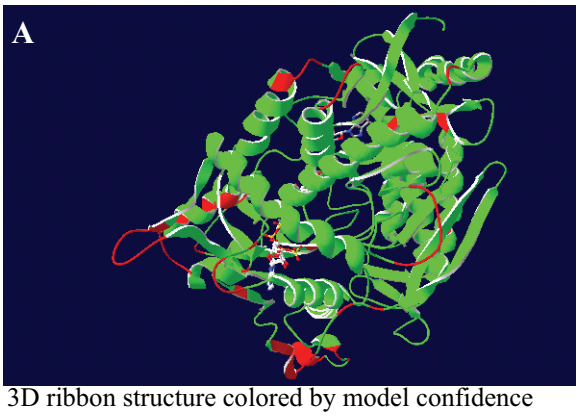

3D ribbon structure colored by model confidence

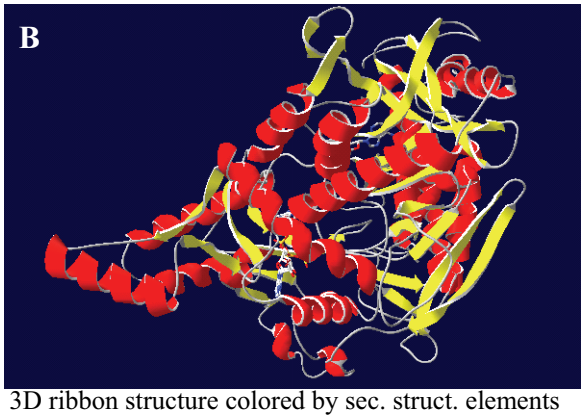

3D ribbon structure colored by sec. struct. elements

AprA model shown from front side

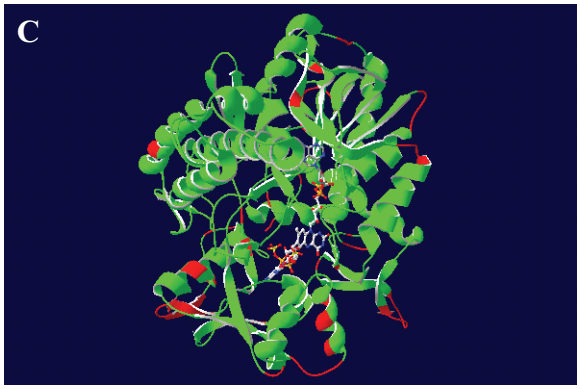

3D ribbon structure colored by model confidence

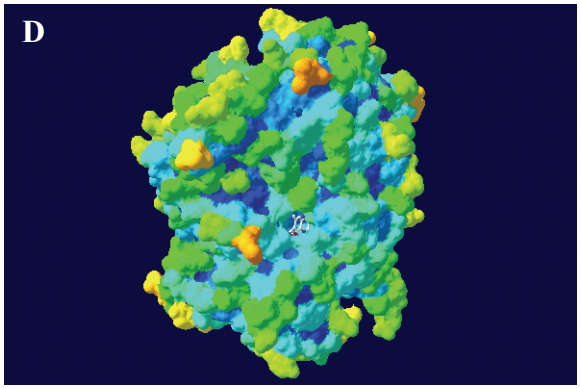

Protein molecular surface colored by accessibility

AprA model shown from top view

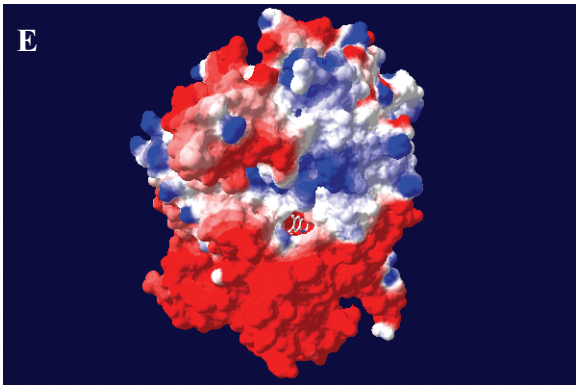

AprA model shown from top view

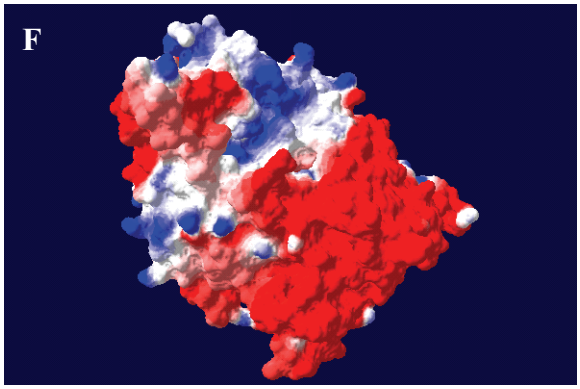

AprA model shown from back side

Protein molecular surface colored by calculated electrostatic potential (electric charge at the molecular surface is colored with a red (negative), white (neutral, and blue (positive) color gradient)

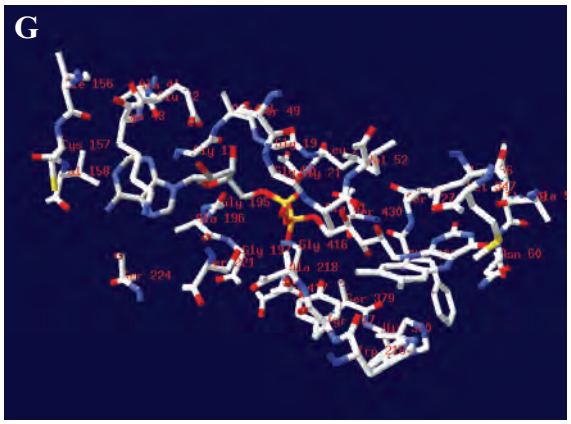

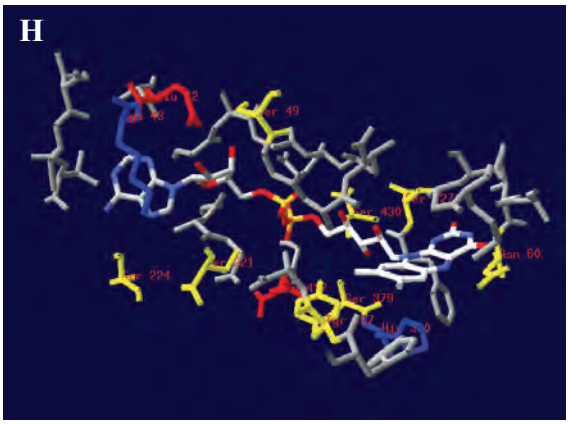

FAD surrounding protein matrix: residues present in a distance of < 4.1Å are shown (amino acids are coloured as follows: positively charged, basic AA, blue; negatively charged, acidic AA, red; polar AA, yellow; and unpolar, uncharged AA, grey)

Cdt. Pelagibacter ubique

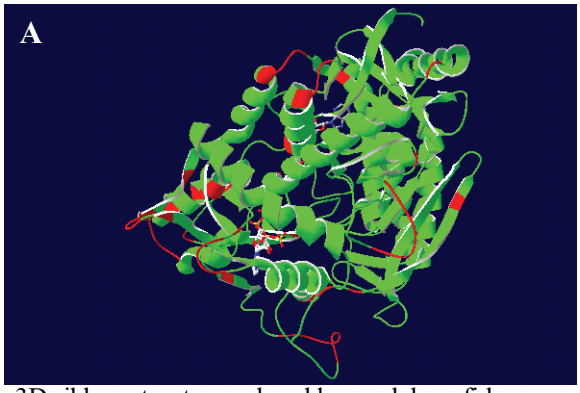

3D ribbon structure colored by model confidence

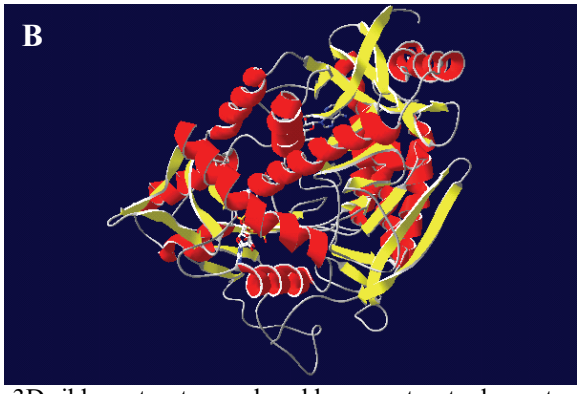

3D ribbon structure colored by sec. struct. elements

AprA model shown from front side

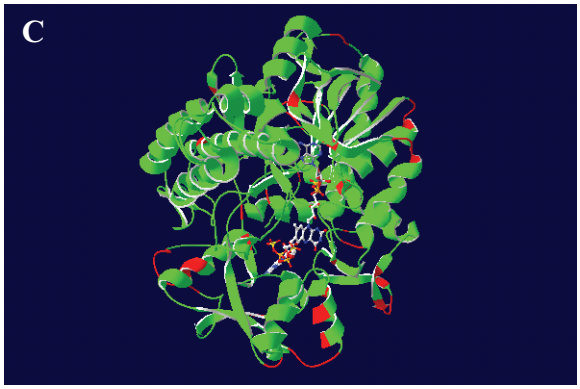

3D ribbon structure colored by model confidence

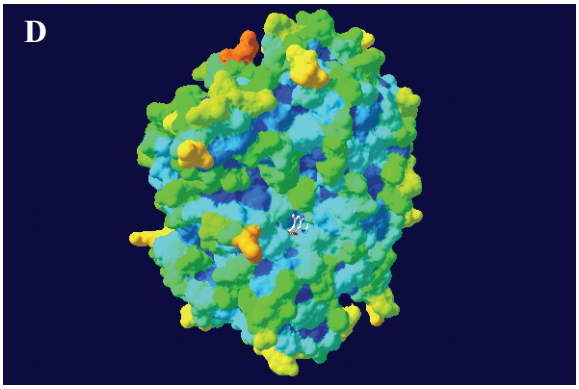

Protein molecular surface colored by accessibility

AprA model shown from top view

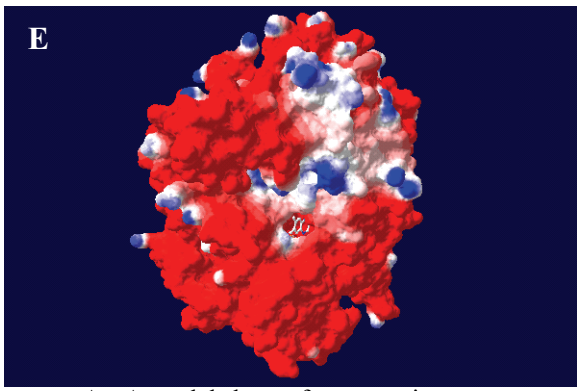

AprA model shown from top view

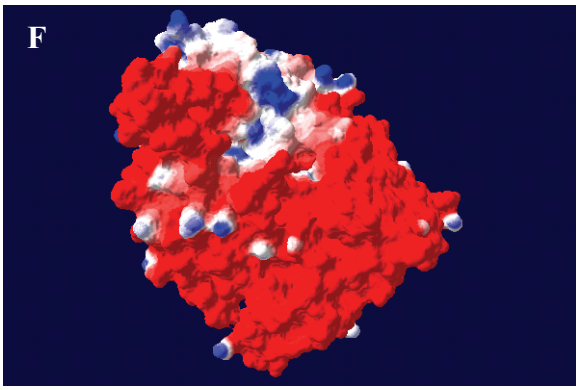

AprA model shown from back side

Protein molecular surface colored by calculated electrostatic potential (electric charge at the molecular surface is colored with a red (negative), white (neutral, and blue (positive) color gradient)

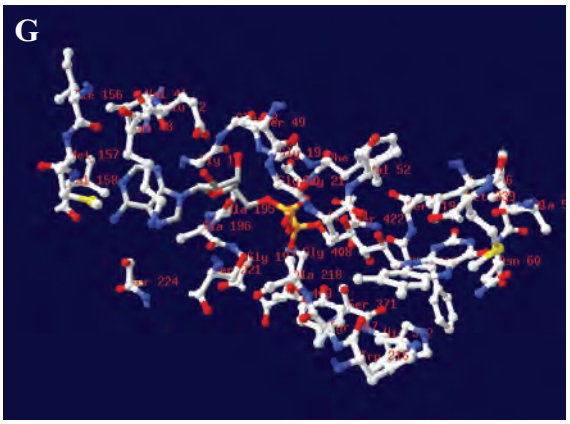

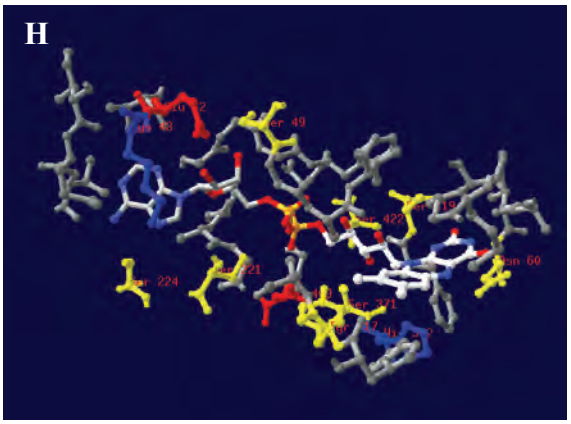

FAD surrounding protein matrix: residues present in a distance of < 4.1Å are shown (amino acids are coloured as follows: positively charged, basic AA, blue; negatively charged, acidic AA, red; polar AA, yellow; and unpolar, uncharged AA, grey)

EBAC2C11

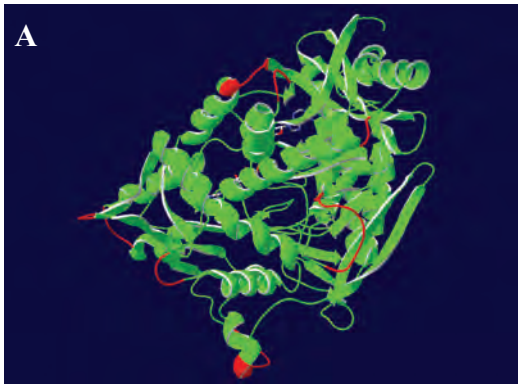

3D ribbon structure colored by model confidence

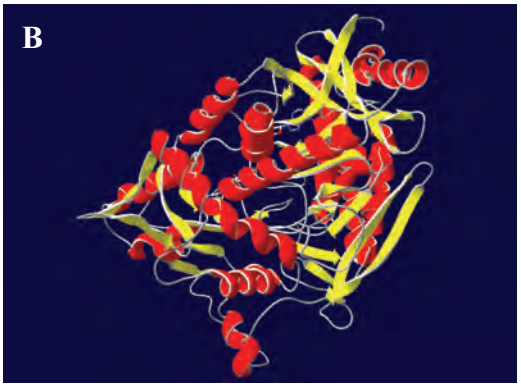

3D ribbon structure colored by sec. struct. elements

AprA model shown from front side

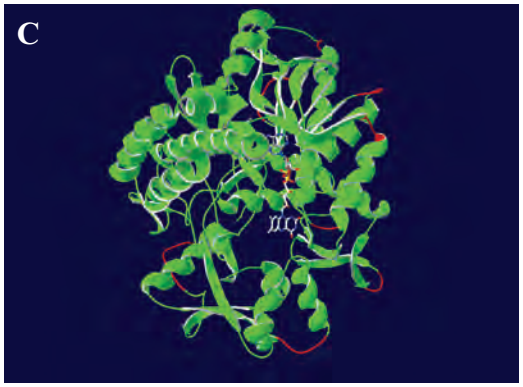

3D ribbon structure colored by model confidence

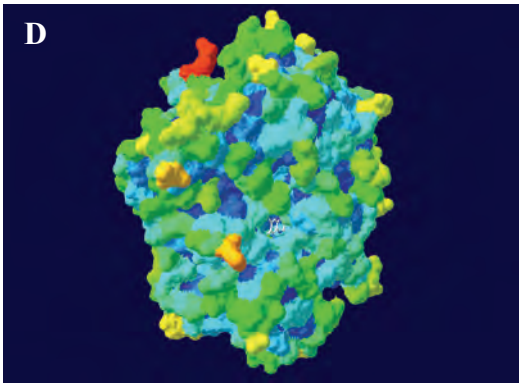

Protein molecular surface colored by accessibility

AprA model shown from top view

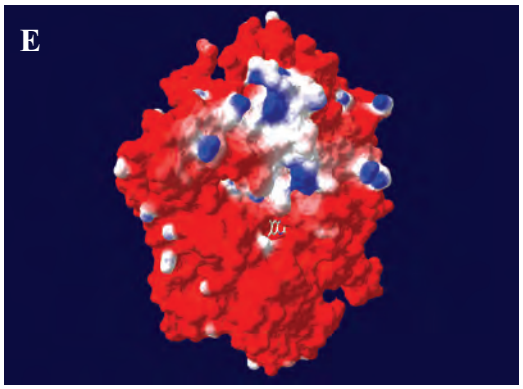

AprA model shown from top view

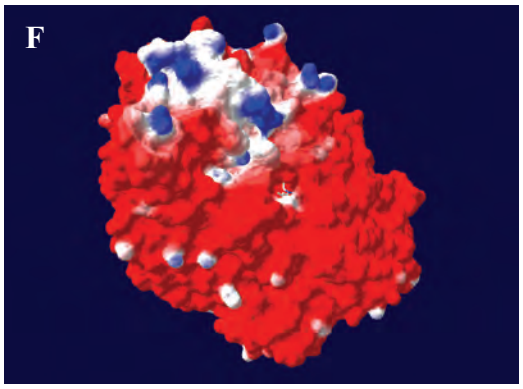

AprA model shown from back side

Protein molecular surface colored by calculated electrostatic potential (electric charge at the molecular surface is colored with a red (negative), white (neutral, and blue (positive) color gradient)

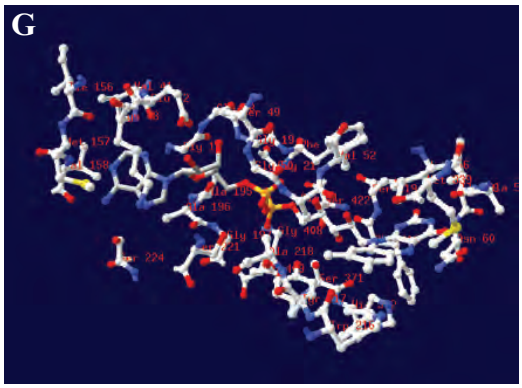

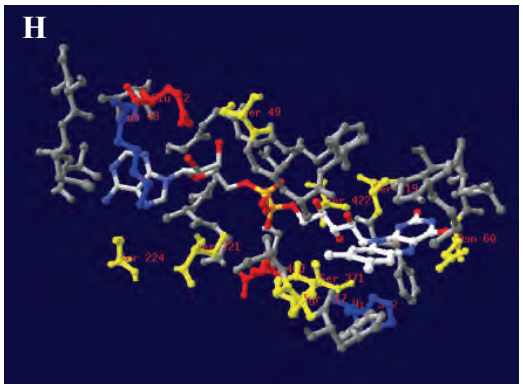

FAD surrounding protein matrix: residues present in a distance of < 4.1Å are shown (amino acids are coloured as follows: positively charged, basic AA, blue; negatively charged, acidic AA, red; polar AA, yellow; and unpolar, uncharged AA, grey)

Crenarchaeal SRP

Pyrobaculum calidifontis

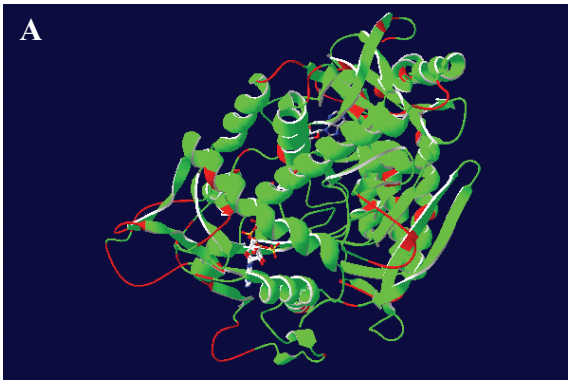

3D ribbon structure colored by model confidence

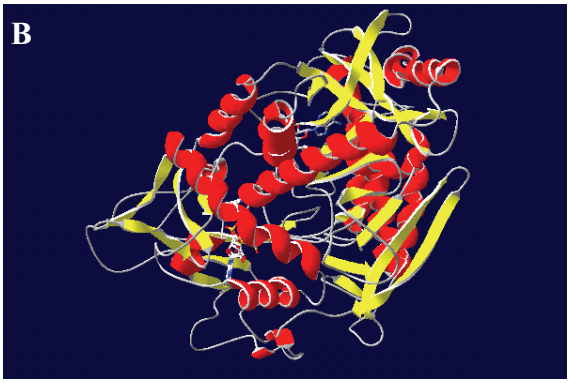

3D ribbon structure colored by sec. struct. elements

AprA model shown from front side

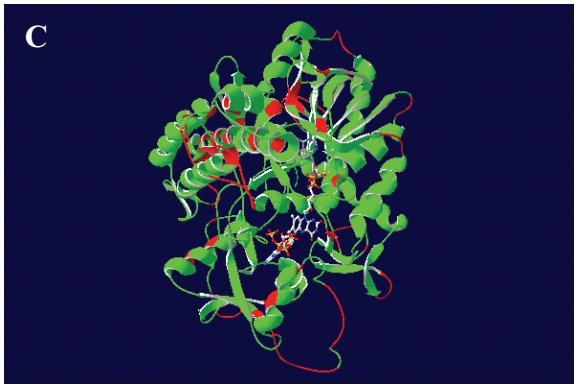

3D ribbon structure colored by model confidence

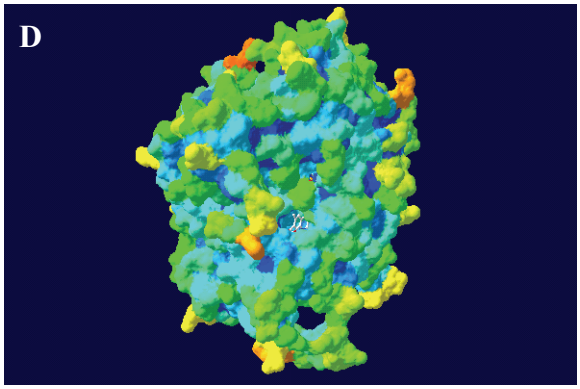

Protein molecular surface colored by accessibility

AprA model shown from top view

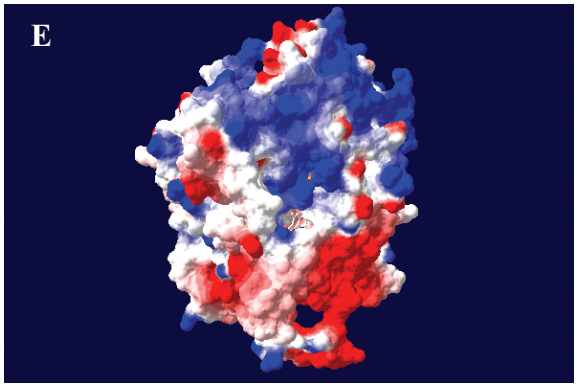

AprA model shown from top view

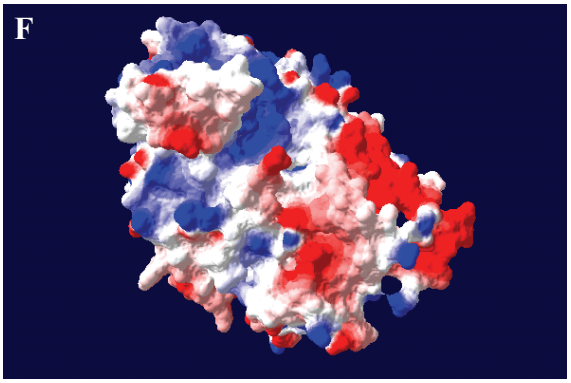

AprA model shown from back side

Protein molecular surface colored by calculated electrostatic potential (electric charge at the molecular surface is colored with a red (negative), white (neutral, and blue (positive) color gradient)

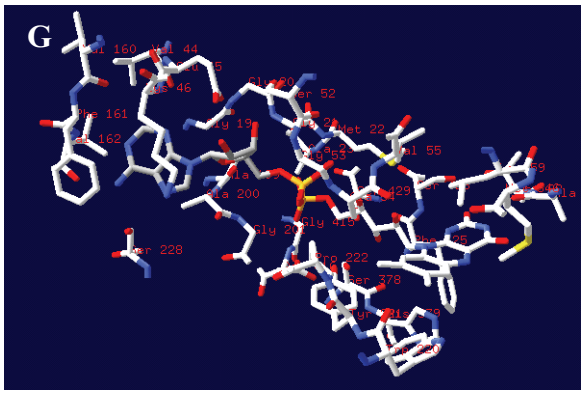

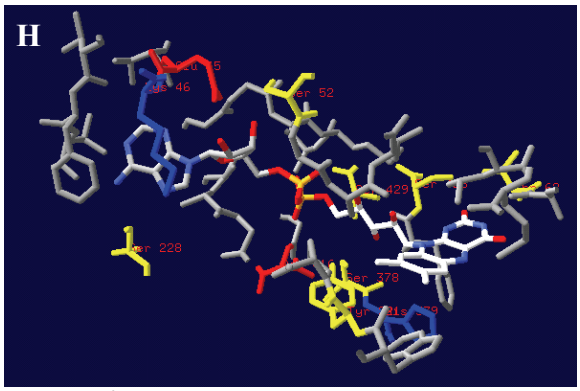

FAD surrounding protein matrix: residues present in a distance of < 4.1Å are shown (amino acids are coloured as follows: positively charged, basic AA, blue; negatively charged, acidic AA, red; polar AA, yellow; and unpolar, uncharged AA, grey)

Caldivirga maquilingensis

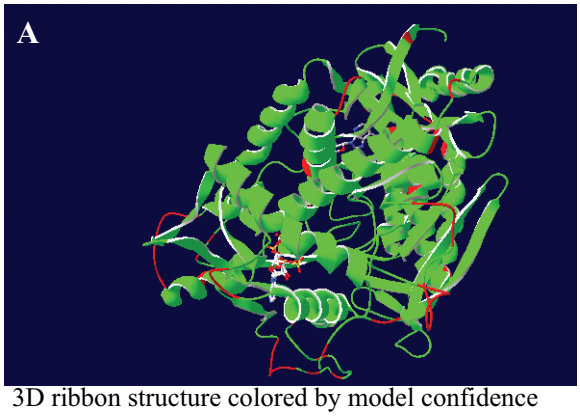

3D ribbon structure colored by model confidence

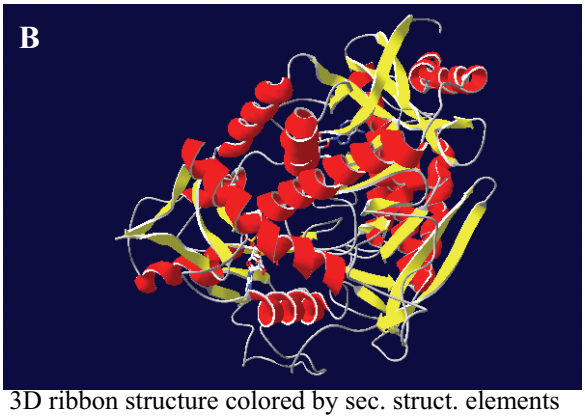

3D ribbon structure colored by sec. struct. elements

AprA model shown from front side

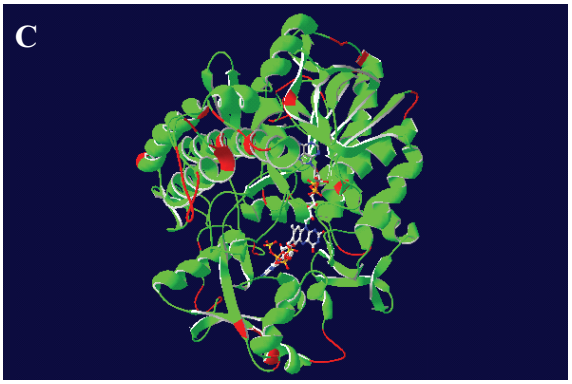

3D ribbon structure colored by model confidence

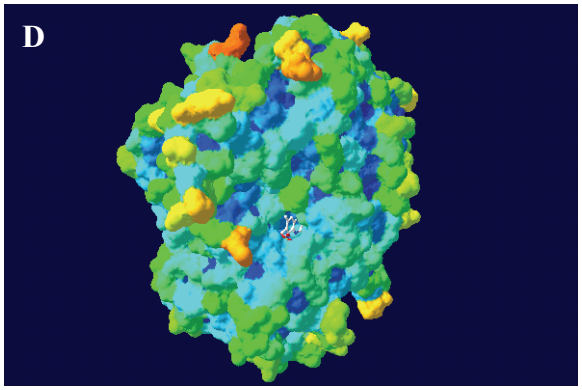

Protein molecular surface colored by accessibility

AprA model shown from top view

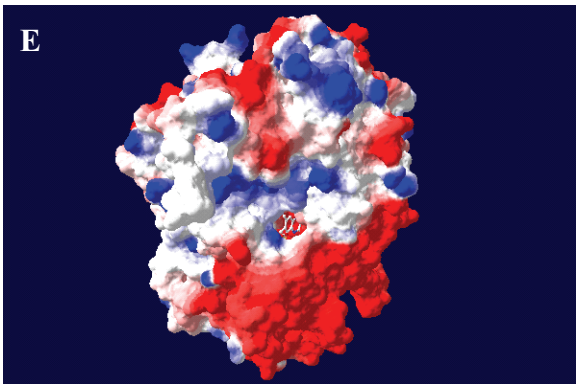

AprA model shown from top view

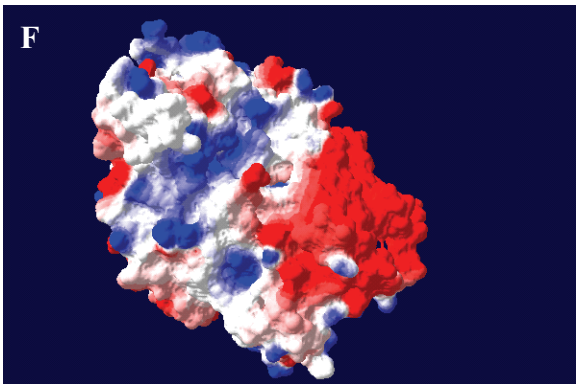

AprA model shown from back side

Protein molecular surface colored by calculated electrostatic potential (electric charge at the molecular surface is colored with a red (negative), white (neutral, and blue (positive) color gradient)

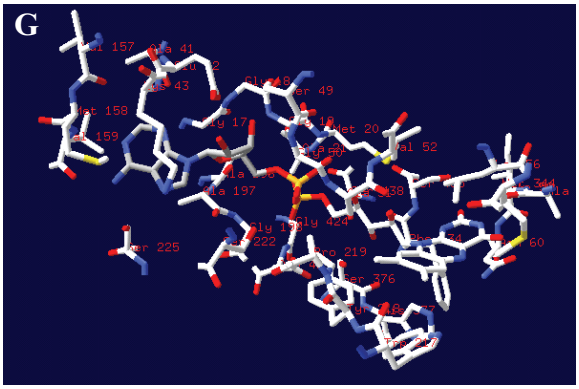

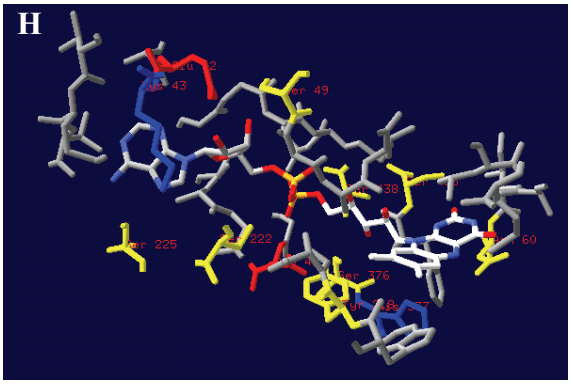

FAD surrounding protein matrix: residues present in a distance of < 4.1Å are shown (amino acids are coloured as follows: positively charged, basic AA, blue; negatively charged, acidic AA, red; polar AA, yellow; and unpolar, uncharged AA, grey)

SRB and related SOB Apr lineage II

Desulfotomaculum reducens

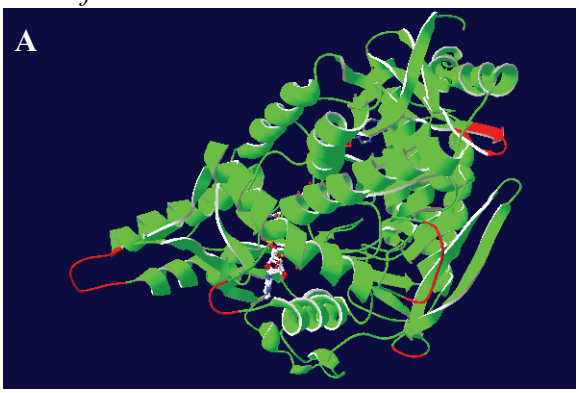

3D ribbon structure colored by model confidence

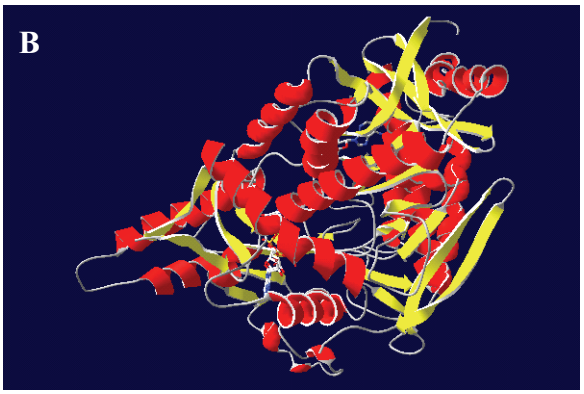

3D ribbon structure colored by sec. struct. elements

AprA model shown from front side

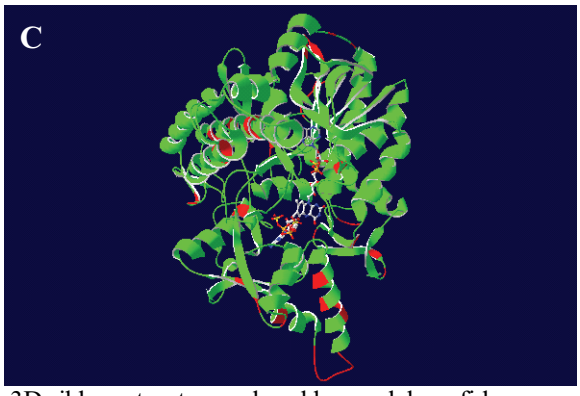

3D ribbon structure colored by model confidence

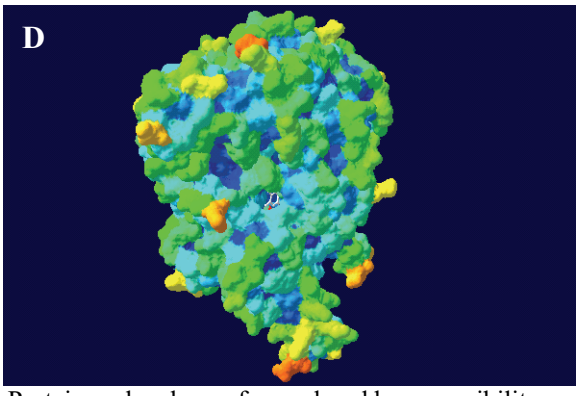

Protein molecular surface colored by accessibility

AprA model shown from top view

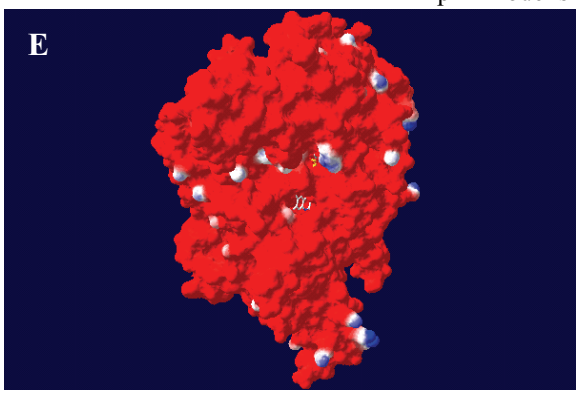

AprA model shown from top view

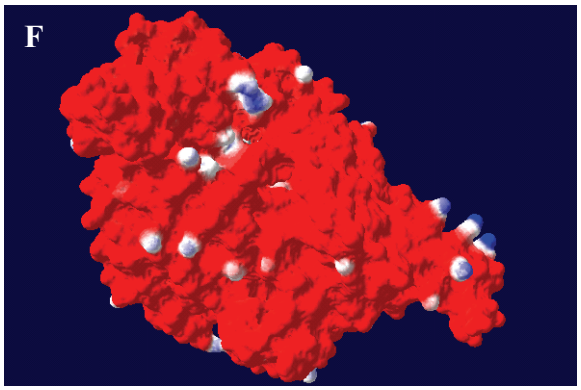

AprA model shown from back side

Protein molecular surface colored by calculated electrostatic potential (electric charge at the molecular surface is colored with a red (negative), white (neutral, and blue (positive) color gradient)

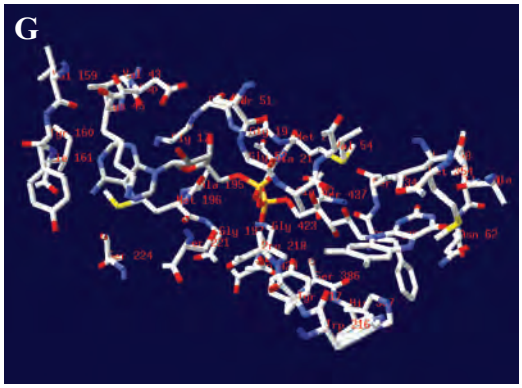

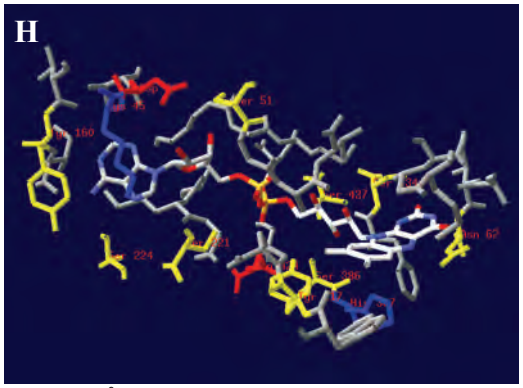

FAD surrounding protein matrix: residues present in a distance of < 4.1Å are shown (amino acids are coloured as follows: positively charged, basic AA, blue; negatively charged, acidic AA, red; polar AA, yellow; and unpolar, uncharged AA, grey)

Syntrophobacter fumaroxidans

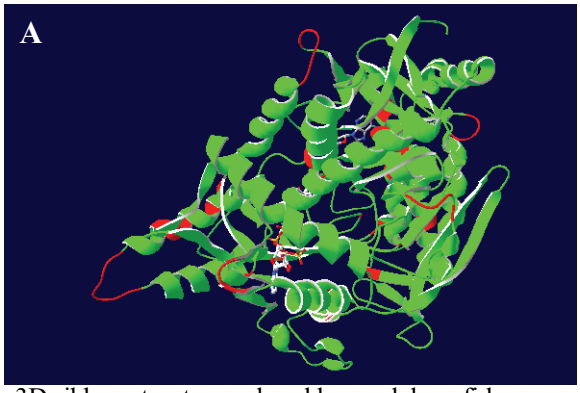

3D ribbon structure colored by model confidence

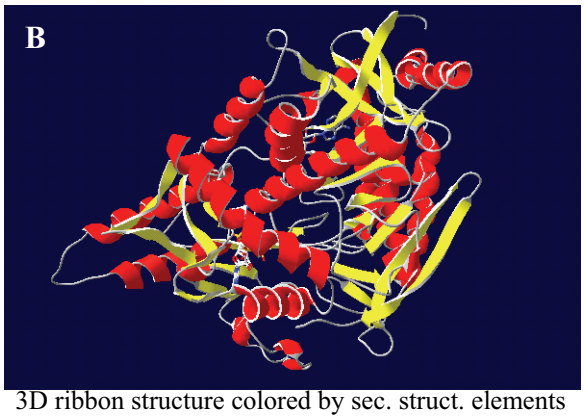

3D ribbon structure colored by sec. struct. elements

AprA model shown from front side

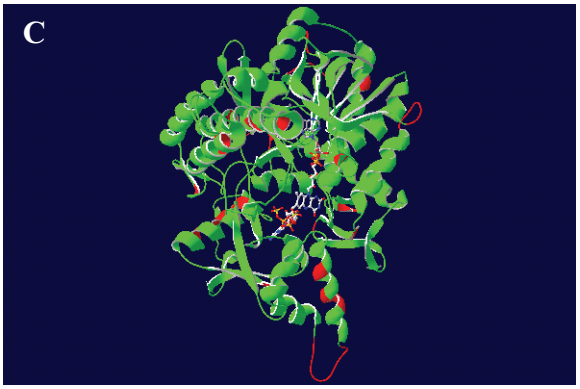

3D ribbon structure colored by model confidence

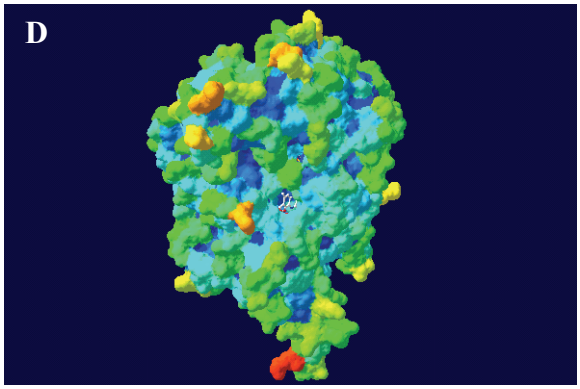

Protein molecular surface colored by accessibility

AprA model shown from top view

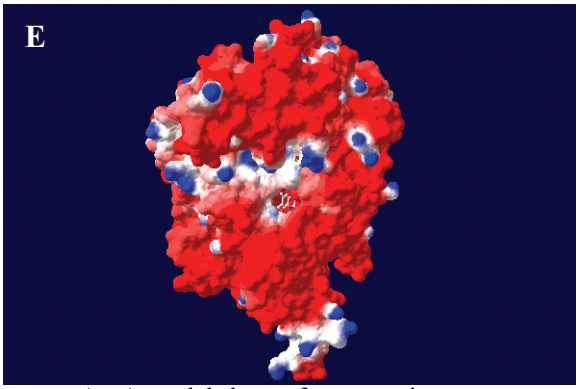

AprA model shown from top view

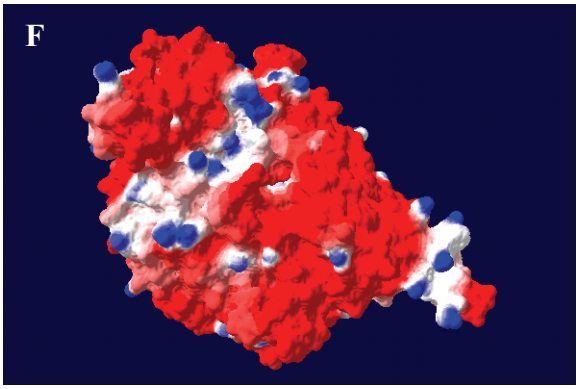

AprA model shown from back side

Protein molecular surface colored by calculated electrostatic potential (electric charge at the molecular surface is colored with a red (negative), white (neutral, and blue (positive) color gradient)

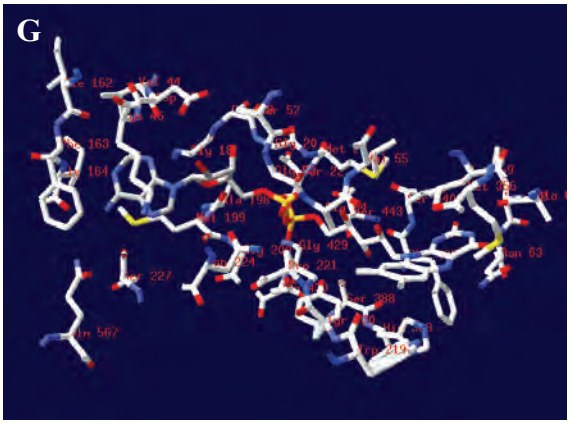

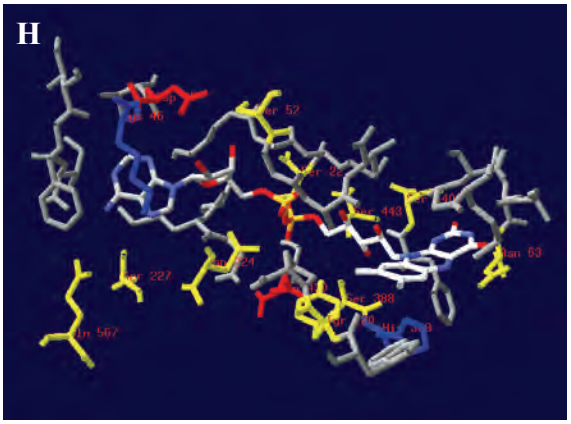

FAD surrounding protein matrix: residues present in a distance of < 4.1Å are shown (amino acids are coloured as follows: positively charged, basic AA, blue; negatively charged, acidic AA, red; polar AA, yellow; and unpolar, uncharged AA, grey)

fosws39f7

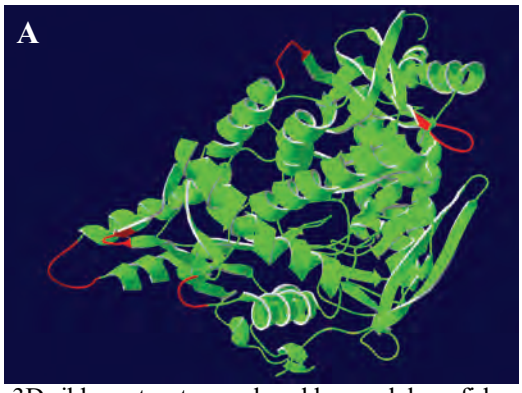

3D ribbon structure colored by model confidence

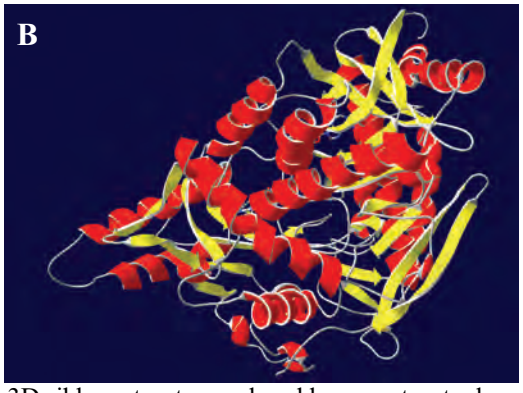

3D ribbon structure colored by sec. struct. elements

AprA model shown from front side

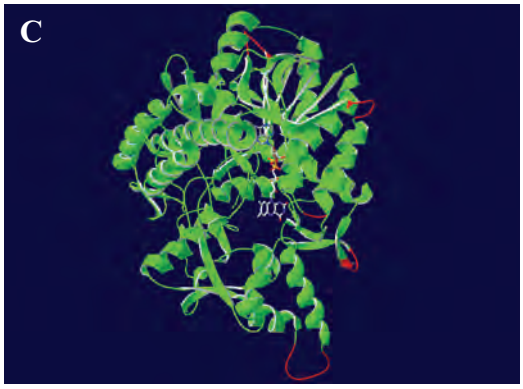

3D ribbon structure colored by model confidence

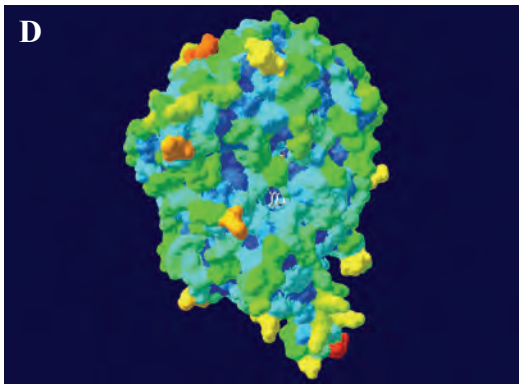

Protein molecular surface colored by accessibility

AprA model shown from top view

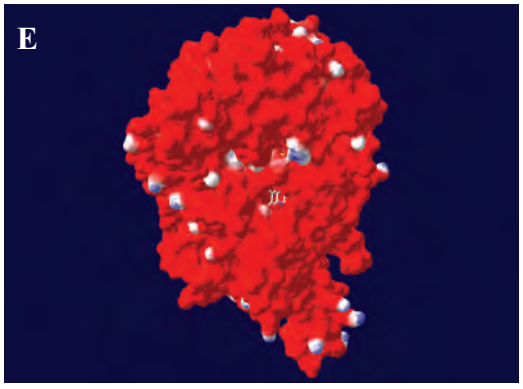

AprA model shown from top view

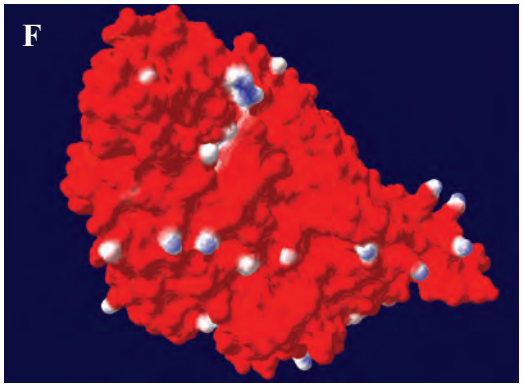

AprA model shown from back side

Protein molecular surface colored by calculated electrostatic potential (electric charge at the molecular surface is colored with a red (negative), white (neutral, and blue (positive) color gradient)

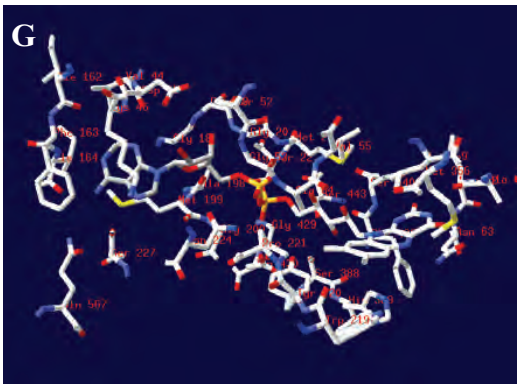

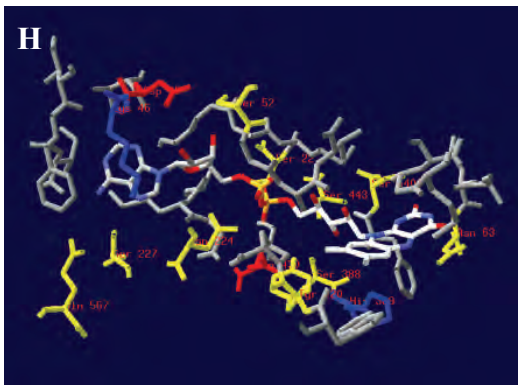

FAD surrounding protein matrix: residues present in a distance of < 4.1Å are shown (amino acids are coloured as follows: positively charged, basic AA, blue; negatively charged, acidic AA, red; polar AA, yellow; and unpolar, uncharged AA, grey)

fosws7f8

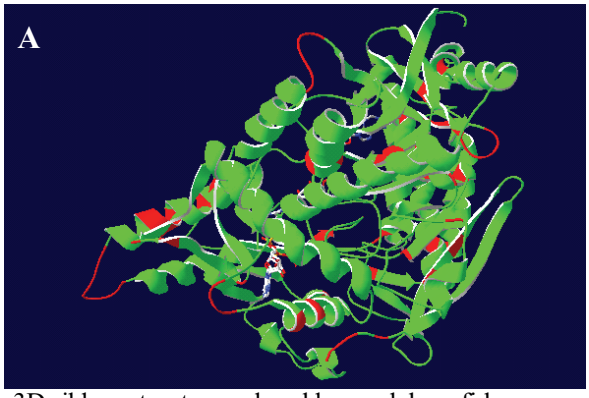

3D ribbon structure colored by model confidence

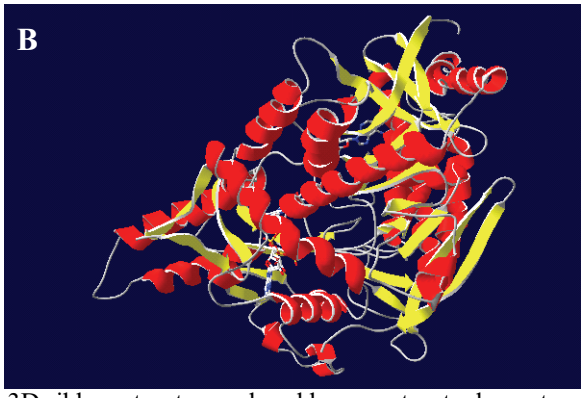

3D ribbon structure colored by sec. struct. elements

AprA model shown from front side

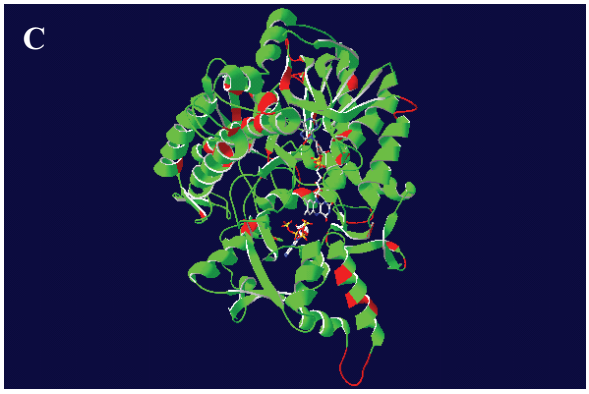

3D ribbon structure colored by model confidence

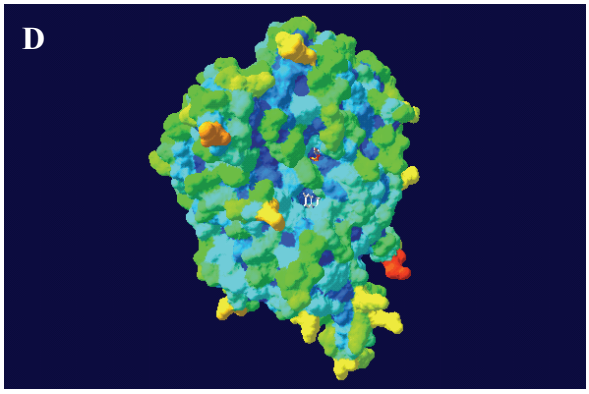

Protein molecular surface colored by accessibility

AprA model shown from top view

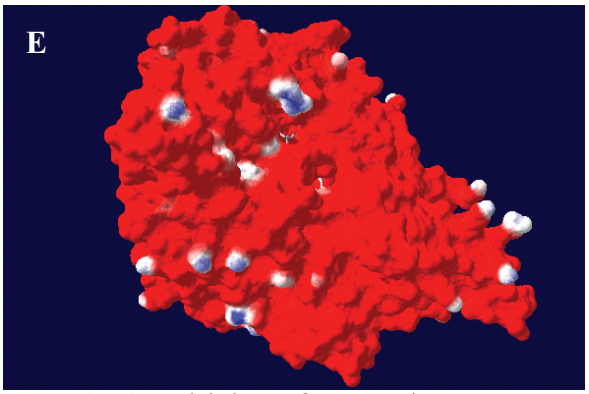

AprA model shown from top view

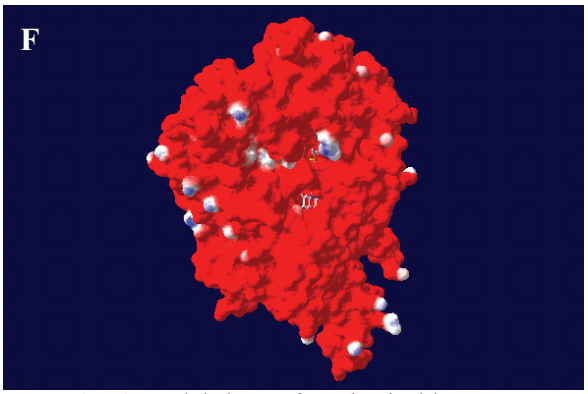

AprA model shown from back side

Protein molecular surface colored by calculated electrostatic potential (electric charge at the molecular surface is colored with a red (negative), white (neutral, and blue (positive) color gradient)

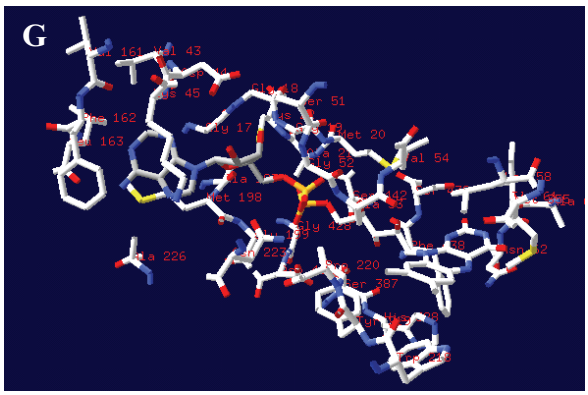

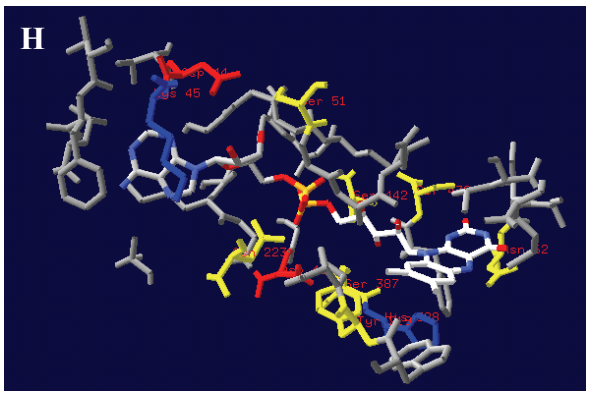

FAD surrounding protein matrix: residues present in a distance of < 4.1Å are shown (amino acids are coloured as follows: positively charged, basic AA, blue; negatively charged, acidic AA, red; polar AA, yellow; and unpolar, uncharged AA, grey)

Thermodesulfobacterium commune

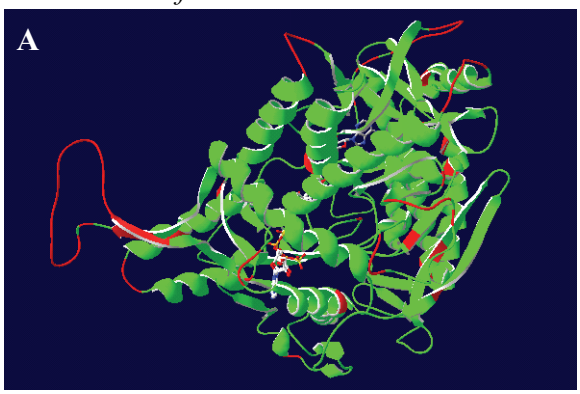

3D ribbon structure colored by model confidence

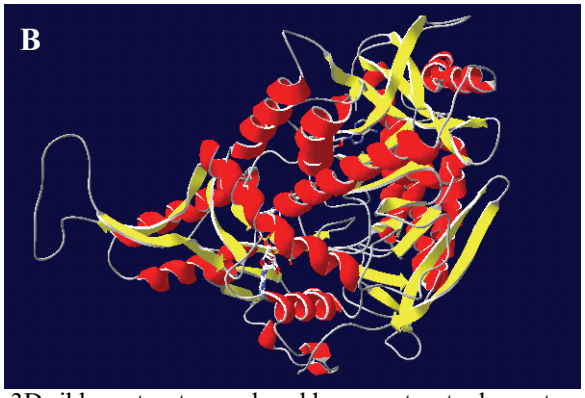

3D ribbon structure colored by sec. struct. elements

AprA model shown from front side

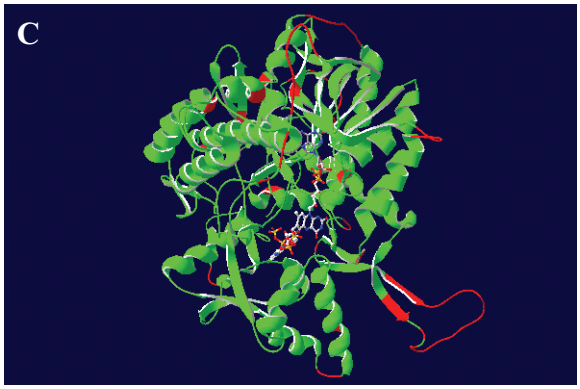

3D ribbon structure colored by model confidence

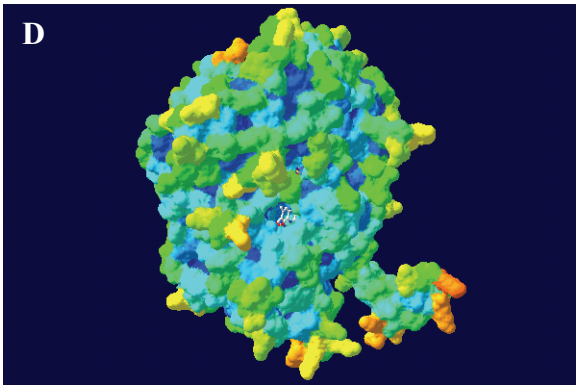

Protein molecular surface colored by accessibility

AprA model shown from top view

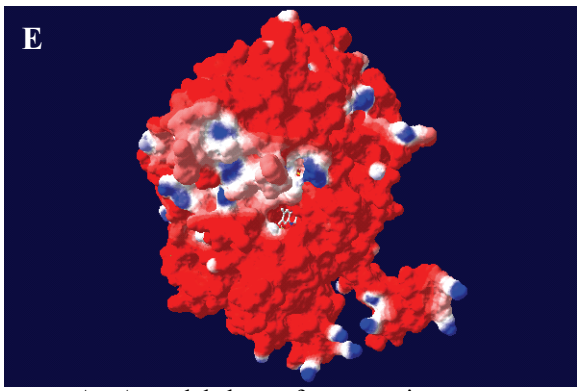

AprA model shown from top view

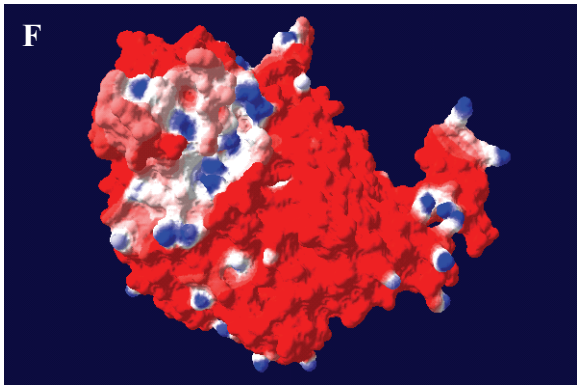

AprA model shown from back side

Protein molecular surface colored by calculated electrostatic potential (electric charge at the molecular surface is colored with a red (negative), white (neutral, and blue (positive) color gradient)

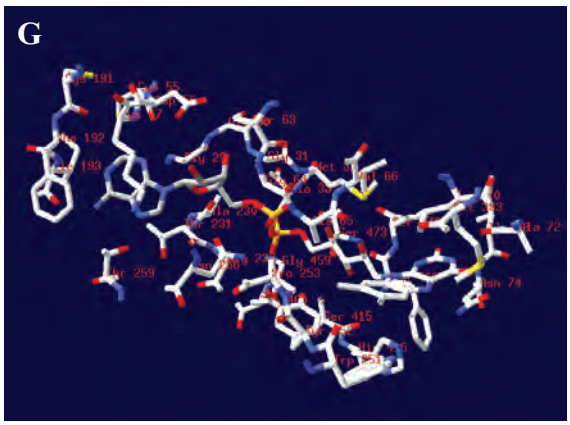

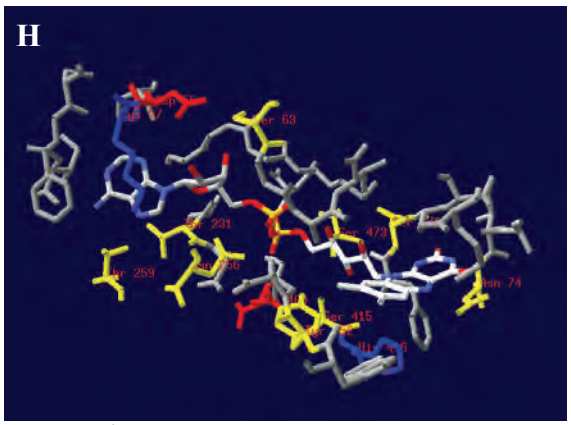

FAD surrounding protein matrix: residues present in a distance of < 4.1Å are shown (amino acids are coloured as follows: positively charged, basic AA, blue; negatively charged, acidic AA, red; polar AA, yellow; and unpolar, uncharged AA, grey)

Desulfovibrio desulfuricans

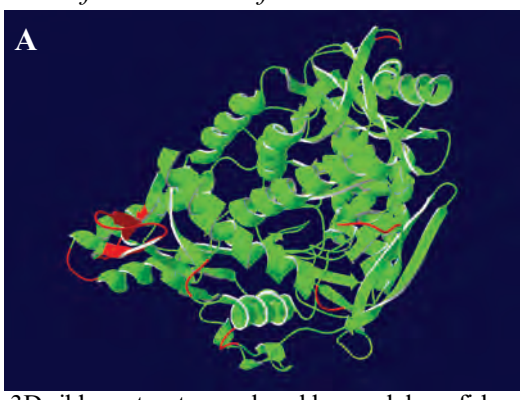

3D ribbon structure colored by model confidence

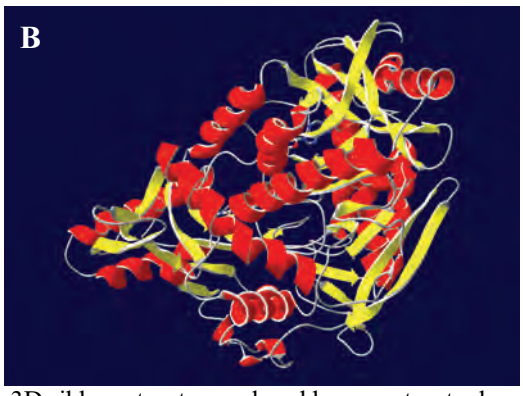

3D ribbon structure colored by sec. struct. elements

AprA model shown from front side

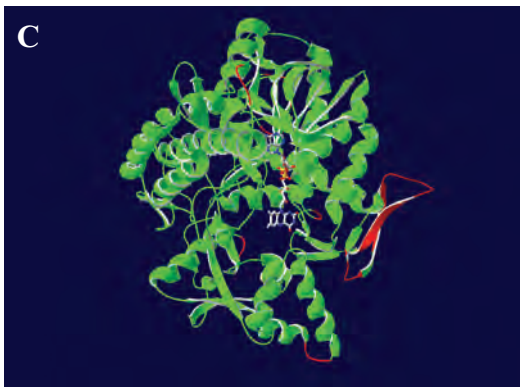

3D ribbon structure colored by model confidence

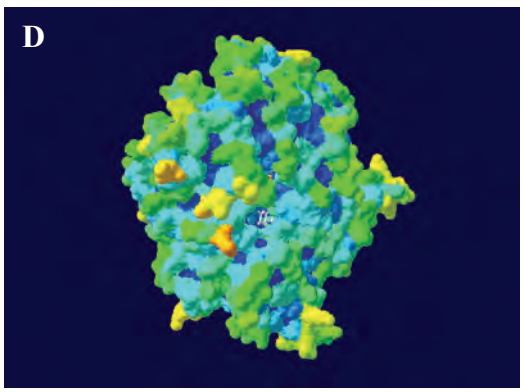

Protein molecular surface colored by accessibility

AprA model shown from top view

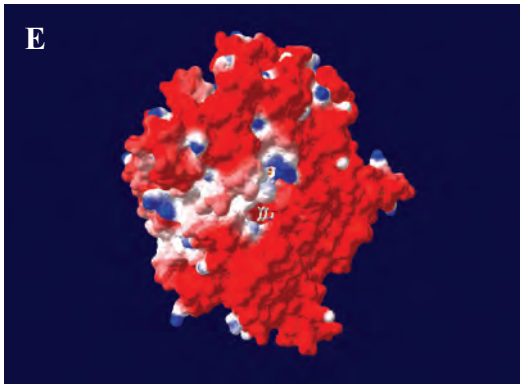

AprA model shown from top view

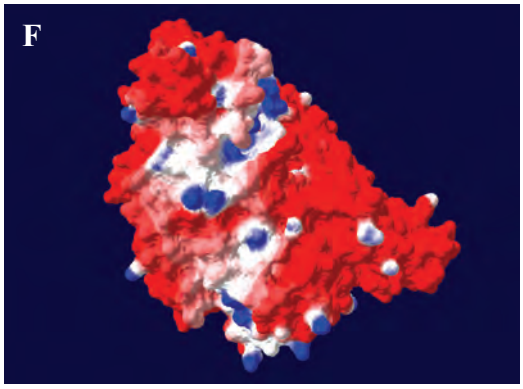

AprA model shown from back side

Protein molecular surface colored by calculated electrostatic potential (electric charge at the molecular surface is colored with a red (negative), white (neutral, and blue (positive) color gradient)

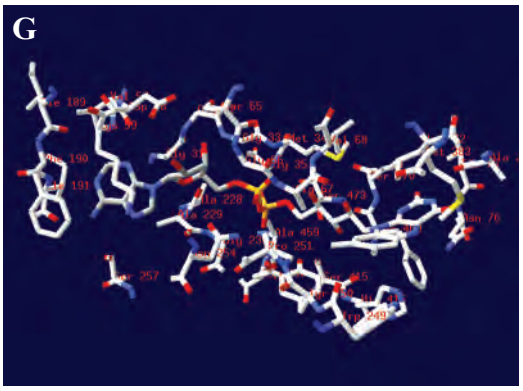

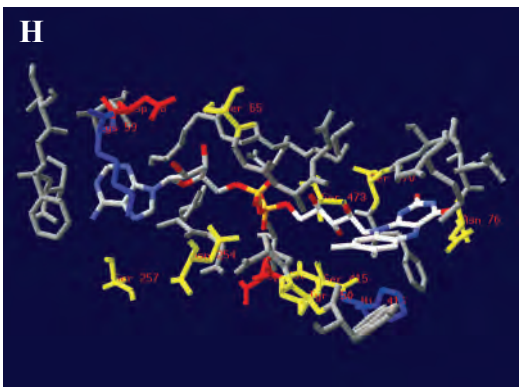

FAD surrounding protein matrix: residues present in a distance of < 4.1Å are shown (amino acids are coloured as follows: positively charged, basic AA, blue; negatively charged, acidic AA, red; polar AA, yellow; and unpolar, uncharged AA, grey)

Desulfovibrio vulgaris

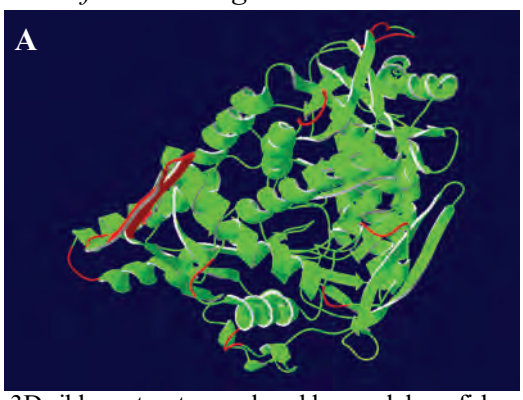

3D ribbon structure colored by model confidence

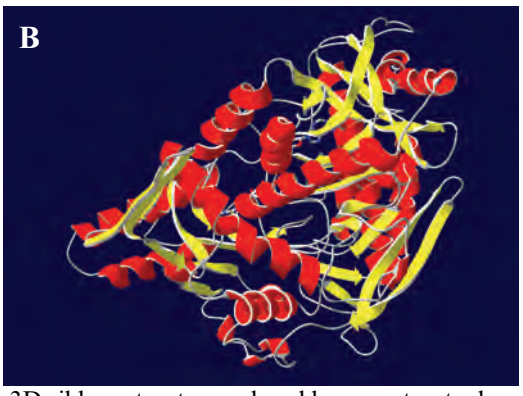

3D ribbon structure colored by sec. struct. elements

AprA model shown from front side

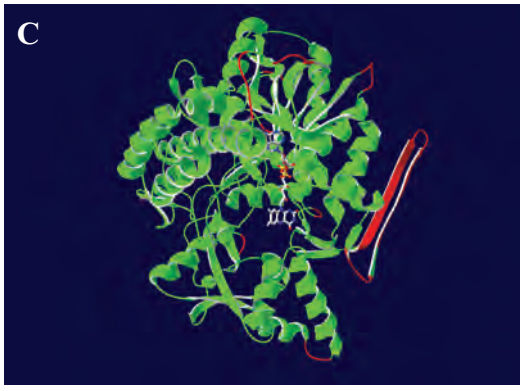

3D ribbon structure colored by model confidence

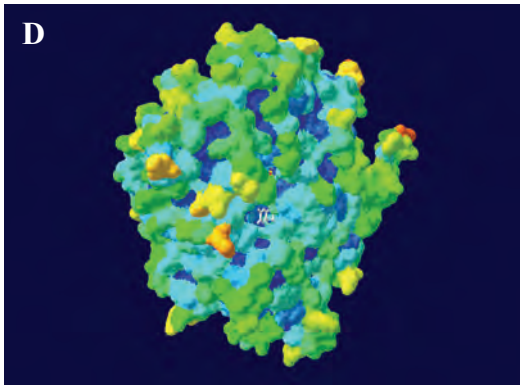

Protein molecular surface colored by accessibility

AprA model shown from top view

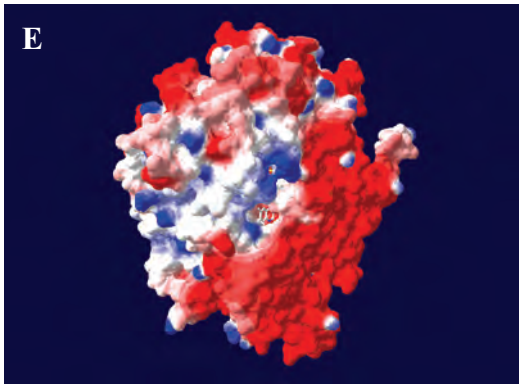

AprA model shown from top view

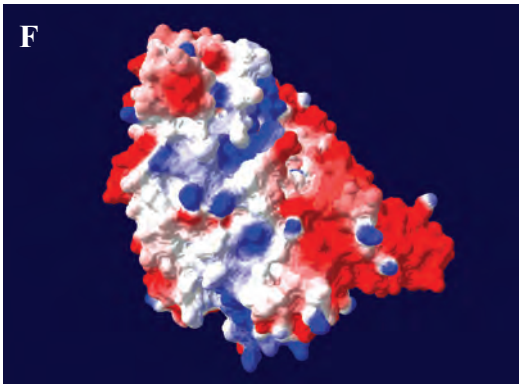

AprA model shown from back side

Protein molecular surface colored by calculated electrostatic potential (electric charge at the molecular surface is colored with a red (negative), white (neutral, and blue (positive) color gradient)

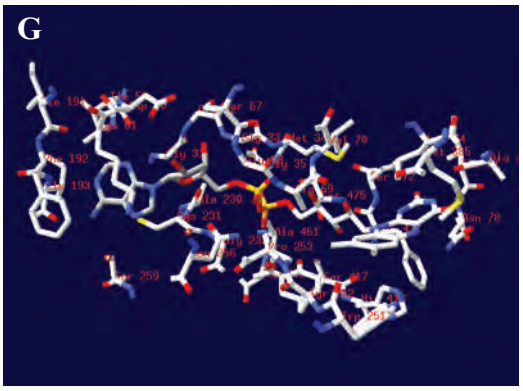

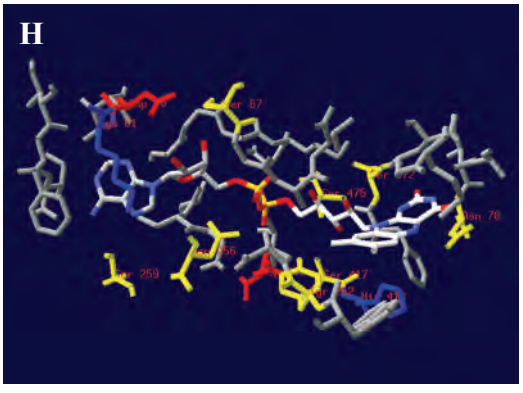

FAD surrounding protein matrix: residues present in a distance of < 4.1Å are shown (amino acids are coloured as follows: positively charged, basic AA, blue; negatively charged, acidic AA, red; polar AA, yellow; and unpolar, uncharged AA, grey)

Desulfobulbus sp.

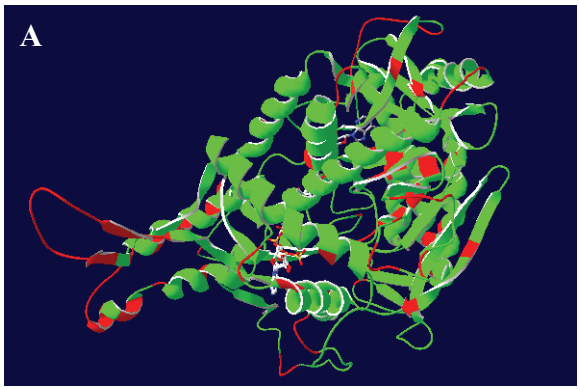

3D ribbon structure colored by model confidence

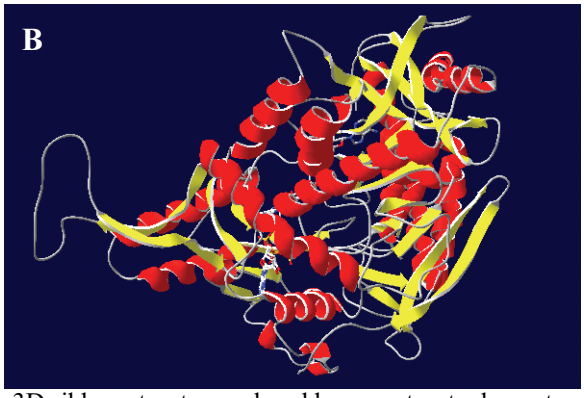

3D ribbon structure colored by sec. struct. elements

AprA model shown from front side

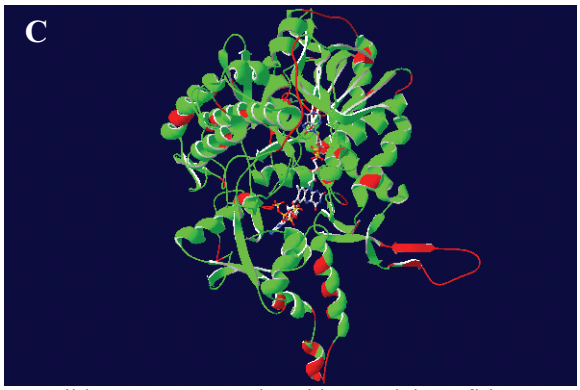

3D ribbon structure colored by model confidence

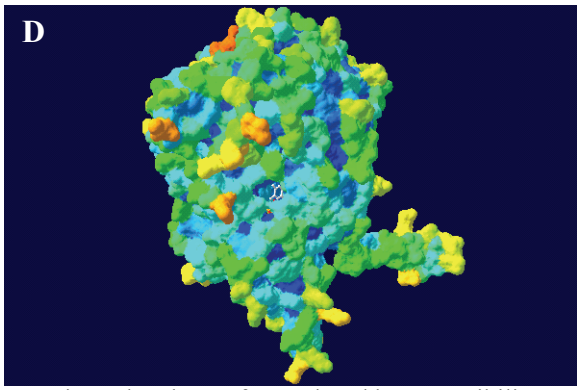

Protein molecular surface colored by accessibility

AprA model shown from top view

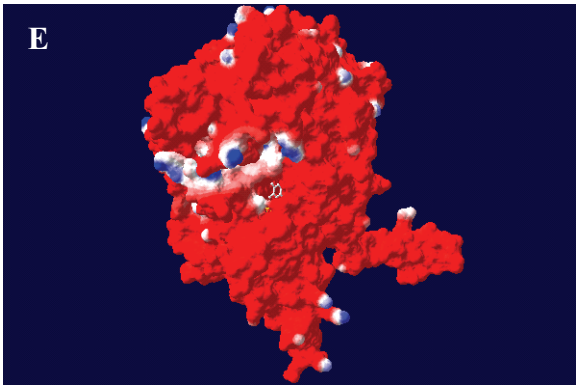

AprA model shown from top view

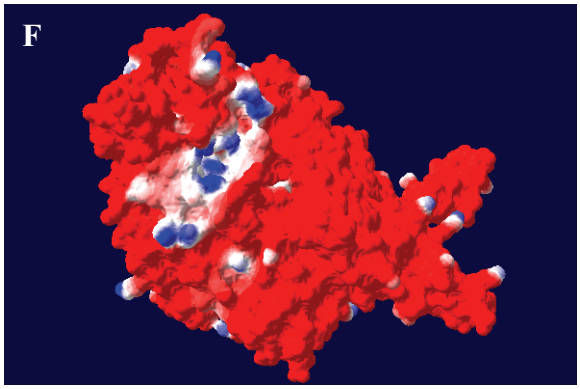

AprA model shown from back side

Protein molecular surface colored by calculated electrostatic potential (electric charge at the molecular surface is colored with a red (negative), white (neutral, and blue (positive) color gradient)

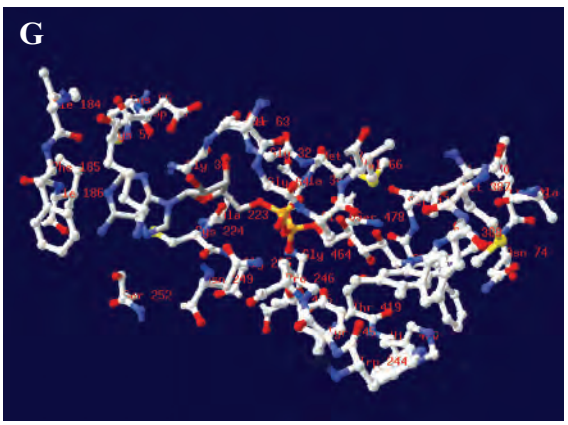

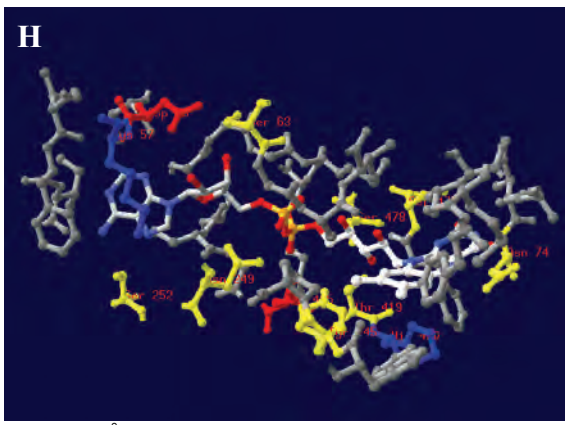

FAD surrounding protein matrix: residues present in a distance of < 4.1Å are shown (amino acids are coloured as follows: positively charged, basic AA, blue; negatively charged, acidic AA, red; polar AA, yellow; and unpolar, uncharged AA, grey)

Desulfotalea psychrophila

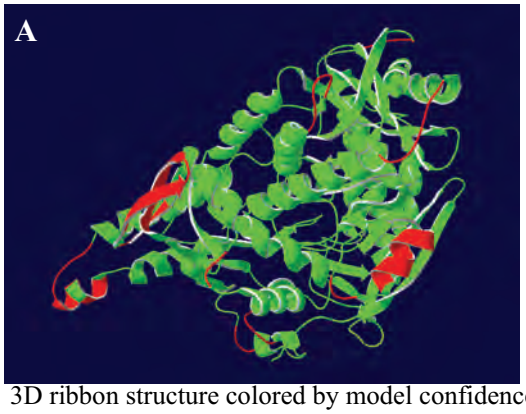

3D ribbon structure colored by model confidence

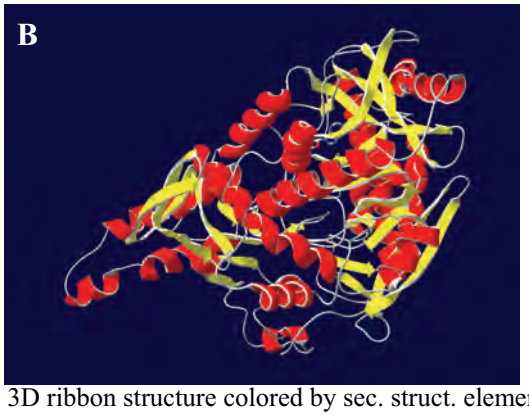

3D ribbon structure colored by sec. struct. elements

AprA model shown from front side

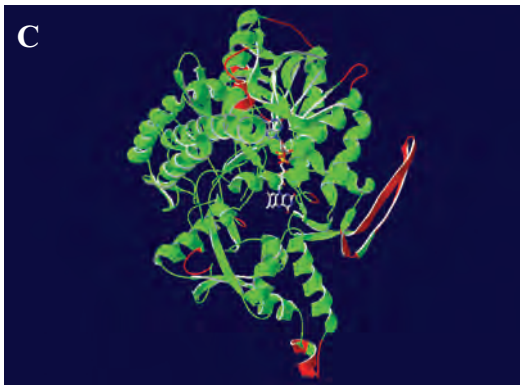

3D ribbon structure colored by model confidence

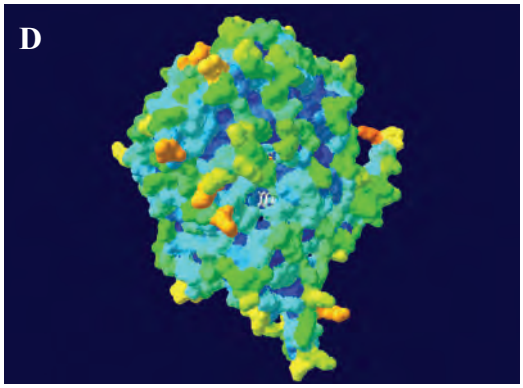

Protein molecular surface colored by accessibility

AprA model shown from top view

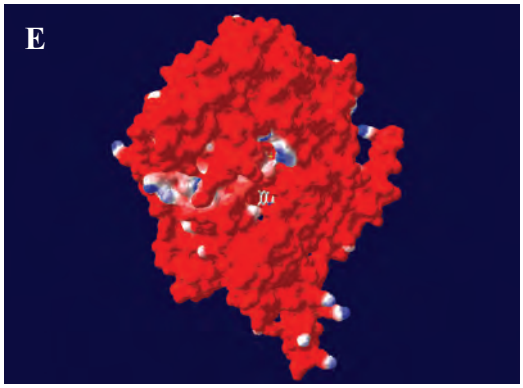

AprA model shown from top view

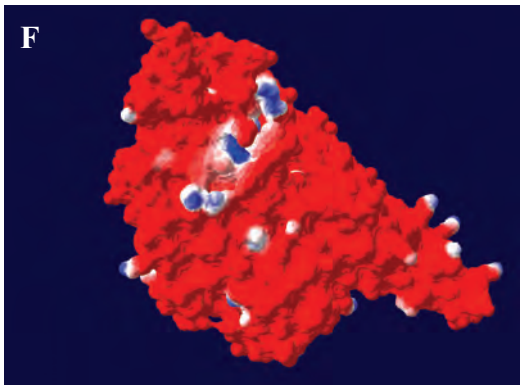

AprA model shown from back side

Protein molecular surface colored by calculated electrostatic potential (electric charge at the molecular surface is colored with a red (negative), white (neutral, and blue (positive) color gradient)

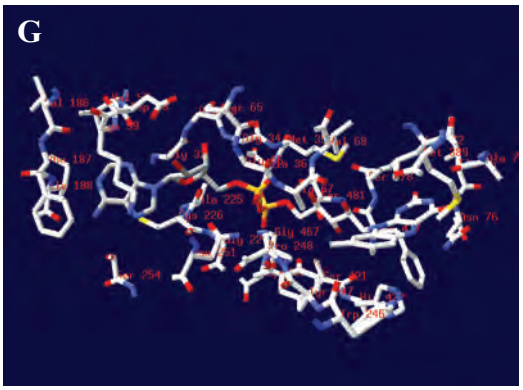

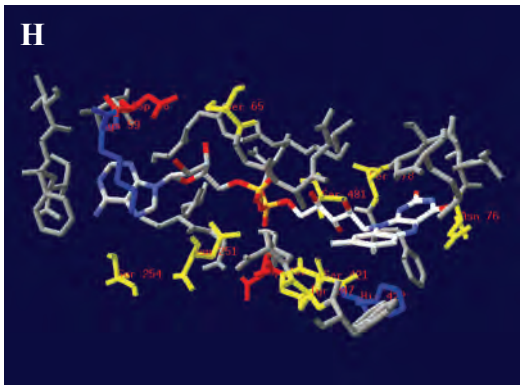

FAD surrounding protein matrix: residues present in a distance of < 4.1Å are shown (amino acids are coloured as follows: positively charged, basic AA, blue; negatively charged, acidic AA, red; polar AA, yellow; and unpolar, uncharged AA, grey)

O. algarvensis Delta 1 symbiont

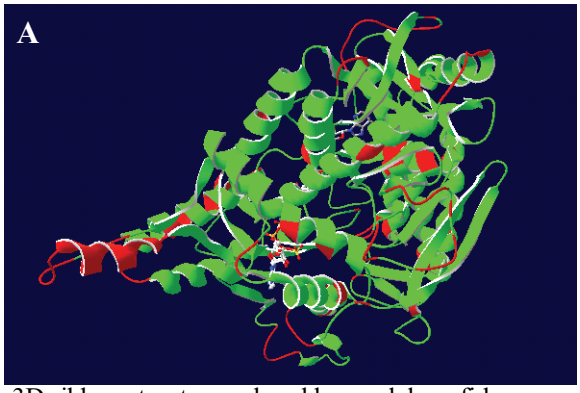

3D ribbon structure colored by model confidence

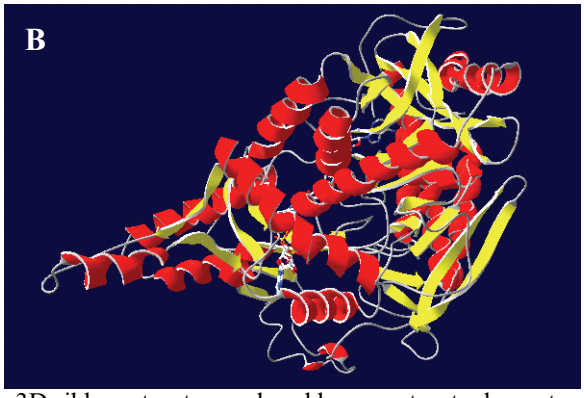

3D ribbon structure colored by sec. struct. elements

AprA model shown from front side

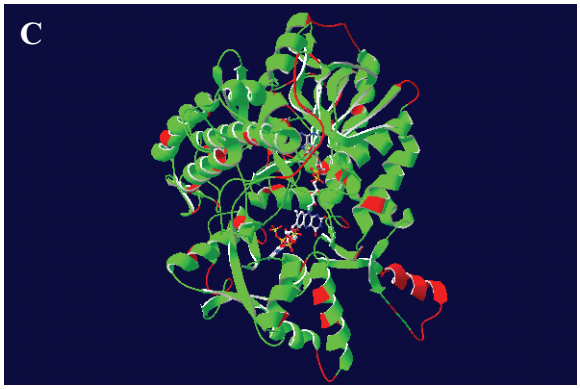

3D ribbon structure colored by model confidence

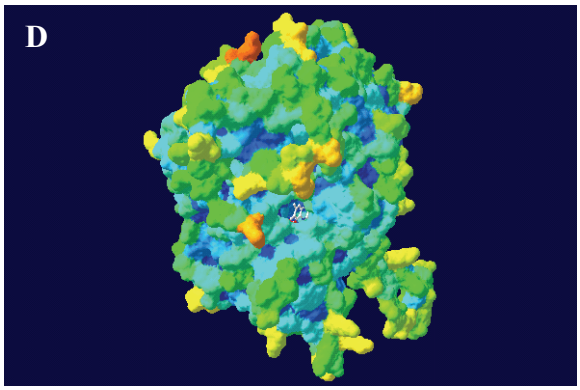

Protein molecular surface colored by accessibility

AprA model shown from top view

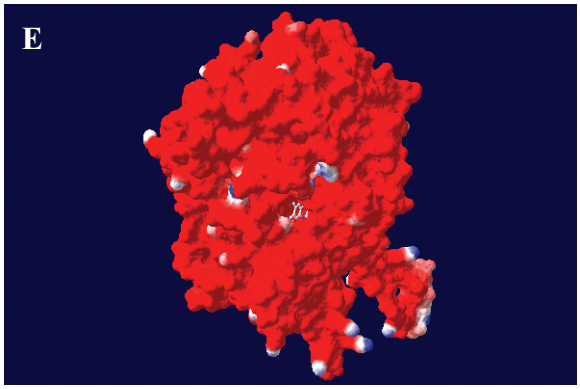

AprA model shown from top view

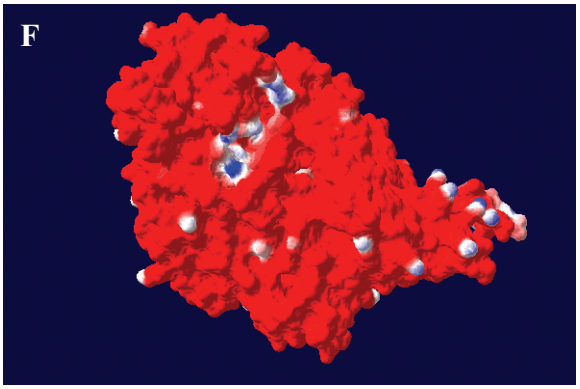

AprA model shown from back side

Protein molecular surface colored by calculated electrostatic potential (electric charge at the molecular surface is colored with a red (negative), white (neutral, and blue (positive) color gradient)

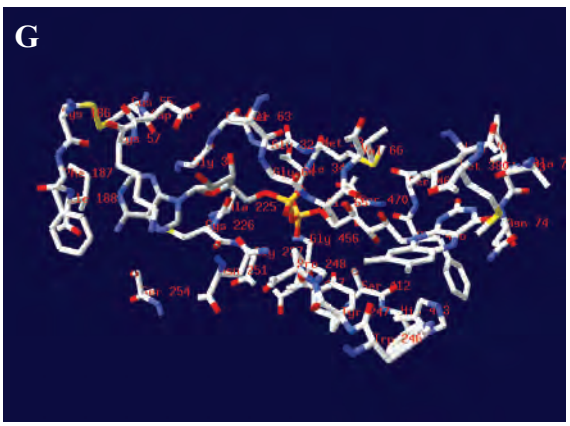

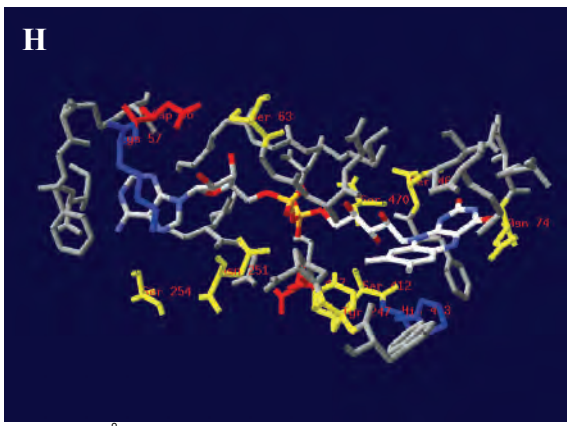

FAD surrounding protein matrix: residues present in a distance of < 4.1Å are shown (amino acids are coloured as follows: positively charged, basic AA, blue; negatively charged, acidic AA, red; polar AA, yellow; and unpolar, uncharged AA, grey)

Thermodesulfovibrio yellowstonii

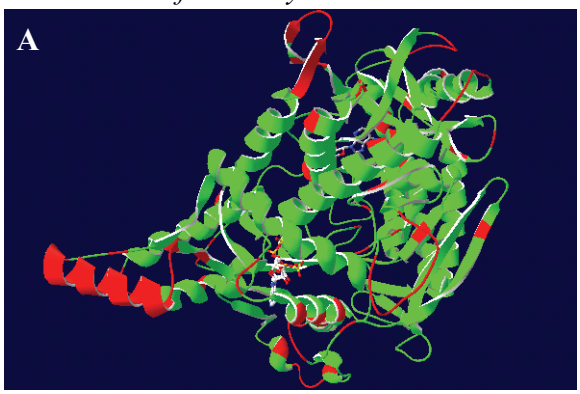

3D ribbon structure colored by model confidence

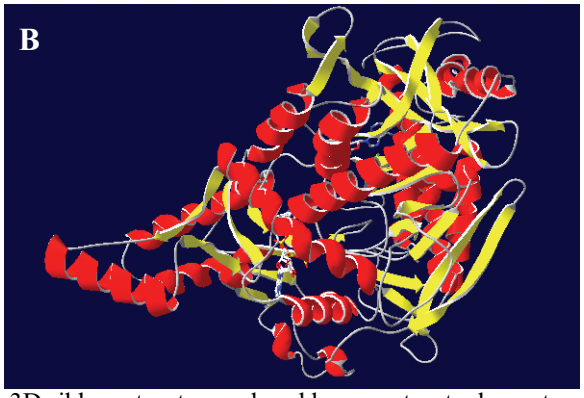

3D ribbon structure colored by sec. struct. elements

AprA model shown from front side

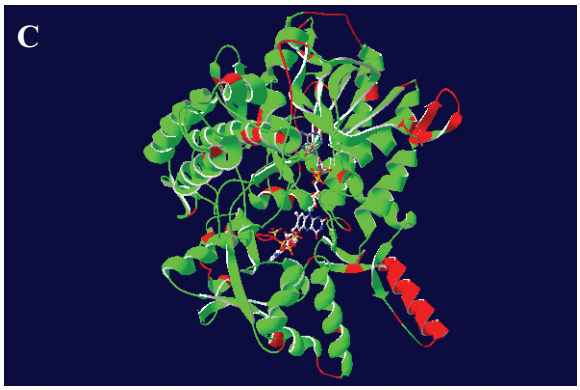

3D ribbon structure colored by model confidence

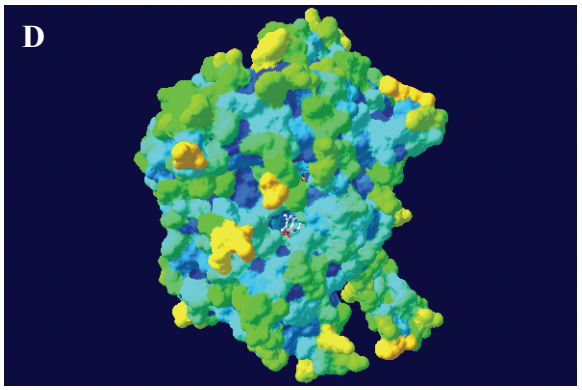

Protein molecular surface colored by accessibility

AprA model shown from top view

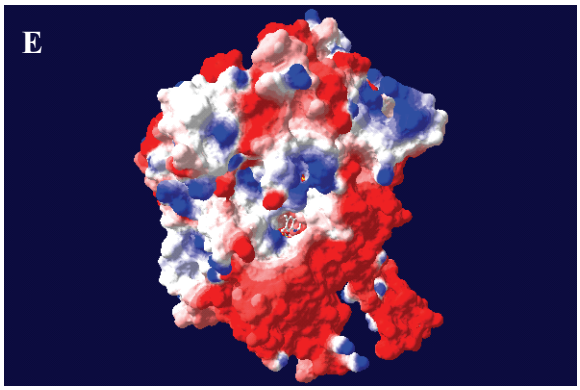

AprA model shown from top view

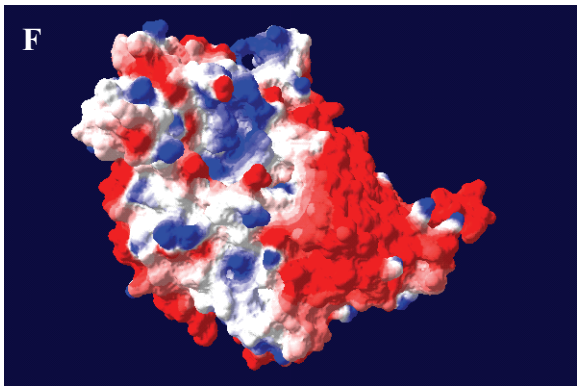

AprA model shown from back side

Protein molecular surface colored by calculated electrostatic potential (electric charge at the molecular surface is colored with a red (negative), white (neutral, and blue (positive) color gradient)

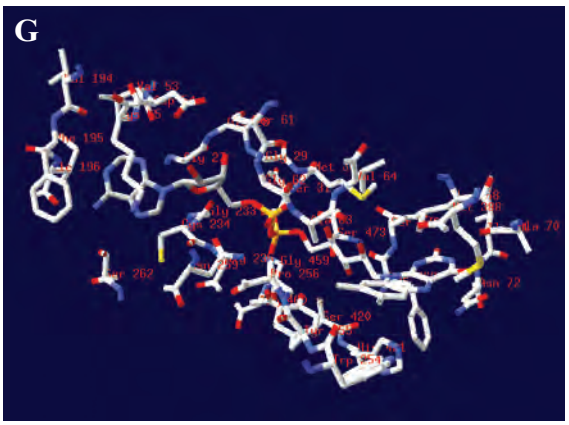

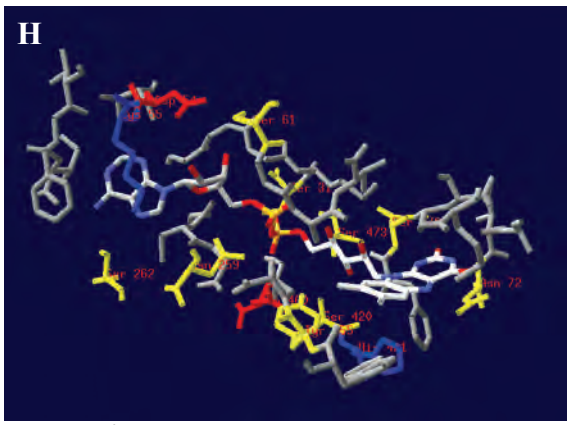

FAD surrounding protein matrix: residues present in a distance of < 4.1Å are shown (amino acids are coloured as follows: positively charged, basic AA, blue; negatively charged, acidic AA, red; polar AA, yellow; and unpolar, uncharged AA, grey)

Chlorobaculum tepidum

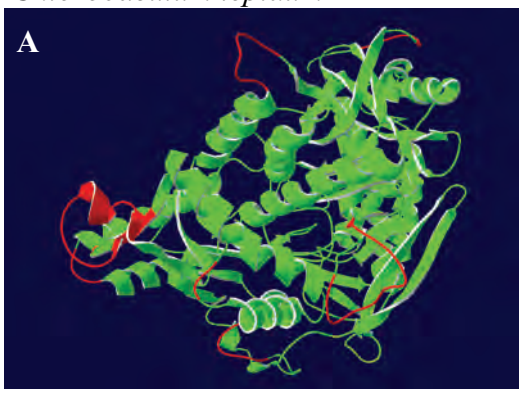

3D ribbon structure colored by model confidence

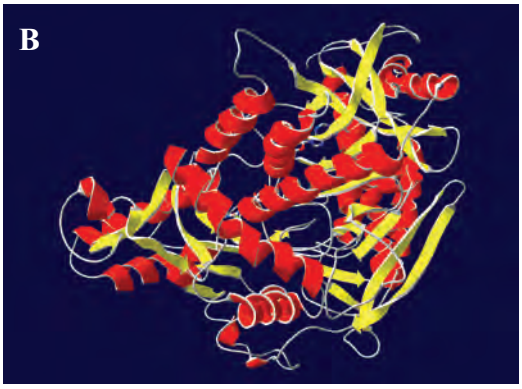

3D ribbon structure colored by sec. struct. elements

AprA model shown from front side

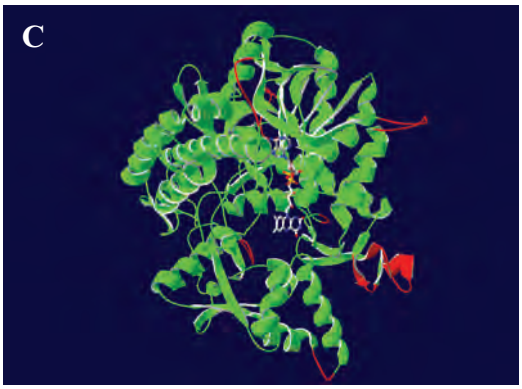

3D ribbon structure colored by model confidence

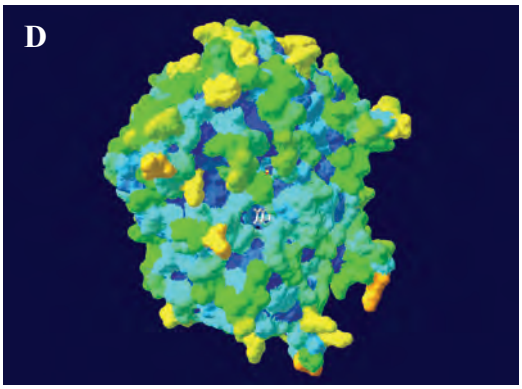

Protein molecular surface colored by accessibility

AprA model shown from top view

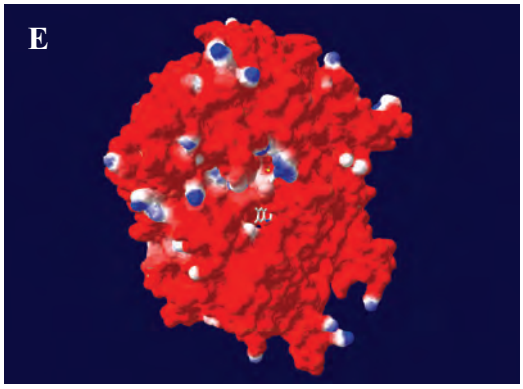

AprA model shown from top view

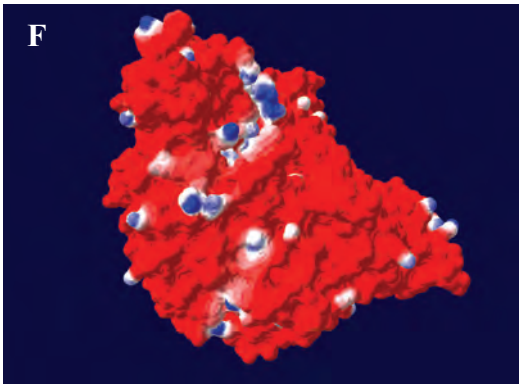

AprA model shown from back side

Protein molecular surface colored by calculated electrostatic potential (electric charge at the molecular surface is colored with a red (negative), white (neutral, and blue (positive) color gradient)

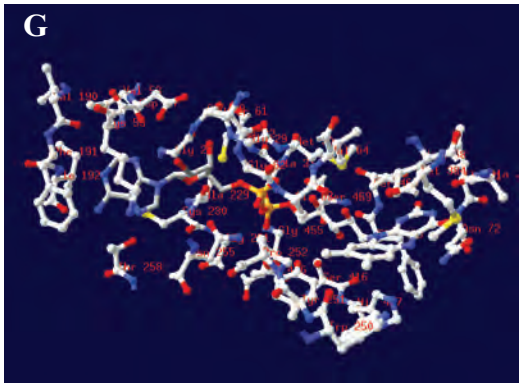

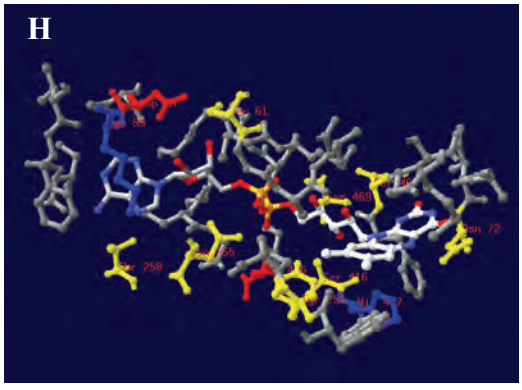

FAD surrounding protein matrix: residues present in a distance of < 4.1Å are shown (amino acids are coloured as follows: positively charged, basic AA, blue; negatively charged, acidic AA, red; polar AA, yellow; and unpolar, uncharged AA, grey)

Thiobacillus denitrificans

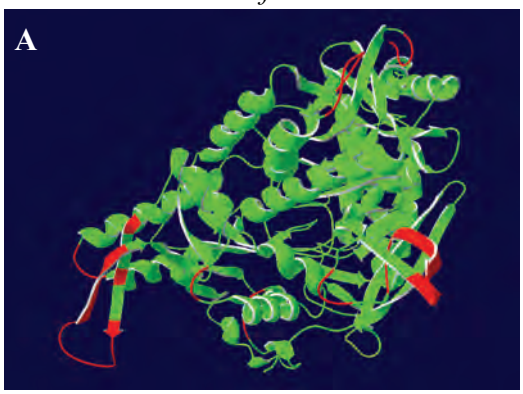

3D ribbon structure colored by model confidence

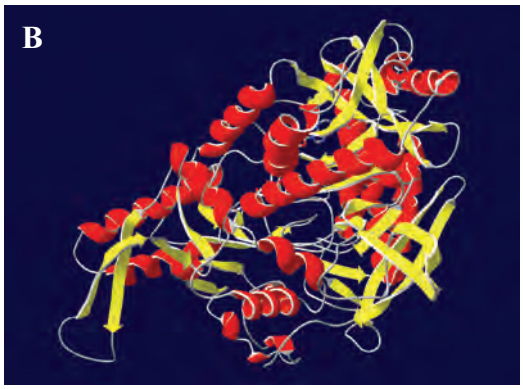

3D ribbon structure colored by sec. struct. elements

AprA model shown from front side

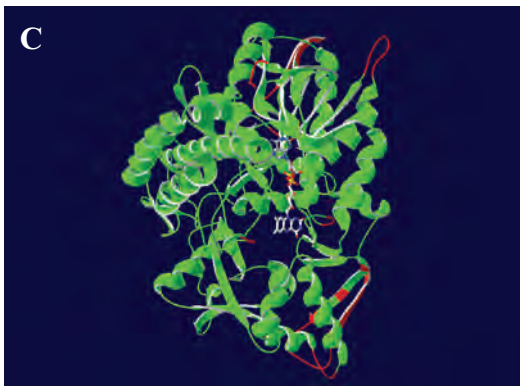

3D ribbon structure colored by model confidence

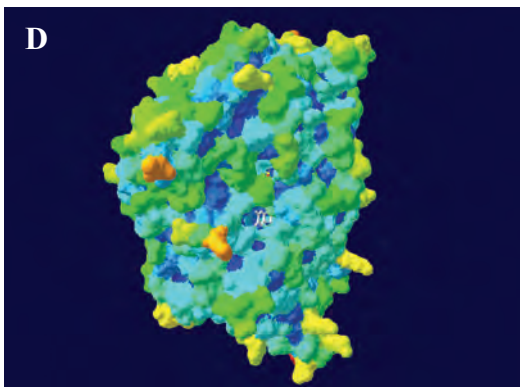

Protein molecular surface colored by accessibility

AprA model shown from top view

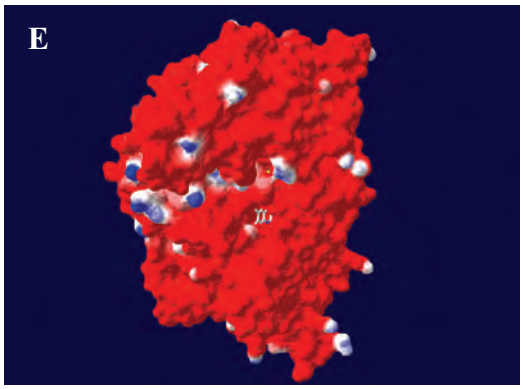

AprA model shown from top view

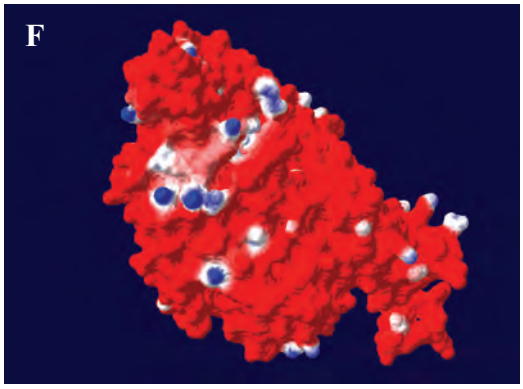

AprA model shown from back side

Protein molecular surface colored by calculated electrostatic potential (electric charge at the molecular surface is colored with a red (negative), white (neutral, and blue (positive) color gradient)

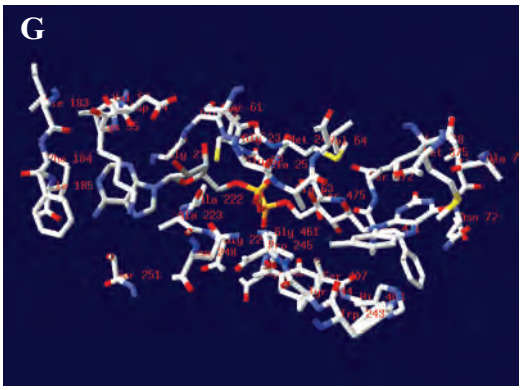

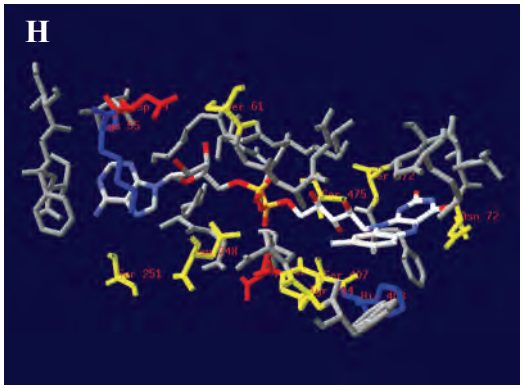

FAD surrounding protein matrix: residues present in a distance of < 4.1Å are shown (amino acids are coloured as follows: positively charged, basic AA, blue; negatively charged, acidic AA, red; polar AA, yellow; and unpolar, uncharged AA, grey)

Supplementary data material Figure S4: APS/ sulfite binding site – active center in AprA models of SRP and SOB (distances of the residues to the N5 atom of FAD are given in Å, isoalloxazine ring interacting residues are green coloured, polar and basic amino acids are coloured in yellow and blue, respectively)

Reference structure *Archaeoglobus fulgidus*

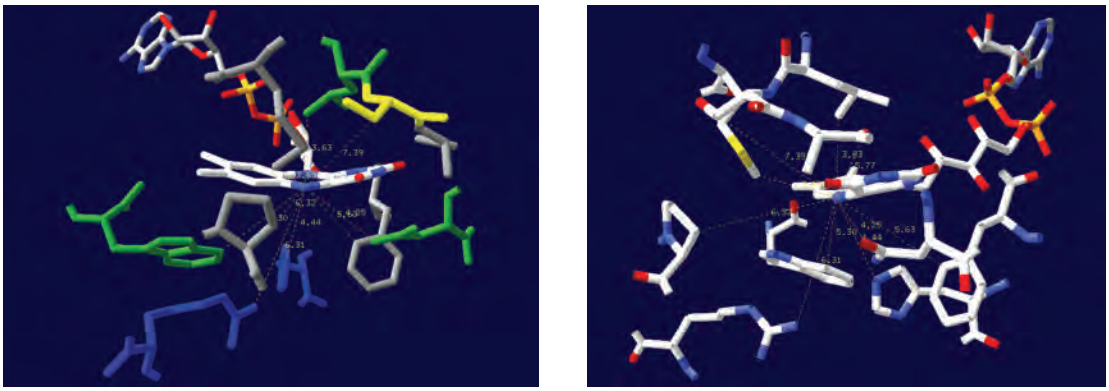

SOB Apr lineage I

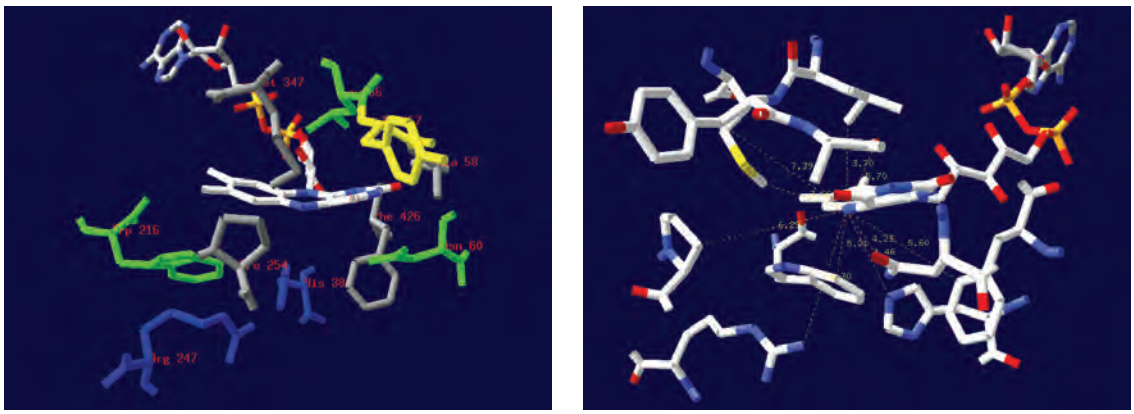

Allochromatium vinosum

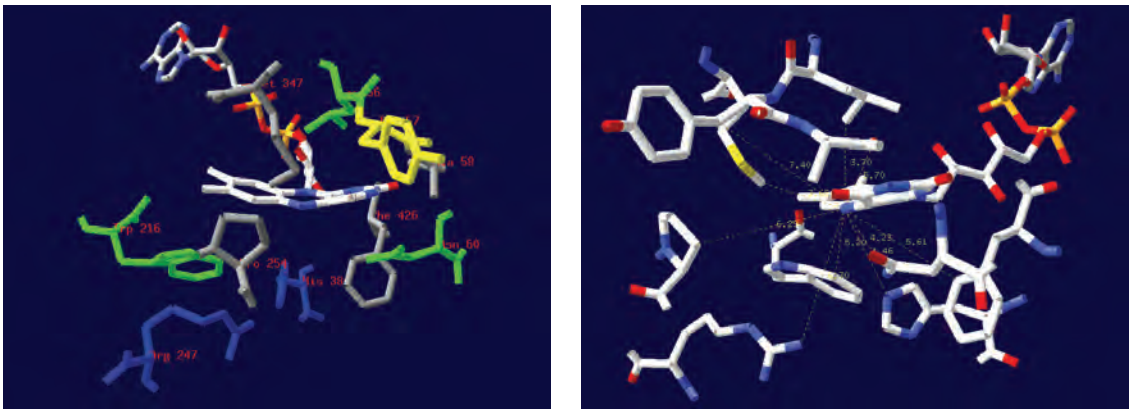

Thiobacillus denitrificans

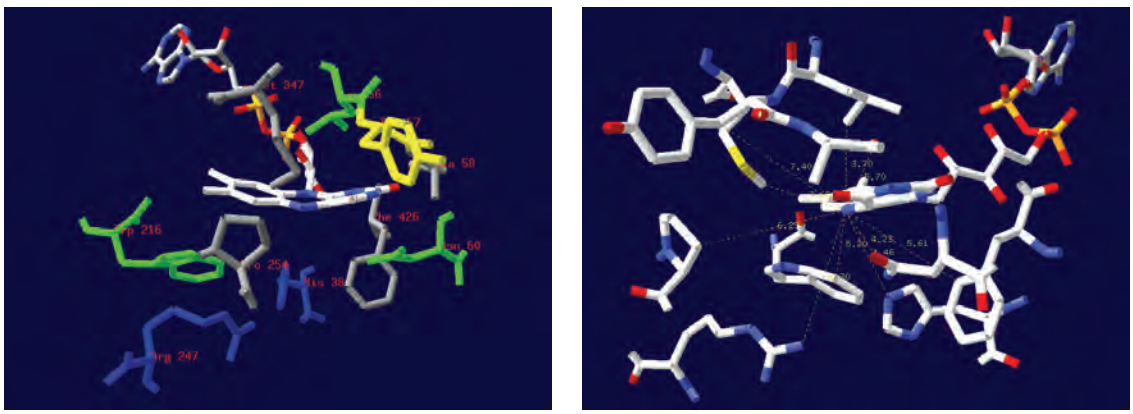

Cdt. Ruthia magnifica

SOB Apr lineage I

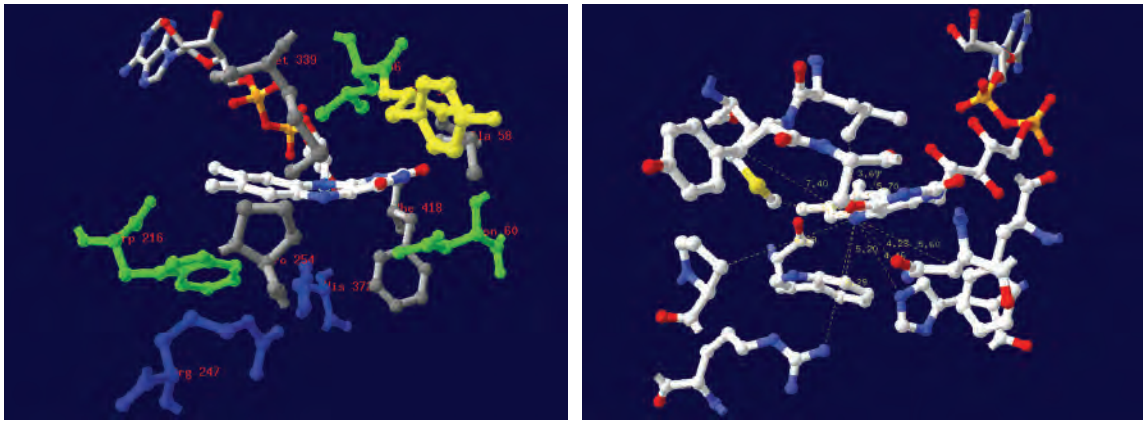

Cdt. Pelagibacter ubique

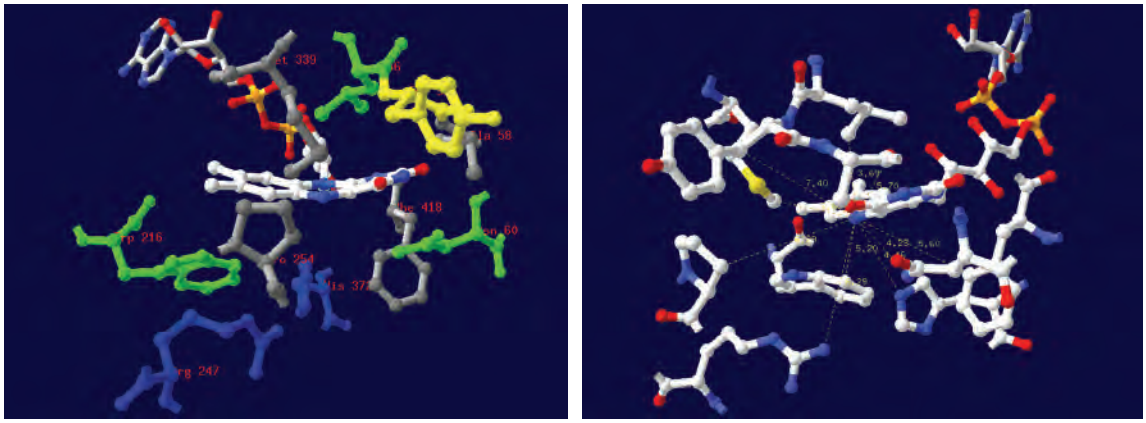

EBAC2C11

Crenarchaeal SRP

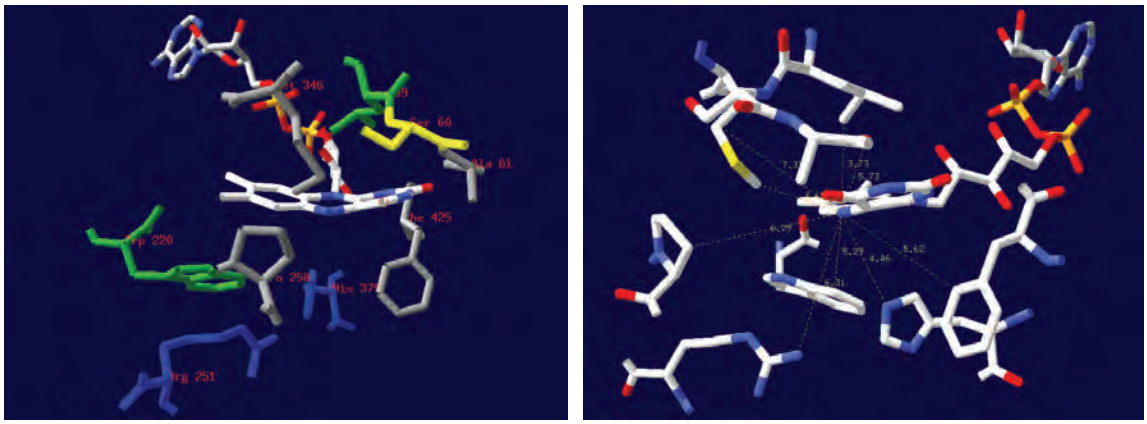

Pyrobaculum calidifontis

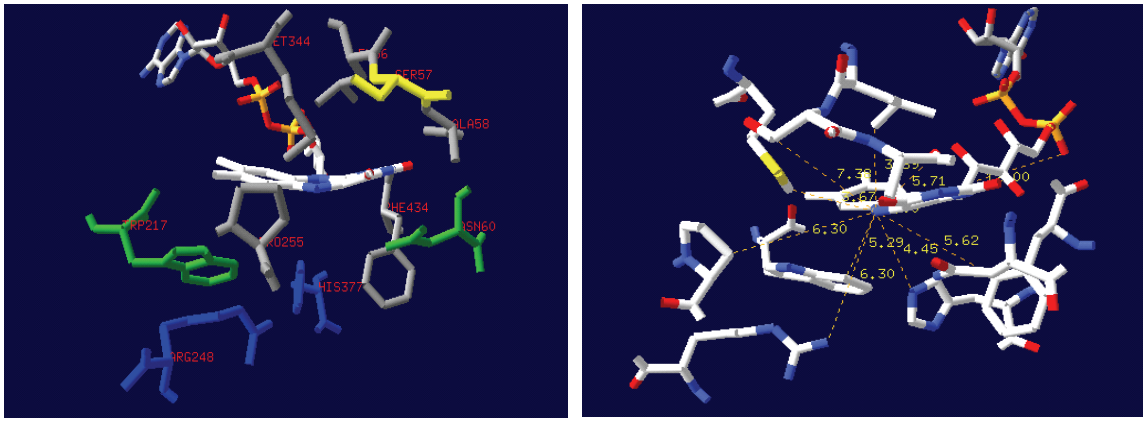

Caldivirga maquilingensis

SRB and related SOB Apr lineage II

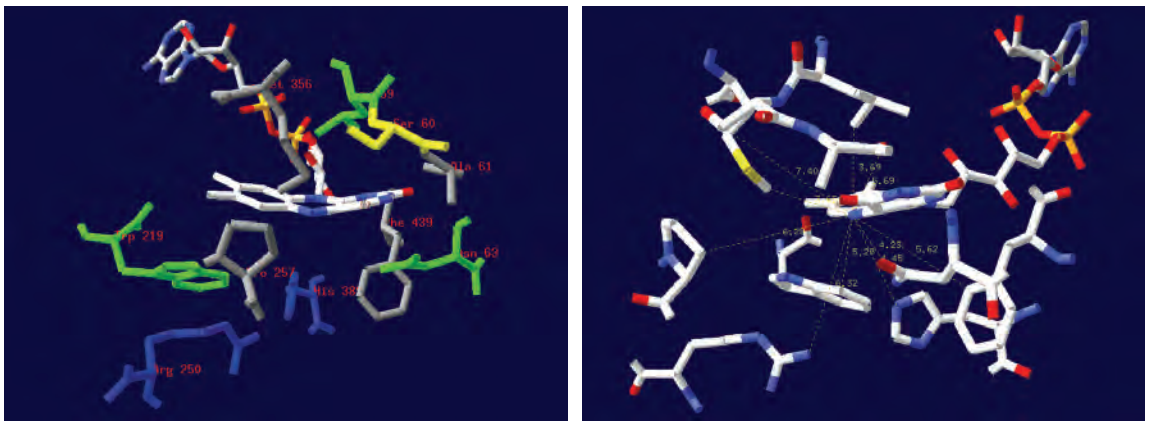

Gram-positive and related deltaproteobacterial SRB

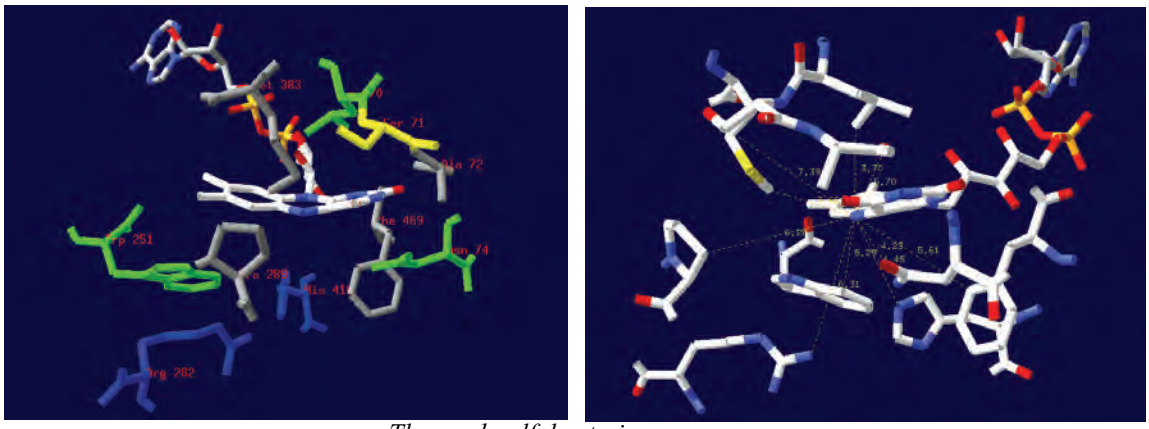

Thermodesulfobacterium commune

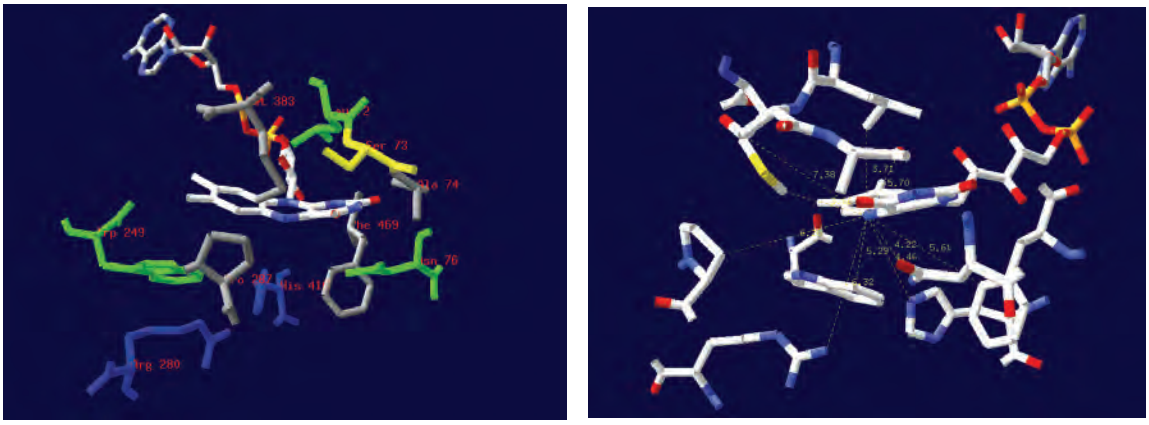

Desulfovibrionaceae

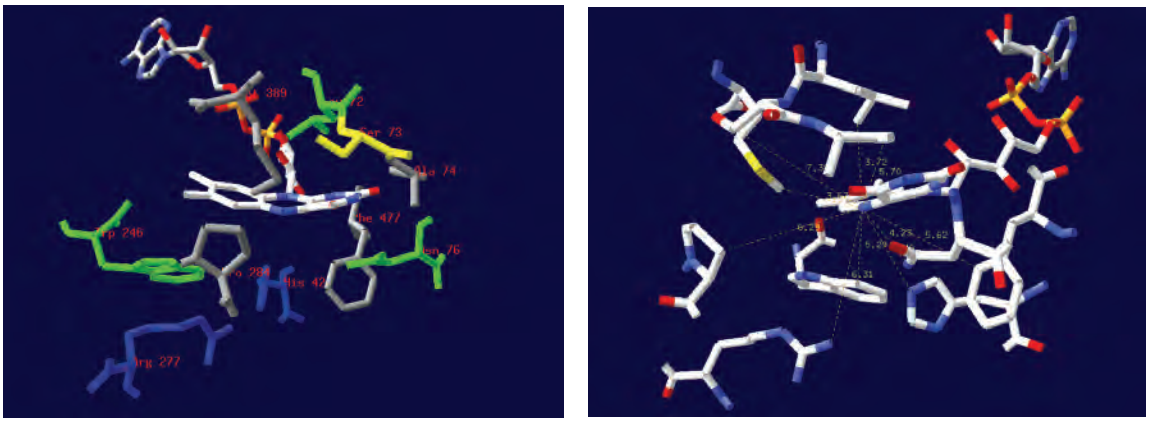

Desulfobulbaceae and *Desulfobacteraceae*

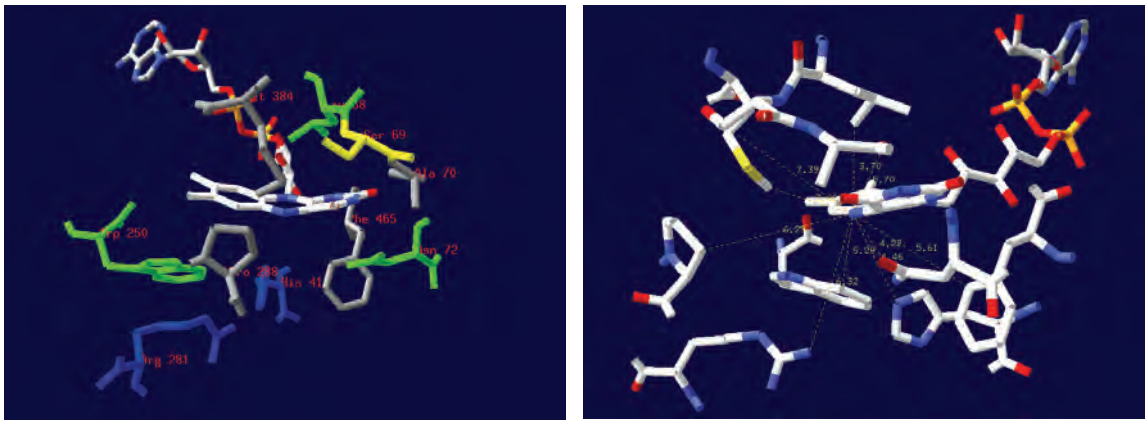

Chlorobaculum tepidum

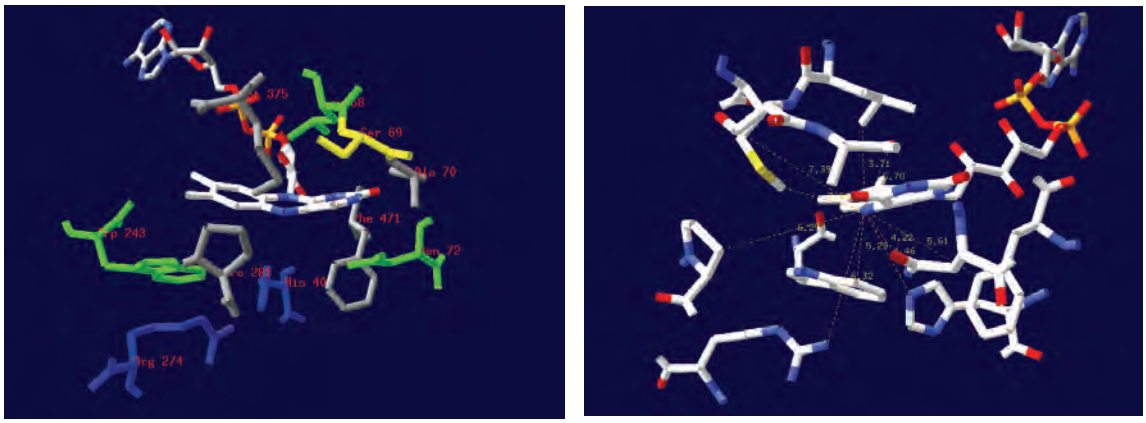

Thiobacillus denitrificans

Supplementary data material Table S4. FAD-binding site: residues adjacent to the FAD cofactor in AprA models of SRP and SOB

Species (no. of AA involved in binding)	FAD-binding domain			Capping domain	
		Isoalloxazine-binding	AA at a distance of < 4.1Å to FAD		AA at a distance of < 4.1Å to FAD
Archaeoglobus fulgidus **(35 AA)**	A2-A261 A394-A487	Leu70, Asn74, Trp234	Gly29, Gly30, Gly31, Phe32, Ser33, Val55, Glu56, Lys57, Ser63, Gly64, Ala65, Val66, Leu70, Ala72, Ile73, Asn74, Val174, Phe175, Ile176, Ala213, Thr214, Gly215, Trp234, Tyr235, Ala236, Asp239, Ser242 Ser397, His398, Gly438, Asp439, Phe448, Ser449, Ser452	A262-A393	**Met365**
SRB and rel. SOB					
Desulfotomaculum reducens **(35 AA)**	A2-A243 A382-A472	Leu58, Asn62, Trp216	Gly17, Gly18, Gly 19, Met20, Ala21, Val43, Asp44, Lys45, Ser51, Gly52, Ala53, Val54, Leu58, Ala60, Ile61, Asn62, Val162, Phe163, Ile164, Gly198, Met199, Gly200, Trp216, Tyr217, Pro218, Ser221, Ser224 Ser386, His387, Gly423, Asp424, Phe433, Ser434, Ser437	A244-A382	**Met354**
Syntrophobacter fumaroxidans **(35 AA)**	A2-A248 A387-A482	Leu58, Asn62, Trp220	Gly17, Gly18, Gly 19, Met20, Ser21, Val43, Asp44, Lys45, Ser51, Gly52, Ala53, Val54, Leu58, Ala60, Ile61, Asn62, Val163, Phe164, Ile165, Ala199, Met200, Gly201, Trp220, Tyr221, Pro222, Asn225, Ser228 Ser390, His391, Gly433, Asp434, Phe443, Ser444, Ser447	A249-A386	**Met358**
fosws7f8 **(36 AA)**	A2-A245 A384-A477	Leu58, Asn62, Trp218	Gly17, Gly18, Gly19, Met20, Ala21, Cys22, Val43, Asp44, Lys45, Ser51, Gly52, Ala53, Val54, Leu58, Ala60, Ile61, Asn62, Val161, Phe162, Leu163, Ala197, Met198, Gly199, Trp218, Tyr219, Pro220, Asn223, Ala226 Ser387, His388, Gly428, Asp429, Phe438, Ser439, Ser442	A246-A383	**Met355**
fosws39f7 **(36 AA)**	A2-A246 A385-A478	Leu59, Asn63, Trp219	Gly18, Gly19, Gly 20, Met21, Ser22, Val44, Asp45, Lys46, Ser52, Gly53, Ala54, Val55, Leu59, Ala61, Leu62?, Asn63, Ile162, Phe163, Ile164, Ala198, Met199, Gly200, Trp219, Tyr220, Pro221, Asn224, Ser227 Ser388, His389, Gly429, Asp430, Phe439, Ser440, Ser443, Gln567	A247-A384	**Met356**
Thermodesulfo-bacterium commune **(35 AA)**	A2-A278 A412-A508	Leu70, Asn74, Trp251	Gly29, Gly30, Gly31, Met32, Ala33, Cys55, Asp56, Lys57, Ser63, Gly64, Ala65, Val66, Leu70, Ala72, Ile73, Asn74, Cys191, Phe192, Ile193, Ala230, Thr231, Gly232, Trp251, Tyr252, Pro253, Asn256, Thr259 Ser415, His416, Gly459, Asp460, Phe469, Ser470, Ser473	A279-A411	**Met383**
Desulfovibrio vulgaris **(35 AA)**	A2-A278 A414-A510	Leu74, Asn78, Trp251	Gly31, Gly32, Gly 33, Met34, Gly35, Ile59, Asp60, Lys61, Ser67, Gly68, Ala69, Val70, Leu74, Ala76, Ile77, Asn78, Ile191, Phe192, Ile193, Ala230, Cys231, Gly232, Trp251, Tyr252, Pro253, Asn256, Ser259 Ser417, His418, Ala461, Asp462, Phe471, Ser472, Ser475	A279-A413	**Met385**
Desulfovibrio desulfuricans **(35 AA)**	A2-A276 A412-A508	Leu72, Asn76, Trp249	Gly31, Gly32, Gly 33, Met34, Gly35, Val57, Asp58, Lys59, Ser65, Gly66, Ala67, Val68, Leu72, Ala74, Ile75, Asn76, Ile189, Phe190, Ile191, Ala228, Ala229, Gly230, Trp249, Tyr250, Pro251, Asn254, Ser257 Ser415, His416, Ala459, Asp460, Phe469, Ser470, Ser473	A277-A411	**Met383**

Desulfotalea psychrophila **(35 AA)**	A2-A273 A418-A515	Leu72, Asn76, Trp246	Gly32, Gly33, Gly 34, Met35, Ala36, Val57, Asp58, Lys59, Ser65, Gly66, Ala67, Val68, Leu72, Ala74, Ile75, Asn76, Val186, Phe187, Ile188, Ala225, Cys226, Gly227, Trp246, Tyr247, Pro248, Asn251, Ser254 Ser421, His422, Gly467, Asp468, Phe477, Ser478, Ser481	A274-A417	**Met389**
***Desulfobulbus* sp. MLMS1** **(35 AA)**	A2-A271 A416-A513	Leu70, Asn74, Trp244	Gly30, Gly31, Gly 32, Met33, Ala34, Val55, Asp56, Lys57, Ser63, Gly64, Ala65, Val66, Leu70, Ala72, Ile73, Asn74, Ile184, Phe185, Ile186, Ala223, Cys224, Gly225, Trp244, Tyr245, Pro246, Asn249, Ser252 Thr419, His420, Gly464, Asp465, Phe474, Ser475, Ser478	A272-A415	**Met387**
***O. algarvensis* Delta 1 symbiont** **(35 AA)**	A2-A273 A409-A505	Leu70, Asn74, Trp246	Gly30, Gly31, Gly 32, Met33, Ala34, Val55, Asp56, Lys57, Ser63, Gly64, Ala65, Val66, Leu70, Ala72, Ile73, Asn74, Val186, Phe187, Ile188, Ala225, Cys226, Gly227, Trp246, Tyr247, Pro248, Asn251, Ser254 Ser412, His413, Gly456 Asp457, Phe466, Ser467, Ser470	A274-A408	**Met380**
Thermodesulfo-vibrio yellowstonii **(35 AA)**	A2-A281 A417-A508	Leu68, Asn72, Trp254	Gly27, Gly28, Gly29, Met30, Ser31, Val53, Asp54, Lys55, Ser61, Gly62, Ala63, Val64, Leu68, Ala70, Ile71, Asn72, Val194, Phe195, Ile196, Gly233, Cys234, Gly235, Trp254, Tyr255, Pro256, Asn259, Ser262 Ser420, His421, Gly459, Asp460, Phe469, Ser470, Ser473	A282-A416	**Met388**
Chlorobaculum tepidum **(36 AA)**	A2-A277 A413-A504	Leu68, Asn72, Trp250	Gly27, Gly28, Gly29, Met30, Ala31, Cys32, Val53, Asp54, Lys55, Ser61, Gly62, Ala63, Val64, Leu68, Ala70, Ile71, Asn72, Val190, Phe191, Ile192, Ala229, Cys230, Gly231, Trp250, Tyr251, Pro252, Asn255, Thr258 Ser416, His417, Gly455, Asp456, Phe465, Ser466, Ser469	A278-A412	**Met384**
***Thiobacillus denitrificans* 25259** **(36 AA)**	A2-A270 A404-A510	Leu68, Asn72, Trp243	Gly21, Gly22, Gly23, Met24, Ala25, Cys26, Val53, Asp54, Lys55, Ser61, Gly62, Ala63, Val64, Leu68, Ala70, Ile71, Asn72, Ile183, Phe184, Ile185, Ala222, Ala223, Gly224, Trp243, Tyr244, Pro245, Asn248, Ser251 Ser407, His408, Gly461, Asp462, Phe471, Ser472, Ser475	A271-A403	**Met375**
Crenarch. SRP					
Caldivirga maquilingensis **(35 AA)**	A2-A244 A373-A474	Leu56, Asn60, Trp217	Gly17, Gly18, Gly19, Met20, Ala21, Ala41, Glu42, Lys43, Ser49, Gly50, Ala51, Val52, Leu56, Ala58, Ile59, Asn60, Val157, Met158, Val159, Ala196, Ala197, Gly198, Trp217, Tyr218, Pro219, Ser222, Ser225 Ser376, His377, Gly424, Asp425, Phe434, Ser435, Ser438	A245-A372	**Met344**
Pyrobaculum calidifontis **(33 AA)**	A2-A247 A375-A466	Leu59, -, (Asn63) Trp220	Gly19, Gly20, Gly21, Met22, Ala23, Val44, Glu45, Lys46, Ser52, Gly53, Ala54, Val55, Leu59, Ala61, Thr62, -, Val160, Phe161, Val162, Ala199, Ala200, Gly201, Trp220, Tyr221, Pro222, -, Ser228 Ser378, His379, Gly415, Asp426, Phe425, Ser426, Ser429	A248-A374	**Met346**
SOB Apr lineage I					
Allochromatium vinosum **(35 AA)**	A2-A243 A376-A466	Leu56, Asn60, Trp216	Gly17, Ala18, Gly 19, Leu20, Gly21, Ala41, Glu42, Lys43, Ser49, Gly50, Ala51, Val52, Leu56, Ala58, Ile59, Asn60, Ile156, Cys157, Val158, Ala195, Ala196, Gly197, Trp216, Tyr217, Ala218, Ser221, Ser224 Ser379, His380, Gly416, Asp417, Phe426, Ser427, Ser430	A244-A375	**Met347**
***Thiobacillus den.itrificans* 25259**	A2-A243 A376-A466	Leu56, Asn60, Trp216	Gly17, Ala18, Gly 19, Leu20, Gly21, Ala41, Glu42, Lys43, Ser49, Gly50, Ala51, Val52, Leu56, Ala58, Ile59, Asn60, Ile156, Cys157, Val158, Gly195, Ala196, Gly197, Trp216, Tyr217, Ala218, Ser221, Ser224	A244-A375	**Met347**

(35 AA)			Ser379, His380, Gly416, Asp417, Phe426, Ser427, Ser430		
***Cdt.* Ruthia magnifica** **(35 AA)**	A2-A247 A379-A469	Leu56, Asn60, Trp219	Gly17, Ala18, Gly 19, Leu20, Gly21, Ala41, Glu42, Lys43, Ser49, Gly50, Ala51, Val52, Leu56, Ala58, Ile59, Asn60, Ile159 Met160, Val161, Gly198, Ala199, Gly200, Trp219, Tyr220, Ala221, Ser224, Ser227 Ser382, His383, Gly419, Asp420, Phe429, Ser430, Ser433	A248-A378	**Met350**
***Cdt.* Pelagibacter ubique** **(35 AA)**	A2-A243 A367-A458	Leu56, Asn60, Trp216	Gly17, Gly18, Gly 19, Met20, Ala21, Val41, Glu42, Lys43, Ser49, Gly50, Ala51, Val52, Leu56, Ala58, Ile59, Asn60, Ile156, Met157, Ile158, Ala195, Ala196, Gly197, Trp216, Tyr217, Ala218, Ser221, Ser224 Ser371, His372, Gly408, Asp409, Phe418, Ser419, Ser422	A244-A366	**Met339**
EBAC2C11 **(35 AA)**	A2-A243 A367-A458	Leu56, Asn60, Trp216	Gly17, Gly18, Gly 19, Phe20, Gly21, Val41, Glu42, Lys43, Ser49, Gly50, Ala51, Val52, Leu56, Ala58, Ile59, Asn60, Ile156, Met157, Val158, Ala195, Ala196, Gly197, Trp216, Tyr217, Ala218, Ser221, Ser224 Ser371, His372, Gly408, Asp409, Phe418, Ser419, Ser422	A244-A366	**Met339**

Supplementary data material Table S5. APS/sulfite-AMP binding site: residues adjacent to the substrates APS/sulfite-AMP in AprA models of SRP and SOB

Species **(no. of AA involved in substrate binding)**	**FAD-binding domain**		**Capping domain**		**AA in a distance of < 5.0Å to (deviations to the *A. fulgidus* AprA template structure are listed and highlighted by red colour)**			
		AA in a distance of < 5.0Å to APS/sulfite-AMP		AA in a distance of < 5.0Å to APS/sulfite-AMP	Sulfate moiety of APS/sulfite	Phosphate moiety of APS/AMP	Ribityl moiety of APS/AMP	Adenine ring of APS/ AMP
Archaeoglobus fulgidus **(22 AA)**	A2-A261 A394-A487	Asn74, Tyr95, Glu141, Trp144, Gln145, Trp234, Phe261 His398, Ser399, His446, Phe448	A262-A393	Arg265, Pro272, Val273, Gly274, Ala275, Phe277, Leu278, Pro311, Thr314, Arg317, Met365	Asn74, Trp234, Arg265, His398, (Phe261, Thr314, Ser399, Met365)	Arg265, Pro272, Val273, Gly274	Tyr95, Glu141, Gln145, Gly274, Leu278, Thr314, His446, Phe448	Gly274, Phe277, Leu278, Pro311, Arg317
SRB and rel. SOB								
Desulfotomaculum reducens **(21 AA)**	A2-A243 A382-A472	Asn62, Tyr80, Trp129, Gln130, Trp216, Phe243 His387, Ser388, His431, Phe433	A244-A382	Arg247, Pro254, Val255, Gly256, Ala257, Phe259, Leu260, Pro293, Ala296, Arg299, Met354	(Thr314 substituted by Ala296)	Identical to ***A. fulgidus***	Glu141 is missing unsubstituted (Thr314 unsubstituted by Ala299)	Identical to ***A. fulgidus***
Syntrophobacter fumaroxidans **(22 AA)**	A2-A248 A387-A482	Asn62, Tyr80, Glu126, Trp129, Gln130, Trp220, Phe247 His391, Ser392, His441, Phe443	A249-A386	Arg251, Pro258, Val259, Gly260, Ala261, Phe263, Leu264, Pro297, Ala300, Arg303, Met358	(Thr314 substituted by Ala299)	Identical to ***A. fulgidus***	Identical to Archglobus fulgidus (Thr314 unsubstituted by Ala299)	Identical to ***A. fulgidus***
fosws7f8 **(22 AA)**	A2-A245 A384-A477	Asn62, Tyr80, Glu126, Trp129, Gln130, Trp218, Phe245 His388, Ser389, His436, Phe438	A246-A383	Arg249, Pro256, Val257, Gly258, Ala259, Phe261, Leu262, Pro295, Ala298, Arg301, Met355	Identical to ***A. fulgidus***	Identical to ***A. fulgidus***	Identical to ***A. fulgidus***	Identical to ***A. fulgidus***
fosws39f7 **(22 AA)**	A2-A246 A385-A478	Asn63, Tyr81, Glu127, Trp130, Gln131, Trp219, Phe246 His389, Ser390, His437, Phe439	A247-A384	Arg250, Pro257, Val258, Gly259, Ala260, Phe262, Leu263, Pro296, Ala299, Arg302, Met356	(Thr314 substituted by Ala299)	Identical to ***A. fulgidus***	Identical to ***A. fulgidus*** (Thr314 unsubstituted by Ala299)	Identical to ***A. fulgidus***
Thermodesulfo-bacterium commune **(20 AA)**	A2-A278 A412-A508	Asn74, Trp158, Gln159, Trp251, Phe278 His416, Ala417, His467, Phe469	A279-A411	Arg282, Pro289, Val290, Gly291, Ala292, Phe294, Leu295, His328, Thr331, Arg334, Met383	(Ser399 substituted by Ala417)	Identical to ***A. fulgidus***	Glu141 is missing unsubstituted Tyr95 is missing unsubstituted	Pro311 is substituted by His328
Desulfovibrio vulgaris **(20 AA)**	A2-A278 A414-A510	Asn78, Trp161, Gln162, Trp251, Phe278 His418, Ser419, His469,	A279-A413	Arg282, Pro289, Val290, Gly291, Ala292, Phe294, Leu295, Val330, Thr333,	Identical to ***A. fulgidus***	Identical to ***A. fulgidus***	Tyr95, Glu141 are missing unsubstituted	Pro311 is missing unsubstituted Additional Aa Val330

		Phe471		Arg336, Met385				
Desulfovibrio desulfuricans **(20 AA)**	A2-A276 A412-A508	Asn76, Trp159, Gln160, Trp249, Phe276 His416, Ser417, His467, Phe469	A277-A411	Arg280, Pro287, Val288, Gly289, Ala290, Phe292, Leu293, Val328, Thr331, Arg334, Met383	Identical to ***A. fulgidus***	Identical to ***A. fulgidus***	Tyr95, Glu141 are missing unsubstituted	Pro311 is missing unsubstituted Additional Aa Val328
Desulfotalea psychrophila **(20 AA)**	A2-A273 A418-A515	Asn76, Trp156, Gln157, Trp246, Phe273 His422, Ser423, His475, Phe477	A274-A417	Arg277, Pro284, Val285, Gly286, Ala287, Phe289, Leu290, Val325, Thr328, Arg331, Met389	Identical to ***A. fulgidus***	Identical to ***A. fulgidus***	Tyr95, Glu141 are missing unsubstituted	Pro311 is missing unsubstituted Additional Aa Val325
***Desulfobulbus* sp. MLMS1** **(19 AA)**	A2-A271 A416-A513	Asn62, Trp154, Gln155, Trp244, Phe271 His420, Ser421, His472, Phe474	A272-A415	Arg275, Pro282, Val283, Gly284, Ala285, Phe287, Leu288, Thr326, Arg329, Met387	Identical to ***A. fulgidus***	Identical to ***A. fulgidus***	Tyr95, Glu141 are missing unsubstituted	Pro311 is missing unsubstituted
***O. algarvensis* Delta 1 symbiont** **(20 AA)**	A2-A273 A409-A505	Asn74, Trp156, Gln157, Trp246, Phe273 His413, Ser414, His464, Phe466	A274-A408	Arg277, Pro284, Val285, Gly286, Ala287, Phe289, Leu290, Ile325, Thr328, Arg331, Met380	Identical to ***A. fulgidus***	Identical to ***A. fulgidus***	Tyr95, Glu141 are missing unsubstituted	Pro311 substituted by Ile325
Thermodesulfovibrio yellowstonii **(22 AA)**	A2-A281 A417-A508	Asn72, Tyr86, Trp156, Gln157, Trp254, Phe281 His421, Ala422, His467, Phe469	A282-A416	Arg285, Pro292, Val293, Gly294, Ala295, Phe297, Leu298, Glu332, Ala333, Thr336, Arg339, Met388	(Ser399 substituted by Ala422)	Identical to ***A. fulgidus***	Glu141 is missing unsubstituted	Pro311 is substituted by additional Aa Glu332 and Ala333
Chlorobaculum tepidum **(22 AA)**	A2-A277 A413-A504	Asn72, Tyr86, Trp152, Gln153, Trp250, Phe277 His417, Ala418, His463, Phe465	A278-A412	Arg281, Pro288, Val289, Gly290, Ala291, Phe293, Leu294, His328, Leu330, Thr332, Arg335, Met384	(Ser399 substituted by Ala418)	Identical to ***A. fulgidus***	Glu141 is missing unsubstituted	Pro311 is substituted by additional Aa His328 and Leu330
***Thiobacillus denitrificans* 25259** **(22 AA)**	A2-A270 A404-A510	Asn72, Trp153, Gln154, Trp234, Phe270 His408, Ser409, His469, Phe471	A271-A403	Arg274, Pro281, Val282, Gly283, Ala284, Phe286, Leu287, Val320, Pro321, Ala322, Ser323, Arg326, Met375	(Thr314 substituted by Ser323)	Identical to ***A. fulgidus***	Tyr95, Glu141 are missing unsubstituted	Pro311 is substituted by additional Aa Val320, Pro321 and Ala322
Crenarch. SRP								
Caldivirga maquilingensis **(24 AA)**	A2-A244 A373-A474	Asn60, Tyr78, Glu124, Trp127, Gln128, Trp217, Phe244 His377, Ala378, His432, Phe434	A245-A372	Val246, Arg248, Pro255, Val256, Gly257, Ala258, Gln260, Leu261, Pro297, Thr299, Thr301, Arg304, Met344	(Ser399 substituted by Ala378 Additional Aa Val249)	Identical to ***A. fulgidus***	Identical to Archglobus fulgidus	Phe277 is substituted by Gln260 Additional Aa Thr299
Pyrobaculum calidifontis **(20 AA)**	A2-A247 A375-A466	Tyr82, Trp132, Gln133, Trp220, Leu247 His379, His423, Phe425	A248-A374	Val249, Arg251, Pro258, Val259, Gly260, Phe261, Tyr263, Leu264, Pro301, Thr304, Arg307, Met346	Asn74 is missing (Asn63 is improper placed) (Ser399 is missing unsubstituted, Additional Aa Val249)	Identical to ***A. fulgidus***	Glu141 is missing unsubstituted	Phe277 is substituted by Tyr263
SOB Apr lineage I								
Allochromatium vinosum	A2-A243 A376-A466	Asn60, Tyr78, Glu125, Trp128, Gln129, Trp216,	A244-A375	Leu245, Arg247, Pro254, Val255, Gly256, Ala257,	Additional Aa Leu245 Phe261 substituted by Ile243	Identical to ***A. fulgidus***	Identical to ***A. fulgidus***	Additional Aa Glu275

(24 AA)		Ile243 His380, Ala381, His424, Phe426		Phe259, Leu260, Glu275, Pro302, Thr305, Arg308, Met347	Ser399 substituted by Ala 381			
***Thiobacillus denitrificans* 25259** **(24 AA)**	A2-A243 A376-A466	Asn60, Tyr78, Glu125, Trp128, Gln129, Trp216, Ile243 His380, Ala381, His424, Phe426	A244-A375	Leu245, Arg247, Pro254, Val255, Gly256, Ala257, Phe259, Leu260, Glu275, Pro302, Thr305, Arg308, Met347	Additional Aa Leu245 Phe261 substituted by Ile243 Ser399 substituted by Ala 381	Identical to ***A. fulgidus***	Identical to ***A. fulgidus***	Additional Aa Glu275
***Cdt.* Ruthia magnifica** **(24 AA)**	A2-A247 A379-A469	Asn60, Tyr78, Glu128, Trp131, Gln132, Trp219, Ile246 His383, Ala384, His427, Phe429	A248-A378	Leu248, Arg250, Pro257, Val258, Gly259, Ala260, Phe262, Leu263, Glu278, Pro305, Thr308, Arg311, Met350	Additional Aa Leu278 Phe261 substituted by Ile246 Ser399 substituted by Ala 384	Identical to ***A. fulgidus***	Identical to ***A. fulgidus***	Additional Aa Glu278
***Cdt.* Pelagibacter ubique** **(22 AA)**	A2-A243 A367-A458	Asn60, Tyr78, Glu125, Trp128, Gln129, Trp216, Ile243 His372, Ala373, His416, Phe418	A244-A366	Leu245, Arg247, Pro254, Val255, Gly256, Ala257, Phe259, Leu260, Thr297, Arg300, Met339	Additional Aa Leu245 Phe261 substituted by Ile243 Ser399 substituted by Ala 373	Identical to ***A. fulgidus***	Identical to ***A. fulgidus***	Pro311 is missing unsubstituted
EBAC2C11 **(23 AA)**	A2-A243 A367-A458	Asn60, Tyr78, Glu125, Trp128, Gln129, Trp216, Ile243 His372, Ala373, His416, Phe418	A244-A366	Leu245, Arg247, Pro254, Val255, Gly256, Ala257, Phe259, Leu260, Pro294, Thr297, Arg300, Met339	Additional Aa Leu245 Phe261 substituted by Ile243 Ser399 substituted by Ala 371	Identical to ***A. fulgidus***	Identical to ***A. fulgidus***	Identical to ***A. fulgidus***

Supplementary data material Table S6. Structure of the active center at the substrate binding site: residues adjacent to the catalytically active N5 atom of FAD in AprA models of SRP and SOB (distances in Å are listed)

Species	FAD-binding domain I	AA adjacent to the N5-FAD atom	distance in Å	Capping domain	AA adjacent to the N5-FAD atom	distance in Å	FAD-binding domain II	AA adjacent to the N5-FAD atom	distance in Å	Helical domain	AA adjacent to the N5-FAD atom
Archaeoglobus fulgidus	A2-A261	Leu 70	3.63	A262-A393	Arg 265	6.31	A394-A487	His 398	4.44	A488-A643	-
		Ser 71	7.39		Pro 272	6.32		Phe 448	5.63		
		Ala 72	5.77		Met 365	3.69					
		Asn 74	4.25								
		Trp 234	5.30								
Desulfotomaculum reducens	A2-A243	Leu 58	3.69	A244-A382	Arg 247	6.32	A383-A472	His 387	4.45	A473-624	-
		Ser 59	7.40		Pro 254	6.28		Phe 433	5.29		
		Ala 60	5.69		Met 354	3.65					
		Asn 62	4.23								
		Trp 216	5.29								
Syntrophobacter fumaroxidans	A2-A248	Leu 58	3.69	A249-A386	Arg 251	6.32	A387-A482	His 391	4.45	A483-A634	-
		Ser 59	7.39		Pro 258	6.28		Phe 443	5.62		
		Ala 60	5.70		Met 358	3.65					
		Asn 62	4.23								
		Trp 220	5.29								
fosws7f8	A2-A245	Leu 58	3.60	A246-A383	Arg 249	6.32	A384-A477	His 388	4.46	A478-A630	-
		Ser 59	7.39		Pro 256	6.29		Phe 438	5.62		
		Ala 60	5.69		Met 355	3.65					
		Asn 62	4.23								
		Trp 218	5.29								
fosws39f7	A2-A246	Leu 59	3.69	A247-A384	Arg 250	6.32	A385-A478	His 389	4.45	A479-A634	-
		Ser 60	7.39		Pro 257	6.29		Phe 439	5.62		
		Ala 61	5.70		Met 356	3.65					
		Asn 63	4.23								
		Trp 219	5.29								
Thermodesulfobacterium commune	A2-A278	Leu 70	3.68	A279-A411	Arg 282	6.31	A412-A508	His 416	4.45	A509-A664	-
		Ser 71	7.39		Pro 289	6.28		Phe 469	5.61		
		Ala 72	5.71		Met 383	3.67					
		Asn 74	4.23								
		Trp 251	5.29								
Desulfovibrio vulgaris	A2-A278	Leu 74	3.72	A279-A413	Arg 282	6.31	A414-A510	His 418	4.46	A511-A664	-
		Ser 75	7.38		Pro 289	6.28		Phe 471	5.62		
		Ala 76	5.70		Met 385	3.67					
		Asn 78	4.23								
		Trp 251	5.29								
Desulfovibrio desulfuricans	A2-A276	Leu 72	3.71	A277-A411	Arg 280	6.32	A412-A508	His 416	4.46	A509-A662	-
		Ser 73	7.38		Pro 287	6.28		Phe 469	5.61		
		Ala 74	5.70		Met 383	3.66					
		Asn 76	4.22								
		Trp 249	5.29								

***Desulfobulbus* sp.**	A2-A271	Leu 70	3.70	A272-A415	Arg 275	6.32	A416-A513	His 420	4.46	A514-A669	-
		Ser 71	7.39		Pro 282	6.29		Phe 474	5.61		
		Ala 72	5.70		Met 387	3.65					
		Asn 74	4.22								
		Trp 244	5.29								
Desulfotalea psychrophila	A2-A273	Leu 72	3.72	A274-A417	Arg 277	6.31	A418-A515	His 422	4.46	A516-A671	-
		Ser 73	7.38		Pro 284	6.29		Phe 477	5.62		
		Ala 74	5.70		Met 389	3.67					
		Asn 76	4.23								
		Trp 246	5.29								
***Olavius algarvensis* Delta 1 symbiont**	A2-A273	Leu 70	3.70	A274-A408	Arg 277	6.32	A409-A505	His 413	4.45	A506-A659	-
		Ser 71	7.39		Pro 284	6.29		Phe 466	5.61		
		Ala 72	5.70		Met 380	3.65					
		Asn 74	4.22								
		Trp 246	5.29								
Thermodesulfovibrio yellowstonii	A2-A281	Leu 68	3.69	A282-A416	Arg 285	6.32	A417-A508	His 421	4.45	A509-A662	-
		Ser 69	7.39		Pro 292	6.29		Phe 469	5.61		
		Ala 70	5.70		Met 388	3.65					
		Asn 72	4.22								
		Trp 254	5.29								
Chlorobaculum tepidum	A2-A277	Leu 68	3.70	A278-A412	Arg 281	6.32	A413-A504	His 417	4.46	A505-A658	-
		Ser 69	7.39		Pro 288	6.29		Phe 465	5.61		
		Ala 70	5.70		Met 384	3.66					
		Asn 72	4.22								
		Trp 250	5.29								
***Thiobacillus denitrificans* 25259**	A2-A270	Leu 68	3.71	A271-A403	Arg 274	6.32	A404-A510	His 408	4.46	A511-A666	-
		Ser 69	7.39		Pro 281	6.29		Phe 471	5.61		
		Ala 70	5.70		Met 375	3.66					
		Asn 72	4.22								
		Trp 243	5.29								
Pyrobaculum calidifontis	A2-A247	Leu 59	3.73	A248-A374	Arg 251	6.31	A375-A466	His 379	4.46	A467-A627	-
		Ser 60	7.37		Pro 258	6.29		Phe 425	5.62		
		Ala 61	5.73		Met 346	3.67					
		Trp 220	5.29								
Caldivirga maquilingensis	A2-A244	Leu 56	3.69	A245-A372	Arg 248	6.30	A373-A474	His 377	4.45	A475-A635	-
		Ser 57	7.38		Pro 255	6.30		Phe 434	5.62		
		Ala 58	5.71		Met 344	3.67					
		Asn 60	4.23								
		Trp 217	5.29								
Allochromatium vinosum	A2-A243	Leu 56	3.70	A244-A375	Arg 247	6.30	A376-A466	His 380	4.46	A467-A620	-
		Tyr 57	7.39		Pro 254	6.29		Phe 426	5.60		
		Ala 58	5.70		Met 347	3.66					
		Asn 60	4.23								
		Trp 216	5.20								
***Thiobacillus denitrificans* 25259**	A2-A243	Leu 56	3.70	A244-A375	Arg 247	6.30	A376-A466	His 380	4.46	A467-A622	-
		Tyr 57	7.40		Pro 254	6.29		Phe 426	5.61		
		Ala 58	5.70		Met 347	3.65					
		Asn 60	4.23								

		Trp 216	5.20							
***Cdt.* Ruthia magnifica**	A2-A247	Leu 56	3.70	A248-A378	Arg 250	6.30	A379-A469	His 383	4.46	A470-A625 -
		Tyr 57	7.39		Pro 257	6.29		Phe 429	5.61	
		Ala 58	5.70		Met 350	3.66				
		Asn 60	4.23							
		Trp 219	5.21							
***Cdt.* Pelagibacter ubique**	A2-A243	Leu 56	3.69	A244-A366	Arg 247	6.30	A367-A458	His 372	4.46	A459-A614 -
		Tyr 57	7.40		Pro 254	6.29		Phe 418	5.60	
		Ala 58	5.70		Met 339	3.65				
		Asn 60	4.23							
		Trp 216	5.19							
EBAC2C11	A2-A243	Leu 56	3.69	A244-A366	Arg 247	6.29	A367-A458	His 372	4.46	A459-A621 -
		Tyr 57	7.40		Pro 254	6.29		Phe 418	5.60	
		Ala 58	5.70		Met 339	3.65				
		Asn 60	4.23							
		Trp 216	5.20							

Danksagung

An dieser Stelle möchte ich meinen Eltern danken, ohne deren Unterstützung und Rückhalt meine Doktorarbeit nicht möglich gewesen wäre.

Weiterer großer Dank gilt

Prof. Dr. Friedrich Widdel für die Bereitstellung des Arbeitsplatzes am Max-Planck-Institut für Marine Mikrobiologie und die Erstellung des Erstgutachtens,

Dr. Jan Küver für die Bereitstellung des Themas, seine Anregungen, Diskussionsbereitschaft, unermüdliche Hilfeleistungen bei der Berechnung von phylogenetischen Stammbäumen und die Erstellung des Zweitgutachtens

sowie der gesamten Arbeitsgruppe Mikrobiologie für die erhaltene Unterstützung und angenehme Arbeitsatmosphäre.